

University of Southampton Research Repository ePrints Soton

Copyright © and Moral Rights for this thesis are retained by the author and/or other copyright owners. A copy can be downloaded for personal non-commercial research or study, without prior permission or charge. This thesis cannot be reproduced or quoted extensively from without first obtaining permission in writing from the copyright holder/s. The content must not be changed in any way or sold commercially in any format or medium without the formal permission of the copyright holders.

When referring to this work, full bibliographic details including the author, title, awarding institution and date of the thesis must be given e.g.

AUTHOR (year of submission) "Full thesis title", University of Southampton, name of the University School or Department, PhD Thesis, pagination

UNIVERSITY OF SOUTHAMPTON FACULTY OF ENGINEERING AND THE ENVIRONMENT INSTITUTE OF SOUND AND VIBRATION

RESEARCH

DISCOMFORT OF SEATED PERSONS EXPOSED TO LOW FREQUENCY LATERAL AND ROLL MOTION

by

George Frederick Beard

Thesis for the degree of Doctor of Philosophy

October 2012

UNIVERSITY OF SOUTHAMPTON

ABSTRACT

FACULTY OF ENGINEERING AND THE ENVIRONMENT INSTITUTE OF SOUND AND VIBRATION RESEARCH

Doctor of Philosophy

DISCOMFORT OF SEATED PERSONS EXPOSED TO LOW FREQUENCY LATERAL AND ROLL MOTION

By George Frederick Beard

Passengers of land transport are exposed to horizontal and rotational oscillations at frequencies less than 1 Hz which may cause vibration discomfort and motion sickness. Previous knowledge of human responses to motion is insufficient for predicting the discomfort caused by low frequencies. The objective of this thesis is to improve understanding of subjective responses to lateral and roll oscillation (presented in isolation and in combination) at frequencies less than 1 Hz in order to establish a predictive model of comfort.

The first of five experiments tested the predictions of a conceptual model of motion sickness. Illness ratings were obtained over a 30-minute exposure to 0.2 Hz fully roll-compensated lateral oscillation where the point of full roll-compensation was either at the seat surface (i.e. 'seat compensation') or at head height (i.e. 'head compensation'). Median illness ratings were greater during 'head compensation', showing some support for the motion sickness model, but differences were not statistically significant. Age, stature and body weight had no effect on illness ratings, but Asians were more than three-times as likely to experience 'mild nausea' than Europeans. It is concluded that differences in the position of full roll-compensation in transport vehicles are less important for motion sickness than inherent differences in passenger populations.

The next four experiments used the method of magnitude estimation to determine the vibration discomfort caused by lateral oscillation, roll oscillation, and fully roll-compensated lateral oscillation with a variety of seating configurations. In the second experiment, lateral acceleration between 0.2 and 1.0 Hz caused less discomfort when sitting with a backrest than when sitting without a backrest on both a rigid seat and on a cushioned train seat; contrary to the predictions of current standards. In the third experiment, 0.25 to 0.4 Hz lateral acceleration in the plane of the seat caused similar discomfort regardless of whether the acceleration was due to lateral oscillation or roll oscillation through the gravitational vector, but above 0.4 Hz, discomfort from the roll was far greater. At frequencies less than 0.5 Hz, fully compensating the lateral acceleration with roll improved comfort compared to uncompensated lateral acceleration, but at greater frequencies, roll-compensation worsened comfort and caused discomfort similar to pure roll oscillation at 1 Hz.

The fourth and fifth experiments examined differences in discomfort caused by the rigidity of the seat pan and the height of the backrest. In the fourth experiment, discomfort was greater on a soft foam seat than on a rigid seat during lateral oscillation below 0.63 Hz, during roll oscillation below 0.5 Hz and during fully roll-compensated lateral oscillation between 0.315 and 0.5 Hz. In the fifth experiment, discomfort was greater without a backrest than with a short backrest for lateral oscillation between 0.315 and 0.5 Hz. Contrary to current standards, discomfort was also greater without a backrest than with a high backrest for lateral oscillation below 1 Hz and for roll oscillation below 0.5 Hz. In addition, sitting with a backrest was beneficial for comfort with fully roll-compensated lateral oscillation between 0.4 and 0.63 Hz.

The results of the five experiments were collated to provide recommendations for the improvement of current vibration standards. On the basis of experiment 1, a new multiplying factor for the prediction of vomiting incidence in an unadapted group of male Asian adults is offered. On the basis of the four discomfort experiments, modifications to current frequency weightings for lateral acceleration and roll acceleration are offered so as to extend the prediction to frequencies less than 0.5 Hz. Guidance for the prediction of discomfort with fully roll-compensated lateral oscillation is also provided. The thesis is concluded with recommendations for future research.

Contents

List of table	sxiii
List of figure	esxv
Acknowled	gementsxxvii
Nomenclati	ırexxix
Chapter 1	Introduction1
Chapter 2	Literature review5
2.1. Ir	ntroduction5
2.2. T	he motion environment5
2.2.1.	Coordinate system5
2.2.2.	Inertia and gravitational forces6
2.2.3.	Rotation9
2.2.4.	Tilt-compensation
2.2.5.	Railway motions
2.3. N	lotion perception
2.3.1.	The vestibular system
2.3.2.	The visual system
2.3.3.	The somatosensory system
2.4. Ir	ovestigation of motion sickness
2.4.1.	Symptoms
2.4.2.	Measurement and evaluation
2.4.3.	Theories of motion sickness
2.5. F	actors influencing motion sickness
2.5.1.	Frequency
2.5.2.	Magnitude
2.5.3.	Multi-axis motion
2.5.4.	Seating and posture
2.5.5.	Inter-subject variability
2.5.6.	Vision44

2.5.7.	Head movements	45
2.6. Mo	del of motion sickness	47
2.7. Inv	estigation of vibration discomfort	47
2.7.1.	Definitions	47
2.7.2.	Measurement and evaluation	47
2.7.3.	Reliability of subjective methods	50
2.8. Fac	ctors influencing vibration discomfort	53
2.8.1.	Frequency	53
2.8.2.	Magnitude	61
2.8.3.	Multi-axis motion	63
2.8.4.	Seating and posture	64
2.9. Mo	del of vibration discomfort	68
2.9.1.	Frequency weightings and axis multiplying factors	68
2.10. Co	nclusion	73
Chapter 3	Equipment and experimental methods	75
3.1. Intr	oduction	75
3.2. Mo	tion simulation equipment	75
3.2.1.	12-m tilting and translating cabin	75
3.2.2.	1-m horizontal simulator	77
3.2.3.	6-axis simulator	79
3.3. Tes	st environment	79
3.3.1.	Motions	79
3.3.2.	Visual field	90
3.3.3.	Noise	90
3.4. Psy	ychophysical methods	91
3.4.1.	Motion sickness	91
3.4.2.	Vibration discomfort	93
3.5. Sta	atistical power and subject sampling	95
3.5.1.	Subjects	95

3.5.2.	Sample power
3.6. Dat	a analysis96
3.6.1.	Software
3.6.2.	Statistical tests
3.7. Saf	ety and ethics
Chapter 4 E	ffects of position of full roll-compensation and subject demographics on motion
sickness	
4.1. Intr	oduction
4.2. Met	hod 101
4.2.1.	Apparatus
4.2.2.	Design
4.2.3.	Motion stimuli
4.2.4.	Subjects
4.2.5.	Measurement of motion sickness
4.3. Res	sults
4.3.1.	Effect of position of full roll-compensation
4.3.2.	Effects of subject characteristics
4.3.3.	Survival analysis
4.4. Dis	cussion
4.4.1.	Effect of position of full roll-compensation
4.4.2.	Ethnicity112
4.5. Cor	nclusion114
Chapter 5 S	seating effects with lateral vibration discomfort
5.1. Intr	oduction115
5.2. Met	hod 117
5.2.1.	Apparatus
5.2.2.	Design
5.2.3.	Motion stimuli
5.2.4.	Subjects
5.2.5.	Analysis

5.3.	Results	122
5.3.1	Rate of growth of vibration discomfort	122
5.3.2	2. Effect of frequency of oscillation on vibration discomfort	123
5.3.3	3. Effect of seating on vibration discomfort	124
5.3.4	4. Location of discomfort	125
5.4.	Discussion	126
5.4.1	1. Rate of growth of discomfort	126
5.4.2	2. Equivalent comfort contours	126
5.4.3	3. Location of discomfort	129
5.5.	Practical implications	130
5.6.	Conclusion	130
Chapter (6 Discomfort caused by lateral, roll and fully roll-compensated lateral osc	cillation 131
6.1.	Introduction	131
6.2.	Method	132
6.2.1	1. Apparatus	132
6.2.2	2. Design	133
6.2.3	3. Motion stimuli	133
6.2.4	4. Subjects	134
6.2.5	5. Analysis	135
6.3.	Results	135
6.3.1	1. Rate of growth of vibration discomfort	135
6.3.2	2. Effect of frequency of oscillation on vibration discomfort	137
6.3.3	3. Effect of direction of oscillation on vibration discomfort	137
6.3.4	4. Effect of magnitude on the frequency-dependence of equivalent con	nfort contours
		137
6.3.5	5. Effect of gender on equivalent comfort contours	139
6.3.6	5. Location of discomfort	139
6.4.	Discussion	140
6.4.1	1. Rate of growth of discomfort	140
6.4.2	2. Effect of frequency of oscillation on discomfort	141

	6.4.3.	Effect of direction of oscillation on discomfort	145
	6.4.4.	Location of discomfort	146
	6.4.5.	Implications for transport	146
6.	5. Con	clusion	147
Cha	pter 7 E	ffect of seat pan stiffness	149
7.	1. Intro	oduction	149
7.	2. Met	nod	150
	7.2.1.	Apparatus	150
	7.2.2.	Design	151
	7.2.3.	Motion stimuli	152
	7.2.4.	Subjects	154
	7.2.5.	Analysis	154
	7.2.6.	Objective measurements	155
7.	3. Res	ults	156
	7.3.1.	Effect of seating on rate of growth of discomfort	156
	7.3.2.	Effect of frequency and direction of oscillation on rate of growth of discomfort	158
	7.3.3.	Effect of seating on vibration discomfort	160
	7.3.4.	Effect of frequency and direction of oscillation on vibration discomfort	160
	7.3.5.	Effect of magnitude on the frequency-dependence of equivalent comfort conto	
	7.3.6.	Location of discomfort	
	7.3.7.	Lateral transmissibility and roll transmissibility of foam cushion	165
	7.3.8.	Effect of magnitude on lateral and roll transmissibility of foam seat	166
7.	4. Disc	cussion	167
	7.4.1.	Rate of growth of discomfort	167
	7.4.2.	Equivalent comfort contours	168
	7.4.3.	The location of discomfort	169
	7.4.4.	Implications for vibration standards	171
7.	5. Con	clusion	174
Cha	nter 8 F	ffect of backrest height	175

8.1.	Introduction	175
8.2.	Method	177
8.2.1	Apparatus	177
8.2.2	2. Design	178
8.2.3	B. Motion stimuli	179
8.2.4	l. Subjects	180
8.2.5	5. Analysis	180
8.3.	Results	182
8.3.1	Rate of growth of discomfort	182
8.3.2	2. Vibration discomfort	184
8.3.3	B. Location of discomfort	188
8.4.	Discussion	189
8.4.1	Rate of growth of discomfort	189
8.4.2	2. Equivalent comfort contours	189
8.4.3	3. The location of discomfort	193
8.4.4	Implications for vibration standards	194
8.5.	Conclusion	197
Chapter	9 Discussion	199
9.1.	Introduction	199
9.2.	Human response to roll-compensated lateral acceleration	199
9.2.1	Mechanisms of motion sickness and physical discomfort	204
9.2.2	2. Model of motion sickness	205
9.2.3	B. Model of discomfort	206
9.3.	Recommendations for vibration standards	209
9.3.1	Motion sickness dose value	209
9.3.2	2. Discomfort from lateral acceleration	210
9.3.3	B. Discomfort from roll acceleration	214
9.3.4	Discomfort from roll-compensated lateral acceleration	217
9.3.5	5. Passenger seating	219

9.4. Ass	essment of adjusted weightings	. 220
9.4.1.	Lateral acceleration	. 223
9.4.2.	Roll acceleration	. 224
9.4.3.	Fully roll-compensated lateral acceleration	. 225
9.5. Res	search methodology	. 226
9.5.1.	Absolute versus relative magnitude estimation	. 226
9.5.2.	Motion sickness bias	. 230
9.5.3.	Effects of fatigue	. 232
9.5.4.	Order effects	. 233
9.5.5.	Range effects	. 234
9.6. Red	commendations for future research	. 235
9.6.1.	Centre-of-rotation	. 235
9.6.2.	Percentage compensation	. 238
9.6.3.	The semantics of discomfort	. 241
9.6.4.	Phase	. 242
Chapter 10	Conclusion	. 243
Appendices		. 245
A.1. Subjec	et consent form	. 245
A.2. Motion	sickness susceptibility questionnaire	. 247
A.3. Subjec	et information questionnaire	. 253
A.4. Subjec	et instructions	. 254
A.4.1. Ex	periment 1	. 254
A.4.2. Ex	periment 2	. 255
A.4.3. Ex	periment 3	. 256
A.4.4. Ex	periment 4	. 257
A.4.5. Ex	periment 5	. 258
A.5. MATLA	AB scripts: Motion generation	. 259
A.5.1. 12	-m tilting and translating cabin	. 259
A.5.2. 1-r	n horizontal simulator	. 264

A.6. Subject demographics 273 A.7. Load-deflection curve (Foam cushion used in Experiment 4) 278 A.8. Frequency-weighted components of lateral, roll and fully-roll compensated lateral motion 279 A.9. Experimental designs 282 A.9.1. Experiment 1 282 A.9.2. Experiment 2 282 A.9.3. Experiment 3 284 A.9.4. Experiment 4 285 A.9.5. Experiment 5 287 A.10. Equations for calculating ride values 289 A.11. Normalisation procedures 290 References 293		A.5.3. 6-axis simulator	266
A.8. Frequency-weighted components of lateral, roll and fully-roll compensated lateral motion 279 A.9. Experimental designs 282 A.9.1. Experiment 1 282 A.9.2. Experiment 2 282 A.9.3. Experiment 3 284 A.9.4. Experiment 4 285 A.9.5. Experiment 5 287 A.10. Equations for calculating ride values 289 A.11. Normalisation procedures 290		A.6. Subject demographics	273
A.9. Experimental designs 282 A.9.1. Experiment 1 282 A.9.2. Experiment 2 282 A.9.3. Experiment 3 284 A.9.4. Experiment 4 285 A.9.5. Experiment 5 287 A.10. Equations for calculating ride values 289 A.11. Normalisation procedures 290		A.7. Load-deflection curve (Foam cushion used in Experiment 4)	278
A.9. Experimental designs 282 A.9.1. Experiment 1 282 A.9.2. Experiment 2 282 A.9.3. Experiment 3 284 A.9.4. Experiment 4 285 A.9.5. Experiment 5 287 A.10. Equations for calculating ride values 289 A.11. Normalisation procedures 290		A.8. Frequency-weighted components of lateral, roll and fully-roll compensated lateral mo	otion
A.9.1. Experiment 1 282 A.9.2. Experiment 2 282 A.9.3. Experiment 3 284 A.9.4. Experiment 4 285 A.9.5. Experiment 5 287 A.10. Equations for calculating ride values 289 A.11. Normalisation procedures 290			279
A.9.2. Experiment 2 282 A.9.3. Experiment 3 284 A.9.4. Experiment 4 285 A.9.5. Experiment 5 287 A.10. Equations for calculating ride values 289 A.11. Normalisation procedures 290		A.9. Experimental designs	282
A.9.3. Experiment 3 284 A.9.4. Experiment 4 285 A.9.5. Experiment 5 287 A.10. Equations for calculating ride values 289 A.11. Normalisation procedures 290		A.9.1. Experiment 1	282
A.9.4. Experiment 4		A.9.2. Experiment 2	282
A.9.5. Experiment 5		A.9.3. Experiment 3	284
A.10. Equations for calculating ride values		A.9.4. Experiment 4	285
A.11. Normalisation procedures		A.9.5. Experiment 5	287
·		A.10. Equations for calculating ride values	289
References		A.11. Normalisation procedures	290
	F	References	293

List of tables

Table 1.1 Objectives of this thesis.	3
Table 2.1 Effect of arbitrary values of angular displacement (θ), distance from centre-of-rotation	n
(H) and frequency of oscillation (f) on vertical (a_z) and lateral (a_y) acceleration	11
Table 2.2 Nominal motion quantities for a train traversing a curve (Persson et al., 2009)	15
Table 2.3 Unweighted coach-lateral accelerations, coach-vertical accelerations and coach roll-	-
velocities measured across 26 journeys on an experimental TGV tilting train (Donohew and Griffin, 2007).	17
Table 2.4 Changes in coach-lateral acceleration, coach-vertical acceleration and coach-roll	
displacement associated with changes in percentage compensation (Donohew, 2006)	19
Table 2.5 Measures of motion sickness susceptibility (Griffin and Howarth, 2000)	28
Table 2.6 Motion sickness illness rating scale (Griffin and Howarth, 2000)	29
Table 2.7 List of common motion sickness symptoms (Griffin and Howarth, 2000)	29
Table 2.8 Types and categories of sensory conflict based on the sensory rearrangement theory (Griffin, 1990).	-
Table 2.9 Quantities of lateral, roll and fully roll-compensated lateral motions and associated	
levels of 'mild nausea', as reported by Howarth and Griffin (2003), Donohew and Griffin (2004))
and Donohew (2006)	35
Table 2.10 Results of field studies investigating effect of inter-subject variables on motion sickness	43
Table 2.11 Distribution of acceleration magnitudes used by Suzuki (1998a)	52
Table 2.12 Summary of laboratory studies investigating vibration discomfort caused by	
translational and rotational oscillation at low frequencies (part 1).	57
Table 2.13 Summary of laboratory studies investigating vibration discomfort caused by	
translational and rotational oscillation at low frequencies (part 2).	58
Table 2.14 Frequency weightings for predicting vibration discomfort with fore-and-aft (x), laterately, vertical (z), roll (r_x), pitch (r_y) and yaw (r_z) vibration between 0.5 and 80 Hz (ISO 2631-1, 1997)	
Table 2.15 Effect of the magnitude of vibration total values (VTV) on estimated comfort levels,	
as provided by ISO 2631-1 (1997)	
Table 3.1 Typical measured accelerations for 'seat compensation' and 'head compensation'	
conditions in Experiment 1. (*Accelerations were filtered using band-pass filters one-third octav	ve
above and below 0.2 Hz)	82

Table 3.2 Percentage error calculations (W_d -weighted error / measured acceleration x 100) fo	r
each frequency of lateral oscillation used in Experiment 2.	85
Table 3.3 Percentage error calculations (W_d -weighted error / measured acceleration x 100) for	r
each frequency of lateral oscillation used in Experiment 3, 4 and 5.	86
Table 3.4 Percentage error calculations (W_e -weighted error / measured acceleration x 100) for	r
each frequency of roll oscillation used in Experiment 3, 4 and 5.	87
Table 3.5 Measures of motion sickness susceptibility (Griffin and Howarth, 2000)	91
Table 3.6 Illness rating (IR) scale used in Experiment 1	92
Table 3.7 Symptom Checklist used in Experiment 1	92
Table 3.8 Median (inter-quartile range) age, height and weight of subjects tested in each	
experiment	95
Table 3.9 Parameters used to calculate statistical power for subject samples used in Experime 1 to 5	
Table 3.10 List of statistical tests used in Experiments 1 – 5	.97
Table 4.1 Motion quantities for the two experimental conditions	
Table 4.2 Result of Cox regression analysis1	09
Table 9.1 Nominal motion quantities at the seat surface and at the head* during roll-	
compensated lateral oscillations (* head assumed to be 800 mm above the seat surface)2	202
Table 9.2 Parameters of the transfer functions for W_d (current weighting) and $W_{d'}$ (adjusted	
weighting) for lateral acceleration.	213
Table 9.3 Parameters of the transfer functions for W_e (current weighting) and W_{e} (adjusted	
weighting) for roll acceleration	216
Table 9.4 List of seating conditions tested in Chapters 5 to 8	219
Table 9.5 Frequency weightings at one-third octave centre frequencies. [Standardised	
weightings W_d and W_e (ISO 8041, 2005) and adjusted weightings W_d and W_e (Section 9.3)].2	221
Table 9.6 Distribution of 78 discomfort responses to test motions equivalent to a subjective	
magnitude of 100 (i.e. equivalent to the reference motion) reported by subjects during	
Experiment 2 and 3	
Table 9.7 Effect of distance from centre-of-rotation* on nominal lateral accelerations at the sea	
and the head+2	
Table 9.8 Effect of percentage compensation on nominal accelerations at the seat and the here.	
during roll-compensated lateral oscillation.	:39
Table 9.9 Effect of the magnitude of vibration total values of estimated comfort levels, as	140
provided by ISO 2631-1 (1997)	42

List of figures

Figure 2.1 The six axes of motion [fore-and-aft (x-axis), lateral (y-axis), vertical (z-axis)] and	
three rotational axes [roll (r_x -axis), pitch (r_y -axis), yaw (r_z -axis)].	6
Figure 2.2 Basicentric coordinate system used to define motion of a seated person at a) the	
back, b) the seat, and c) the feet.	8
Figure 2.3 Gravitational (F_g , F_p , F_n '), normal (F_n) and frictional (F_n) forces associated with a statement of the statement of	ıtic
object placed on a Earth-horizontal surface (a) and a surface inclined through angle θ (b)	8
Figure 2.4 The inertial force (F_1), the normal force (F_n), the gravitational force (F_g) and the	
resultant gravito-inertial force (GIF) imposed on a basicentric coordinate system undergoing	
lateral acceleration (a _y).	9
Figure 2.5 Horizontal (Y_d) and vertical (V_d) displacement of a point distance (H) from the centrof-rotation (CoR) during angular displacement (θ)	
Figure 2.6 Example of tilt-compensation technique for sinusoidal lateral and roll motion at 0.2	
Hz. Inertial lateral acceleration (a_y) and gravitational lateral acceleration (a_g) are 180° out-of-	
phase, thereby resulting in zero lateral acceleration (a_r) at the centre-of-rotation (CoR) (i.e. the	Э
position of full roll-compensation).	12
Figure 2.7 The reduction of lateral centripetal acceleration associated with a) track cant, and be)
an active tilting suspension mechanism (adapted from Persson, Goodall and Sasaki, 2009)	15
Figure 2.8 Power spectral densities for vertical (z -axis), lateral (y -axis) and roll (r_x -axis)	
acceleration measured on a tilting and a non-tilting train (adapted from Persson, 2008)	16
Figure 2.9 Magnitudes of coach-lateral acceleration, coach-vertical acceleration and coach-	
referenced roll velocity across seven octave-band frequencies between 0.015 and 1.0 Hz	
calculated from journey 3 and 4 (adapted from Donohew and Griffin, 2007)	18
Figure 2.10 Example lateral vibration waveform measured at the carbody floor of a railway	
vehicle in Japan (Suzuki 1998b).	19
Figure 2.11 Example distribution of peak lateral accelerations measured on a Japanese railwa	ìу
vehicle. Test run 2 was on the same portion of track, but at 15 km/h faster than test run 1	
(Suzuki, 1998a)	20
Figure 2.12 Anatomy of the inner ear, consisting of the vestibular system and the cochlear	
(Haslwanter, 2008)	21
Figure 2.13 Orientation and sensitivity of stereocilia and kinocilium (a). Stereocilia are polarise	∍d
in the same direction in the cristae (b), but reverse their polarity in the region of the striola	
(dotted line) in the utricular macula (c) and saccular macula (d) (adapted from Goldberg and	
Fernandez, 2011)	22

Figure 2.14 Orientation of the semi-circular canals (adapted from Jacobson, Newman and Kartush, 1993)
Figure 2.15 Structure of the crista (consisting of the cupula and the ampullary crest) within the semi-circular canals. Velocity changes in the endolymphatic fluid in the canals stimulates movement of the cupula, causing the 'hair-cells' to generate a nerve impulse (adapted from NASA, 2002)
Figure 2.16 Structure of otolith organs (utricle and saccule) (adapted from NASA, 2002)25
Figure 2.17 Optic flow fields during lateral movement or rotary movement about a fixed point (a), forward movement (b) and backward movement (c). Arrows are velocity vectors representing apparent movement of objects in the visual field (adapted from Horseman, Macauley and Barnes, 2011).
Figure 2.18 Motion sickness frequency weighting W_f with a band-pass filter at 0.08 and 0.63 Hz (ISO 2631-1, 1997)30
Figure 2.19 Effect of frequency (Hz) on motion sickness caused by fore-and-aft oscillation, as reported by Golding and colleagues (Golding and Markey, 1996; Golding, Finch and Stott, 1997; Golding, Mueller and Gresty, 2001)
Figure 2.20 The effect of frequency (Hz) on motion sickness caused by uncompensated lateral oscillation and fully roll-compensated lateral oscillation, as reported by Donohew (2006) and Donohew and Griffin (2009).
Figure 2.21 The percentage of subjects to report 'mild nausea' during exposure to roll oscillation (Howarth and Griffin, 2003), lateral oscillation (Donohew and Griffin, 2004) and fully roll-compensated lateral oscillation (Donohew, 2006). Full motion quantities are shown in Table 2.9.
Figure 2.22 Asymptotic and realizable frequency weightings for lateral acceleration and vertical acceleration, <i>W</i> _f (figure adapted from Donohew and Griffin, 2004)
Figure 2.23 Comparison of the nauseogenicity of Earth-horizontal and Earth-vertical oscillation with supine and seated posture (adapted from Golding <i>et al.</i> , 1995)42
Figure 2.24 Examples of visual stimuli used in motion sickness experiment reported by Butler and Griffin (2006), adapted from Butler (2008).
Figure 2.25 Conceptual model of motion sickness
Figure 2.26 Effect of range of acceleration magnitudes on mean discomfort ratings (Suzuki, 1998a). Description of magnitude ranges given in Table 2.11
Figure 2.27 Equivalent comfort contours for fore-and-aft (x-axis) and lateral (y-axis) motion 59
Figure 2.28 Equivalent comfort contours for pitch (<i>r_y</i> -axis) and roll (<i>r_x</i> -axis) motion60
Figure 2.29 Equivalent comfort contours representing subjective magnitudes from 25 to 300, where 100 equals discomfort caused by a 1.0 ms ⁻² r.m.s. fore-and-aft (top) or lateral (bottom) reference motion. Median absolute percention thresholds (solid line with symbols) and the range

of stimuli used (dotted lines) are also shown. Figure adapted from Morioka and Griffin (2006a).
Figure 2.30 Seat-to-head transmissibility during lateral and fore-and-aft oscillation between 0.2 and 16 Hz for 'back-on' and 'back-off' postures (adapted from Paddan and Griffin, 1988) 65
Figure 2.31 Equivalent comfort contours for lateral, fore-and-aft, roll and pitch oscillation with and without a backrest and four-point harness (Wyllie and Griffin, 2007; 2009)
Figure 2.32 Current model for predicting vibration discomfort (ISO 2631-1, 1997)
2631-1, 1997)
Figure 3.1 Schematic view of the 12-metre horizontal simulator (from Donohew, 2006) 76
Figure 3.2 Approximate 12-m tilting and translating simulator peak acceleration limits. [Rotational displacement represented as the peak acceleration in the plane of the seat, i.e. due to gravity]
Figure 3.3 Approximate 1-m horizontal simulator peak acceleration limits
Figure 3.4 Approximate 6-axis motion simulator peak acceleration limits
Figure 3.5 Illustration of Pulsar Iterative Control System (ICS) procedure
Figure 3.6 Accelerometer measurement locations on 12-m tilting and translating cabin 82
Figure 3.7 Comparison of desired and measured horizontal acceleration waveforms for a typical 30-second segment of 'seat compensation' condition in Experiment 1 (12-m tilting and translating cabin)
Figure 3.8 Comparison of desired and measured horizontal acceleration waveforms for a typical 30-second segment of 'head compensation' condition in Experiment 1 (12-m tilting and translating cabin)
Figure 3.9 Comparison of desired and measured lateral acceleration waveforms at 0.25, 0.5 and 1.0 Hz used in Experiment 2 (1-m horizontal simulator)
Figure 3.10 Comparison of desired and measured lateral acceleration waveforms for lateral oscillation at 0.25, 0.5 and 1.0 Hz used in Experiment 3, 4 and 5 (6-axis simulator)
Figure 3.11 Comparison of desired and measured lateral acceleration waveforms for roll oscillation at 0.25, 0.5 and 1.0 Hz used in Experiment 3, 4 and 5 (6-axis simulator) 89
Figure 3.12 Annotated illustration of SIT-BAR used to measure translational and rotational motion at the seat-buttock interface (adapted from Whitham and Griffin, 1977)
Figure 4.1 Mean illness ratings reported each minute for seat compensation and head compensation. Exposure to roll-compensated lateral oscillation occurred between 5 and 35 minutes
Figure 4.2 The percentage of subjects to reach each illness rating with seat compensation and head compensation

Figure 4.3 Mean illness ratings reported each minute by 20 European and 40 Asian subjects. Exposure to roll-compensated lateral oscillation occurred between 5 and 35 minutes
Figure 4.4 The percentage of European and Asian subjects to reach each illness rating 108
Figure 5.1 Diagrammatic representation of experimental apparatus (train seat and rigid seat
positioned adjacent on 1-metre horizontal simulator)117
Figure 5.2 The four seating conditions: (a) train seat with backrest, (b) train seat without
backrest, (c) rigid seat with backrest, and (d) rigid seat without backrest118
Figure 5.3 Labelled diagram of the human body (body map) used by subjects to indicate the
location of most discomfort in Part 3
Figure 5.4 Example waveform of transient lateral motion stimuli (0.5 Hz oscillation at 0.2 ms ⁻²
r.m.s.)
Figure 5.5 Rates of growth of discomfort for lateral oscillation on a rigid seat and a cushioned
train seat with and without backrests. Medians and inter-quartile ranges for 12 subjects 123
Figure 5.6 Equivalent comfort contours adjusted to represent discomfort equivalent to 0.5 Hz at
0.2 ms $^{-2}$ r.m.s. on a rigid seat with backrest (i.e. a subjective magnitude, Ψ , of 100). Medians
and inter-quartile ranges for 12 subjects
Figure 5.7 Percentage of subjects reporting most discomfort at the head, neck, or shoulders
(top), or at the buttocks (ischial tuberosities) (bottom) during exposure to lateral oscillation
across all frequencies with each seating condition. Data from 12 subjects pooled across all
three magnitudes of oscillation
Figure 5.8 Comparison of median equivalent comfort contours from current study with previous
data for lateral oscillation on a rigid seat with and without backrest and frequency weighting W_d .
The levels of the contours have been adjusted to represent discomfort equivalent to 0.5 Hz at
0.2 ms ⁻² r.m.s. on a rigid seat with backrest128
Figure 6.1 Illustration of rigid seat with backrest
Figure 6.2 Example waveforms for 1.0-Hz oscillation showing the acceleration in the plane of
the seat for lateral oscillation, roll oscillation, and fully roll-compensated lateral oscillation 134
Figure 6.3 Median rates of growth of discomfort for lateral, roll, and fully roll-compensated lateral
oscillation. Upper and lower error bars show 75th and 25th percentiles, respectively 136
Figure 6.4 Median equivalent comfort contours for lateral, roll, and fully roll-compensated lateral
oscillation, each producing discomfort equal to that arising from lateral oscillation at 0.5 Hz, 0.2
ms- 2 r.m.s (i.e. a subjective magnitude, Ψ , of 100)
Figure 6.5 The effect of acceleration magnitude on median equivalent comfort contours caused
by lateral, roll, and fully roll-compensated lateral oscillation. Contours represent discomfort
equal to subjective magnitudes of 50, 63, 80, 100, 125, 160, and 200138

Figure 6.6 Median equivalent comfort contours for lateral, roll, and fully roll-compensated lateral oscillation for males (\Im) and females (\Im), each producing discomfort equal to that arising from lateral oscillation at 0.5 Hz, 0.2 ms ⁻² rms (i.e. a subjective magnitude, Ψ , of 100)
Figure 6.7 Location on the body where subjects felt discomfort caused by lateral, roll, and fully roll-compensated lateral oscillation at frequencies from 0.25 to 1.0 Hz
Figure 6.8 Effect of frequency of oscillation on equivalent comfort contours for lateral oscillation. Contours normalised to represent discomfort equal to that caused by lateral acceleration at 0.5 Hz 0.2 ms ⁻² r.m.s. on a rigid seat with backrest (i.e. a subjective magnitude, Ψ , of 100) 141
Figure 6.9 Effect of frequency of oscillation on equivalent comfort contours for roll oscillation expressed in terms of rotational acceleration (rads ⁻² r.m.s.). Contours normalised to represent discomfort equal to that caused by lateral acceleration at 0.5 Hz 0.2 ms ⁻² r.m.s. on a rigid seat with backrest (i.e. a subjective magnitude, Ψ , of 100)
Figure 6.10 Frequency-weighted accelerations corresponding to median equivalent comfort contours for roll oscillation. Values calculated using asymptotic acceleration weightings given in BS 6841 (1987) that have been extrapolated horizontally at frequencies less than 0.5 Hz 143 Figure 7.1 Illustration of the two seat-pan conditions (a) rigid seat; (b) foam cushion
Figure 7.1 mustration of the two seat-pair conditions (a) rigid seat, (b) roam cushion. In 1900 Figure 7.2 Body map used by subjects to indicate the location of discomfort caused by lateral, roll and fully roll-compensated lateral oscillation
Figure 7.3 Example waveforms for 1.0-Hz oscillation showing the acceleration in the plane of the seat for lateral oscillation, roll oscillation, and fully roll-compensated lateral oscillation 153
Figure 7.4 Median rates of growth of discomfort for lateral, roll and fully roll-compensated lateral oscillation on the rigid seat and the foam seat. Upper and lower error bars show 75th and 25th percentiles, respectively
Figure 7.5 Effect of seating on adjusted median equivalent comfort contours for lateral oscillation, roll oscillation, and fully roll-compensated lateral oscillation. Contours, expressed as the component of lateral acceleration in the plane of the seat, represent discomfort equal to that arising with 0.5-Hz lateral oscillation at, 0.2 ms ⁻² r.m.s. on the rigid seat (i.e. a subjective magnitude, Ψ , of 100).
Figure 7.6 Effect of direction of oscillation on median equivalent comfort contours for the rigid seat and the foam cushion. Contours, expressed as the component of lateral acceleration in the plane of seat, represent discomfort equal to that arising from 0.5-Hz lateral oscillation at 0.2 ms ⁻² r.m.s. on the rigid seat (i.e. a subjective magnitude, Ψ , of 100)
Figure 7.7 The effect of acceleration magnitude on median equivalent comfort contours caused by lateral oscillation, roll oscillation, and roll-compensated lateral oscillation on the rigid seat and the foam cushion. Contours, expressed as the component of lateral acceleration in the plane of seat, represent discomfort equal to subjective magnitudes of 50, 63, 80, 100, 125, 160 and 200. The level of the contours should not be compared across seats

Figure 7.8 Percentage of subjects reporting discomfort localised at the ischial tuberosities when sitting on the rigid seat and on the foam cushion during exposure to lateral oscillation, roll
oscillation, and fully roll-compensated lateral oscillation across all frequencies162
Figure 7.9 Percentage of subjects reporting discomfort localised at the upper thighs, lower
thighs or lower legs when sitting on the rigid seat and on the foam cushion during exposure to
lateral oscillation, roll oscillation, and fully roll-compensated lateral oscillation across all
frequencies
Figure 7.10 Median lateral transmissibility of the foam cushion during exposure to lateral
oscillation, roll oscillation, and fully roll-compensated lateral oscillation at 0.1, 0.2, and 0.4 ms ⁻²
r.m.s. at frequencies from 0.25 to 1.0 Hz
Figure 7.11 Median roll transmissibility of the foam cushion during exposure to roll oscillation
and roll-compensated lateral oscillation at 0.1, 0.2, and 0.4 ms ⁻² r.m.s. at frequencies from 0.25
to 1.0 Hz
Figure 7.12 Effect of magnitude of oscillation on the median roll velocity measured at the seat-
body interface of the foam cushion during exposure to lateral oscillation and roll oscillation at
frequencies between 0.25 and 1.0 Hz
Figure 7.13 Root-sums-of-squares of frequency-weighted measured components at the seat-
body interface during lateral oscillation, roll oscillation, and fully roll-compensated lateral
oscillation on a rigid seat and on a foam cushion. Components weighted using axis multiplying
factors and asymptotic weightings extrapolated horizontally at frequencies less than 0.5 Hz
without band-pass filtering (BS 6841, 1987). Median data calculated across 20 subjects 170
Figure 7.14 Comparison of equivalent comfort contours for lateral oscillation on rigid and
cushioned seats without a backrest and the reciprocals of the asymptotic and the realisable
versions of frequency weighting W_d for lateral acceleration (BS 6841, 1987). Contours for rigid
seats normalised to unity at 1 Hz
Figure 7.15 Comparison of equivalent comfort contours for roll oscillation on rigid and cushioned
seats without a backrest and the reciprocals of the asymptotic and the realisable versions of
frequency weighting W_e for roll acceleration (BS 6841, 1987). Contours normalised to unity at 1
Hz173
Figure 8.1 Illustration of the three backrest conditions (a) no backrest; (b) short backrest; (c)
high backrest
Figure 8.2 Body map used by subjects to indicate the location of discomfort caused by lateral,
roll and fully roll-compensated lateral oscillation
Figure 8.3 Example waveforms for 1.0-Hz oscillation showing the acceleration in the plane of
the seat for lateral oscillation, roll oscillation, and fully roll-compensated lateral oscillation 180
Figure 8.4 Median rates of growth of discomfort for lateral oscillation, roll oscillation, and fully
roll-compensated lateral oscillation with no backrest, a short backrest and a high backrest.
Upper and lower error bars show 75 th and 25 th percentiles, respectively

Figure 8.5 Effect of backrest height on adjusted median equivalent comfort contours for lateral, roll and fully roll-compensated lateral oscillation. Contours represent discomfort equal to that arising from lateral oscillation at 0.5 Hz, 0.2 ms ⁻² r.m.s. on a rigid seat without backrest (i.e. a subjective magnitude, Ψ , of 100).
Figure 8.6 Effect of direction on median equivalent comfort contours for the three seat configurations (no backrest, short backrest, and high backrest). Contours represent discomfort equal to that arising from lateral oscillation at 0.5 Hz 0.2 ms $^{-2}$ r.m.s. on a rigid seat without backrest (i.e. a subjective magnitude, Ψ , of 100).
Figure 8.7 Effect of magnitude on equivalent comfort contours for lateral, roll and fully roll-compensated lateral oscillation on rigid seat without a backrest, with a short backrest and with a high backrest. Contours represent subjective magnitudes of 50, 63, 80, 100, 125, 160 and 200.
Figure 8.8 Comparison of median rates of growth of discomfort for lateral, roll and fully roll-compensated lateral oscillation in the current study with those reported previously
Figure 8.9 Comparison of equivalent comfort contours for roll oscillation from the current study with those reported previously.
Figure 8.10 Comparison of current frequency-weightings with inverted median equivalent comfort contours for lateral, roll and fully roll-compensated lateral oscillation on all backrest conditions. Contours (normalised to unity at 1 Hz) represent subjective magnitudes of 50, 63, 80, 100, 125, 160 and 200
Figure 9.1 Comparison of mean illness ratings during 30-minute exposures to fully roll-compensated sinusoidal lateral oscillation at 0.2 Hz
Figure 9.2 Effect of percentage compensation at the seat surface during 30-minute exposures to roll-compensated lateral oscillation at 0.2 Hz
Figure 9.3 Components of Earth-lateral acceleration required to produce equivalent discomfort (solid line) and mean illness ratings (dotted line; Donohew, 2006) associated with fully roll-compensated lateral oscillation between 0.05 and 1 Hz. [Equivalent comfort contours calculated from the mean of all contours reported in Experiments 3, 4 and 5]
Figure 9.4 Effect of frequency of uncompensated lateral oscillation on motion sickness (Donohew and Griffin, 2004) and physical discomfort (Experiment 3, 4 and 5) (grey lines indicate fully roll-compensated motion).
Figure 9.5 Conceptual model of motion sickness caused by combined lateral and roll oscillation.
Figure 9.6 Equivalent comfort contours for lateral oscillation, roll oscillation (expressed as lateral acceleration in the plane of the seat, ms ⁻² r.m.s.) and fully roll-compensated lateral oscillation (expressed as the Earth-lateral acceleration component, ms ⁻² r.m.s.). Contours constructed from the mean of all equivalent comfort contours defined in Experiments 2 to 5

208
Figure 9.8 Equivalent comfort contours for inertial lateral acceleration (i.e. due to lateral displacement) from Experiments 2, 3, 4 and 5. [Mean equivalent comfort contour calculated across the ten conditions shown in bold]
Figure 9.9 Equivalent comfort contours for gravitational lateral acceleration (i.e. due to roll displacement) from Experiment 3, 4 and 5. [Mean equivalent comfort contour calculated across the six conditions shown in bold].
Figure 9.10 Mean equivalent comfort contours for inertial lateral acceleration (i.e. due to lateral displacement) and gravitational lateral acceleration (i.e. due to roll displacement) calculated across all conditions in Experiment 2, 3, 4 and 5, and normalised W_d (BS 6841, 1987) and W_d (adjusted) weightings
Figure 9.11 Standardised weighting W_d (ISO 8041, 2005) and adjusted weighting $W_{d'}$ for predicting discomfort from lateral acceleration. Weightings achieved with band-limiting filter defined in Table 9.2.
Figure 9.12 Equivalent comfort contours for roll acceleration from Experiment 3, 4 and 5. [Mean equivalent comfort contour calculated across the six conditions shown in bold]
Figure 9.13 Mean equivalent comfort contours for roll acceleration calculated across all conditions in Experiment 3, 4 and 5, and normalised W_e (BS 6841, 1987) and W_e (adjusted) weightings.
Figure 9.14 Standardised weighting W_e (ISO 8041, 2005) and adjusted weighting W_e for predicting discomfort from roll acceleration. Weightings achieved with band-limiting filter defined in Table 9.3
Figure 9.15 Equivalent comfort contours for fully roll-compensated lateral acceleration from Experiment 3, 4 and 5, expressed in terms of the component of Earth-lateral acceleration. [Mean equivalent comfort contour calculated across the six conditions shown in bold]218 Figure 9.16 Mean equivalent comfort contours for fully roll-compensated lateral acceleration
calculated across all conditions in Experiment 3, 4 and 5, and normalised W_e (BS 6841, 1987) and W_e (adjusted) weightings.
Figure 9.17 Overall ride values (i.e. root-sums-of-squares of weighted components) for lateral oscillation on a rigid seat with no backrest, with a short backrest and with a high backrest, frequency-weighted using current (ISO 8041, 2005) and adjusted (Section 9.3) weightings222
Figure 9.18 Overall ride values (i.e. root-sums-of-squares of weighted components) for roll oscillation on a rigid seat with no backrest, with a short backrest and with a high backrest, frequency-weighted using current (ISO 8041, 2005) and adjusted (Section 9.3) weightings223
Figure 9.19 Overall ride values (i.e. root-sums-of-squares of weighted components) for fully roll-compensated lateral oscillation on a rigid seat with no backrest, with a short backrest and with a

high backrest, frequency-weighted using current (ISO 8041, 2005) and adjusted (Section 9.3) weightings.
Figure 9.20 Distribution of lateral subjective magnitude estimates using the method of magnitude estimation with and without a reference (estimates reported without reference have been normalised), using all data collated from Experiments 2 to 5
Figure 9.21 Median rates of growth of discomfort for lateral oscillation on a rigid seat with backrest obtained from magnitude estimates with a reference (Experiment 3) and without a reference (Experiment 5). Upper and lower error bars show 75 th and 25 th percentiles, respectively.
Figure 9.22 Distribution of standardised residuals when using magnitude estimation with and without reference, using all data collated from Experiments 2 to 5. Normal distribution indicated by solid line.
Figure 9.23 Median coefficients of determination (R^2) for least squares regression when using magnitude estimation with and without reference. Upper and lower errors bars indicate 75th and 25th percentiles, respectively
Figure 9.24 Percentage of subjects reporting sensations associated with motion sickness during exposure to lateral oscillation, roll oscillation and fully roll-compensated lateral oscillation (median values from Experiment 2, 3, 4 and 5)
Figure 9.25 Effect of stimuli presentation order on subjective discomfort ratings obtained for lateral oscillation at 0.5 Hz and 0.4 ms ⁻² r.m.s. in Experiments 3 – 5
Figure 9.26 Distribution of discomfort responses to test motions equivalent to a subjective magnitude of 100 (i.e. equivalent to the reference motion); a) boxplot showing median and interquartile range, and; b) scatterplot showing 78 individual responses
Figure 9.27 Illustration of the position of the centre-of-rotation relative to a seated subject used to calculate nominal quantities given in Table 9.7
Figure 9.28 Nominal predictions of the effect of increasing the vertical height of the centre-of-rotation from 0 to 1.6 m above the seat surface on the level of equivalent comfort contours for lateral oscillation, roll oscillation and fully-roll compensated lateral oscillation
Figure 9.29 Nominal predictions of the frequency-dependence of equivalent comfort contours for uncompensated lateral oscillation and 25%, 50%, 75% and 100% roll-compensated lateral oscillation (with constant Earth-lateral acceleration)
Figure 9.30 Nominal predictions of the frequency-dependence of equivalent comfort contours for roll oscillation and 25%, 50%, 75% and 100% roll-compensated lateral oscillation (with constant roll displacement).

DECLARATION OF AUTHORSHIP

I, GEORGE FREDERICK BEARD,

declare that the thesis entitled

DISCOMFORT OF SEATED PERSONS EXPOSED TO LOW FREQUENCY LATERAL AND ROLL MOTION

and the work presented in the thesis are both my own, and have been generated by me as the result of my own original research. I confirm that:

- this work was done wholly or mainly while in candidature for a research degree at this University;
- where any part of this thesis has previously been submitted for a degree or any other qualification at this University or any other institution, this has been clearly stated;
- where I have consulted the published work of others, this is always clearly attributed;
- where I have quoted from the work of others, the source is always given. With the
 exception of such quotations, this thesis is entirely my own work;
- I have acknowledged all main sources of help;
- where the thesis is based on work done by myself jointly with others, I have made clear exactly what was done by others and what I have contributed myself;
- parts of this work have been published as:
 - Beard, G.F. and Griffin, M.J. (2012). Motion sickness caused by rollcompensated lateral acceleration: effects of centre-of-rotation and subject demographics. Proceedings of the Institution of Mechanical Engineers, Part F: Journal of Rail and Rapid Transit. DOI: 10.1177/0954409712460981.
 - Beard, G.F. and Griffin, M.J. (2012). Discomfort during lateral acceleration:
 Influence of seat cushion and backrest. Applied Ergonomics.
 http://dx.doi.org/10.1016/j.apergo.2012.11.009.
 - Beard, G.F. and Griffin, M.J. (2012). Discomfort caused by low frequency lateral oscillation, roll oscillation, and roll-compensated lateral oscillation. Ergonomics.
 DOI: 10.1080/00140139.2012.729613.

Signed:	
Date:	.12/10/2012

Acknowledgements

I owe a debt of gratitude to many people who have offered their help and support throughout the past three years.

First and foremost, I would like to sincerely thank my supervisor, Professor Michael J. Griffin, for his perpetual guidance and encouragement all the way through my PhD studies. Without his valuable time and assistance, completion of this thesis would not have been possible.

I would also like to express my gratitude to the members of the Human Factors Research Unit, past and present, who are always on hand, and always willing, to share their knowledge and expertise. Particular thanks must go to Dr Chris Lewis and Dr Martin Toward for teaching me how to use the motion simulators, and to the family of technicians (Peter, Gary and Weidong) for 'kitting them out' with whatever I needed!

I must also thank my parents, John and Helen, for their everlasting encouragement. Their own personal experiences of completing PhD theses were an inspiration to complete one of my own.

Last, but by no means least, my thanks go out to my girlfriend, partner, best friend, and housemate, Katie, for her advice and care when it was most necessary, and for pretending to understand what I have been doing these past 3 years!

Nomenclature

g Gravitational acceleration (± 9.81 ms⁻²) r.m.s. Root-mean-square F_g Gravitational force F_p Force imposed on an object positioned on an inclined surface F_n Normal force perpendicular to the plane of a surface F_n' Gravitational force perpendicular to the surface (opposite to the normal force) F_i Inertial force exerted on an object under dynamic conditions Vertical acceleration (ms-2) a_z Lateral acceleration (ms⁻²) a_{v} a_g Lateral acceleration due to gravity (ms⁻²) a_c Centrpetal acceleration imposed on an object traversing a curve Resultant acceleration in the plane of a track imposed on a rail vehicle a_r Total angle (°) given by track cant and carbody tilt θ_{total} **GIF** Gravito-inertial force V_d Vertical displacement (m) Y_d Lateral displacement (m) MSDV Motion sickness dose value (ms-1.5) VI Vomiting incidence (%) IR Illness rating SS Symptom score Ψ Subjective magnitude (i.e. discomfort) Physical magnitude (i.e. r.m.s. acceleration) Exponent in Stevens' power law (i.e. rate of growth of discomfort) n Constant in Stevens' power law MTVV Maximum transient vibration value (ms-2 r.m.s.) Vibration dose value (ms^{-1.75}) **VDV** PCT / TCT Discomfort due to perceived curve transitions



Chapter 1

Introduction

The transport industry faces an increasing demand to provide the growing population with safe, reliable, efficient and fast means of travel. Modern advances in technology have allowed for substantial developments in high-speed vehicles which may help with this demand.

High-speed rail typically utilises 'custom' built continuous-weld rail track with dedicated rights of way, limited crossings and few curves. Straight tracks are preferred so as to avoid excessive lateral centripetal forces associated with traversing curves at speed. Where straight tracks are not possible however, lateral forces may be reduced by tilting the vehicle into the curve; a technique achieved with the use of tilting train sets. In the United Kingdom, for example, topographical restrictions limit the opportunity for building high-speed rail track, so a more viable option is to implement tilting train technology.

The passenger experience on transport is governed by vehicle climate, seating configurations, journey durations, crowdedness and exposure to noise and vibration. Passengers of tilting trains, and other forms of land transport, are exposed to horizontal and rotational forces which may affect the comfort of the journey. There has been considerable research into the effects on comfort of transport vibration transmitted through vehicle structures to seated occupants, and methods for predicting vibration discomfort have been defined in British and International standards (BS 6841, 1987; ISO 2631-1, 1997). However, previous research has typically focused on vibration where the frequency of oscillation is greater than 1 Hz, with less work involving frequencies less than this. Since the forces associated with cornering in land transport typically occur at very low frequencies, it is of great value to understand the implications of these motions on passenger comfort.

Horizontal and rotational oscillation at frequencies less than 1 Hz may lead to motion sickness ("vomiting, nausea or malaise provoked by actual or perceived motion of the body or its surroundings"; Griffin, 1990, p. 831) or physical discomfort associated with disturbance to sitting posture. This thesis is concerned with understanding both the motion sickness and the vibration discomfort resulting from low frequency horizontal and rotational motions which are common in

land transport, to allow for predictions of the passenger experience on board current, and future, high-speed vehicles.

The specific objectives of this thesis, and the chapter in which they are addressed, are shown in Table 1.1. Chapter 2 includes a literature review of previous work concerning the motion sickness and vibration discomfort of seated passengers, and the equipment and experimental methods used in this thesis are presented in Chapter 3. The main body of work is contained in Chapter 4 to 8, which report five original experimental studies investigating the effect of lateral oscillation, roll oscillation and fully roll-compensated lateral oscillation on motion sickness and vibration discomfort across a variety of motion and environmental conditions. A discussion of the methods and results of the five experiments is included in Chapter 9, along with recommendations for current vibration standards and future research. The conclusions of the thesis are presented in Chapter 10.

Included in the Appendices are the subject consent form, motion sickness susceptibility questionnaire (*MSSQ*), subject information questionnaire and subject instructions, the MATLAB scripts for generating motion signals for each of the three motion simulators, a list of the demographics of subjects tested across the five experiments, the load-deflection curve for the foam cushion used in Experiment 4 (Chapter 7) and the frequency-weighted components of lateral and roll motion using the adjusted weightings defined in Chapter 9.

Table 1.1 Objectives of this thesis.

Objective	Chapter		
Establish the state of knowledge on the effect of motion and environmental variables on a) the development of motion sickness and b) the causation of physical discomfort	Literature review (Chapter 2)		
Establish experimental methods for evaluating psychophysical relationships	Equipment and experimental methods (Chapter 3)		
Test conceptual model of motion sickness	Effects of centre-of-rotation and subject demographics on motion sickness (Chapter 4)		
Assess the impact of seating on lateral vibration discomfort	Seating effects with lateral vibration discomfort (Chapter 5)		
	Discomfort caused by lateral, roll and fully roll- compensated lateral oscillation (Chapter 6)		
Determine effects of frequency, direction and seating on discomfort caused by lateral, roll and fully roll-compensated lateral oscillations	Effect of seat-pan stiffness (Chapter 7)		
	Effect of backrest height (Chapter 8)		
Collate the findings from experimental work. Assess the implications for development of a new predictive model. State recommendations for future work.	General discussion (Chapter 9)		
Demonstrate original contribution to knowledge.	Conclusions (Chapter 10)		

Chapter 2

Literature review

2.1. Introduction

This chapter presents a discussion of previous literature. The objectives were four-fold: (1) clarify the physical principles necessary to understand the motion environment (Section 2.2); (2) establish the physiological mechanisms of the body responsible for the perception of motion (Section 2.3); (3) determine the psychophysical procedures necessary to study subjective responses to motion (Section 2.4 and 2.7), and; (4) understand the state of current knowledge concerning the discomfort and the motion sickness caused by low frequency horizontal and rotational oscillation (Section 2.5 and 2.8). As a result of this review, a model of motion sickness and a model of vibration discomfort is visualised in Section 2.6 and 2.9, respectively. The conclusions of the literature review are presented in Section 2.10.

2.2. The motion environment

2.2.1. Coordinate system

Motion may be defined in terms of three translational axes [fore-and-aft (x-axis), lateral (y-axis), vertical (z-axis)] and three rotational axes [roll (r_x axis), pitch (r_y axis), yaw (r_z axis)] (Griffin, 1990; see Figure 2.1). To study human response to motion, the six axes are typically defined in a 'basicentric' coordinate system, i.e. human-referenced co-ordinates originating at a point at which motion (vibration or shock) enters the body (Griffin, 1990). In a normal seated posture, vibration may transmit to the body from the seat surface, the backrest, and from the floor. Basicentric co-ordinates for the seated human body are therefore typically defined at these three input locations (see Figure 2.2).

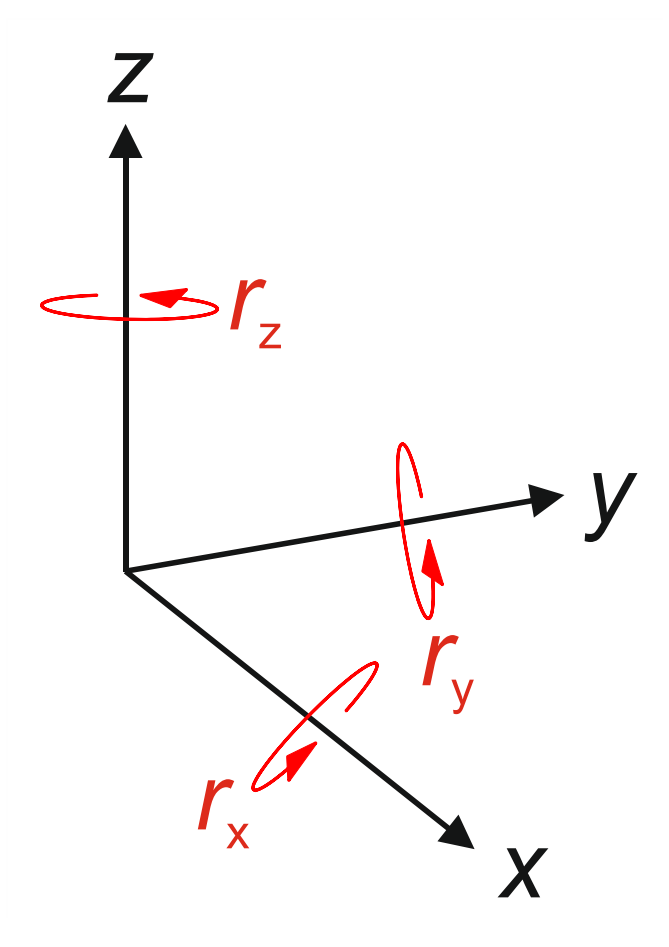


Figure 2.1 The six axes of motion [fore-and-aft (x-axis), lateral (y-axis), vertical (z-axis)] and three rotational axes [roll (r_x -axis), pitch (r_y -axis), yaw (r_z -axis)].

2.2.2. Inertia and gravitational forces

Under static conditions, an object resting on an Earth-horizontal surface is subjected to a gravitational force (F_g) and a normal force (F_n) perpendicular to the plane of the surface (Figure 2.3a). The gravitational force is proportional to the mass of the object (m) and the gravitational acceleration (g), such that:

Equation 2.1:
$$F_g = m \times g$$

where g is equal to 9.81 ms⁻² (in the terrestrial environment). The normal force (F_n) is the force exerted upon an object that is in contact with another stable object (e.g. the upward supportive force of a seat acting on a seated human body). If the horizontal plane is tilted (e.g. Figure 2.3b), then the object will often slide down the surface of that plane with a force parallel to the surface (F_p), dependent on the degree of incline (θ) and the frictional force (F_n) of the surface, such that:

Equation 2.2:
$$F_p = m \times g \times \sin \theta - F_f$$

The gravitational force perpendicular to the surface (F_n) is opposite to the normal force (F_n) and is determined by:

Equation 2.3:
$$F_n' = -F_n = m \times g \times \cos \theta$$

Ignoring the frictional force allows the resultant incline force (F_p) to be estimated from the gravitational acceleration and the degree of incline. Normalising with respect to the object mass determines the rate at which the object moves down the inclined surface, i.e. the acceleration (a_g):

Equation 2.4:
$$a_g = g \times \sin \theta$$

Under dynamic conditions, an object is also subjected to an inertial force (F_i) , dependent on the dynamic properties of the motion (i.e. the acceleration, a) and the object mass, such that:

Equation 2.5:
$$F_i = -m \times a$$

In the terrestrial environment, gravitational forces and inertial forces are indistinguishable (Einstein, 1908, as cited by, Donohew, 2006). The resultant, known as the gravito-inertial force (*GIF*), is the vector sum of the gravitational and inertial forces:

Equation 2.6:
$$GIF = \sqrt{F_i^2 + F_g^2}$$

The relationship between these forces is illustrated in Figure 2.4, showing a seated person undergoing translational acceleration in the lateral direction (*y*-axis).

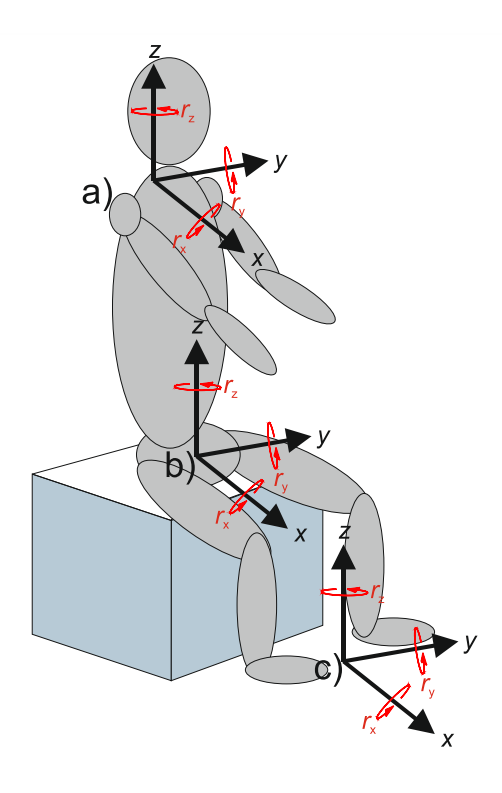


Figure 2.2 Basicentric coordinate system used to define motion of a seated person at a) the back, b) the seat, and c) the feet.

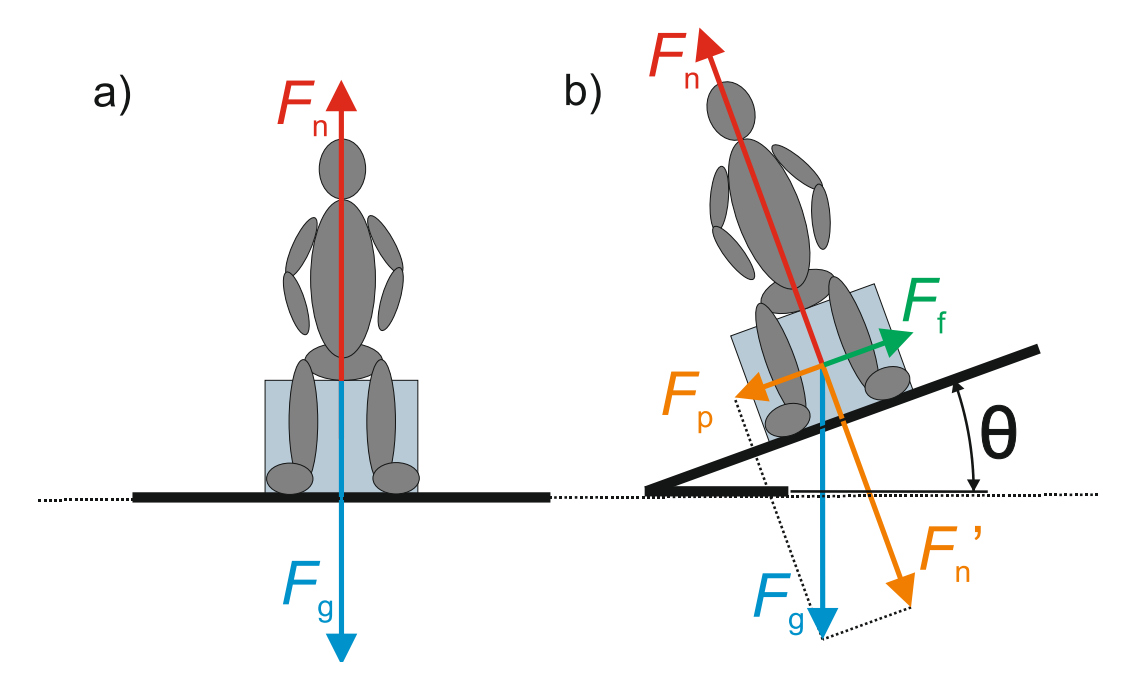


Figure 2.3 Gravitational (F_9 , F_p , F_n), normal (F_n) and frictional (F_n) forces associated with a static object placed on a Earth-horizontal surface (a) and a surface inclined through angle θ (b).

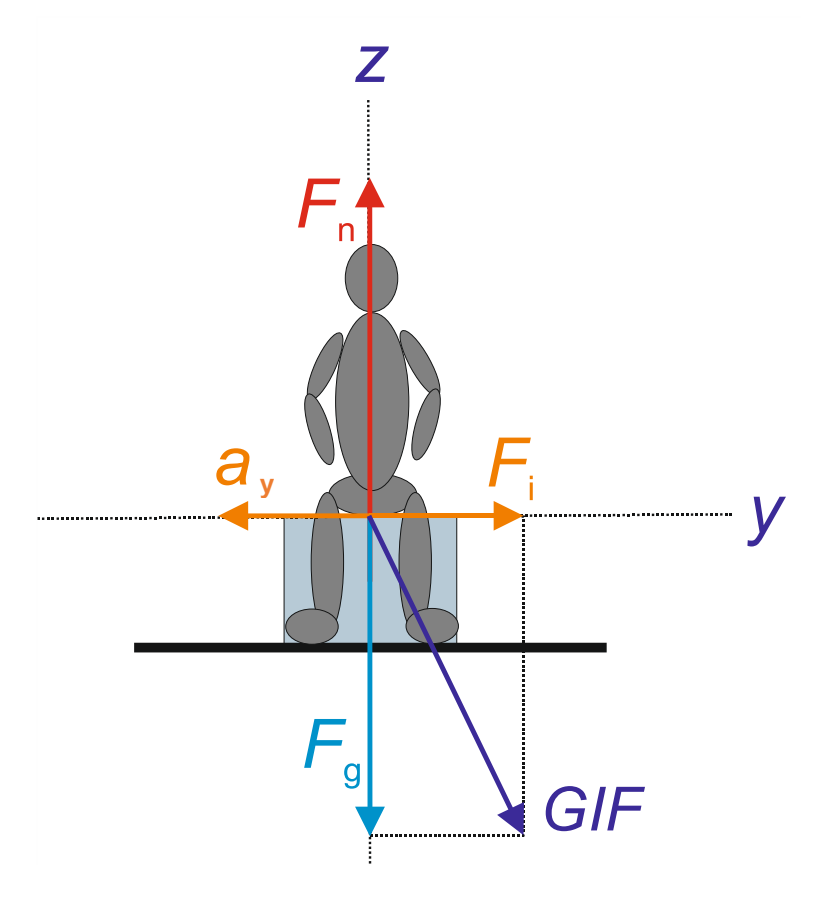


Figure 2.4 The inertial force (F_1) , the normal force (F_n) , the gravitational force (F_g) and the resultant gravito-inertial force (GIF) imposed on a basicentric coordinate system undergoing lateral acceleration (a_y) .

2.2.3. Rotation

If exposed to a rotational displacement (θ), an object will be subjected to a vertical (V_d) and horizontal (Y_d) displacement dependent on the distance (H) from the centre-of-rotation¹ (see Figure 2.5). The vertical displacement (V_d) is determined by:

Equation 2.7:
$$V_d = H - \cos \theta \times H$$

The horizontal displacement (Y_d) is determined by:

Equation 2.8:
$$Y_d = \sin \theta \times H$$

where θ_d is the rotational displacement in degrees. Alternatively, the horizontal displacement may be estimated by:

¹ The stationary point in space about which an object rotates, in the absence of any translational movement.

Equation 2.9:
$$Y_d' = \frac{\theta_d}{360} \times 2\pi \times H$$

where Y_d' is the estimated horizontal displacement.

Assuming the motion is sinusoidal, the vertical (a_z) and lateral (a_y) acceleration imposed on the object away from the centre-of-rotation for pure rotational motion can be estimated according to the frequency (f), such that:

Equation 2.10:
$$A = (2 \times \pi \times f)^2 \times D$$

where A is the lateral (a_y) or vertical (a_z) acceleration and D is the lateral (Y_d) or vertical (V_d) displacement.

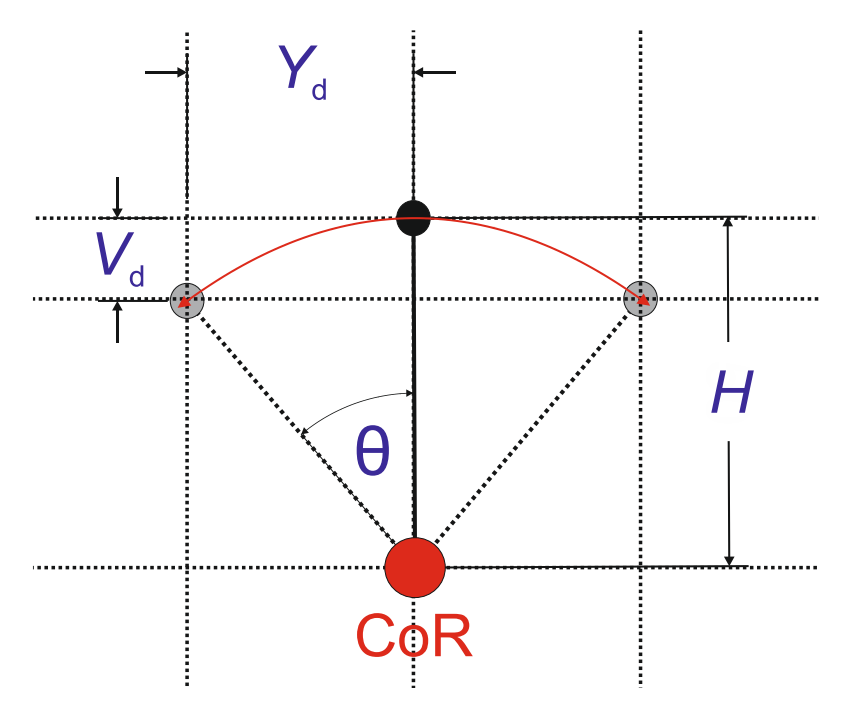


Figure 2.5 Horizontal (Y_d) and vertical (V_d) displacement of a point distance (H) from the centre-of-rotation (CoR) during angular displacement (θ).

The effect of angular displacement (θ), distance from the centre-of-rotation (H), and the frequency of oscillation (f) on vertical (a_z) and lateral (a_y) acceleration is shown in Table 2.1. Equation 2.10 implies that the magnitude of acceleration required to achieve a constant displacement increases by a factor of 4 as the frequency doubles. This relationship is illustrated by the arbitrary values of angular, vertical and horizontal acceleration shown in Table 2.1. Increasing either the distance from the centre-of-rotation or the angular displacement by a factor of 2 also doubles the magnitude of horizontal acceleration. Increasing the distance from the centre-of-rotation by a factor of 2 also doubles the magnitude of vertical acceleration, however

increasing the angular displacement by a factor of 2 causes a two-fold increase in horizontal acceleration but a four-fold increase in vertical acceleration.

Table 2.1 Effect of arbitrary values of angular displacement (θ), distance from centre-of-rotation (H) and frequency of oscillation (f) on vertical (a_z) and lateral (a_y) acceleration.

Frequency (Hz)	Distance from centre- of- rotation (m)	Angular displacement (°)	Angular acceleration (°/s²)	Vertical displacement (m)	Vertical acceleration (m/s²)	Lateral displacement (m)	Lateral acceleration (m/s²)
f	Н	θ	<i>θ</i> a	$V_{ m d}$	V _a	Y _d	$\boldsymbol{a}_{\!\scriptscriptstyle y}$
0.125	1	1	0.6169	0.0002	0.0001	0.0175	0.0108
0.250	1	1	2.4674	0.0002	0.0004	0.0175	0.0431
0.500	1	1	9.8696	0.0002	0.0015	0.0175	0.1723
1.000	1	1	39.4784	0.0002	0.0060	0.0175	0.6891
2.000	1	1	157.9137	0.0002	0.0241	0.0175	2.7564
0.125	2	1	0.6169	0.0003	0.0002	0.0349	0.0215
0.250	2	1	2.4674	0.0003	0.0008	0.0349	0.0861
0.500	2	1	9.8696	0.0003	0.0030	0.0349	0.3445
1.000	2	1	39.4784	0.0003	0.0120	0.0349	1.3782
2.000	2	1	157.9137	0.0003	0.0481	0.0349	5.5128
0.125	1	2	1.2337	0.0006	0.0004	0.0349	0.0215
0.250	1	2	4.9348	0.0006	0.0015	0.0349	0.0862
0.500	1	2	19.7392	0.0006	0.0060	0.0349	0.3447
1.000	1	2	78.9568	0.0006	0.0240	0.0349	1.3786
2.000	1	2	315.8273	0.0006	0.0962	0.0349	5.5145
0.125	2	2	1.2337	0.0012	0.0008	0.0698	0.0431
0.250	2	2	4.9348	0.0012	0.0030	0.0698	0.1723
0.500	2	2	19.7392	0.0012	0.0120	0.0698	0.6893
1.000	2	2	78.9568	0.0012	0.0481	0.0698	2.7572
2.000	2	2	315.8273	0.0012	0.1924	0.0698	11.0289

2.2.4. Tilt-compensation

An object exposed to translational horizontal motion and rotational motion simultaneously will be subjected to an inertial force (Equation 2.5) and a gravitational force parallel to the inclined surface (Equation 2.2, Figure 2.3b). Since the two forces are indistinguishable (Einstein, 1908; Donohew, 2006), the resultant force acting on the object is equal to the vector sum of the gravitational force and the inertial force. If the forces are polar opposites, then the resultant

force will be smaller than either of the two components presented in isolation. This principle, known as 'tilt-compensation', means that a rotational motion can be added to a horizontal motion to reduce the magnitude of the resultant force. The magnitude of 'compensation' (often expressed as a percentage) is dependent on the ratio between the magnitude of the gravitational force and the magnitude of the inertial force, the phase between the two motions, and the frequency of the two motions. An example of 100% compensation achieved with sinusoidal 0.2-Hz lateral acceleration and roll acceleration is shown in Figure 2.6. The components of lateral acceleration at the position of full roll-compensation are shown for the inertial force (Equation 2.5), the gravitational force (Equation 2.4) and the resultant force. In this case, the inertial lateral acceleration (a_y) and the gravitational lateral acceleration (a_g) are 180 out-of-phase, resulting in zero lateral acceleration (a_r) (i.e. at the position of full roll-compensation. Tilt-compensation is discussed in greater detail in Section 2.2.5 with respect to tilting train technology.

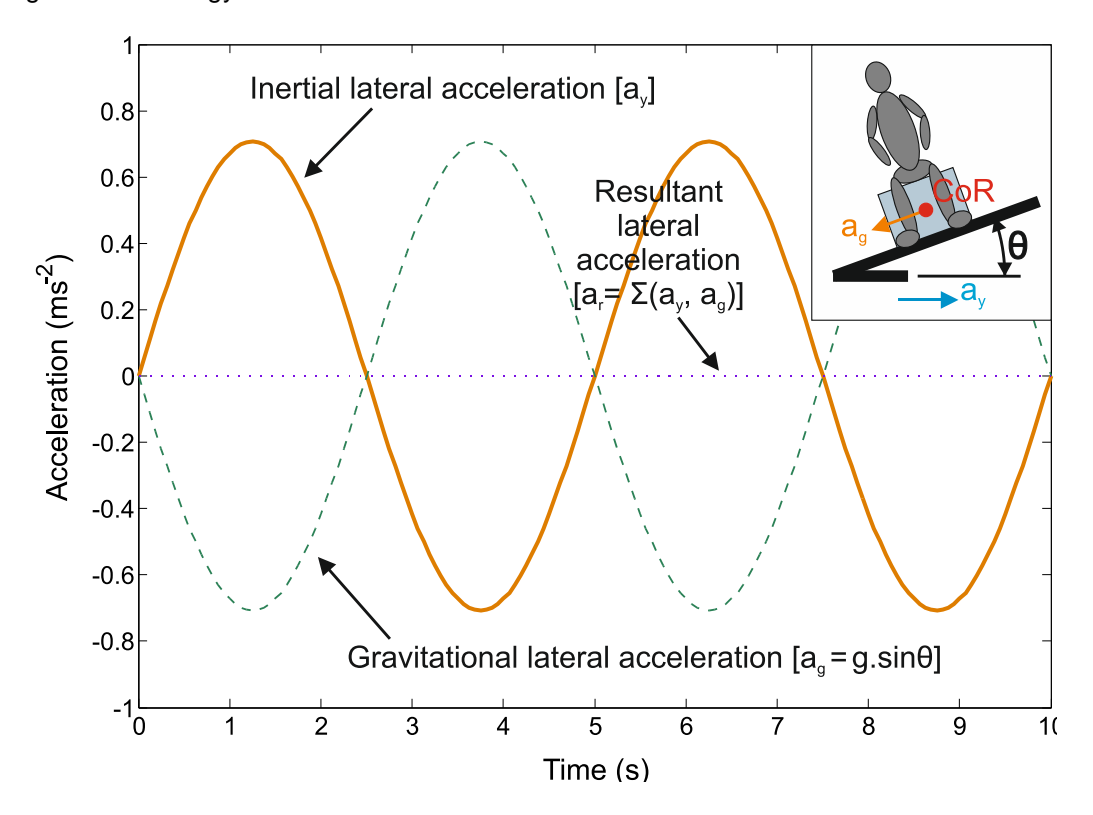


Figure 2.6 Example of tilt-compensation technique for sinusoidal lateral and roll motion at 0.2 Hz. Inertial lateral acceleration (a_y) and gravitational lateral acceleration (a_g) are 180° out-of-phase, thereby resulting in zero lateral acceleration (a_r) at the centre-of-rotation (CoR) (i.e. the position of full roll-compensation).

2.2.5. Railway motions

The theoretical basis for understanding the motion environment has been established in Section 2.2. In order to understand the practical implications of motion sickness and vibration discomfort research for the railway industry, this Section aims to determine the characteristics of typical motions measured in track vehicles (non-tilting and tilting passenger trains).

2.2.5.1. Curvilinear motion

The topography of the Earth dictates that land vehicles must traverse curves in the road or track. An object moving through space in a curvilinear vector is subjected to a centripetal acceleration, a_c , dependent on the vehicle speed, V, and the curve radius, R, such that (Harris *et al.*, 1998):

Equation 2.11:
$$a_c = \frac{V^2}{R}$$

For passengers of most land vehicles, the centripetal acceleration due to curvilinear motion occurs in the lateral direction. The impact of this lateral centripetal acceleration on comfort is of great importance to both passengers and vehicle manufacturers.

2.2.5.2. Track vehicles

When assessing passenger comfort on railway vehicles, the motion environment is often compared between non-tilting trains and those equipped with tilting suspension mechanisms. Traditionally, the lateral centripetal forces associated with traversing curves are reduced by limiting train speed and introducing appropriate track cant. The cant of a track (also known as 'superelevation') is defined as the difference in height between the inner rail and the outer rail (Klauser, 2005). The concept of track cant utilises the physical principles outlined in Section 2.2.4, i.e., a lateral centripetal acceleration (see 2.2.4) may be reduced with appropriate roll displacement due to the gravitational force parallel to an inclined plane (see also Figure 2.6). Under quasi-static conditions, the resultant acceleration in the plane of the track, a_r , is given by the lateral centripetal acceleration, a_c , and the track cant angle, θ , such that:

Equation 2.12:
$$a_r = a_c \times \cos \theta - g \times \sin \theta$$

where *g* is the gravitational acceleration (Donohew, 2006). It follows from Equation 2.11 and Equation 2.12 that the resultant lateral force experienced in the plane of the track is dependent on the cant angle, the track radius and the vehicle speed. For a given cant angle and curve radius, the vehicle speed at which the resultant force equals zero is denoted the 'balance speed' (Klauser, 2005). Deviations from the balance speed result in lateral forces greater than zero: at higher speeds this is known as 'cant deficiency' (which defines the increase in cant, in

mm, required to achieve zero resultant force) and at lower speeds this is known as 'cant excess' (which defines the reduction in cant, in mm, required to achieve zero resultant force).

In contrast to conventional non-tilting trains, tilting trains are equipped with tilting suspension mechanisms which effectively allow for increases in the balance speed by introducing additional roll of the train carriage so as to compensate for any cant deficiency. Tilting trains are principally divided into two categories: passive (or natural) tilting and active tilting (Persson *et al.*, 2009). In a passive tilting mechanism, the mechanical pivot point about which the carbody rotates is higher than the carbody centre-of-gravity, meaning that the lateral centripetal forces associated with traversing a curve (see Section 2.2.5.1) cause the lower portion of the carbody to swing outwards in the direction opposite the curve. In an actively tilting mechanism, hydraulic or electrodynamic actuators drive the carbody roll. The roll may be triggered via one of two control modes: a 'reactive mode' which senses the beginning and end of curves via accelerometers fixed to the front-wheel set or the bogie, or; a 'predictive mode' which senses the curve via a Global Positioning System (GPS) and a database of track parameters (Cohen *et al.*, 2011). Passively-tilted trains tend to have a higher pivot points than actively-tilted trains (Hitachi, 2009).

Tilting mechanisms are used in conjunction with the cant of the track, therefore the total angle of roll experienced by passengers, θ_{total} , is determined by the sum of the cant angle, θ_{C} , and carbody angle, θ_{T} , such that:

Equation 2.13:
$$\theta_{total} = \theta_C + \theta_T$$

The implementation of this technique in a rail vehicle using track cant and carbody tilt is illustrated in Figure 2.7a and Figure 2.7b, respectively.

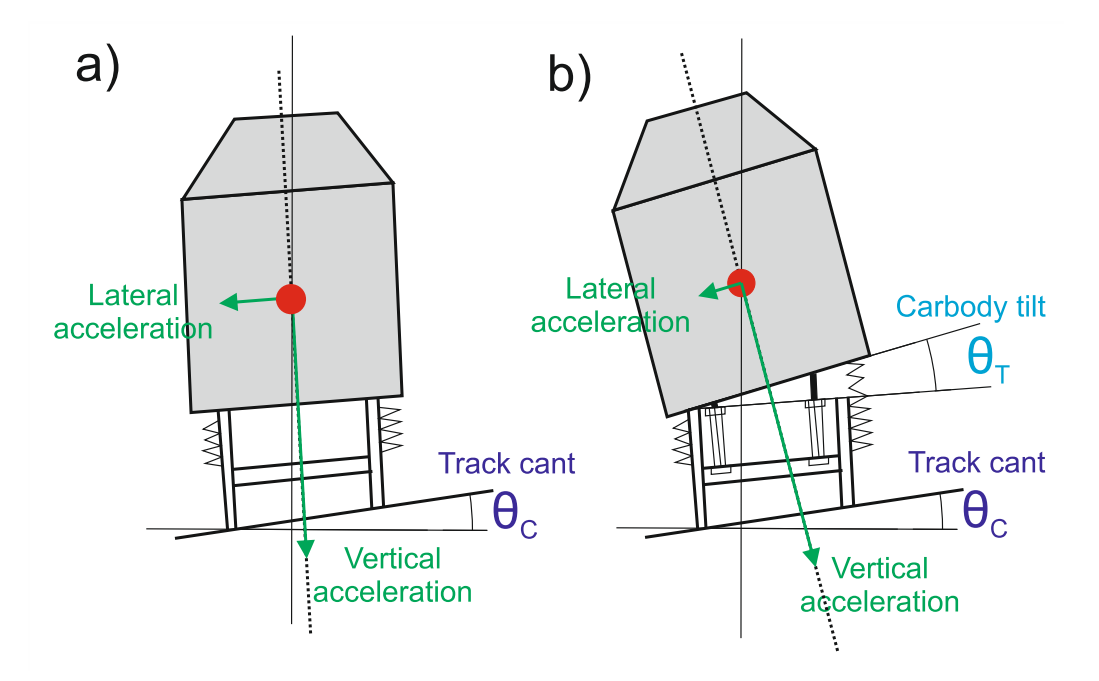


Figure 2.7 The reduction of lateral centripetal acceleration associated with a) track cant, and b) an active tilting suspension mechanism (adapted from Persson, Goodall and Sasaki, 2009).

Typical motion quantities experienced on a train traversing a curve with various amounts of tilt are shown in Table 2.2 (Persson *et al.*, 2009). Here it can be seen that with a constant curve radius, R, the resultant lateral acceleration, y, associated with increasing vehicle speed, S, may be held constant with appropriate increases in track cant, θ_T , or carbody tilt, θ_c . Increases in roll angle, either from the track cant or the carbody tilt, are also associated with increases in vertical acceleration, z (see Section 2.2.3).

Table 2.2 Nominal motion quantities for a train traversing a curve (Persson et al., 2009).

Speed (km/h)	Radius (m)	Track tilt angle (°)	Carbody tilt angle (°)	Lateral acceleration (ms ⁻²)	Vertical acceleration (ms ⁻²)	
S	R	$oldsymbol{ heta}_{ au}$	$\boldsymbol{\theta_{C}}$	У	z	
104	1000	0.00	-1.00	1.00	0.00	
153	1000	5.70	-1.00	1.00	0.15	
200	1000	5.70	6.50	1.00	0.44	

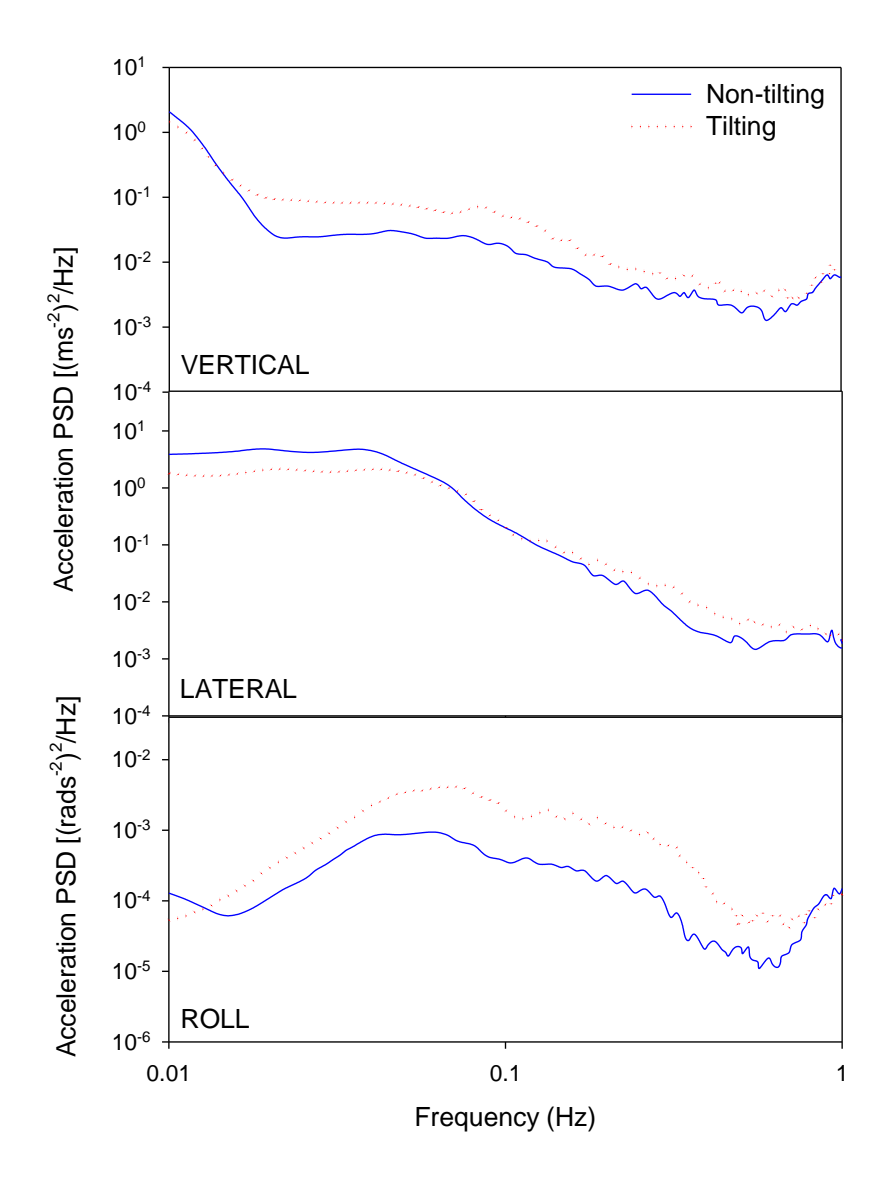


Figure 2.8 Power spectral densities for vertical (*z*-axis), lateral (*y*-axis) and roll (*r*_x-axis) acceleration measured on a tilting and a non-tilting train (adapted from Persson, 2008).

This relationship is supported by acceleration measurements made on a track vehicle between Kristiansand and Vegardshei in Norway (Persson, 2008). (A four-car class BM73 tilting train, from Norwegian State Railways, was used – with the tilt inactive during the non-tilting test). Between about 0.02 and 0.8 Hz, the magnitude of vertical acceleration and roll acceleration was greater in the tilting train than the non-tilting train, but at frequencies less than about 0.05 Hz, lateral acceleration was greater in the non-tilting than in the tilting train (see Figure 2.8).

Table 2.3 Unweighted coach-lateral accelerations, coach-vertical accelerations and coach roll-velocities measured across 26 journeys on an experimental TGV tilting train (Donohew and Griffin, 2007).

Journey number	Target cant deficiency (mm)	Carbody tilt (Y/N)	Target % compensation (where specified)	Coach- lateral acceleration (ms ⁻² r.ms.)	Coach- vertical acceleration (ms ⁻² r.m.s.)	Coach- roll velocity (°/s r.m.s.)
1	280	Υ	-	0.43	0.15	1.25
2	280	Υ	-	0.43	0.15	1.41
3	300	Υ	-	0.45	0.14	1.22
4	300	Υ	-	0.46	0.13	1.42
5	260	Υ	-	0.37	0.12	1.21
6	260	Υ	-	0.42	0.13	1.19
7	220	N	0	0.79	0.09	0.56
8	220	N	0	0.73	0.09	0.66
9	160	N	0	0.67	0.09	0.58
10	260	Υ	-	0.41	0.15	1.35
11	150	Υ	100	0.16	0.13	1.35
12	150	Υ	100	0.17	0.12	1.06
13	150	N	-	0.62	0.11	0.68
14	150	N	-	0.61	0.11	0.60
15	220	Υ	55	0.53	0.15	1.15
16	220	Υ	55	0.42	0.14	0.83
17	260	Υ	65	0.44	0.16	1.46
18	260	Υ	65	0.46	0.16	1.26
19	260	Υ	45	0.62	0.15	1.21
20	260	Υ	45	0.61	0.15	1.04
21	280	Υ	55	0.40	0.13	1.21
22	280	Υ	55	0.51	0.17	1.26
23	300	Υ	55	0.58	0.17	1.41
24	300	Υ	55	0.60	0.17	1.22
25	300	Υ	-	0.52	0.18	1.50
26	300	Υ	-	0.54	0.18	1.28

The lateral acceleration, vertical acceleration and roll velocity were also measured on board an experimental TGV between Paris and Toulouse in France (Donohew and Griffin, 2007). Unweighted motion quantities (measured in train coach-referenced co-ordinates at the centre of the passenger carbody) for 26 journeys are shown in Table 2.3. Supportive of Persson's (2008) claims, it is clear that the vertical acceleration and roll velocity increase in magnitude when the carbody tilt is active. It can also be seen that lateral acceleration is highest with high cant

deficiency but no active tilt. Example magnitudes of lateral acceleration, vertical acceleration and roll velocity from journey 3 and 4 (listed in Table 2.3) for octave-band frequencies between 0.015 and 1.0 Hz are shown in Figure 2.9. Here it can be seen that peak magnitudes tend to occur at frequencies less than 0.5 Hz, with some evidence of decreasing magnitude with decreasing frequency below 0.0315 Hz (Donohew, 2006).

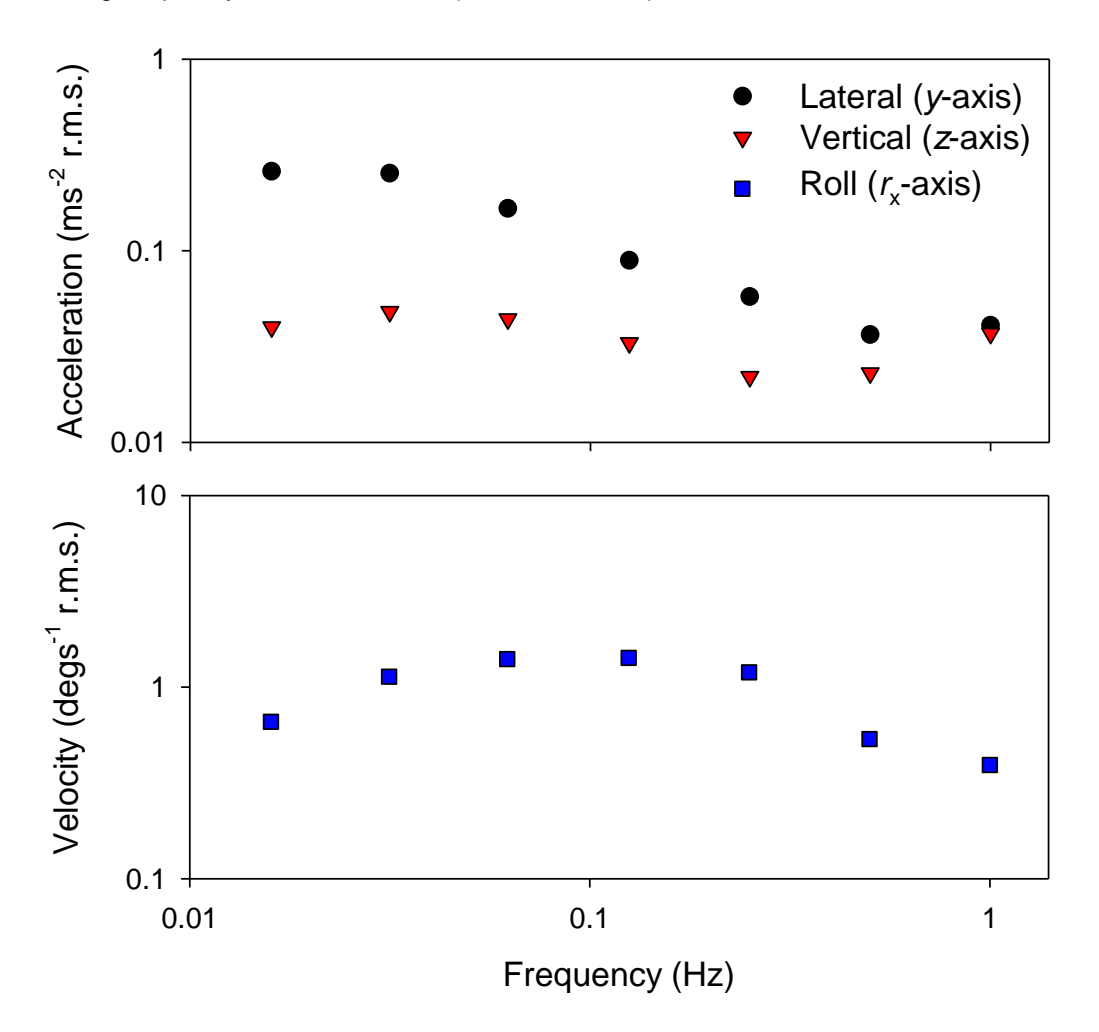


Figure 2.9 Magnitudes of coach-lateral acceleration, coach-vertical acceleration and coach-referenced roll velocity across seven octave-band frequencies between 0.015 and 1.0 Hz calculated from journey 3 and 4 (adapted from Donohew and Griffin, 2007).

In an assessment of the magnitudes of lateral, vertical and roll motion typically experienced on board tilting trains, Donohew (2006) concluded that with constant Earth-lateral acceleration but increasing percentage roll-compensation, the coach-lateral acceleration decreases, the coach-vertical acceleration increases and the coach-roll displacement increases. The ranges of

magnitudes at which these changes occurred during measurement on an experimental TGV are shown in Table 2.4.

Table 2.4 Changes in coach-lateral acceleration, coach-vertical acceleration and coach-roll displacement associated with changes in percentage compensation (Donohew, 2006).

Earth-lateral acceleration (ms ⁻² r.m.s.)	Change in compensation (%)	Change in coach- lateral acceleration (ms ⁻² r.m.s.)	Change in coach- vertical acceleration (ms ⁻² r.m.s.)	Change in coach-roll displacement (°/s² r.m.s.)
Constant (~1.16)	Increase	Decrease	Increase	Increase
	(42 - 86)	(0.67 - 0.16)	(0.11 - 0.13)	(3.14 - 6.64)
Constant	Increase	Decrease	Increase	Increase
(1.62)	(54 - 67)	(0.76 - 0.54)	(0.17 - 0.20)	(5.13 - 6.43)

An example acceleration time history for lateral motion measured at carbody floor of a Japanese railway vehicle is provided in Figure 2.10 (Suzuki, 1998b). The lateral motion is largely random in nature, but does include some periodic features and other vibration events (a peak magnitude is indicated by the arrow, likely due to the train passing a level crossing or turnout; Suzuki, 1998b). The distribution of peak lateral accelerations measured over a 20-minute period (and then divided into 5-second blocks) is shown in Figure 2.11 (Suzuki, 1998a). Measurements were made twice on the same portion of track (a mountainous area of Japan with several curves); in the second test run the train travelled approximately 15 km/h faster than in the first test run. Peak lateral accelerations are most common around 0.5 ms⁻², but the probability of greater magnitudes of vibration increases with increasing train speed.

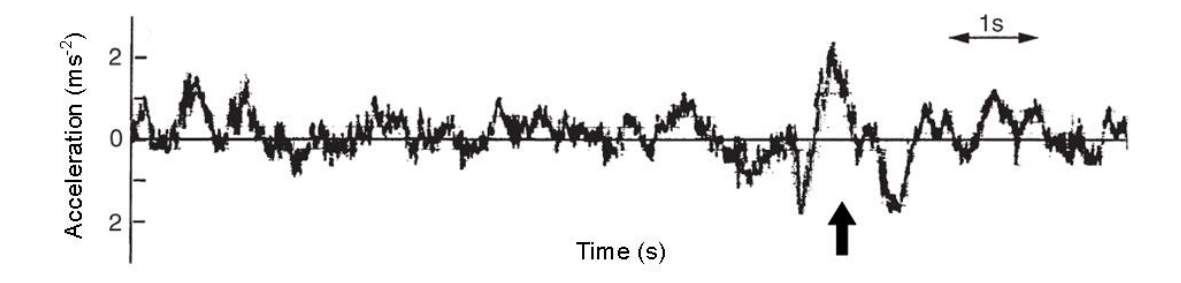


Figure 2.10 Example lateral vibration waveform measured at the carbody floor of a railway vehicle in Japan (Suzuki 1998b).

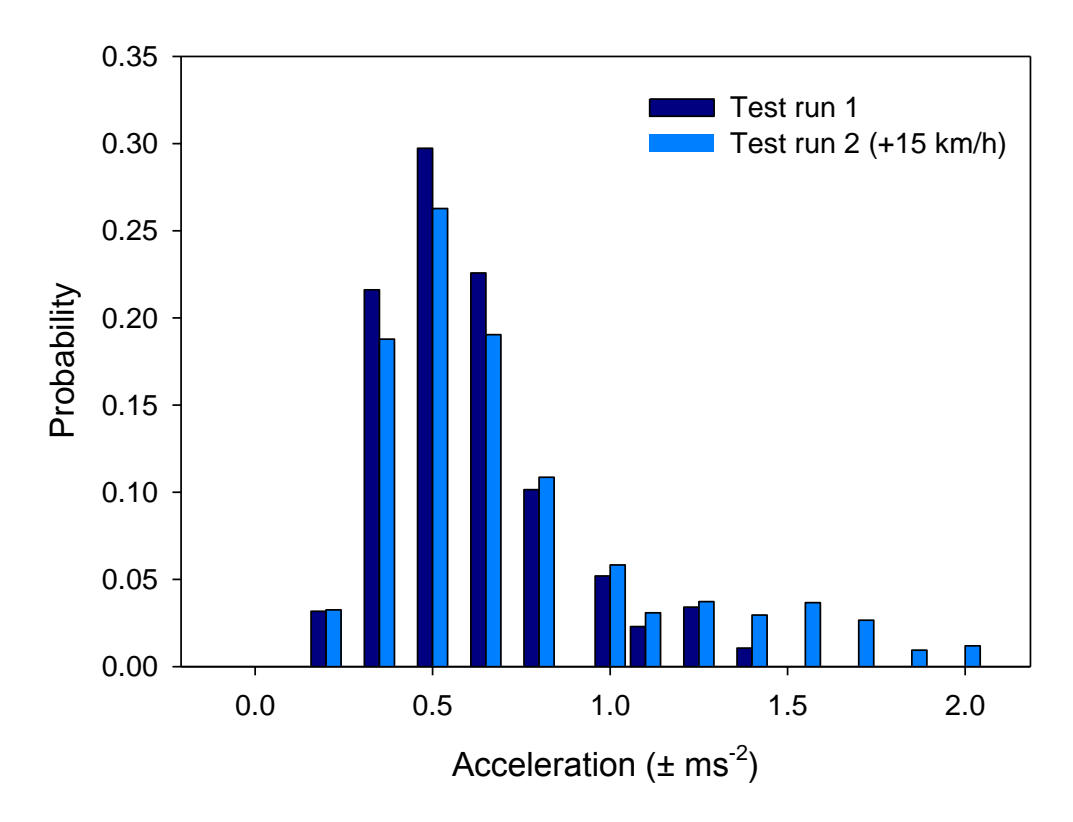


Figure 2.11 Example distribution of peak lateral accelerations measured on a Japanese railway vehicle. Test run 2 was on the same portion of track, but at 15 km/h faster than test run 1 (Suzuki, 1998a).

2.3. Motion perception

To understand the effects of motion on the comfort of people, one must first understand the physiological mechanisms responsible for motion perception. In this respect, three human sensory systems are of interest: (i) the vestibular system (i.e. the organs of balance in the inner ear); (ii) the visual system (i.e. the eyes), and; (iii) the somatosensory system (i.e. the receptors in the skin, muscles and joints). Information from each of these systems is collated by the Central Nervous System (CNS) to provide an interpretation of the motion event and its effect on the body. Each of the three systems is discussed in this Section.

2.3.1. The vestibular system

A diagrammatic representation of the inner ear is shown in Figure 2.12. There are five organs of balance within the vestibular system – three semi-circular canals (horizontal [or lateral], anterior and posterior) which are sensitive to rotational acceleration, and two otoliths (utricle and saccule) which are sensitive to translational (horizontal and vertical) acceleration. The five end

organs are (approximately) orthogonally aligned so as to detect motion in any of the six directions. The horizontal, anterior and posterior semi-circular canals are roughly aligned so as to detect yaw, roll and pitch rotations, respectively. The utricule and saccule otoliths are aligned to detect horizontal and vertical translation, respectively. The maculae of the utricule and the saccule, and the cristae of the semi-circular canals house vestibular sensory epithelium, responsible for the perception of motion.

2.3.1.1. Sensory epithelium

In the vestibular system, the sensory epithelial cells are hair-like structures known as stereocilia and kinocilium. There are approximately 50-100 stereocilia for every kinocilium, which is thicker and longer in structure (NDBC, 2012). Stereocilia are arranged in a staircase formation with the height of the cells increasing with decreasing proximity to the kinocilium (Figure 2.13). When stereocilia are displaced towards the kinocilium, the neuron firing rate increases (hyperpolarisation) and the vestibular nerve exhibits an excitatory signal (Goldberg and Fernandez, 2011). Conversely, when stereocilia are displaced away from the kinocilium, the neuron firing rate decreases (depolarisation) and the vestibular nerve exhibits an inhibitory signal. In the cristae of the semi-circular canals, stereocilia are polarised in the same direction, but in the maculae of the otoliths, the polarisation reverses in the region of the striola (facing away from the striola in the saccular macula and towards the striola in the utricular macula) (see Figure 2.13).

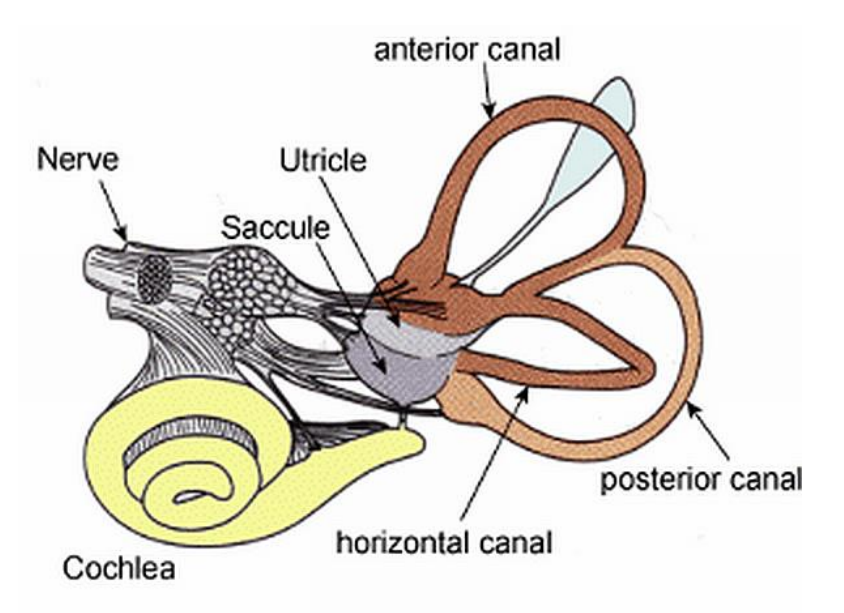


Figure 2.12 Anatomy of the inner ear, consisting of the vestibular system and the cochlear (Haslwanter, 2008).

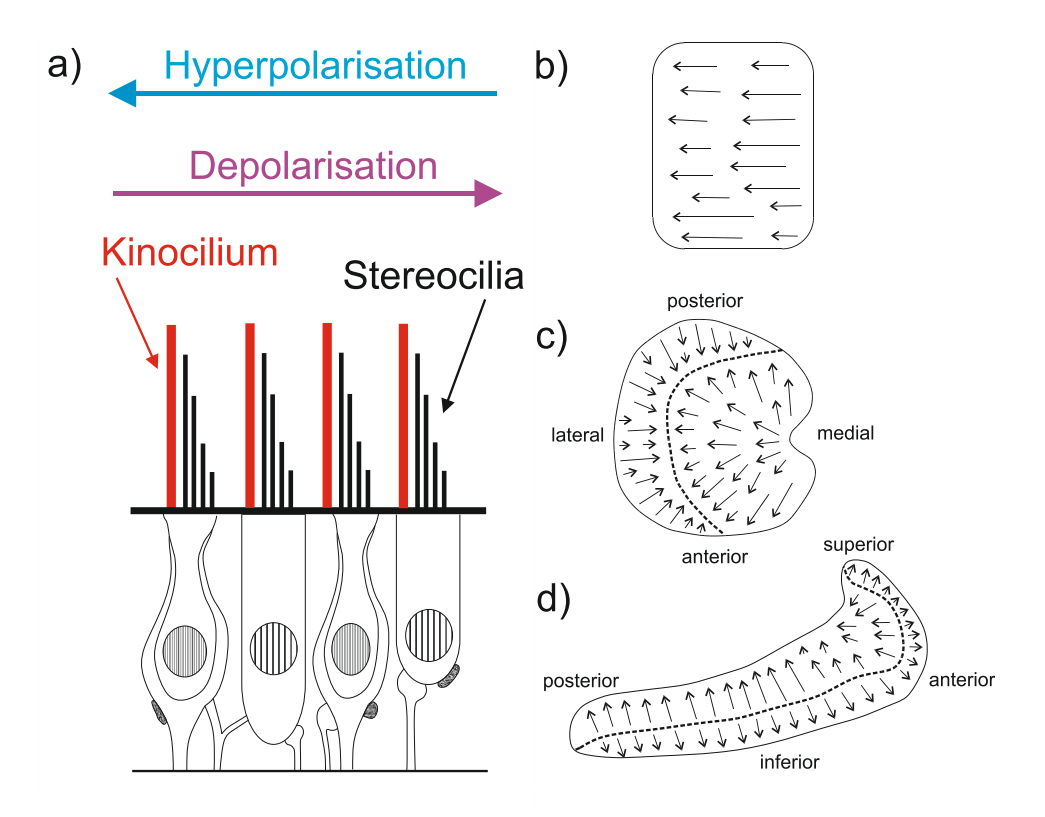


Figure 2.13 Orientation and sensitivity of stereocilia and kinocilium (a). Stereocilia are polarised in the same direction in the cristae (b), but reverse their polarity in the region of the striola (dotted line) in the utricular macula (c) and saccular macula (d) (adapted from Goldberg and Fernandez, 2011).

Whilst the sensory mechanisms of the otoliths and the semi-circular canals are grounded in the same physical principles, their structures are inherently different (NASA, 2002). The structure of the cristae of the semi-circular canals and the maculae of the otoliths is discussed in greater detail in Section 2.3.1.2 and 2.3.1.3, respectively.

2.3.1.2. Semi-circular canals

The semi-circular canals on the left and right side of the head act as functional pairs of sensory organs (Figure 2.14). The lateral canals sit approximately in the horizontal plane, and are thus sensitive to yaw motion of the head (in basicentric coordinates – see Figure 2.2). The anterior canal on the left side of the head is parallel to the posterior canal on the right side of the head, and vice versa, and are responsible for detecting roll and pitch motion (in basicentric coordinates). This pairing allows for the direction of rotation to be detected via two means; an excitatory (hyperpolarising) signal on one side and an inhibitory (depolarising) signal on the other.

Each semi-circular canal is a ring-like structure consisting of a thin membrane surrounded by perilymphic fluid and connected to a bony tube via connective tissue. The membranous tube is filled with a fluid-like substance called endolymph. At the base of each tube, the vestibular nerve breaches into an enlarged cavity known as the ampulla. Stereocilia extend from the end of the vestibular nerve into the ampullary crest, atop which sits the wedge-shaped gelatinous structure of the cupula. The cupula forms a fluid-tight partition by extending to the horizontal and vertical internal walls of the membranous tube (NDBC, 2012). Together, the structure of the ampullary crest and the cupula is known as the crista (see Figure 2.15).

Inertial forces imposed on the canal causes relative movement between the endolymphatic fluid and the cupula (see Figure 2.15). An inhibitory or an excitatory nerve impulse (depending on the direction of movement – see Figure 2.13) is caused by the resultant depolarisation or hyperpolarisation, respectively, of the stereocilia and kinocilium cells. The deflection of the cupula and thus the firing rate of the resultant nerve impulse is proportional to head angular velocity (Bos and Bles, 2002, as cited by, Donohew, 2006). Since the density of the cupula is approximately equal to that of the surrounding endolymph, the structure does not react to gravitational forces (unlike the otolith organs).

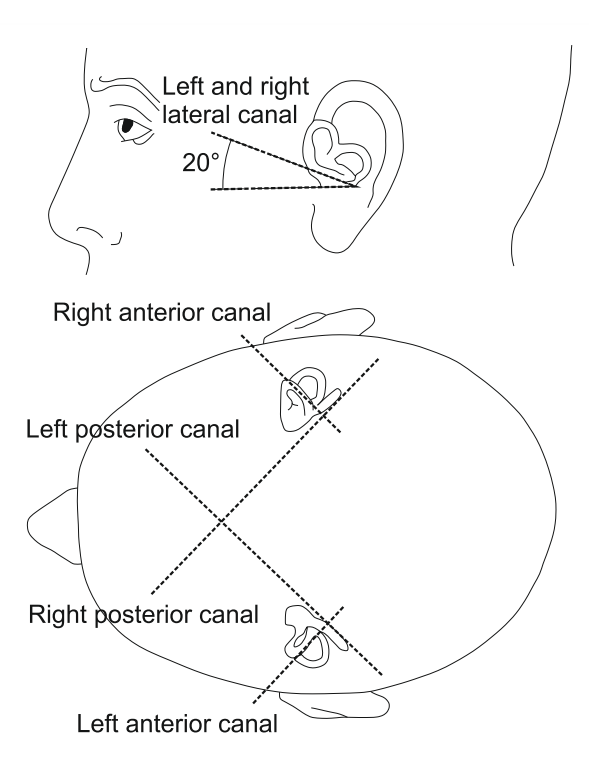


Figure 2.14 Orientation of the semi-circular canals (adapted from Jacobson, Newman and Kartush, 1993).

2.3.1.3. Otolith organs

The function of the otolith organs also depends on the inertial deflection of hair cells in order to produce action potentials in the vestibular nerve cells. The vestibular nerve fibres penetrate the utricule and saccule in an area known as the macula, which consists of a collection of hair cells and supporting cells (see Figure 2.16). Above this structure sits a gelatinous otolithic membrane which houses groups of calcium carbonate crystals known as the otoliths. The otoliths are key to the sensory function of the organ, as they increase the density of the otolithic membrane giving the structure more inertia allowing it to respond to gravity. (NASA, 2002). The saccular macula sits on the anterior vertical wall of the saccule, whilst the utricular macula sits horizontally in the anterior portion of the utricle (known as the utricular recess).

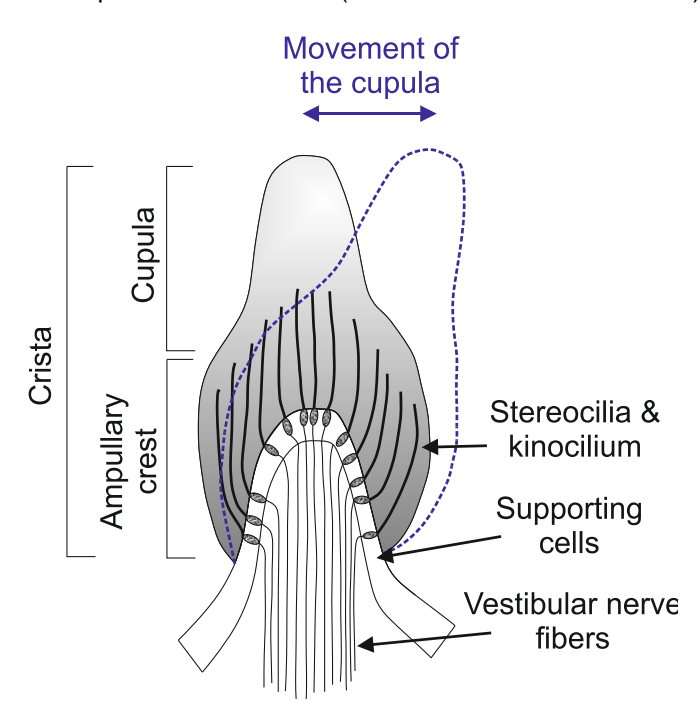


Figure 2.15 Structure of the crista (consisting of the cupula and the ampullary crest) within the semi-circular canals. Velocity changes in the endolymphatic fluid in the canals stimulates movement of the cupula, causing the 'hair-cells' to generate a nerve impulse (adapted from NASA, 2002).

Inertial and gravitational forces imposed on the utricle and saccule cause relative movement between the otoliths and the macula. This displacement stimulates the hair cells which triggers a vestibular nerve impulse. The otolith organs react to translational acceleration in the horizontal (utricle) and the vertical (saccule) plane, and gravitational acceleration associated with tilts of the head (see Equation 2.2, Section 2.2.2). "Like all linear accelerometers, [the otoliths] respond to specific gravito-inertial force (*GIF*), which is the sum of the specific force associated with

gravity and the specific inertial force due to linear acceleration" (Park *et al.*, 2006, p. 486), so stimulation of the otoliths via inertial acceleration is indistinguishable from that via gravitational acceleration (Griffin, 1990).

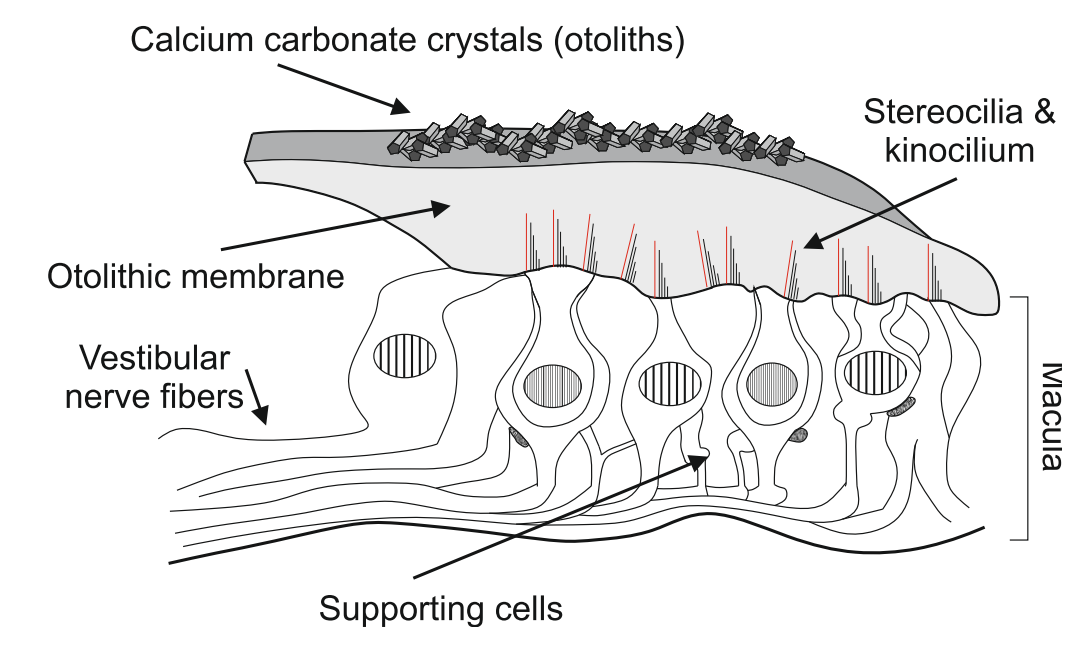


Figure 2.16 Structure of otolith organs (utricle and saccule) (adapted from NASA, 2002).

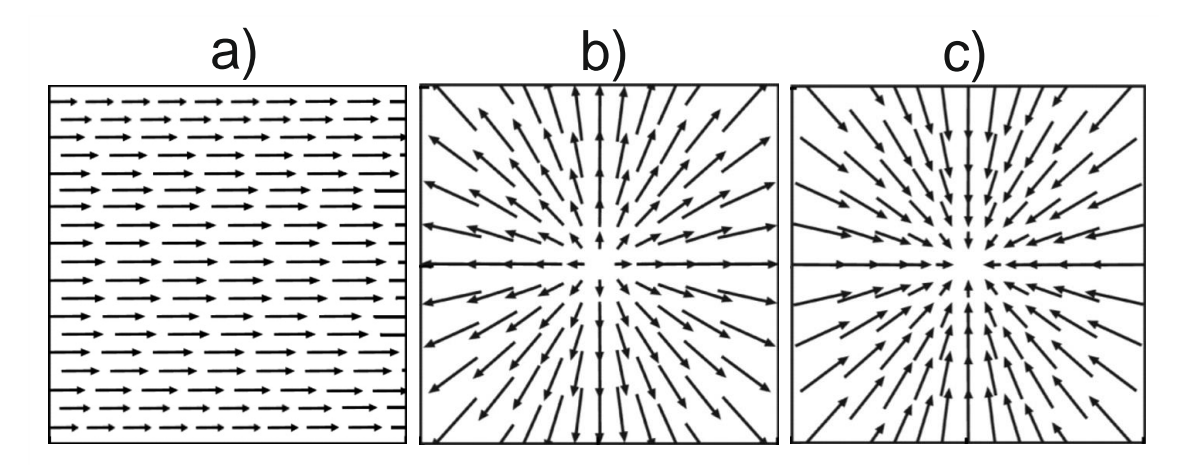


Figure 2.17 Optic flow fields during lateral movement or rotary movement about a fixed point (a), forward movement (b) and backward movement (c). Arrows are velocity vectors representing apparent movement of objects in the visual field (adapted from Horseman, Macauley and Barnes, 2011).

2.3.2. The visual system

Motion is interpreted by the visual system through the recognition of changing patterns of light focussed on the retina, known as 'optic flow' (Figure 2.17).

When fixated on an object in the moving environment, the peripheral optical information forms an 'optic flow' in the visual field. Movement of light in the optic flow originates from the focal point in the visual field, known as the focus of expansion, acting as velocity vectors providing information on the speed and direction of motion. Optic flow is generated by relative movement between the head and the visual field, which may include movement of the head, movement of the visual field, or movement of both the head and the visual field (Joseph, 2008). This perceptual system allows the interpretation of motion trajectory as well as object depth, distance and shape (Heeger and Simoncelli, 1993).

2.3.3. The somatosensory system

The somatosensory system includes a number of modalities including the cutaneous senses and proprioception (Tsuchitani, 1997). Cutaneous receptors are located in the skin and respond to changes in pressure and temperature. Proprioceptors are located in the muscles and joints, providing information on the position, orientation and movement of the body. Proprioceptors respond to static forces acting on joints, muscles and tendons indicating the position and orientation of specific limbs, and dynamic changes to those forces indicating movement of specific limbs (Tsuchitani, 1997). Proprioception is essential for aiding motor control, therefore the integration of proprioceptive signals with those from the vestibular and visual systems is likely to be vital for the interpretation of low frequency oscillations which may disturb posture and balance.

2.4. Investigation of motion sickness

2.4.1. Symptoms

The phenomenon of motion sickness has been of interest to scientists for centuries; Erasmus Darwin noted in 1796 that "...when first we go on ship-board, where the movements of ourselves, and the movements of the large waves are both new to us, the vertigo is almost unavoidable with the terrible sickness, which attends it". Today, motion sickness is a common disturbance characterised as "vomiting (emesis), nausea or malaise provoked by actual or perceived motion of the body or its surroundings" (Griffin, 1990, p. 831).

Individual susceptibility to motion sickness varies considerably (e.g. Bos *et al.*, 2007) and therefore the signs and symptoms of this phenomenon depend on the characteristics of the person and other environmental factors. Any combination of headaches, yawning, drowsiness, bodily warmth, increased salivation, cold sweating, dizziness, increased respiration rate, nausea and vomiting may be experienced by sufferers of motion sickness. The condition may begin with 'a feeling of discomfort in the upper abdomen' and 'an increasing feeling of being unwell' (NHS, 2011). Symptoms can develop at any time during exposure to a provocative stimulus; however it is common for the severity of symptoms to increase with the duration of provocation (e.g. Lawther and Griffin, 1987).

2.4.2. Measurement and evaluation

Historically, motion sickness has been objectively quantified by observing the vomiting incidence of people exposed to provocative stimuli (Griffin, 1990). Vomiting incidence expressed as a percentage of the total number of people exposed is known as the motion sickness incidence, or MSI (O'Hanlon and McCauley, 1973). The MSI may be objective, but vomiting is not the most common symptom, and rarely appears first, therefore its practicality as a measure of motion sickness is limited (Joseph, 2008). Today, more ethical and practical procedures are used to measure the development of motion sickness.

2.4.2.1. Motion sickness susceptibility

Questionnaires designed to assess the degree of 'motion sickness susceptibility' have taken many forms including The Reason and Brand Motion Sickness Susceptibility Questionnaire (Reason and Brand, 1975) and it's revised form (Golding, 1998), the Pensacola Motion History Questionnaire (Kennedy *et al.*, 1990) and the ISVR Motion Sickness Susceptibility Questionnaire (Reid, 1991). The latter questionnaire (reported by Griffin and Howarth, 2000) has been utilised in a substantial body of work at the Institute of Sound and Vibration Research at The University of Southampton (e.g. Butler and Griffin, 2006; Donohew and Griffin, 2009; Holmes, 1996; 1997; 1998; Howarth, 1999; Howarth, Martino and Griffin, 1999; Joseph and Griffin, 2007; 2008; Lobb, 1999; Mills and Griffin, 2000; Webb, 1997; 1998; 1999; Woodman and Griffin, 1997). The questionnaire consists of 16-parts designed to examine self-reports of "individual exposure to motion in various forms of transport...and the occurrence of illness and vomiting in these forms of transport during the past year" (Griffin and Howarth, 2000, p. 2). The frequency of motion sickness symptoms experienced in different forms of transport and a self-rated susceptibility to motion sickness is also obtained; leading to the determination of nine measures of motion sickness susceptibility (see Table 2.5).

Table 2.5 Measures of motion sickness susceptibility (Griffin and Howarth, 2000).

Measures of motion sickness susceptibility	Code
Travel frequency in the past year	<i>T</i> _(yr.)
Illness frequency while travelling in the past year	Itravel(yr.)
Vomiting frequency while travelling in the past year	V _{travel(yr.)}
Illness susceptibility in transport in the past year	I _{susc.(yr.)}
Vomiting susceptibility in transport in the past year	V _{susc.(yr.)}
Total susceptibility to vomiting	V _{total}
Total susceptibility to motion sickness	M _{total}
Susceptibility to motion sickness in land transport	Mand
Susceptibility to motion sickness in non-land transport	M _{nland}

2.4.2.2. Motion sickness severity and symptoms

Previous research has adopted various forms of 'illness rating scales' to assess the severity of motion sickness symptoms (e.g. Golding and Kerguelen, 1992; Förstberg *et al.*, 1998; Suzuki *et al.*, 2005; Joseph and Griffin, 2007). Well-being on railway transport has been rated on a four-point scale ranging from 'I felt all right' to 'I felt absolutely dreadful, and a five-point scale ranging from 'very bad' to 'very good' (Förstberg *et al.*, 1998; Suzuki *et al.*, 2005), whilst in laboratory simulations, a seven-point illness rating scale ranging from 'no symptoms' to 'moderate nausea, and want to stop' has often been used (e.g. Golding and Kerguelen, 1992; Howarth and Griffin, 2003; Joseph and Griffin, 2008a; 2008b; Donohew and Griffin, 2009). Whilst the wording varies, all the rating scales share terms to describe escalating severity of 'well-being' or 'sickness'. An example seven-point illness rating scale (presented by Griffin and Howarth, 2000) can be seen in Table 2.6.

Illness rating scales provide a method for determining the severity of motion sickness symptoms, but it is also useful to assess the type of symptoms experienced by passengers. To achieve this, Griffin and Howarth (2003) defined a 'symptom checklist' used to determine the incidence of 10 common symptoms of motion sickness (see Table 2.7).

Table 2.6 Motion sickness illness rating scale (Griffin and Howarth, 2000).

Rating	ng Corresponding feelings			
0	No symptoms			
1	Any symptoms, however slight			
2	Mild symptoms			
3	Mild nausea			
4	Mild to moderate nausea			
5	Moderate nausea but can continue			
6	Moderate nausea and want to stop			

Table 2.7 List of common motion sickness symptoms (Griffin and Howarth, 2000).

Motion sickness symptoms				
Yawning	Bodily warmth			
Increased salivation	Stomach awareness			
Cold sweating	Dizziness			
Headache	Dry mouth			
Nausea	Drowsiness			

2.4.2.3. Prediction of motion sickness

A prediction of the effects of motion frequency, magnitude and duration on the incidence of motion sickness can be made from measured motion quantities in a given transport environment. The motion sickness dose value (*MSDV*), proposed by Lawther and Griffin (1987), is defined in British (BS 6841, 1987) and International standards (ISO 2631-1, 1997):

Equation 2.14:
$$MSDV \ ms^{-1.5} = \left(\int_0^T a^2(t)dt\right)^{\frac{1}{2}}$$

where T is the motion exposure duration in seconds and a(t) is acceleration. It follows that the MSDV is also determined by multiplying the root-mean-square (r.m.s.) acceleration by the square root of the motion exposure duration, such that:

Equation 2.15:
$$MSDV \ ms^{-1.5} = a_{r.m.s.} \times T^{\frac{1}{2}}$$

where $a_{r.m.s.}$ is the r.m.s. acceleration. The MSDV is a cumulative function, i.e., a dose, whereby sickness increases equally with a doubling of the acceleration magnitude or a quadrupling of the duration of motion. Habituation to motion and recovery of motion sickness symptoms is not incorporated in the function, however the MSDV is limited to motion durations up to about 6 hours, so habituation is unlikely to affect the prediction of sickness.

The likely vomiting incidence may also be approximated from the MSDV:

Equation 2.16:
$$VI(\%) = MSDV \times K_m$$

where VI is the percentage of people likely to vomit, and K_m is a constant dependent on the characteristics of the exposed population. For a "mixed population of unadapted male and female adults" K_m may be equal to 1/3 (ISO 2631-1, 1997, p 27).

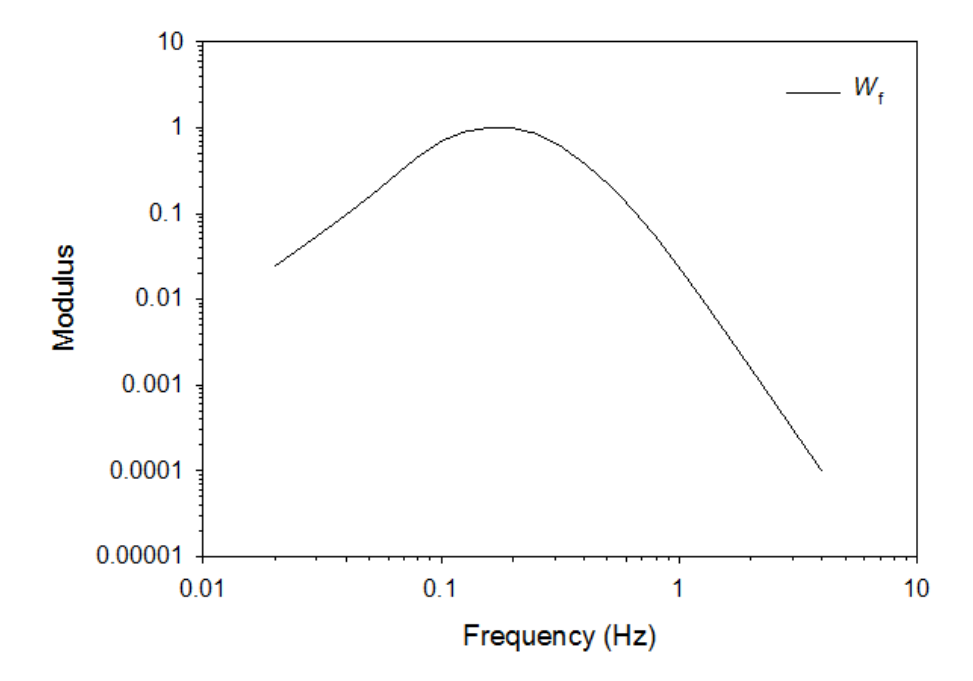


Figure 2.18 Motion sickness frequency weighting W_f with a band-pass filter at 0.08 and 0.63 Hz (ISO 2631-1, 1997).

To account for the effects of frequency on motion sickness the a(t) and $a_{r.m.s.}$ components in Equation 2.14 and Equation 2.15, respectively, are frequency weighted using the W_t weighting function (BS 6841, 1987; ISO 2631-1, 1997; see Figure 2.18). It is principally advised that the

function is only applied to sickness caused by vertical oscillation in the range 0.1 to 0.5 Hz, although 'realisable' values outside this range can be achieved with high-pass and low-pass filters at 0.08 and 0.63 Hz, respectively (BS 6841, 1987). The effects of frequency on motion sickness incidence are discussed in greater detail in Section 2.5.1.

2.4.3. Theories of motion sickness

2.4.3.1. Evolutionary hypothesis

Treisman (1977) argues that since motion sickness is prevalent in such a wide range of species, from birds and fish to horses and monkeys, an evolutionary explanation for the condition must exist. One such explanation theorises that motion sickness is a result of the vestibular system serving as a natural 'toxin detector'. The ingestion of toxins can lead to disturbances in the visual, vestibular or proprioceptive systems, and when the brain recognises these changes it provokes an emetic response in an attempt to rid the body of toxins. Since exposure to certain types of motion will trigger similar disturbances to the visual, vestibular or proprioceptive systems, it is possible motion sickness is simply an unfortunate by-product of an important survival mechanism.

Table 2.8 Types and categories of sensory conflict based on the sensory rearrangement theory (Griffin, 1990).

	Category of conflict			
Type of conflict	Visual (A) – Vestibular (B)	Canal (A) – Otolith (B)		
Type I A signals different from B	Visual and vestibular simultaneously signal different information	Semi-circular canals and otolith organs simultaneously signal different information		
Type IIa A signals, not B	Visual system signals in the absence of an expected vestibular signal	Semi-circular canals signal in the absence of an expected otolith signal		
Type IIb B signals, not A	Vestibular system signals in the absence of an expected visual signal	Otoliths signal in the absence of an expected semi-circular canal signal		

2.4.3.2. Sensory conflict theory

As discussed in Section 2.3, motion information is processed by three sensory pathways; the vestibular system, the visual system and the somatosensory system. The sensory conflict theory assumes that motion sickness is caused by conflicting information received by one or more of these sensory systems (Reason and Brand, 1975). Since the vestibular system is integral to the generation of motion sickness, 'conflict' is principally defined as 'inter-sensory' (between the visual and vestibular systems), or 'intra-sensory' (between the semi-circular canals and the otolith organs within the vestibular system). However, a simple conflict between sensory signals is an insufficient explanation of motion sickness, since it does not account for the mechanism of habituation (Griffin, 1990).

2.4.3.3. Sensory rearrangement theory

The ideas of sensory conflict were further developed by Reason (1978) into the sensory rearrangement theory. Rather than conflicting sensory signals, the basis of this theory states that motion sickness arises from a difference between 'sensed' and 'expected' sensory signals. Sensed signals are defined as the actual resultant stimulation of the vestibular or visual organs during exposure to a motion or visual stimulus. Expected signals are defined as the 'usual' stimulation of those sensory organs, derived from previous exposures to the same, or similar, environmental stimuli. Griffin (1990) provides a summary of the types of 'conflict' which may occur according to this theory (see Table 2.8). Since expected signals are thought to arise from a combination of inherent processes and what has been 'learned' from previous experiences, the theory is able to incorporate a mechanism for habituation.

2.5. Factors influencing motion sickness

2.5.1. Frequency

The incidence of motion sickness is highly dependent on the frequency of oscillation. With vertical oscillation, 0.53 Hz causes markedly less sickness than 0.22, 0.27 and 0.37 Hz (Alexander *et al.*, 1945, as cited by, Donohew, 2006), and the incidence of sickness decreases with increasing frequency between 0.167 and 0.7 Hz (O'Hanlon and McCauley, 1973; McCauley *et al.*, 1976). Frequency weighting W_f , proposed by Lawther and Griffin (1987), suggests sensitivity to vertical acceleration is constant between 0.125 and 0.25 Hz, but decreases by 12 dB per octave above and 6 dB per octave below this range. The weighting therefore predicts vertical oscillation is most provocative at frequencies between 0.125 and 0.25 Hz.

Similar effects of frequency have been shown with horizontal oscillation. The time required for 12 subjects to reach 'moderate nausea' decreased with the frequency of ±3.6 ms⁻² fore-and-aft oscillation between 0.205 and 1.0 Hz (Golding and Markey, 1996; Golding, Finch and Stott, 1997). Moderate nausea was reported by 75% of subjects during 0.35 Hz oscillation and by 17% of subjects during 1 Hz oscillation. Greater sickness was also reported with ±1.0 ms⁻² fore-and-aft oscillation at 0.2 Hz than at 0.1 and 0.4 Hz, suggesting the frequency dependence is similar to that for vertical oscillation (Golding, Mueller and Gresty, 2001). This work by Golding and colleagues suggests a 'motion sickness maximum' at 0.2 Hz (see Figure 2.19), which may be explained by a frequency-dependent phase discrepancy in the processing of motion stimuli (Golding *et al.*, 2001).

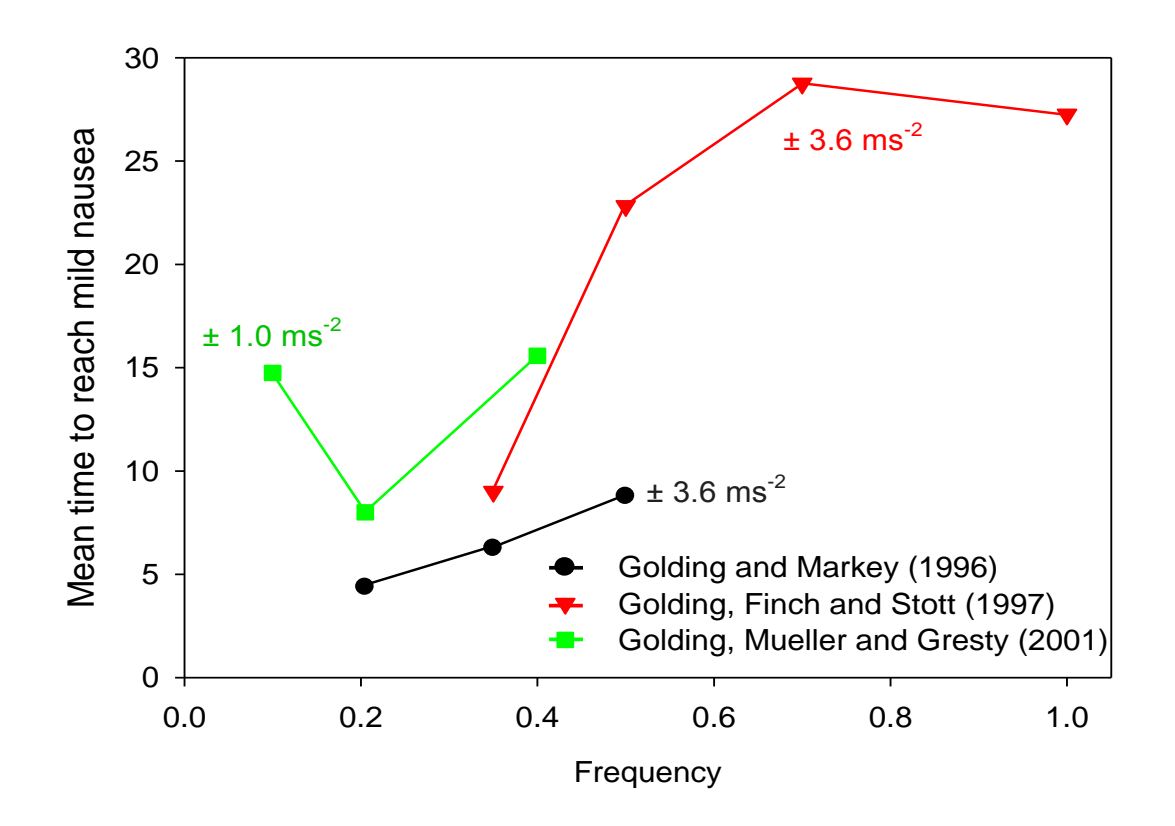


Figure 2.19 Effect of frequency (Hz) on motion sickness caused by fore-and-aft oscillation, as reported by Golding and colleagues (Golding and Markey, 1996; Golding, Finch and Stott, 1997; Golding, Mueller and Gresty, 2001)

With ±1.0 ms⁻¹ lateral oscillation, motion sickness increased with frequency between 0.0315 and 0.2 Hz (Donohew and Griffin, 2004). The greatest proportion of subjects reported illness at 0.2 Hz, consistent with the existence of a 'motion sickness maximum' around this frequency (Golding *et al.*, 1996; 1997; 2001). Between 0.315 and 0.8 Hz, lateral oscillation with a constant

perk jerk (1.96 ms⁻³) revealed no significant differences in motion sickness, suggesting an "acceleration frequency weighting with a gain proportional to frequency" in this range (Donohew, 2006, p 126).

Fully roll-compensated lateral oscillation (i.e. with a zero resultant acceleration at the position of roll-compensation, in this case the seat surface) lead to an increasing incidence of motion sickness with increasing frequency between 0.05 and 0.2 Hz (constant Earth-lateral velocity, ±1.0 ms⁻¹), but decreasing motion sickness incidence between 0.315 and 0.8 Hz (constant Earth-lateral jerk, ±1.96 ms⁻³) (Donohew, 2006). Fully-roll compensated lateral oscillation was more provocative than lateral oscillation presented alone, however the frequency dependence of motion sickness responses appears to be similar (Figure 2.20; Donohew and Griffin, 2004).

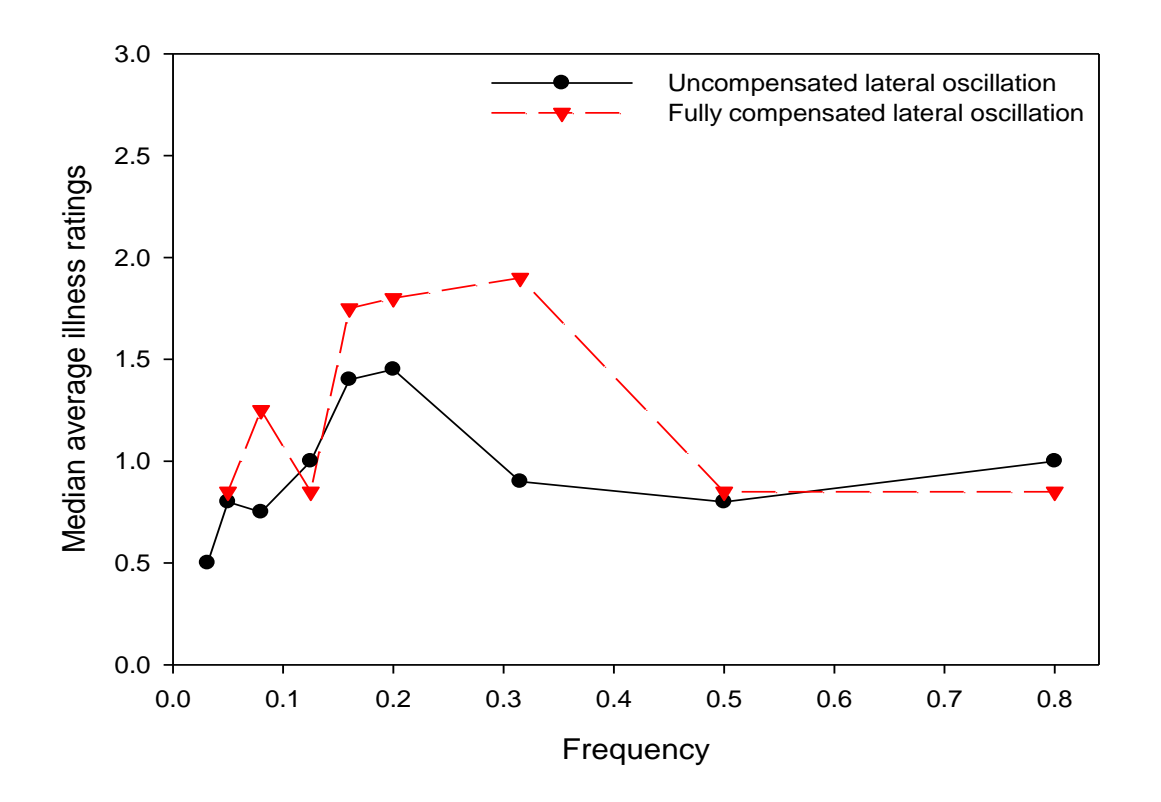


Figure 2.20 The effect of frequency (Hz) on motion sickness caused by uncompensated lateral oscillation and fully roll-compensated lateral oscillation, as reported by Donohew (2006) and Donohew and Griffin (2009).

Similar provocation of motion sickness was found with ± 0.5 ms⁻¹ fore-and-aft and lateral oscillation, however interestingly no differences in sickness were found between oscillation at 0.2 and 0.8 Hz (Griffin and Mills, 2002a). With a constant peak velocity of ± 0.5 ms⁻¹, sinusoidal oscillation at 0.2 Hz yields an acceleration of ± 0.63 ms⁻² whilst at 0.8 Hz it is ± 2.51 ms⁻². In this

case the substantially larger acceleration at 0.8 Hz negated the frequency-dependence of motion sickness.

Table 2.9 Quantities of lateral, roll and fully roll-compensated lateral motions and associated levels of 'mild nausea', as reported by Howarth and Griffin (2003), Donohew and Griffin (2004) and Donohew (2006).

Study	Frequency (Hz)	Roll displacement (± °)	Roll acceleration (± °/s²)	Earth-lateral acceleration (± m/s²)	Lateral acceleration in the plane of the seat (± m/s²)	Proportion of subjects to reach "mild nausea" (%)
	0.025	8	0.20	0.00	1.37	10
Howarth and	0.05	8	0.79	0.00	1.37	10
Griffin (2003) - Roll	0.1	8	3.16	0.00	1.37	5
oscillation	0.2	8	12.63	0.00	1.37	15
	0.4	8	50.53	0.00	1.37	15
	0.0315	0	0.00	0.20	0.20	4
	0.05	0	0.00	0.31	0.31	10
	0.08	0	0.00	0.51	0.51	15
Donohew and	0.125	0	0.00	0.79	0.79	30
Griffin (2004) - Lateral	0.16	0	0.00	1.00	1.00	45
oscillation	0.2	0	0.00	1.26	1.26	55
	0.315	0	0.00	0.99	0.99	20
	0.5	0	0.00	0.63	0.63	35
	0.8	0	0.00	0.39	0.39	10
	0.05	1.83	0.18	0.31	0	25
	0.08	2.93	0.74	0.5	0	35
Donohew	0.125	4.58	2.83	0.79	0	20
(2006) - Fully roll-	0.16	5.85	5.91	1.01	0	60
compensated lateral	0.2	7.3	11.53	1.26	0	75
oscillation	0.315	5.76	22.56	0.99	0	60
	0.5	3.67	36.22	0.63	0	45
	0.8	2.27	57.35	0.39	0	30

The effect of the frequency of roll oscillation on motion sickness incidence has also been investigated previously (Howarth and Griffin, 2003). With ±8° roll oscillation, low levels of motion sickness were reported with no significant differences between 0.025, 0.05, 0.1, 0.2 and 0.4 Hz. The quantities of this roll oscillation, along with quantities of lateral oscillation and fully roll-compensated lateral oscillation used by previous authors, are shown in Table 2.9. The

magnitudes of lateral acceleration in the plane of the seat surface (i.e. \pm ms⁻², due to roll through gravity – see Section 2.2.2) used by Howarth and Griffin (2003) were greater than those used by Donohew and Griffin (2004), yet the incidence of 'mild nausea' was lower in with roll oscillation than with lateral oscillation. Likewise, the magnitudes of roll acceleration (\pm °/s²) used by Howarth and Griffin (2003) were greater than those used by Donohew (2006), but there was greater sickness in the latter study. This evidence suggests that roll oscillation (as studied by Howarth and Griffin, 2003) is not as provocative of motion sickness as lateral oscillation (studied by Donohew and Griffin, 2004) or fully roll-compensated lateral oscillation (studied by Donohew, 2006). The percentage of subjects to report 'mild nausea' in each of these three conditions is illustrated in Figure 2.21.

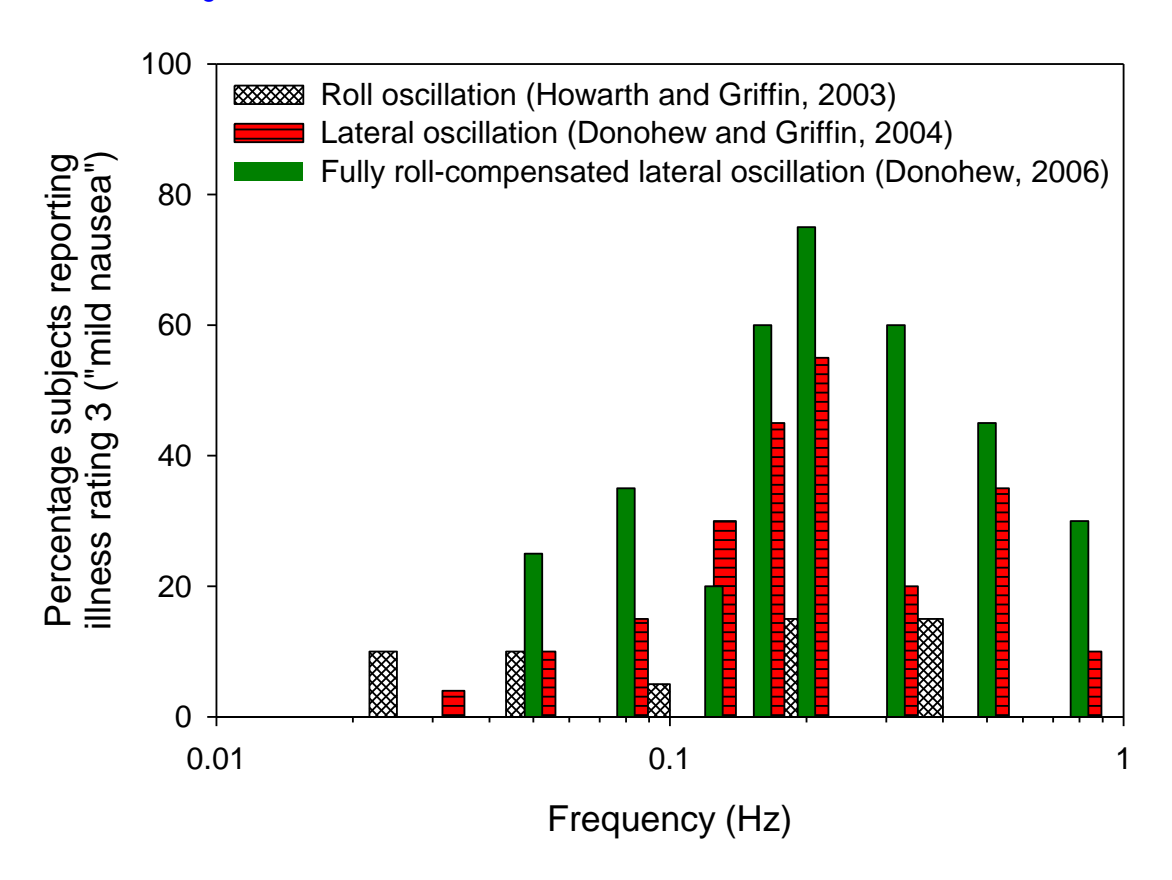


Figure 2.21 The percentage of subjects to report 'mild nausea' during exposure to roll oscillation (Howarth and Griffin, 2003), lateral oscillation (Donohew and Griffin, 2004) and fully roll-compensated lateral oscillation (Donohew, 2006). Full motion quantities are shown in Table 2.9.

It is clear that a frequency-dependence of motion sickness exists for vertical, lateral, fore-and-aft and fully roll-compensated lateral oscillation, but frequency weighting W_i for vertical oscillation is the only prediction method defined in current standards (BS 6841, 1987; ISO 2631-1, 1997). An acceleration frequency weighting for lateral oscillation was constructed by

Donohew and Griffin (2004) using the incidence of subjects reaching an illness rating of 3 (mild nausea). The asymptotic weighting (shown in Figure 2.22) is constant between 0.0315 to 0.25 Hz and decreases in proportion to displacement between 0.25 and 0.8 Hz. In relation to $W_{\rm f}$, the lateral weighting suggests greater sensitivity to lateral oscillation than vertical oscillation at frequencies less than 0.1 Hz.

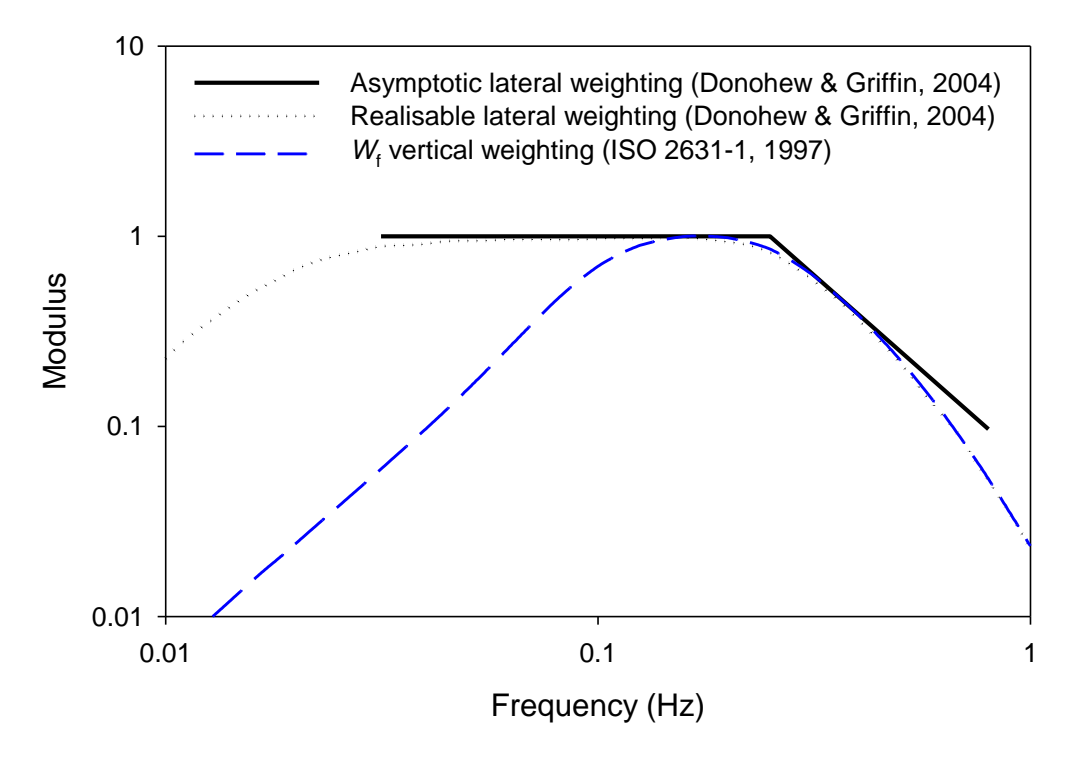


Figure 2.22 Asymptotic and realizable frequency weightings for lateral acceleration and vertical acceleration, *W*_f (figure adapted from Donohew and Griffin, 2004).

The frequency-dependence of motion sickness caused by uncompensated and fully roll-compensated lateral oscillation may be similar (Donohew and Griffin, 2004; Donohew, 2006; Donohew and Griffin, 2009). However, the development of a frequency weighting for roll-compensated lateral oscillation may not be straight-forward; previous authors have concluded that motion sickness caused by fully roll-compensated lateral oscillation may not be well predicted from any one component of the motion, e.g. the subject-lateral force, the Earth-lateral force or the roll displacement (Donohew and Griffin, 2004; 2009).

In land-based vehicles, low frequency translational accelerations occur predominantly in the horizontal plane, whereas accelerations in the vertical plane occur at higher frequencies. Horizontal oscillation is therefore the likely primary cause of motion sickness in land transport. In high-curve-speed railway vehicles (HCSRVs), peak horizontal accelerations occur between 0.5 and 1.0 Hz, whereas in traditional railway vehicles accelerations peaked above 1 Hz (Ueno et

al., 1986). In a survey of 119 passengers and 100 staff conducted on the same vehicles, a greater incidence of motion sickness was identified on the HCSRVs than on traditional vehicles, showing support for a frequency-dependence of motion sickness.

2.5.2. Magnitude

The 'magnitude' of a motion may refer to the displacement, velocity, acceleration or jerk. The incidence and severity of motion sickness is highly dependent on the motion magnitude. With 0.37 Hz vertical oscillation, sickness increased with increasing acceleration magnitude (Alexander *et al.*, 1945; O'Hanlon and McCauley, 1973; McCauley *et al.*, 1976). Between 0.22 and 0.53 Hz, the increase in sickness did not increase linearly between ±1.96 ms⁻² and ±6.38 ms⁻²; instead the intermediate magnitudes were most provocative (Alexander *et al.*, 1945, as cited by Donohew, 2006). It is possible that the magnitude-dependence of motion sickness plateaus after a certain level of acceleration.

The incidence of motion sickness increased with acceleration between 0.28 and 1.11 ms⁻² r.m.s. during exposure to horizontal (i.e. fore-and-aft and lateral) oscillation at 0.15 Hz (Griffin and Mills, 2002b). The magnitude-dependence of motion sickness was similar for fore-and-aft and lateral oscillation. Sickness also increased with acceleration magnitude between 0.22 and 0.89 ms⁻² r.m.s. with fore-and-aft oscillation at 0.2 Hz (Joseph, 2008).

With roll and pitch oscillation, the incidence of sickness increased with displacement magnitude between ±1.83° and ±7.32°, with no differences reported between the two directions (Joseph and Griffin, 2008a).

Magnitude-dependence was also tested with 50% roll-compensated lateral oscillation at 0.1 Hz (Joseph and Griffin, 2008b). Subjects were exposed to 60 minutes of motion consisting of four different 15-minute periods of high (H) magnitude oscillation (±1.26 ms⁻², ±3.66°) and low (L) magnitude oscillation (±0.63 ms⁻², ±1.83°). Greater sickness was reported with four periods of high magnitude oscillation (i.e. HHHH) than with four periods of low magnitude oscillation (i.e. LLLL). No differences were found between intermediate conditions with equal motion sickness dose values (i.e. LHHL and HLHL).

The motion sickness dose value (MSDV) (Equation 2.14), proposed by Lawther and Griffin (1987) and defined in British and International standards (BS 6841, 1987; ISO 2631-1, 1997), can be used to predict the effects of acceleration magnitude, frequency and duration on motion sickness caused by vertical oscillation. Since the MSDV predicts the frequency-dependence using W_f it is principally advised that the function is only used to predict sickness caused by vertical oscillation (BS 6841, 1987; ISO 2631-1, 1997).

2.5.3. Multi-axis motion

Exposure to motion in multiple axes of translation and rotation is more provocative of motion sickness than exposure to motion in only one axis. Pitch motion at 0.08 Hz between ± 0.098 and ± 0.216 ms⁻² and roll motion at 0.05 to 0.07 Hz between ± 0.029 and ± 0.137 ms⁻² combined with vertical motion at 0.1 Hz between ± 0.196 and ± 0.343 ms⁻² was highly provocative of sickness, whilst the same pitch, roll and vertical motions presented in isolation caused low levels of sickness (Wertheim *et al.*, 1998).

With roll-compensated lateral oscillations, the development of motion sickness is highly dependent on the percentage compensation (i.e. the degree to which the acceleration due to roll reduces the Earth-lateral acceleration). In a survey of 80 passengers on board a Swedish tilting train, there was approximately 4 times less motion sickness with 55% roll-compensation than with 70% compensation (Förstberg *et al.*, 1998) and greatest sickness was reported with 100% roll-compensated lateral motions (Förstberg, 2000). Tilting train sickness has also been correlated with tilt-compensation, tilt velocity (Donohew and Griffin, 2007) and lateral acceleration between 0.25 and 0.315 Hz (Suzuki *et al.*, 2005). Likewise in the laboratory, motion sickness was greatest with 75% and 100% roll-compensated lateral oscillation at 0.1 and 0.2 Hz (Donohew and Griffin, 2010). At 0.2 Hz, 50% roll-compensation was less provocative of sickness than 0% roll-compensation, indicating that some reduction of Earth-lateral acceleration is beneficial for comfort (Donohew and Griffin, 2010).

The degree of roll-compensation of lateral acceleration may be achieved by varying the roll displacement magnitude or the phase difference between the two components. With 0.2 Hz rollcompensated lateral oscillation (±1.26 ms⁻² r.m.s. and ±7.32°), motion sickness varied with the phase difference between the lateral and the roll (Joseph and Griffin, 2007). Four different phase relationships were tested (with associated percentage compensation): 1) 0° delay (100%); 2) 14.5° delay (75%); 3) 29° delay (50%); and 4) 29° advance (50%). (A phase delay indicates the roll motion occurred after the lateral motion, and a phase advances indicates the reverse). Greatest sickness occurred with a phase delay of 0° (100% compensation), showing support for previous research into the effects of percentage compensation on motion sickness (e.g. Förstberg, 2000; Donohew, 2006), and sickness decreased with increasing phase delay between 14.5° and 29°. Interestingly, a 29° phase advance was less provocative of motion sickness than a 29° phase delay, despite offering the same 50% compensation. A pre-existing phase discrepancy between sensory transduction in the otoliths and semi-circular canals suggested by Golding et al. (2001) and later by Joseph (2008) may explain this result. If the effects of an existing phase discrepancy are attenuated by a 29° phase advance (where the roll motion precedes the lateral motion) then this should result in a reduction of sensory conflict and

therefore less sickness. It is suggested that any phase discrepancy between the semi-circular canals and the otoliths is fixed and peaks at 0.2 Hz; therefore the phase-dependence of motion sickness should differ depending on the frequency of oscillation, if the theory is correct (Joseph, 2008).

The phase difference between the lateral and roll components have also been investigated in the field. Cohen *et al.* (2011) found greater tilting train sickness with reactive tilt modes (where the tilt is determined by accelerometers positioned on the train carriage) than with predictive tilt modes (where the tilt is determined according to a database of track telemetry and the geographical position of the train). The roll acceleration and deceleration at the start and at the end of the curves was greater during the predictive mode than the reactive mode, and the tilt of the carriage was more closely synchronised with the tilt of the GIF in the predictive mode. It was concluded that these dynamic differences must account for the observed differences in sickness; i.e. "if the roll occurred close to the onset of lateral acceleration... there was little of no motion sickness" [Cohen *et al.*, 2011, p. 3772]. Contrary to the authors' claims, the findings by Joseph and Griffin (2007) do not support this conclusion; sickness was greatest with a 0° phase discrepancy between the lateral and roll components and decreased with increasing phase delay.

The degree of motion sickness was not different with a 0° and a 180° phase difference between 0.1 Hz fore-and-aft oscillation at ±1.26 ms⁻² and 0.1 Hz pitch oscillation at ±3.69° (Joseph, 2008). The resultant Earth-horizontal acceleration at the position of roll-compensation was 0.63 ms⁻² with a 0° phase difference and 1.89 ms⁻² with a 180° phase difference, suggesting that the difference in vestibular stimulation between these two conditions was not sufficient for producing a difference in sickness.

The sensory rearrangement theory states that motion sickness arises from inter- or intrasensory conflict in the visual and/or vestibular systems (Reason and Brand, 1975), which may explain the previous reports of motion sickness caused by roll-compensated lateral oscillation. Pure roll motion of the head stimulates both the semi-circular canals and the otoliths (due to the gravitational force associated with an inclined plane – see Section 2.2.2). Integration of the neural signals from the otoliths and from the semi-circular canals allow for the correct interpretation of this motion as 'head rotation' (Park *et al.*, 2006). However, roll-compensated lateral motion will stimulate the semi-circular canals without the normally expected stimulation of the otoliths (because the gravitational component of the roll will 'compensate' for the lateral acceleration – see Section 2.2.4). With fully roll-compensated lateral oscillation, there can therefore be two conflicting interpretations of the motion based either on the response from the semi-circular canals (i.e. roll motion) or the (lack of) response from the otoliths (i.e. no roll). With

lower levels of roll-compensation (e.g. 50%) there will be some otolith stimulation, but at a lower magnitude than normally expected with a head rotation – consistent with a reduction in motion sickness (e.g. Donohew and Griffin, 2010). Without roll-compensation, lateral acceleration stimulates the otolith organs in the absence of any accompanying stimulation of the semi-circular canals – consistent with high levels of motion sickness (e.g. Donohew and Griffin, 2004).

Previous work investigating the motion sickness caused by roll-compensated lateral oscillation has only addressed the case where the position of full roll-compensation is located at the seat surface. Because rotational motion causes translational acceleration away from the centre-ofrotation (see Section 2.2.3), fully roll-compensated lateral acceleration with the position of roll compensation at the seat surface will not fully roll-compensate for lateral acceleration at the head (i.e. where the vestibular organs are located). Full roll-compensation of lateral acceleration at approximate head height will result in even less stimulation of the otoliths than when the position of full roll-compensation is at the seat surface (because the gravitational component of the roll will truly offset the lateral acceleration at the head). On the basis of the sensory rearrangement theory, this condition would therefore result in greater sensory conflict, and greater sickness. Validation of this theory would provide further support for the sensory rearrangement theory of motion sickness. In a tilting train, the position of full roll-compensation will be dependent on the magnitude of Earth-lateral motion, the magnitude of roll motion, and the location of the mechanical pivot point about which the carbody rotates. Since the location of the pivot point differs between tilting railway vehicles (see Section 2.2.5), knowledge of its influence on motion sickness is of interest to passengers and vehicle manufacturers alike.

2.5.4. Seating and posture

Seating configuration and sitting posture inevitably varies between passengers and between vehicles. The provocation of motion sickness during exposure to low frequency oscillation is highly dependent on posture. Linear oscillation through the head-body z-axis at 0.3 Hz (±1.8 ms⁻² r.m.s), resulted in less sickness when subjects were positioned in a supine posture than when they were seated upright (Golding and Kerguelen, 1992). It is suggested that "the decreased necessity for postural control in the supine as opposed to the upright seated posture may be the critical factor" for motion sickness (Golding and Kerguelen, 1992, p. 496).

When seated upright, 0.35 Hz Earth-horizontal oscillation at ±3.6 ms⁻² caused greater sickness than the same motion in the Earth-vertical direction (Golding *et al.*, 1995). With Earth-vertical motion through the head-body x-axis, subjects lying supine reported less sickness than seated subjects, however differences were not statistically significant. From this work it can be

concluded that: 1) linear oscillation through the head-body x-axis is more nauseogenic than linear oscillation through the head-body z-axis (Golding and Kerguelen, 1992); and 2) sitting upright results in greater motion sickness than lying supine postures (Golding *et al.*, 1995) (see Figure 2.23).

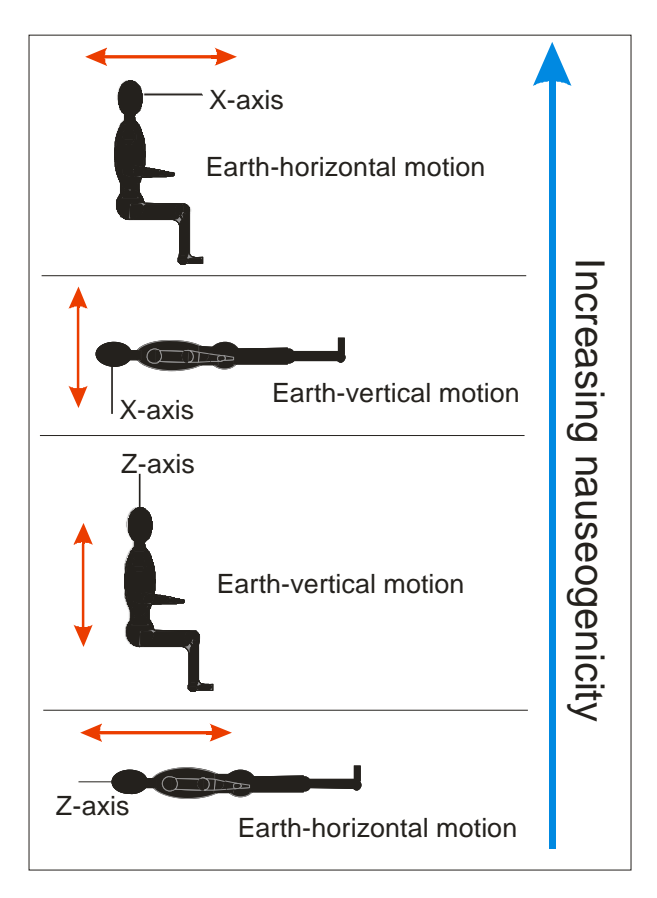


Figure 2.23 Comparison of the nauseogenicity of Earth-horizontal and Earth-vertical oscillation with supine and seated posture (adapted from Golding *et al.*, 1995)

The configuration of the seat may also affect the level of motion sickness. With 0.25 Hz fore-and-aft and lateral oscillation at ±0.7 ms⁻², sitting on a low backrest chair resulted in a greater incidence of sickness than sitting on a high backrest chair (Mills and Griffin, 2000). The reduction in head and upper body movement when seated on a high backrest chair may have reduced the stimulation of the vestibular organs therefore leading to less sickness. Contrary to these findings, the presence or absence of a backrest was not found to affect motion sickness caused by 0.2 Hz fore-and-aft oscillation (Joseph, 2008), suggesting the effect of backrest may be mediated by other factors.

2.5.5. Inter-subject variability

The variability of motion sickness susceptibility in passengers has been investigated in various forms of transport (e.g. Lawther and Griffin, 1988; Turner and Griffin, 1999a; 1999b; Turner et al., 2000; Bos et al., 2007). The findings of these studies are summarised in Table 2.10.

Table 2.10 Results of field studies investigating effect of inter-subject variables on motion sickness.

		•		Inter-subje	ct variables	
Author	Transport type	No. of subjects	Age	Gender	Experience	Other
Lawther and Griffin (1988)	Ship	20,029	Decreasing sickness with increasing age	Females more susceptible than males	-	Vomiting incidence related to anti-sickness tablets and alcohol consumption
Bos <i>et al.</i> (2007)	Ship	3,121	Decreasing sickness with increasing age above 15, increase in sickness from childhood to adolescence	Females more susceptible than males	Greater susceptibility in those with previous history of sickness	-
Turner and Griffin (1999a ; 1999b)	Road coach	3256	Decreasing sickness with age over 15	Females more susceptible than males	Greater susceptibility in those with previous history of sickness	Lower sickness with a good view of road ahead, lower sickness in those who travel frequently
Turner <i>et al.</i> (2000)	Airplane	923	Decreasing sickness with increasing age	Females more susceptible than males	Greater susceptibility in those with previous history of sickness	Sickness greater in those who took anti-motion sickness tablets

There is consistent evidence of a greater susceptibility to motion sickness in females than males and a reduction in susceptibility with increasing age above about 15 years old. Below 15, there is a tendency for sickness susceptibility to increase rapidly from childhood. Passengers with a previous history of motion sickness tend to be more susceptible to subsequent bouts of sickness, suggesting little habituation. There is also some evidence for greater sickness in those who take anti-motion sickness tablets. It is unlikely that anti-sickness drugs contribute to sickness, but rather those passengers who are most likely to suffer from sickness take the drugs in an attempt to relieve their symptoms.

2.5.6. Vision

It is commonly believed that the symptoms of motion sickness can be alleviated by staring at the horizon. An explanation for the apparent beneficial effects of this behaviour is rooted in sensory rearrangement theory, which states that one cause of motion sickness is a conflict between visual and vestibular sensory information (Reason and Brand, 1975). The visual-dependency of motion sickness has since been quantified in laboratory research.

Motion sickness caused by roll and pitch oscillation was examined in three different visual conditions in a tilting room; 1) covered windows – no visual reference of the external environment; 2) uncovered windows – partial view of the external environment; and, 3) covered windows with an artificial horizon projected onto the wall (Rolnick and Bles, 1989). Greatest sickness was reported with covered windows and no visual reference of the external environment, suggesting that either a partial external view or an artificial horizon alleviated the onset of motion sickness. The findings have practical implications for reducing seasickness on naval vessels where sailors are required to work below deck.

The severity of sickness caused by 0.3 Hz linear oscillation at ±1.8 ms⁻² increased when subjects were required to perform a visual search task compared to when their eyes were closed (Golding and Kerguelen, 1992). In line with the sensory rearrangement theory, visual input during the search task would have been incongruous with the concurrent vestibular input, therefore leading to increased conflict and a greater incidence of sickness (Reason and Brand, 1975).

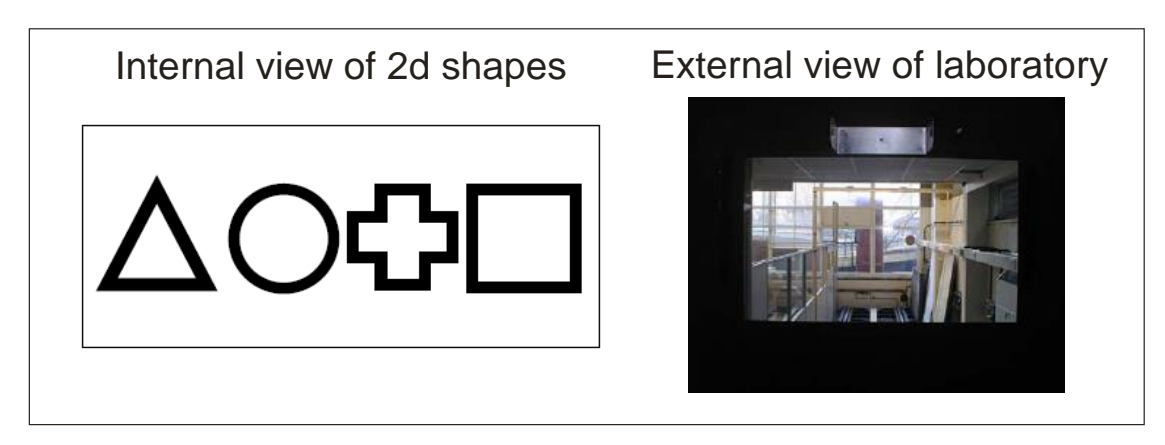


Figure 2.24 Examples of visual stimuli used in motion sickness experiment reported by Butler and Griffin (2006), adapted from Butler (2008).

Contrary to these findings, there was no visual-dependence of motion sickness caused by 0.25 Hz fore-and-aft and lateral oscillation at 0.7 ms⁻² r.m.s. (Mills and Griffin, 2000). However, subjects in this experiment did not have access to an external view; therefore even with the

eyes open there may not have been enough congruent visual information available to reduce the sensory conflict. But, with 0.1 Hz fore-and-aft oscillation at 0.89 ms⁻² r.m.s no differences in sickness were identified between six visual conditions (see Figure 2.24): 1) internal view of 2D shapes; 2) external view of 2D shapes; 3) external view of six horizontal lines; 4) 3D external view; 5) no view; and, 6) internal collimated view of 2D shapes (Butler and Griffin, 2006, see Figure 2.24). In contrast to the sensory rearrangement theory, this finding suggests that conflicting signals between the visual and vestibular sensory systems are not the primary cause of motion sickness induced by 0.1 Hz fore-and-aft oscillation.

However, with 0.1 Hz combined fore-and-aft and pitch oscillation (0.89 ms⁻² r.m.s., ±3.69°), motion sickness was greater with an internal view of shapes than with an external view of the laboratory or with no view at all (Butler, 2008). Coupled with the result reported by Butler and Griffin (2006), this finding suggests that the alleviating effect of an external view may only occur when the provocative motion involves both translation and rotation.

Unlike in conventional trains, the inward tilt of a tilting train traversing a curve means that passengers with an external view observe the external landscape tilting upwards (if looking inwards from the curve) or downwards (if looking outwards from the curve) whilst remaining approximately aligned with the GIF (Neimer *et al.*, 2001). On an actively-tilted train exhibiting 60% compensation, the level of sickness was greater with an external view of the landscape than when the external view was covered; suggesting sickness arose from a visual-vestibular conflict (Neimer *et al.*, 2001; see section 2.4.3).

2.5.7. Head movements

Voluntary and involuntary movements of the head during exposure to translational and rotational oscillation may attenuate or accentuate provocative stimulation of the vestibular organs. During continuous yaw rotation, 30° forward pitch movements of the head lead to greater sickness than the same magnitude of backward pitch movements (Woodman and Griffin, 1997). As well as altering the stimulation of the otoliths and/or the semi-circular canals, head movements may activate appropriate proprioceptive sensory systems which serve to reduce the onset of motion sickness.

Subjects who actively aligned their head with the gravito-inertial force (GIF) when exposed to 0.2 Hz fore-and-aft motion (±3.1 ms⁻²), reported less motion sickness than subjects who misaligned their head with the GIF (Golding *et al.*, 2003). The findings are synonymous with the observation that drivers experience less sickness than passengers, as they are more easily able to adjust their body and head position according to the magnitude of vehicle motion.

Interestingly, passive alignment of the head with the GIF using a mechanical seat-tilting system

caused greater sickness than passive misalignment of the head with the GIF. Here, the findings are synonymous with a greater incidence of sickness on tilting trains than non-tilting trains.

Sitting with a backrest lowers the displacement of the head relative to the seat during 0.2 Hz fore-and-aft oscillation, but head displacement was not found to be associated with the prevalence of sickness, suggesting "fore-and-aft motion of the head relative to the cabin was not a principal determinant of motion sickness" (Joseph, 2008, p. 142). It appears that whether the head and body is actively or passively moved during motion exposure directly affects the likelihood of motion sickness. Possibly, the addition of proprioceptor signals to the sensory system during voluntary motor control may help to reduce the nauseogenicity of certain motion stimuli.

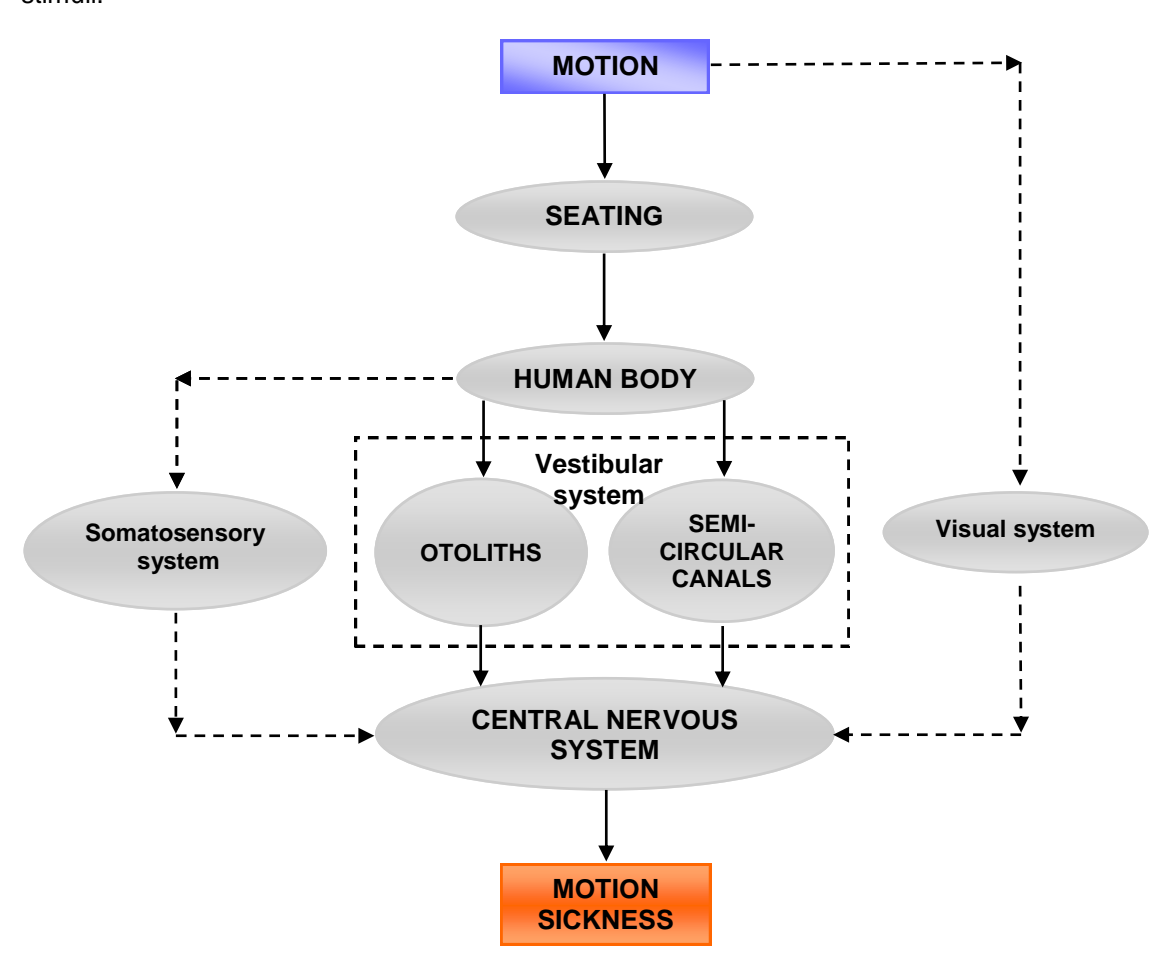


Figure 2.25 Conceptual model of motion sickness.

2.6. Model of motion sickness

It is clear from the literature discussed in Section 2.4 and 2.5 that motion sickness is dependent on the motion characteristics, the seating configuration and subsequent sitting posture, the transmission of motion through the body to the organs of balance, and the interpretation of vestibular, visual and somatosensory nerve impulses. From this understanding it is possible to construct a conceptual model of motion sickness caused by low frequency motion (see Figure 2.25).

2.7. Investigation of vibration discomfort

2.7.1. Definitions

The psychology of 'comfort' is complex. Comfort may be "a reaction of a person to either an environment [physical conditions] or situation [social conditions]" (Richards, 1980, p.16). It is a bipolar concept, with positive attributes at one end of the scale, i.e. subjective well-being, and negative attributes at the other, i.e. subjective distress. "Comfort [may be] associated with feelings of relaxation and well-being, whereas discomfort seems to be associated with biomechanical factors [such as] joint angles, muscle contractions and pressure distribution" (Zhang, 1996, as cited by Schust *et al.*, 2010, p. 735). Branton (1972) argues comfort may only be defined by the absence of *dis*comfort, since discomfort, but not comfort, can be quantified (as cited by Thuong, 2011). Nevertheless, many authors have attempted to measure both comfort and discomfort responses (e.g. Kyung *et al.*, 2008; Kyung and Nussbaum, 2008).

'Travelling comfort' has been defined as the overall comfort during an entire journey, and may be split into three categories: (i) 'riding comfort', experienced within the vehicle itself; (ii) 'local comfort', experienced at service stations, waiting rooms, etc., and; (iii) 'organisational comfort' due to the quality and reliability of the service (Mayr, 1959, cited in Oborne, 1978b, p. 45). Under this definition, the focus of this discussion falls under the definition of 'riding comfort', i.e. the comfort (or discomfort) resulting from experiences within a transport vehicle. More specifically, this chapter examines the impact of the *vibration environment* within transport vehicles, which may elicit positive responses, indicating comfort, or negative responses, indicating discomfort (Griffin, 1990). The 'vibration discomfort', therefore, may be defined as the extent to which individuals associate negative attributes to a given vibration stimulus.

2.7.2. Measurement and evaluation

The subjective nature of comfort and discomfort implies that they must be measured by asking people (Richards, 1990). Studying *psychological* responses to *physical* stimuli is known as

psycho-physics. Psychophysical methods enable the psychological perception of physical stimuli to be quantified. In the simplest form, this may involve placing someone in a given vibration environment and asking whether they or not they are comfortable. More usefully, other formal methods such as rating scales, magnitude production or magnitude estimation may be used to obtain more complex and more detailed quantitative information than simple binary responses (Stevens, 1975; Richards, 1990).

When studying vibration discomfort, it is useful to generate equivalent comfort contours which express changes in the magnitude of discomfort associated with changes in the magnitude of vibration (Griffin, 1990). An equivalent comfort contour may cover any range of frequencies, is defined for specific criteria (such as direction, duration, seating configuration, or posture) and represents a specific subjective magnitude (i.e. level of discomfort). The methods required to produce equivalent comfort contours are discussed below.

2.7.2.1. Rating scales

"The rating scale is a method of subjective assessment which is used quite extensively in both psychological and ergonomics investigation to provide the researcher with quantitative judgements of stimulus quantities" (Oborne, 1976, p. 201). This method may take many forms: such as a linear scale – where a straight line of fixed length is used by subjects to indicate where on a given dimension a certain stimulus falls, or; a category scale – where subjects choose from pre-defined semantic meanings to indicate the stimulus sensation. In the case of vibration research, rating scales allow subjects to assign semantic meanings to vibration stimuli in order to describe their level of vibration discomfort (e.g. slightly uncomfortable, uncomfortable, extremely uncomfortable and so on).

Whilst the linear scale cannot give quantitative meaning to ratings (other than those at the extremes of the scale), the category scale is subject to bias from alternative interpretation of the 'categories' and only provides a crude assessment of sensation (Oborne, 1976). Both scales also suffer from being inherently ordinal, restricting the ability to accurately compare and contrast the meaning of individual ratings.

2.7.2.2. Magnitude production

The method of magnitude production typically involves presenting subjects with pairs of vibration stimuli. To quantify discomfort, subjects are require to physically adjust the magnitude of a 'test' stimulus until it causes a specific level of discomfort relative to that caused by a 'reference' stimulus. For example, subjects may be asked to adjust a test stimulus relative to the reference stimulus until it caused the same discomfort, half as much discomfort, twice as much

as discomfort, and so on. The reference stimulus may be fixed over a whole experiment (method of constant stimuli) or it may be varied (method of 'moving reference'). Magnitude production allows for equivalent comfort contours to be produced simply and directly, without the need for further data processing (Thuong, 2011). However, since subjects will inherently try to avoid exposure to uncomfortable stimuli, it has been suggested that the method may lead to a bias toward low magnitude motions (Griffin, 1990).

Alternatively, subjects may be required to adjust the magnitude of vibration stimuli to match a specific semantic meaning (e.g. slightly uncomfortable, uncomfortable, etc.). This method is subject to the same limitations as conventional linear rating scales (see Section 2.7.2.1).

2.7.2.3. Magnitude estimation

The method of magnitude estimation requires subjects to rate the subjective magnitude of the sensation produced by a physical stimulus, by assigning numerical values to that stimulus (Stevens, 1975). Typically, this may involve comparing the discomfort caused by a series of 'test' vibration stimuli to that caused by a 'reference' vibration stimulus. The reference stimulus may be assigned a constant numerical value, usually 100, and magnitude estimates are given proportional to this value. For example, if the test vibration causes twice as much discomfort as the reference vibration then a value of 200 would be given, or if it causes half as much discomfort then a value of 50, and so on. As with magnitude production, the reference stimulus may be fixed or it may be varied over the course of an experiment.

Alternatively, magnitude estimation may be used without a reference. In this case subjects are required to assign a numerical value to stimuli using an absolute judgement, but whilst still retaining proportionality between judgements (i.e. 100 indicates half as much discomfort as 200). Some authors argue in favour of magnitude estimation without reference instead of with reference (e.g. Green and Luce, 1974; Stevens, 1975; Zwislocki and Goodman, 1980), implying that absolute methods allow subjects to make 'free' and 'unconstrained' perceptual judgements. Other authors suggest that absolute methods elicit greater response variability which lowers statistical power (Mellers, 1983).

Producing equivalent comfort contours from magnitude estimates is less straight-forward than using the method of magnitude production and require additional data processing (Thuong, 2011). Typically, Stevens' power law (Stevens, 1975) is used to relate magnitude estimates to physical vibration magnitudes by performing linear regressions (see Section 2.7.2.5).

2.7.2.4. Cross-modality matching

The method of magnitude production and the method of magnitude estimation may also use multi-model matching techniques. With multi-modality (or cross-modality) matching, the subjective sensation associated with one physical stimulus is compared to some other physical quantity. For example, the discomfort caused by vibration may be compared to the loudness of a sound or the length of a line, allowing the rates of growth of the two modalities to be derived simultaneously (Stevens, 1975).

Two stimuli (e.g. vibration and sound) may be presented as simultaneous physical stimuli, and subjects could be required to rate the discomfort caused by a single stimulus only (e.g. vibration). This method can be used to understand the interactive nature of multiple physical quantities on subjective sensation (Griffin, 1990).

2.7.2.5. Stevens' power law

Stevens' power law (Stevens, 1975) suggests the physical magnitudes of stimuli (Φ) are related to the subjective sensation magnitudes (Ψ) as shown in Equation 2.17:

Equation 2.17:
$$\psi = k \varphi^n$$

where the exponent (n) is the rate of growth of sensation (e.g. vibration discomfort) and k is a constant. Logarithmic transformation of this equation (see Equation 2.18) allows the exponent n and the constant k to be determined through a linear regression.

Equation 2.18:
$$\log_{10} \psi = \log_{10} k + n \log_{10} \varphi$$

Using this method with a range of magnitudes at each frequency of interest allows equivalent comfort contours to be constructed across a desired frequency range (Griffin, 1990).

2.7.3. Reliability of subjective methods

2.7.3.1. Rating scales vs. magnitude estimation

The parameters of a rating scale may include the length of the scale and the words (and/or numbers) used to portray semantic meaning to vibration. As stated by Huddleston (1965), "different words mean different things to different people in different contexts" (as cited by Oborne and Clarke, 1975, p.68), therefore the variability in the construction of vibration rating scales may cause undesired variability in subjective responses. To quantify the extent of this bias, Oborne and Clarke (1975) examined vibration discomfort rated by 20 male standing subjects exposed to vertical oscillation between 3 and 30 Hz using 5 types of rating scale, 6 sets of descriptive words (termed 'scale ends') and the method of magnitude estimation. In

general there was high concordance between discomfort ratings across the various psychophysical methods. The pattern of discomfort responses did not differ greatly between rating scale type, or when alternative descriptive terms were employed (e.g. "smooth – rough", "weak – strong", "pleasant – unpleasant", or "comfortable – uncomfortable". Furthermore, whilst the level of equivalent comfort contours constructed using rating scales tended to be greater than those constructed using magnitude estimation, the frequency response profile remained consistent. However, the distribution of ratings given using magnitude estimation was far greater than when using any of the rating scale methods, which allowed for a "tenfold increase in 'scale length'" (Oborne and Clark, 1975, p. 77). This therefore has a distinct advantage over rating scale methods when investigating a set of motion stimuli which are likely to elicit a wide range of discomfort responses.

2.7.3.2. The stability of equivalent comfort contours

If equivalent comfort contours are to be used to determine the true human response to whole-body vibration, then the stability of these methods over time must be assessed. Discomfort ratings were measured twice over a period of 1 to 66 days, using the method of magnitude production with vertical sinusoidal oscillation between 3 and 80 Hz (Oborne, 1978a). Equivalent comfort contours for 20 standing subjects (11 female, 9 male) were similar in shape for the first and second session and 'test-retest' correlation coefficients were above 0.9 for all but one subject. The findings show that high intra-subject reliability can be achieved using equivalent comfort contours generated with intensity matching methods.

2.7.3.3. Range effects

Based on Stevens' power law (Stevens, 1975, see Section 2.7.2.5), subjective sensation magnitudes (i.e. vibration discomfort) are related to physical stimuli (i.e. vibration magnitude) through linear regression. The resulting regression coefficients (and thus the resulting equivalent comfort contours) are dependent on the range of physical magnitudes *and* the range of subjective magnitudes. Ratings of discomfort are affected by the range of vibration stimuli presented (e.g. Suzuki, 1998a, see Table 2.11 and Figure 2.26), so the choice of vibration magnitudes can affect the subsequent shape of equivalent comfort contours. In laboratory research, the choice of vibration stimuli will often be governed by equipment limitations (for example, see Section 3.2), but it will also be important to consider: (1) the range of magnitudes experienced in a given environment, for example a car or train, and; (2) the number of vibration stimuli required for a satisfactory linear regression.

					Peak	lateral	accele	ration (±ms ⁻²)				
	0.35	0.50	0.65	0.80	0.95	1.10	1.25	1.40	1.55	1.70	1.85	2.00	Total
Range 1	4	15	14	8	3	2	1	1					48
Range 2	3	10	12	7	3	3	2	2	2	2	1	1	48
Range 3					4	15	14	8	3	2	1	1	48
Range 4	4	4	4	4	4	4	4	4	4	4	4	4	48

Table 2.11 Distribution of acceleration magnitudes used by Suzuki (1998a).

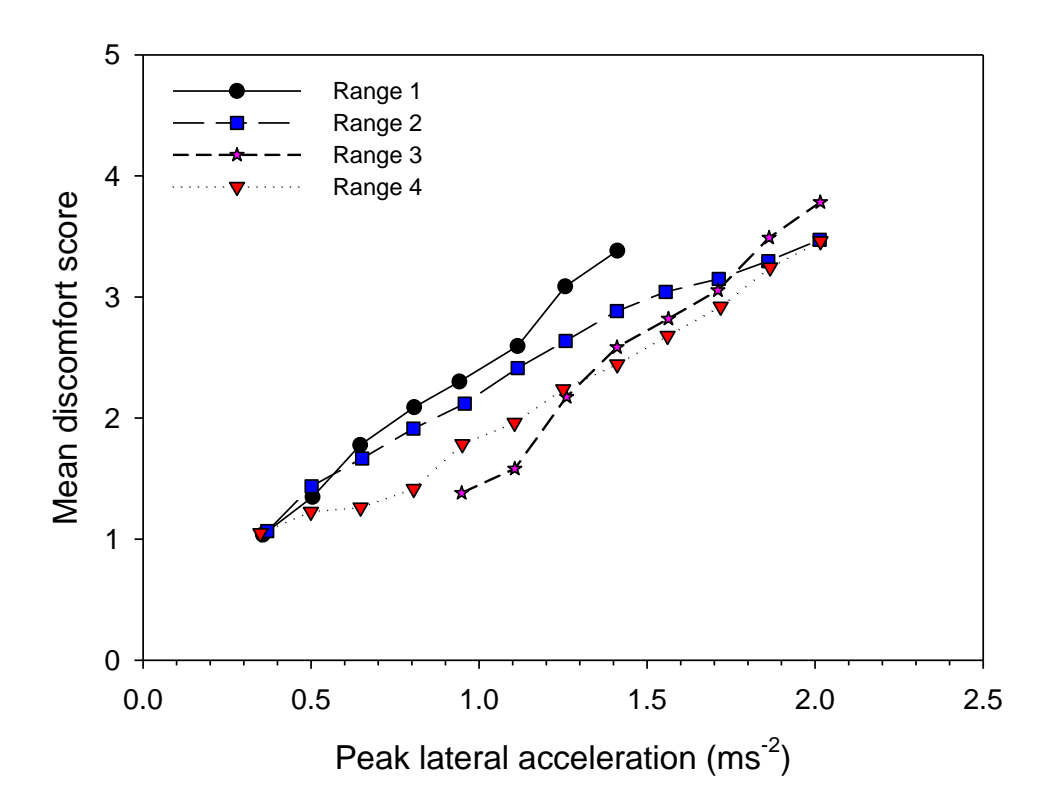


Figure 2.26 Effect of range of acceleration magnitudes on mean discomfort ratings (Suzuki, 1998a). Description of magnitude ranges given in Table 2.11.

2.7.3.4. Order effects

Stevens (1975) raises the issue of order effects, where the order of presentation of stimuli can affect subsequent psychophysical judgements. With vibration discomfort experiments, an order effect may occur because of: a) the order of presentation of reference and test stimuli in magnitude estimation or magnitude production methods, and; b) the order of presentation of test stimuli in relative or absolute judgement methods. There may be a tendency for subjects to 'under adjust' test stimuli presented after a reference in magnitude production (Fairly and Griffin,

1988), or overestimate the discomfort of test stimuli after a reference in magnitude estimation (Griffin and Whitham, 1980). Judgements of comfort may also be lower for the second presentation of motion stimuli, suggesting possible effects of time on subjective sensation (Schust *et al.*, 2010).

Test stimuli presented in ascending magnitude order elicit "strikingly different" judgements than test stimuli presented in descending magnitude order (Stevens, 1975, p. 23). The effect of this bias would be reduced by presenting all test stimuli in a random order. When using magnitude estimation with a reference, the bias reported by Griffin and Whitham (1980) may be reduced by presenting the 'reference-test' sequence twice in succession. However, this will double the total duration of the experiment, so the influence of subject fatigue must be considered.

2.8. Factors influencing vibration discomfort

Vibration discomfort has been the focus of much research for many decades. This section is principally focussed on previous research into vibration discomfort caused by horizontal (fore-and-aft and lateral) oscillation and rotational (roll and pitch) oscillation at low frequencies. Table 2.12 and Table 2.13 provide a summary of the methodology and experimental conditions used in previous laboratory studies investigating vibration discomfort with low frequency translational and rotational motions. The findings and implications of this research are discussed in the following sections.

2.8.1. Frequency

The discomfort caused by horizontal and rotational motion is highly dependent on the frequency of oscillation. Equivalent comfort contours for lateral, fore-and-aft, roll and pitch generated by previous researchers are shown in As shown by Figure 2.28, sensitivity to pitch and roll motion decreases with increasing frequency above 1 Hz with a flat rigid seat pan, with no backrest and a stationary footrest (Parsons and Griffin, 1978; 1982).

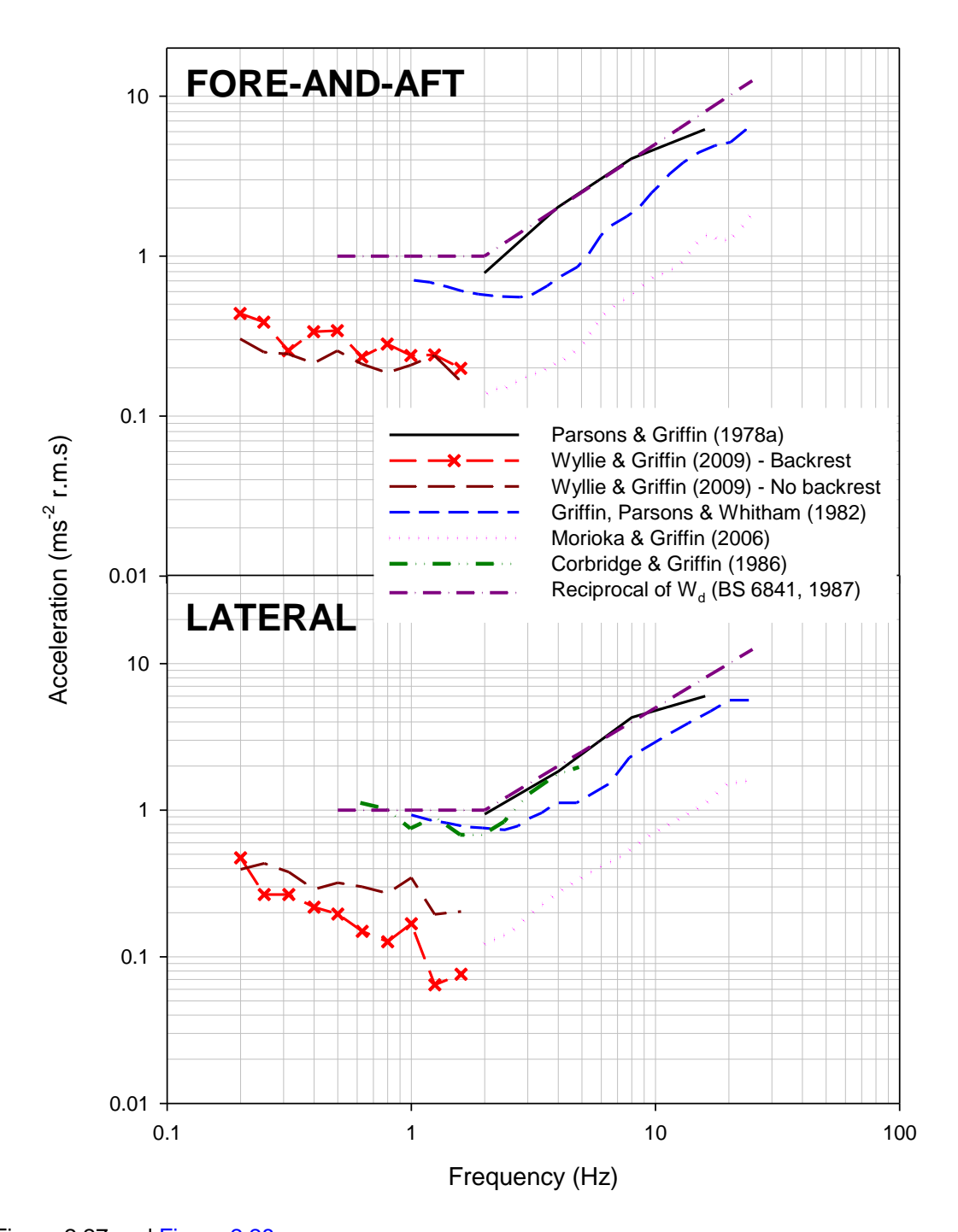


Figure 2.27 and Figure 2.28.

As shown by As shown by Figure 2.28, sensitivity to pitch and roll motion decreases with increasing frequency above 1 Hz with a flat rigid seat pan, with no backrest and a stationary footrest (Parsons and Griffin, 1978; 1982).

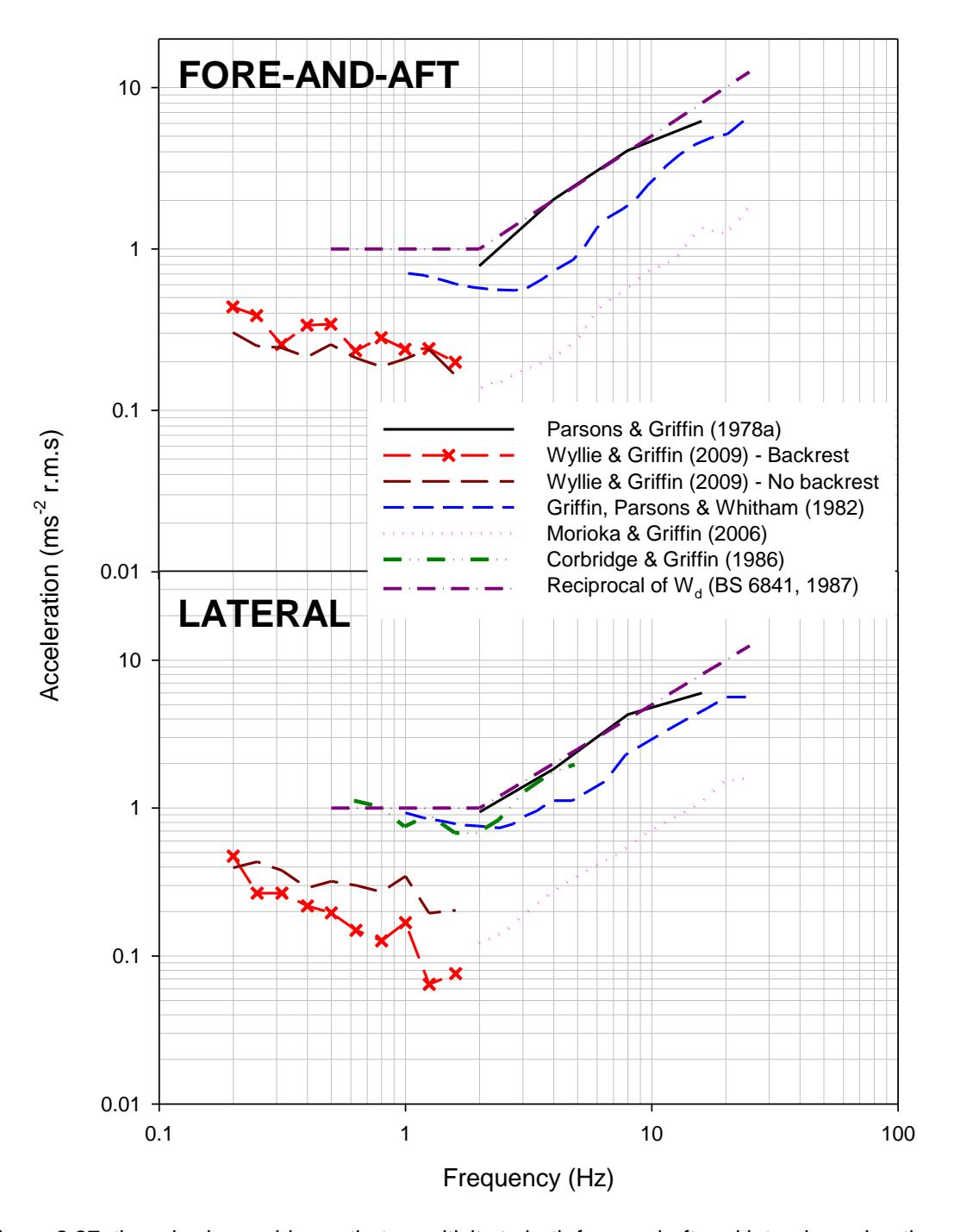


Figure 2.27, there is clear evidence that sensitivity to both fore-and-aft and lateral acceleration decreases with increasing frequency above 2 Hz with a flat rigid seat pan and stationary footrest (Parsons and Griffin, 1978; 1982), a flat rigid seat pan and a 400 mm backrest (Corbridge and Griffin, 1986a), a contoured rigid seat pan and stationary foot- and hand-rests (Morioka and Griffin, 2006a) and a flat rigid seat pan with a shoulder-height backrest and four-point harness (Wyllie and Griffin, 2007; 2009).

The equivalent comfort contours show minimum values between 1 and 2 Hz, indicating greatest sensitivity to fore-and-aft and lateral motion in this frequency range. There is less data available for motions below 1 Hz, but research with a flat rigid seat pan and a 400 mm backrest (Corbridge and Griffin, 1986) and a flat rigid seat pan with and without a shoulder-height backrest and four-point harness (Wyllie and Griffin, 2007; 2009) suggests decreasing sensitivity with decreasing frequency of lateral and fore-and-aft oscillation. There are no obvious differences in the frequency-dependence of the equivalent comfort contours between lateral and fore-and-aft oscillation, and this observation is supported by previous authors (e.g. Miwa, 1967; Parsons and Griffin, 1978a; Griffin, et al., 1982a; Morioka and Griffin, 2006a).

Standardised frequency weighting W_d predicts discomfort proportional to fore-and-aft and lateral acceleration between 0.5 and 1.0 Hz and decreasing sensitivity above this range (BS 6841 1987; ISO 2631-1 1997). Frequency weighting W_d is not intended for use at frequencies less than 0.5 Hz or greater than 80 Hz, but 'realisable' values may be obtained outside this range with high-pass and low-pass filtering at 0.4 and 100 Hz, respectively.

Table 2.12 Summary of laboratory studies investigating vibration discomfort caused by translational and rotational oscillation at low frequencies (part 1).

Author(s)	Frequency (Hz)	Axes	Magnitude	Waveform	Method	Seating/posture	Visual conditions	Subjects
Miwa (1967)	0.5 - 300	х, у	±0.0315 - 1.0 ms ⁻²	sinusoidal	limits	Flat rigid seat, with rigid backrest, 'dangling' feet		10 (all male)
Fothergill and Griffin (1977)	3 - 40	Z	0.35 - 1.4 ms ⁻² r.m.s.	sinusoidal	magnitude production	Flat rigid seat, no backrest, stationary	Eyes open, facing dark wall	10 (all male)
Griffin and Whitham (1977)	3.15	y, z	0.7 - 1.4 ms ⁻² r.m.s.	sinusoidal	magnitude production	Flat rigid seat, no backrest, stationary	Eyes open, facing dark wall	8 (all male)
Parsons and Griffin (1978)	2 - 16	x, y, z, r _x , r _y	•	sinusoidal	magnitude production	Flat rigid seat, no backrest, stationary	Eyes open, facing dark wall	10 (all male)
Griffin and Whitham (1978)	4, 16	Z	0.41 - 2.46 ms ⁻² r.m.s.	sinusoidal	forced-choice (constant	Flat rigid seat, no backrest, stationary	Eyes open, facing dark wall	Eyes open, 112 (56 men, 28 facing dark wall women, 17 boys,
Whitham and Griffin (1978) – part 1	2 - 64	Z	1 ms ⁻² r.m.s.	sinusoidal	Location of discomfort	Flat rigid seat, no backrest, stationary		75 (30 men, 30 women, 11 boys,
Whitham and Griffin (1978) – part 2	2 - 64	x, y	1 ms ⁻² r.m.s.	sinusoidal	Location of discomfort	Flat rigid seat, no backrest, stationary		10 (all male)
Whitham and Griffin (1978) – part 3	2 - 64	Z	0.5, 2 ms ⁻² r.m.s.	sinusoidal	Location of discomfort	Flat rigid seat, no backrest, stationary		10 (all male)
Griffin <i>et al.</i> (1982b)	1 – 63	x, x	0.5, 1.25 ms ⁻² r.m.s.	sinusoidal	magnitude estimation	Flat rigid seat, no backrest, stationary		36 (18 male, 18 female)
Parsons and Griffin (1982) – part 1	1 - 31.5	f_x , f_y , f_z	4.5 - 31.5 rads ⁻² r.m.s.	sinusoidal	magnitude production	Flat rigid seat, no backrest, stationary	Eyes open, restricted view	12 (all male)
Parsons and Griffin (1982) – part 2	1 - 31.5	fx, fy, fz	4.5 - 31.5 rads ⁻² r.m.s.	sinusoidal	magnitude production	Flat rigid seat, no backrest, stationary	Eyes open, restricted view	36 (18 male, 18 female)
Donati <i>et al.</i> (1983)	1 – 20	x, y, z	±1.2, 1.6 ms ⁻²	sinusoidal, narrow-band	intensity matching	Flat rigid seat, no backrest		81 (66 male, 15 female)
Corbridge and Griffin (1986) - part 1	0.5 - 5	Z	0.04 - 2 ms ⁻² r.m.s.	sinusoidal	forced-choice (constant	Flat rigid seat, flat vertical 400 mm		40 (20 male, 20 female)
Corbridge and Griffin (1986) - part 2	0.5 - 4	Z	0.1 - 1 ms ⁻² r.m.s.	narrow-band random	forced-choice (constant	Flat rigid seat, flat vertical 400 mm		10 (all male)
Corbridge and Griffin (1986) - part 3	0.5 - 5	^	0.4 - 3.15 ms ⁻² r.m.s.	sinusoidal	forced-choice (constant	Flat rigid seat, flat vertical 400 mm		20 (all male)

Table 2.13 Summary of laboratory studies investigating vibration discomfort caused by translational and rotational oscillation at low frequencies (part 2).

Author(s)	Frequency (Hz)	Axes	Magnitude	Waveform	Method	Seating/posture	Visual conditions	Subjects
Fairley and Griffin (1988)	2.5 - 10	x, z		sinusoidal	magnitude production	Flat rigid seat, no backrest, stationary footrest	Eyes open, restricted view	16 (male)
Brett and Griffin (1991)	0 - 3.15	У	1.0 ms ⁻² r.m.s.	broad-band random	seat-to-head transmissibility	Flat rigid seat, hard foam backrests (0 to 700 mm	Eyes open, restricted view	16 (all male)
Jang and Griffin (1999)	4	Z	0.25 - 1.6 ms ⁻² r.m.s.	sinusoidal	magnitude estimation	Flat rigid seat, with and without thigh contact. no	-	12 (10 male, 2 female)
Jang and Griffin (2000)	2.5 - 6.3	Z	0.25 - 1.6 ms ⁻² r.m.s.	sinusoidal	magnitude estimation	Flat rigid seat, with and without thigh contact. no	-	12 (10 male, 2 female)
Ebe and Griffin (2000a)	2.5, 5.5	Z	0.25 - 0.5 ms ⁻² r.m.s.	narrow-band random	paired comparison	Foam seat cushions (50 - 120 mm thickness), no backrest	1	12 (all male)
Ebe and Griffin (2000b)	0.8 - 20	Z	0.125 - 2 ms ⁻² r.m.s.	broad-band random	magnitude estimation	Rigid seat pan, foam seat cushions (42.8 - 52.4 kg.m ³), no backrest	-	20 (all male)
Matsumoto and Griffin (2001)	3, 9, 12	Z	±1.0 ms ⁻²	sinusoidal, shocks	paired comparison	Flat rigid seat, no backrest, no footrest	Eyes open, restricted view	20 (10 male, 10 female)
Morioka and Griffin (2006a)	2 - 315	x, y, z	0.02 - 1.25 ms ⁻¹ r.m.s.	sinusoidal	magnitude estimation	Contoured rigid seat, no backrest, stationary footrest. stationary hand	Eyes open	36 (all male)
Wyllie and Griffin (2007)	0.2 - 1.6	y, r _x	0.063 - 0.63 ms ⁻² r.m.s.	sinusoidal	magnitude estimation	Flat rigid seat, with and without flat shoulder-height backrest and harness	Blindfolded, no view	12 (all male)
Hacaambwa and Giacomin (2007)	0.5 - 50.5	×	±0.01 - 0.86 ms ⁻²	broad-band random	magnitude estimation, BORG CR-10 scale	Flat rigid seat, no backrest	-	16 (8 male, 8 female)
Wyllie (2007)	0.2 - 1.6	ľx, fy	0.16 - 0.5 ms ⁻² r.m.s.	sinusoidal	magnitude estimation	Flat rigid seat, no backrest, 'head still' and 'move-with'		12 (all male)
Wyllie and Griffin (2009)	0.2 - 1.6	x, r _y	0.05 - 0.63 ms ⁻² r.m.s.	sinusoidal	magnitude estimation	Flat rigid seat, with and without flat shoulder-height backrest and harness	Blindfolded, no view	12 (all male)

As shown by Figure 2.28, sensitivity to pitch and roll motion decreases with increasing frequency above 1 Hz with a flat rigid seat pan, with no backrest and a stationary footrest (Parsons and Griffin, 1978; 1982).

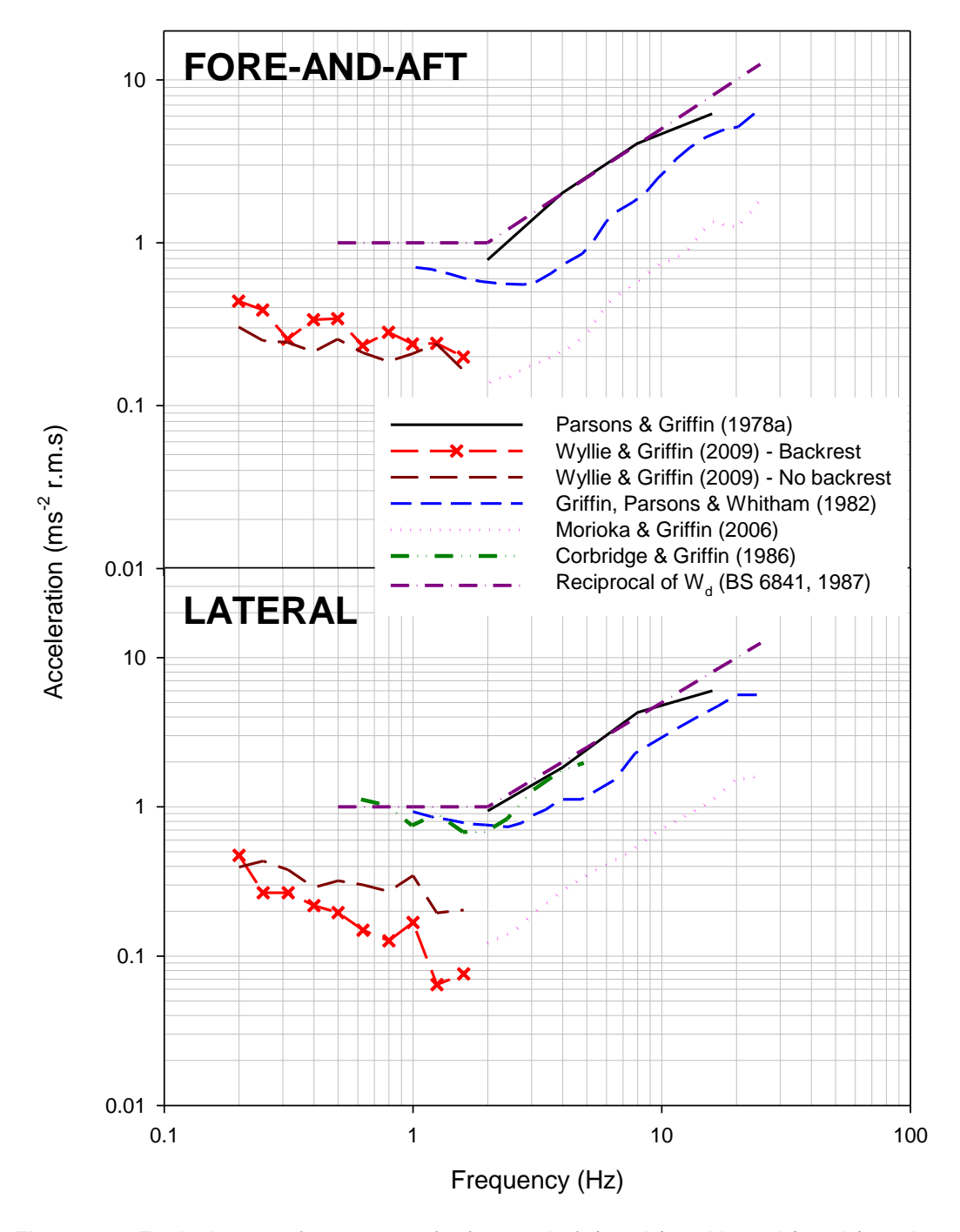


Figure 2.27 Equivalent comfort contours for fore-and-aft (x-axis) and lateral (y-axis) motion.

Sensitivity to roll oscillation with no backrest and pitch oscillation with and without backrest and four-point harness increases with decreasing frequency below 1 Hz (Wyllie and Griffin, 2007; 2009). But sensitivity to roll oscillation on a rigid seat with backrest and four-point harness is proportional to roll acceleration between 0.5 and 1.0 Hz, and then increases with decreasing frequency between 0.2 and 0.5 Hz (Wyllie and Griffin, 2007).

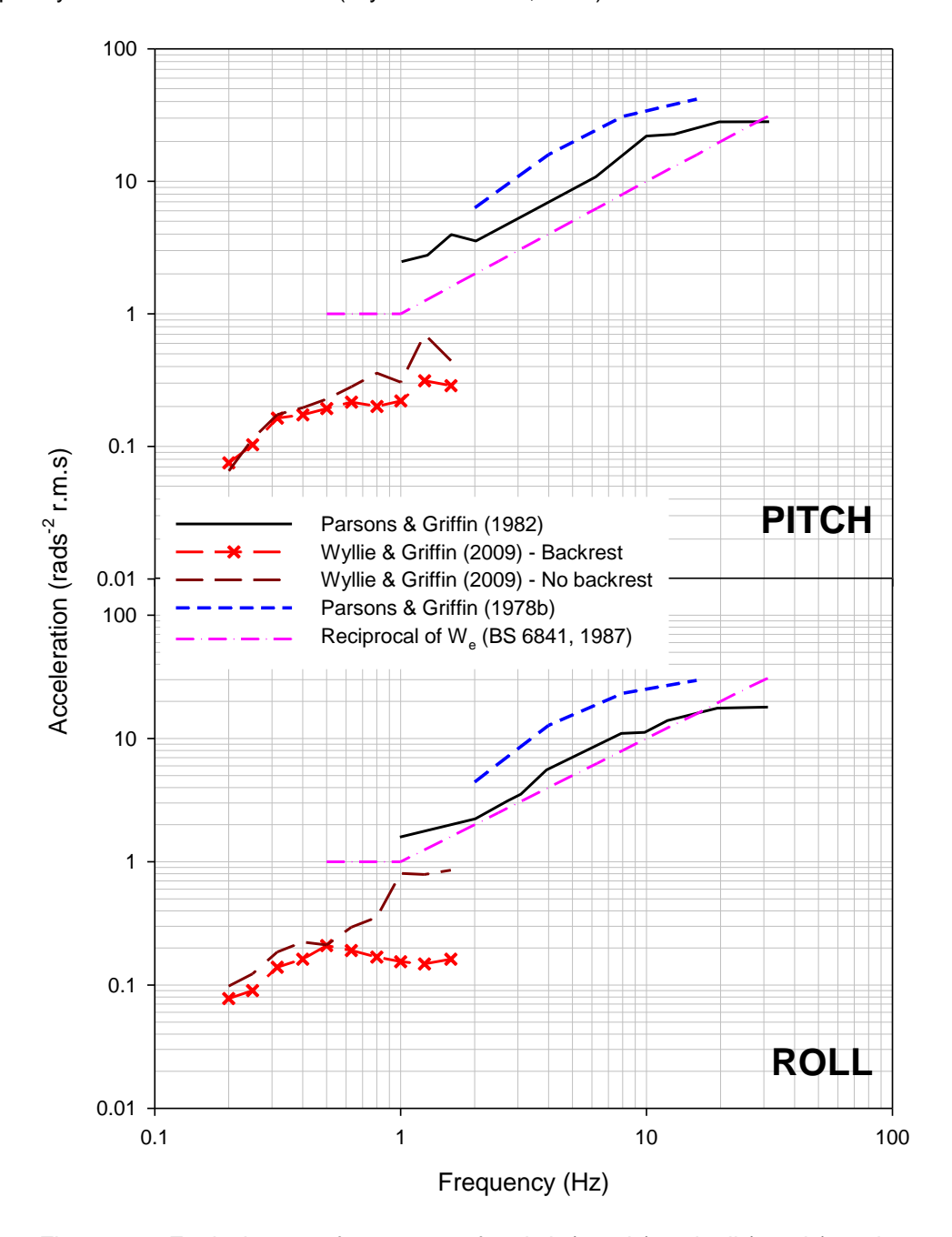


Figure 2.28 Equivalent comfort contours for pitch (r_y -axis) and roll (r_x -axis) motion.

Standardised frequency weighting W_e predicts decreasing sensitivity to roll and pitch motion with increasing frequency above 1 Hz, and sensitivity proportional to rotational acceleration between 0.5 and 1.0Hz (BS 6841 1987; ISO 2631-1 1997). This weighting may therefore only be appropriate for predicting discomfort from roll oscillation between 0.5 and 1.0 Hz when there is a backrest and four-point harness (see Figure 2.28, Wyllie and Griffin, 2007).

As with W_d , this weighting is intended for use between 0.5 to 80 Hz, but realisable values may be obtained outside this range with band-pass filtering at 0.4 and 100 Hz. However, halving the frequency (e.g. from 1.0 to 0.5 Hz) with constant rotational acceleration will increase the rotational displacement by a factor of 4. With large rotational displacements below 0.5 Hz, the translational acceleration due to gravity (e.g. in the plane of the seat) may give a better prediction of discomfort (Wyllie and Griffin, 2007; 2009), therefore the application of realisable values from frequency weighting W_d may be more appropriate in this range.

Oborne and Boarer (1982) showed that the concepts (i.e. 'parts of body shaken', 'attributes of vibration', etc.) used by 100 standing subjects to rate discomfort from vertical vibration changed with frequency between 2.4 and 40 Hz. Whitham and Griffin (1978) showed that the localisation of discomfort in seated subjects is dependent on oscillation frequency between 2 and 64 Hz. It is likely that the frequency-dependence of discomfort is due to the human biodynamic response and the transmission of motion to different parts of the body.

Since the equivalent comfort contours were constructed using horizontal and rotational oscillation at various magnitudes, the level of the contours should not be directly compared. The effect of magnitude on equivalent comfort contours is discussed in Section 2.8.2.

2.8.2. Magnitude

The 'magnitude' of a motion may refer to the displacement, velocity, acceleration or jerk. As well as being frequency-dependent, the discomfort caused by horizontal and rotational motion is dependent on the magnitude of oscillation.

The relationship between subjective sensation (e.g. vibration discomfort) and physical stimuli (e.g. vibration magnitude) is represented by Stevens' power law (Stevens, 1975; see Section 2.7.2.5). Despite the assumptions of the law, the value of the exponent, n, has been shown to vary significantly with the frequency of horizontal and rotational oscillation in a variety of seating arrangements (e.g. Miwa, 1968; Howarth and Griffin, 1988; Wyllie and Griffin, 2007; 2009). The changes in subjective magnitude associated with changes in physical magnitude are dependent on the exponent (i.e. rate of growth of discomfort). Therefore if the exponent is dependent on

vibration frequency, then it follows that the shape of equivalent comfort contours is dependent on vibration magnitude.

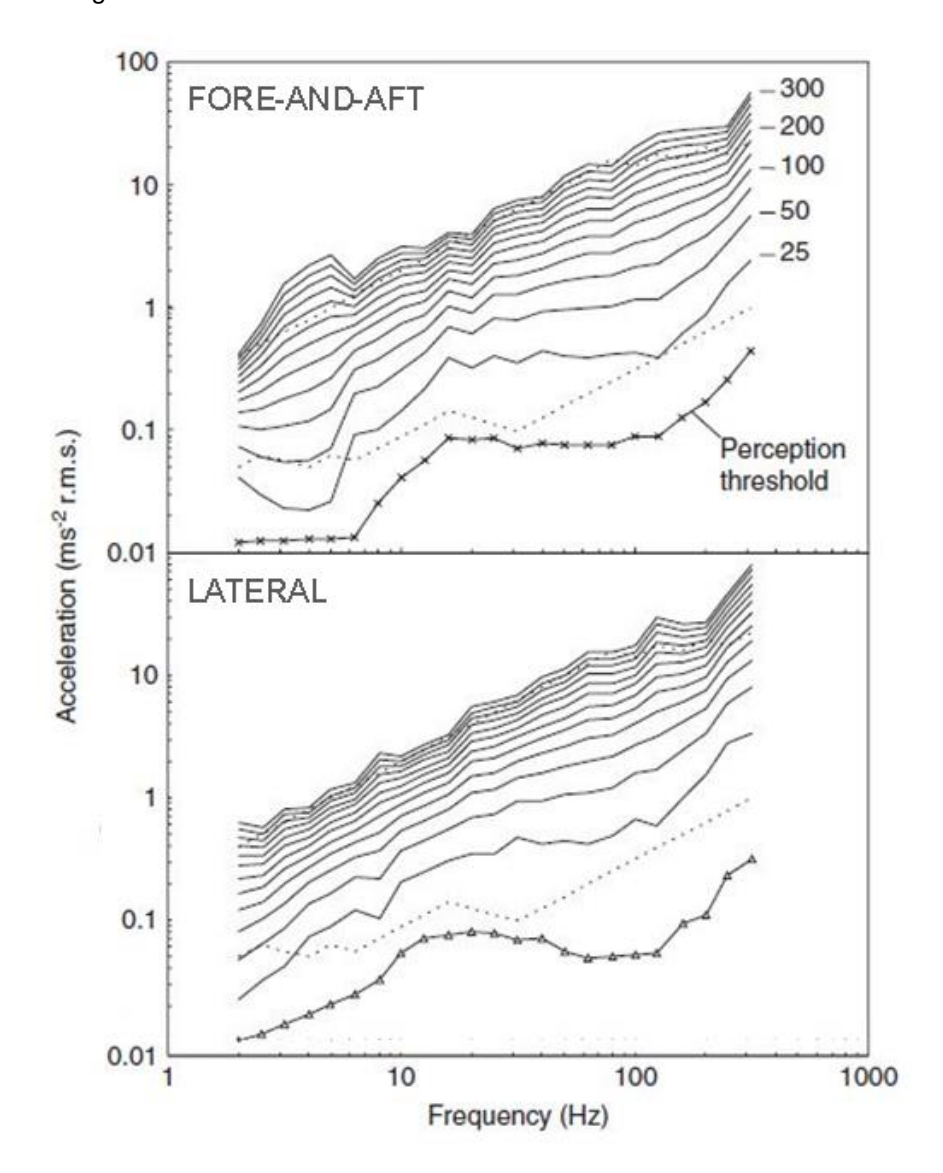


Figure 2.29 Equivalent comfort contours representing subjective magnitudes from 25 to 300, where 100 equals discomfort caused by a 1.0 ms⁻² r.m.s. fore-and-aft (top) or lateral (bottom) reference motion. Median absolute perception thresholds (solid line with symbols) and the range of stimuli used (dotted lines) are also shown. Figure adapted from Morioka and Griffin (2006a).

The magnitude-dependence of equivalent comfort contours for fore-and-aft and lateral oscillation from 2 to 300 Hz on a rigid seat with no backrest and stationary foot- and hand-rests is shown in Figure 2.29 (adapted from Morioka and Griffin, 2006a).

The shape of equivalent comfort contours approximate to perception thresholds at the lowest sensation magnitude (i.e. 25), and then conform to a shape representing constant velocity as the sensation magnitude increases to 300 (Morioka and Griffin, 2006a). The magnitude-dependence of discomfort in fact alters the frequency-dependence, and thus the relative discomfort caused by different frequencies of motion will differ depending on the magnitude of oscillation. "For example, a 4 ms⁻² r.m.s. fore-and-aft vibration produced more than [twice as much discomfort] at 20 Hz than at 100 Hz, whereas 0.4 ms⁻² r.m.s. fore-and-aft vibration" at 20 and 100 Hz produced similar discomfort (Morioka and Griffin, 2006a, p. 767).

The magnitude-dependence of vibration discomfort has been both confirmed and contested by previous authors. When seated on a rigid seat without backrest, the severity of discomfort increased with increasing magnitude (between 0.5 and 2.0 ms⁻² r.m.s.) of 2 to 64 Hz fore-and-aft and lateral vibration (Whitham and Griffin, 1978). But with a rigid seat with no backrest and a stationary footrest, the shape of equivalent comfort contours for lateral and fore-and-aft oscillation between 1 and 64 Hz did not vary with increasing magnitude (0.5, 0.8 and 1.25 ms⁻² r.m.s.) of a 10 Hz vertical reference vibration (Griffin, Whitham and Parsons, 1982a). Additionally with 1 to 31.5 Hz roll and pitch motion on a rigid seat with no backrest, equivalent comfort contours were independent of the magnitude (0.5 and 1.25 ms⁻² r.m.s.) of a 10 Hz vertical reference (Parsons and Griffin, 1982). The discrepancy in findings may be explained by the differences in the seating configuration used in these studies (i.e. stationary vs. moving footrest, and stationary vs. no hand rest).

A magnitude-dependence of discomfort with hand-transmitted vibration may be explained by the existence of multiple sensory receptors in the hands which react differently to certain frequencies and magnitudes of vibration (Morioka and Griffin, 2006b). The magnitude-dependence of discomfort with whole-body vibration is less well explained, but is likely due to the complexity of the human sensory system (incorporating visual, vestibular and proprioceptive information) and the non-linearity of the human biodynamic response (Morioka and Griffin 2006a; Thuong, 2011).

"A magnitude-dependence in equivalent comfort contours means that no single linear frequency weighting can provide accurate predictions of subjective judgements of discomfort caused by whole-body vibration" (Morioka and Griffin, 2006a, p. 771).

2.8.3. Multi-axis motion

The effect of 'rotational-compensation' of horizontal acceleration on vibration discomfort has not been investigated by previous authors, but the relative discomfort caused by lateral and roll motions, and by fore-and-aft and pitch motions, between 0.2 and 1.6 Hz has been addressed by

Wyllie and Griffin (2007; 2009). On a rigid seat with and without a backrest and four-point harness, sensitivity to translational acceleration in the plane of the seat (i.e. due to the component of gravity from rotation) increased with frequency for lateral, roll, fore-and-aft and pitch oscillation. Above 0.5 Hz without a backrest, and above 0.8 Hz with a backrest, sensitivity to acceleration in the plane of the seat was greater during roll oscillation than during lateral oscillation. Likewise, above 0.8 Hz without a backrest and above 0.4 Hz with a backrest, sensitivity to acceleration in the plane of the seat was greater during pitch oscillation than during fore-and-aft oscillation.

Since the translational and rotational oscillations used by Wyllie and Griffin (2007; 2009) yielded the same horizontal acceleration in the plane of the seat, the additional discomfort caused by rotations above 0.4 Hz must be due to: a) the translational acceleration experienced above and below the centre-of-rotation (i.e. at the extremities of the body), or; b) the rotational acceleration imposed on the body. If the latter is true, then rotational acceleration may be a useful predictor of roll- or pitch-compensated horizontal motions, since the translational acceleration with these motions may be negligible.

Additionally, the findings have implications for the prediction of discomfort in transport vehicles caused by rotational oscillations in the range 0.4 to 1.6 Hz since it is crucial whether the "acceleration is caused by translation or caused by rotation through the gravity vector" (Wyllie and Griffin, 2007, p. 2650).

2.8.4. Seating and posture

The configuration of the seat and the subsequent sitting posture affects the transmission of motion to the body and therefore the resulting vibration discomfort. The seating in transport vehicles differs considerably, from the shape and composition of the seat pan, to the height and angle of the backrest, therefore it is of great importance to understand the impact of these factors on discomfort.

At frequencies between 0.2 and 16 Hz, the seat-to-head transmissibility of random horizontal oscillation was increased by the presence of a short backrest, most notably with fore-and-aft oscillation (Paddan and Griffin, 1988; 1992, see Figure 2.30). This increase may be due to: a) the additional input (i.e. at the backrest) of vibration to the upper body, or; b) the associated change in posture which may alter resonance frequencies of the body (Paddan and Griffin, 1988; 1992). The backrest angle may also affect body dynamics: with random fore-and-aft oscillation between 0.25 and 20 Hz, the resonance frequency increased above 4 Hz and the transmissibility at resonance increased with increasing backrest inclination from 90° (i.e. vertical) to 105° (Abdul-Jalil and Griffin, 2007). With random lateral oscillation between 0 and

3.15 Hz, the movement of the head relative to the seat decreased with increasing height of backrest between 0 and 700 mm, implying the degree of lateral support increased with backrest height (Brett and Griffin, 1991).

The configuration of the seating clearly affects the movement of the body during exposure to motion. If vibration discomfort with low frequency translational and rotational oscillation is dependent on the displacement of the head and upper body relative to the seat, then Brett and Griffin's (1991) findings suggest a high backrest may be beneficial for passengers. However, if lateral support forces the upper body to move with the motion, then rotational motions which involve translational components at points away from the centre-of-rotation (see Section 2.2.3) may cause greater discomfort if seated with a full-height backrest. One should also be cautious when generalising results from experiments involving random vibration to alternative motion environments.

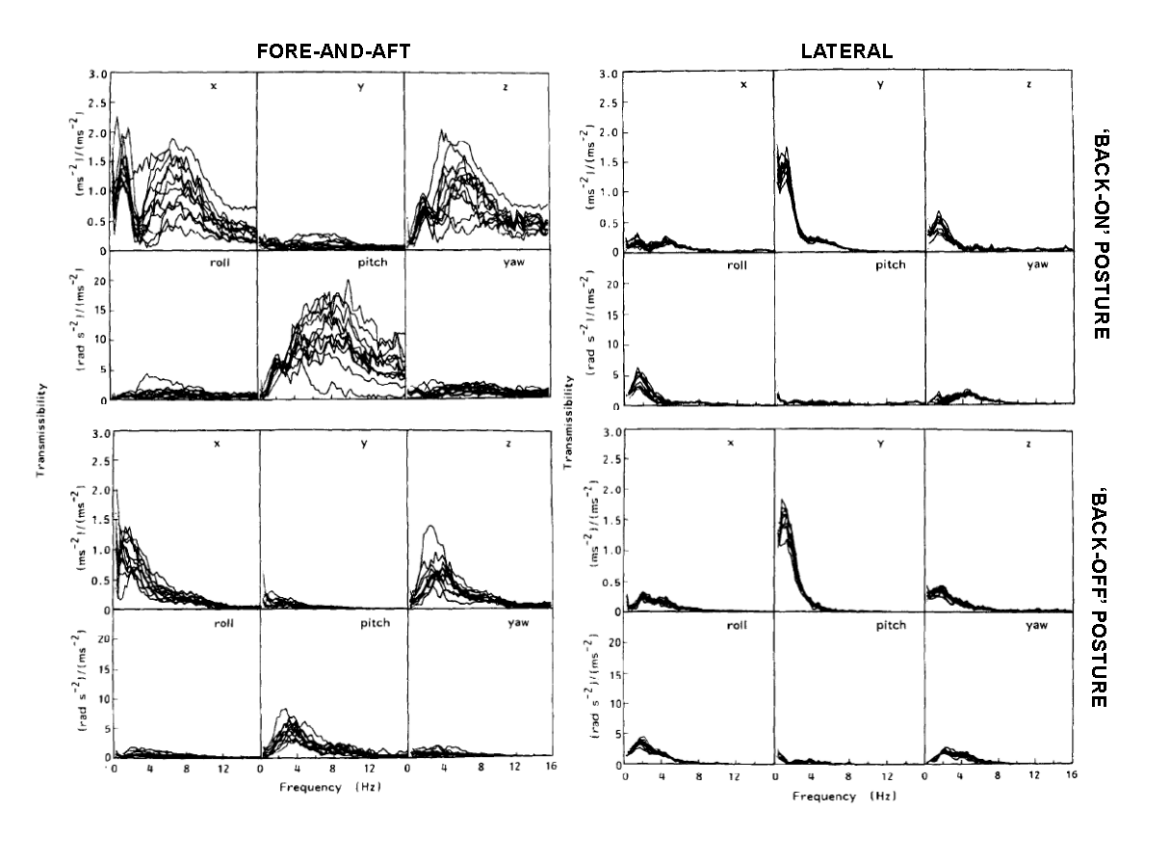


Figure 2.30 Seat-to-head transmissibility during lateral and fore-and-aft oscillation between 0.2 and 16 Hz for 'back-on' and 'back-off' postures (adapted from Paddan and Griffin, 1988).

The effect of backrest contact on vibration discomfort has been investigated by Parsons *et al.*, (1982) and Wyllie and Griffin (2007; 2009). Subjects sat on a rigid seat with backrest reported decreasing discomfort with increasing frequency of fore-and-aft and lateral vibration of the back

between 2.5 and 63 Hz, suggesting discomfort from vibration at the back elicits a similar frequency response as vibration at the seat (Parsons *et al.*, 1982). Above 2 Hz, contact with a backrest increased discomfort from fore-and-aft and lateral oscillation relative to sitting with no backrest. The detrimental effect of backrest was larger with fore-and-aft than with lateral oscillation.

Equivalent comfort contours for lateral, fore-and-aft, roll and pitch oscillation between 0.2 and 1.6 Hz with and without a backrest and four-point harness (Wyllie and Griffin, 2007; 2009) are shown in Figure 2.31. With lateral oscillation between 0.5 Hz and 1.6 Hz, and with roll oscillation and pitch oscillation between 0.63 and 1.6 Hz, vibration discomfort was greater when sitting with a backrest and four-point harness than when sitting with no backrest (Wyllie and Griffin, 2007; 2009). Conversely, sitting with a backrest and harness reduced discomfort caused by fore-and-aft oscillation between 0.25 and 1.25 Hz (Wyllie and Griffin, 2009).

With all four directions investigated (lateral, fore-and-aft, roll and pitch), there was a greater incidence of discomfort localised at the head, neck or shoulders when seated with a backrest than when seated without a backrest (Wyllie and Griffin, 2007; 2009), suggesting the backrest increased the transmission of motion to these locations. Subjects seated with a full-height backrest and harness were not given a headrest, so there may have been relative movement between the head and the shoulders (or strain in the neck muscles preventing this movement) which lead to greater discomfort in this region. Interestingly, a backrest and harness was only detrimental for comfort with lateral, roll and pitch oscillation, and not during fore-and-aft oscillation.

The presence of a backrest may serve to stabilise the body during oscillation, reducing the muscular effort required to maintain an upright posture and thereby reducing discomfort. Alternatively a backrest may increase discomfort by increasing the transmission of vibration to the upper body and head or by reducing the ability of seated persons to make compensatory movements. During roll and pitch oscillation, there were no differences in discomfort between a 'move-with' posture (where subjects maintained a seat-referenced vertical orientation) and a 'head-still' posture (where subjects maintained an Earth-vertical orientation) (Wyllie, 2007). This suggests that an inability to make 'compensatory movements' (i.e. due to a backrest and harness) during exposure to rotational oscillation is not sufficient for explain discomfort.

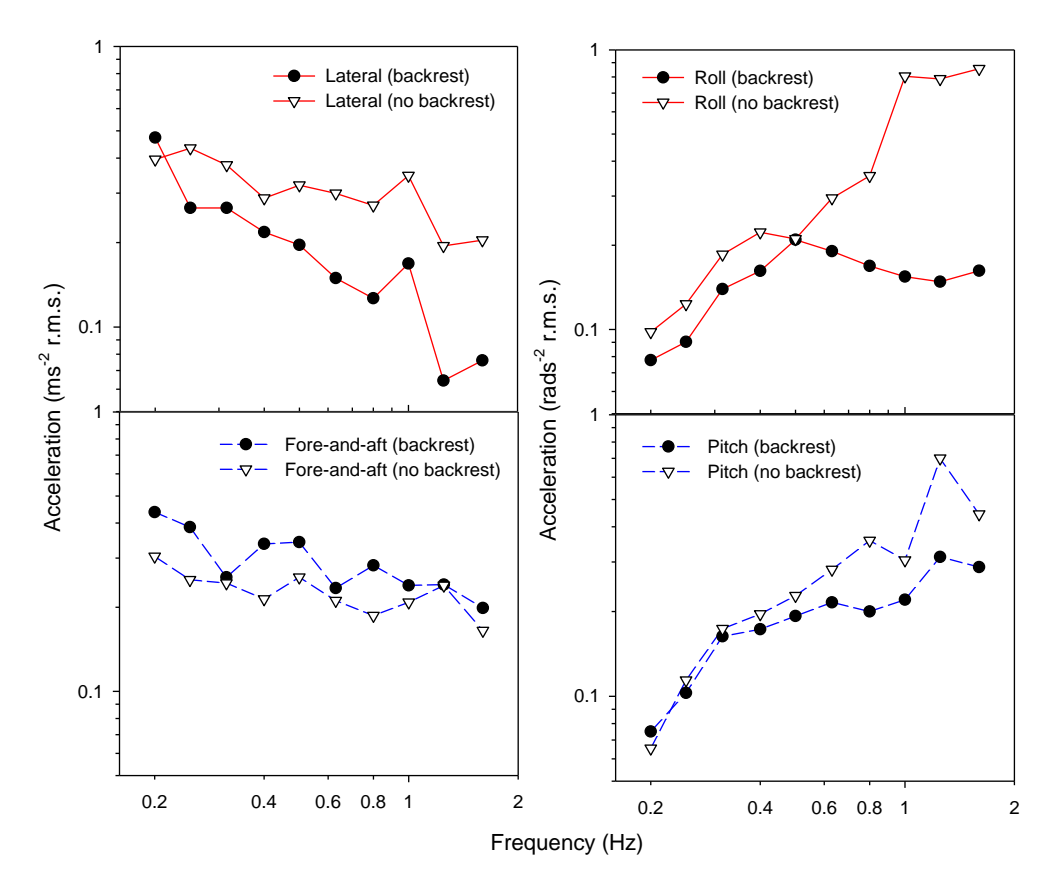


Figure 2.31 Equivalent comfort contours for lateral, fore-and-aft, roll and pitch oscillation with and without a backrest and four-point harness (Wyllie and Griffin, 2007; 2009).

The seating conditions investigated by Wyllie and Griffin (2007; 2009) represent, perhaps, two extremes of the lateral support offered to the body; a) no backrest, offering no support, or: b) full-height backrest with a tightly fastened four-point harness, offering full lateral support but forcing the upper body to move with the motion. Further investigation with 'intermediary' types of backrest (with 'intermediate' levels of lateral support) is necessary to understand the implications for transport.

For lateral and fore-and-aft oscillation at the back, British Standard 6841 (1987) suggests the use of frequency weighting W_d with an axis multiplying factor of 0.5 and W_c with an axis multiplying factor of 0.8, respectively. These weightings suggest discomfort caused by lateral and fore-and-aft acceleration at the back will be approximately 50% and 80%, respectively, of that caused by acceleration at the seat surface (if the seat is rigid and there is no other source of vibration discomfort, e.g., at the feet). Whilst this may be true for high frequencies, evidence suggests the effects of backrest are more complex below 2 Hz.

The backrest is not the only aspect of seating which may affect the vibration discomfort of seated occupants. On a rigid seat with no backrest and a stationary footrest, sensitivity to roll and pitch oscillation between 1.6 and 31.5 Hz decreased with increasing footrest height (Parsons *et al.*, 1982). With different inputs at the seat and at the feet, vibration discomfort is dependent on the magnitude of the motion, the relative movement between the two inputs (i.e. the phase) and the seat-thigh contact (Jang and Griffin, 1999; 2000). Increasing the height of the footrest will reduce seat-thigh contact which may benefit comfort.

The arrangement of passenger seating relative to the moving vehicle is also likely to affect the vibration discomfort of passengers. With roll and pitch motion between 2 and 16 Hz, sensitivity increased with increasing distance from the centre-of-rotation (Parsons and Griffin, 1978). As subjects were moved farther from the centre-of-rotation, the frequency response of equivalent comfort contours became more similar to those produced by translation alone, suggesting that the translational component of the rotation became more dominant in the perception of discomfort.

2.9. Model of vibration discomfort

2.9.1. Frequency weightings and axis multiplying factors

Current national vibration standards (BS 6841, 1987) and international vibration standards (ISO 2631-1, 1997) provide guidance for the prediction of discomfort in seated and standing persons exposed to translational and rotational vibration. Evaluation of vibration discomfort can be split into three main steps:

- 1. Frequency-weight single-axis vibration
- 2. Apply multiplying factors for posture and measurement location
- 3. Combine multiple axes of vibration into a single prediction

An illustration of this procedure is shown in Figure 2.32. The frequency weightings and multiplying factors for each axis of vibration and the associated posture or measurement location to which they apply are shown in Table 2.14 (Note: Wk in ISO 2631-1 replaces Wb in BS 6841). The standards define the frequency weightings as realisable filters. Guidance is principally limited to frequencies between 0.5 and 80 Hz, however values outside this range are achieved after applying a band-pass filter at 0.4 and 100 Hz. The W_c , W_d , W_e , W_j and W_k realisable weightings with the band-limiting filter are shown in Figure 2.33.

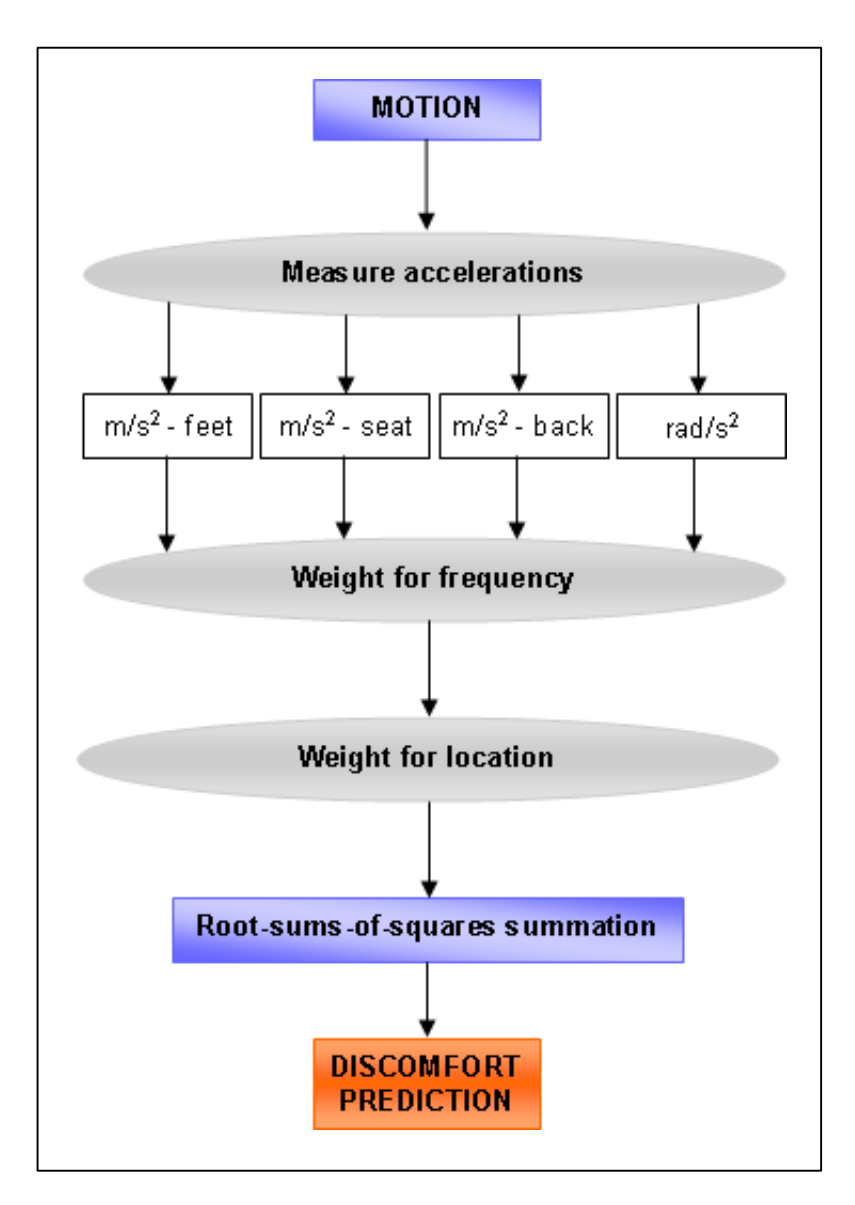


Figure 2.32 Current model for predicting vibration discomfort (ISO 2631-1, 1997).

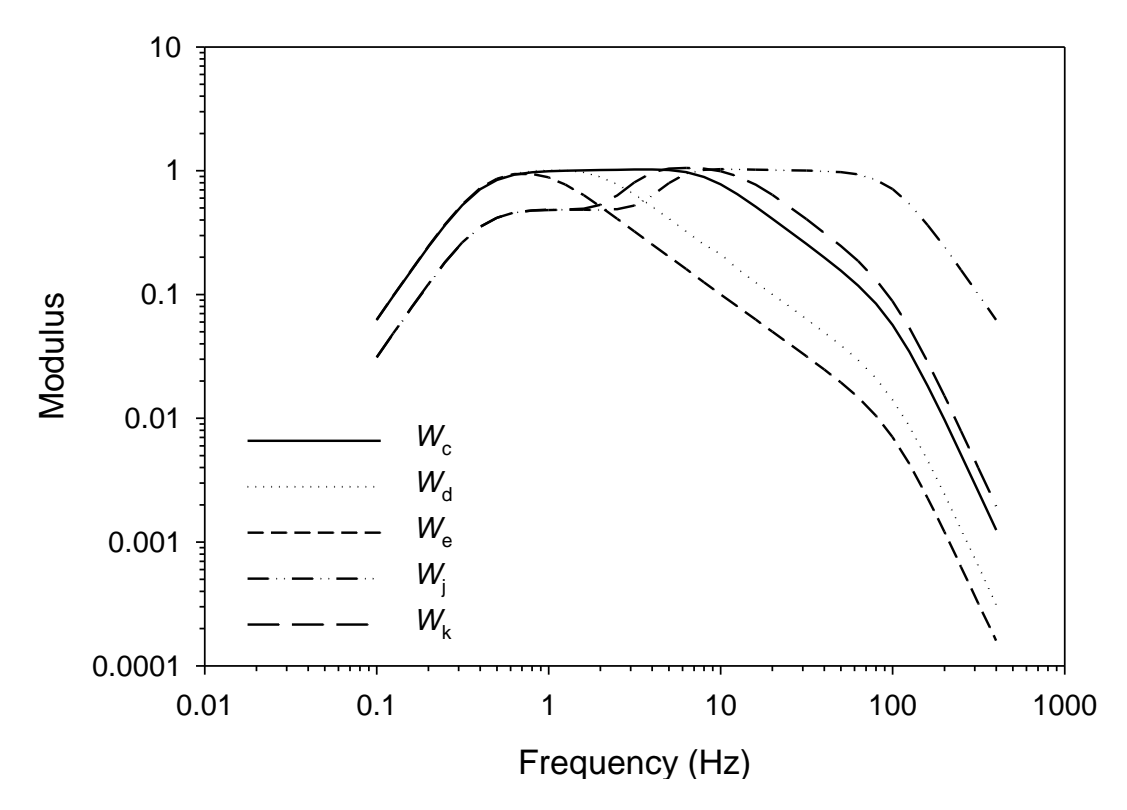


Figure 2.33 Discomfort frequency weightings with a band-pass filter at 0.4 and 100 Hz (ISO 2631-1, 1997).

Once the effects of frequency, posture and measurement position are accounted for (using the frequency weightings and multiplying factors shown in Table 2.14), each component of the vibration may be evaluated using the root-mean-square (r.m.s.) averaging method. The r.m.s. is calculated as follows:

Equation 2.19:
$$a_{w} = \left[\frac{1}{T} \int_{0}^{T} a_{w}^{2}(t) dt\right]^{\frac{1}{2}}$$

where a_w is the frequency-weighted r.m.s. acceleration, $a_w(t)$ is the frequency-weighted acceleration, and T is the duration of measurement. It should be noted that in some cases "it is not possible to evaluate human response to vibration using the frequency-weighted r.m.s acceleration" (ISO 2631-1, 1997, p. 25). For example, ISO 2631-1 recommends the r.m.s. is not used if the crest factor (the ratio between the peak acceleration and the r.m.s. acceleration) is greater than 9.0. But, BS 6841 1987 recommends the r.m.s. is not used for motions with a crest factor greater than 6.0, so the correct procedure is not clear. A number of methods other than the crest factor exist for detecting shocks (Schust *et al.*, 2012), including the use of 'boundary values' with the maximum transient vibration value (MTVV) or the vibration dose value (VDV) (see Equation 2.22 and Equation 2.23 below).

With motions containing shocks or with transient vibrations, the standards recommend the use of the running r.m.s. method (Equation 2.20) or the fourth-power vibration dose value (Equation 2.21).

Equation 2.20:
$$MTVV = MAX\{a_w(t_0)\} = \left[\frac{1}{\tau} \int_{t_0 - \tau}^{t_0} [a_w(t)]^2 dt\right]^{\frac{1}{2}}$$

where MTVV (maximum transient vibration value) is the maximum of frequency-weighted r.m.s. acceleration, $a_w(t_0)$, at instantaneous time point, t_0 , τ is the size of the integration window (1 second is recommended), T is the measurement duration and $a_w(t)$ is the frequency-weighted acceleration.

Equation 2.21:
$$VDV = \left[\int_0^T [a_w(t)]^4 dt\right]^{\frac{1}{4}}$$

where VDV is the vibration dose value (ms-1.75), T is the measurement duration and aw(t) is the frequency-weighted acceleration. These methods are more sensitive to peaks in the acceleration by including a short integration time window (in the case of the running r.m.s.) or the fourth instead of the second power (in the case of the vibration dose value). It is suggested that the MTVV or the VDV be used if the conditions of Equation 2.22 or Equation 2.23 are satisfied:

Equation 2.22:
$$\frac{MTVV}{r.m.s.} > 1.5$$

Equation 2.23:
$$\frac{VDV}{r \, m \, s \times \tau^{1/4}} > 1.75$$

The standards therefore imply that the *MTVV* or the *VDV* should be used if they give substantially different values from the r.m.s. method. Using the alternative methods when the values are similar to the r.m.s. would also be logical, as this would imply equivalence between the methods (Thuong, 2011).

In stage 3, the overall discomfort can be assessed by calculating the total vibration value, as shown in Equation 2.24.

Equation 2.24:
$$a_v = \left[a_x^2 + a_y^2 + a_z^2 + a_{R_x}^2 + a_{R_y}^2 + a_{R_z}^2 \right]^{\frac{1}{2}}$$

where a_v is the total vibration value, a_x , a_y , a_z , a_{Rx} , a_{Ry} , and a_{Rz} are the frequency-weighted r.m.s. accelerations in fore-and-aft, lateral, vertical, pitch, roll and yaw axes, respectively. The vibration total value may be used to combine r.m.s. accelerations across multiple axes or multiple measurement locations into a single prediction of discomfort.

Table 2.14 Frequency weightings for predicting vibration discomfort with fore-and-aft (x), lateral (y), vertical (z), roll (r_x), pitch (r_y) and yaw (r_z) vibration between 0.5 and 80 Hz (ISO 2631-1, 1997).

Weighting	Axis	Measurement position / Posture	Multiplying factor
W c	Х	Seat-Back	0.8
	Х	Seat	1
	У	Seat	1
	Х	Standing	1
147	У	Standing	1
$W_{ m d}$	X	Recumbent	1
	У	Recumbent	1
	У	Seat-Back	0.5
	Z	Seat-Back	0.4
	r _x	Seat	0.63
<i>W</i> e €	r y	Seat	0.4
	r _z	Seat	0.2
W _j	Z	Recumbent	1
	Х	Feet (sitting)	0.25
	У	Feet (sitting)	0.25
W_k	Z	Feet (sitting)	0.4
	Z	Seat	1
	Z	Standing	1

Table 2.15 Effect of the magnitude of vibration total values (VTV) on estimated comfort levels, as provided by ISO 2631-1 (1997).

VTV (ms ⁻²)	Estimated comfort level
< 0.315	not uncomfortable
0.315 - 0.63	a little uncomfortable
0.5 - 1.0	fairly uncomfortable
0.8 - 1.6	uncomfortable
1.25 - 2.5	very uncomfortable
> 2.0	extremely uncomfortable

As a final step, the standards provide guidance on the interpretation of vibration total values in terms of the 'likely comfort reaction' of exposed persons (see Table 2.15). The semantic interpretation of vibration and the perception of comfort will vary considerably across the population and is highly dependent on environmental context. For example, a vibration at a magnitude perceived to be typical for a car would likely be appalling in a building. Furthermore, there is no indication of how to handle vibration total values which fall across two categories (e.g. 2.2 ms⁻²). For these reasons, the guidance should be read with some caution.

2.10. Conclusion

Low frequency horizontal and rotational oscillation (at frequencies less than 1.0 Hz) may cause motion sickness (due to provocative stimulation of the vestibular, visual and somatosensory systems) or physical vibration discomfort (due to disturbances in balance or sitting posture or due to the transmission of motion to specific body parts). Motions at these frequencies have been measured in railway vehicles (and other land transport) therefore it is important for transport operators to understand the implications of the motion environment on passenger comfort. Low frequency horizontal centripetal accelerations associated with cornering may be reduced with the addition of appropriate roll acceleration (i.e. roll-compensation); a technique which is adopted by tilting trains to allow for higher speeds without excessive lateral forces.

The incidence of motion sickness with roll-compensated lateral oscillation at frequencies less than 1 Hz has been documented in previous research. The incidence of sickness increases with the level of roll-compensation between 50% and 100%, but low levels of compensation may be less provocative than uncompensated lateral oscillation. Pure roll oscillation does not cause substantial sickness. The frequency-dependence of sickness remains consistent across uncompensated and compensated lateral motions, with the incidence of sickness increasing with decreasing frequency below 1 Hz and reaching a 'maximum' around 0.2 Hz.

The orientation of the body affects the transmission of motion to the upper body and head, therefore the stimulation of the vestibular organs, and the level of motion sickness, is influenced by seating and posture. Motion sickness is greater in passengers seated upright than those lying supine. Gender, age and previous experience are also consistent correlates with the incidence of sickness on many forms of transport.

Previous motion sickness research has only tested roll-compensated lateral motions where the position of full roll-compensation is at the seat surface. The position of full roll-compensation may differ between tilting rail vehicles, therefore knowledge of its influence on passenger

sickness is of interest. Such empirical research may also help to substantiate (or invalidate) the sensory rearrangement theory of motion sickness.

No previous studies have systematically investigated the effects of roll-compensated lateral oscillation on vibration discomfort. Vibration discomfort is highly dependent on the frequency of oscillation. The discomfort caused by pure horizontal acceleration and pure roll acceleration exhibit different frequency dependencies. Sensitivity to horizontal acceleration increases with increasing frequency between 0.2 and 2 Hz and then decreases with frequency above this range. Sensitivity to rotational acceleration tends to decrease with increasing frequency from 0.2 Hz. Above about 0.5 Hz, acceleration in the plane of the seat caused by roll (or pitch) motion through the gravitational vector causes greater discomfort than that caused by lateral (or fore-and-aft) motion. Current British and International standards do not offer a complete method of predicting discomfort with motions at frequencies less than 0.5 Hz.

The configuration of seating and the sitting posture greatly affect the transmission of motion to the body and the subsequent severity and location of vibration discomfort. Understanding of the effects of backrest on vibration discomfort with motions below 1 Hz is incomplete. Current standards suggest discomfort caused by lateral acceleration at the back will be approximately 50% of that caused by acceleration at the seat surface, however previous research suggests the effects of backrest are more complex with motions below 2 Hz.

This literature review has identified areas where further research is required. Knowledge of the effect of the position of full roll-compensation on motion sickness may improve the application of motion sickness research and help to validate a conceptual model of motion sickness. However, the majority of previous research on low frequency horizontal and rotational motions is focussed on the development of motion sickness rather than the causation of physical discomfort; therefore it is the primary aim of this thesis to focus on the latter. Thorough investigation of the frequency-dependence of lateral oscillation, roll oscillation and roll-compensated lateral oscillation at frequencies less than 1.0 Hz will add to the current knowledge offered in British and International standards. Additionally, experiments are needed to ease the ambiguity of the effect of seating on vibration discomfort caused by low frequency oscillation.

Chapter 3

Equipment and experimental methods

3.1. Introduction

This chapter details the experimental apparatus and research methods used during the work presented in this thesis.

3.2. Motion simulation equipment

The five experiments described in this thesis utilised three different human-rated motion simulators, located in the Human Factors Research Unit of the Institute of Sound and Vibration Research at the University of Southampton, Southampton, United Kingdom.

3.2.1. 12-m tilting and translating cabin

The tilting and translating cabin (HFRU, 2012a) is a bespoke simulator capable of reproducing horizontal (e.g. lateral or fore-and-aft) and rotational (e.g. roll or pitch) motions at frequencies up to 1 Hz. The simulator operates with maximum peak-to-peak horizontal displacements up to 12 metres, and peak rotational angles of up to 10 degrees (see Figure 3.1). Full details of the limits when generating fully compensated horizontal motions are provided in Figure 3.2.

The simulator is driven by two AC asynchronous induction motors rated at 15 kW r.m.s for the horizontal motion and 1.5 kW r.m.s for the rotational motion. Voltage signals for horizontal and the rotational motors are generated using the *HVLab* toolbox within Mathworks MATLAB software (version R2010a). Example MATLAB scripts (i.e. m-files) are shown in Appendix A.4.1.

Horizontal and rotational motions were monitored by the operator using a Thurlby (type 1504) voltmeter and a HFRU roll displacement meter, respectively. A potentiometer built into the HFRU signal amplifier allowed for small adjustments (±120 mV) to the horizontal and rotational signals, to counter any signal offsets.

Subjects were housed in a 2 m x 1.2 m x 1.7 m cabin fitted to the simulator platform.

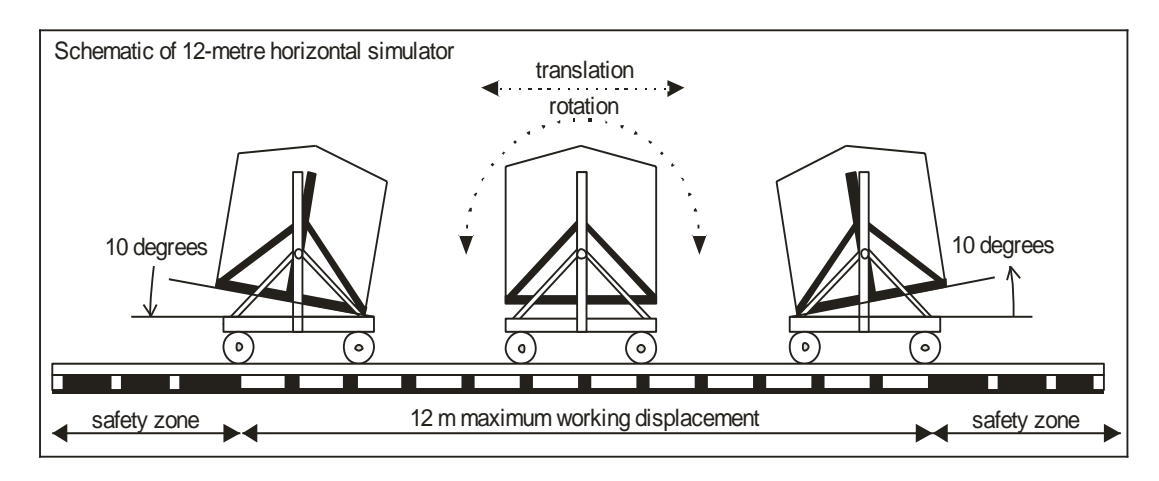


Figure 3.1 Schematic view of the 12-metre horizontal simulator (from Donohew, 2006).

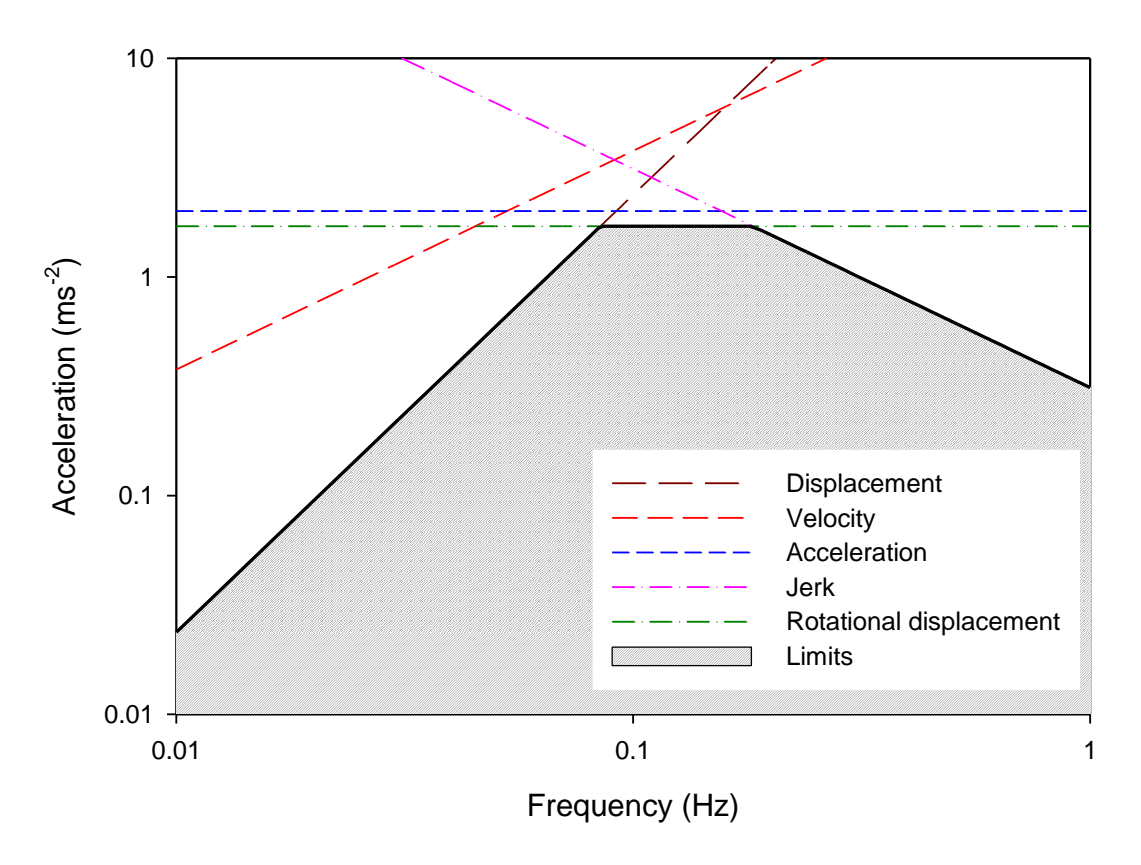


Figure 3.2 Approximate 12-m tilting and translating simulator peak acceleration limits.

[Rotational displacement represented as the peak acceleration in the plane of the seat, i.e. due to gravity].

3.2.2. 1-m horizontal simulator

The horizontal simulator (HFRU, 2012b) is an electro-hydraulic vibrator capable of producing horizontal oscillation between 0 and 50 Hz with peak-to-peak displacements up to 1 metre and peak accelerations up to 6 ms⁻² (see Figure 3.3).

A Pulsar Digital Controller provided by Servotest Systems was used to control the simulator. Motion waveforms are generated for a single-axis in a Servotest file format (i.e. '.sef') using the *HVLab* toolbox within MATLAB. An example MATLAB script (i.e. m-file) is shown in Appendix A.4.2.

Subjects were placed on seating fixed to the 1 m x 1.75 m simulator platform.

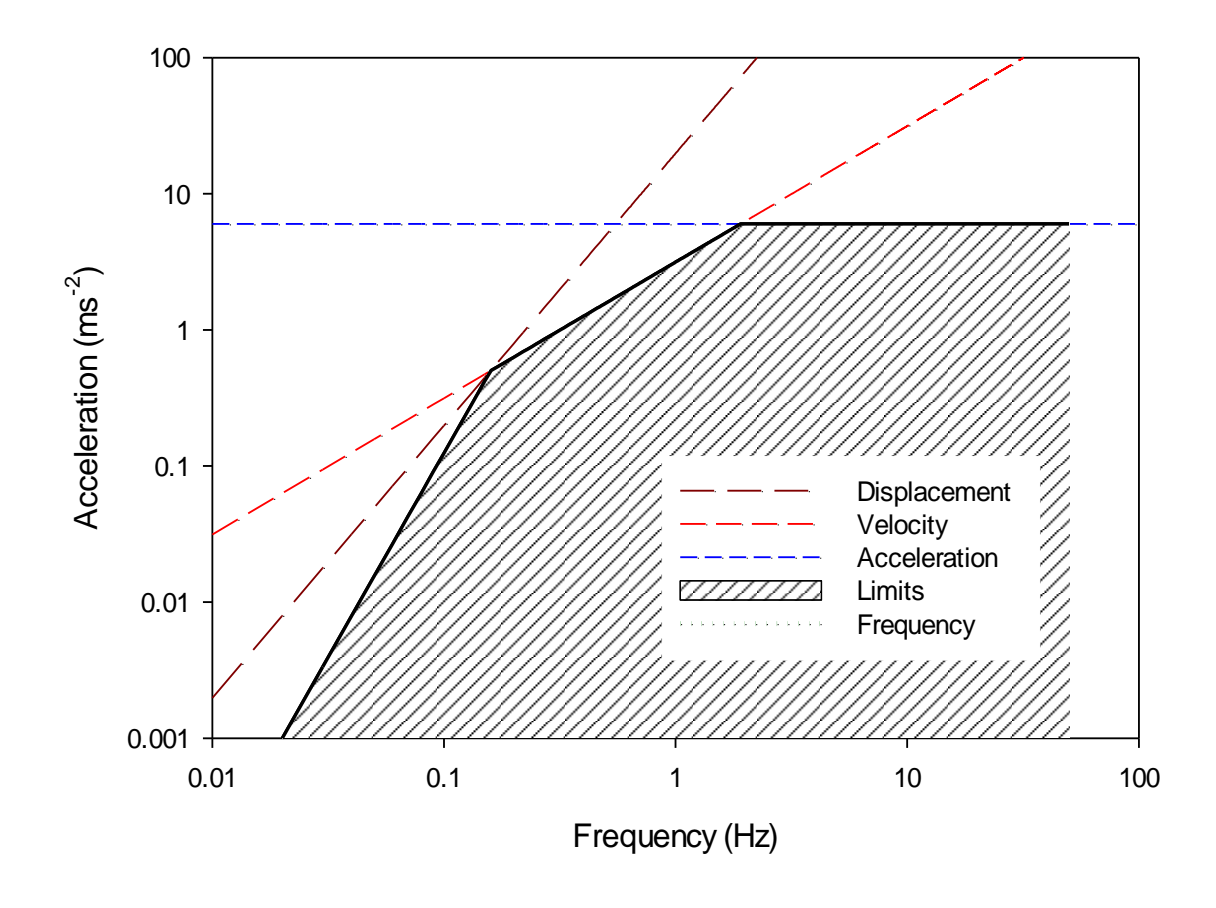


Figure 3.3 Approximate 1-m horizontal simulator peak acceleration limits.

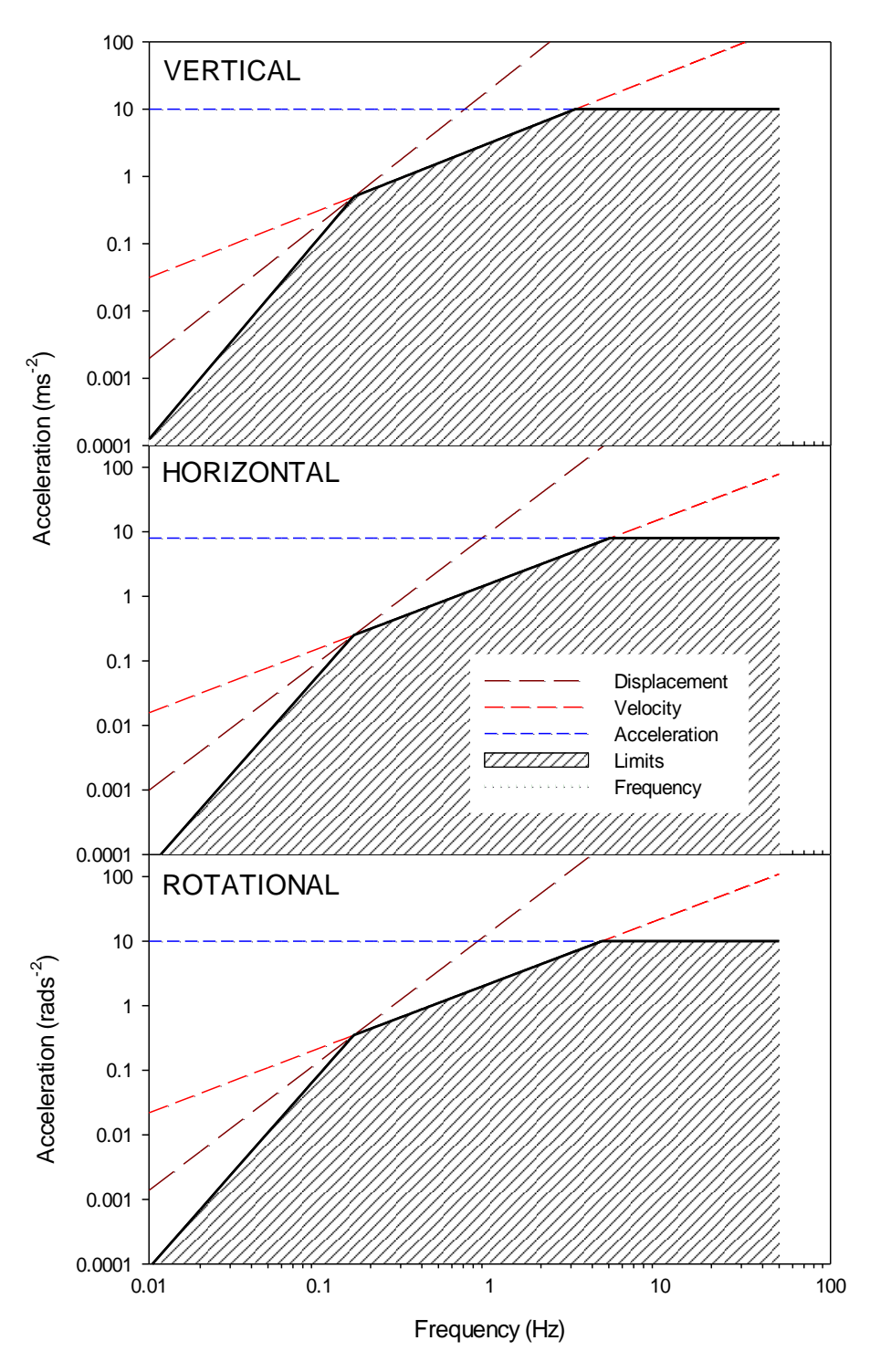


Figure 3.4 Approximate 6-axis motion simulator peak acceleration limits

3.2.3. 6-axis simulator

The 6-axis motion simulator (HFRU, 2012c) can reproduce complex motions between 0 and 50 Hz in any of three translation axes (fore-and-aft, lateral, and vertical) and three rotational axes (roll, pitch, and yaw). The simulator operates with a maximum vertical displacement of ±0.5 metres, a maximum horizontal displacement of ±0.25 metres, and a maximum rotational angle of about ±20 degrees. Maximum accelerations are ±10 ms⁻² and ±10 rads⁻² for translation and rotation, respectively. Full details of the approximate motion limits for vertical, horizontal and rotational motion are shown in Figure 3.4.

The simulator was controlled by a Servotest Pulsar Digital Controller. Motion waveforms are generated for all 6-axes in a Servotest file format (i.e. '.sef') using the *HVLab* toolbox within MATLAB. An example MATLAB script (i.e. m-file) is shown in Appendix A.4.3.

Seating and other equipment (up to 1000 kg) can be attached to the 3 m x 2 m simulator platform.

3.3. Test environment

3.3.1. Motions

This Section details the procedure used to generate motion stimuli for all five experiments described in this thesis, including quality control methods used to ensure the accuracy of motion stimuli.

3.3.1.1. Motion generation

All motions were generated using a script (i.e. m-file) within MATLAB software. Each of the three simulators required a different script.

For Experiment 1 (Chapter 4), sinusoidal waveforms were generated for lateral motion and roll motion by defining the input frequency, the peak horizontal acceleration, the proportion of roll-compensation (i.e. 0 to 1), and the signal duration (see Appendix A.4.1.). Motion signals were sampled at 50 samples per second and equalised by adjusting the scaling factor between the voltage inverter input and the velocity output (initially set at 0.5 ms⁻¹/volt for horizontal motion) through comparison of the target motion with the actual motion generated. This procedure accounted for any offsets in the system.

For Experiments 2, 3, 4 and 5 (Chapter 5, 6, 7 and 8) motion waveforms were generated using a similar MATLAB script (see Appendix A.4.2. and A.4.3.), but signals were equalised using the PULSAR Iterative Control System (ICS) provided by Servotest Systems (see Section 3.3.1.2).

Details of the measurement systems used during the five experiments are provided in section 3.3.1.4.

3.3.1.2. PULSAR equalisation procedure

The PULSAR Iterative Control System (ICS) consists of a two-stage process for creating a digital drive signal in order to reproduce a desired motion signal on a servo-hydraulic simulator (either the 1-m horizontal simulator, or the 6-axis simulator – see Section 3.2.). An illustration of this process is provided in Figure 3.5.

In the first stage, a matrix of transfer functions (known as the System Matrix) between the system response (the output) and the system drive (the input) is calculated using a Fast Fourier Transform (FFT) in the frequency domain. To calculate the System Matrix, ICS generates an input function in the form of a white noise signal. The frequency content of the white noise must be representative of the desired motion signal in order to ensure correct identification of the System Matrix over the frequency range of interest. A digital drive signal is then created using the Inverse System Matrix.

In the second stage, the digital drive file is replayed in an iterative process which adjusts the signal according to the error between the measured response and the desired response. The process is repeated until the desired signal is achieved (or the error between the measured response and the desired response is sufficiently low).

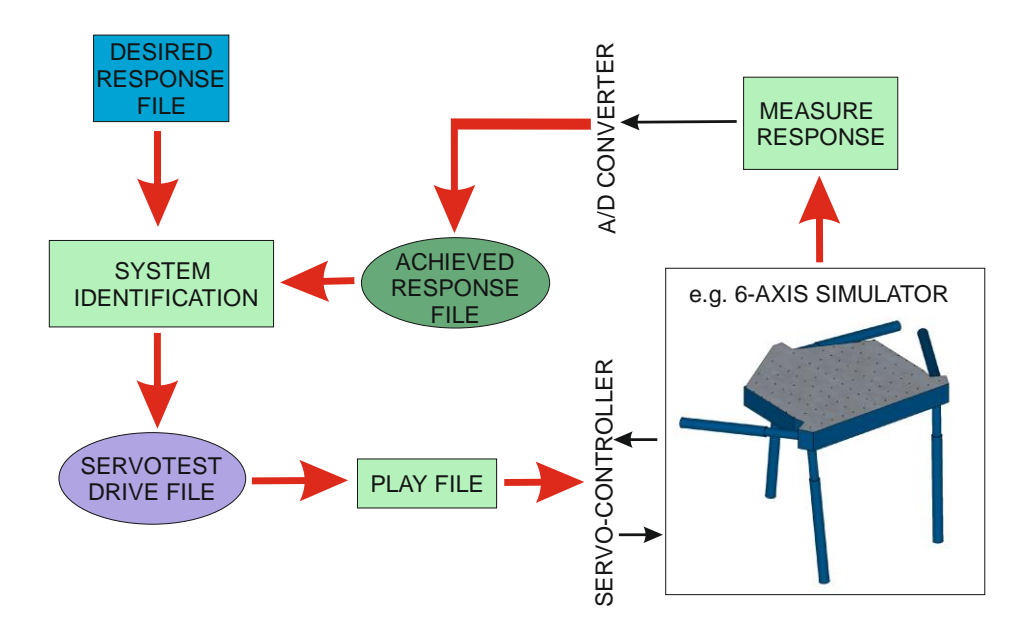


Figure 3.5 Illustration of Pulsar Iterative Control System (ICS) procedure.

3.3.1.3. Waveform distortion

Adjustment of the scaling factor between the voltage inverter input and the velocity output (in Experiment 1; Chapter 4) and the Pulsar ICS equalisation procedure (in Experiment 2 - 5; Chapter 5 - 8) ensured that the target magnitude of acceleration was achieved for each motion stimulus; however it was also necessary to assess the waveform distortion for all three motion simulators.

Previous research demonstrated that waveform distortion is independent of the presence of subjects (Thuong, 2011) so the distortion on all simulators was calculated without subjects. Two methods have been used to assess the level of distortion in motion signals, Equation 3.1 (Griffin, 1990), and Equation 3.2:

Equation 3.1: Distortion (%) =
$$\frac{\sqrt{a_t^2 - a_d^2}}{a_d} \times 100$$

where a_t is the total measured acceleration (ms⁻² r.m.s.), and a_d is the measured acceleration (ms⁻² r.m.s.) filtered over a one-third octave band centred on the desired frequency.

Equation 3.2:
$$Error (\%) = \frac{RMS(a_i - a_m)}{a_{rms}} \times 100$$

where a_i is the input acceleration time history (i.e. desired), and a_m is the measured acceleration time history (i.e. achieved). The r.m.s. of $a_i - a_m$ was calculated and divided by a_{rms} , the total r.m.s. acceleration of the measured time history (ms⁻² r.m.s.).

Experiment 1 (Chapter 4) used sinusoidal motion stimuli, therefore Equation 3.1 was used to estimate distortion (see Table 3.1). Experiment 2 to 5 (Chapter 5 to 8) used transient motion stimuli, therefore Equation 3.2 was used to estimate distortion (see Table 3.2, Table 3.3 and Table 3.4).

In order to account for human sensitivity to motion, measured accelerations were frequency-weighted using appropriate filters defined in ISO 8041 (2005). For Experiment 1, accelerations were weighted using $W_{\rm f}$ to account for motion sickness sensitivity. For Experiment 2, 3, 4 and 5, accelerations were weighted using $W_{\rm d}$ (for lateral acceleration) and $W_{\rm e}$ (for roll acceleration) to account for discomfort sensitivity.

3.3.1.3.1. 12-m tilting and translating cabin

Waveform distortion on the 12-m tilting and translating cabin was calculated using a 0.2 Hz horizontal sinusoidal signal at ±1.26 ms⁻² and ±1.41 ms⁻². Accelerations were recorded in the range 0 to 5 Hz and sampled at 50 samples per second. Typical unweighted and *W*_f-weighted horizontal accelerations (ms⁻² r.m.s.) measured at the carriage, at the seat surface and at head

height (see Figure 3.6) and the percentage distortion for motions used in the 'seat compensation' and 'head compensation' conditions are shown in Table 3.1. Example acceleration waveforms for a 30-second segment of the motion signal used in the 'seat compensation' and 'head compensation' conditions are shown in Figure 3.7 and Figure 3.8, respectively.

Table 3.1 Typical measured accelerations for 'seat compensation' and 'head compensation' conditions in Experiment 1. (*Accelerations were filtered using band-pass filters one-third octave above and below 0.2 Hz).

			Measured acceleration (ms-2 r.m.s.)						
	Measurement	Measurement location (ms-2 r.m.s.). Desired acceleration (ms-2 r.m.s.). Unweighted Unweighted Unweighted Unweighted		Unweighted			W₁ – weighted		
Condition				Unfiltered	Filtered*	Distortion (%)			
	Carriage	0.8910	0.7576	0.7015	28.00	0.7453	0.7253	17.40	
Seat compensation	Seat	0.0000	0.0175	0.0019	-	0.0020	0.0019	=	
·	Head	=	0.0319	0.0135	-	0.0145	0.0139	-	
	Carriage	0.9970	0.9444	0.8846	26.01	0.9399	0.9122	17.44	
Head compensation	Seat	-	0.0230	0.0125	-	0.0133	0.0129	-	
'	Head	0.0000	0.0122	0.0022	-	0.0025	0.0023	=	

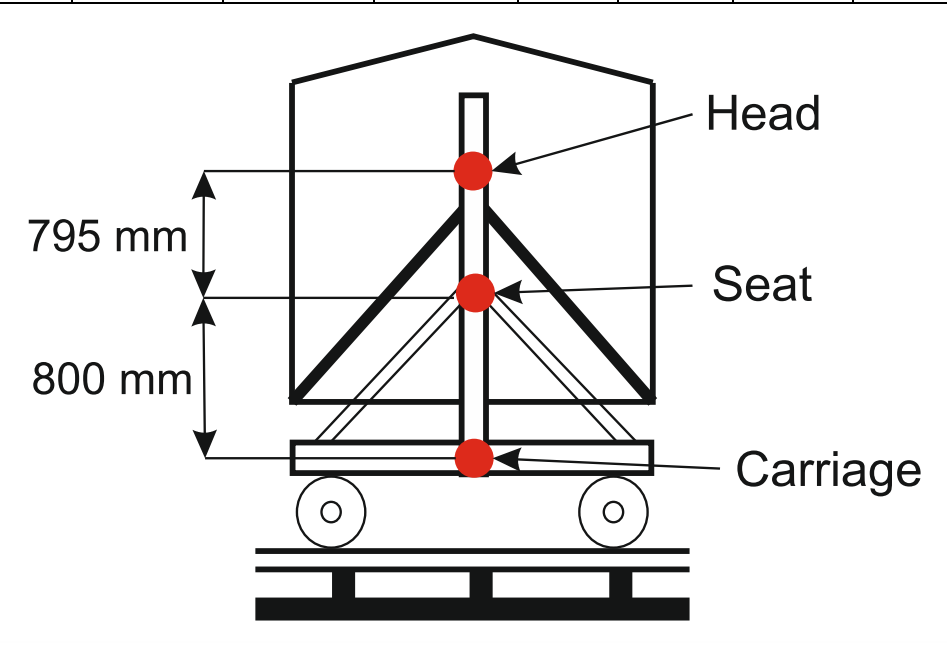


Figure 3.6 Accelerometer measurement locations on 12-m tilting and translating cabin.

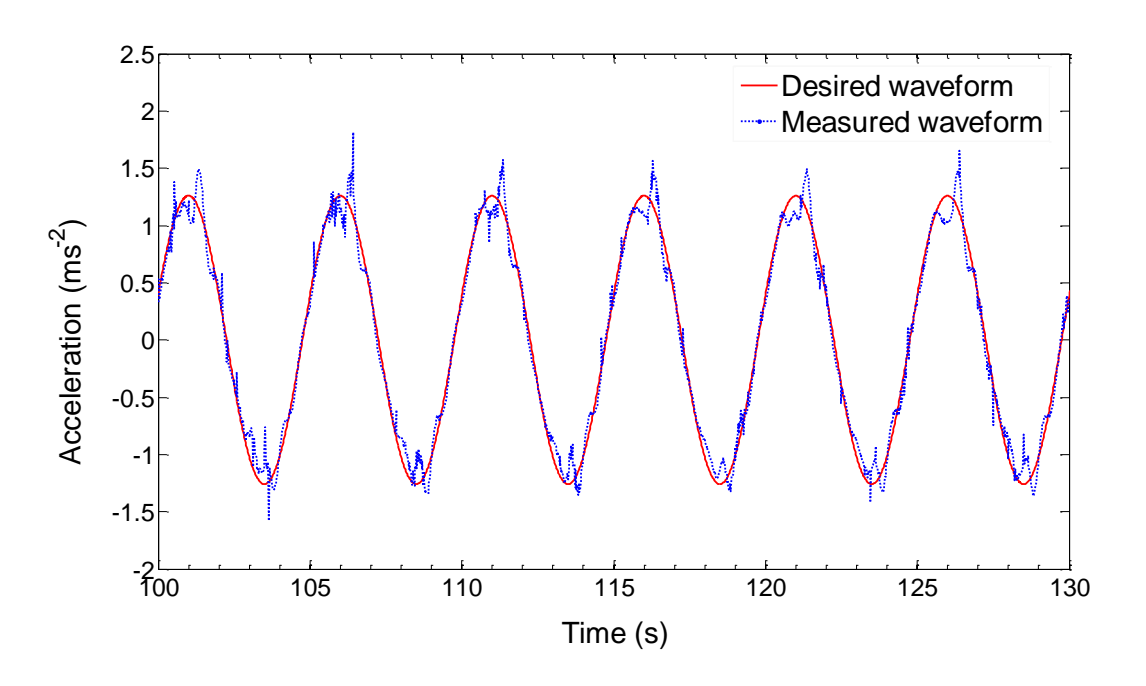


Figure 3.7 Comparison of desired and measured horizontal acceleration waveforms for a typical 30-second segment of 'seat compensation' condition in Experiment 1 (12-m tilting and translating cabin).

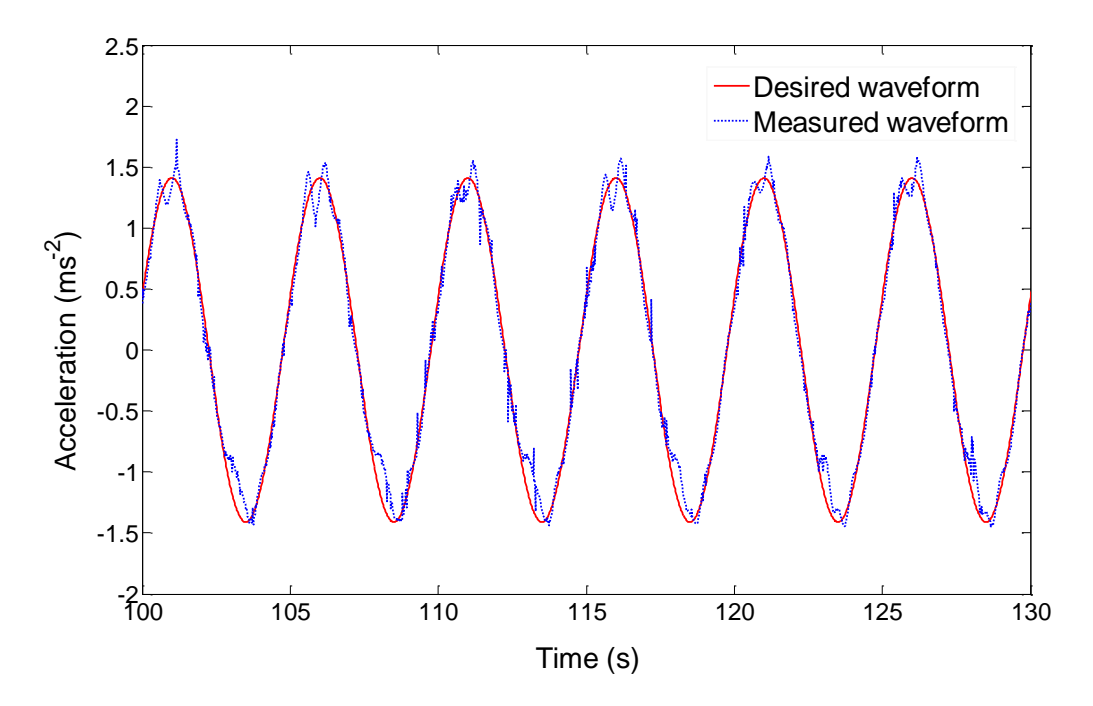


Figure 3.8 Comparison of desired and measured horizontal acceleration waveforms for a typical 30-second segment of 'head compensation' condition in Experiment 1 (12-m tilting and translating cabin).

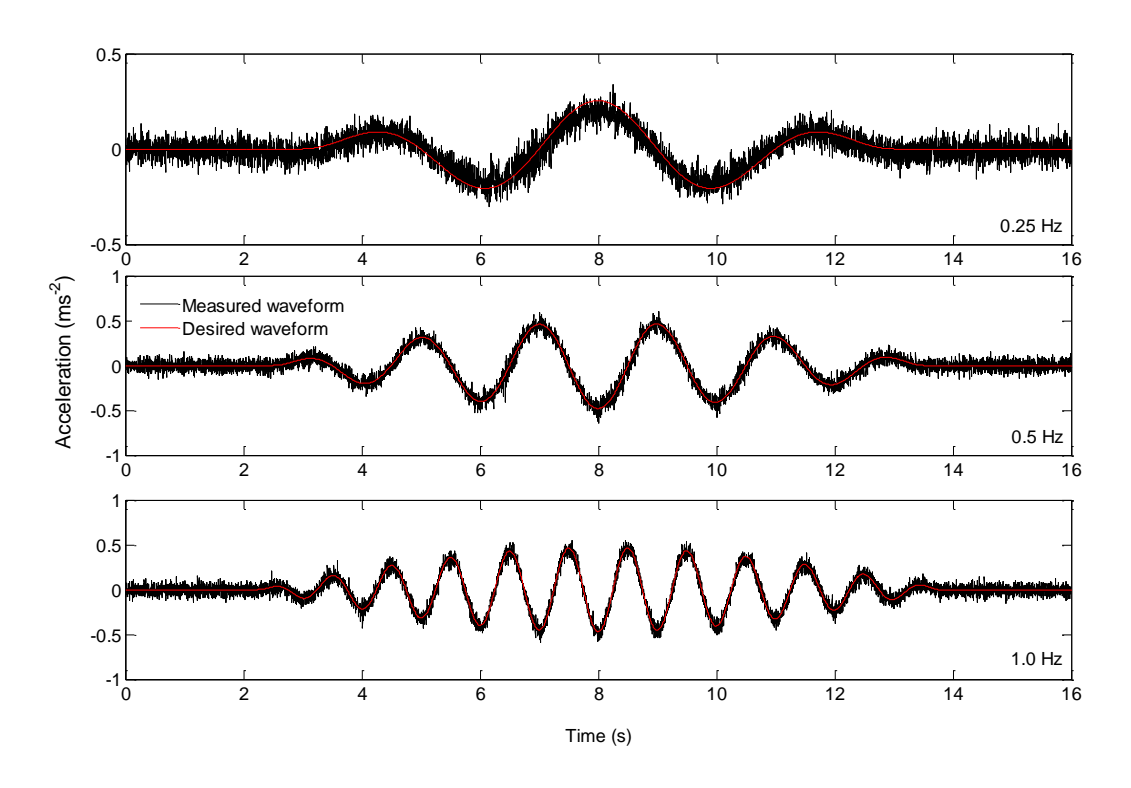


Figure 3.9 Comparison of desired and measured lateral acceleration waveforms at 0.25, 0.5 and 1.0 Hz used in Experiment 2 (1-m horizontal simulator).

3.3.1.3.2. <u>1-m horizontal simulator</u>

Distortion on the 1-m horizontal simulator was calculated using sinusoidal lateral acceleration at each of eight preferred one-third octave centre frequencies from 0.2 to 1.0 Hz at three magnitudes (low, medium and high). Accelerations were recorded in the range 0 to 128 Hz and sampled at 256 Hz. Typical lateral accelerations (ms⁻² r.m.s.) measured on the platform and the corresponding percentage error (Equation 3.2) for each frequency of lateral oscillation are shown in Table 3.2. Example acceleration waveforms for 0.2, 0.5 and 1.0 Hz motion are shown in Figure 3.9. (Note: because the waveforms are transient and not pure tones, frequencies other than those stated will be present in the spectrum).

Table 3.2 Percentage error calculations (*W*_d-weighted error / measured acceleration x 100) for each frequency of lateral oscillation used in Experiment 2.

Frequency (Hz)	Target acceleration (ms ⁻² r.m.s.)	Measured acceleration (ms ⁻² r.m.s.)	Error (ms ⁻² r.m.s.)	W _d - weighted error (ms ⁻² r.m.s.)	Error (%)
	0.1	0.092	0.046	0.006	6.522
0.2	0.2	0.171	0.061	0.009	5.263
	0.25	0.203	0.069	0.011	5.419
	0.1	0.094	0.047	0.008	8.511
0.25	0.2	0.176	0.016	0.015	8.738
	0.4	0.341	0.011	0.028	8.211
	0.1	0.104	0.049	0.008	7.692
0.315	0.2	0.177	0.013	0.016	9.202
	0.4	0.357	0.087	0.027	7.563
	0.1	0.104	0.042	0.006	5.769
0.4	0.2	0.196	0.047	0.010	5.102
	0.4	0.386	0.060	0.017	4.404
	0.1	0.109	0.047	0.007	6.422
0.5	0.2	0.203	0.050	0.009	4.433
	0.4	0.397	0.053	0.011	2.771
	0.1	0.108	0.049	0.008	7.407
0.63	0.2	0.202	0.028	0.015	7.556
	0.4	0.392	0.055	0.025	6.439
	0.1	0.109	0.047	0.006	5.505
0.8	0.2	0.199	0.028	0.013	6.347
	0.4	0.389	0.054	0.025	6.488
	0.1	0.112	0.050	0.006	5.357
1	0.2	0.205	0.047	0.006	2.927
	0.4	0.395	0.048	0.012	3.038

3.3.1.3.3. <u>6-axis simulator</u>

For Experiment 3, 4 and 5 (Chapter 6, 7 and 8), distortion on the 6-axis simulator was calculated for lateral and roll signals at each of seven preferred one-third octave centre frequencies from 0.25 to 1.0 Hz at three magnitudes. Accelerations were recorded in the range 0 to 128 Hz and sampled at 256 samples per second. Typical lateral accelerations (ms⁻² r.m.s.) measured in the plane of the seat surface during lateral oscillation and roll oscillation on the platform and the corresponding percentage error for each frequency of lateral and roll oscillation are shown in Table 3.3 and Table 3.4, respectively. Example acceleration time histories for

0.25, 0.5 and 1.0 Hz lateral and roll motion are shown in Figure 3.10 and Figure 3.11, respectively. (Note: because the waveforms are transient and not pure tones, frequencies other than those stated will be present in the spectrum).

Table 3.3 Percentage error calculations (W_d -weighted error / measured acceleration x 100) for each frequency of lateral oscillation used in Experiment 3, 4 and 5.

Frequency (Hz)	Target acceleration (ms ⁻² r.m.s.)	Measured acceleration (ms ⁻² r.m.s.)	Error (ms ⁻² r.m.s.)	W _d - weighted error (ms ⁻² r.m.s.)	Error (%)
	0.100	0.103	0.018	0.006	6.158
0.250	0.160	0.163	0.020	0.008	5.050
	0.200	0.203	0.026	0.013	6.363
	0.100	0.103	0.019	0.009	8.561
0.315	0.200	0.203	0.030	0.015	7.601
	0.315	0.316	0.039	0.026	8.149
	0.100	0.104	0.020	0.008	7.971
0.400	0.200	0.205	0.026	0.014	6.828
	0.400	0.408	0.042	0.030	7.279
	0.100	0.105	0.021	0.011	10.067
0.500	0.200	0.208	0.029	0.020	9.510
	0.400	0.414	0.055	0.048	11.629
	0.100	0.103	0.016	0.005	4.840
0.630	0.200	0.205	0.021	0.008	3.991
	0.400	0.409	0.027	0.015	3.591
	0.100	0.104	0.020	0.010	9.119
0.800	0.200	0.207	0.029	0.018	8.465
	0.400	0.410	0.056	0.049	11.905
	0.100	0.104	0.020	0.006	6.242
1.000	0.200	0.206	0.026	0.012	5.647
	0.400	0.410	0.036	0.019	4.746

Table 3.4 Percentage error calculations (*W*_e-weighted error / measured acceleration x 100) for each frequency of roll oscillation used in Experiment 3, 4 and 5.

Frequency (Hz)	Target acceleration (ms ⁻² r.m.s.)	Measured acceleration (ms ⁻² r.m.s.)	Error (ms ⁻² r.m.s.)	W _e - weighted error (ms ⁻² r.m.s.)	Error (%)
	0.100	0.101	0.012	0.003	3.201
0.250	0.160	0.161	0.014	0.004	2.392
	0.200	0.202	0.018	0.006	3.223
	0.100	0.102	0.015	0.004	3.814
0.315	0.200	0.202	0.017	0.005	2.561
	0.315	0.318	0.027	0.008	2.501
	0.100	0.100	0.014	0.004	3.944
0.400	0.200	0.198	0.021	0.006	3.205
	0.400	0.396	0.033	0.020	5.126
	0.100	0.103	0.018	0.005	4.731
0.500	0.200	0.203	0.022	0.006	3.112
	0.400	0.406	0.032	0.014	3.440
	0.100	0.102	0.021	0.007	6.762
0.630	0.200	0.202	0.026	0.011	5.453
	0.400	0.403	0.045	0.020	4.929
	0.100	0.120	0.027	0.012	9.771
0.800	0.200	0.235	0.021	0.018	7.801
	0.400	0.422	0.029	0.037	8.752
	0.100	0.114	0.032	0.013	11.626
1.000	0.200	0.221	0.044	0.024	10.835
	0.315	0.349	0.075	0.041	11.819

3.3.1.4. Motion measurement

In Experiment 1 (Chapter 4), horizontal acceleration was measured at three locations (see Figure 3.6) using Setra Systems capacitive accelerometers (type 141A) mounted to the chassis of the simulator carriage, on the cabin wall at the mechanical pivot point, and on the cabin wall 800 mm above the mechanical pivot point.

In Experiment 2 (Chapter 5), horizontal acceleration was measured using a Sundstrand Data Control Inc. accelerometer (type QA 800) fixed to the platform of the 1-m horizontal simulator.

In Experiments 3, 4 and 5 (Chapter 6, 7 and 8) acceleration was measured in three translational axes (fore-and-aft, lateral and vertical) and three rotational axes (roll, pitch and yaw) using FGP (Measurement Specialities) micro-machined silicon sensors (type FA101A2) fixed to the platform of the 6-axis simulator. Additionally, lateral acceleration in the plane of the seat, and

rotational velocity at the seat surface was measured using a Silicon Design capacitive micromachined translational accelerometer (type 2260) and a BAE Systems single-axis VSG bipolar rotational gyro, respectively.

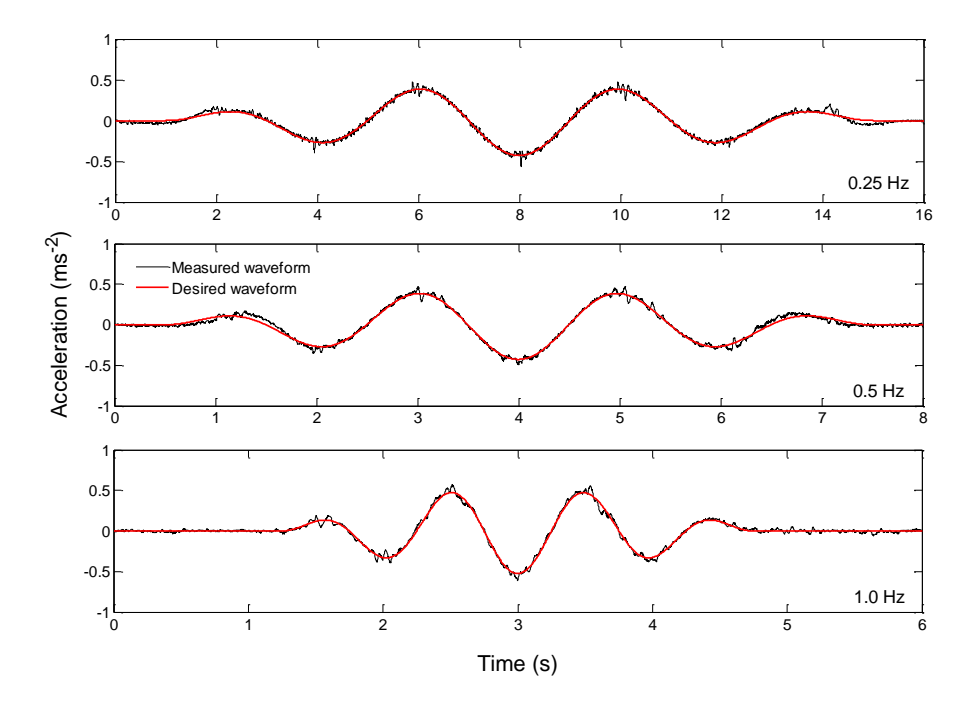


Figure 3.10 Comparison of desired and measured lateral acceleration waveforms for lateral oscillation at 0.25, 0.5 and 1.0 Hz used in Experiment 3, 4 and 5 (6-axis simulator).

In Experiment 4 (Chapter 7), lateral acceleration and rotational velocity was also measured at the seat-body interface between the foam cushion and the ischial tuberosities using a Seat Interface for Transducers indicating Body Acceleration Received (SIT-BAR; see Figure 3.12), which consisted of a translational piezo-resistive Endevco accelerometer (type 2265) and a BAE System single-axis VSG bipolar rotational gyro.

After amplification (using HFRU-ISVR built accelerometer amplifiers) the measured acceleration signals were interfaced with the computer via a 16-channel breakout-box (Laplace Instruments) and were subsequently low-pass filtered at 2 Hz (Experiment 1) or 50 Hz (Experiment 2 – 5) using an anti-aliasing filter PC card (Techfilter) prior to A/D conversion.

Where possible, transducers were calibrated using the gravity acceleration (±1 g) and had a DC response.

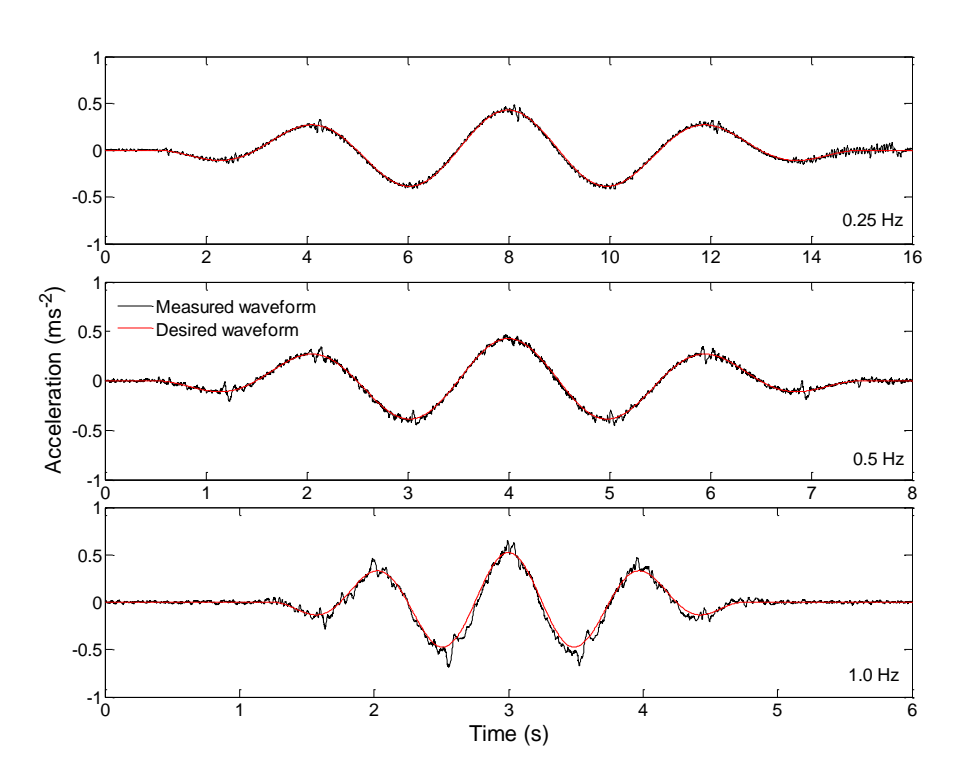


Figure 3.11 Comparison of desired and measured lateral acceleration waveforms for roll oscillation at 0.25, 0.5 and 1.0 Hz used in Experiment 3, 4 and 5 (6-axis simulator).

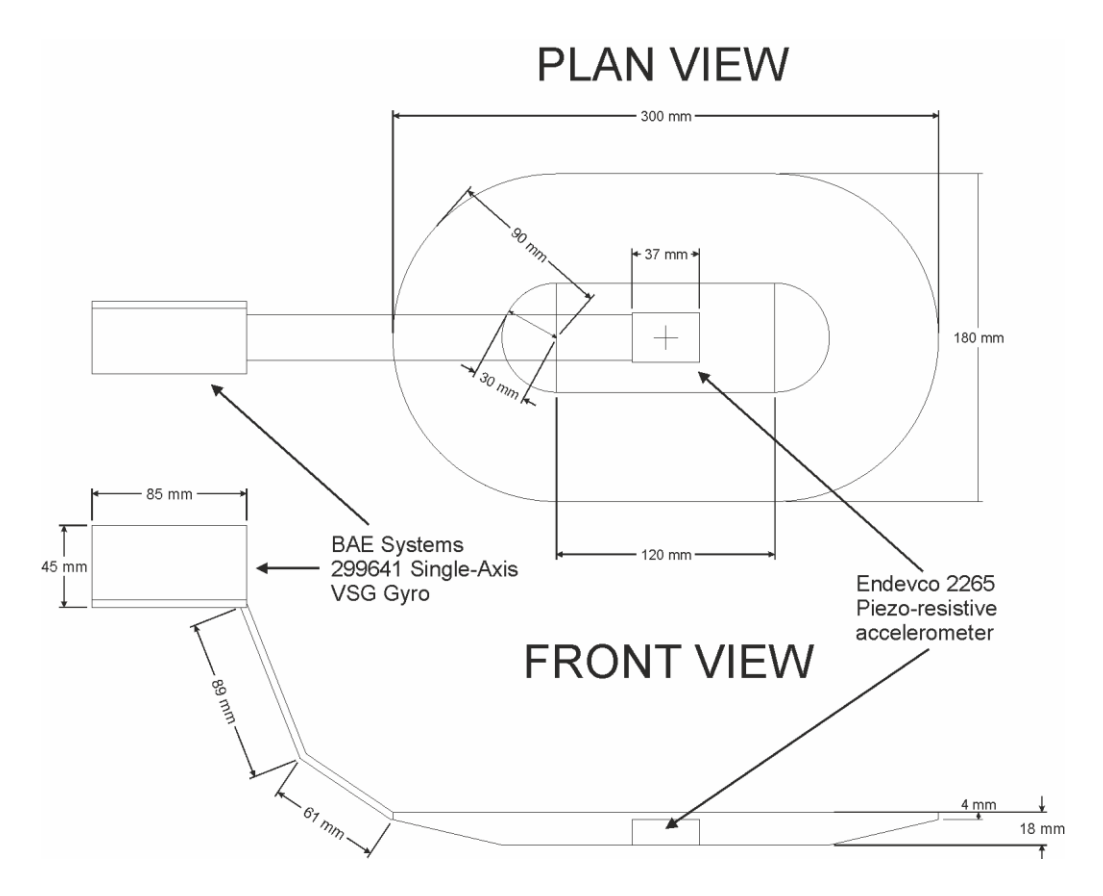


Figure 3.12 Annotated illustration of SIT-BAR used to measure translational and rotational motion at the seat-buttock interface (adapted from Whitham and Griffin, 1977).

3.3.2. Visual field

The visual field may affect the perception of vibration at low frequencies (e.g. Moxley *et al.*, 2012) and the development of motion sickness with combined translation and rotation (e.g. Butler, 2008). In all five experiments, therefore, subjects were required to close their eyes during motion exposure in order to limit variability in subjective responses due to vision.

3.3.3. Noise

Audible noise was an inevitable by-product associated with the generation of motion stimuli on all three motion simulators. With the simulators powered on and idling, the sound pressure level (SPL) of this noise when measured at the location of the subjects was 58.2 dB(A) on the 12-m tilting and translating cabin, 53.1 dB(A) on the 1-m horizontal simulator and 44.3 dB(A) on the 6-axis simulator.

'White' noise is a type of noise that combines all the different frequencies of sound, so it is useful to mask other noises. Therefore in order to mask the unwanted simulator noise, subjects

in all five experiments wore headphones producing white noise at 65 dB(A). White noise was produced using a bespoke HFRU Noise System designed by the Human Factors Research Unit at the University of Southampton. The SPL of the white noise was calibrated according to British Standard 11904⁻² (2004) using a 'Kemar' (Knowles Electronics Manikin for Acoustic Research) consisting of an artificial ear (GRAS Type IEC 700) with an embedded microphone (GRAS Type 40AG), a calibrator (Brüel & Kjær Type 4231) and a sound level meter (Brüel & Kjær Type 2250). The SPL was determined by A-weighting (BS ISO 10845, 1995) the one-third octave band spectra of the sound waves measured by the B&K sound level meter.

In all experiments, the experimenter communicated with subjects via a microphone connected to the headphones which interrupted the white noise.

3.4. Psychophysical methods

3.4.1. Motion sickness

In the first experiment, three quantities of motion sickness were assessed: (1) motion sickness susceptibility; (2) the development of motion sickness symptoms, and; (3) the type of motion sickness symptoms. The first quantity was obtained using a Motion Sickness Susceptibility Questionnaire (MSSQ) defined by Griffin and Howarth (2000). This 16-part questionnaire is used to calculate nine measures of motion sickness susceptibility relating to the proportion of illness experienced in previous journeys on land and non-land vehicles (see Table 3.5). An example copy of the MSSQ can be found in the Appendices. The procedure for calculating these measures is detailed by Griffin and Howarth (2000). The MSSQ was completed by all subjects in Experiment 1 prior to motion exposure.

Table 3.5 Measures of motion sickness susceptibility (Griffin and Howarth, 2000).

Measures of motion sickness susceptibility	Code
Travel frequency in the past year	T _(yr.)
Illness frequency while travelling in the past year	Itravel(yr.)
Vomiting frequency while travelling in the past year	V _{travel(yr.)}
Illness susceptibility in transport in the past year	I _{susc.(yr.)}
Vomiting susceptibility in transport in the past year	V _{susc.(yr.)}
Total susceptibility to vomiting	V_{total}
Total susceptibility to motion sickness	<i>M</i> total
Susceptibility to motion sickness in land transport	Mand
Susceptibility to motion sickness in non-land transport	M _{nland}

The development of motion sickness and the type of motion sickness symptoms were assessed using a 7-point illness rating scale (Table 3.6) and 10-item symptom checklist (Table 3.7), respectively, defined by Griffin and Howarth (2000). The illness rating (IR) scale ranges from 0 (no symptoms) to 6 (moderate nausea, and want to stop). Illness ratings were obtained every minute for a 5-minute acclimatisation period, a 30-minute exposure period, and a 15-minute recovery period. If subjects indicated an illness rating of 1 or higher, they were asked to list which of the 10 symptoms on the symptom checklist they were experiencing. The symptom checklist was also completed at the end of the 15-minute recovery period.

Table 3.6 Illness rating (IR) scale used in Experiment 1.

Rating	Corresponding feelings		
0	No symptoms		
1	Any symptoms, however slight		
2	Mild symptoms		
3	Mild nausea		
4	Mild to moderate nausea		
5	Moderate nausea but can continue		
6	Moderate nausea and want to stop		

Table 3.7 Symptom Checklist used in Experiment 1.

Motion sickness symptoms				
Yawning	Bodily warmth			
Increased salivation	Stomach awareness			
Cold sweating	Dizziness			
Headache	Dry mouth			
Nausea	Drowsiness			

3.4.2. Vibration discomfort

3.4.2.1. The method of magnitude estimation

The four experiments investigating vibration discomfort (Chapter 5, 6, 7 and 8) utilised the method of magnitude estimation. In magnitude estimation tasks, subjects are exposed to a stimulus (i.e. a vibration) and required to assign a numerical value reflecting the subsequent subjective sensation (i.e. discomfort). As described in Section 2.7.2.3, magnitude estimation may be used with or without a reference. With a reference, subjects are required to assign numerical values to describe the discomfort caused by a series of test stimuli relative to a reference stimulus (usually constant throughout the experiment). Typically the magnitude of the reference motion is selected such that it falls approximately in the middle of the full range of magnitudes used (Stevens, 1975). Without a reference, subjects are required to assign any numerical value which they feel is appropriate to describe the discomfort caused by each test vibration.

In Experiment 2 and 3 (Chapter 5 and 6), the method of magnitude estimation with a reference was used. In both cases, a 0.5 Hz lateral motion at 0.2 ms⁻² r.m.s. was selected as the reference. However, in Experiment 4 and 5 (Chapter 7 and 8), the method of magnitude estimation was used without a reference. Due to the number of conditions tested in these two experiments, it was convenient to reduce the duration of the experimental procedure (i.e. by removing the reference). The validity of using magnitude estimation without a reference has been demonstrated previously (Green and Luce, 1974; Stevens, 1975; Zwislocki and Goodman, 1980).

Since motions at frequencies less than 1 Hz can cause both motion sickness and physical discomfort (see Chapter 2), three steps were taken to ensure that the subjective ratings of physical discomfort obtained in Experiments 2 to 5 (Chapter 5 to Chapter 8) were not influenced by sensations of motion sickness. Firstly, the order in which motion signals were presented was fully randomised in the discomfort experiments. Motions at around 0.2 Hz are most provocative of motion sickness, with sensitivity decreasing with increasing frequency (see Chapter 2). Randomisation of the presentation order avoids sequential exposure to the lowest frequencies, therefore reducing the likelihood of motion sickness. Secondly, the discomfort experiments utilised short duration motion stimuli (approximately 12 seconds in Experiment 2 - Chapter 5 - and 3.5 cycles in Experiment 3 to 5 - Chapter 6 to Chapter 8), and frequent rest breaks. Lastly, as a quality control in case the first two steps were not effective, subjects were asked whether they experienced motion sickness symptoms during exposure to motion in the discomfort

experiments. The influence of motion sickness bias on discomfort ratings is discussed further in section 9.5.2.

3.4.2.2. Stevens' power law

Stevens' power law (Stevens, 1975) was used to relate the subjective magnitude estimates (Ψ) obtained in Experiment 2 - 5 (Chapter 5 - 8) to the physical acceleration magnitudes of vibration stimuli (Φ), as shown in Equation 3.3:

Equation 3.3:
$$\psi = k \varphi^n$$

where the exponent (n) is the rate of growth of vibration discomfort and k is a constant. Logarithmic transformation of this equation allows the exponent n and the constant k to be determined through a linear regression:

Equation 3.4:
$$\log_{10} \psi = \log_{10} k + n \log_{10} \varphi$$

In the vibration discomfort experiments, each frequency of motion was presented at, nominally, eight acceleration magnitudes (except where simulator limitations restricted this range - see Chapter 5 - 8). Estimates of k and n could therefore be obtained for each frequency, subject and direction of motion using values of $log_{10}(\Psi)$ and $log_{10}(\Phi)$ obtained in each experiment. The physical acceleration magnitude (Φ) corresponding to a given subjective magnitude (Ψ) (i.e. 50, 63, 80, 100, 125, 160 and 200) were then determined using Equation 3.5:

Equation 3.5:
$$\varphi = [\psi / k]^{(1/n)}$$

Equivalent comfort contours were constructed by plotting the acceleration magnitude required to produce a given subjective magnitude (i.e. 50, 63, 80, 100, 125, 160 or 200) as a function of frequency.

There are three different methods which can be used to construct median equivalent comfort contours: (1) performing linear regressions on individual sets of magnitude estimates for each subject and using Equation 3.5 with individual n and k estimates; (2) performing linear regressions on individual sets of magnitude estimates for each subject and using Equation 3.5 with median n and k estimates pooled across all subjects; or (3) performing linear regressions on median magnitude estimates pooled across all subjects and using Equation 3.5 on the resultant pooled n and k estimates. The third option has the added benefit of more available data points for the linear regression, but for Experiment 2, 3, 4 and 5 the first option was selected because it allows for appropriate statistical testing on the rates of growth of discomfort n and equivalent comfort contours.

3.5. Statistical power and subject sampling

3.5.1. Subjects

All subjects were volunteers recruited from the staff and student population of the University of Southampton, Southampton, United Kingdom. In order to limit any variability due to gender and age (e.g. Bos *et al.*, 2007), subject samples were predominantly limited to males aged 18 to 35 years old (except for Experiment 3 – Chapter 6 – where both males and females were tested in order to assess the effects of gender). All subjects completed a health questionnaire before testing (see Appendix A.1.). Full details of the 143 subjects tested across the five experiments are provided in Appendix A.6. Median and inter-quartile data for the subjects is shown in Table 3.8.

Table 3.8 Median (inter-quartile range) age, height and weight of subjects tested in each experiment.

Experiment	No. of subjects	Age (years)	Stature (m)	Weight (kg)
1	60	24.0 (3.0)	1.75 (0.09)	70.0 (13.6)
2	12	25.5 (2.8)	1.75 (0.10)	70.9 (22.0)
3	30	27.0 (4.8)	1.69 (0.08)	61.6 (16.6)
4	20	26.0 (5.8)	1.79 (0.10)	63.1 (17.5)
5	21	25.0 (7.0)	1.76 (0.09)	73.4 (18.4)
All	143	25.0 (5.0)	1.75 (0.11)	67.0 (16.9)

3.5.2. Sample power

The statistical power refers to the probability that a statistical test will be able to correctly reject the null hypothesis, thereby avoiding a Type II error (a false negative). The statistical power for the five experiments described in this thesis (Chapter 4 - 8) was calculated on the basis of previous similar research (see Table 3.9). Mean illness ratings during exposure to 0.2 Hz uncompensated lateral oscillation and 0.2 Hz fully roll-compensated lateral oscillation (Donohew, 2006), equivalent comfort contours for lateral oscillation on a rigid seat with and without backrest (Wyllie, 2008), and equivalent comfort contours for lateral and roll oscillation on a rigid seat with backrest (Wyllie, 2008) were used to estimate statistical power for Experiment 1, Experiment 2, 4 and 5, and Experiment 3, respectively. Because there is no simple method of calculating power for non-parametric statistics, power calculations were made on the basis of equivalent parametric tests.

3.6. Data analysis

3.6.1. Software

Microsoft Excel 2010 was used to record and process the subjective data. IBM SPSS Statistics (version 19) was used for statistical analysis of the data. Mathworks MATLAB (version R2010a) and Systat Inc. SigmaPlot (version 11) were used for graphical illustration of the results. IBM SamplePower (version 3) was used to compute estimates of statistical power. The *HVLab* toolbox (version 1.1; developed by the Human Factors Research Unit, University of Southampton) within MATLAB was used for signal processing.

Table 3.9 Parameters used to calculate statistical power for subject samples used in Experiment 1 to 5.

Experiment number	Number of subjects	Test	Mean difference	Pooled standard deviation	Significance level	Power	Data source
1	60	Independent samples t- test*	0.8	1.4	0.05	0.61	Donohew (2006)
2	12	Paired samples t-test#	0.1	0.2	0.05	0.72	Wyllie (2008)
3	30	Paired samples t- test [%]	0.2	0.2	0.05	0.99	Wyllie (2008)
4	20	Paired samples t-test#	0.1	0.2	0.05	0.93	Wyllie (2008)
5	21	Paired samples t-test#	0.1	0.2	0.05	0.94	Wyllie (2008)

^{*} Difference between illness ratings with 0.2 Hz fully roll-compensated lateral oscillation and 0.2 Hz uncompensated lateral oscillation

3.6.2. Statistical tests

Alignment of the current data with the assumptions of parametric statistical tests could not be guaranteed; therefore non-parametric statistics were used for all five experiments (see Table 3.10).

[#] Difference between discomfort due to lateral oscillation on a rigid seat with and without backrest

 $^{\% \ \}mathsf{Difference} \ \mathsf{between} \ \mathsf{discomfort} \ \mathsf{due} \ \mathsf{to} \ \mathsf{lateral} \ \mathsf{oscillation} \ \mathsf{and} \ \mathsf{roll} \ \mathsf{oscillation} \ \mathsf{on} \ \mathsf{a} \ \mathsf{rigid} \ \mathsf{seat} \ \mathsf{with} \ \mathsf{backrest}$

Difference between *n* related

binary variables

Experiment Test **Purpose** Difference between 2 Mann-Whitney U test independent groups 1 Influence of multiple Cox regression (survival variables on a single timeanalysis) dependent variable Correlation between 2 Spearman rank-order correlation coefficient variables Wilcoxon matched pairs Difference between 2 related variables test 2, 3, 4, 5 Difference between n related Friedman two analysis of variables variance Difference between 2 related McNemar change test binary variables

Table 3.10 List of statistical tests used in Experiments 1 - 5.

3.7. Safety and ethics

5

All the experiments were approved by the Ethics Committee of the Faculty of Engineering and The Environment at the University of Southampton. All subjects were paid volunteers recruited from the staff and student population of the University of Southampton, who gave full informed consent before participating (see consent from in Appendix A.1. and subject instructions in Appendix A.4.). Subjects were free to terminate the experiment at any time without consequence or needing to provide a reason.

Cochran's Q test

Full risk assessments were performed for each experiment and approved by the appropriate Safety Officer before the commencement of research.

Chapter 4

Effects of position of full roll-compensation and subject demographics on motion sickness

4.1. Introduction

Motion sickness is characterised by an unpleasant combination of symptoms, including pallor, sweating, nausea and vomiting (Treisman, 1977). Symptoms may be caused by translational or rotational motion of the body, or by visual stimulation with no motion of the body (Griffin, 1990).

Passengers in tilting trains and some other forms of transport experience motions that can provoke motion sickness. When travelling at speed and turning to the left or right, the resultant lateral forces can be reduced by 'tilting into the turn'. When traversing a curve in a tilting train, this is known as 'compensation', because the gravitation force arising from a roll to the left 'compensates' for a lateral centripetal force to the right, and vice versa.

Whilst the incidence of motion sickness on non-tilting trains may be low (e.g. Kaplan, 1964; Ueno *et al.*, 1986), reports of sickness on high-speed tilting vehicles suggest tilt compensation increases motion sickness (e.g., Ueno *et al.*, 1986; Bromberger, 1996; Förstberg *et al.*, 1998; Suzuki *et al.*, 2005; Donohew and Griffin, 2007; 2009; Persson, 2010). On the Swedish X2000 tilting train, 14.5% of passengers reported sickness with 70% tilt-compensation, but there was less sickness with 55% compensation (Förstberg *et al.*, 1998). Lateral motions in the frequency range 0.25 to 0.32 Hz have been reported to be particularly provocative of sickness (Suzuki *et al.*, 2005). In Japanese passively-tilted high curve speed rail vehicles, where horizontal

acceleration is greatest at frequencies less than 1 Hz, nausea was reported by 26% of passengers compared to 4% of passengers in non-tilting vehicles where acceleration is greatest at frequencies higher than 1 Hz (Ueno *et al.*, 1986). Laboratory studies have found that fully roll-compensated lateral oscillation (i.e., 100% tilt compensation) is more provocative of motion sickness than lateral oscillation presented without the compensation, with some evidence of greatest sensitivity to acceleration around 0.2 Hz (Donohew and Griffin, 2009).

The sensory rearrangement theory states that motion sickness arises from conflict between, or within, the visual and vestibular systems (Reason and Brand, 1975). Intra-sensory conflict within the vestibular system (arising from an unusual combination of stimulation of the otoliths and the semi-circular canals) will occur with combined lateral and roll motion of the head. Without lateral acceleration, roll movements of the head stimulate both the semi-circular canals and the otoliths in a way normally interpreted as head rotation. With lateral acceleration, if the head rolls so as to 'fully compensate' for the lateral acceleration, the semi-circular canals will respond to the roll without the normally expected otolithic response (because the gravitational component arising from the roll offsets the component arising from the lateral acceleration). This allows two alternative, and conflicting, interpretations of the motion based either on the response from the semi-circular canals (i.e. roll motion) or the response from the otoliths (i.e. no roll).

Previous research has investigated how motion sickness depends on the frequency, the magnitude, and the phase of combined lateral and roll oscillation when full compensation occurs at the seat surface (Joseph and Griffin, 2007; 2008; Donohew and Griffin, 2009). In those studies, the roll motions were selected to produce the gravitational forces required to compensate the lateral acceleration at the seat, and they were therefore not of the magnitude required to compensate the lateral acceleration at the head, resulting in some otolithic stimulation even in 'fully compensated' conditions. No previous experiment has investigated the motion sickness associated with roll-compensated lateral oscillation with the position of full roll-compensation at head height. Passively-tilted trains tend to have higher pivot points than actively-tilted trains (Hitachi, 2009), which may influence the position of full roll-compensation, and it has been suggested that there is a greater incidence of sickness with passive tilting (Bromberger, 1996). It is therefore of practical importance to understand the extent to which the position of full roll-compensation influences motion sickness.

Factors that influence the motion sickness susceptibility of passengers have been investigated in various forms of transport (Lawther and Griffin, 1986; 1988; Turner and Griffin, 1999; 2000). Females have been found more susceptible to motion sickness than males among 20,029 passengers on ships (Lawther and Griffin, 1988), 3,256 road coach passengers (Turner and

Griffin, 1999), and 923 aircraft passengers (Turner *et al.*, 2000). A pattern of decreasing susceptibility with increasing age has also been reported (Lawther and Griffin, 1988; Turner and Griffin, 1999).

The motion sickness caused by roll-compensated lateral oscillation is dependent on the frequency, the magnitude, and the duration of the motion, the characteristics of passengers, and the transport environment, but there is currently insufficient understanding to develop a predictive model showing the influence of all of these factors on motion sickness. One aim of the experiment reported here was to determine whether the sickness caused by roll-compensated lateral oscillation differed when full compensation was achieved at the seat surface or at the head, in order to establish whether this aspect of the design of tilting trains (i.e. the height of the centre-of-roll), influences the motion sickness of rail passengers. It was hypothesised that sickness would be greater when full compensation occurred at the head than when full compensation occurred at the seat. The study was also designed to investigate whether three passenger characteristics that have rarely been considered (ethnic origin, stature, and body weight) influence susceptibility to motion sickness.

4.2. Method

4.2.1. Apparatus

Motions were produced using a simulator capable of 12 metres of lateral oscillation and up to 10 degrees of roll oscillation in the Human Factors Research Unit of the Institute of Sound and Vibration Research at the University of Southampton.

Subjects sat on a first-class train seat inside a closed simulator cabin (2.0 m high x 1.9 m wide x 1.3 m deep) with no external view. Subjects sat blindfolded in relaxed upright postures with the backrest and headrest supporting their upper-body, their hands on their laps, and feet flat on the floor. A loose lap belt was worn for safety.

Subjects were headphones producing white noise at 65 dB(A) to mask noises of the simulator. The experimenter communicated with subjects via the headphones by interrupting the white noise. Subjects were monitored via a video camera.

4.2.2. Design

The study used an independent groups (between-subjects) design. Subjects were assigned alternately to one of the two experimental conditions (i.e., 'seat compensation' or 'head

compensation'), resulting in 30 subjects per condition. Subjects were seated in the cabin for 50 minutes, including a 5-minute acclimatisation period, a 30-minute motion period, and a 15-minute recovery period. Subjects were tested one-at-a-time and experimental sessions lasted approximately one hour.

4.2.3. Motion stimuli

Two motion conditions were investigated using an independent samples (between-subjects) design. In one condition, combined lateral and roll oscillation provided full roll-compensation at the seat surface (i.e. 'seat compensation'). In the other condition, with very similar motions, full roll-compensation occurred at head height (i.e. 'head compensation').

Subjects were exposed to 0.2-Hz sinusoidal roll oscillation combined in-phase with 0.2 Hz sinusoidal lateral oscillation. When full roll-compensation was at the seat, ±7.3° of roll was combined with ±1.26 ms⁻² of lateral oscillation (i.e., the same motions employed in some previous research; Donohew and Griffin, 2009). When full roll-compensation was at the head, ±7.3° of roll was combined with ±1.41 ms⁻² of lateral oscillation. The head was assumed to be located 800 mm above the seat surface (the median sitting eye height for British men aged 19 to 45 years is 795 mm; Pheasant, 1996). The motions were measured throughout all exposures and found to be accurate to within 5%. The motions at the seat and at the head are shown in Table 4.1.

4.2.4. Subjects

The subjects were 60 healthy male staff and students of the University of Southampton aged between 18 and 30 years (median = 24.0, inter-quartile range, IQR = 3.0), with weights between 50 and 160 kg (median = 70.0, IQR = 14.9) and statures between 163 and 198 cm (median = 175.0, IQR = 9.8). Full details of the subject demographics can be found in the Appendices.

4.2.5. Measurement of motion sickness

The experiment utilised a 16-part motion sickness susceptibility questionnaire (*MSSQ*), a 7-point illness rating scale ranging from 0 ('no symptoms') to 6 ('moderate nausea and want to stop') and a symptom checklist identifying 10 common motion sickness symptoms (i.e., yawning, increased salivation, stomach awareness, bodily warmth, headache, nausea, dry mouth, cold sweating, dizziness and drowsiness) (Griffin and Howarth, 2000). The *MSSQ* was completed prior to motion exposure. Subjects then entered the simulator cabin and illness ratings were recorded every minute from 5 minutes before motion started, during the 30 minutes

of motion exposure, and during a 15-minute period after motion had ceased. If an illness rating of 1 ('any symptoms, however slight') or higher was given, subjects were asked to indicate the symptoms they were experiencing using the symptom checklist.

If subjects reported an illness rating of 6 before the end of the motion exposure, the motion was stopped, and a rating of 6 was assumed for the remaining motion period. The recovery period was defined as the 15-minute period commencing immediately after the cessation of motion: either after 35 minutes or after a subject reached an illness rating of 6.

At the end of the experiment, subjects completed a symptom checklist indicating which of the 10 symptoms, if any, they had experienced whilst in the cabin.

Table 4.1 Motion quantities for the two experimental conditions².

Condition	Frequency (Hz)	Earth-lateral displacement (± m)	Earth-lateral acceleration (± ms ⁻²)	Roll displacement (± degrees)	Resultant lateral acceleration at the head (± ms ⁻²)
1: Seat compensation	0.20	0.80	1.26	7.30	0.15
2: Head compensation	0.20	0.89	1.41	7.30	0.00

4.3. Results

4.3.1. Effect of position of full roll-compensation

4.3.1.1. Population demographics

Responses to the MSSQ indicated that 'total susceptibility to motion sickness', M_{total} (median = 8.0, IQR = 8.8) for the sample of 60 subjects was similar to the 'normal' population (Griffin and

² Desired motion quantities are shown here. See section 3.3.1.3.1 for full details of waveforms used.

Howarth, 2000). Between the two motion conditions, there were no significant differences in subject age, stature, weight, or motion sickness susceptibility (p > 0.30; Mann-Whitney U).

4.3.1.2. Illness ratings

In both conditions, illness ratings increased over the 30-minute motion exposures and decreased during the 15-minute post-motion period (Figure 4.1). Over the 30-minute exposures, mean illness ratings were greater with 'head compensation' (mean, M = 2.80, standard deviation, SD = 1.83) than with 'seat compensation' (M = 2.26, SD = 1.61), but the difference was not statistically significant (p = 0.23; Mann-Whitney U). Maximum illness ratings (i.e., the highest rating reported during motion) were also greater with head compensation (M = 3.90, SD = 1.92) than with seat compensation (M = 3.57, SD = 1.91), but the difference was also not statistically significant (p = 0.51; Mann-Whitney U). Similarly, more subjects reached the higher illness ratings with head compensation (Figure 4.2).

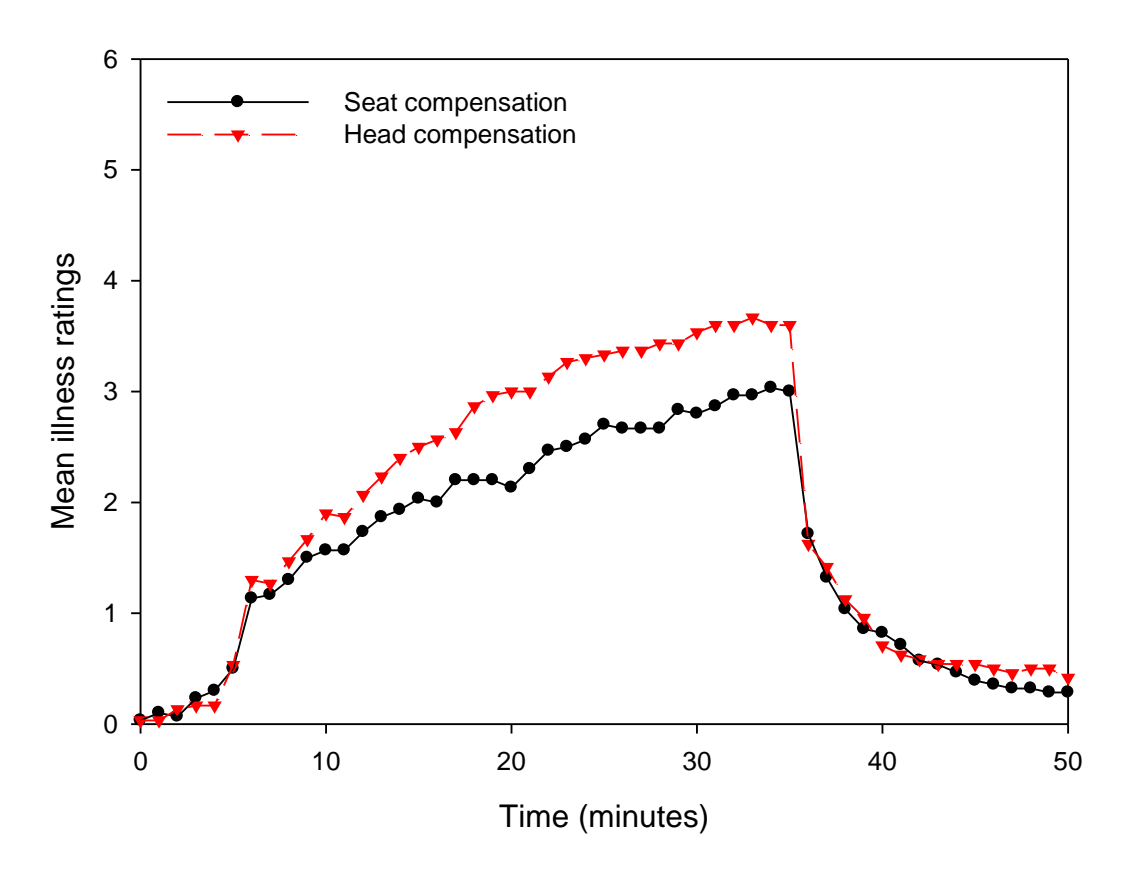


Figure 4.1 Mean illness ratings reported each minute for seat compensation and head compensation. Exposure to roll-compensated lateral oscillation occurred between 5 and 35 minutes.

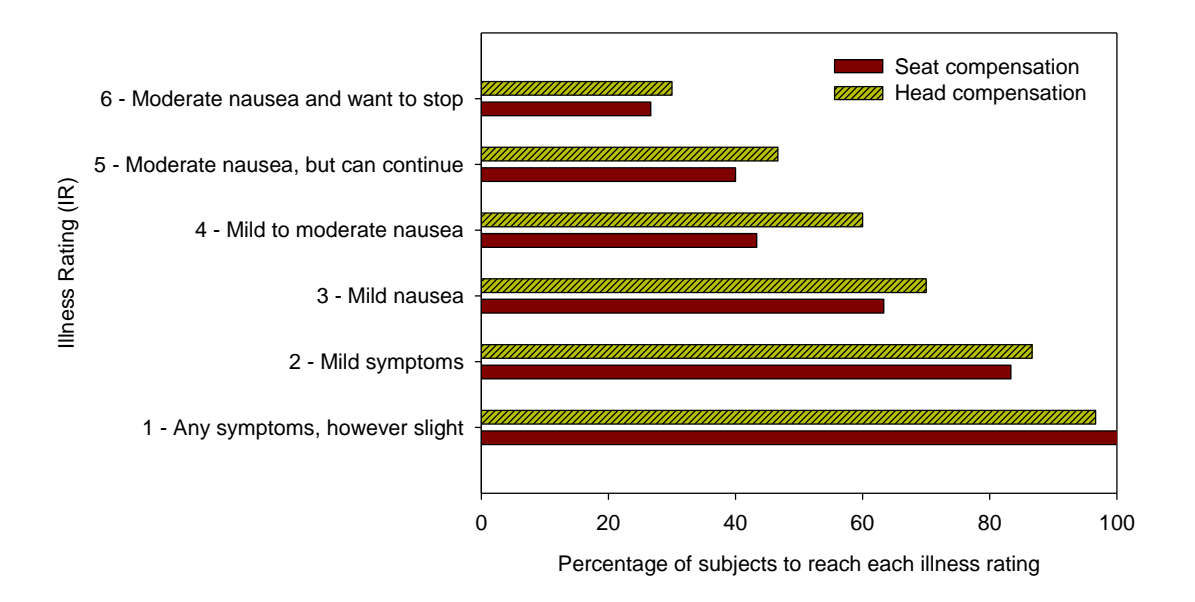


Figure 4.2 The percentage of subjects to reach each illness rating with seat compensation and head compensation.

4.3.1.3. Symptom scores

The total number of symptoms reported by each subject at the end of the study was taken as their 'total symptom score' (with a maximum of 10). The mean total symptom scores for the two conditions were similar (M = 5.00 and 5.03) and not significantly different (p = 0.93; Mann-Whitney U). 'Nausea' was reported by 77% of subjects experiencing 'head compensation' and by 67% of subjects experiencing 'seat compensation', with the difference not statistically significant (p = 0.39; Mann-Whitney U).

The total number of symptoms reported by each subject every minute over the duration of their motion exposure, divided by the duration of their exposure, was taken as their 'normalised cumulative total symptom score'. This measure compensates for a subject terminating exposure before the end of the planned 30-minute period. The 'normalised cumulative total symptom scores' were not significantly different between 'head compensation' (M = 1.72, SD = 1.07) and 'seat compensation' (M = 1.40, SD = 0.69, p = 0.28; Mann-Whitney U).

4.3.1.4. Recovery

A total of 17 subjects reported an illness rating of 6 (moderate nausea and want to stop) before the end of the 30-minute exposure to motion. Eight of these experienced seat compensation and nine experienced head compensation. The mean illness ratings at the end of the motion period were 3.00 for 'seat compensation' and 3.60 for 'head compensation', but not significantly different (p = 0.31; Mann-Whitney U). The mean illness ratings over the 15-minute recovery period were 0.62 for 'seat compensation' and 0.74 for 'head compensation', and not significantly different (p = 0.68; Mann-Whitney U). The mean illness ratings at the end of the 15-minute recovery period were 0.29 for 'seat compensation' and 0.42 for 'head compensation' and not significantly different (p = 0.31; Mann-Whitney U). (For eight subjects, two with seat compensation and six with head compensation, illness ratings were not obtained during recovery because they terminated the experiment, so their recovery data are not included in the analysis of mean illness ratings).

At the end of the recovery period, of the 52 subjects with recovery data, 82% of those experiencing 'seat compensation' reported an illness rating of 0, compared to 71% of those experiencing 'head compensation'.

4.3.2. Effects of subject characteristics

4.3.2.1. Population demographics

The 60 subjects were grouped based on their self-reported ethnic origin. Forty subjects reported their ethnic origin as Chinese, Indian or other Asian, and were thus grouped under the heading 'Asian'. Twenty subjects reported their ethnic origin as White British or European and were grouped under the heading 'European'. Fifty percent of the 'Asian' group experienced seat compensation and 50% experienced head compensation. Likewise, 50% of the 'European' group experienced seat compensation and the other 50% experienced head compensation. Subject age and height were not significantly different between Asian and European subjects (p = 0.06 and 0.15, respectively; Mann-Whitney U). Subject weight was significantly greater for Europeans (M = 75.15 kg, SD = 9.16) than for Asians (M = 70.09 kg, SD = 19.89, p < 0.01; Mann-Whitney U). No significant differences were found between Asian and European subjects for any of the six measures of motion sickness susceptibility (Griffin and Howarth, 2000), $I_{Susc.(yr.)}$, $V_{Susc.(yr.)}$, V_{total} , M_{hand} and M_{nland} (p > 0.35; Mann-Whitney U).

4.3.2.2. Illness ratings

For both the European and the Asian subjects, mean illness ratings increased over the 30-minute exposures to motion, and decreased during the 15-minute post-motion period (Figure 4.3). The mean illness ratings reported during the 30-minute exposures to motion were significantly greater for Asians (M = 3.01, SD = 1.74) than for Europeans (M = 1.57, SD = 1.27, P < 0.01; Mann-Whitney U). Likewise, maximum illness ratings were significantly greater for the

Asians (M = 4.33, SD = 1.83) than for the Europeans (M = 2.55, SD = 1.47, p < 0.001; Mann-Whitney U). This pattern was reflected in the percentage of Asian and European subjects to reach each illness rating (Figure 4.4).

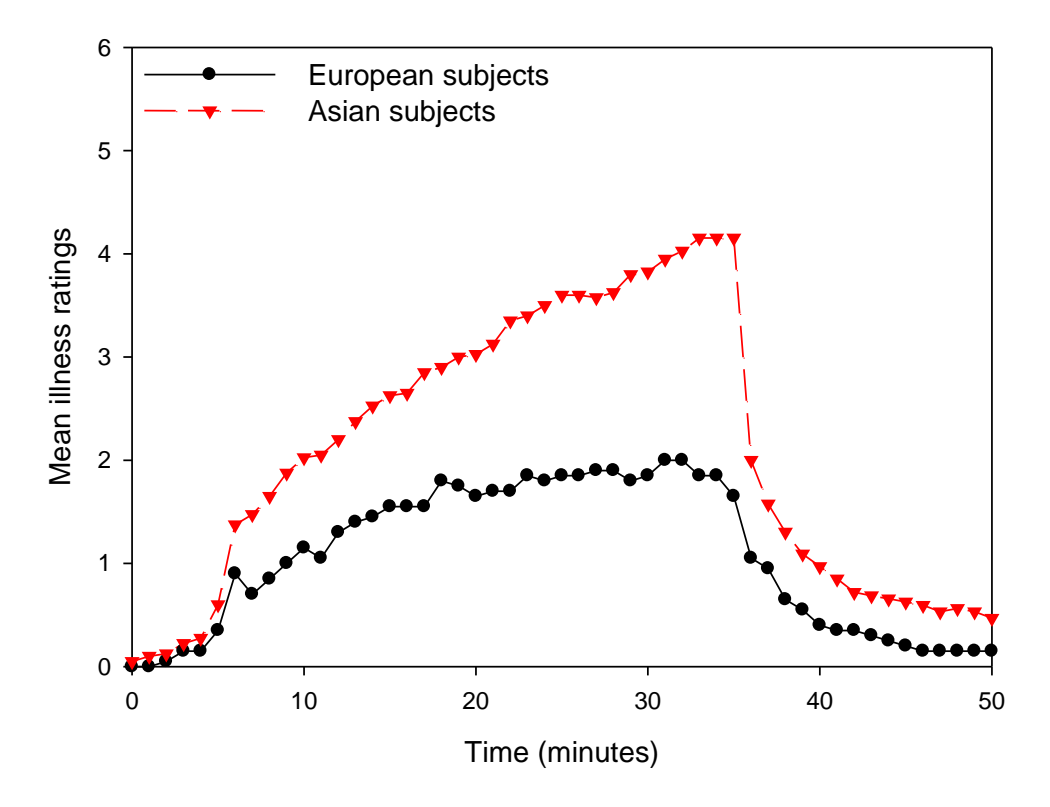


Figure 4.3 Mean illness ratings reported each minute by 20 European and 40 Asian subjects. Exposure to roll-compensated lateral oscillation occurred between 5 and 35 minutes.

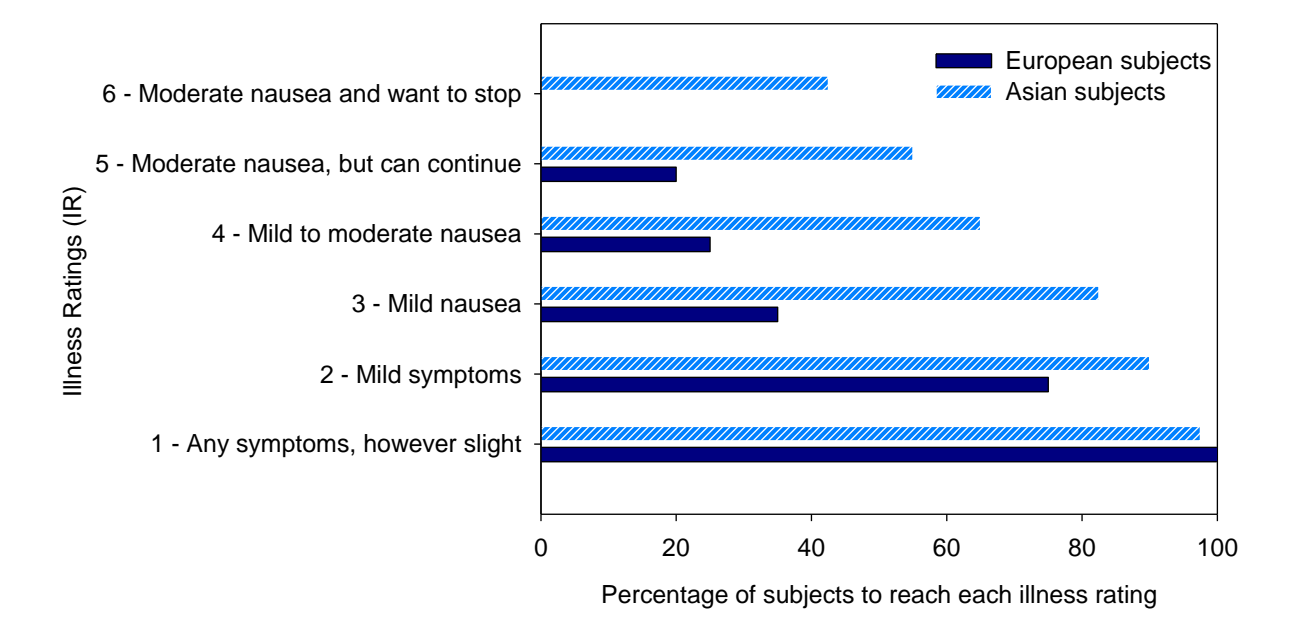


Figure 4.4 The percentage of European and Asian subjects to reach each illness rating.

4.3.2.3. Symptom scores

The 'total symptom scores' reported by Asians and Europeans at the end of their exposures to motion (M = 5.20 and 4.65, respectively) were not significantly different (p = 0.25; Mann-Whitney U). However, 80% of the Asians reported 'nausea' on the symptom checklist compared to 55% of the Europeans (p = 0.045; Mann-Whitney U).

The 'normalised cumulative total symptom scores' were significantly greater for Asians (M = 1.72, SD = 0.86) than for Europeans (M = 1.24, SD = 0.92) (p = 0.03; Mann-Whitney U).

4.3.2.4. Recovery

A total of 17 Asian subjects reported an illness rating of 6 (moderate nausea and want to stop) before the end of the 30-minute motion exposure. No European subjects reported an illness rating of 6 during the study.

During the recovery period, illness ratings decreased for both Asian and European subjects (Figure 4.3). The mean illness ratings at the end of the motion were 4.15 for Asians and 1.65 for Europeans, and significantly different (p < 0.001; Mann-Whitney U). The mean illness ratings over the 15-minute recovery period were 0.86 for Asians and 0.39 for Europeans, but not significantly different (p = 0.13; Mann-Whitney U). The mean illness ratings at the end of the 15-

minute recovery period were 0.47 for Asians and 0.15 for Europeans, and were marginally non-significantly different (p = 0.09; Mann-Whitney U). (For eight Asian subjects, illness ratings were not measured during the recovery period due to these subjects terminating the experiment, so these data were not included in the analysis of illness ratings during the recovery period).

At the end of the recovery period, of the 52 subjects for whom recovery period data were recorded, 90% of European subjects reported an illness rating of 0, compared with 69% of Asian subjects.

4.3.3. Survival analysis

A Cox regression survival analysis was used to examine the influence of the experimental conditions, subject age, stature, weight, and ethnic origin on the occurrence of the first report of illness rating 3 (mild nausea) during the 30-minute motion period. The covariates were entered into the Cox regression model simultaneously and the results are shown in Table 4.2. The Cox analysis revealed no significant influence of the experimental conditions (i.e. 'seat compensation' versus 'head compensation') on the probability of subjects reporting an illness rating of 3 ($e\beta$ = 1.167, p = 0.65). However, there was a threefold ($e\beta$ = 3.64) increase in the risk of reaching an illness rating of 3 for Asians compared to Europeans (p < 0.01). Subject age, stature, and weight did not significantly influence the likelihood of reaching an illness rating of 3 (mild nausea).

Table 4.2 Result of Cox regression analysis.

Predictor variable	Reference	Exp (β)	Significance level
Compensation at the head	Compensation at the seat	1.167	0.654
Age	-	1.056	0.462
Height	-	0.964	0.257
Weight	-	1.009	0.503
Asian ethnicity	European ethnicity	3.636	0.003

4.4. Discussion

4.4.1. Effect of position of full roll-compensation

The motion was provocative of motion sickness in both conditions, with more than 65% of subjects across both conditions reaching an illness rating of at least 3 ('mild nausea') (Figure 4.2). This is consistent with previous studies that have found fully roll-compensated lateral oscillation at 0.2 Hz highly provocative of sickness (Joseph and Griffin, 2007; Donohew and Griffin, 2009). The mean illness ratings increased rapidly after the start of motion (i.e., at 5 minutes) and decreased rapidly after cessation of motion (i.e. at 35 minutes) with the majority of subjects fully recovering before the end of the 15-minute recovery period. Previous studies with these motions have found similar patterns, consistent with this motion being associated with a quick onset and quick recovery of motion sickness symptoms (e.g. Joseph and Griffin, 2008).

Consistent with the hypothesis, mean illness ratings were greater when full compensation was at head height than when it was at the seat surface (Figure 4.1). However, analysis of both the illness ratings and the symptom scores showed that the differences in these measures of motion sickness between these two levels of compensation were not statistically significant, so the hypothesis was not substantiated. The findings suggest that any effect of increasing the height of the position of full roll-compensation from the level of the seat to 800 mm above the seat is small compared to other influences on motion sickness. However, the underlying model suggesting greater sickness with 100% compensation at the head than with 100% compensation at the seat has not been disproved, and it might be substantiated with greater numbers of subjects or greater control of other factors influencing sickness.

The study achieved 100% compensation at the seat and the head by combining ±7.3° of roll with each of two magnitudes of lateral acceleration (i.e., ±1.26 ms⁻² or ±1.41 ms⁻², respectively) (Table 4.1). It would also have been possible to achieve 100% compensation at the seat and the head by combining ±1.26 ms⁻² of lateral acceleration with each of two magnitudes of roll (i.e., ±7.3° or ±6.6°, respectively). The chosen conditions involved the same roll angle but increased translational acceleration when there was 100% compensation at the head. The increase in translational acceleration might be expected to increase sickness, but the increase in mean illness ratings was not statistically significant in this study. If instead, the experiment had been conducted with the same translational acceleration but reduced roll angle when there was 100% compensation at the head, it might be expected that the sickness would have been even less than reported in the current 'head compensation' condition (Joseph and Griffin, 2008),

and therefore even less likely to be significantly greater than with 100% compensation at the seat.

With 'head compensation', the resultant lateral acceleration at the head was not exactly zero, principally due to some distortion in the translational motion. In the octave band centred on 0.2 Hz, the resultant lateral acceleration measured 800 mm above the seat was ±0.18 ms⁻² with 'seat compensation' and ±0.07 ms⁻² with 'head compensation'. The difference of ±0.11 ms⁻² is probably greater than the threshold for detecting 0.2-Hz lateral oscillation, although thresholds for perceiving this type of motion are not well established and the detection of the oscillatory motion may be intermittent and not yield a clear perception of either the timing or the direction of the motion. Whether or not the difference was perceptible, the difference in otolithic stimulation between 'seat compensation' and 'head compensation' was not sufficient to cause a significant difference in sickness. The difference would be greater with greater magnitudes of oscillation and the position of full roll-compensation might then have greater influence on motion sickness.

In tilting railway vehicles, passengers experience lateral, vertical, and roll motions that are influenced by track geometry, vehicle suspension, and tilt mechanisms (Persson, 2010). The position of full roll-compensation associated with track cant will typically be lower than that associated with a carbody tilting mechanism. This study investigated the simplified situation where roll motion is used to compensate for lateral acceleration, with two alternative positions of full roll-compensation, but the difference in location was not selected to compare differences between track cant and carbody tilt. Reductions of lateral acceleration arising from the cant of the track and carbody tilt increase acceleration in a direction normal to the floor of the vehicle (i.e., in the z-axis of the seat passenger). If motion sickness increases when there is increased compensation, increases in these 'vertical' accelerations will be associated with increases in motion sickness (Donohew and Griffin, 2007; Persson et al., 2009; Persson, 2010). In this laboratory study the vertical acceleration was ±0.16 ms⁻² and ±0.18 ms⁻² in the seat compensation and head compensation conditions, respectively. Over the 30-minute exposure to motion, the motion sickness dose values corresponding to these accelerations are approximately 4.8 and 5.4 ms^{-1.5}, respectively, which would be expected to result in about two percent of the population vomiting according to both BS 6841 (1987) and ISO 2631-1 (1997). In fact, 27% (eight subjects) in the 'seat compensation' condition and 30% (nine subjects) in the 'head compensation' condition stopped their exposures within 30 minutes, presumably because they feared imminent vomiting.

The position of the mechanical pivot point differs between different designs of tilting train, with higher pivot points in some Japanese passive tilting mechanisms than some European active

tilting mechanisms (Hitachi, 2009). Although greater incidence of motion sickness has been reported in passively-tilted trains than actively-tilted trains (Bromberger, 1996), the current findings suggest differences in the height of the position of full roll-compensation may not be sufficient to explain differences in sickness.

The position of the centre-of-rotation with pure rotational motion can also be expected to influence responses other than motion sickness (e.g., passenger comfort and stability), with greater vibration discomfort as the distance between the seat surface and the centre-of-rotation increases (Parsons and Griffin, 1978). With low frequencies of roll combined with lateral acceleration, the influence of the position of the full roll-compensation on the physical comfort and stability of passengers has not been systematically investigated. The present study of motion sickness may assist the consideration of alternative designs but contributes only a part of the required information.

4.4.2. Ethnicity

There were no significant effects on motion sickness of subject age, weight, or stature but a highly significant effect of ethnic origin. Asians reported higher illness ratings and more motion sickness symptoms than Europeans and had significantly increased risk of reaching an illness rating of 3 ('mild nausea') (Table 4.2).

An apparent 'hyper-susceptibility' to motion sickness in Asian subjects has been documented previously. With visually-induced sickness in a rotating optokinetic drum, Chinese subjects reported significantly greater sickness than European-American or African-American subjects (Stern *et al.*, 1993). A follow-up study with American-born subjects with Asian parents, European-American, and African-American subjects found similar results, suggesting environmental factors associated with living in Asia were not sufficient to explain the findings (Stern *et al.*, 1996). When exposed to constant velocity rotation in yaw while making pitch movements of the head, Chinese subjects were reported to have significantly shorter 'rotation tolerance times' than Caucasian subjects, although motion sickness susceptibility scores reported by the Chinese subjects before testing "did not reflect their higher susceptibility during the subsequent test" (Klosterhalfen *et al.*, 2005, p. 1054), and there were no significant differences in susceptibility scores between Caucasians and Chinese subjects. This may suggest the Chinese subjects were less aware of their increased susceptibility to provocative motion stimuli relative to the Caucasians, consistent with the present study where no significant differences were found between the susceptibility scores of Europeans and Asians. Likewise,

with 'pseudorotation' in a vection drum, rotation tolerance time was significantly less in Chinese subjects than in White subjects (Klosterhalfen *et al.*, 2006).

Although the visual motion stimuli used in the above studies may have caused sickness in a fundamentally different way from the combined lateral and roll oscillation used in the present study, there is a similar pattern of greater susceptibility to motion sickness in Asian compared to European subjects, suggesting genetic influences are responsible. In mono-zygotic and dizygotic twins, approximately 53% of the variation in sickness susceptibility in a study sample has been attributed to genetic factors (Reavley *et al.*, 2006). Genetic influences were greatest during childhood and decreased as age increased. The study was limited to females, assumed common environmental factors across pairs of twins, and was susceptible to questionnaire response bias, but nevertheless suggests a basis for understanding the role of genetic factors in motion sickness susceptibility.

The alpha 2-adrenergic receptor genes may be associated with motion sickness susceptibility (Finley *et al.*, 2004), with allelic variations in this gene in the Chinese population accounting for the observed pattern of increased susceptibility (Liu *et al.*, 2002). Motion sickness research supported by advances in genetic screening may help to explain the hyper-susceptibility to motion sickness in Asians or, conversely, the reduced susceptibility in Europeans.

The language used in motion sickness susceptibility questionnaires, instructions sheets, and any verbal instructions given by experimenters may be a barrier to understanding differences between subjects with different languages. In the present study, all participants were deemed sufficiently proficient to study at degree level in the English language, having proven their ability by passing English language exams, and not all the subjects classified as 'European' were native-English speakers. Care was taken to ensure that subjects understood the instructions before entering the simulator cabin and it seems unlikely that language differences were the main cause of the observed differences between Asians and Europeans.

The findings have implications for the selection of subjects in motion sickness research, the design of motion sickness susceptibility questionnaires, and the development of anti-motion sickness measures. When constructing a sample population for motion sickness research, differences in susceptibility between ethnic groups require consideration so as to minimise bias, especially when using experimental designs with independent groups. In motion sickness susceptibility questionnaires, Asians may tend to underestimate their susceptibility to motion sickness relative to Europeans. However, the findings suggest that the need to understand and

Effects of position of full roll-compensation and subject demographics on motion sickness

control the causes of motion sickness, including the motions in tilting trains, may be greater in Asian than in European populations.

4.5. Conclusion

With fully roll-compensated 0.2-Hz lateral oscillation, no significant differences in motion sickness were found with full compensation of lateral forces at the seat surface or 800 mm above the seat surface (i.e. at the average sitting eye height). Subject age, weight, and stature did not have a significant effect on motion sickness, but Asian subjects reported significantly greater motion sickness symptoms than Europeans, consistent with previous reports of ethnic differences in motion sickness susceptibility. It is concluded that differences in susceptibility between Asians and Europeans have a greater effect on motion sickness than the height of the position of full roll-compensation during roll-compensated lateral acceleration.

Chapter 5

Seating effects with lateral vibration discomfort

5.1. Introduction

When a moving vehicle changes the direction of travel, the drivers and passengers must counteract lateral forces if they are to remain upright. While standing or walking, postural stability may be maintained by holding or leaning on a support, or adjusting the location of the feet (e.g., Thuong and Griffin, 2011; Sari and Griffin, 2010). While seated, postural stability is maintained by friction from contact with a backrest (e.g., Corlett and Eklund, 1984; Carcone and Keir, 2007), by differential downward forces at the ischial tuberosities and at the feet (e.g. Helander *et al.*, 1987; Coelho and Dahlman, 1999; Porter *et al.*, 2003), and by muscle activity (e.g., Seidel, 1988; Robertson and Griffin, 1989; Farah *et al.*, 2006; Gallais, 2007). In Chapter 4 it was demonstrated that, at 0.2 Hz, reducing these lateral forces with appropriate tilt-compensation is highly provocative of motion sickness. Lateral forces may also result in physical discomfort (e.g., Miwa, 1967; Donati, 1983; Corbridge and Griffin, 1986; Wyllie and Griffin, 2007), but there has been little systematic investigation of how this discomfort depends on the characteristics of the lateral motion or the characteristics of the seating.

When sitting on a flat horizontal rigid seat with a flat vertical rigid backrest, the discomfort caused by lateral sinusoidal acceleration has been reported to be greatest at frequencies of oscillation between 1.25 and 2.0 Hz (Corbridge and Griffin, 1986). When sitting on a similar rigid seat, both with and without a backrest, sensitivity to lateral acceleration caused by either lateral motion or roll through the gravity vector, was found to increase with increasing frequency of oscillation from 0.2 to 1.6 Hz (Wyllie and Griffin, 2007). At frequencies less than 0.4 Hz, lateral

acceleration in the plane of the seat arising from roll through the gravity vector caused similar discomfort to the same acceleration produced by lateral oscillation. However, at frequencies greater than 0.4 Hz, roll oscillation caused greater discomfort than the equivalent lateral oscillation. Compared to sitting with no backrest, wearing a four-point harness with a full height backrest increased discomfort from lateral oscillation at frequencies greater than 0.4 Hz and increased discomfort from roll oscillation at frequencies greater than 0.63 Hz (Wyllie and Griffin, 2007).

During lateral oscillation at frequencies between 0.5 and 3.15 Hz, the relative displacement between the head and the seat decreases with increasing height of a backrest (Brett and Griffin, 1991), suggesting that taller backrests offer greater lateral support (i.e., forcing the upper-body to move in-phase with the motion). Any discomfort from the muscular exertion required to maintain an upright posture may therefore be expected to reduce when there is increased lateral support from a backrest. Conversely, discomfort may be increased due to the increased transmission of vibration to the upper-body when supported by a backrest, consistent with greater discomfort when wearing a four-point harness with a backrest than when not using a backrest (Wyllie and Griffin, 2007) – suggesting the increased transmission of motion to the upper-body when wearing the harness with a backrest was a more dominant cause of discomfort than either relative motion between the head and the seat or the muscular effort required to maintain an upright posture when sitting without the harness or a backrest.

Currently standardised methods of predicting discomfort caused by whole-body vibration suggest greater vibration discomfort with more contact points between the body and the vibrating environment (e.g., BS 6841, 1987; ISO 2631-1, 1997). This implies that contact with the backrest of a seat will always increase vibration discomfort, even if it stabilises the body during low frequency lateral oscillation. The standards imply that vibration discomfort can be predicted from the acceleration at the interfaces between the body and a seat (e.g., at the ischial tuberosities and at the back). Since the transmission of very low frequency translational vibration to the body is independent of seat compliance (ignoring any roll on compliant seating), the standardised methods predict similar discomfort with rigid and compliant seats at low frequencies.

Previous research has found that backrests affect the movement of the body and can increase vibration discomfort, broadly consistent with current standards for evaluating vibration with respect to discomfort, yet it is widely assumed that seats with backrests are more comfortable. The experiment described here was designed to quantify the extent to which the discomfort caused by lateral oscillation in the range 0.2 to 1.0 Hz depends on backrest support and seat

cushioning. It was hypothesised that the discomfort caused by lateral acceleration would increase as the frequency of oscillation increased from 0.2 to 1.0 Hz, but that the frequency-dependence of discomfort would depend on the both the presence of a backrest and whether the seat was cushioned.

5.2. Method

5.2.1. Apparatus

Motions were produced by a simulator capable of 1-metre of horizontal oscillation. A train seat and a rigid seat were positioned adjacent to each other on the 1.0 by 1.5 m motion platform (Figure 5.1). The seats were orientated so that horizontal displacement of the simulator platform provided lateral oscillation.

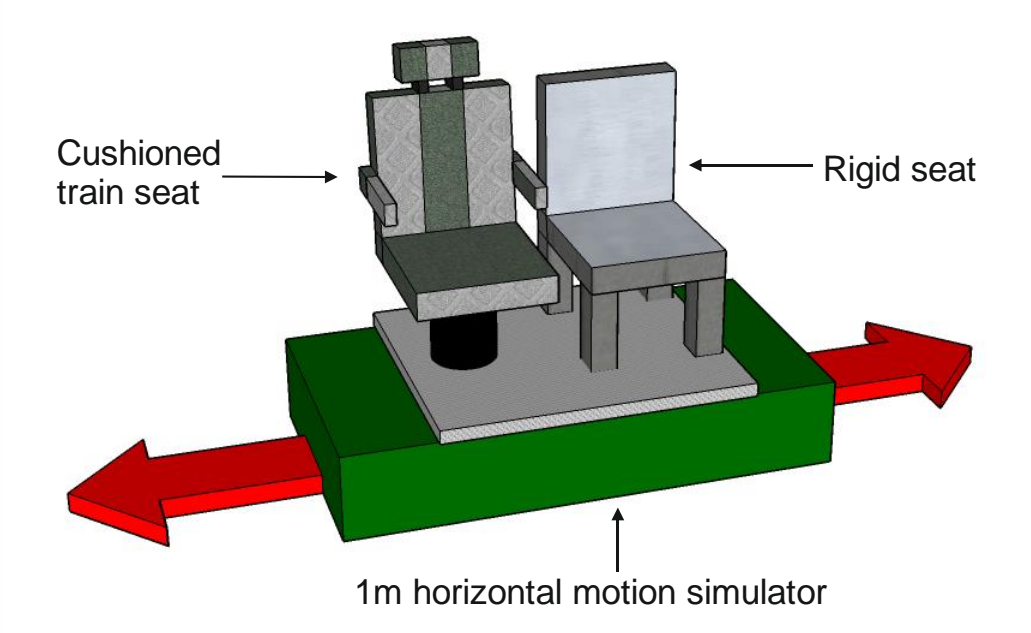


Figure 5.1 Diagrammatic representation of experimental apparatus (train seat and rigid seat positioned adjacent on 1-metre horizontal simulator).

The rigid seat consisted of a flat horizontal seat pan (510 by 400 mm), located 480 mm above the motion platform, and a flat vertical backrest (645 by 650 mm). The surfaces of the seat pan and the backrest were covered in hard rubber less than 2-mm thick to increase surface friction. The train seat consisted of a cushioned seat pan (510 by 400 mm) located 420 mm above the motion platform with a cushioned backrest (520 by 740 mm) inclined by 31 degrees relative to

gravity (SAE J826, 2008). The backrest was contoured both vertically and horizontally. Cushioned horizontal armrests, 270 mm above the seat pan, were not used.

Subjects were asked to maintain comfortable upright postures with their hands on their laps and their feet flat on the floor. When backrest contact was required, subjects were asked to ensure the whole back (but not the head) was in contact with the backrest. During motion exposure, subjects wore headphones producing white noise at 65 dB(A) in order to mask any sounds from the simulator. The experimenter communicated with subjects through a microphone connected to headphones which interrupted the white noise. Subjects wore a loose lap belt for safety.

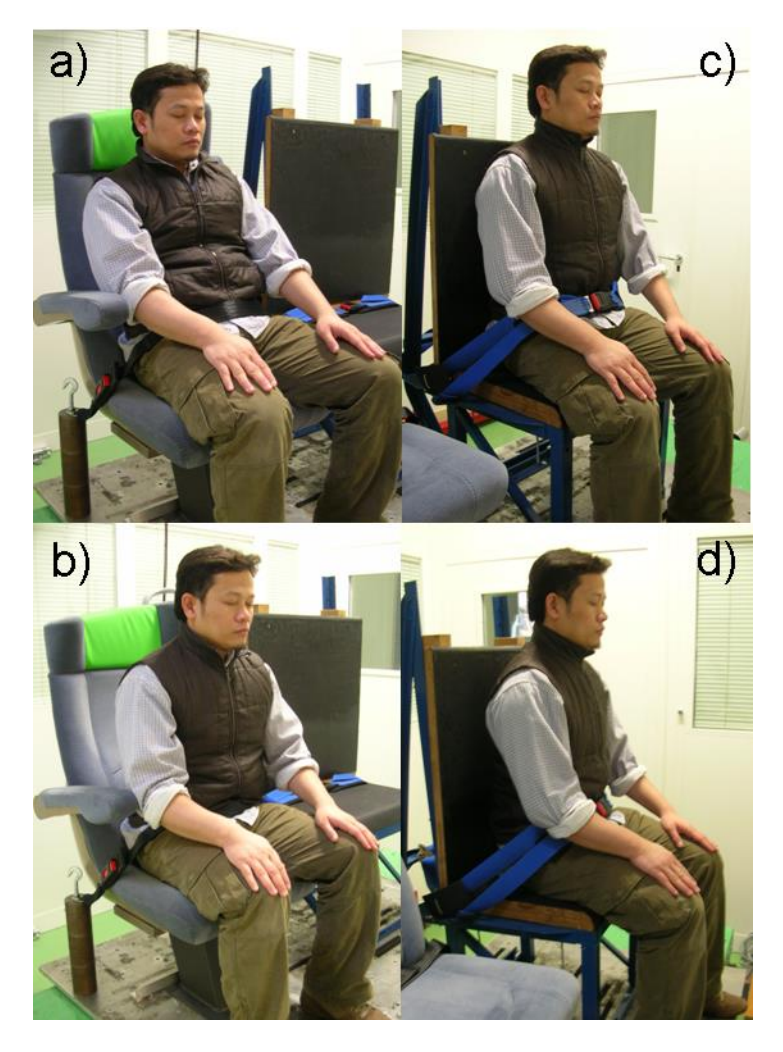


Figure 5.2 The four seating conditions: (a) train seat with backrest, (b) train seat without backrest, (c) rigid seat with backrest, and (d) rigid seat without backrest.

5.2.2. Design

The experiment adopted a repeated measures (within-subjects) design. Subjects were exposed to a series of pairs of motion stimuli whilst seated in one of four seating conditions (the rigid seat with and without backrest contact, and the cushioned train seat with and without backrest contact – see Figure 5.2) in each of four experimental sessions. The method of magnitude estimation was used to rate the discomfort of test stimuli relative to the discomfort caused by a reference stimulus. At the start of each session, subjects were trained on the method of magnitude estimation by judging the length of lines relative to a reference line, and by judging the discomfort of a set of practice motion stimuli.

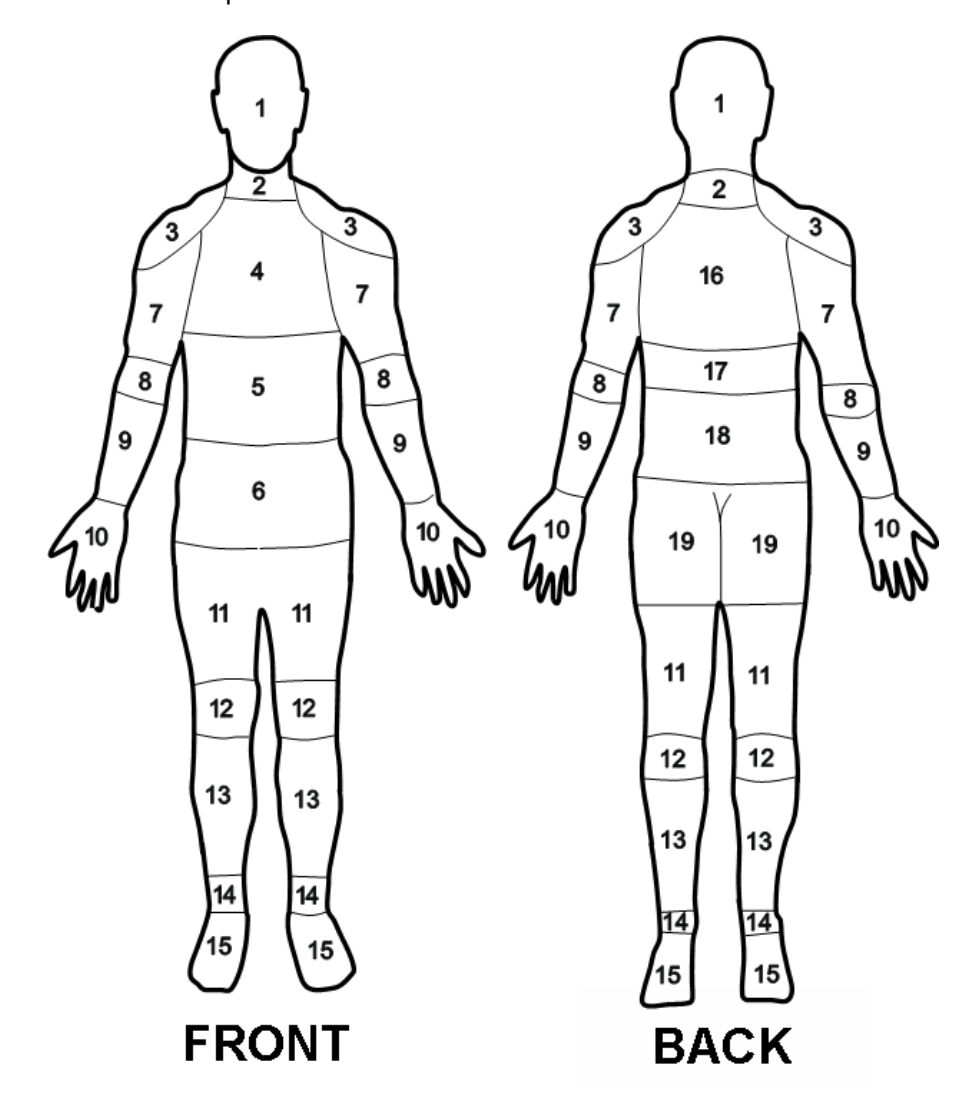


Figure 5.3 Labelled diagram of the human body (body map) used by subjects to indicate the location of most discomfort in Part 3.

Each session consisted of three parts. In part 1 (equivalent comfort contours) subjects were required to rate the discomfort of test stimuli relative to the discomfort caused by a reference stimulus (0.5-Hz lateral oscillation at 0.2 ms⁻² r.m.s.), where the reference and test stimuli were presented in the same seating condition. In part 2 (cross-over test) subjects rated the discomfort of test stimuli relative to the discomfort caused by a reference stimulus, where the reference and the test stimuli were presented in different seating conditions. In part 3 (body map) subjects indicated the location of the body where they felt *most* discomfort using a labelled diagram of the body (Figure 5.3).

The order of presentation of motion stimuli within each session was fully randomised for each subject. The order of the four sessions was varied for each subject using a Latin square.

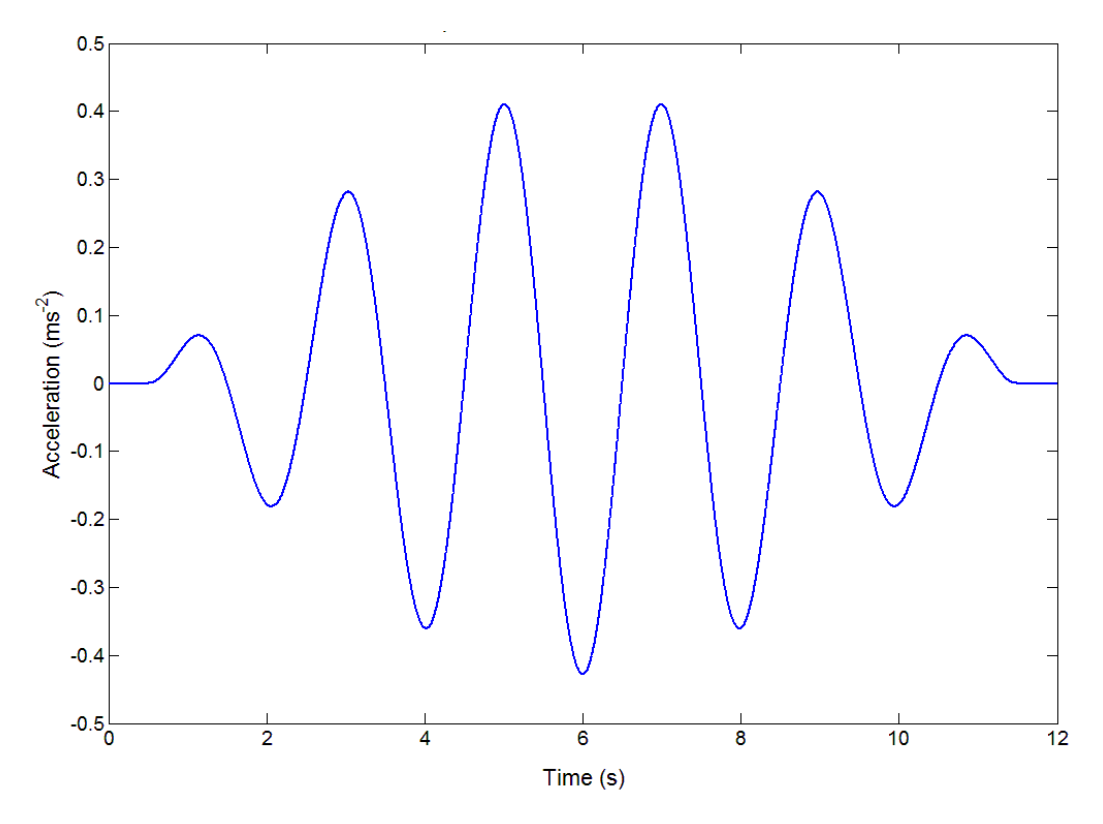


Figure 5.4 Example waveform of transient lateral motion stimuli (0.5 Hz oscillation at 0.2 ms⁻² r.m.s.).

5.2.3. Motion stimuli

Lateral oscillatory motion was presented at each of the eight preferred one-third octave centre frequencies from 0.2 to 1.0 Hz. In part 1 (equivalent comfort contours), each frequency was presented at eight magnitudes (in logarithmic series between 0.08 and 0.40 ms⁻² r.m.s.), except

for 0.2 Hz where the two highest magnitudes were not presented due to simulator displacement limitations. The same reference motion was used throughout the experiment: a 0.5-Hz lateral oscillation at 0.2 ms⁻² r.m.s. In part 2 (cross-over test), eight magnitudes were presented at 0.5 Hz only. In part 3 (body map), each frequency was presented at 0.08, 0.16 and 0.40 ms⁻² r.m.s. (except for 0.2 Hz, where 0.25 ms⁻² r.m.s. was the highest magnitude possible). All motion stimuli were transient waveforms of approximately 11-s duration (to the nearest half-cycle) generated from the product of a sine wave of the desired frequency and a half-sine of the same duration (Figure 5.4). All motions were generated within MATLAB (version R2009 research) using the *HVLab* toolbox (version 1.0).

5.2.4. Subjects

Twelve healthy male volunteers aged 18 to 30 years participated in the experiment (median age 25.5 years, inter-quartile range, IQR 2.8 years; median weight 70.9 kg, IQR 22.0 kg; median stature 1.75 m, IQR 0.10 m). Subjects were recruited from the staff and student population of the University of Southampton. Full details of the subject demographics can be found in the Appendices.

5.2.5. Analysis

The physical magnitudes of the motion stimuli (Φ) were related to the subjective magnitude estimates (Ψ) using Stevens' power law, shown in Equation 5.1 (Stevens, 1975).

Equation 5.1:
$$\psi = k \varphi^n$$

The exponent, *n*, (i.e. the rate of growth of discomfort) and the constant, *k*, were determined by performing linear regression on the logarithmic transformation of Equation 5.1 (see Equation 5.2).

Equation 5.2:
$$\log_{10} \psi = \log_{10} k + n \log_{10} \varphi$$

Values for n and k were determined for each individual subject for each frequency and seating condition. Equivalent comfort contours for a subjective magnitude (Ψ) of 100 were calculated for each subject and seating condition using Equation 5.2.

The data from part 2 (cross-over test) were used to calculate correction factors in order to adjust the equivalent comfort contours obtained from the test 1 data, so that the relative discomfort experienced across different seating conditions could be examined. Correction factors were calculated using Equation 5.3.

Equation 5.3 Correction factor =
$$(\varphi_{\text{Cross-over}}) / (\varphi_{\text{Part 1}})$$

where $\varphi_{Part 1}$ is the acceleration magnitude of a 0.5 Hz test motion in part 1 which caused discomfort equal to that caused by a 0.5 Hz, 0.20 ms⁻² r.m.s. reference in the same seating condition as the test stimulus, and $\varphi_{Cross-over}$ is acceleration magnitude of a 0.5 Hz test motion in part 2 (cross-over test) which caused discomfort equal to that caused by a 0.5 Hz, 0.20 ms⁻² r.m.s. reference in a different seating condition as the test stimulus. The rigid seat with a backrest was used as a common reference, so that the relative discomfort caused by the other three seating conditions could be compared on one axis. The acceleration magnitudes used to define $\varphi_{Part 1}$ and $\varphi_{Cross-over}$ were median values calculated from the 12 subjects. Relative equivalent comfort contours for the four seating conditions were generated by applying the correction factors to the median equivalent comfort contours calculated from part 1. Individual equivalent comfort contours from part 1 were also adjusted using the same correction factors in order to allow statistical comparisons across seating conditions.

The data from part 3(body map) were used to assess the effect of frequency and magnitude of lateral oscillation on the location of most discomfort.

The Friedman test was used to test for an overall effect of frequency and seating on the rates of growth in discomfort (*n*) and the equivalent comfort contours. The Wilcoxon matched pairs test was used to examine specific differences in rates of growth in discomfort (*n*) and equivalent comfort contours between frequencies and seating conditions. The McNemar dichotomous variables test was used to examine differences in the location of discomfort across specific seating conditions. The median rates of growth of discomfort (*n*) and median equivalent comfort contours were used to identify overall trends in the data.

5.3. Results

5.3.1. Rate of growth of vibration discomfort

The rate of growth of discomfort varied with the frequency of vibration for the rigid seat with backrest (p = 0.003; Friedman), but not for the rigid seat without backrest, or for the train seat, either with or without backrest (p = 0.047, 0.948 and 0.110, respectively; Figure 5.5). The seating condition had no significant effect on the rate of growth of discomfort at any frequency (p > 0.05; Friedman).

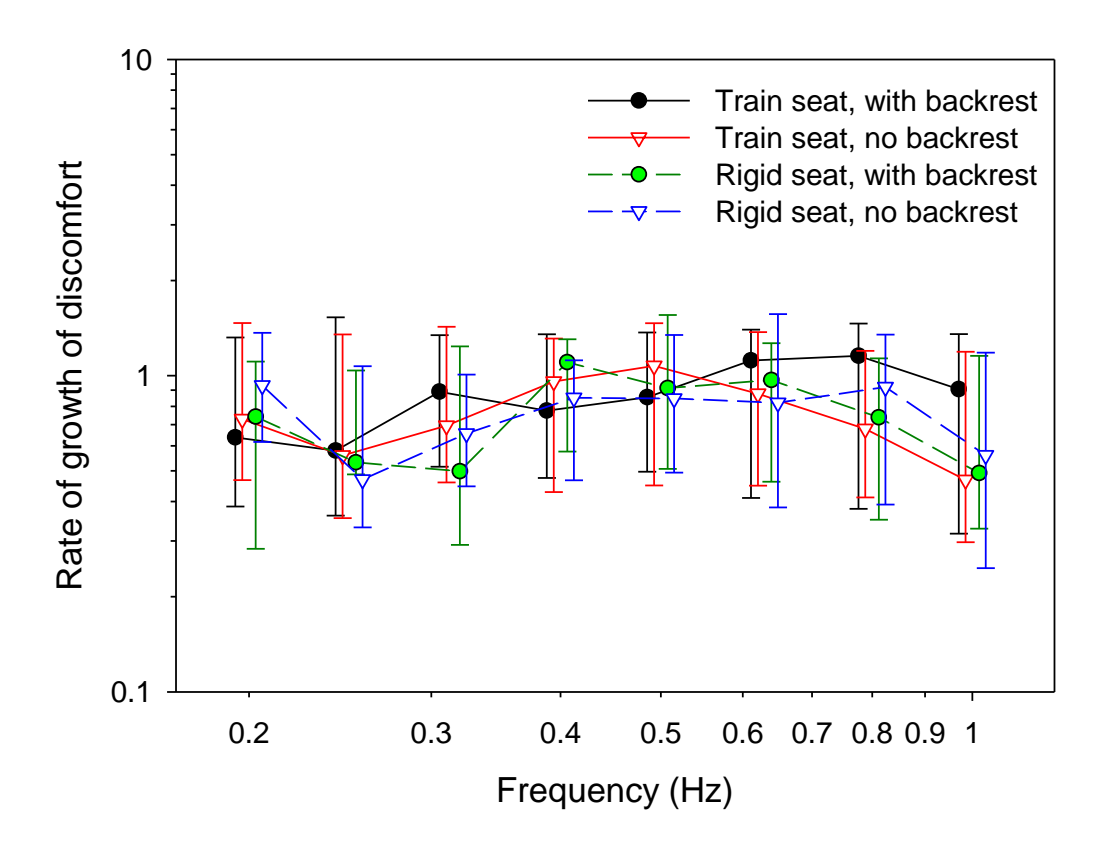


Figure 5.5 Rates of growth of discomfort for lateral oscillation on a rigid seat and a cushioned train seat with and without backrests. Medians and inter-quartile ranges for 12 subjects.

5.3.2. Effect of frequency of oscillation on vibration discomfort

Equivalent comfort contours obtained from each subject in each seating condition were adjusted (as described above) to determine the vibration magnitude required at each frequency to produce vibration discomfort equivalent to that caused by the common reference motion: $0.5 \, \text{Hz}$ $0.20 \, \text{ms}^{-2} \, \text{r.m.s.}$ lateral oscillation on the rigid seat with backrest (Figure 5.6). The frequency-dependence of equivalent comfort contours will change with the magnitude of the vibration (e.g., Morioka and Griffin, 2006a). However, because there was no difference in the rate of growth of discomfort between seating conditions, the relative discomfort between seats will be independent of vibration magnitude. The equivalent comfort contours shown here are therefore constructed for only one magnitude of vibration. The acceleration associated with equivalent comfort decreased with increasing frequency of vibration for the train seat with backrest (p = 0.009; Friedman) and the rigid seat without backrest (p = 0.022), but not for the train seat without backrest (p = 0.054) or the rigid seat with backrest (p = 0.125; Friedman).

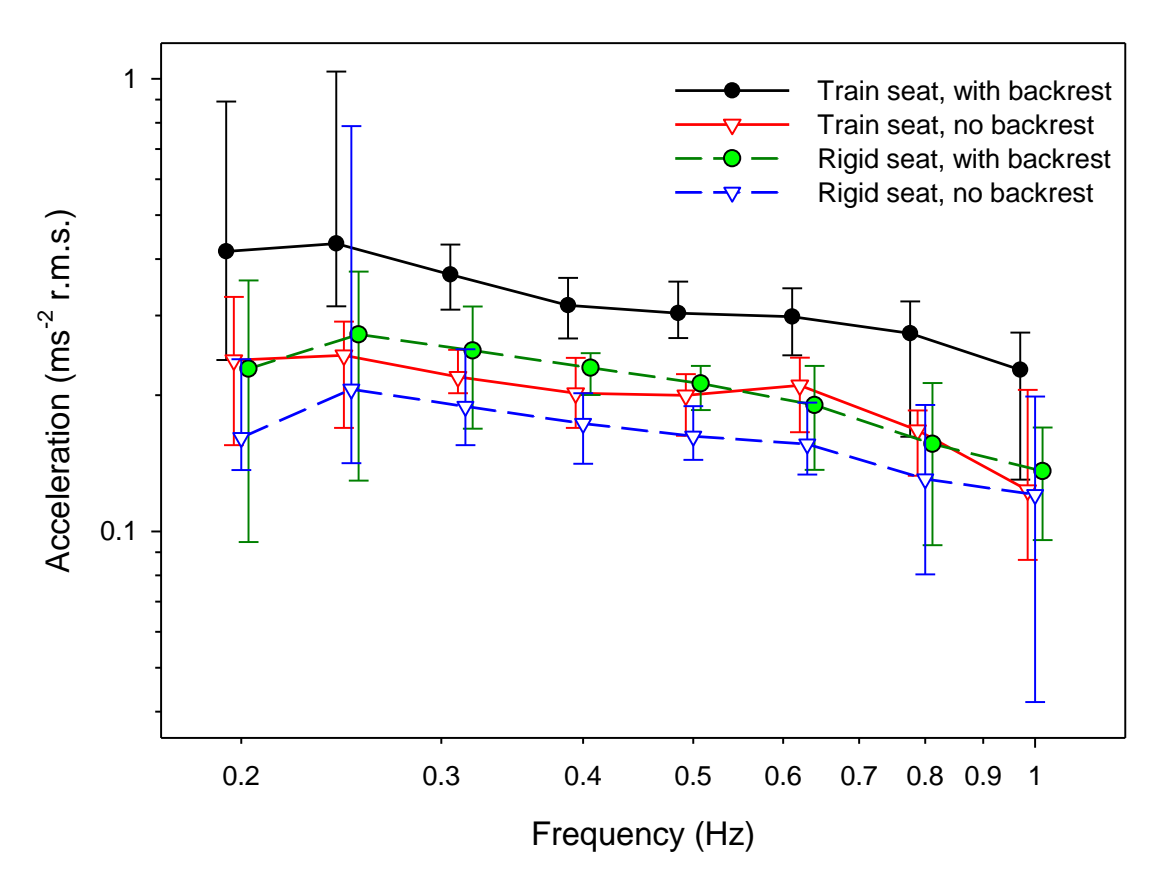


Figure 5.6 Equivalent comfort contours adjusted to represent discomfort equivalent to 0.5 Hz at $0.2~\text{ms}^{-2}$ r.m.s. on a rigid seat with backrest (i.e. a subjective magnitude, Ψ , of 100). Medians and inter-quartile ranges for 12 subjects.

5.3.3. Effect of seating on vibration discomfort

At every frequency, the adjusted equivalent contours were highly dependent on seating condition (p < 0.01; Friedman). Greater magnitudes of lateral oscillation were required to cause equivalent discomfort when seated on the train seat with backrest than when seated on: (i) the train seat without backrest, at all frequencies except 0.2 and 1.0 Hz (p < 0.01; Wilcoxon), (ii) the rigid seat with backrest, at all frequencies except 0.315 and 1.0 Hz (p < 0.01), and (iii) the rigid seat without backrest, at all frequencies except 0.25 and 0.315 Hz (p < 0.01). Lower magnitudes of lateral oscillation were required to cause discomfort on the rigid seat without backrest than on both the train seat without backrest at 0.63 Hz (p < 0.01; Wilcoxon) and on the rigid seat with backrest at 0.4 and 0.63 Hz (p < 0.01; Wilcoxon).

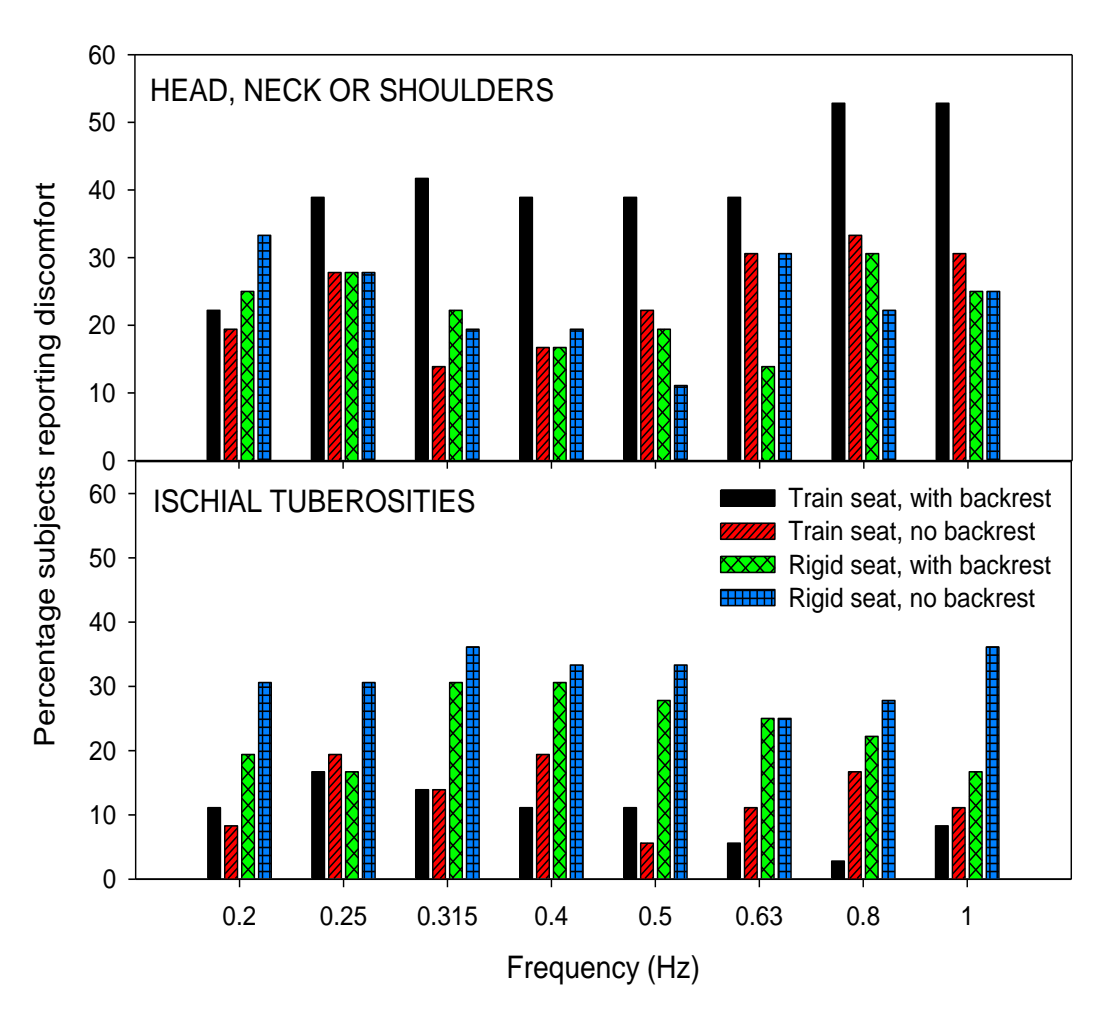


Figure 5.7 Percentage of subjects reporting most discomfort at the head, neck, or shoulders (top), or at the buttocks (ischial tuberosities) (bottom) during exposure to lateral oscillation across all frequencies with each seating condition. Data from 12 subjects pooled across all three magnitudes of oscillation.

5.3.4. Location of discomfort

There were no clear effects of the magnitude of oscillation on the locations in the body where subjects felt most discomfort, so the data were pooled across the three magnitudes at each frequency. Greatest discomfort occurred more frequently at the head, neck, or shoulders during 0.5-Hz oscillation on the train seat with backrest than on the rigid seat without backrest (p = 0.006; McNemar). Greatest discomfort occurred more frequently at the ischial tuberosities on the rigid seat (with and without backrest) than on the train seat without backrest during 0.5-Hz oscillation (p = 0.008 and 0.006, respectively; McNemar), and more frequently on the rigid seat

without backrest than on the train seat with backrest during 1-Hz oscillation (p = 0.006; McNemar). These patterns are illustrated in Figure 5.7. No other statistically significant differences in the location of greatest discomfort were found.

5.4. Discussion

5.4.1. Rate of growth of discomfort

A greater rate of growth of discomfort implies a greater increase in the magnitude of discomfort associated with a unit increase in the magnitude of acceleration. Rates of growth of discomfort did not vary between conditions with and without backrest on either the rigid seat or the train seat, although there were statistically significant changes with the frequency of lateral oscillation on the rigid seat with backrest but not on the train seat. Previous research with lateral oscillation on a rigid seat reported no effects on the rate of growth of discomfort when using a rigid backrest and four-point harness, consistent with the present study (Wyllie and Griffin, 2007). During lateral oscillation of a rigid seat without backrest, the previous study found decreasing rates of growth of discomfort with increasing frequency of oscillation from 0.2 to 1.6 Hz, with a more consistent effect of frequency than found here. The present study investigated acceleration magnitudes between 0.08 and 0.40 ms⁻² r.m.s. with a 0.5-Hz reference at 0.20 ms⁻² r.m.s., somewhat less uncomfortable than the 0.2 to 0.63 ms⁻² r.m.s. range with a 0.5-Hz reference at 0.315 ms⁻² r.m.s. used by Wyllie and Griffin (2007). Stevens (1975) assumed the exponent in the power law was independent of the magnitude of physical stimuli, but this may not apply with all physical stimuli – a dependence of the rate of growth of discomfort on vibration magnitude might explain the discrepancy between the current findings and those reported by Wyllie and Griffin (2007).

5.4.2. Equivalent comfort contours

In all four seating conditions, the lateral acceleration required to produce equivalent discomfort decreased by approximately 3 dB per octave as the frequency increased from 0.2 to 1.0 Hz (i.e., sensitivity increased with increasing frequency). A similar effect of frequency has been reported for lateral vibration of a rigid seat without backrest over the frequency range 0.2 to 1.6 Hz, but a greater rate of decrease (approximately 6 dB/octave) was found for a rigid seat with four-point harness and backrest (Wyllie and Griffin, 2007; Figure 6). This is consistent with the harness reducing discomfort at lower frequencies but increasing discomfort at higher frequencies.

At all frequencies, lateral oscillation caused least discomfort when sitting on the train seat with backrest. Compared to the rigid seat without backrest (i.e., the seat associated with greatest discomfort), the train seat with backrest allowed approximately a two-fold increase in vibration magnitude for the same level of vibration discomfort (Figure 5.6). The rigid seat without backrest and the cushioned train seat without backrest produced similar discomfort at all frequencies (Figure 5.6), consistent with no large differences in discomfort during lateral oscillation at 1 Hz when seated on a flat rigid seat without backrest or a foam cushion without backrest as reported by Moxley *et al.* (2011).

It has been suggested that the overall discomfort, ψ , of a seat can be predicted by summing the static discomfort, ψ_s , and the dynamic discomfort, ψ_v (Ebe and Griffin, 2000):

Equation 5.4
$$\psi = a + b\phi_s^{n_s} + c\varphi_v^{n_v}$$

where φ_s is a measure of the seat pan stiffness (causing static discomfort), n_s is the rate of growth of static discomfort, φ_v is the vibration acceleration magnitude (causing dynamic discomfort), n_v is the rate of growth of dynamic discomfort, and a, b, and c are constants. Without asking subjects to distinguish between static and dynamic discomfort, the present study found that greater vibration magnitudes were required to cause a given level of discomfort on the train seat with backrest than on the other three seat conditions. The above model (Equation 5.4) allows the possibility that the greater comfort on the train seat with backrest was partially due to greater static comfort with this seat.

A lower magnitude of lateral acceleration was required to produce equivalent discomfort on the rigid seat without backrest than on the rigid seat with backrest, indicating that the backrest reduced discomfort (with a statistically significant benefit at 0.4 and 0.63 Hz). This differs from the increasingly detrimental effect of a backrest with harness as the frequency increases from 0.2 to 1.0 Hz (Wyllie and Griffin, 2007; Figure 5.8). This detriment is also apparent at 1.6 and 2 Hz when comparing contours obtained with a backrest without harness by Corbridge and Griffin (1986) with those obtained with backrest and harness by Wyllie and Griffin (2007), as shown in Figure 5.8. The increased discomfort with a four-point harness may be due to increased transmission of motion to the upper-body resulting in increased forces at the neck.

In current standards, the discomfort caused by lateral acceleration at frequencies greater than 0.5 Hz is predicted using frequency weighting W_d (BS 6841, 1987; ISO 2631-1, 1997). The asymptotic version of this weighting has sensitivity to acceleration which is independent of frequency from 0.5 to 2 Hz and then falls in inverse proportion to frequency from 2 to 80 Hz. The realisable version of the frequency weighting has a gradual transition around 2 Hz and a high

pass filter at 0.4 Hz. The reciprocal of the realisable frequency weighting W_d shows some similarity to the current and previous equivalent comfort contours for low frequency lateral oscillation, even though the weighting is not intended for application to frequencies less than 0.5 Hz (Figure 5.8). However, relative to other frequencies, it seems that the realisable W_d weighting tends to underestimate the discomfort caused by frequencies less than about 0.3 Hz, except when restrained against a backrest by a harness.

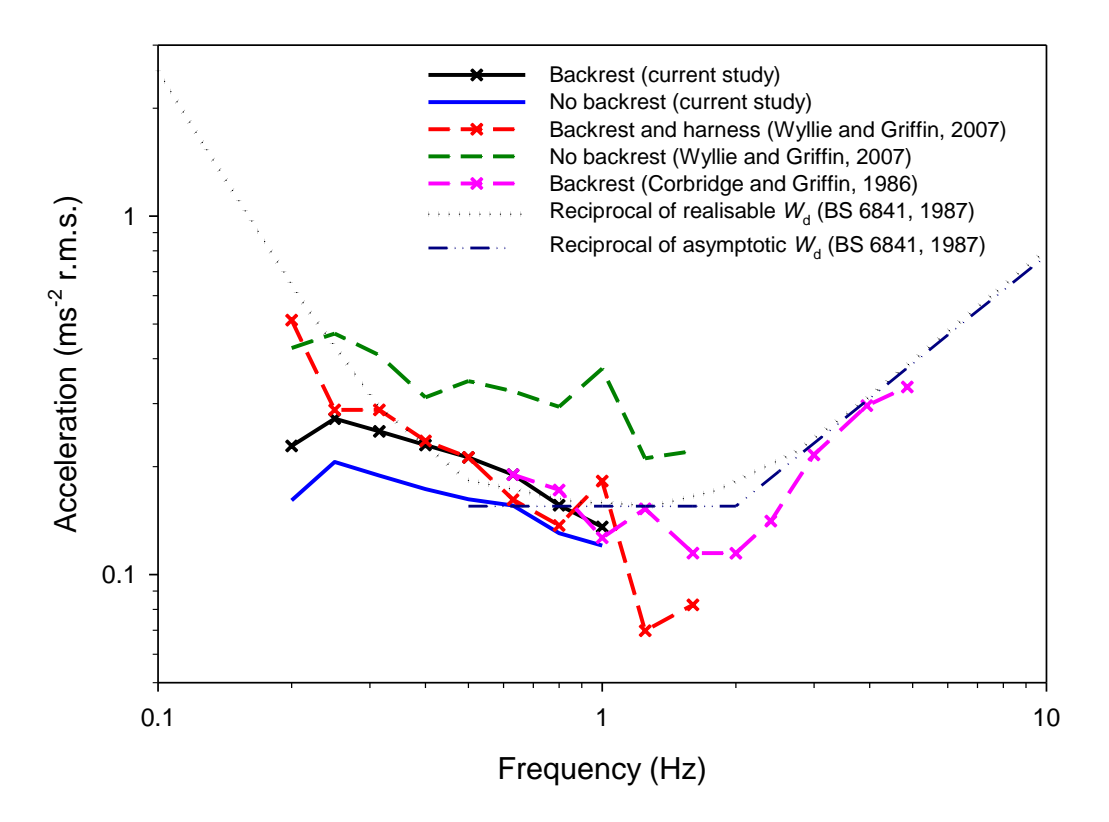


Figure 5.8 Comparison of median equivalent comfort contours from current study with previous data for lateral oscillation on a rigid seat with and without backrest and frequency weighting W_d . The levels of the contours have been adjusted to represent discomfort equivalent to 0.5 Hz at 0.2 ms⁻² r.m.s. on a rigid seat with backrest.

Irrespective of the frequency-dependence, the level of the equivalent comfort contours depends on the seating conditions. British standard 6841 (1987) and International standard 2631-1 (1997) advocate the use of frequency weighting W_d to predict discomfort caused by both lateral oscillation at the seat and lateral acceleration at the backrest, but with sensitivity at the backrest half that at the seat (i.e., a 0.5 multiplying factor is used for lateral acceleration at the backrest). An 'overall ride value' can be predicted from the root-sums-of-squares (r.s.s.) of all weighted inputs, so contact with vibration at a backrest will increase the overall ride value and imply

increased discomfort (Griffin, 2007). If the vibration at the seat and the backrest is the same, the r.s.s. of the weighted vibration at the seat and the back will be about 12% greater when vibration at the backrest is included. Wyllie and Griffin (2007) found that wearing a full harness that forced contact with a backrest increased discomfort, although the increase varied with frequency and was greater than implied by the standards over the range 0.8 to 1.6 Hz. The present study with both a rigid seat and a train seat found that leaning against a backrest without a harness tended to reduce discomfort at all frequencies between 0.2 and 1.0 Hz. It seems that an intermediate situation is optimum: contact with a backrest can help to reduce movements responsible for discomfort but forcing the back to move with a backrest can increase strain in the body. Without a harness, people may be able, to some extent, to control their contact with a backrest so that it is beneficial and not detrimental.

5.4.3. Location of discomfort

During 0.5-Hz lateral oscillation, the location of greatest discomfort occurred more frequently at the head, neck, and shoulders on the train seat with backrest than in any of the other three seating conditions (Figure 5.7). Either the train seat with backrest increased discomfort at the head, neck, and shoulders or it decreased discomfort at other locations of the body. The 740 mm high backrest resulted in most subjects having the tops of their shoulders in contact with the seat, which is likely to have increased the transmission of vibration to the shoulders, neck, and head (Paddan and Griffin, 1988). The contouring of the train seat backrest also provided lateral support so the upper-body was less free to make compensatory adjustments during oscillation. The contact with the backrest may have increased lateral acceleration of the upper-body, and without support for the head this may have resulted in greater strain around the neck. When sitting with the backrest there may also have been reduced discomfort at other locations, leaving the head, neck, and shoulders as the dominant locations for discomfort. For example, the backrest may have reduced back muscle activity associated with maintaining an upright posture during lateral oscillation.

During lateral oscillation between 2 and 64 Hz on a rigid seat without backrest, discomfort was localised mainly at the ischial tuberosities (Whitham and Griffin, 1978). In this study, greatest discomfort also occurred most frequently at the ischial tuberosities when sitting on the rigid seat without backrest during 0.5-Hz and 1-Hz oscillation (Figure 5.7). When stationary and sitting upright, the weight of the body is supported with similar pressure at both ischial tuberosities, but during lateral oscillation with no backrest the sway of the body is partially restrained by alternating increases in pressure at the two ischial tuberosities. Backrests help to reduce pressure on the ischial tuberosities when static (e.g., Vos *et al.*, 2006; Kyung and Nussbaum,

2008) and also help to constrain the swaying of the body during oscillation. The reduction in the weight supported at the ischial tuberosities and the decreased need to control sway by increasing pressure, is consistent with reduced discomfort at the ischial tuberosities when sitting with a backrest during low frequency lateral oscillation.

5.5. Practical implications

The characteristics of a seat and the sitting posture have been shown to influence the severity of vibration discomfort, and the location of discomfort, caused by low frequency lateral vibration. With a rigid seat and a compliant train seat, contact with the backrest reduced the discomfort caused by all frequencies of lateral acceleration between 0.2 and 1.0 Hz. It seems reasonable to assume that the backrests reduced the muscular exertion that is otherwise required to maintain an upright posture during low frequency lateral oscillation (Robertson and Griffin, 1989). Reduced pressure at the ischial tuberosities on the train seat may explain why lateral acceleration caused less discomfort on the train seat than the rigid seat. Other factors associated with the configuration of a backrest (e.g., backrest height, inclination, and curvature) may also affect motion discomfort, with effects that may be expected to depend on the type of motion (e.g., lateral oscillation or roll oscillation; Chapter 6). The prediction of seating comfort in an environment with low frequency acceleration should therefore consider how the seat characteristics control the motions of the seat occupant as well as how the motion is transmitted through the seat to the surface of the human body.

5.6. Conclusion

The discomfort caused by lateral acceleration increases with increasing frequency of oscillation from 0.2 to 1.0 Hz. When applied with a band-limiting filter, the frequency weighting W_d in current standards gives a useful indication of how discomfort depends on the frequency of lateral oscillation in the range 0.3 to 1.0 Hz, but it underestimates the discomfort caused by lower frequencies. Current standards predict that contact with a backrest will increase vibration discomfort, but low frequency lateral acceleration causes less discomfort when sitting supported by a backrest than when sitting on the same seat without backrest support. Sitting on a rigid seat, either with or without a backrest, resulted in greater motion discomfort than sitting on a compliant seat, with greater incidence of discomfort at the ischial tuberosities. The combination of a compliant seat cushion with a high, contoured, slightly reclined backrest was associated with least discomfort from lateral motions in the frequency range 0.2 to 1.0 Hz.

Chapter 6

Discomfort caused by lateral, roll and fully roll-compensated lateral oscillation

6.1. Introduction

The lateral centripetal accelerations which occur when a vehicle traverses a curve are determined by the vehicle speed and the curve radius. The findings from Chapter 5 show that the discomfort caused by such lateral motions is dependent on the vehicle seating. Reductions of the lateral acceleration felt within the vehicle are achieved if the vehicle rolls so that it remains aligned with the gravito-inertial force. In tilting trains, 'roll-compensation' is employed to allow high-speeds through curves without unacceptable horizontal forces. The combination of low frequency rotational and translational motion can increase motion sickness, as seen in tilting trains (e.g., Ueno *et al.* 1986, Bromberger 1996, Förstberg *et al.* 1998, Donohew and Griffin 2007, Persson 2010) and in laboratory simulations (e.g., Donohew and Griffin 2007, 2009, Joseph and Griffin 2007, 2008, Chapter 4). Increases in peak roll acceleration have been correlated with increases in the discomfort of high-speed rail passengers (e.g. Suzuki *et al.* 1999, 2001), but there has been little systematic study of the effect of the roll-compensation of lateral oscillation on physical discomfort.

The study reported here was designed to determine the relative discomfort caused by lateral oscillation, roll oscillation, and fully roll-compensated lateral oscillation. From previous studies it was anticipated that with frequencies of oscillation less than about 0.4 Hz, pure lateral acceleration would cause similar discomfort to pure roll oscillation when there was the same

acceleration in the plane of the seat. At these frequencies, discomfort was expected to be reduced when lateral acceleration was combined with the equivalent roll oscillation (i.e., it was 'roll-compensated'). With frequencies of oscillation greater than about 0.4 Hz, it was expected that with the same acceleration in the plane of the seat, lateral oscillation would cause less discomfort than roll oscillation, and roll-compensation would be less effective.



Figure 6.1 Illustration of rigid seat with backrest.

6.2. Method

6.2.1. Apparatus

Motions were produced by a six-axis motion simulator in the Human Factors Research Unit of the Institute of Sound and Vibration Research at the University of Southampton. The simulator was capable of ± 0.5 m vertical motion, ± 0.25 m horizontal motion, and about $\pm 20^{\circ}$ of rotational motion. Subjects sat on a rigid seat positioned so that the centre of the seat surface was at the centre of the motion platform (approximately 2.5 m by 3.0 m).

The seat consisted of a rigid flat horizontal seat pan (51 by 46 cm) located 40 cm above the platform surface, and a rigid flat vertical backrest (62 by 40 cm). The surface of the seat pan was covered in hard rubber less than 2 mm in thickness to increase surface friction. A square block of 5-cm thick foam (40 by 40 cm, 35 kg/m³, 150 N) was placed on the backrest to increase surface friction and provide lateral support for the upper-body (see Figure 6.1).

Subjects were asked to maintain comfortable upright postures ensuring full contact with the backrest, with their hands on their laps and their feet flat on the platform of the simulator. Subjects wore a loose lap belt for safety.

During motion exposure, subjects were headphones producing white noise at 65 dB(A) in order to mask the sounds of the simulator. The experimenter communicated with subjects through a microphone connected to the headphones by interrupting the white noise.

6.2.2. Design

The study used a repeated measures (within-subjects) design. The experiment consisted of two parts. In part 1 (equivalent comfort contours) subjects used the method of magnitude estimation to rate the discomfort produced by lateral, roll, and fully roll-compensated lateral oscillations (i.e., the test stimuli) relative to the discomfort produced by a lateral oscillation (i.e., the reference stimulus). In part 2 (body map), for every stimulus, the subjects used a labelled diagram of the body to indicate where they felt discomfort choosing as many locations as they felt appropriate. The order of presentation of motion stimuli within each experimental part was fully randomised for each subject. At the start of each session, subjects were trained on the method of magnitude estimation by judging the length of lines relative to a reference line, and by judging the discomfort of a set of practice motion stimuli.

6.2.3. Motion stimuli

The motion stimuli consisted of seven frequencies at the preferred one-third octave centre frequencies from 0.25 to 1.0 Hz. Each frequency was presented at, nominally, eight magnitudes in logarithmic series from 0.08 to 0.40 ms⁻² r.m.s. (Due to simulator limitations, five magnitudes of lateral oscillation (0.08 to 0.20 ms⁻² r.m.s.) were presented at 0.25 Hz and seven magnitudes (0.08 to 0.315 ms⁻² r.m.s.) at 0.315 Hz. Seven magnitudes of roll oscillation (equivalent to 0.08 to 0.315 ms⁻² r.m.s.) were presented at 1.0 Hz. Seven magnitudes of roll-compensated oscillation were presented at 0.8 Hz (0.08 to 0.315 ms⁻² r.m.s.) and six magnitudes (0.08 to 0.25 ms⁻² r.m.s.) at 1.0 Hz).

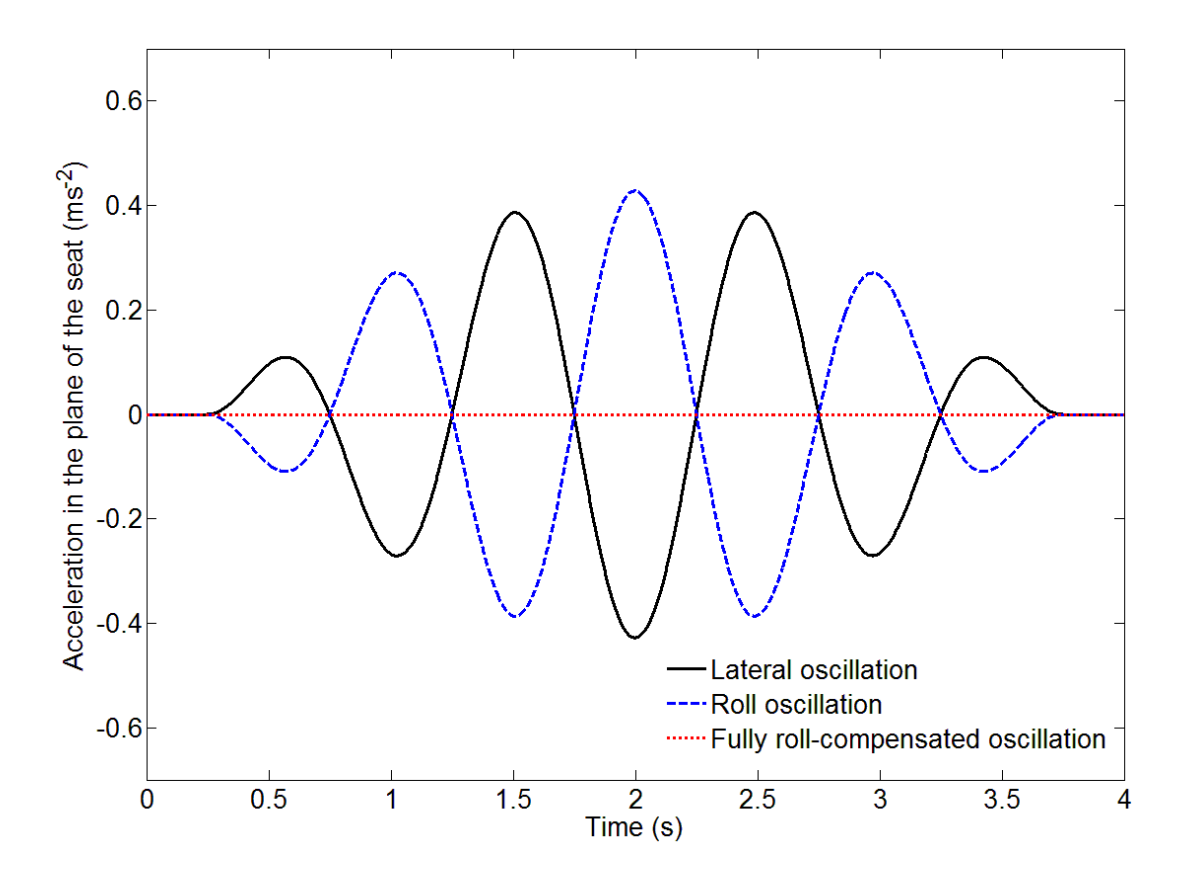


Figure 6.2 Example waveforms for 1.0-Hz oscillation showing the acceleration in the plane of the seat for lateral oscillation, roll oscillation, and fully roll-compensated lateral oscillation.

For roll oscillation, the magnitude was defined by the acceleration in the plane of the seat (i.e., due to gravity). For roll-compensated lateral oscillation, the lateral oscillation and the roll oscillation were combined 180° out-of-phase such that the resultant acceleration in the plane of the seat was zero. This procedure is illustrated in Figure 6.2 which shows the acceleration waveform in the plane of the seat for lateral, roll, and roll-compensated oscillation at 0.5 Hz. All motion stimuli were transient waveforms with a 3.5 cycle duration (as shown in Figure 6.2) generated from the product of a sine wave of the desired frequency and a half-sine of the same duration. The motions were generated within MATLAB (version R2010a research) using the *HVLab* toolbox (version 1.0).

6.2.4. Subjects

Fifteen male and fifteen female volunteers aged between 19 and 30 years participated in the experiment (median age 27.0 years, inter-quartile range, IQR = 4.8 years; median weight 61.6 kg, IQR 16.6 kg; median stature 1.69 m, IQR 0.08 m). Subjects were recruited from the staff and

student population of the University of Southampton. Full details of the subject demographics can be found in the Appendices.

6.2.5. Analysis

The physical magnitudes of the motion stimuli, Φ , were related to the subjective magnitude estimates, Ψ , using Stevens' power law (Stevens 1975):

Equation 6.1:
$$\psi = k \varphi^n$$

The exponent, *n*, (i.e., the rate of growth of discomfort) and the constant, *k*, were determined by performing linear regression on the logarithmic transformation of Equation 6.1:

Equation 6.2:
$$\log_{10} \psi = \log_{10} k + n \log_{10} \varphi$$

Values for n and k were determined for each individual subject for each frequency and direction of oscillation. Equivalent comfort contours for subjective magnitudes, Ψ , of 50, 63, 80, 100, 125, 160, and 200 were calculated for each subject and direction using Equation 6.1.

The non-parametric Friedman test was used to investigate the overall effects of frequency and direction on the rates of growth of discomfort, n, and the equivalent comfort contours. The Wilcoxon matched-pairs signed ranks test was used to examine specific differences in rates of growth in discomfort and equivalent comfort contours between frequencies and directions. The median rates of growth of discomfort and median equivalent comfort contours were used to identify overall trends in the data.

6.3. Results

6.3.1. Rate of growth of vibration discomfort

The rate of growth of discomfort, n, varied with the frequency of oscillation for all three types of oscillation (Figure 6.3; p < 0.001; Friedman), with a decreasing rate of growth of discomfort with increasing frequency of oscillation (p < 0.001; Spearman).

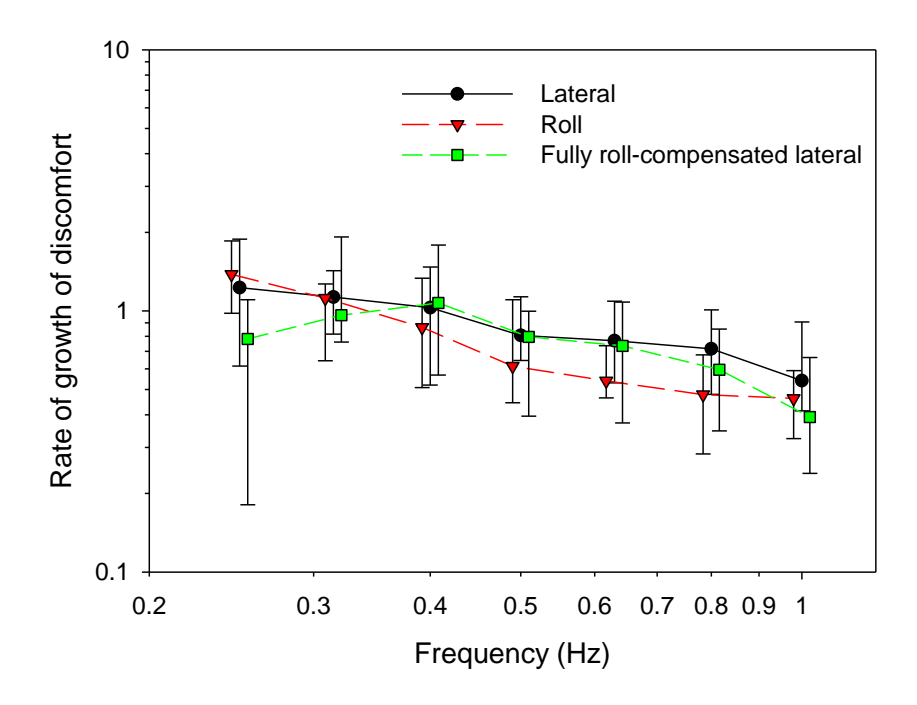


Figure 6.3 Median rates of growth of discomfort for lateral, roll, and fully roll-compensated lateral oscillation. Upper and lower error bars show 75th and 25th percentiles, respectively.

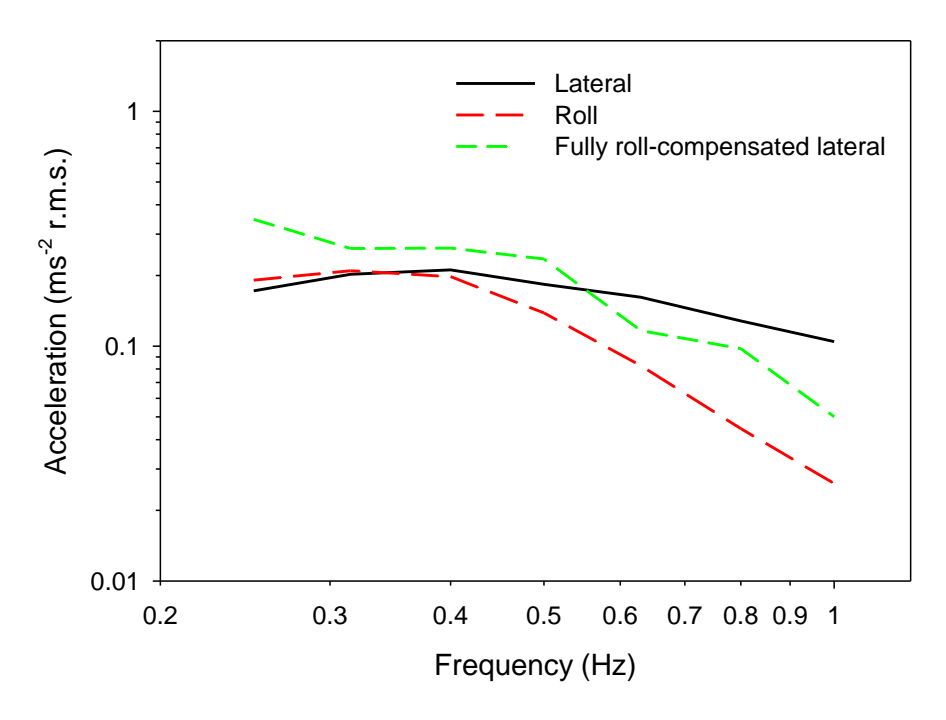


Figure 6.4 Median equivalent comfort contours for lateral, roll, and fully roll-compensated lateral oscillation, each producing discomfort equal to that arising from lateral oscillation at 0.5 Hz, 0.2 ms⁻² r.m.s (i.e. a subjective magnitude, Ψ , of 100).

The rate of growth of discomfort depended on the type of oscillation at all frequencies except 0.315 and 0.5 Hz (p < 0.04; Friedman). The rate of growth of discomfort was greater for lateral oscillation than roll oscillation at 0.63, 0.8, and 1.0 Hz (p < 0.01; Wilcoxon), and greater for roll oscillation than roll-compensated oscillation at 0.25 Hz (p < 0.01; Wilcoxon). There was no effect of gender on the rate of growth of discomfort for any motion at any frequency (p > 0.12; Mann-Whitney U).

6.3.2. Effect of frequency of oscillation on vibration discomfort

For all three types of oscillation, the acceleration required to produce a subjective magnitude of 100 (i.e., the discomfort caused by 0.5-Hz lateral oscillation at 0.2 ms $^{-2}$ r.m.s.) varied with the frequency of oscillation (Figure 6.4; p < 0.001; Friedman). For lateral oscillation and roll oscillation the acceleration required for a subjective magnitude of 100 was approximately constant between 0.25 and 0.4 Hz, but declined from 0.4 to 1.0 Hz at approximately 5 dB per octave for lateral oscillation and at approximately 12 dB per octave for roll oscillation. For fully roll-compensated lateral oscillation, the acceleration required for equivalent comfort reduced at approximately 3 dB per octave from 0.25 to 0.5 Hz, and at approximately 12 dB per octave from 0.5 to 1.0 Hz.

6.3.3. Effect of direction of oscillation on vibration discomfort

At all seven frequencies, the acceleration required to produce a subjective magnitude of 100 differed between the three types of oscillation (p < 0.001; Friedman). Equivalent comfort contours for lateral oscillation and roll oscillation did not differ at frequencies less than 0.4 Hz (p > 0.07; Wilcoxon) but were greater for lateral oscillation than roll oscillation between 0.4 and 1.0 Hz (p < 0.02; Wilcoxon). Equivalent comfort contours were greater for roll-compensated lateral oscillation than pure lateral oscillation at frequencies less than 0.5 Hz (p < 0.02; Wilcoxon) but were greater for lateral oscillation than roll-compensated lateral oscillation at frequencies greater than 0.5 Hz (p < 0.02; Wilcoxon). Equivalent comfort contours were greater for roll-compensated lateral oscillation than pure roll oscillation at all frequencies except 1.0 Hz (p < 0.02; Wilcoxon).

6.3.4. Effect of magnitude on the frequency-dependence of equivalent comfort contours

Equivalent comfort contours were calculated for subjective magnitudes between 50 and 200 (Figure 6.5). The magnitude of acceleration had a large effect on the shape of the equivalent comfort contours, as a result of the change in the rate of growth of discomfort with frequency as

shown in Figure 6.3. However, as the frequency-dependence of the rate of growth of discomfort is similar for all three motions, the relative positions of the contours are similar at all magnitudes.

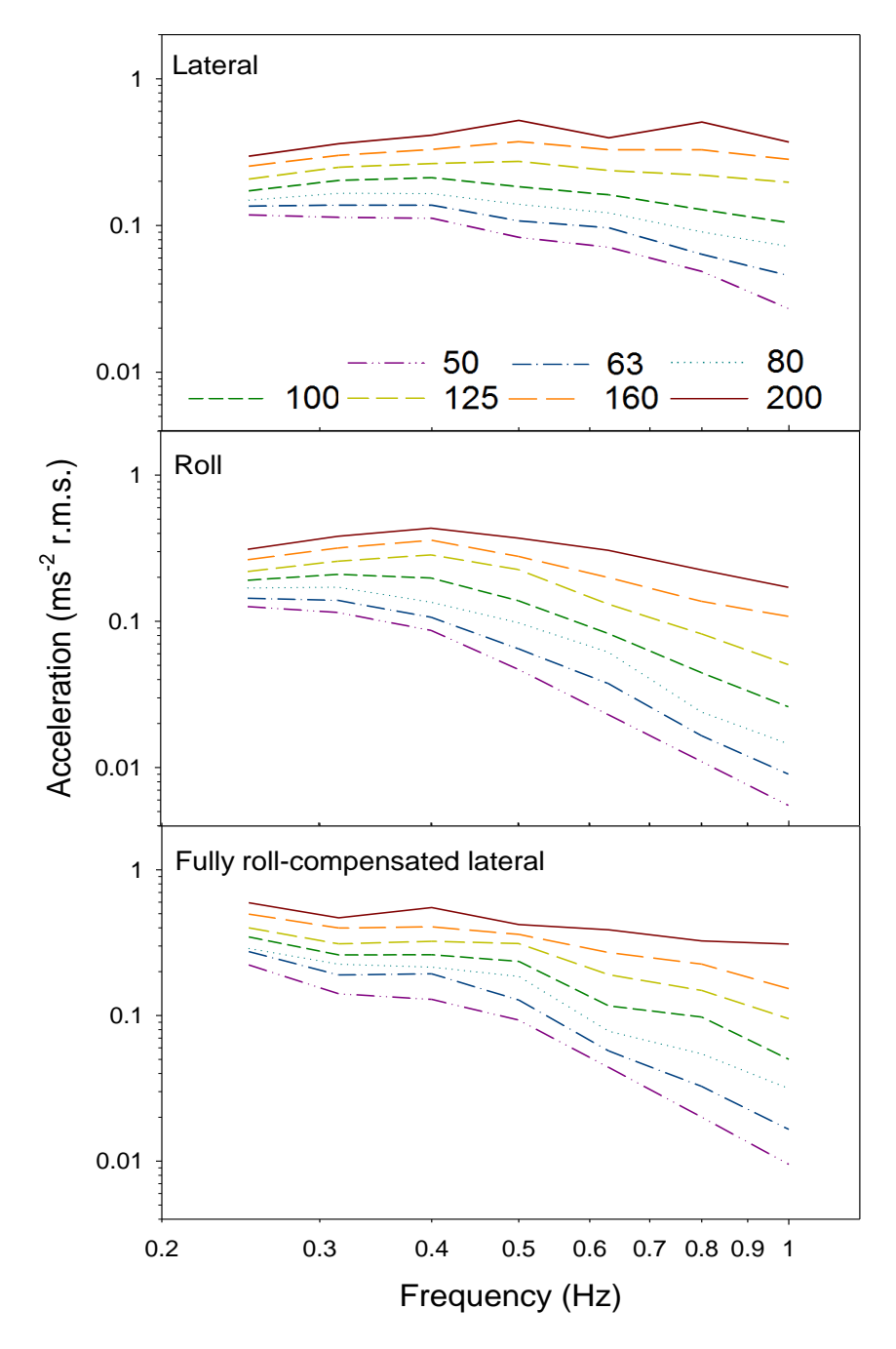


Figure 6.5 The effect of acceleration magnitude on median equivalent comfort contours caused by lateral, roll, and fully roll-compensated lateral oscillation. Contours represent discomfort equal to subjective magnitudes of 50, 63, 80, 100, 125, 160, and 200.

6.3.5. Effect of gender on equivalent comfort contours

Median equivalent comfort contours representing a subjective magnitude of 100 for each type of oscillation were similar in males and females (Figure 6.6). After Bonferroni correction, the only statistically significant difference suggested that, relative to the reference motion, the females were more sensitive to lateral oscillation at 1 Hz than males (p = 0.01; Mann-Whitney U).

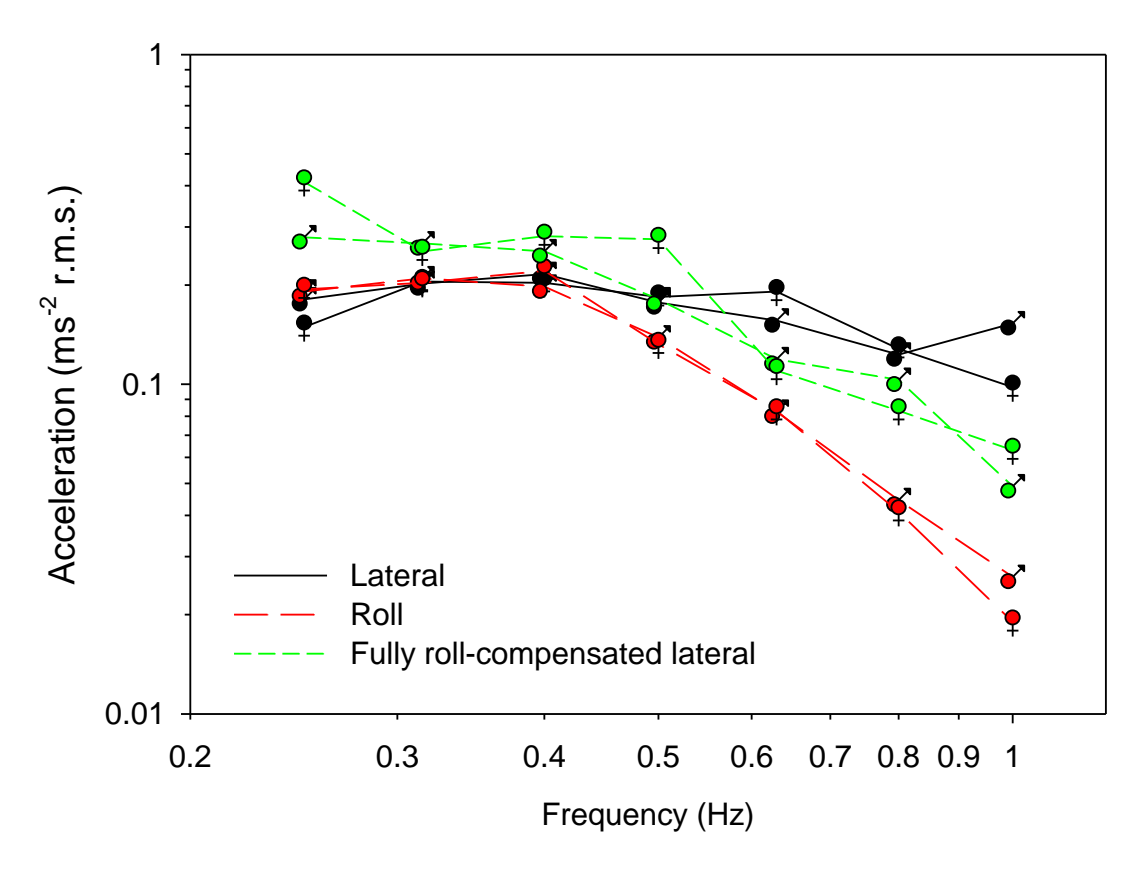


Figure 6.6 Median equivalent comfort contours for lateral, roll, and fully roll-compensated lateral oscillation for males (\circlearrowleft) and females (\updownarrow), each producing discomfort equal to that arising from lateral oscillation at 0.5 Hz, 0.2 ms⁻² rms (i.e. a subjective magnitude, Ψ , of 100).

6.3.6. Location of discomfort

After pooling judgements from the low magnitude and the high magnitude exposures, more subjects reported discomfort at the head, neck, shoulders, and upper-back with roll oscillation than with roll-compensated lateral oscillation at 0.315 and 0.4 Hz (p < 0.01; McNemar). There was a trend for greater incidence of discomfort at the ischial tuberosities with lateral oscillation and roll oscillation than with roll-compensated lateral oscillation, which reached significance at 0.315 and 0.8 Hz (p < 0.02; McNemar). At 0.315 and 0.4 Hz, more subjects reported 'no

discomfort' with fully roll-compensated lateral oscillation than with roll oscillation (p < 0.01; McNemar). No other significant trends in the location of discomfort were identified.

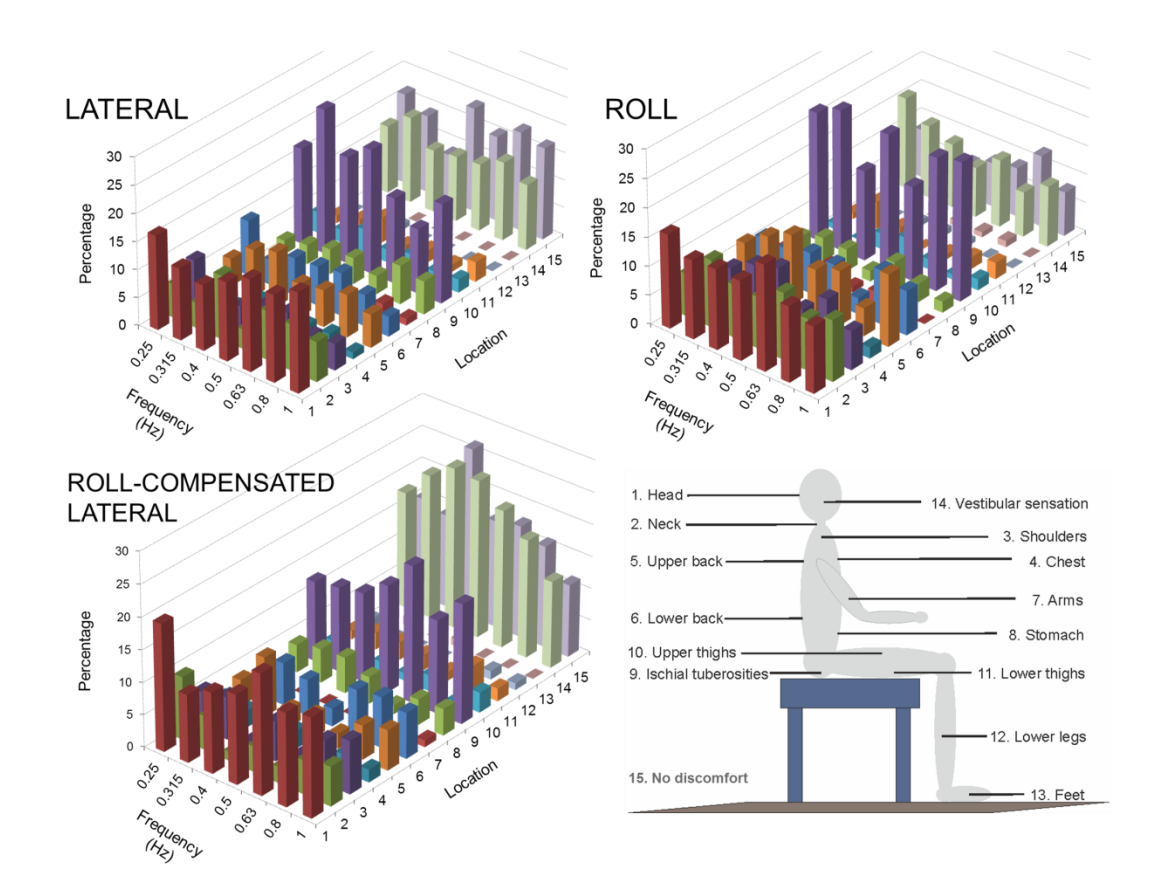


Figure 6.7 Location on the body where subjects felt discomfort caused by lateral, roll, and fully roll-compensated lateral oscillation at frequencies from 0.25 to 1.0 Hz.

6.4. Discussion

6.4.1. Rate of growth of discomfort

The median rates of growth of discomfort for lateral oscillation, roll oscillation, and fully roll-compensated lateral oscillation decreased as the frequency increased from 0.25 to 1.0 Hz, indicating greater sensitivity to changes in acceleration magnitude at lower frequencies. The equivalent comfort contours therefore show greater dispersion at higher frequencies (Figure 6.5). Similar findings have been reported with lateral and roll oscillation between 0.2 and 1.6 Hz on a rigid seat with and without a backrest and four-point harness (Wyllie and Griffin 2007). The rate of growth of discomfort was greater for lateral oscillation than for roll oscillation at

frequencies between 0.63 and 1.0 Hz, suggesting greater sensitivity to changes in the magnitude of roll oscillation than changes in the magnitude of lateral oscillation. The different rates of growth for lateral oscillation and roll oscillation mean that the relative importance of these axes, as shown in Figure 6.4, will vary with the magnitude of the motion. However, at frequencies greater than 0.63 Hz, sensitivity to roll oscillation is so much greater than sensitivity to lateral oscillation that roll will often be the dominant cause of discomfort if the two motions have similar magnitudes.

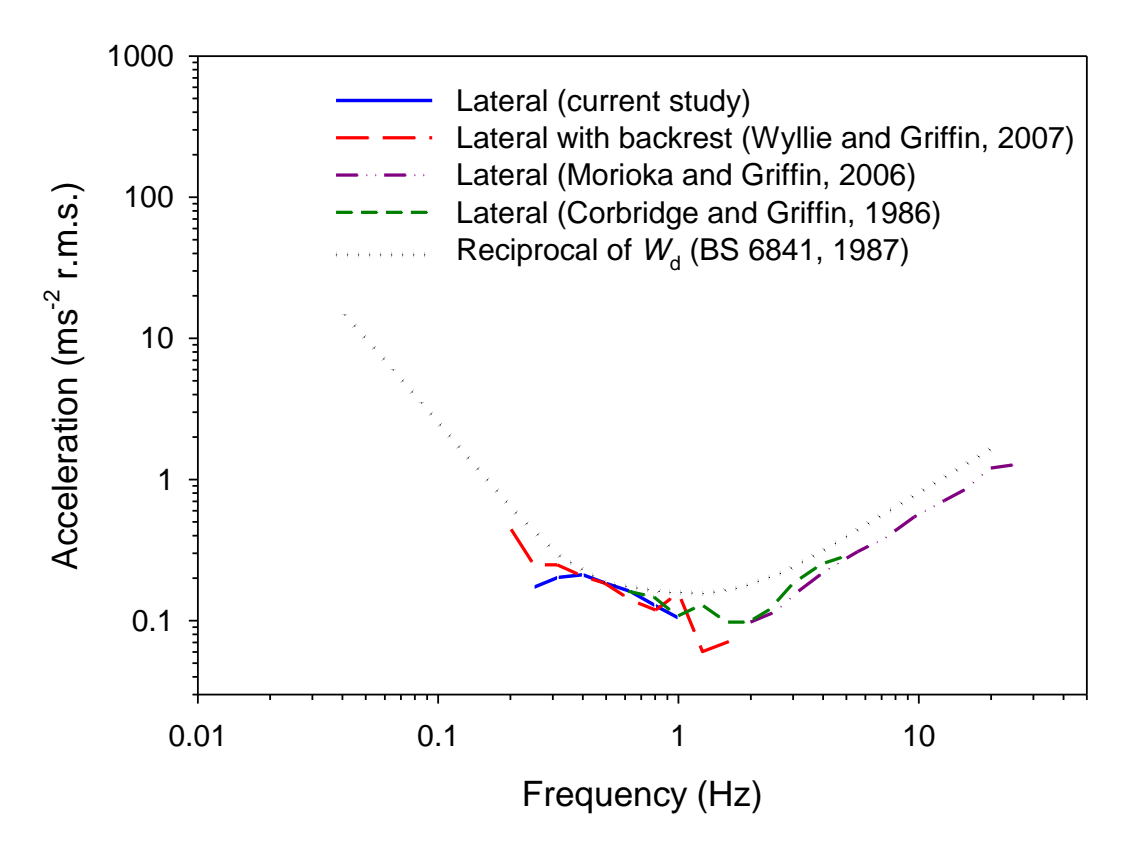


Figure 6.8 Effect of frequency of oscillation on equivalent comfort contours for lateral oscillation. Contours normalised to represent discomfort equal to that caused by lateral acceleration at 0.5 Hz 0.2 ms⁻² r.m.s. on a rigid seat with backrest (i.e. a subjective magnitude, Ψ , of 100).

6.4.2. Effect of frequency of oscillation on discomfort

The equivalent comfort contours for lateral oscillation and roll oscillation are compared with those reported previously in Figure 6.8 and Figure 6.9. The figures show increasing sensitivity to lateral acceleration from 0.2 to 2.0 Hz, but decreasing sensitivity at higher frequencies. In the present study, as the frequency of oscillation increased from 0.5 to 1.0 Hz, the acceleration required for equivalent discomfort decreased by approximately 5 dB per octave for lateral

acceleration, by 12 dB per octave for the lateral acceleration caused by roll, and by 12 dB per octave for the lateral acceleration associated with fully roll-compensated lateral oscillation. For lateral oscillation and roll oscillation of a rigid seat with backrest and harness, equivalent comfort contours from 0.2 to 1.6 Hz declined at approximately 6 dB and 12 dB per octave, respectively (Wyllie and Griffin 2007), broadly consistent with the current findings. The somewhat steeper contours reported previously are consistent with a four-point harness reducing sensitivity at low frequencies, but increasing sensitivity at high frequencies.

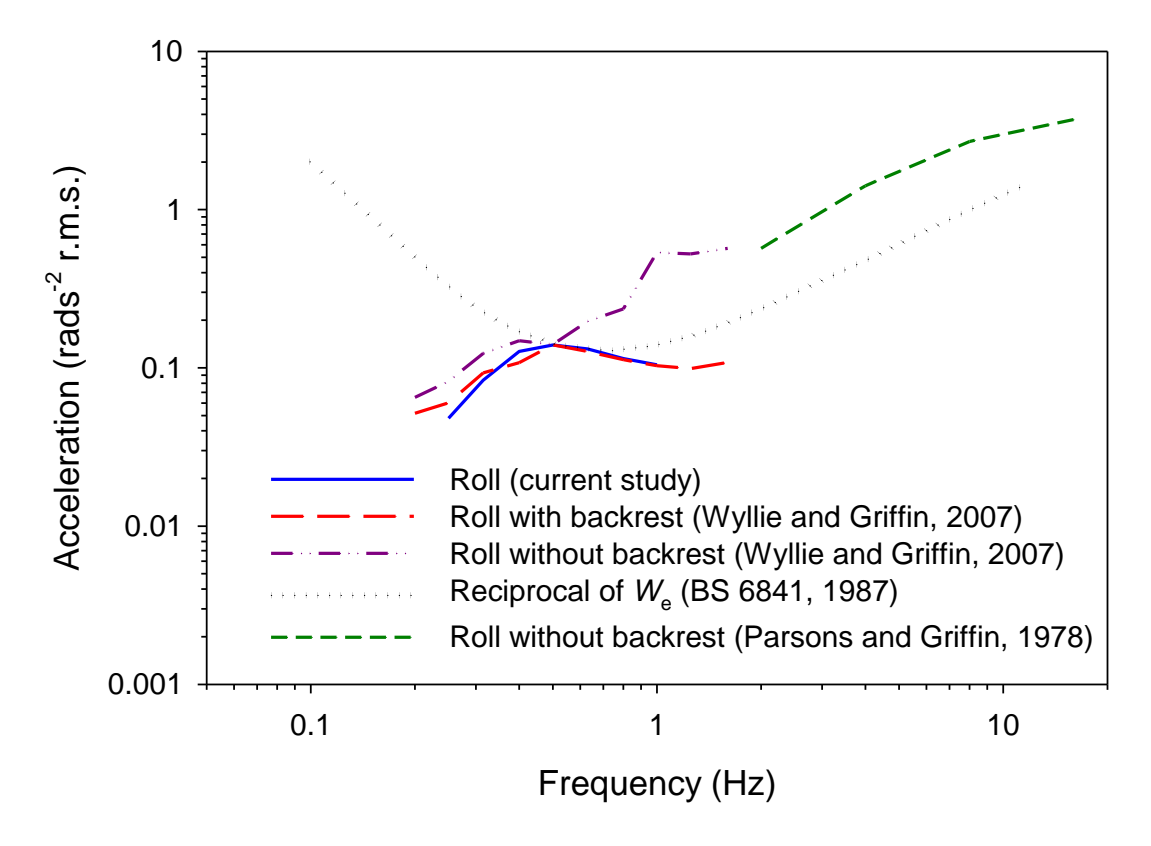


Figure 6.9 Effect of frequency of oscillation on equivalent comfort contours for roll oscillation expressed in terms of rotational acceleration (rads- 2 r.m.s.). Contours normalised to represent discomfort equal to that caused by lateral acceleration at 0.5 Hz 0.2 ms- 2 r.m.s. on a rigid seat with backrest (i.e. a subjective magnitude, Ψ , of 100).

Frequency weighting W_d , suggested for evaluating lateral seat acceleration in BS 6841 (1987) and ISO 2631-1 (1997), appears to offer a close approximation to the experimental contours for lateral acceleration in the plane of the seat (Figure 6.8). For lateral acceleration at a backrest, the standards suggest the same frequency weighting but with a multiplying factor of 0.5, indicating less sensitivity to acceleration at the back than at the seat. The combination of the two weightings assumes discomfort is slightly greater when seated with a backrest than when

seated without a backrest. Studies of the discomfort caused by lateral acceleration when seated with a rigid flat backrest (with and without a four-point harness) and a cushioned backrest (with contours) have produced mixed conclusions (e.g., Wyllie and Griffin 2007; Chapter 5). Further investigation of how the motion of the body and discomfort is influenced by the characteristics of a backrest may assist the optimisation of seats.

As roll oscillation increases in frequency from 0.2 to 1.6 Hz, increased sensitivity to lateral acceleration in the plane of the seat caused by the roll (i.e., the acceleration due to gravity) has been reported when sitting on a rigid seat with backrest and a four-point harness (Wyllie and Griffin 2007). The equivalent comfort contours in the present study show a similar trend (Figure 6.5). When expressed in terms of rotational acceleration (rad.s⁻² r.m.s.), equivalent comfort contours for a rigid seat with backrest show sensitivity increasing at approximately 9 dB per octave as the frequency increases from 0.25 to 0.5 Hz and then remaining approximately constant from 0.5 to 1.0 Hz (Figure 6.9). However, sensitivity to rotational acceleration of a rigid seat without a backrest increased at approximately 6 dB per octave from 0.2 to 1.6 Hz (Wyllie and Griffin 2007) and from 2 to 16 Hz (Parsons and Griffin 1978, Figure 6.9).

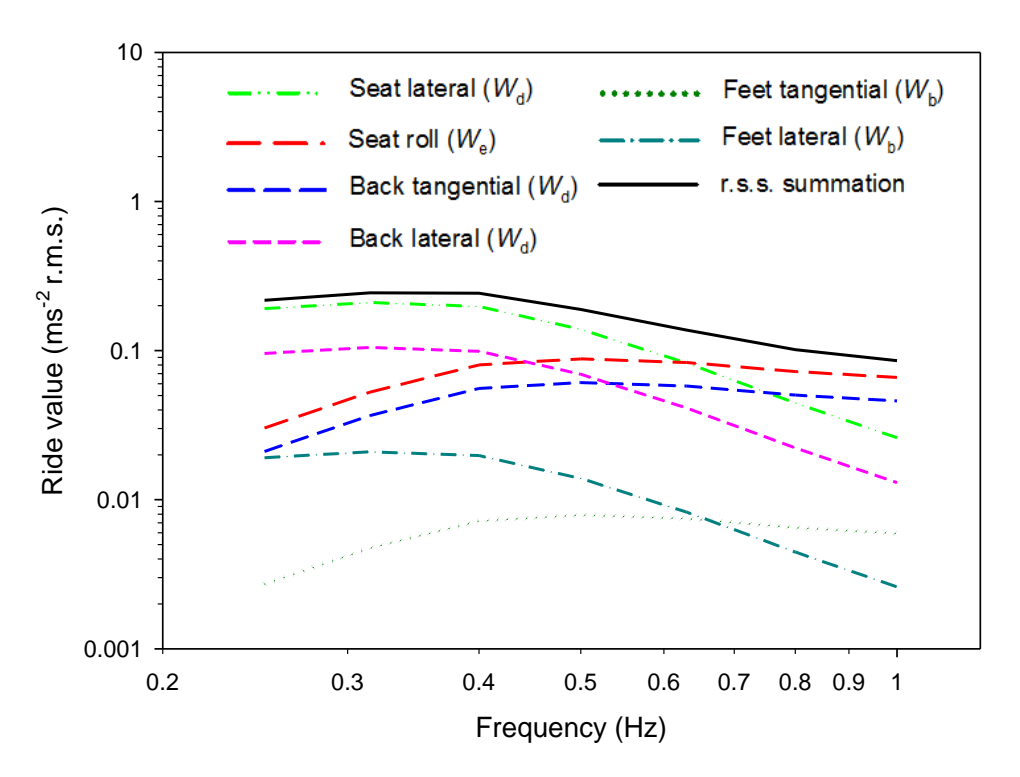


Figure 6.10 Frequency-weighted accelerations corresponding to median equivalent comfort contours for roll oscillation. Values calculated using asymptotic acceleration weightings given in BS 6841 (1987) that have been extrapolated horizontally at frequencies less than 0.5 Hz.

Frequency weighting W_e , is suggested for evaluating roll acceleration in BS 6841 (1987) and ISO 2631-1 (1997), but appears to give an inaccurate representation of the frequency-dependence of the discomfort caused by roll oscillation of rigid seats (both with and without backrests) over the frequency range 0.2 to 1.6 Hz (Figure 6.9). With fully roll-compensated lateral acceleration, the lateral acceleration at the seat is zero and predictions of discomfort are solely dependent on the rotational acceleration (assuming the position of full roll-compensation is at the seat surface and the translational motions at the backrest and footrest arising from roll are negligible). The accuracy of frequency weighting W_e at low frequencies is therefore crucial for predicting the discomfort associated with fully roll-compensated lateral oscillations.

Using the root-sums-of-squares summation method and the frequency weightings as defined in current standards (BS 6841 1987, ISO 2631-1 1997), Wyllie and Griffin (2007) showed how seven component ride values arising from roll oscillation of a seat may contribute to vibration discomfort: lateral acceleration at the seat surface, the backrest, and the foot support (due to these not being at the centre of roll), translational acceleration at the seat, the back, and the feet (arising from the gravitational component due to roll, $g.\sin\theta$), and rotational acceleration at the seat surface (see Appendix A.10. for a list of equations relating to each of these components). For roll oscillations of a rigid seat with backrest that caused similar discomfort at all frequencies, the root-sums-of-squares summation of these seven components declined with increasing frequency, indicating discomfort was underestimated at high frequencies or, conversely, overestimated at low frequencies (Wyllie and Griffin 2007). The current results are consistent with this conclusion (Figure 6.10).

With fully roll-compensated lateral oscillation, if the component ride values for the horizontal accelerations and the translational accelerations due to roll were measured separately they would have opposite polarities. The root-sums-of-squares of all such values will ignore polarity and cannot be expected to provide an appropriate prediction of ride comfort. However, if at each location the discomfort is caused by the vector sum of the horizontal acceleration and the acceleration due to gravity, it would be appropriate to measure the resultant acceleration (e.g., using a single translational accelerometer) at each location. The present findings suggest this would provide an appropriate indication of discomfort for frequencies of oscillation less than about 0.4 Hz, but that it would underestimate discomfort at frequencies greater than about 0.4 Hz.

6.4.3. Effect of direction of oscillation on discomfort

The level of the equivalent comfort contours representing a subjective magnitude of 100 was similar for lateral and roll oscillation at 0.4 Hz and lower frequencies (Figure 6.4), suggesting lateral acceleration in the plane of the seat can predict discomfort in this frequency range irrespective of whether the acceleration is caused by lateral oscillation or roll oscillation. At frequencies greater than 0.4 Hz, lateral acceleration in the plane of the seat caused more discomfort when it was produced by roll oscillation than when it was produced by lateral oscillation. Differences in the discomfort caused by lateral and roll oscillation increased as the frequency increased from 0.4 to 1.0 Hz, consistent with (Wyllie and Griffin 2007).

At frequencies less than about 0.5 Hz, the acceleration of the equivalent comfort contour was greater for roll-compensated lateral oscillation than for uncompensated lateral oscillation, consistent with the 'compensation' reducing discomfort. In this frequency range, the discomfort associated with roll-compensated lateral acceleration was similar to that caused by uncompensated lateral acceleration with half the magnitude of lateral acceleration. However, at 0.63 Hz and higher frequencies, roll-compensated lateral oscillation caused more discomfort than uncompensated lateral oscillation.

Subjects exposed to roll-compensated lateral oscillation experienced zero lateral acceleration at the seat surface (i.e., at the position of full roll-compensation) but there was lateral acceleration above and below this position (due to translation arising from the roll). The magnitude of the lateral acceleration increased with increasing distance from the position of full roll-compensation and with increasing frequency of oscillation, so the extremities of the body experienced the greatest lateral acceleration during these motions. The feet experienced lateral acceleration of the vibrator table and the head experienced lateral acceleration as a result of the roll motion of the body centred on the seat surface. This translational acceleration at the feet, the head, and other parts of the body can be expected to have contributed to the increased discomfort with roll oscillation at the higher frequencies.

It is also necessary to consider the effect of rotational acceleration (rads⁻²) on discomfort. To achieve full roll-compensation of lateral acceleration, α , the angle of roll, θ , must satisfy:

Equation 6.3:
$$\alpha = g \times \sin \theta$$
 (where $g = \text{gravitational component}$)

The relationship between α and θ remains constant regardless of frequency, but as the frequency doubles the magnitude of rotational acceleration required to achieve an angular displacement, θ , increases by a factor of 4. Whilst a roll oscillation of 0.5 Hz may yield the same rotational displacement (and therefore the same lateral acceleration in the plane of the seat) as

a 1.0-Hz roll oscillation, the magnitude of rotational acceleration at 1.0 Hz will be four times as great. This rapid growth in rotational acceleration with increasing frequency may explain the increased discomfort caused by roll oscillation and fully-roll compensated lateral oscillation at frequencies greater than 0.5 Hz.

6.4.4. Location of discomfort

Fully roll-compensated lateral oscillation caused less discomfort at the ischial tuberosities than both uncompensated lateral oscillation and pure roll oscillation, confirming the expectation of 'balanced' lateral forces at the seat surface (i.e., at the position of full roll-compensation). Reports of 'no discomfort' were most frequent with fully roll-compensated oscillation at frequencies less than 0.5 Hz, consistent with little discomfort in this frequency range (see Figure 6.4). Roll oscillation at 1 Hz caused greatest discomfort at the head, neck, shoulders, and upper-back, consistent with previous work (Wyllie and Griffin 2007). Compared to sitting on a rigid seat with no backrest, discomfort caused by roll oscillation is greater when seated with a backrest and four-point harness (Wyllie and Griffin 2007). This may be explained by the increased transmission of lateral and roll vibration to the head and upper-body when sitting with a backrest (Paddan and Griffin 1988, 1992) or an inability to make compensatory movements when sitting against a backrest. No difference in discomfort between a 'head still' posture (where the upper-body maintained an Earth-vertical orientation) and a 'move-with' posture (where the upper-body moved in-line with the seat) when exposed to roll and pitch oscillation (Wyllie 2007), suggests voluntary postural control does not offer a complete explanation.

6.4.5. Implications for transport

The findings have implications for the measurement of low frequency vibration in transport. Passengers of land vehicles are exposed to horizontal and rotational forces when traversing curves and passing over undulations. The discomfort caused by low frequency lateral and roll oscillations is usually estimated from the resultant translational acceleration in "the lateral axis of the vehicle disregarding whether the measured acceleration arises from lateral acceleration or the component of gravity, i.e., g.sin θ caused by roll" (Wyllie and Griffin 2007, p. 2650). At frequencies greater than 0.5 Hz, fully roll-compensated lateral oscillation causes greater discomfort than pure lateral oscillation, so the resultant translational acceleration alone is clearly insufficient for predicting discomfort in vehicles. An understanding of the discomfort caused by roll oscillation is necessary to predict the discomfort caused by oscillation at these frequencies.

The findings also have implications for the design of vehicles where the suspension influences roll at frequencies in the range 0.5 to 1.0 Hz (e.g., in tilting trains; Ueno *et al.* 1986; Förstberg

2000; Cohen *et al.*, 2011). The discomfort associated with lateral centripetal acceleration while traversing curves at high speed can be reduced by roll-compensation, but only with motions at frequencies less than about 0.5 Hz. Roll-compensation of lateral acceleration at frequencies greater than 0.5 Hz is likely to worsen passenger comfort and so other techniques for minimising adverse effects of these motions will be required.

6.5. Conclusion

The discomfort caused by lateral oscillations with frequencies less than about 0.5 Hz can be reduced by appropriate roll oscillations. However, with frequencies greater than about 0.5 Hz, roll-compensation increases the discomfort caused by lateral oscillation.

At frequencies less than about 0.5 Hz, frequency weighting the lateral acceleration in the plane of the seat (using standardised weighting W_d) provides a useful prediction of the discomfort caused by lateral oscillation, roll oscillation, and combined lateral and roll oscillation. At frequencies between about 0.5 and 1.0 Hz, the additional contribution of any rotational acceleration is required to predict discomfort, but the root sums-of-squares method using frequency weighting W_e is not sufficient in its current form in this frequency range. Improved understanding of the factors influencing the discomfort caused by low frequency roll oscillation is required, particularly for predicting discomfort caused by fully roll-compensated lateral oscillation where lateral acceleration in the plane of the seat is zero.

The design of vehicles with tilt compensation requires caution if compensation of lateral acceleration occurs at frequencies greater than 0.5 Hz, as this is likely to worsen passenger comfort.

Chapter 7

Effect of seat pan stiffness

7.1. Introduction

It was shown in Chapter 5 that lateral vibration discomfort is dependent on the configuration of seating, but the effects of seating with low frequency motions containing roll are still unknown. In Chapter 6, it was shown that both pure roll oscillation and fully roll-compensated lateral oscillation cause greater discomfort than pure lateral oscillation at frequencies greater than 0.63 Hz. The purpose of the experiments described in this chapter, and in the next (Chapter 8), was to determine whether the discomfort caused by these motions is dependent on seating.

The optimisation of the design of a seat should include consideration of many factors, including the shape, the width, and the height of the seat pan and the backrest, and the seat cushioning, all of which may influence both the static discomfort of seat occupants and their vibration discomfort. The ability of seated occupants to maintain postural stability during low frequency lateral oscillation depends on the composition of the seat pan. Soft cushions tend to reduce the maximum pressure at the seat-buttock interface (Sprigle *et al.*, 1990), which may improve static comfort (e.g., Ebe and Griffin, 2000). However, the compliance of a cushion might be expected to impair lateral stability. Understanding the trade-offs between static and dynamic seat comfort is necessary to optimise the overall comfort of seated passengers (Ebe and Griffin, 2000), but there has been little systematic investigation with non-vertical vibration.

Current vibration standards suggest how vibration discomfort can be predicted from the acceleration measured at the seat-body interfaces (i.e., between the buttocks and the seat pan, between the back and the backrest, and between the feet and footrest) for frequencies between 0.5 and 80 Hz (BS 6841, 1987; ISO 2631-1, 1997). In many forms of transport, people are exposed to lower frequencies of horizontal and rotational oscillations that can also cause

discomfort. How to predict the discomfort caused by such motions, and how discomfort depends on the configuration of seating is not well understood.

The experiment reported here was designed to quantify differences in vibration discomfort when sitting on a rigid seat and when sitting on a foam cushion during lateral oscillation, roll oscillation, and fully roll-compensated lateral oscillation at frequencies between 0.25 and 1.0 Hz. It was hypothesised that reduced stability when sitting on the cushion would result in increased vibration discomfort. If motion at the subject seat interface is a good basis for predicting discomfort, measurements of the transmission of motion through the cushion should indicate differences in vibration discomfort between the rigid seat and the cushioned seat.

7.2. Method

7.2.1. Apparatus

Motions were produced by a six-axis motion simulator in the Human Factors Research Unit of the Institute of Sound and Vibration Research at the University of Southampton. The simulator is capable of ± 0.5 m vertical motion, ± 0.25 m horizontal motion, and $\pm 20^{\circ}$ of rotational motion. Subjects sat on a seat positioned so that the centre of the seat surface was at the centre of the motion platform (approximately 2.5 m by 3.0 m) and at the centre-of-rotation.

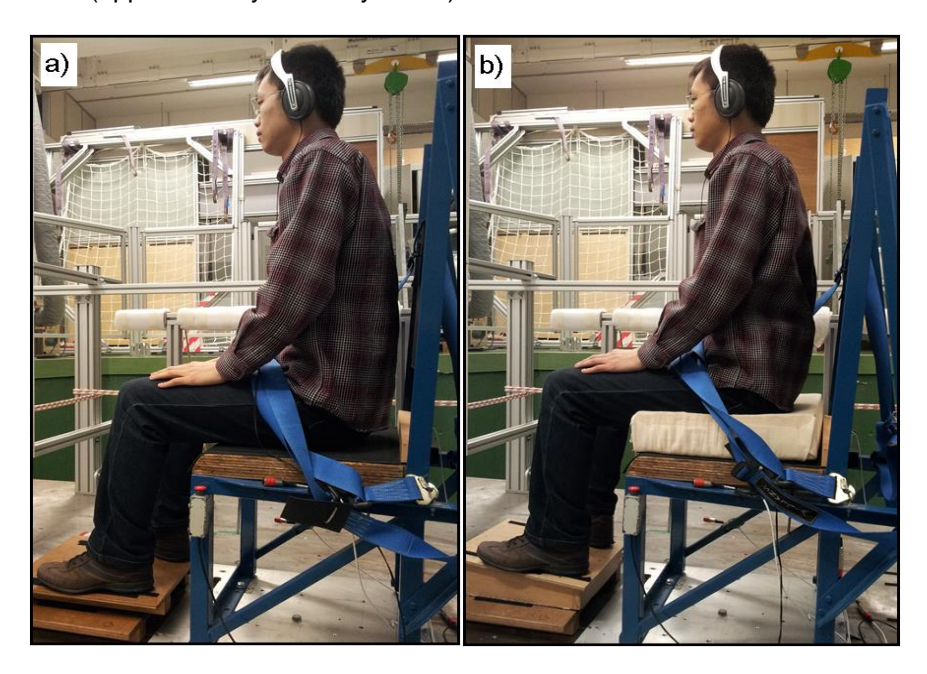


Figure 7.1 Illustration of the two seat-pan conditions (a) rigid seat; (b) foam cushion.

The seat was rigid and consisted of a flat horizontal seat pan (510 by 400 mm) located 480 mm above the motion platform. The surface of the seat pan was covered with rigid rubber (less than 2 mm in thickness) to increase surface friction. When needed, a block of foam (400 by 400 by 100 mm, with a density of 62.5 kg/m³, and a stiffness of 7.73 N/mm – see section Appendices) was secured to the surface of the rigid seat.

Subjects were provided with an adjustable height footrest to allow the same sitting posture across both seating conditions (i.e., with their thighs parallel to the floor). Subjects were asked to maintain comfortable upright postures without contacting the backrest, with their hands on their laps and their feet flat on the footrest (see Figure 7.1). Subjects wore a loose lap belt for safety.

Subjects wore headphones producing white noise at 65 dB(A) to mask the sounds of the simulator. The experimenter communicated with subjects through a microphone connected to the headphones by interrupting the white noise.

Lateral acceleration and rotational velocity were measured on the rigid seat (using a Silicon Design 2260 capacitive translational accelerometer and a BAE Systems 299641-0100 Single-Axis VSG Bipolar rotational gyro), and at the seat-body interface between the foam cushion and the ischial tuberosities using a SIT-BAR (Seat Interface for Transducers indicating Body Acceleration Received; Whitham and Griffin, 1977) with a translational piezo-resistive accelerometer (Endevco 2265) and a rotational gyro (BAE Systems 299641-0100 Single-Axis VSG Bipolar).

7.2.2. Design

The study used a repeated measures (within-subjects) design. Subjects were exposed to a series of motion stimuli while seated in one of two seating conditions (the rigid seat or the foam cushioned seat) in each of two experimental sessions (conducted on separate days). At the start of each session, subjects were trained on the method of absolute magnitude estimation using a set of practice motion stimuli (consisting of all three directions of oscillation at the lowest and highest magnitudes – see section 7.2.3).

Each session consisted of four parts. In part 1 (equivalent comfort contours) subjects used the method of magnitude estimation to rate the discomfort produced by lateral, roll, and fully roll-compensated lateral motion at seven frequencies of oscillation from 0.25 to 1.0 Hz (at magnitudes between 0.08 and 0.4 ms⁻² r.m.s.), on either the rigid seat or the foam cushion. In part 2 (body map) subjects used a labelled diagram of the body (Figure 7.2) to indicate where they felt discomfort during exposure to lateral oscillation, roll oscillation, and fully roll-

compensated lateral oscillation at a single magnitude (0.2 ms⁻² r.m.s.) of each frequency. Subjects were free to choose as many locations as they felt appropriate. In part 3 (relative discomfort) subjects used magnitude estimation to rate the discomfort caused by 0.5-Hz lateral oscillations between 0.08 and 0.4 ms⁻² r.m.s. when sitting on both the rigid seat and the foam cushion. In part 4 (objective test) subjects were exposed to three magnitudes of lateral oscillation, roll oscillation, and fully roll-compensated lateral oscillation at the seven frequencies from 0.25 to 1.0 Hz whilst sitting on the foam cushion with the SIT-BAR (Figure 3.12).

The order of presentation of motion stimuli within each part of the experiment was fully randomised for each subject. The order of the two seating conditions was alternated for each subject such that half the subjects sat on the rigid seat first and half sat on the foam cushion first.

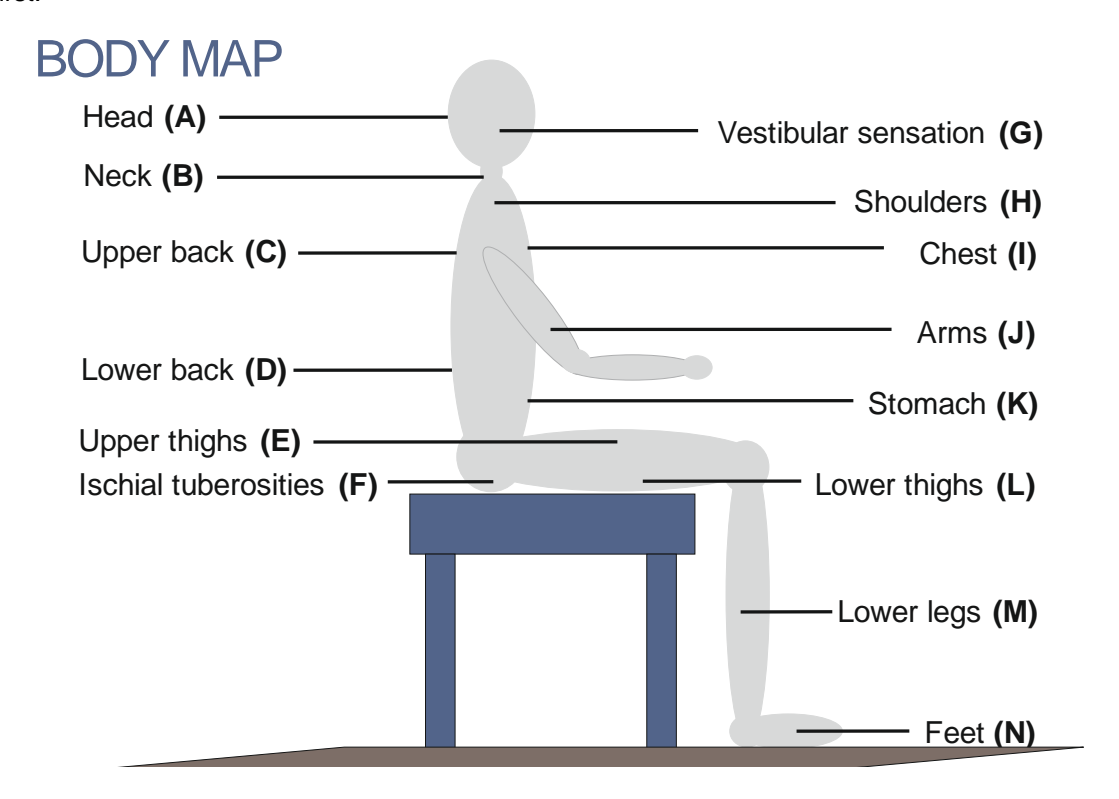


Figure 7.2 Body map used by subjects to indicate the location of discomfort caused by lateral, roll and fully roll-compensated lateral oscillation.

7.2.3. Motion stimuli

The motion stimuli consisted of seven frequencies at the preferred one-third octave centre frequencies from 0.25 to 1.0 Hz. Each frequency was presented at, nominally, eight magnitudes in logarithmic series from 0.08 to 0.40 ms⁻² r.m.s. (Due to simulator limitations, five magnitudes

of lateral oscillation (0.08 to 0.20 ms⁻² r.m.s.) were presented at 0.25 Hz and seven magnitudes (0.08 to 0.315 ms⁻² r.m.s.) at 0.315 Hz. Seven magnitudes of roll oscillation (equivalent to 0.08 to 0.315 ms⁻² r.m.s.) were presented at 1.0 Hz. Seven magnitudes of roll-compensated oscillation were presented at 0.8 Hz (0.08 to 0.315 ms⁻² r.m.s.) and six magnitudes (0.08 to 0.25 ms⁻² r.m.s.) at 1.0 Hz.

For roll oscillation, the magnitude was defined by the acceleration in the plane of the seat (i.e., due to gravity). For roll-compensated lateral oscillation, the lateral oscillation and the roll oscillation were combined 180° out-of-phase such that the resultant acceleration in the plane of the seat was zero. This procedure is illustrated in Figure 7.3 which shows the acceleration waveform in the plane of the seat for lateral, roll, and roll-compensated oscillation at 0.5 Hz. All motion stimuli were transient waveforms with a 3.5 cycle duration (as shown in Figure 7.3) generated from the product of a sine wave of the desired frequency and a half-sine of the same duration. The motions were generated within MATLAB (version R2010a research) using the *HVLab* toolbox (version 1.0).

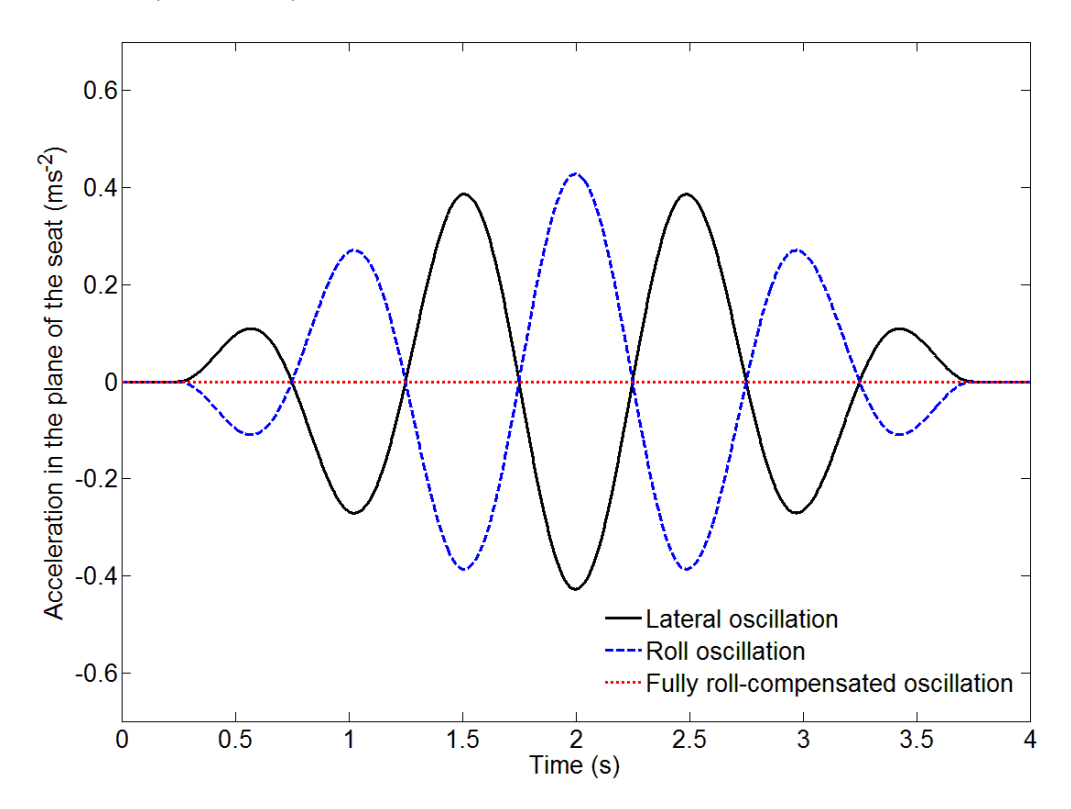


Figure 7.3 Example waveforms for 1.0-Hz oscillation showing the acceleration in the plane of the seat for lateral oscillation, roll oscillation, and fully roll-compensated lateral oscillation.

7.2.4. Subjects

Twenty healthy male volunteers aged between 18 and 32 years participated in the experiment (median age 26.0 years, inter-quartile range, IQR, 5.8 years; median weight 79.0 kg, IQR 17.6 kg; median stature 1.79 m, IQR 0.10 m). Subjects were recruited from the staff and student population of the University of Southampton. Full details of the subject demographics can be found in the Appendices.

7.2.5. Analysis

The physical magnitudes, φ , of the motion stimuli were related to the subjective magnitude estimates, ψ , using Stevens' power law (Stevens, 1975):

Equation 7.1:
$$\psi = k \varphi^n$$

The exponent, n, (i.e., the rate of growth of discomfort) and the constant, k, were determined by performing linear regression on the logarithmic transformation of Equation 7.1:

Equation 7.2:
$$\log_{10} \psi = \log_{10} k + n \log_{10} \varphi$$

Lateral oscillation of the rigid seat at a frequency of 0.5 Hz and a magnitude of 0.2 ms⁻² r.m.s. was selected as a 'common reference' for constructing equivalent comfort contours. A 'normalisation' factor was determined in order to normalise the data for all subjects such that the reference condition was assigned a value of 100. Normalisation factors were calculated using Equation 7.3:

Equation 7.3: Normalisation factor =
$$(100 / \psi_{Reference})$$

where $\psi_{\text{Reference}}$ is the subjective magnitude corresponding to the reference condition, obtained through linear regression of Equation 7.2. Normalisation factors were determined for each subject.

Values for n and k were determined for each individual subject for each frequency and direction of oscillation using normalised magnitude estimates from part 1 (equivalent comfort contours). Equivalent comfort contours for normalised subjective magnitudes, Ψ , of 50, 63, 80, 100, 125, 160, and 200 were calculated for each subject and all three directions of oscillation using Equation 7.1.

The data from part 2 (body map) were used to assess the effect of seating and the frequency of lateral oscillation, roll oscillation and fully roll-compensated lateral oscillation on the location of discomfort.

The data from part 3 (relative discomfort) were used to calculate a 'seat-pan factor' to adjust the equivalent comfort contours for the foam cushion (obtained in part 1) so that discomfort relative to the rigid seat could be examined. The seat-pan factor was calculated using Equation 7.4:

Equation 7.4 Seat-pan factor =
$$(\varphi_{Relative}) / (\varphi_{Foam})$$

where φ_{Foam} is the acceleration magnitude of a 0.5-Hz lateral test motion on the foam cushion in part 1 (equivalent comfort contours) that was given a subjective magnitude of 100, and $\varphi_{\text{Relative}}$ is the acceleration magnitude of a 0.5-Hz lateral test motion on the foam cushion in part 3 (relative discomfort) that was given a subjective magnitude of 100. The acceleration magnitudes used to define φ_{Foam} and $\varphi_{\text{Relative}}$ were median values calculated from the 20 subjects. Relative equivalent comfort contours for the rigid seat and the foam cushion were generated by applying the seat-pan factors to the median equivalent comfort contours for the foam cushion calculated from part 1. Individual equivalent comfort contours from part 1 were also adjusted using the same seat-pan factors in order to allow for statistical comparisons across seating conditions.

The non-parametric Friedman test was used to investigate the overall effect of frequency, direction and seat pan stiffness on the rates of growth of discomfort and the equivalent comfort contours. The Wilcoxon matched-pairs signed ranks test was used to examine specific differences in rates of growth of discomfort and equivalent comfort contours between seating conditions, frequencies, and directions. The McNemar dichotomous test was used to test for significant trends in the body map data. Median rates of growth of discomfort and median equivalent comfort contours were used to identify overall trends in the data. The Bonferroni correction was used where there were multiple comparisons.

7.2.6. Objective measurements

The 'lateral transmissibility' (T_y) of the foam was calculated with three magnitudes of lateral oscillation, roll oscillation, and fully roll-compensated lateral oscillation at each of the seven preferred one-third octave centre frequencies from 0.25 to 1.0 Hz. The transmissibility was calculated by dividing the lateral acceleration at the seat-body interface of the foam cushion ($a_{y-\text{foam}}$) by the acceleration on the rigid seat surface ($a_{y-\text{rigid}}$):

Equation 7.5:
$$T_y = a_{y-foam} / a_{y-rigid}$$

For the same motions, roll transmissibility (T_{roll}) of the foam cushion was calculated by dividing the rotational velocity at the seat-body interface of the foam cushion ($v_{roll-foam}$) by the rotational velocity on the rigid seat surface ($v_{roll-rigid}$):

Equation 7.6:
$$T_{roll} = v_{roll-foam} / v_{roll-rigid}$$

7.3. Results

7.3.1. Effect of seating on rate of growth of discomfort

Median rates of growth of discomfort for the three directions of oscillation (lateral, roll, and fully roll-compensated lateral) on the two types of seat (rigid and foam) are shown as a function of frequency in Figure 7.4.

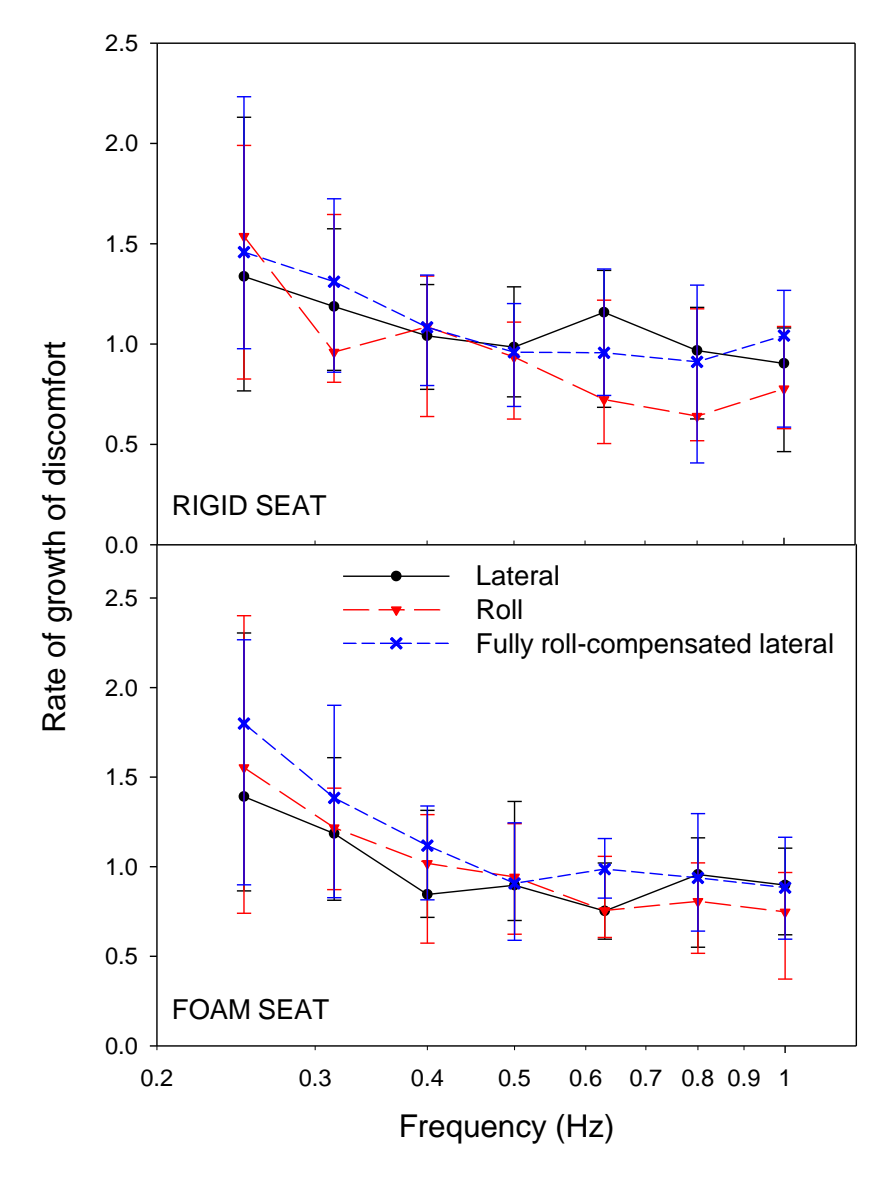


Figure 7.4 Median rates of growth of discomfort for lateral, roll and fully roll-compensated lateral oscillation on the rigid seat and the foam seat. Upper and lower error bars show 75th and 25th percentiles, respectively.

The seat pan type did not have a significant effect on the rate of growth of discomfort for any direction or frequency of oscillation (p > 0.05; Wilcoxon), except for 0.63-Hz lateral oscillation where the rate of growth of discomfort was greater on the rigid seat than the foam cushion (p = 0.005; Wilcoxon).

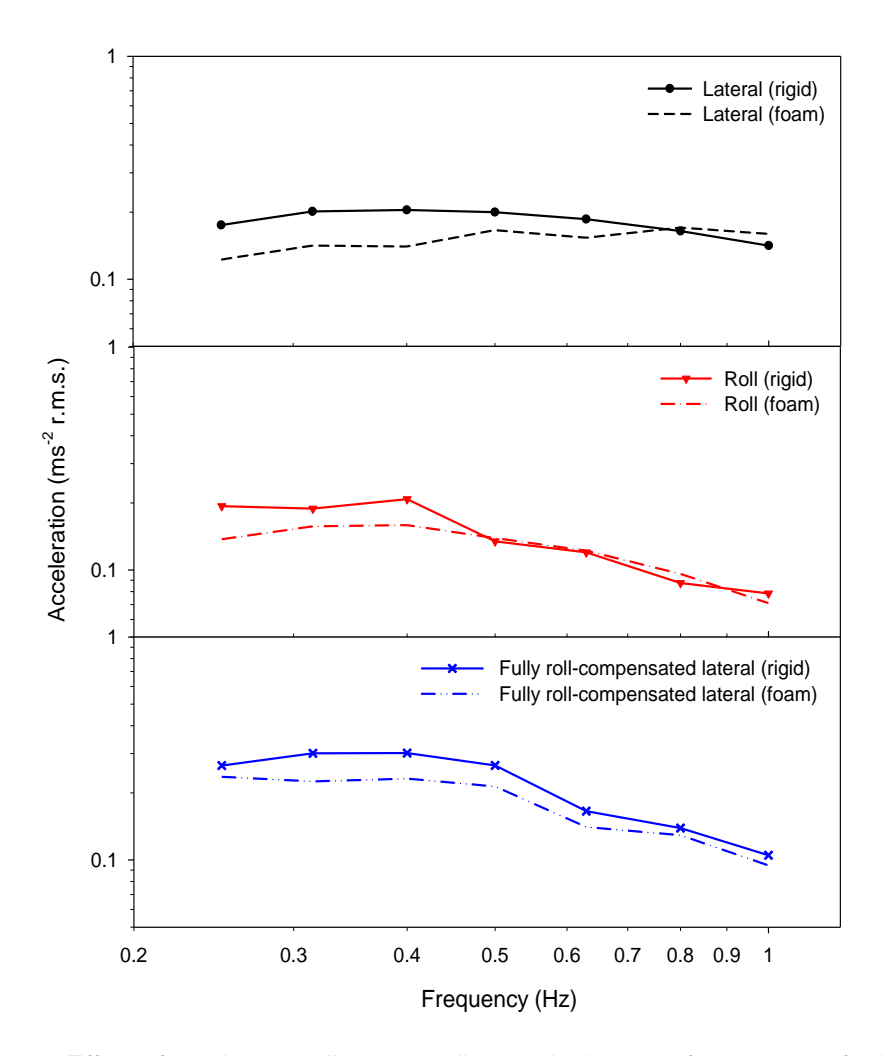


Figure 7.5 Effect of seating on adjusted median equivalent comfort contours for lateral oscillation, roll oscillation, and fully roll-compensated lateral oscillation. Contours, expressed as the component of lateral acceleration in the plane of the seat, represent discomfort equal to that arising with 0.5-Hz lateral oscillation at, 0.2 ms $^{-2}$ r.m.s. on the rigid seat (i.e. a subjective magnitude, Ψ , of 100).

7.3.2. Effect of frequency and direction of oscillation on rate of growth of discomfort

Rates of growth discomfort varied with the frequency of oscillation for all directions (lateral, roll, and fully roll-compensated lateral) of oscillation on both the rigid seat and the foam cushion (p < 0.001; Friedman; see Figure 7.4). On both seats, rates of growth of discomfort were negatively correlated with frequency for lateral oscillation (rigid seat: R = -0.287, p = 0.001, foam cushion: R = -0.276, p = 0.001; Spearman), roll oscillation (rigid seat: R = -0.354, p < 0.001, foam cushion: R = -0.361, p < 0.001; Spearman) and fully roll-compensated lateral oscillation (rigid seat: R = -0.284, p = 0.001, foam cushion: R = -0.304, p < 0.001; Spearman).

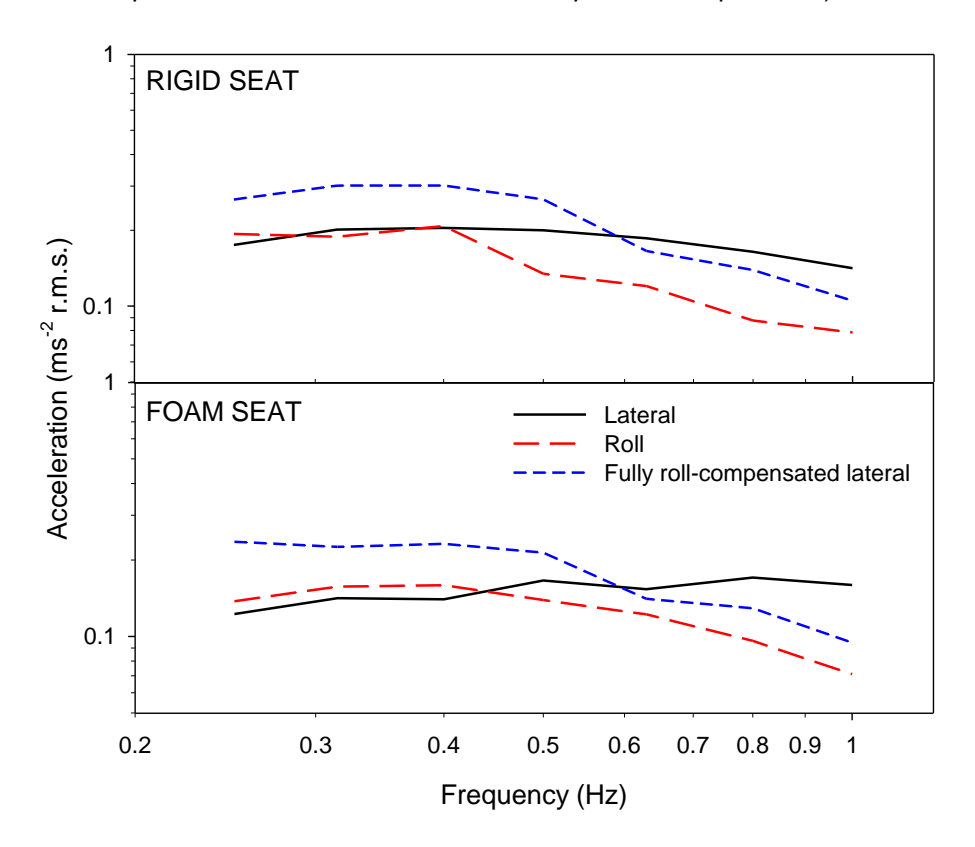


Figure 7.6 Effect of direction of oscillation on median equivalent comfort contours for the rigid seat and the foam cushion. Contours, expressed as the component of lateral acceleration in the plane of seat, represent discomfort equal to that arising from 0.5-Hz lateral oscillation at 0.2 ms⁻² r.m.s. on the rigid seat (i.e. a subjective magnitude, Ψ , of 100).

On the rigid seat, there was no significant effect of the direction of oscillation on the rates of growth of discomfort at any frequency (p > 0.05; Friedman) except for 0.63 Hz (p = 0.019; Friedman) and 1.0 Hz (p = 0.032; Friedman). However, further analysis with the Bonferroni

correction revealed no specific significant differences in the rates of growth of discomfort at these frequencies (p > 0.167; Wilcoxon). On the foam cushion, there was no significant effect of the direction of oscillation on the rates of growth of discomfort at any frequency (p > 0.05; Friedman).

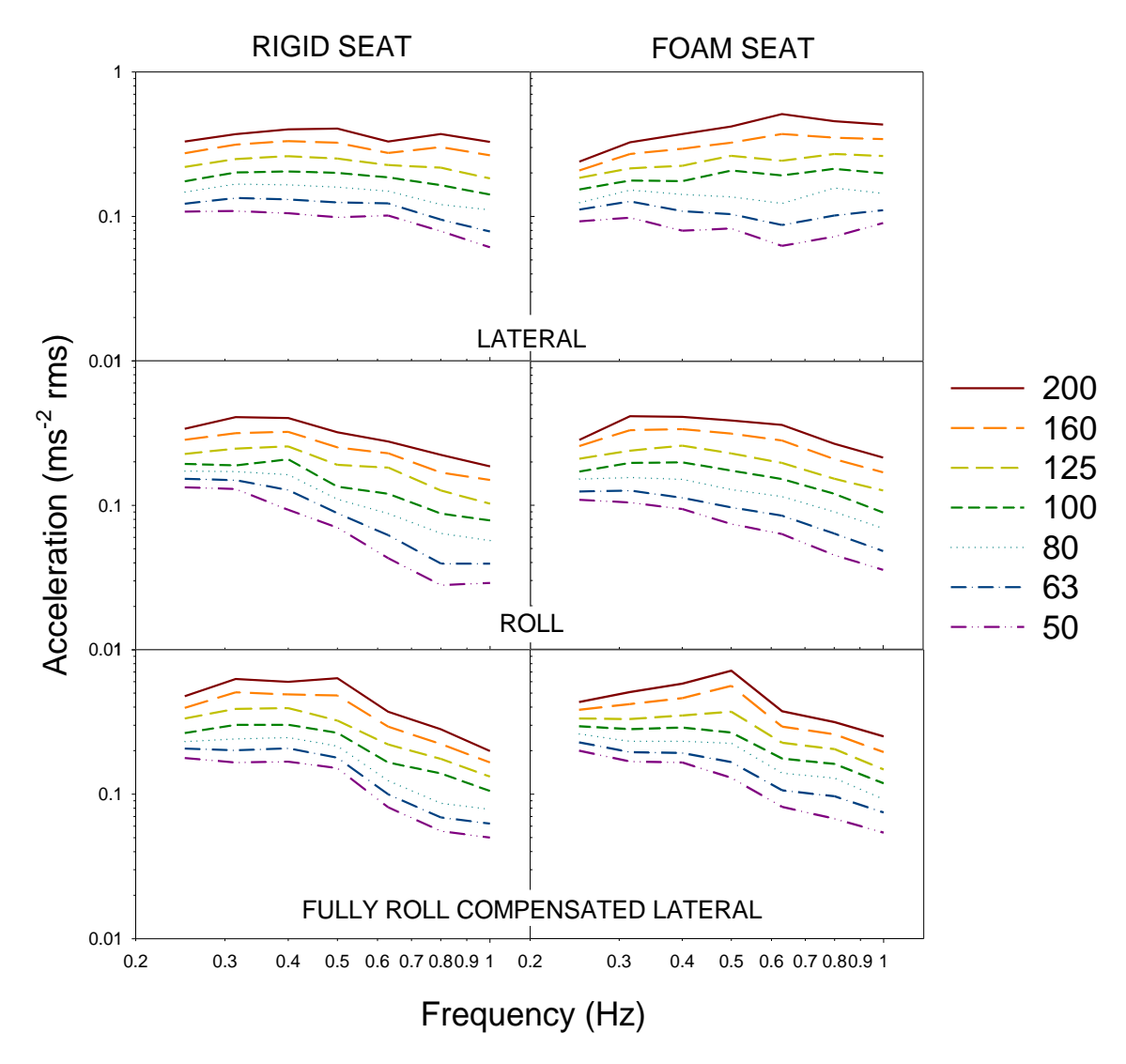


Figure 7.7 The effect of acceleration magnitude on median equivalent comfort contours caused by lateral oscillation, roll oscillation, and roll-compensated lateral oscillation on the rigid seat and the foam cushion. Contours, expressed as the component of lateral acceleration in the plane of seat, represent discomfort equal to subjective magnitudes of 50, 63, 80, 100, 125, 160 and 200. The level of the contours should not be compared across seats.

7.3.3. Effect of seating on vibration discomfort

The median equivalent comfort contours representing discomfort equivalent to that produced by 0.5-Hz lateral oscillation at $0.2~{\rm ms}^{-2}$ r.m.s. on a rigid seat without backrest (i.e., a subjective magnitude of 100) are shown in Figure 7.5. Equivalent comfort contours are expressed in terms of the lateral acceleration in the plane of the seat with both lateral oscillation (i.e., acceleration due to lateral displacement) and with roll oscillation (i.e., acceleration due to roll displacement through the gravitational vector). For roll-compensated lateral oscillation, the resultant acceleration in the plane of the seat was zero, but the lateral component of the motion was used to enable the contours for all three directions to be compared (Section 2.3). With lateral oscillation, there was a significant effect of the foam on the acceleration required to produce a subjective magnitude of 100 at 0.25, 0.315, 0.4 and 0.5 Hz (p < 0.01; Wilcoxon). Similarly, there was a significant effect of foam at 0.25 and 0.315 Hz for roll oscillation (p < 0.015; Wilcoxon), and at 0.315, 0.4 and 0.5 Hz for fully roll-compensated lateral oscillation (p < 0.019; Wilcoxon). With all three directions of oscillation, there was greater sensitivity to acceleration with the foam cushion than with the rigid seat (at the frequencies specified above).

7.3.4. Effect of frequency and direction of oscillation on vibration discomfort

The level of the equivalent comfort contours corresponding to a subjective magnitude of 100 varied with the frequency of oscillation for all three directions of oscillation on the rigid seat (p < 0.001; Friedman), and for roll oscillation and fully roll-compensated lateral oscillation on the foam cushion (p < 0.001; Friedman). The frequency of oscillation did not have a significant effect on the equivalent comfort contour for lateral oscillation with the foam cushion (p = 0.211; Friedman). With the rigid seat, the acceleration equivalent comfort contours were approximately constant between 0.25 and 0.4 Hz and then declined between 0.4 and 1.0 Hz, by approximately 3 dB and 6 dB per octave for lateral oscillation and roll oscillation, respectively. With fully roll-compensated oscillation of the rigid seat, the acceleration contours were approximately constant between 0.25 and 0.5 Hz and declined by approximately 8 dB per octave between 0.5 and 1.0 Hz. With the foam cushion, the acceleration equivalent comfort contours were approximately constant between 0.25 and 0.5 Hz and declined between 0.5 and 1.0 Hz by approximately 6 dB and 7 dB per octave for roll oscillation and fully roll-compensated lateral oscillation, respectively.

The effect of the direction of oscillation on median equivalent comfort contours representing discomfort equivalent to that produced by 0.5-Hz lateral oscillation at 0.2 ms⁻² r.m.s. on a rigid seat without backrest (i.e., a subjective magnitude of 100) is shown in Figure 7.6. . The level of

the equivalent comfort contours was dependent on the direction of oscillation across all frequencies for both the rigid seat and the foam cushion (p < 0.01; Friedman). On the rigid seat, the equivalent comfort contours for lateral oscillation were greater than for roll oscillation (i.e., a greater magnitude of oscillation was needed to produce the same discomfort) at 0.5 Hz and higher frequencies (p < 0.001; Wilcoxon), lower than fully roll-compensated lateral oscillation at 0.5 Hz and lower frequencies (p < 0.001; Wilcoxon), but greater than fully roll-compensated lateral oscillation at frequencies greater than 0.5 Hz (p < 0.002; Wilcoxon). Equivalent comfort contours for roll oscillation were lower than for fully roll-compensated lateral oscillation at all frequencies (p < 0.016; Wilcoxon). On the foam cushion, equivalent comfort contours for lateral oscillation were greater than roll oscillation at 0.8 and 1.0 Hz (p < 0.001; Wilcoxon), lower than fully roll-compensated lateral oscillation at 0.5 Hz and lower frequencies (p < 0.002; Wilcoxon), but greater than fully roll-compensated lateral oscillation at frequencies greater than 0.63 Hz (p < 0.009; Wilcoxon). Equivalent comfort contours for roll oscillation were lower than for fully roll-compensated lateral oscillation at 0.63 Hz and lower frequencies (p < 0.005; Wilcoxon).

7.3.5. Effect of magnitude on the frequency-dependence of equivalent comfort contours

Equivalent comfort contours were calculated for subjective magnitudes from 50 to 200 for the rigid seat and the foam cushion (Figure 7.7). Consistent with the dependence of the rate of growth of discomfort with frequency (as shown in Figure 7.4), the magnitude of oscillation had a large influence on the frequency-dependence of the contours for all directions of oscillation with both the rigid seat and the foam cushion.

7.3.6. Location of discomfort

The location of discomfort during lateral oscillation and during roll oscillation was dependent on the seating condition, with the greatest differences between the rigid seat and the foam cushion at the ischial tuberosities (Figure 7.8) and at the legs (Figure 7.9). During lateral oscillation, there were fewer reports of discomfort at the ischial tuberosities (significant at 0.4 Hz, p = 0.004; McNemar), but more reports of discomfort in the legs (significant at 0.315 Hz, p = 0.021; McNemar) on the foam cushion than on the rigid seat. During roll oscillation, there was a lower incidence of discomfort at the ischial tuberosities on the foam cushion than on the rigid seat (significant at 0.4 and 1.0 Hz, p = 0.022 and 0.039, respectively; McNemar).

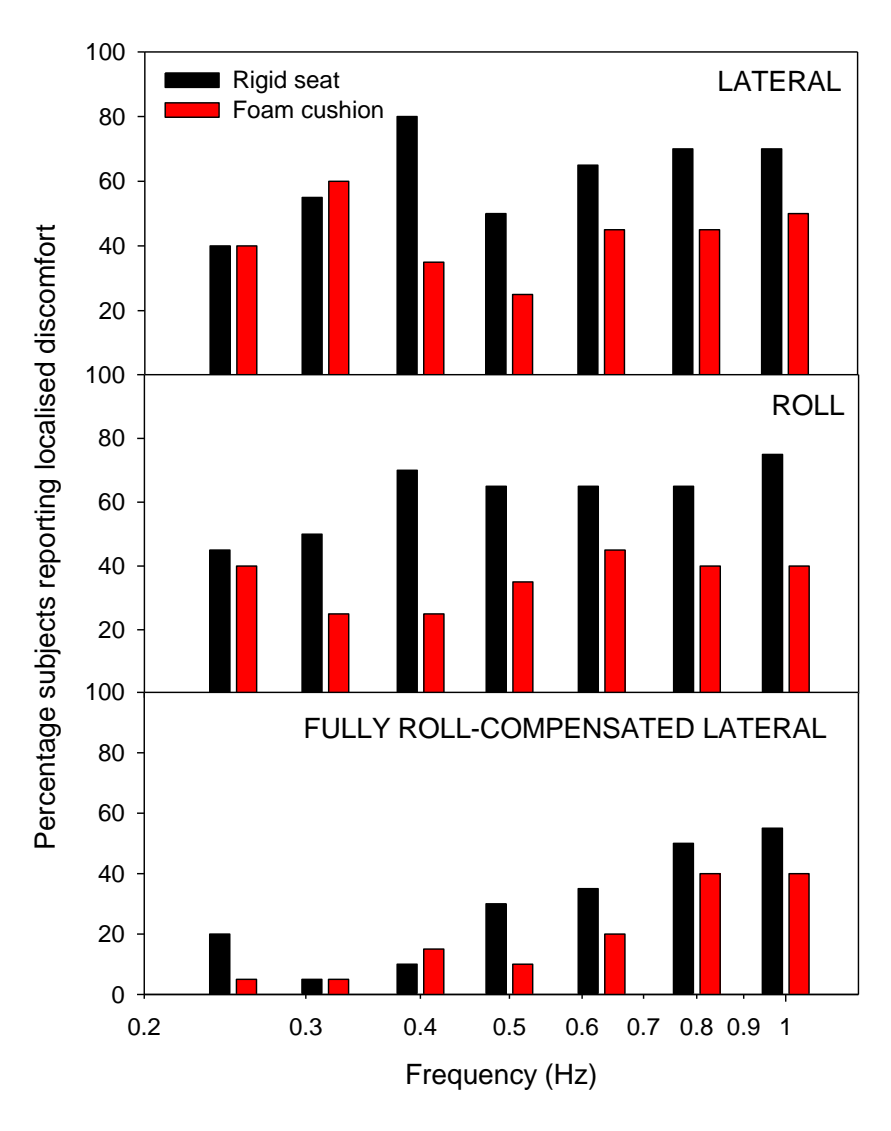


Figure 7.8 Percentage of subjects reporting discomfort localised at the ischial tuberosities when sitting on the rigid seat and on the foam cushion during exposure to lateral oscillation, roll oscillation, and fully roll-compensated lateral oscillation across all frequencies.

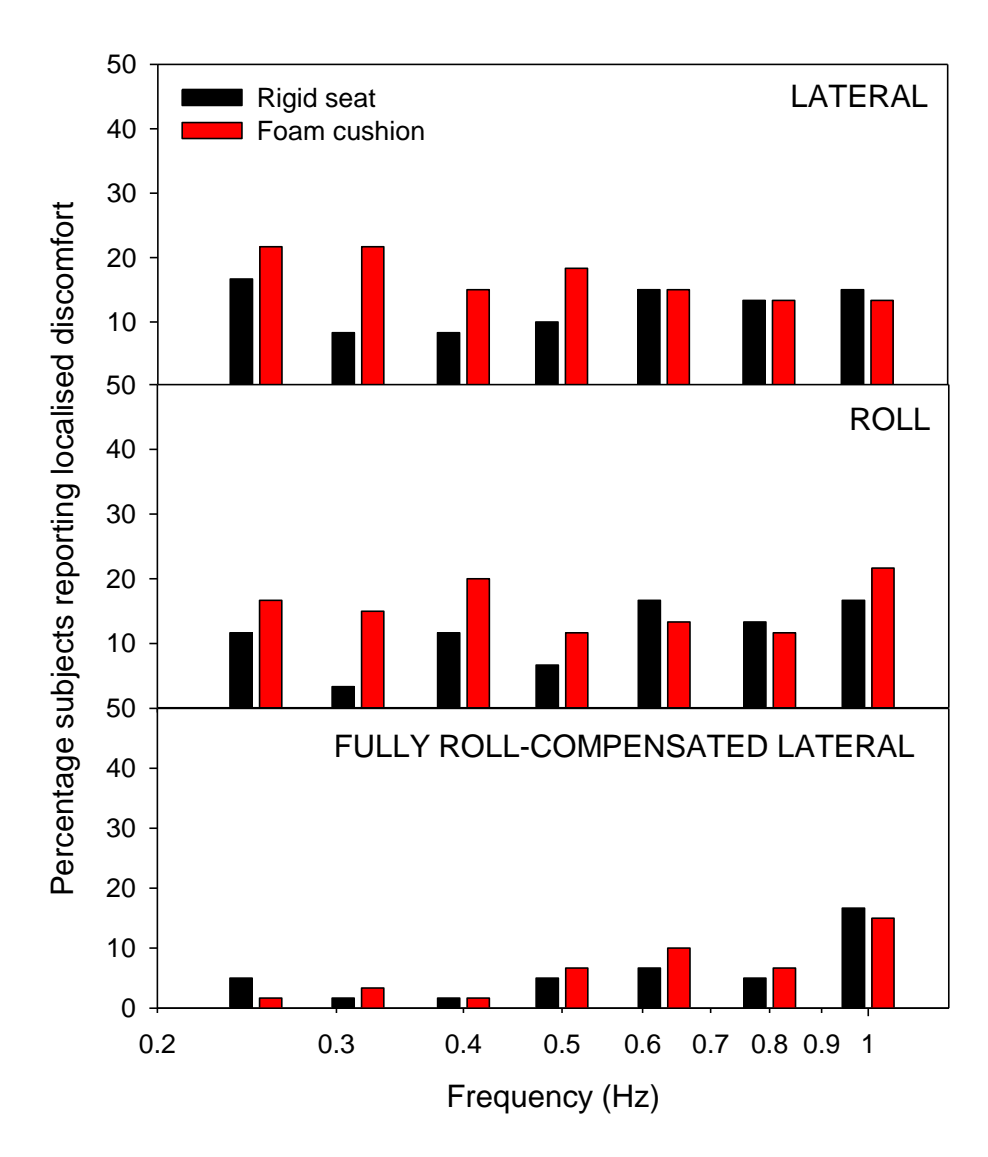


Figure 7.9 Percentage of subjects reporting discomfort localised at the upper thighs, lower thighs or lower legs when sitting on the rigid seat and on the foam cushion during exposure to lateral oscillation, roll oscillation, and fully roll-compensated lateral oscillation across all frequencies.

The direction of oscillation also influenced the location of discomfort. The incidence of discomfort at the ischial tuberosities was greater with lateral oscillation and with roll oscillation than with fully roll-compensated lateral oscillation (significant at 0.25 and 0.315 Hz on the foam cushion, p < 0.05, and at 0.315 and 0.4 Hz on the rigid seat, p < 0.01; McNemar). Discomfort at the legs was greater during lateral oscillation than with fully roll-compensated lateral oscillation (significant at 0.25 Hz on the rigid seat, p = 0.031, and at frequencies less than 0.5 Hz on the

foam cushion, p < 0.05; McNemar), and greater with roll oscillation than with fully roll-compensated lateral oscillation (significant at 0.25, 0.315 and 0.4 Hz on the foam cushion, p < 0.05; McNemar). The incidence of discomfort localised at the head, the neck, or the shoulders was greater with roll oscillation than with lateral oscillation (significant at 0.8 Hz on the foam cushion, p = 0.004; McNemar). The incidence of discomfort at the lower back was greater with lateral oscillation and with roll oscillation than with fully roll-compensated lateral oscillation (significant at 0.25 Hz, p < 0.05; McNemar). No other statistically significant differences in the location of discomfort data were identified.

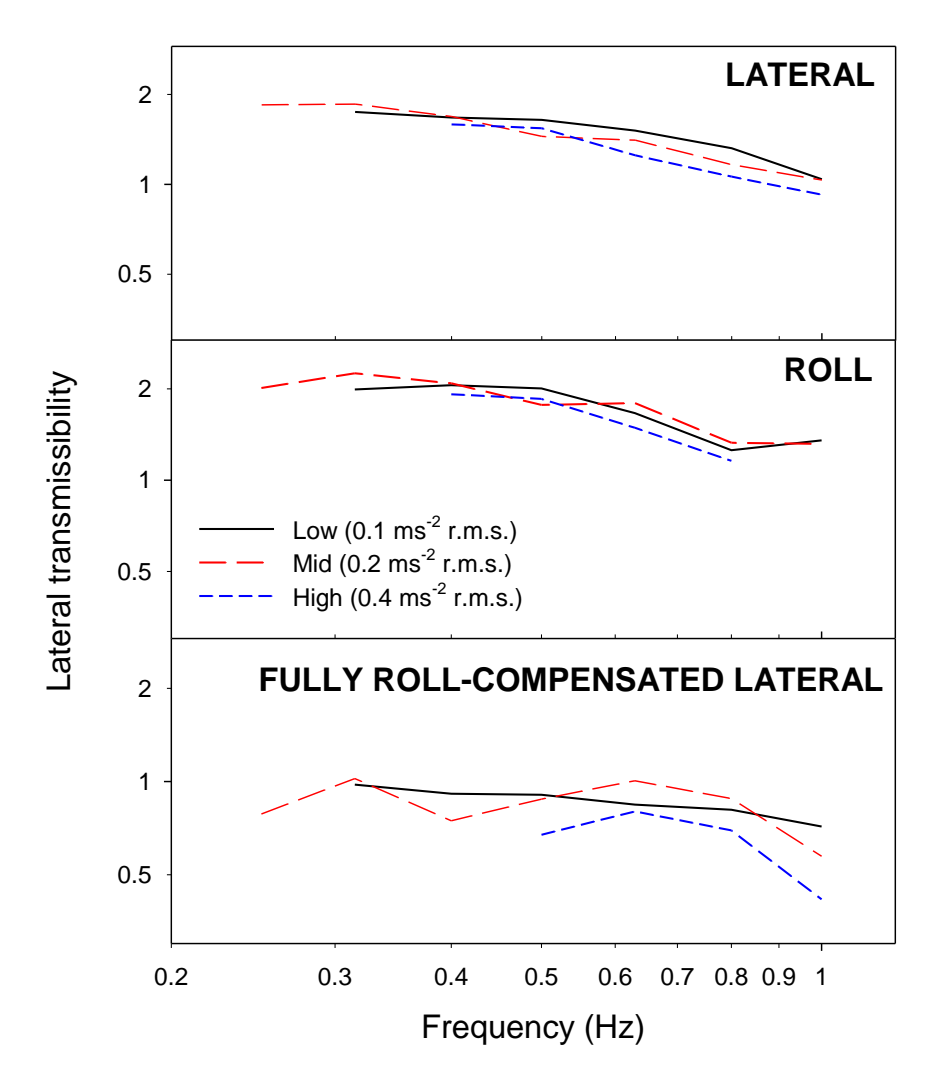


Figure 7.10 Median lateral transmissibility of the foam cushion during exposure to lateral oscillation, roll oscillation, and fully roll-compensated lateral oscillation at 0.1, 0.2, and 0.4 ms⁻² r.m.s. at frequencies from 0.25 to 1.0 Hz.

7.3.7. Lateral transmissibility and roll transmissibility of foam cushion

The 'lateral transmissibility' of the foam cushion was calculated by dividing the lateral acceleration measured at the seat-body interface by the lateral acceleration of the rigid seat (Equation 7.5), for all three directions of oscillation, all seven frequencies of oscillation, and three magnitudes of oscillation (Figure 7.10). For all three directions, the lateral transmissibility was dependent on the frequency of oscillation (p < 0.001; Friedman), decreasing with increasing frequency from 0.25 to 1.0 Hz by approximately 2 dB per octave.

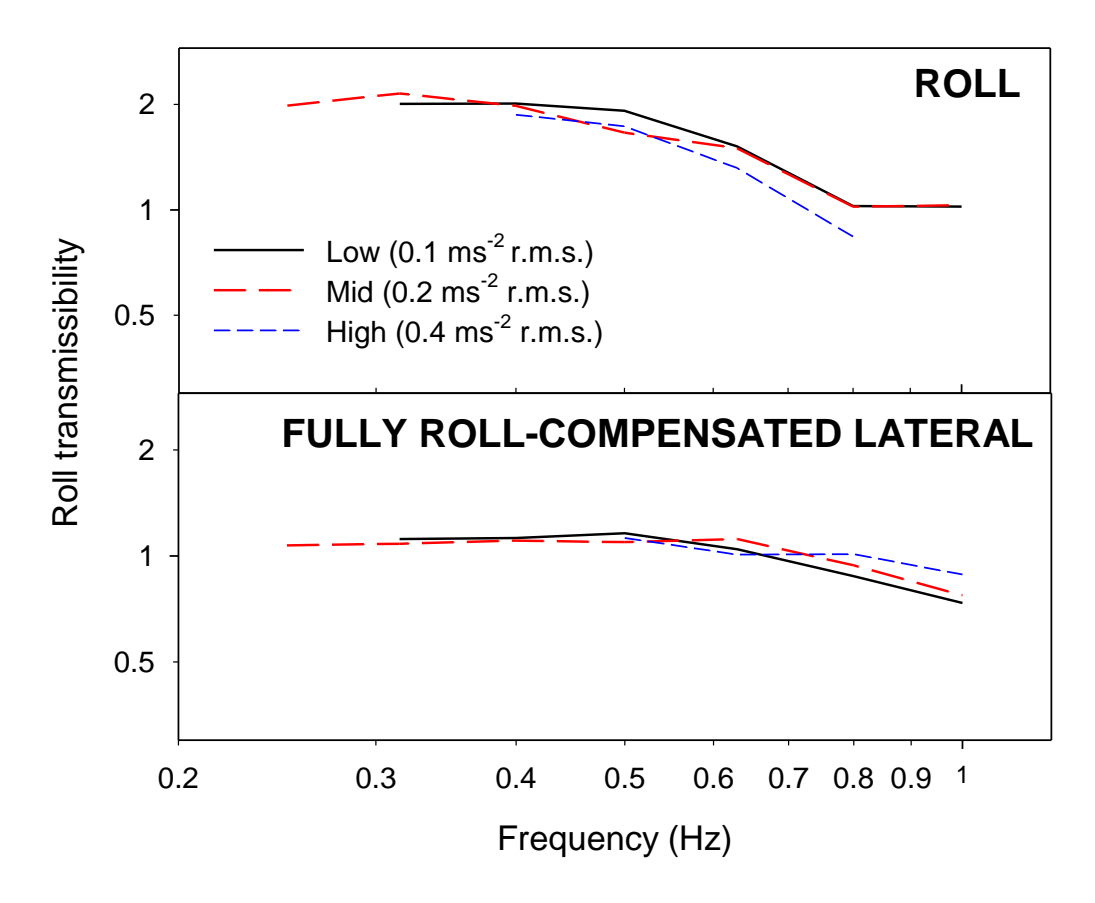


Figure 7.11 Median roll transmissibility of the foam cushion during exposure to roll oscillation and roll-compensated lateral oscillation at 0.1, 0.2, and 0.4 ms⁻² r.m.s. at frequencies from 0.25 to 1.0 Hz.

The direction of oscillation also affected lateral transmissibility at all frequencies (p < 0.001; Friedman), being greater with roll oscillation than lateral oscillation at all frequencies greater than 0.25 Hz (p < 0.01; Wilcoxon) and greater with roll oscillation than fully roll-compensated lateral oscillation at all frequencies (p < 0.01; Wilcoxon) except 0.5 Hz (p = 0.017; Wilcoxon).

The 'roll transmissibility' of the foam was calculated by dividing the roll velocity measured at the seat-body interface by the roll velocity measured on the rigid seat (Equation 7.6). The roll transmissibility was not measured with lateral oscillation. The roll transmissibility of the foam was highly dependent on the frequency of lateral oscillation (Figure 7.11; p < 0.001; Friedman), decreasing from 0.25 to 1.0 Hz by approximately 3 dB per octave with roll oscillation and approximately 1 dB per octave with fully roll-compensated lateral oscillation.

Roll transmissibility was greater during roll oscillation than during fully roll-compensated lateral oscillation (p < 0.01 all frequencies except at 0.8 Hz where p = 0.189; Wilcoxon).

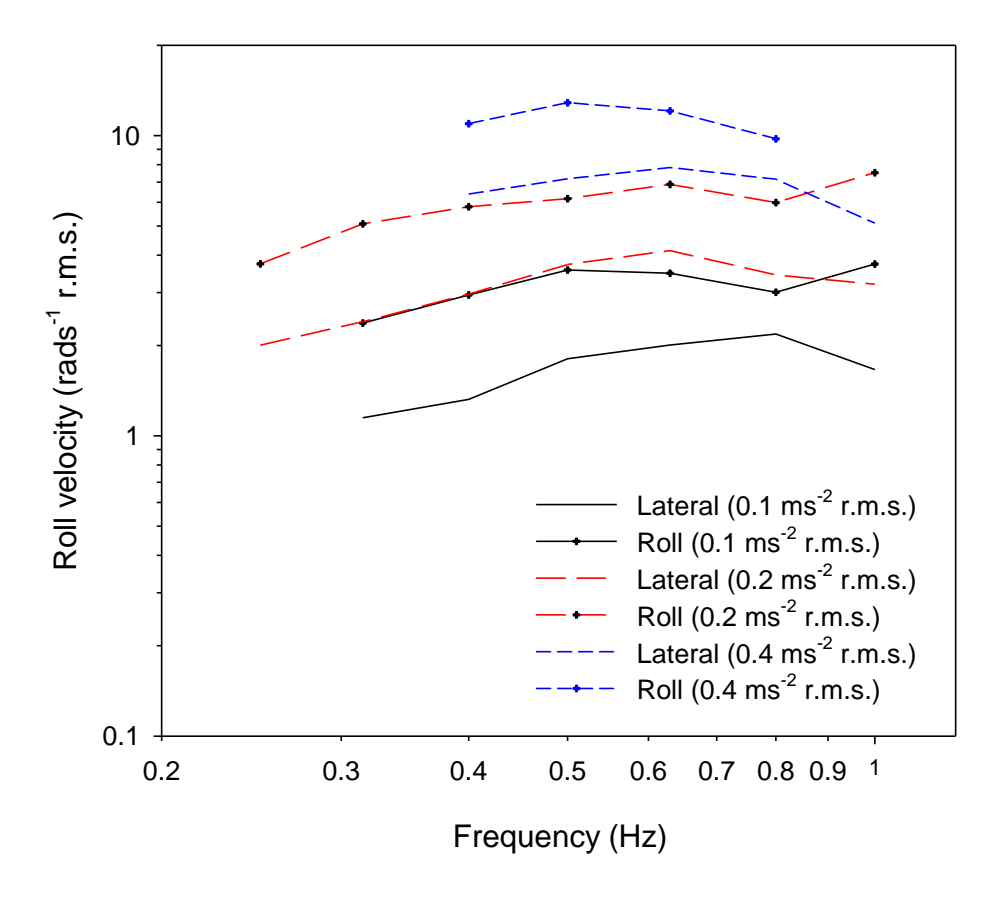


Figure 7.12 Effect of magnitude of oscillation on the median roll velocity measured at the seatbody interface of the foam cushion during exposure to lateral oscillation and roll oscillation at frequencies between 0.25 and 1.0 Hz.

7.3.8. Effect of magnitude on lateral and roll transmissibility of foam seat

The lateral transmissibility of the foam tended to decrease with increasing magnitude of oscillation, with statistically significant reductions at 0.4, 0.8 and 1.0 Hz with lateral oscillation, at

0.4, 0.63 and 0.8 Hz with roll oscillation, and at 0.315 Hz and from 0.5 to 1.0 Hz with fully roll-compensated lateral oscillation (p < 0.05; Friedman).

The roll transmissibility of the foam was dependent on the magnitude of roll oscillation at 0.4 and 0.8 Hz and the magnitude of fully roll-compensated lateral oscillation at 0.315 Hz and from 0.5 to 1.0 Hz (p < 0.05; Friedman). The roll transmissibility tended to decrease with increasing magnitude of roll oscillation, but increase with increasing magnitude of fully roll-compensated lateral oscillation.

The roll oscillations experienced at the seat-body interface during lateral oscillation and during roll oscillation are compared for three magnitudes in Figure 7.12. It may be seen that roll oscillation on the foam at the seat-body interface was approximately double during roll oscillation than during lateral oscillation.

7.4. Discussion

7.4.1. Rate of growth of discomfort

The rate of growth of discomfort (i.e., the exponent in Stevens' power law) describes the relation between changes in the magnitude of the oscillation and changes in the magnitude of discomfort (Stevens, 1975). In a previous study using a rigid seat with backrest, the median rates of growth of discomfort varied over the range 0.54 to 1.23 with lateral oscillation, 0.48 to 1.38 with roll oscillation, and 0.39 to 1.07 with fully roll-compensated oscillation at frequencies between 0.25 and 1.0 Hz, with greater rates of growth at lower frequencies (Chapter 6). With the same motions, similar rates of growth of discomfort were found in the current study with a rigid seat and a foam cushion, both without backrest. During lateral oscillation and roll oscillation of a rigid seat without backrest, and with both a backrest and a four-point harness, the rate of growth of discomfort was independent of seating condition, and also decreased with increasing frequency of oscillation (Wyllie and Griffin, 2007). The current and previous findings suggest the rate of growth is independent of seating characteristics, but highly dependent on the frequency of oscillation. The large decrease in the rate of growth of discomfort with increasing frequency means the shapes of low frequency equivalent comfort contours change with the magnitude of oscillation (Figure 7.7). This has implications for the characteristics of a suitable frequency weighting, because a frequency weighting appropriate for low magnitudes will be inappropriate for high magnitudes (Wyllie and Griffin, 2007).

For a rigid seat with backrest, there were greater rates of growth of discomfort with lateral oscillation than roll oscillation at frequencies between 0.63 and 1.0 Hz, and greater rates of

growth with roll oscillation than fully roll-compensated lateral oscillation at 0.25 Hz (Chapter 6). The present study without a backrest found no statistically significant effects of the direction of oscillation on rates of growth of discomfort for either the rigid seat or the foam cushion, but similar trends can be seen in the median data (Figure 7.4). Differing rates of growth of discomfort for lateral oscillation and roll oscillation imply that the relative importance of these axes (as shown in Figure 7.6) will vary with the magnitude of the motion. Nevertheless, it seems reasonable to expect that at frequencies between 0.5 and 1.0 Hz, lateral acceleration in the plane of the seat due to roll oscillation will produce greater discomfort than the same acceleration arising from lateral oscillation with: (i) a rigid seat without backrest (Wyllie and Griffin, 2007; current study), (ii) a foam cushion without backrest (current study), (iii) a rigid seat with backrest (Chapter 6), and (iv) a rigid seat with backrest and four-point harness (Wyllie and Griffin, 2007). At frequencies greater than about 0.5 Hz, sensitivity to roll oscillation tends to be much greater than sensitivity to lateral oscillation having the same acceleration in the plane of the seat (Chapter 6).

7.4.2. Equivalent comfort contours

Compared to a flat rigid seat pan, a foam cushion might be expected to reduce the discomfort caused by low frequency oscillation by distributing the pressure at the principal seat-body interface (i.e., the ischial tuberosities) so that variations in pressure during oscillation do not reach values as great as with a rigid seat. Alternatively, a foam cushion might be expected to increase discomfort by amplifying the motion at the ischial tuberosities and reducing postural stability. During lateral oscillation at frequencies less than 0.63 Hz, during roll oscillation at frequencies less than 0.4 Hz, and during fully roll-compensated lateral oscillation at frequencies less than 0.63 Hz, sensitivity to lateral acceleration in the plane of the seat was greater when seated on a foam cushion than when seated on a rigid seat, suggesting that the latter explanation is appropriate (i.e., the cushion reduced postural stability). Nevertheless, with lateral oscillation at frequencies less than 0.63 Hz, no statistically significant differences in discomfort were found between a rigid seat and a cushioned train seat without backrest (Chapter 5). Although softer cushions reduce the peak pressure at the ischial tuberosities and can improve static comfort (e.g., Ebe and Griffin, 2000), some soft seats will reduce dynamic comfort. The identification of the properties of seat cushions required to optimise pressure distributions without detrimental effects on postural stability, and the complementary role of backrests in providing stability, merits further research so as to assist the optimisation of seats for transport.

For both the rigid seat and the foam cushion and all three directions of oscillation, the acceleration magnitude required to produce equivalent discomfort (i.e., a subjective magnitude

of 100) was highly dependent on the frequency of oscillation, except for lateral oscillation on the foam cushion which was independent of frequency (Figure 7.5 and Figure 7.6). For the rigid seat, the equivalent comfort contours from 0.4 to 1.0 Hz declined at approximately 3 dB, 6 dB, and 8 dB per octave for lateral oscillation, roll oscillation, and fully roll-compensated lateral oscillation, respectively. For the foam cushion, the equivalent comfort contours from 0.5 to 1.0 Hz declined at 6 dB and 7 dB per octave for roll oscillation and fully roll-compensated lateral oscillation, respectively. Previous studies have reported marginally steeper contours when sitting with a backrest (Chapter 6) and when sitting with both a backrest and a four-point harness (Wyllie and Griffin, 2007), consistent with: (i) a full height backrest increasing sensitivity to lateral and roll oscillation at frequencies between 0.5 and 1.0 Hz relative to 'no backrest', and (ii) a four-point harness increasing sensitivity to lateral and roll oscillation at frequencies between 0.5 and 1.0 Hz relative to sitting with a full height backrest without a harness.

7.4.3. The location of discomfort

During lateral oscillation and during roll oscillation, there was a greater incidence of discomfort at the ischial tuberosities on the rigid seat than on the foam cushion (statistically significant at 0.4 and 1.0 Hz). Greater discomfort at the ischial tuberosities has been found on a rigid seat without backrest than a cushioned train seat during 1-Hz lateral oscillation (Chapter 5). Pressure at the ischial tuberosities may be reduced by leaning back on a backrest (e.g., Vos et al, 2006; Kyung and Nussbaum, 2008). During lateral and roll oscillation, each ischial tuberosity is subjected to alternating downward forces. This is consistent with the lower incidence of discomfort at the ischial tuberosities during fully roll-compensated lateral oscillation, where forces are balanced at the seat surface (Chapter 6; current chapter). Relative to sitting on the rigid seat, the soft foam cushion used in the current study may have reduced the pressure at the ischial tuberosities and thereby reduced discomfort in this region.

During lateral oscillation there was a greater incidence of discomfort in the legs (i.e., upper thighs, lower thighs and lower legs – see Figure 7.2) on the foam cushion than on the rigid seat (statistically significant at 0.315 Hz). This is consistent with the lateral and roll transmissibility of the cushion being greater than unity (Figure 7.10) requiring subjects to exert greater muscular effort to maintain postural stability on the foam cushion than on the rigid seat. The roll of the upper body resulting from lateral oscillation when sitting without a backrest may put stress on the leg muscles (e.g., the quadriceps and hamstrings in the thighs, and/or the gastrocnemius and soleus muscles in the calves) (Mandapuram *et al.*, 2005). A greater necessity to exert the leg muscles when seated on the foam cushion may account for the increased incidence of discomfort in this region. This is also consistent with the reduced incidence of discomfort in the

legs during fully roll-compensated lateral oscillation, where the lateral forces are balanced at the seat surface.

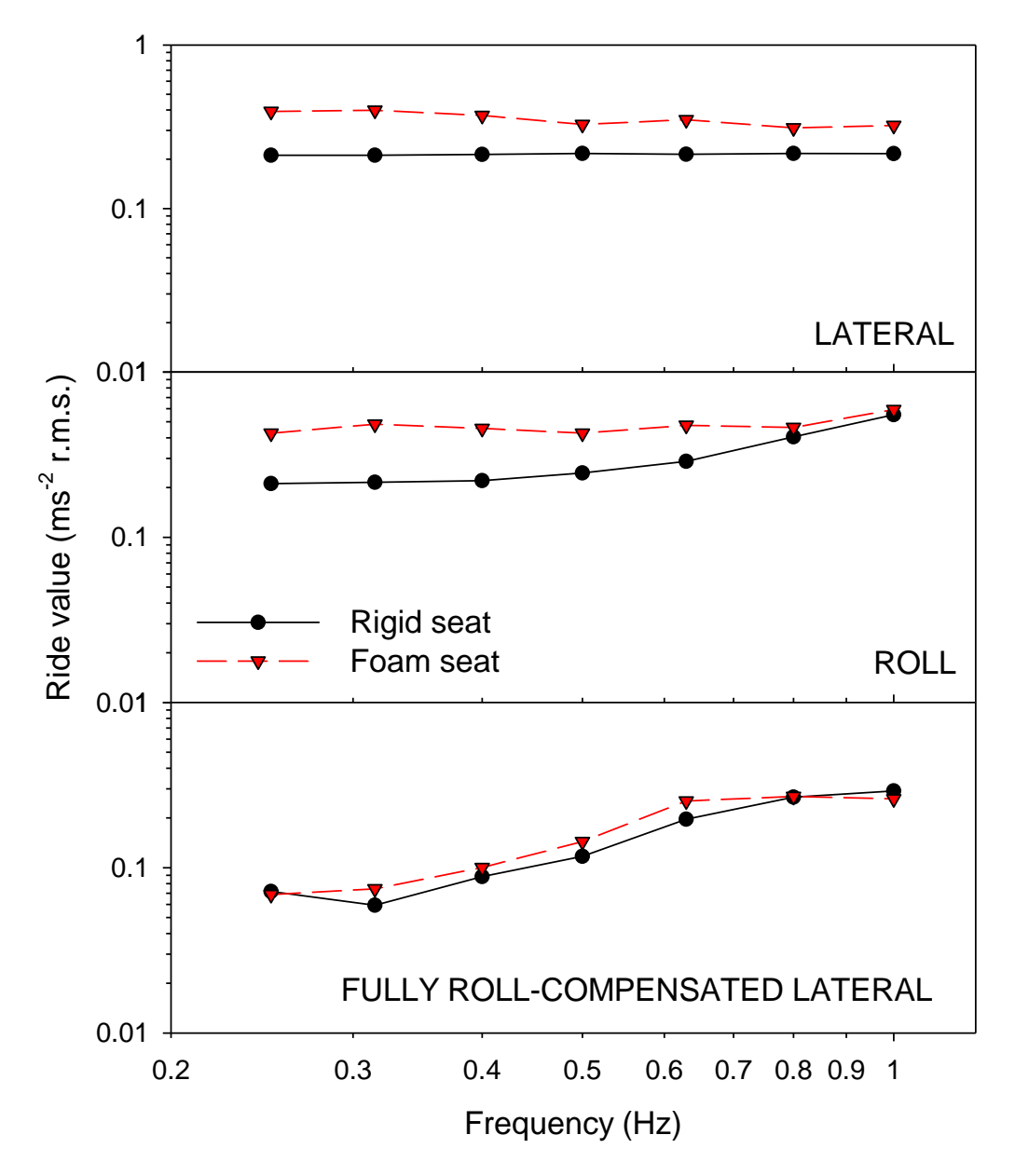


Figure 7.13 Root-sums-of-squares of frequency-weighted measured components at the seat-body interface during lateral oscillation, roll oscillation, and fully roll-compensated lateral oscillation on a rigid seat and on a foam cushion. Components weighted using axis multiplying factors and asymptotic weightings extrapolated horizontally at frequencies less than 0.5 Hz without band-pass filtering (BS 6841, 1987). Median data calculated across 20 subjects.

When seated on a rigid seat with backrest (Chapter 6) or a rigid seat with backrest and harness (Wyllie and Griffin, 2007), there was a greater incidence of discomfort at the head, neck and shoulders than at other locations of the body during 1-Hz roll oscillation. In the current study, there was greater discomfort at the head, neck, or shoulders during roll oscillation than during lateral oscillation when seated on the foam cushion (significant at 0.8 Hz), but not when seated on the rigid seat. The transmission of lateral acceleration to the upper body increases with increasing height of a backrest (Brett and Griffin, 1991), but on a compliant seat without backrest, the displacement of the head relative to the seat surface will depend on the capability of the seated occupant to maintain a stable upright posture. Poor stability on the foam cushion may have led to an amplification of the motion (indicated by a lateral and roll transmissibility greater than unity during 0.8-Hz roll oscillation – Figure 7.10 and Figure 7.11), and a subsequent increase in discomfort in the upper body.

7.4.4. Implications for vibration standards

British Standard 6841 (1987) and International Standard 2631-1 (1997) suggest asymptotic frequency weighting $W_{\rm d}$ for lateral acceleration and frequency weighting $W_{\rm e}$ (with a multiplying factor of 0.63) for roll acceleration. Although both weightings are intended for predicting discomfort caused by vibration at frequencies in the range 0.5 to 80 Hz, realisable weightings are achieved with a high-pass filter (at 0.4 Hz) and a low-pass filter (at 100 Hz) and can be applied to evaluate motions containing energy outside this frequency range.

The standards suggest discomfort can be predicted from frequency-weighted measurements of translational and rotational acceleration at the seat-body interfaces (i.e., at the floor beneath the feet, between the seat-pan and the ischial tuberosities, and between the back and a backrest). Weighting each component appropriately and calculating the root-sums-of-squares (i.e., r.s.s.) over all components is assumed to allow for the effects of different frequencies, different directions, and different input locations on vibration discomfort. Vibration is measured at the seat-body interfaces, so differences in the transmission of vibration though different seats will be reflected in the predicted vibration discomfort with different seats.

With lateral and roll oscillation of a seat without backrest, five components may contribute to discomfort: (i) lateral acceleration in the plane of the seat (ms⁻²), (ii) lateral acceleration in the plane of the seat due to roll (i.e., g.sin θ , ms⁻²), (iii) roll acceleration at the seat surface (rads⁻²), (iv) lateral acceleration at the feet (ms⁻²), and (v) lateral acceleration at the feet due to roll (i.e., g.sin θ , ms⁻²). The frequency-weighted acceleration caused by low frequency oscillation at the feet has been shown to be relatively small (Wyllie and Griffin, 2007; Chapter 6) so the current

analysis focuses on lateral and roll acceleration at the seat surface. If the standardised methods are correct, the root-sums-of-squares of the lateral and roll acceleration measured at the seat-body interface should yield similar conclusions to the equivalent comfort contours in Figure 7.5.

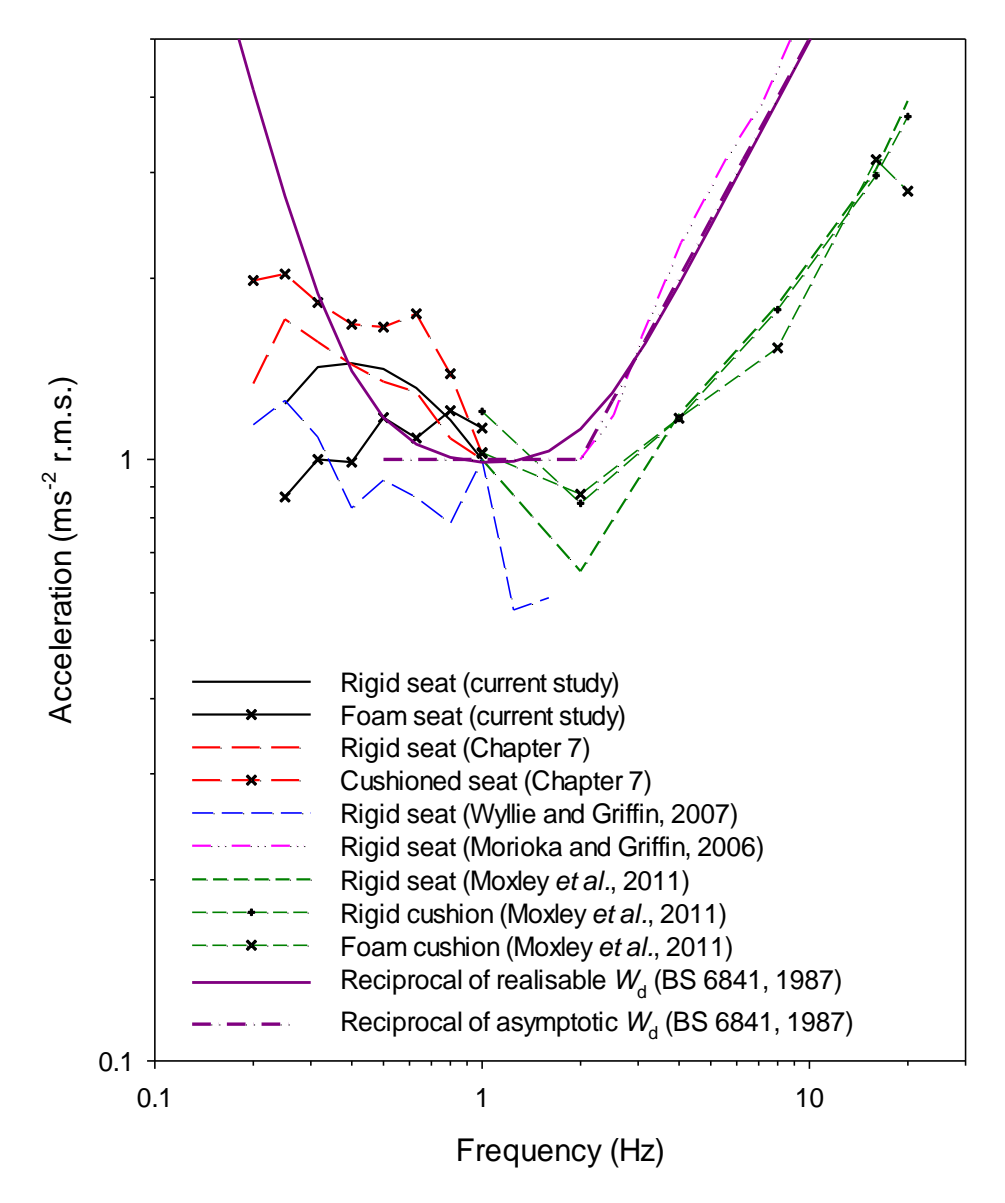


Figure 7.14 Comparison of equivalent comfort contours for lateral oscillation on rigid and cushioned seats without a backrest and the reciprocals of the asymptotic and the realisable versions of frequency weighting W_d for lateral acceleration (BS 6841, 1987). Contours for rigid seats normalised to unity at 1 Hz.

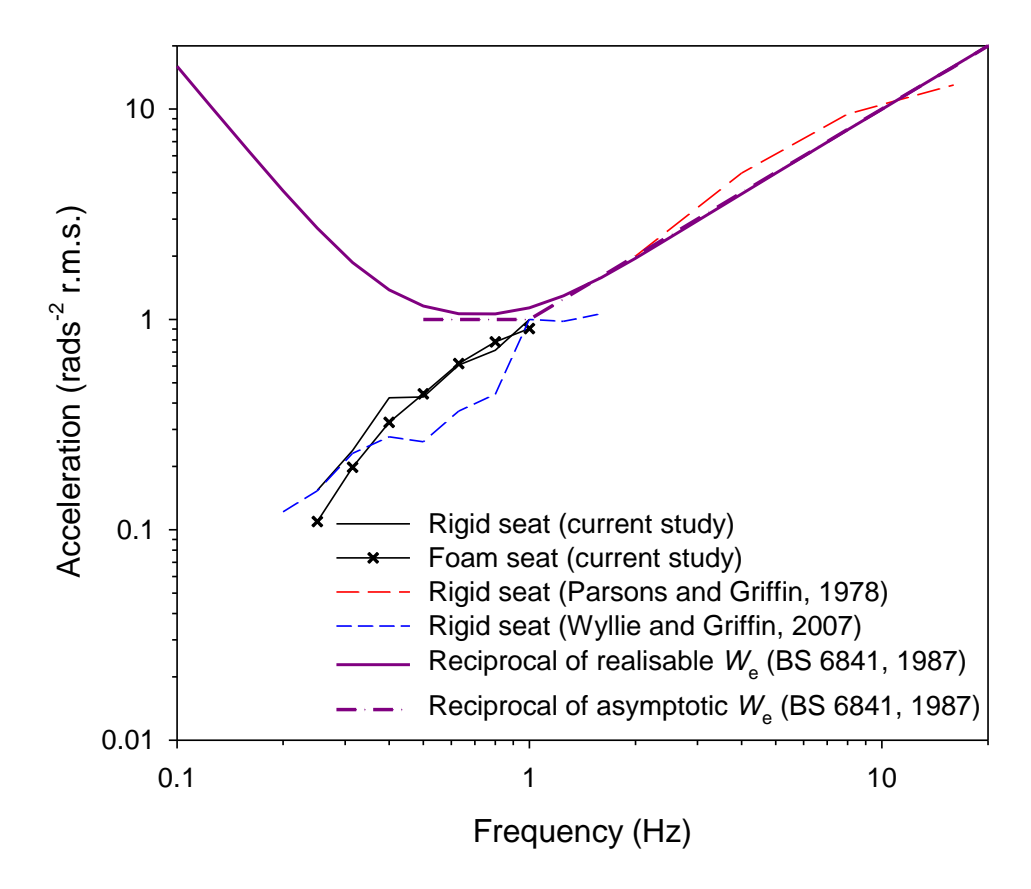


Figure 7.15 Comparison of equivalent comfort contours for roll oscillation on rigid and cushioned seats without a backrest and the reciprocals of the asymptotic and the realisable versions of frequency weighting *W*_e for roll acceleration (BS 6841, 1987). Contours normalised to unity at 1 Hz.

The root-sums-of-squares of the frequency-weighted lateral and roll accelerations measured at the seat-buttock interface on the rigid seat and the foam cushion during exposure to lateral oscillation, roll oscillation, and fully roll-compensated lateral oscillation at $0.2~{\rm ms}^{-2}$ r.m.s. are shown in Figure 7.13. The frequency weightings used were the asymptotic forms of weightings $W_{\rm d}$ and $W_{\rm e}$ horizontally extrapolated to frequencies less than $0.5~{\rm Hz}$. The standardised methods predict greater vibration discomfort on the foam cushion than on the rigid seat at all frequencies with lateral oscillation, at frequencies less than $0.8~{\rm Hz}$ with roll oscillation, and at frequencies between $0.25~{\rm and}~0.8~{\rm Hz}$ with fully roll-compensated lateral oscillation. This is broadly consistent with the equivalent comfort contours shown in Figure 7.5. However, the frequency-dependence of the r.s.s. predictions (Figure 7.13) is not consistent with the frequency-dependence of equivalent comfort contours (Figure 7.5), and the predicted magnitude of the differences in discomfort between the seats in Figure 7.13 is greater than implied by the

equivalent comfort contours in Figure 7.5. This suggests the extrapolated asymptotic frequency weightings with the multiplying factors defined in the standards may not be wholly appropriate for predicting the discomfort caused by lateral oscillation and roll oscillation at all frequencies in the range 0.2 to 1.0 Hz.

When extrapolated to frequencies less than 0.5 Hz, the asymptotic forms of the frequency weightings W_d and W_e (BS 6841, 1987) are unity between 0.25 and 1.0 Hz. Therefore, in Figure 7.13, the total vibration values predict no effect of frequency on discomfort caused by lateral oscillation at 0.2 ms⁻² r.m.s. on a rigid seat, because the acceleration is constant across all frequencies. A more accurate reflection of the effects of the frequency of lateral oscillation may be obtained using the realisable W_d weighting (i.e., with high-pass and low-pass filters at 0.4 and 100 Hz, respectively; BS 6841, 1987), as demonstrated in Figure 7.14. However, it is clear that neither the extrapolated asymptotic weighting nor the band-pass filtered realisable weighting W_e offers an accurate prediction of the discomfort from roll acceleration at frequencies less than about 1 Hz (see Figure 7.15).

7.5. Conclusion

Both the lateral transmissibility and the roll transmissibility of a foam cushion were greater than unity at frequencies in the range 0.25 to 1 Hz, causing greater vibration discomfort from both lateral oscillation and roll oscillation when seated on the foam cushion than when seated on a rigid seat. There was greater discomfort in the legs and the lower back when seated on the foam cushion, suggesting greater muscular exertion was required to maintain postural stability than when seated on the rigid seat, which mainly caused discomfort at the ischial tuberosities.

On both the rigid seat and the cushioned seat without backrest, measurements of the frequency-weighted acceleration at the seat-body interface gave approximate predictions of the discomfort caused by lateral oscillations, roll oscillations and fully roll-compensated lateral oscillations in the frequency range 0.25 to 1.0 Hz, but the predictions could be improved at the lowest frequencies by adjustments to the standardised weightings. This is particularly evident for motions containing components of roll, since frequency-weighting W_e used to evaluate roll acceleration is insufficient to predict discomfort at frequencies less than about 1 Hz. Since predictions of the discomfort caused by fully roll-compensated lateral acceleration are dependent on the W_e -weighted roll acceleration, the current standards do not provide a good understanding of the effect of these motions on passenger comfort.

Chapter 8

Effect of backrest height

8.1. Introduction

The configuration of vehicle seating influences the transmission of motions to the body and the postural support offered to the body (e.g., Griffin, 1975; Oborne *et al.*, 1981; Chapter 7). For example, with lateral oscillation at frequencies less than 3.15 Hz, movements of the head relative to the seat decreased as the height of a backrest increased to 700 mm (Brett and Griffin, 1991). At frequencies between 0.2 and 16 Hz, the transmission of vibration to the head can be increased by even a short backrest, most notably with fore-and-aft oscillation (Paddan and Griffin, 1988, 1994). Backrest inclination can influence the fore-and-aft resonance frequency of a backrest and the backrest transmissibility at resonance (Abdul-Jalil and Griffin, 2007). Different motions of the body with different backrests may be associated with the additional input of vibration at the back or a change of posture altering the dynamic characteristics of the body (Paddan and Griffin, 1988, 1994).

Differences in body motions when sitting in different seats might imply differences in the discomfort of seat occupants, but there has been little previous study of the effects of backrests on the discomfort caused by horizontal and rotational oscillations at low frequencies (e.g., less than 1 Hz). The backrests of the seats in different forms of transport differ considerably, from no backrest, to simple short backrests, or simple flat backrests, or full-height contoured and cushioned backrests. The preferred sitting posture also varies, depending on the type of activity and the transport (e.g., Kamp *et al.*, 2011).

With fore-and-aft and lateral oscillation at frequencies between 2.5 and 63 Hz, contact with a backrest increased discomfort relative to sitting with no backrest (Parsons *et al.*, 1982). At frequencies less than this range (0.2 to 1.0 Hz), lateral oscillation caused less discomfort with a backrest than without a backrest when seated on both a rigid seat and a cushioned train seat (Chapter 5). Between 0.5 and 1.6 Hz, lateral oscillation, roll oscillation, and pitch oscillation caused greater discomfort when seated with a backrest and four-point harness than when sitting

without a backrest (Wyllie and Griffin, 2007, 2009). Conversely, a backrest and harness reduced discomfort caused by fore-and-aft oscillation at frequencies between 0.25 and 1.25 Hz (Wyllie and Griffin, 2009). It seems that a backrest with a four-point harness restrains the head and the upper body, which can be beneficial for comfort when exposed to fore-and-aft oscillation but detrimental for comfort when exposed to lateral, roll and pitch oscillation. With both horizontal oscillation (fore-and-aft and lateral) and rotational oscillation (roll and pitch) at low frequencies, there was a greater incidence of discomfort at the head, neck or shoulders when sitting with a backrest and restrained by a four-point harness than when sitting without a backrest, suggesting the backrest increased the motions or the forces at these locations (Wyllie and Griffin, 2007, 2009).

Sitting with a semi-reclined backrest (reclined to 22.5°, 45° or 67.5°) during sinusoidal vertical oscillation at frequencies between 2 and 64 Hz tended to reduce discomfort relative to sitting with an upright backrest (i.e., 90°) or lying fully recumbent (i.e., 0°) (Paddan *et al.*, 2012). Similarly, the discomfort caused by vertical and fore-and-aft oscillation at frequencies around the principal body resonance was lower when seated with an inclined posture (30° or 60°) or a recumbent posture (0°) compared to an upright posture (90°) (Basri and Griffin, 2011, 2012). The reduction in discomfort with reclined postures may be associated with a reduction in intradiscal pressure to the spine, compared to when sitting upright (Paddan *et al.*, 2012).

It is clear from these studies that the effects of backrests on vibration discomfort depend on the frequency and direction of the motion and the configuration of the seat. British Standard 6841 (1987) and International Standard ISO 2631-1 (1997) suggest the use of frequency weighting W_d (with an axis multiplying factor of 0.5) for evaluating lateral vibration of a backrest and frequency weighting W_c (with an axis multiplying factor of 0.8), for evaluating fore-and-aft vibration of a backrest. The standards imply an additive effect of backrest vibration on discomfort (the weighted components at the seat and backrest are summed using the root-sums-of-squares), so contact with a backrest will always increase the predicted vibration discomfort. Although this may be true for some frequencies, the evidence suggests the effects of backrest on discomfort are more complex at low frequencies (e.g., less than about 1 Hz).

This study was designed to determine the extent to which backrest height influences the discomfort caused by lateral oscillation, roll oscillation, and fully roll-compensated lateral oscillation at frequencies between 0.25 and 1.0 Hz. On the basis of previous research, it was anticipated that discomfort would increase with increasing acceleration magnitude and increasing frequency for all three directions (Chapter 6). Sitting with a backrest was expected to reduce the muscular effort required to maintain an upright posture during lateral oscillation,

thereby reducing discomfort, with the level of reduction dependent on the backrest height. However the increased transmission of motion to the upper body and the head with a full-height backrest was expected to increase discomfort during roll oscillation, with any detrimental effects of a backrest most notable at the highest frequencies.

8.2. Method

8.2.1. Apparatus

Motions were produced by a six-axis motion simulator in the Human Factors Research Unit of the Institute of Sound and Vibration Research at the University of Southampton. The simulator was capable of ± 0.5 m vertical motion, ± 0.25 m horizontal motion, and about $\pm 20^{\circ}$ of rotational motion. Subjects sat on a rigid seat positioned so that the centre of the seat surface was at the centre of the motion platform (approximately 2.5 m by 3.0 m).

The seat consisted of a flat rigid seat pan (510 by 400 mm) located 480 mm above the motion platform. The surface of the seat pan was covered in a hard rubber less than 2 mm in thickness to increase surface friction. Subjects sat with one of three backrest configurations: (i) without a backrest, (ii) with a short rigid backrest 295 mm high by 600 mm wide), and (iii) with a high rigid backrest (650 mm high by 600 mm wide). Both backrests were contoured in shape so as to provide lateral support to the body (Figure 8.1).

Subjects were asked to maintain comfortable upright postures, with their backs in full contact with any backrest, and their hands on their laps and their feet flat on the floor (i.e., platform of the motion simulator). If necessary, subjects were provided with a footrest to ensure a sitting posture with the thighs parallel to the floor. Subjects wore a loose lap belt for safety.

During motion exposure, subjects wore headphones producing white noise at 65 dB(A) in order to mask the sounds of the simulator. The experimenter communicated with subjects through a microphone connected to the headphones by interrupting the white noise.

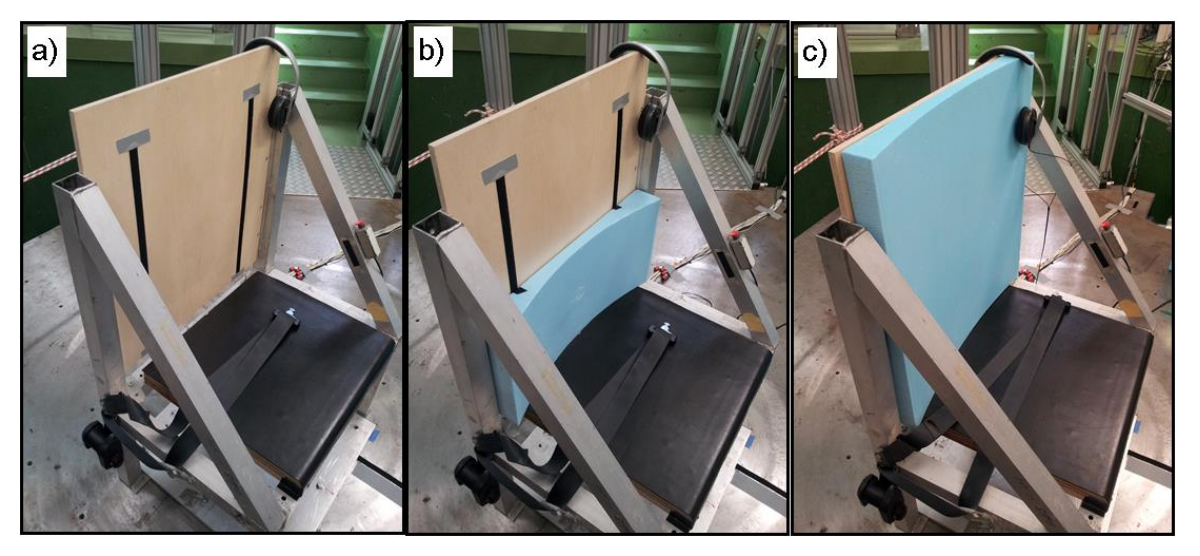


Figure 8.1 Illustration of the three backrest conditions (a) no backrest; (b) short backrest; (c) high backrest.

8.2.2. Design

The experiment adopted a repeated measures (within-subjects) design. Subjects were exposed to a series of motion stimuli whilst seated in one of the three seating conditions (without backrest, short backrest, and high backrest – see Figure 8.1) in each of three experimental sessions (conducted on separate days). At the start of each session, subjects were trained on the method of absolute magnitude estimation using a set of practice motion stimuli (consisting of all three directions of oscillation at the lowest and highest magnitudes – see section 8.2.3).

Each session consisted of three parts. In part 1 (equivalent comfort contours) subjects used the method of absolute magnitude estimation to rate the discomfort produced by lateral oscillation, roll oscillation, and fully roll-compensated lateral oscillation at frequencies between 0.25 and 1.0 Hz whilst seated in one of the backrest conditions. In part 2 (relative discomfort) subjects used absolute magnitude estimation to rate discomfort caused by 0.5-Hz lateral oscillation where motions were experienced both without a backrest and with either the short backrest or the high backrest. In part 3 (body map), for every stimulus, the subjects used a labelled diagram of the body (Figure 8.2) to indicate where they felt discomfort, choosing as many locations as they felt appropriate.

The order of presentation of motion stimuli within each experimental part was fully randomised for each subject. The order of the three experimental sessions was varied for each subject using a Latin square.

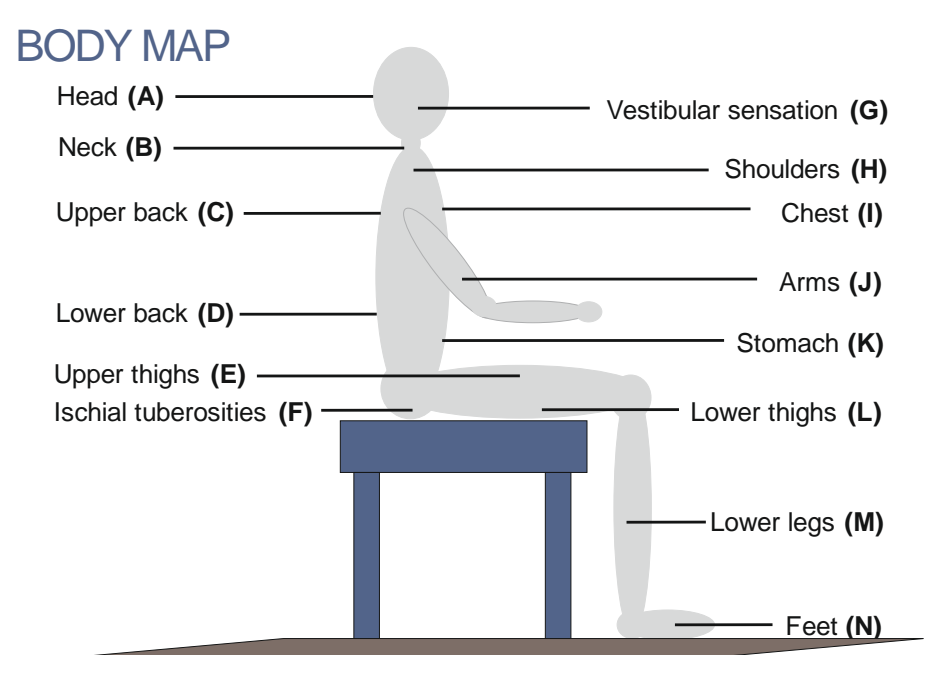


Figure 8.2 Body map used by subjects to indicate the location of discomfort caused by lateral, roll and fully roll-compensated lateral oscillation.

8.2.3. Motion stimuli

The motion stimuli consisted of seven frequencies at the preferred one-third octave centre frequencies from 0.25 to 1.0 Hz. Each frequency was presented at, nominally, eight magnitudes in logarithmic series from 0.08 to 0.40 ms⁻² r.m.s. (Due to simulator limitations, five magnitudes of lateral oscillation (0.08 to 0.20 ms⁻² r.m.s.) were presented at 0.25 Hz and seven magnitudes (0.08 to 0.315 ms⁻² r.m.s.) at 0.315 Hz. Seven magnitudes of roll oscillation (equivalent to 0.08 to 0.315 ms⁻² r.m.s.) were presented at 1.0 Hz. Seven magnitudes of roll-compensated oscillation were presented at 0.8 Hz (0.08 to 0.315 ms⁻² r.m.s.) and six magnitudes (0.08 to 0.25 ms⁻² r.m.s.) at 1.0 Hz).

For roll oscillation, the magnitude was defined by the acceleration in the plane of the seat (i.e., due to gravity). For roll-compensated lateral oscillation, the lateral oscillation and the roll oscillation were combined 180° out-of-phase such that the resultant acceleration in the plane of the seat was zero. This procedure is illustrated in Figure 8.3, which shows the acceleration waveform in the plane of the seat for lateral oscillation, roll oscillation, and roll-compensated lateral oscillation at 0.5 Hz. All motion stimuli were transient waveforms with a 3.5 cycle duration (as shown in Figure 8.3) generated from the product of a sine wave of the desired frequency

and a half-sine of the same duration. The motions were generated within MATLAB (version R2010a research) using the *HVLab* toolbox (version 1.0).

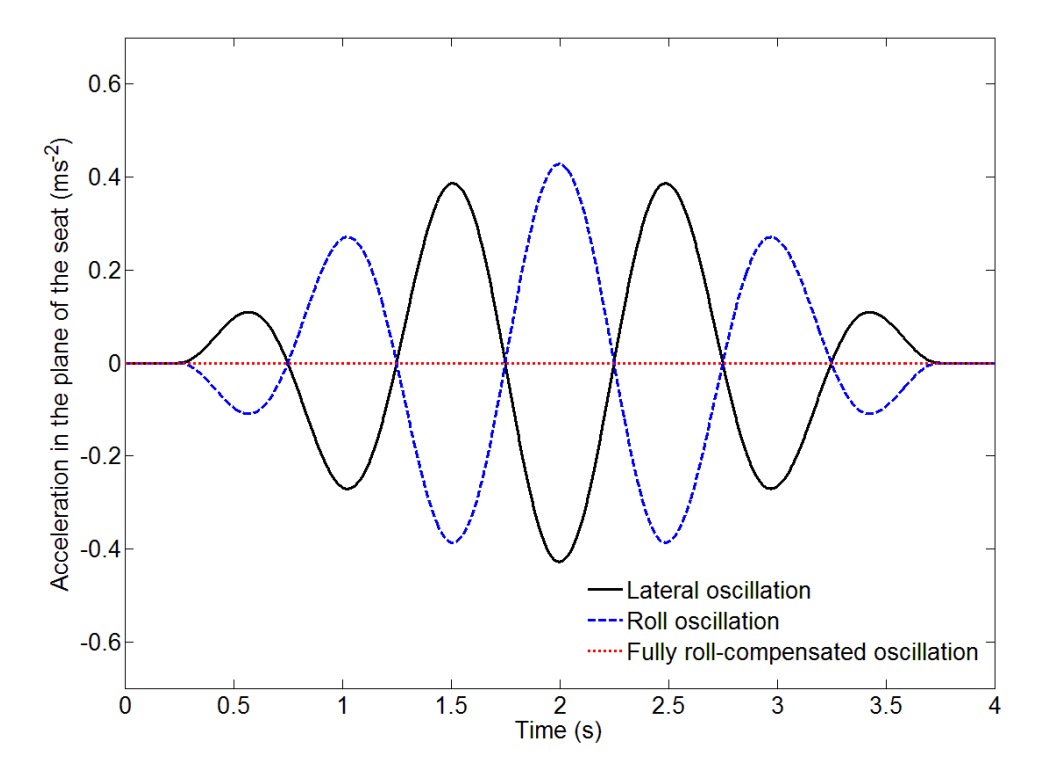


Figure 8.3 Example waveforms for 1.0-Hz oscillation showing the acceleration in the plane of the seat for lateral oscillation, roll oscillation, and fully roll-compensated lateral oscillation.

8.2.4. Subjects

Twenty-one male volunteers aged between 19 and 33 years (median age 25.0 years, interquartile range, IQR, 7.0 years; median weight 71.3 kg, IQR 19.0; median stature 1.76 m, IQR 0.08 m) participated in the experiment. Subjects were recruited from the staff and student population of the University of Southampton. Full details of the subject demographics can be found in the Appendices.

8.2.5. Analysis

The physical magnitudes, φ , of the motion stimuli were related to the subjective magnitude estimates, ψ , using Stevens' power law (Stevens, 1975):

Equation 8.1:
$$\psi = k \varphi^n$$

The exponent, n, (i.e., the rate of growth of discomfort) and the constant, k, were determined by performing linear regression on the logarithmic transformation of Equation 8.1:

Equation 8.2:
$$\log_{10} \psi = \log_{10} k + n \log_{10} \varphi$$

Lateral oscillation of the rigid seat without backrest at a frequency of 0.5 Hz and a magnitude of 0.2 ms⁻² r.m.s. was selected as a 'common reference' for constructing equivalent comfort contours. A 'normalisation' factor was determined in order to normalise the data for all subjects such that the reference condition was assigned a value of 100. Normalisation factors were calculated using Equation:

Equation 8.3: Normalisation factor =
$$(100 / \psi_{Reference})$$

where $\psi_{\text{Reference}}$ is the subjective magnitude corresponding to the reference condition, obtained through linear regression of Equation 8.2. Normalisation factors were determined for each subject.

Values for n and k were determined for each individual subject for each frequency and direction of oscillation using normalised magnitude estimates from part 1 (equivalent comfort contours). Equivalent comfort contours for normalised subjective magnitudes, Ψ , of 50, 63, 80, 100, 125, 160, and 200 were calculated for each subject and all three directions of oscillation using Equation 8.1.

The data from part 2 (relative discomfort) were used to calculate a 'backrest factor' to adjust the equivalent comfort contours for the seat with a short backrest, and for the seat with a high backrest (obtained in part 1) so that discomfort relative to the seat without backrest could be examined. The backrest factor was calculated using Equation 8.4:

Equation 8.4: Backrest factor =
$$(\varphi_{NoBackrest}) / (\varphi_{Backrest})$$

where $\varphi_{\text{Backrest}}$ is the acceleration magnitude of a 0.5-Hz lateral test motion in part 2 that caused discomfort equivalent to a subjective magnitude of 100 on the seat with either a short or high backrest, and $\varphi_{\text{NoBackrest}}$ is the acceleration magnitude of a 0.5-Hz lateral test motion in part 2 that caused discomfort equivalent to a subjective magnitude of 100 on the seat without backrest. Relative equivalent comfort contours for the short backrest and the high backrest configurations were adjusted by applying the backrest factors to the individual equivalent comfort contours for the short and high backrest constructed from the part 1 data.

The data from part 3 (body map) were used to assess the effect of backrest and the frequency of lateral oscillation, roll oscillation, and fully roll-compensated lateral oscillation on the location of discomfort.

The non-parametric Friedman test was used to investigate the overall effect of frequency of oscillation, direction of oscillation, and backrest height on the rates of growth of discomfort and the equivalent comfort contours. The Wilcoxon matched-pairs signed ranks test was used to examine specific differences in rates of growth of discomfort and equivalent comfort contours between backrest conditions, frequencies, and directions. The McNemar dichotomous test was used to test for significant trends in the body map data. Median rates of growth of discomfort and median equivalent comfort contours were used to identify overall trends in the data. The Bonferroni correction was used where there were multiple comparisons.

8.3. Results

8.3.1. Rate of growth of discomfort

8.3.1.1. Effect of backrest height

Median rates of growth of discomfort for the three directions of oscillation (lateral, roll and fully roll-compensated lateral) on the three seat configurations (no backrest, short backrest, and high backrest) are shown in Figure 8.4.

The height of the backrest had no significant effect on the rate of growth of discomfort, except with 0.4-Hz lateral oscillation (p = 0.023; Friedman) and 0.8- and 1.0-Hz roll oscillation (p = 0.023 and 0.013, respectively; Friedman).

8.3.1.2. Effect of frequency of oscillation

Rates of growth discomfort varied with the frequency of oscillation for all directions (lateral, roll and fully roll-compensated lateral oscillation) with all three backrest configurations (no backrest, short backrest and high backrest) (p < 0.003; Friedman; Figure 8.4), except for lateral oscillation with no backrest and with the short backrest (p > 0.05; Friedman) and fully roll-compensated lateral oscillation with the high backrest (p = 0.301; Friedman).

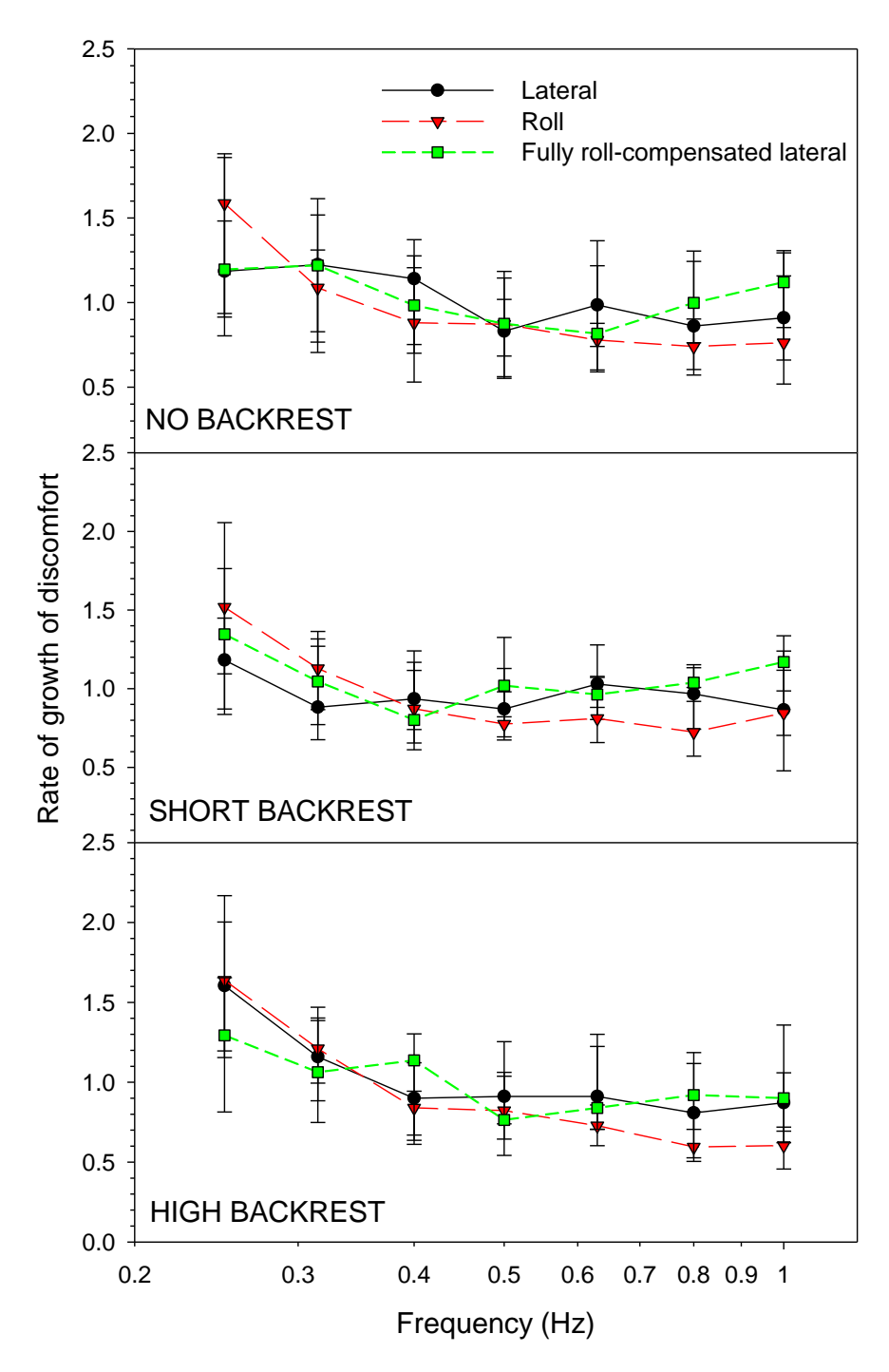


Figure 8.4 Median rates of growth of discomfort for lateral oscillation, roll oscillation, and fully roll-compensated lateral oscillation with no backrest, a short backrest and a high backrest.

Upper and lower error bars show 75th and 25th percentiles, respectively.

For lateral oscillation with the high backrest, the rate of growth of discomfort was negatively correlated with frequency (R = -0.424, p < 0.001; Spearman). In all backrest conditions with roll oscillation, the rate of growth of discomfort was negatively correlated with frequency (R < -0.334, p < 0.001; Spearman). With fully roll-compensated lateral oscillation there were no significant correlations between the rate of growth of discomfort and the frequency of oscillation (p > 0.05; Spearman).

8.3.1.3. Effect of direction of oscillation

Rates of growth of discomfort varied with the direction of oscillation in some conditions: with no backrest at 0.63 Hz and 1.0 Hz (p = 0.013 and 0.007, respectively; Friedman); with the short backrest at 0.63 Hz and 1.0 Hz (p = 0.023 and 0.031, respectively; Friedman), and; with the high backrest at 0.25 Hz, 0.8 Hz and 1.0 Hz (p = 0.024, 0.012 and 0.001, respectively; Friedman).

8.3.2. Vibration discomfort

8.3.2.1. Effect of backrest height

The height of the backrest influenced the magnitude of vibration required to produce discomfort equivalent to a subjective magnitude of 100 for lateral oscillation (at all frequencies except 0.8 and 1.0 Hz; p < 0.031; Friedman), for roll oscillation (at all frequencies except 0.4, 0.63 and 0.8 Hz; p < 0.018; Friedman) and for fully roll-compensated lateral oscillation (at all frequencies except 0.25, 0.63 and 0.8 Hz; p < 0.05; Friedman) (Figure 8.5).

During lateral oscillation, the discomfort was greater without backrest than with the short backrest at 0.315, 0.4 and 0.5 Hz (p < 0.003; Wilcoxon) and greater without a backrest than with the high backrest at all frequencies except 1 Hz (p < 0.011; Wilcoxon). The discomfort caused by lateral oscillation did not differ significantly between the short backrest and the high backrest (p > 0.05; Wilcoxon).

Likewise, roll oscillation caused greater discomfort without a backrest than with the high backrest at frequencies from 0.25 to 0.5 Hz (p < 0.013; Wilcoxon), but there was greater discomfort with the high backrest than without a backrest or with the short backrest at 1 Hz (p < 0.008; Wilcoxon).

Discomfort caused by fully roll-compensated lateral oscillation was greater without backrest than with the short backrest at 0.4 Hz (p = 0.003; Wilcoxon) and greater without a backrest than with the high backrest at 0.5 and 0.63 Hz (p < 0.011; Wilcoxon).

No other statistically significant effects of backrest height on equivalent comfort contours were found.

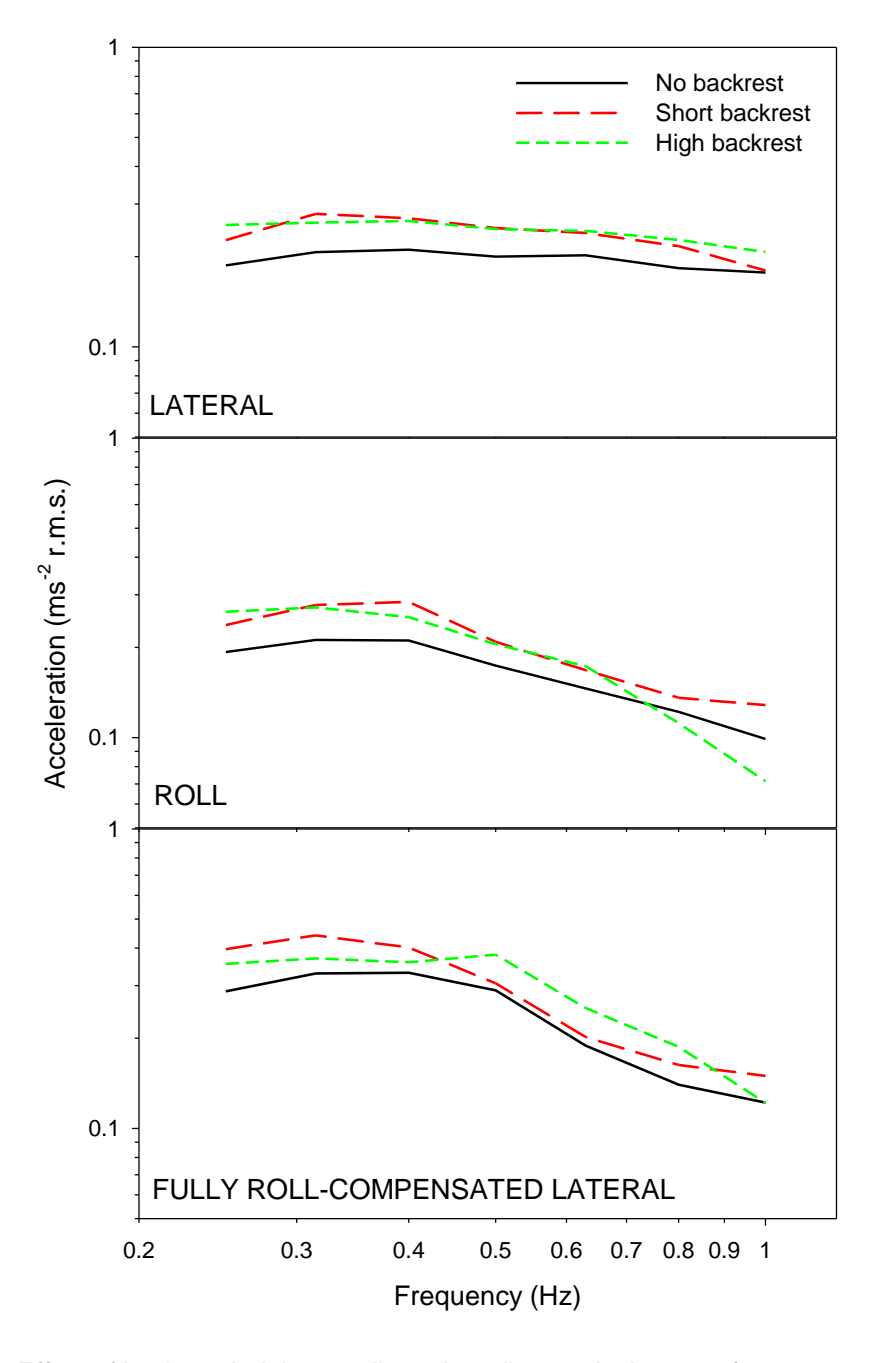


Figure 8.5 Effect of backrest height on adjusted median equivalent comfort contours for lateral, roll and fully roll-compensated lateral oscillation. Contours represent discomfort equal to that arising from lateral oscillation at 0.5 Hz, 0.2 ms⁻² r.m.s. on a rigid seat without backrest (i.e. a subjective magnitude, Ψ , of 100).

8.3.2.2. Effect of frequency and direction of oscillation

The frequency of oscillation influenced the acceleration required to produce a subjective magnitude of 100 with lateral oscillation, roll oscillation, and fully roll-compensated lateral oscillation with all three backrest conditions (Figure 8.5; p < 0.011; Friedman).

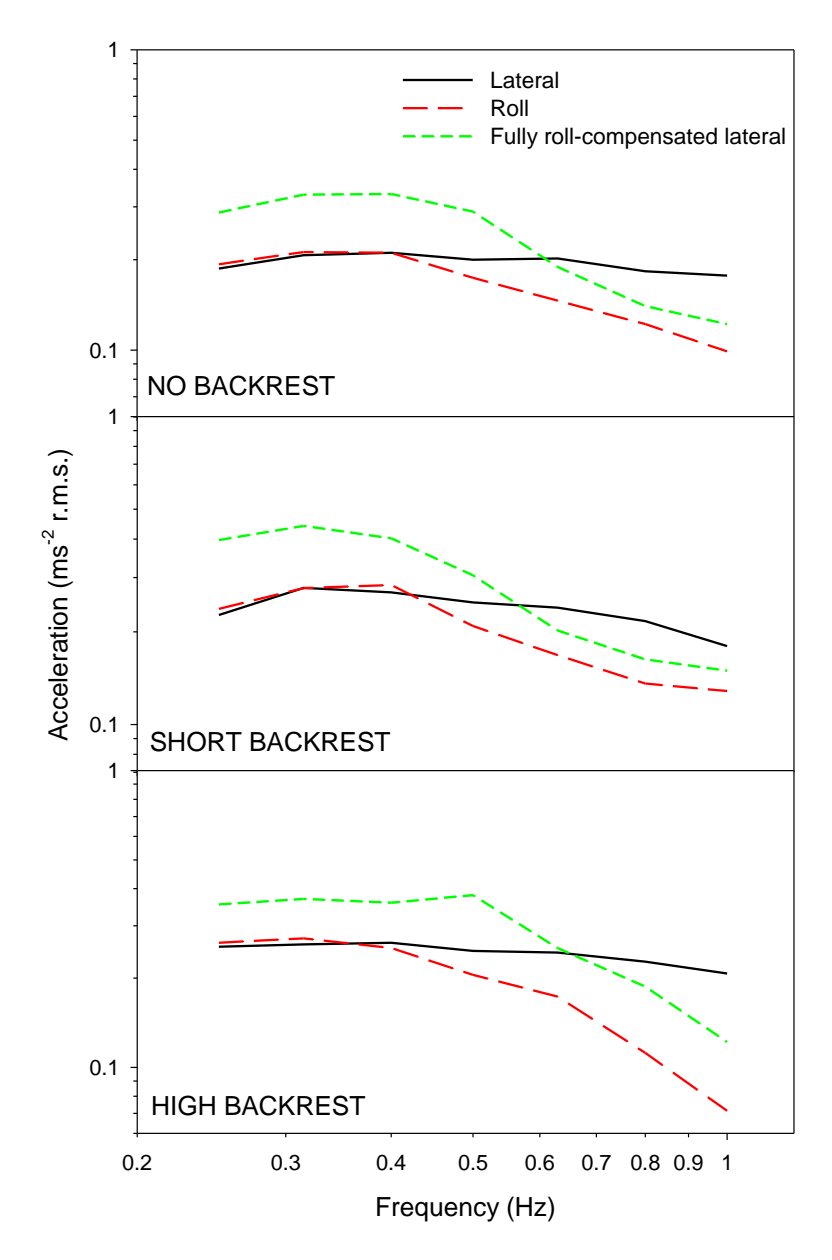


Figure 8.6 Effect of direction on median equivalent comfort contours for the three seat configurations (no backrest, short backrest, and high backrest). Contours represent discomfort equal to that arising from lateral oscillation at 0.5 Hz 0.2 ms⁻² r.m.s. on a rigid seat without backrest (i.e. a subjective magnitude, Ψ , of 100).

Without backrest, the equivalent comfort contour for lateral oscillation had approximately constant acceleration from 0.315 to 0.63 Hz, but declined from 0.63 to 1.0 Hz at approximately 1 dB per octave. For roll oscillation the contour had approximately constant acceleration from 0.315 to 0.4 Hz, but declined at approximately 6 dB per octave from 0.4 to 1.0 Hz. For fully roll-compensated lateral oscillation, the equivalent comfort had approximately constant acceleration from 0.315 to 0.4 Hz, but declined at approximately 7 dB per octave from 0.4 to 1.0 Hz.

With the short backrest, the equivalent comfort contour for lateral oscillation had approximately constant acceleration from 0.315 to 0.5 Hz, but declined at approximately 3 dB per octave from 0.5 to 1.0 Hz. For roll oscillation the contour had approximately constant acceleration from 0.315 to 0.4 Hz, but declined at 6 dB per octave from 0.4 to 1.0 Hz. For fully roll-compensated lateral oscillation, the contour had approximately constant acceleration from 0.25 to 0.4 Hz, but declined at 6 dB per octave from 0.4 to 1.0 Hz.

With the high backrest, the equivalent comfort contour for lateral oscillation had approximately constant acceleration from 0.25 to 0.4 Hz, but declined at approximately 2 dB per octave from 0.4 to 1.0 Hz. For roll oscillation the contour had approximately constant acceleration from 0.25 to 0.4 Hz, but declined at 9 dB per octave from 0.4 to 1.0 Hz. For fully roll-compensated lateral oscillation, the contour had approximately constant acceleration from 0.25 to 0.5 Hz, but declined at 9 dB per octave from 0.5 to 1.0 Hz.

With all three backrest heights, the acceleration required to produce a subjective magnitude of 100 differed with the direction of oscillation at all frequencies (p < 0.001; Friedman; Figure 8.6). The effect of direction was similar to that reported in Chapters 6 and 7.

8.3.2.3. Effect of magnitude of oscillation

Equivalent comfort contours were calculated for subjective magnitudes between 50 and 200 (Figure 8.7). For lateral oscillation on a rigid seat with the high backrest, and for roll oscillation with all three backrest conditions, the dispersion of equivalent comfort contours representing subjective magnitudes between 50 and 200 can be seen to increase with increasing frequency from 0.25 to 1.0 Hz, consistent with the negative correlation between the rate of growth of discomfort and the frequency of oscillation (see Figure 8.4). The shape of the equivalent comfort contours for fully roll-compensated lateral oscillation is most affected by the magnitude of oscillation in the range 0.4 to 0.5 Hz, consistent with the smaller rates of growth of discomfort in this range.

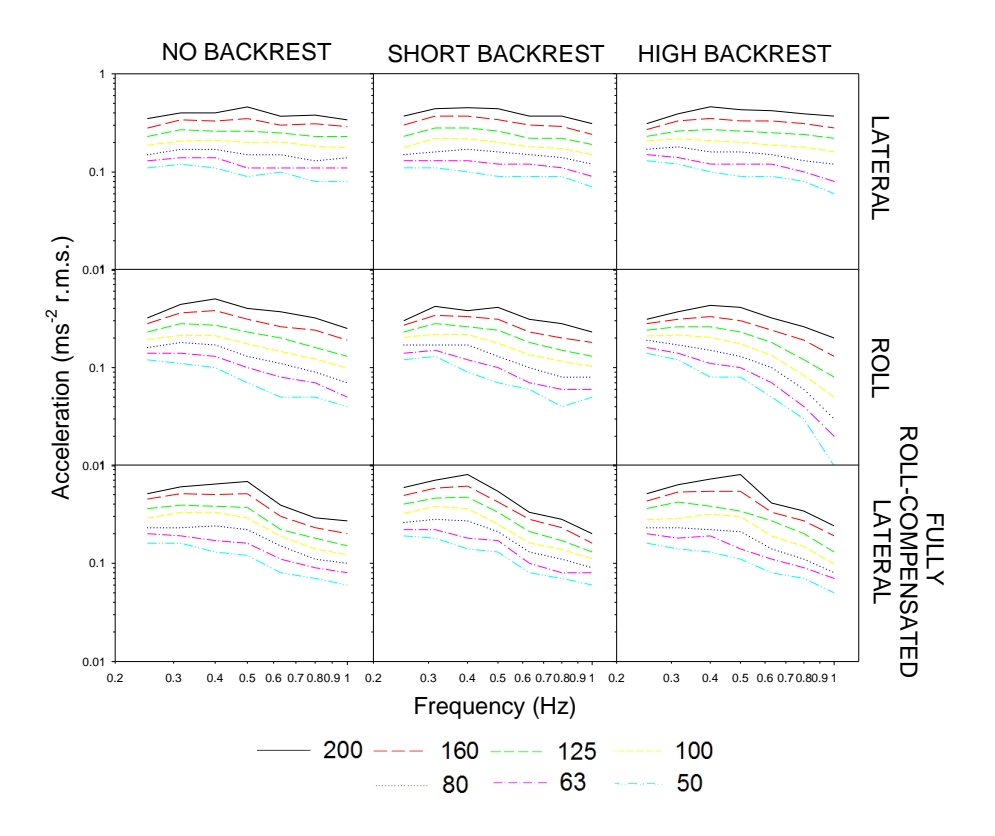


Figure 8.7 Effect of magnitude on equivalent comfort contours for lateral, roll and fully roll-compensated lateral oscillation on rigid seat without a backrest, with a short backrest and with a high backrest. Contours represent subjective magnitudes of 50, 63, 80, 100, 125, 160 and 200.

8.3.3. Location of discomfort

The incidence of discomfort at the shoulders, upper back, stomach, ischial tuberosities and lower thighs was dependent on the height of the backrest (p < 0.05; Cochran's Q). Discomfort at the upper back was more frequent with a high backrest than with either no backrest or a short backrest during 0.8-Hz lateral oscillation (p = 0.008; McNemar). Discomfort at the ischial tuberosities was more frequent when sitting with no backrest than when sitting with a short backrest during 1.0-Hz lateral oscillation (p = 0.008; McNemar). No other statistically significant effects of backrest on the location of discomfort were found.

The incidence of discomfort at the neck, shoulders, upper back, stomach, ischial tuberosities, lower thighs, and lower legs was found to be dependent on the direction of oscillation (p < 0.05; Cochran's Q). However, post-hoc analysis with the Bonferroni correction revealed no statistically significant specific differences in the location of discomfort between lateral

oscillation, roll oscillation, and fully roll-compensated lateral oscillation at any frequency with any of the three backrests.

8.4. Discussion

8.4.1. Rate of growth of discomfort

Median rates of growth of discomfort varied between 0.6 and 1.6, consistent with those reported previously with similar motions on a rigid seat without backrest and with a 550-mm backrest (Chapter 5 and Chapter 6; see Figure 8.8). The type of backrest had very little effect on the rate of growth of discomfort, except for 0.8 Hz and 1.0 Hz roll oscillation where the rate of growth of discomfort was least with the high backrest. Similarly, a full-height backrest with four-point harness did not influence rates of growth of discomfort reported previously (Wyllie and Griffin, 2007). A low rate of growth of discomfort implies that a unit increase in the physical magnitude of oscillation results in only a slight increase in discomfort. The findings therefore suggest less sensitivity to changes in the magnitude of roll oscillation at 0.8 and 1.0 Hz when sitting with a high backrest than when sitting with either a short backrest or no backrest..

Median rates of growth of discomfort decreased with increasing frequency of oscillation (Figure 8.4), except for lateral oscillation without backrest and with the short backrest and for fully roll-compensated lateral oscillation with the high backrest. Reductions in the rate of growth with increasing frequency for lateral and roll oscillation have been reported previously for a rigid seat with a full-height backrest (Chapter 6), a rigid seat with full-height backrest and four-point harness (Wyllie and Griffin, 2007), a rigid seat without backrest (Wyllie and Griffin, 2007; Chapter 7), and a foam seat without backrest (Chapter 7). A decreasing rate of growth of discomfort with increasing frequency implies that an increase in motion magnitude causes a greater increase in discomfort at low frequencies than at high frequencies. As a result, the dispersion of equivalent comfort contours for subjective magnitudes between 50 and 200 increases with increasing frequency of oscillation, as shown in Figure 8.7.

8.4.2. Equivalent comfort contours

Under static conditions, a backrest is designed to encourage a comfortable posture by reducing the muscular strain imposed on the spine whilst maintaining proper lumbar lordosis (Corlett and Eklund, 1984). The current study investigated the advantages (or disadvantages) of sitting with two heights of backrest during exposure to low frequency horizontal and rotational motions. During lateral oscillation at frequencies less than 0.63 Hz, there was less discomfort when

sitting with a short backrest than sitting without a backrest. The 295 mm short backrest provided support for the lumbar region of the back, which may have reduced the muscular effort required to maintain an upright sitting posture during lateral motion. The thoracic region of the back was unsupported by the short backrest, so subjects either allowed their upper body to sway with the motion or used muscle activity to retain a vertical posture. During lateral oscillation at all frequencies less than 1 Hz, there was less discomfort sitting with a high backrest than sitting without a backrest. The addition of lateral support to the thoracic region of the back with a high backrest reduced upper body sway and the reduced discomfort may be associated with reduced muscular activity in maintaining a stable posture. However, during lateral oscillation there were no statistically significant differences in discomfort between the short backrest and the high backrest.

Although the median equivalent comfort contours suggest the short backrest reduced discomfort caused by roll oscillation, no statistically significant effects were found. Compared to sitting with no backrest or the short backrest, the high backrest reduced discomfort at frequencies from 0.25 to 0.63 Hz but increased discomfort at 1.0 Hz. At the lower frequencies, the lateral support offered by the high backrest may have reduced the muscle activity required to maintain an upright posture during roll oscillation. If the lateral acceleration in the plane of the seat due to roll through the gravity vector is constant, then the lateral acceleration of the backrest produced by roll oscillation increases with increasing height above the position of full roll-compensation (the seat surface) and with increasing frequency of oscillation. Therefore, with 1-Hz roll oscillation there was a greater magnitude of lateral acceleration at the top of the backrest than with lower frequencies of roll oscillation. Increased transmission of lateral acceleration to the upper body and the head with the full-height backrest may account for the increased discomfort (Paddan and Griffin, 1988, 1994; Brett and Griffin, 1991).

Similar to the current study, the discomfort caused by lateral oscillation between 0.2 and 1.0 Hz was less with a full-height backrest than without a backrest for both a rigid seat and a cushioned seat (Chapter 5). However, during lateral oscillation between 0.4 and 1.6 Hz and during roll oscillation between 0.63 and 1.6 Hz, discomfort was greater with a full-height backrest and a four-point harness than without a backrest (Wyllie and Griffin, 2007). Subjects were securely fastened to the seat with the four-point harness and unable to move the upper back or shoulders relative to the backrest, so increased transmission of lateral and roll oscillation to the upper body and head may have increased discomfort. The addition of the harness may have extended the detrimental effects of a high backrest seen with 1-Hz roll oscillation in the current study to lower frequencies (i.e., to 0.63 Hz).

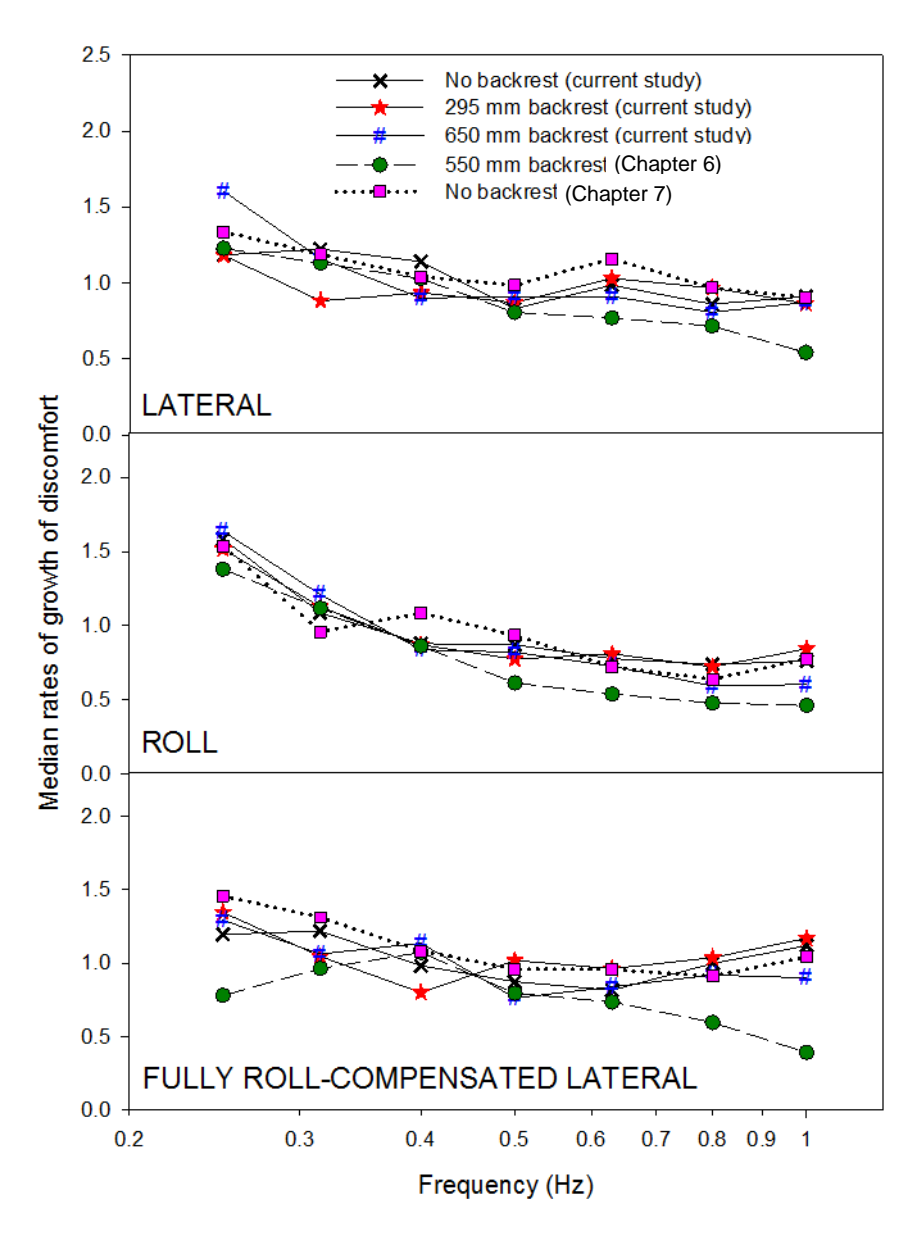


Figure 8.8 Comparison of median rates of growth of discomfort for lateral, roll and fully roll-compensated lateral oscillation in the current study with those reported previously.

Equivalent comfort contours were highly dependent on the frequency of oscillation. When sitting without a backrest, equivalent comfort contours for lateral oscillation required approximately constant acceleration at frequencies from 0.315 to 0.63 Hz, then declined by about 1 dB per octave between 0.63 and 1.0 Hz. Contours for roll oscillation and fully-roll compensated lateral oscillation were approximately constant between 0.315 and 0.4 Hz then declined by 6 dB and 7 dB per octave, respectively, between 0.4 and 1.0 Hz. Similar findings for a rigid seat without

backrest have been reported previously (Wyllie and Griffin, 2007; Chapter 7). Previous equivalent comfort contours for a rigid seat without backrest at these frequencies and at frequencies greater than this range suggest increasing sensitivity to lateral acceleration with increasing frequency up to about 2 Hz and decreasing sensitivity at greater frequencies (Griffin *et al.*, 1982; Morioka and Griffin, 2006a).

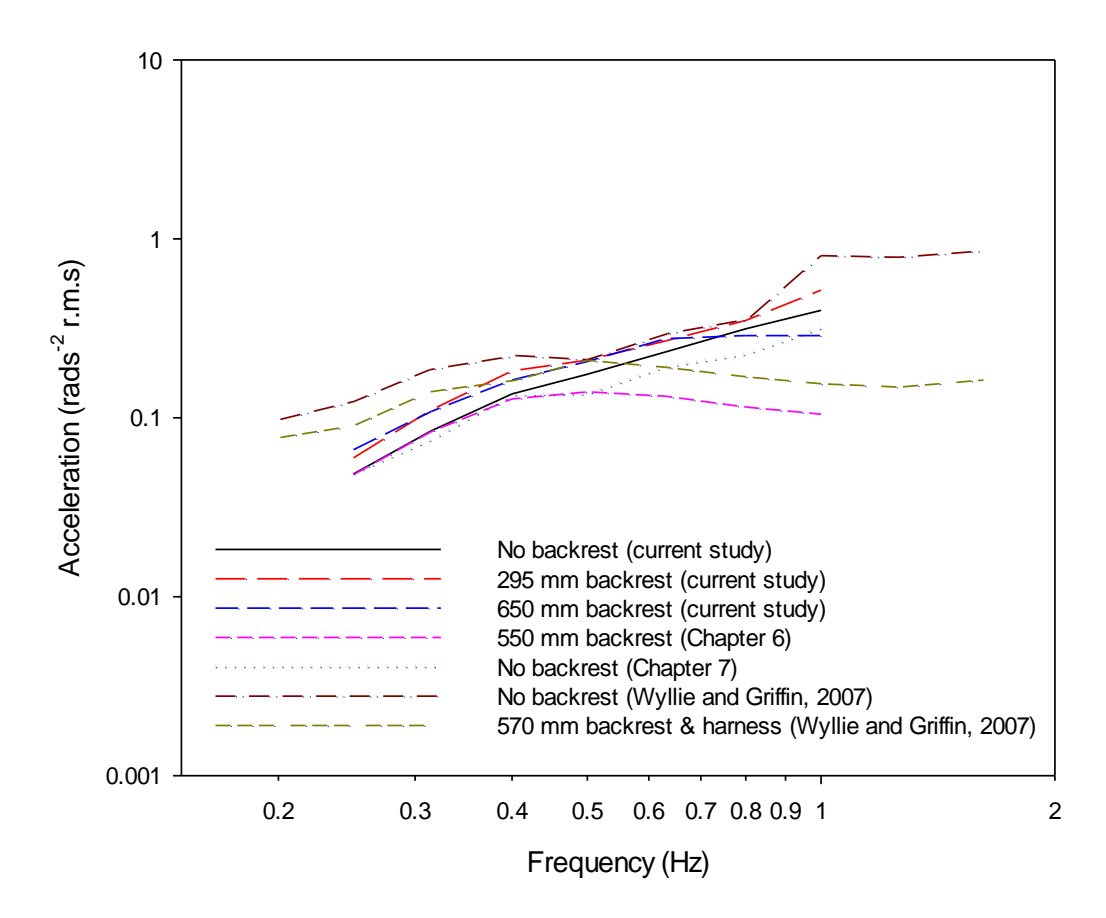


Figure 8.9 Comparison of equivalent comfort contours for roll oscillation from the current study with those reported previously.

When sitting with either a short backrest (295 mm) or a high backrest (650 mm), the frequency dependence of equivalent comfort contours for lateral oscillation was roughly similar, remaining constant between 0.25 and 0.5 Hz and declining by approximately 3 dB per octave above this range. However, during roll oscillation and fully roll-compensated lateral oscillation the frequency-dependence of equivalent comfort contours was dependent on the height of the backrest. When expressed in terms of acceleration in the plane of the seat (ms⁻² r.m.s.), the contours have approximately constant acceleration between 0.25 and 0.4 Hz with both

backrests, but decline between 0.4 and 1.0 Hz at approximately 6 dB per octave with the short backrest and at approximately 9 dB per octave with the high backrest. Previous equivalent comfort contours for roll oscillation (expressed in rotational acceleration – rads⁻² r.m.s.) on a rigid seat with a 550-mm high backrest (Chapter 6) and a rigid seat with a 570-mm high backrest and four-point harness (Wyllie and Griffin, 2007) are compared with those from the current study in Figure 8.9. With the 295-mm high backrest and with no backrest, the roll acceleration required to cause a given level of discomfort increases with increasing frequency from 0.2 to 1.0 Hz. With the taller backrests, the level of equivalent comfort contours remains approximately constant at frequencies between about 0.5 and 1.0 Hz, suggesting sensitivity is proportional to roll acceleration in this range. The frequency-dependence of equivalent comfort contours is consistent with high backrests increasing the discomfort caused by roll oscillation, especially at higher frequencies.

Using a rigid seat with a 550-mm high backrest, a rigid seat without a backrest, and a foam seat without a backrest, full roll-compensation of lateral acceleration reduced discomfort at frequencies less than about 0.5 Hz, but increased discomfort at higher frequencies (Chapter 6 and Chapter 7). Similar findings are seen here when using a rigid seat with no backrest, a 295-mm high backrest, and a 650-mm high backrest. This implies that the physical discomfort associated with traversing curves at high-speed (e.g., in tilting trains) can be reduced by appropriate roll-compensation techniques if the motions occur at frequencies less than about 0.5 Hz. In this range of frequencies, full roll-compensation of lateral accelerations may cause nausea in some passengers (e.g. Ueno *et al.*, 1986; Förstberg *et al.*, 1998; Donohew and Griffin, 2009). At frequencies greater than about 0.5 Hz, roll-compensation is likely to worsen the physical comfort of passengers.

8.4.3. The location of discomfort

At the higher frequencies tested (significant at 0.8-Hz), discomfort during lateral oscillation was more frequently localised at the upper back when sitting with a high backrest than when sitting with no backrest or a short backrest. This is consistent with a high backrest increasing the transmission of lateral acceleration to the upper body (Paddan and Griffin, 1988; Brett and Griffin, 1991). Greater discomfort has also been reported at the head, neck or shoulders when seated with a full-height backrest and four-point harness and it was suggested that the "backrest prevented the torso moving so as to reduce the acceleration reaching the head and neck" (Wyllie and Griffin, 2007, p. 2651). Despite a greater incidence of discomfort at the upper back with the high backrest than without a backrest, the overall level of discomfort reported during lateral oscillation when sitting with a high backrest was less than when sitting with no backrest

(Figure 8.5). This suggests that an increased incidence of discomfort at the upper back associated with sitting with a high backrest was mediated by a reduction in the incidence of discomfort at other locations of the body.

Also with high frequencies of lateral oscillation (significant at 1-Hz), the discomfort at the ischial tuberosities was greatest when sitting with no backrest, consistent with previous findings (Chapter 6 and Chapter 7). Sitting upright without a backrest requires the pelvis to be rolled forward. The pressure on the ischial tuberosities in this posture may be reduced by leaning back against a backrest (e.g. Vos *et al.*, 2006; Kyung and Nussbaum, 2008). Discomfort while exposed to lateral oscillation may result from the downward forces that occur alternately at each ischial tuberosity. Full roll-compensation of lateral oscillation, which balances the lateral forces at the seat surface, has been reported to reduce discomfort at the ischial tuberosities (Chapter 6 and Chapter 7).

8.4.4. Implications for vibration standards

National and International vibration standards suggest that, at every frequency of oscillation, discomfort from lateral acceleration at the backrest and discomfort from lateral acceleration at the seat surface may be predicted with the same frequency-weighting (i.e. W_d) but with sensitivity at the backrest half that at the seat (BS 6841, 1987; ISO 2631-1, 1997). Using the root-sums-of-squares method to summate these components of lateral acceleration implies an additive effect of backrest vibration on discomfort. The current findings indicate that the discomfort caused by lateral oscillation is lowered by the presence of a short backrest (at frequencies less than 0.63 Hz) and by a high backrest (at frequencies less than 1 Hz). The same effect of backrest was found for lateral acceleration caused by the gravitational component of roll at frequencies less than 0.63 Hz. The increase in discomfort predicted by current standards when using a backrest is therefore incorrect in this frequency range.

BS 6841 (1987) and ISO 2631-1 (1997) advise that lateral acceleration is frequency-weighted with a filter (i.e., W_d) and scaled by an appropriate multiplying factor (i.e., 0.5 for a lateral vibration at a backrest, 1.0 for lateral vibration at a seat). A positive multiplying factor would be required for lateral vibration at the backrest for frequencies greater than 1 Hz (where backrest vibration increases discomfort – e.g. Parsons *et al.*, 1982), but a negative multiplying factor would be required at some frequencies less than 1 Hz (where a backrest can reduce discomfort – current study). This requires acceleration spectra to be split into two bands. Alternatively, those concerned with the prediction of discomfort in vehicles should be made aware that a

backrest is likely to reduce the discomfort caused by lateral acceleration at frequencies less than about 0.8 Hz.

Current standards are not intended for predicting the discomfort caused by frequencies less than 0.5 Hz, but the applicability of weighting W_d (for lateral acceleration) and W_e (for roll acceleration) can be considered for frequencies in the range 0.2 to 0.5 Hz. The frequency weightings W_d and W_e are compared with median equivalent comfort contours for each backrest height and direction of motion in Figure 8.10. (The equivalent comfort contours shown in Figure 8.5 have been inverted and normalised to unity at 1 Hz).

For all seating conditions (i.e. no backrest, 295-mm backrest and 650-mm backrest), frequency weighting W_d appears to offer a reasonable approximation to the inverted equivalent comfort contours for frequencies between 0.315 and 1.0 Hz, regardless of the sensation magnitude. But, at frequencies less than 0.315 Hz, W_d appears to underestimate discomfort, particularly at high magnitudes and when seated with a full-height backrest.

Frequency weighting W_e is approximately constant between 0.5 and 1.0 Hz, suggesting that discomfort is approximately proportional to roll acceleration in this range. However, the magnitude-dependence of equivalent comfort contours for roll acceleration (shown in Figure 8.10) indicates that a single weighting is not appropriate for predicting discomfort at frequencies less than 1 Hz. The magnitude-dependence of equivalent comfort contours varies with the backrest condition. Without a backrest and with a short backrest, equivalent comfort contours are approximately inversely proportional to rotational displacement at the highest magnitudes and inversely proportional to rotational velocity at the lowest magnitudes. At the highest magnitudes of roll acceleration on a seat with a full-height backrest, contours are approximately inversely proportional to rotational displacement at all frequencies between 0.25 and 1.0 Hz. At the lowest magnitudes, the contours are approximately constant between 0.5 and 1.0 Hz and inversely proportional to constant velocity at frequencies less than this range.

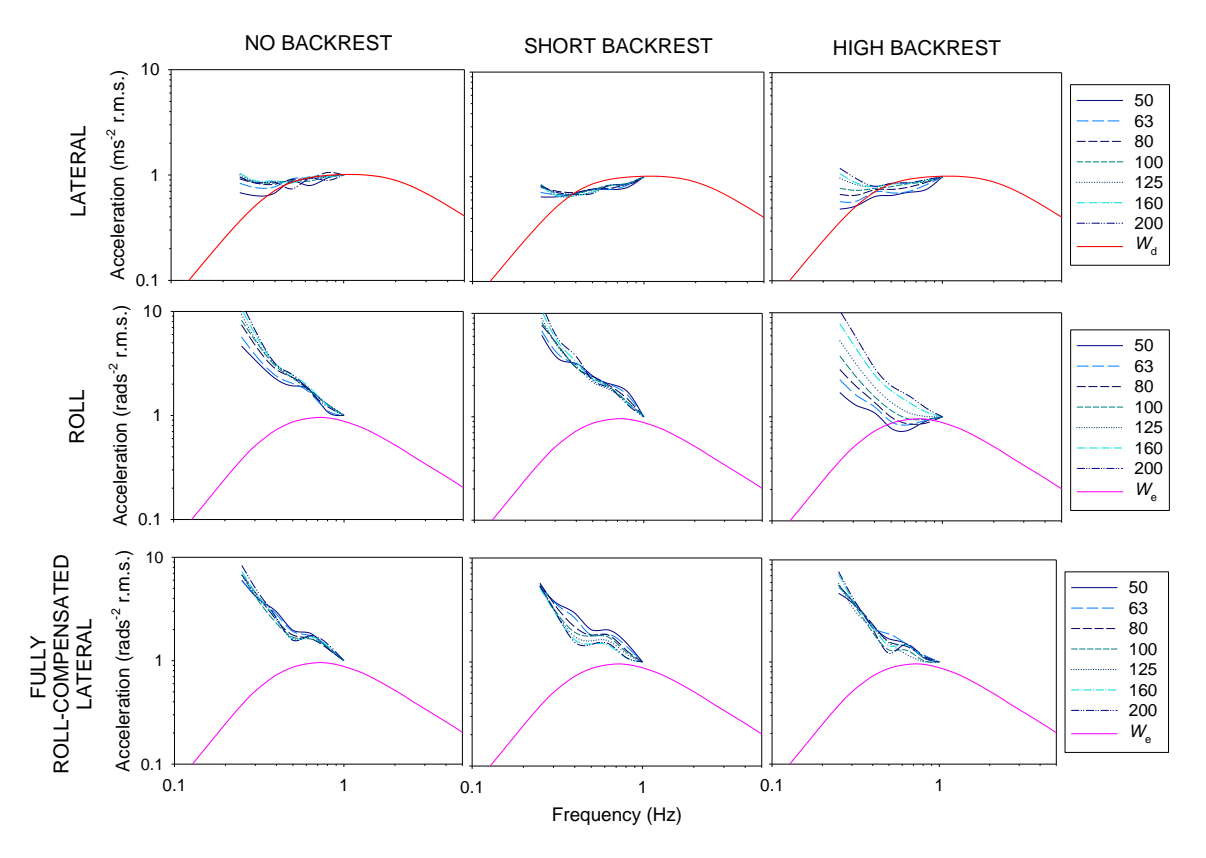


Figure 8.10 Comparison of current frequency-weightings with inverted median equivalent comfort contours for lateral, roll and fully roll-compensated lateral oscillation on all backrest conditions. Contours (normalised to unity at 1 Hz) represent subjective magnitudes of 50, 63, 80, 100, 125, 160 and 200.

With fully roll-compensated lateral oscillation, the lateral acceleration in the plane of the seat at the seat surface (i.e., at the position of full roll-compensation) was zero, therefore using a frequency-weighting for lateral acceleration to predict discomfort is inappropriate. When expressed in terms of rotational acceleration (rads-2 r.m.s.), inverted equivalent comfort contours for fully roll-compensated lateral oscillation (with all 3 backrest conditions) are approximately inversely proportional to constant roll displacement at frequencies less than 0.5 Hz (Figure 8.10). The contours are proportional to constant roll acceleration between 0.5 and 0.8 Hz, and then approximately inversely proportional to constant roll velocity between 0.8 and 1.0 Hz. It seems that as the frequency increases above about 0.5 Hz, discomfort from fully roll-compensated lateral motion may be predicted from a frequency weighting similar to that for pure roll oscillation.

8.5. Conclusion

National and International vibration standards predict an additive effect of vibration of a backrest on discomfort in the frequency range 0.5 to 80 Hz, but the current findings suggest a backrest is beneficial for comfort during lateral oscillation at frequencies less than 1.0 Hz, during roll oscillation at frequencies less than 0.63 Hz and during fully roll-compensated lateral oscillation between 0.4 and 0.63 Hz. With no backrest, discomfort due to lateral oscillation was mostly localised at the ischial tuberosities, but with lateral oscillation of a full-height backrest discomfort was mainly localised at the upper back. Frequency weighting $W_{\rm d}$ for lateral acceleration offers an approximate prediction of discomfort in the range 0.315 to 1.0 Hz, but underestimates discomfort below this range. Frequency weighting $W_{\rm e}$ for roll acceleration is inappropriate for predicting discomfort at frequencies less than 1 Hz. It is concluded that for seats with no backrest or a short backrest, a weighting approximately inversely proportional to constant roll displacement may predict discomfort from roll acceleration in the range 0.25 to 1.0 Hz. No single frequency weighting is appropriate for predicting discomfort caused by roll acceleration on a seat with a full-height backrest at all magnitudes.

Chapter 9

Discussion

9.1. Introduction

In this chapter, the research findings reported in Chapters 4 to 8 are collated in order to present a model of motion sickness (Section 9.2.2), a model of vibration discomfort (Section 9.2.3) and recommendations for current vibration standards (Section 9.3) relating to the prediction of human responses to low frequency horizontal and rotational oscillation. To assess the strengths and limitations of the work, a discussion of the research methodology is also presented (Section 9.5). The chapter concludes with recommendations for future research (Section 9.6).

9.2. Human response to roll-compensated lateral acceleration

Horizontal and rotational motions at frequencies less than 1 Hz may cause motion sickness or physical discomfort. At these frequencies, the magnitude of lateral acceleration may be reduced through the addition of appropriate roll motion (i.e. roll-compensation – see Section 2.2.4). The work presented in this thesis has shown that 0.2-Hz fully roll-compensated lateral oscillation is highly provocative of motion sickness (Experiment 1 – Chapter 4) but causes little physical vibration discomfort (Experiment 3, 4 and 5 – Chapters 6, 7 and 8).

The development of motion sickness with very similar motion conditions was also investigated previously. Figure 9.1 shows mean illness ratings during 30-minute exposures to 100% roll-compensated lateral oscillation at 0.2 Hz (where the position of full roll-compensation was at the seat surface) as reported in Chapter 4, and by Donohew and Griffin (2009) and Joseph and Griffin (2007). The development of sickness is similar across the three studies, which show a gradual increase in mean illness ratings from 0 ('no symptoms') to around 3 ('mild nausea') over the 30-minute exposure period.

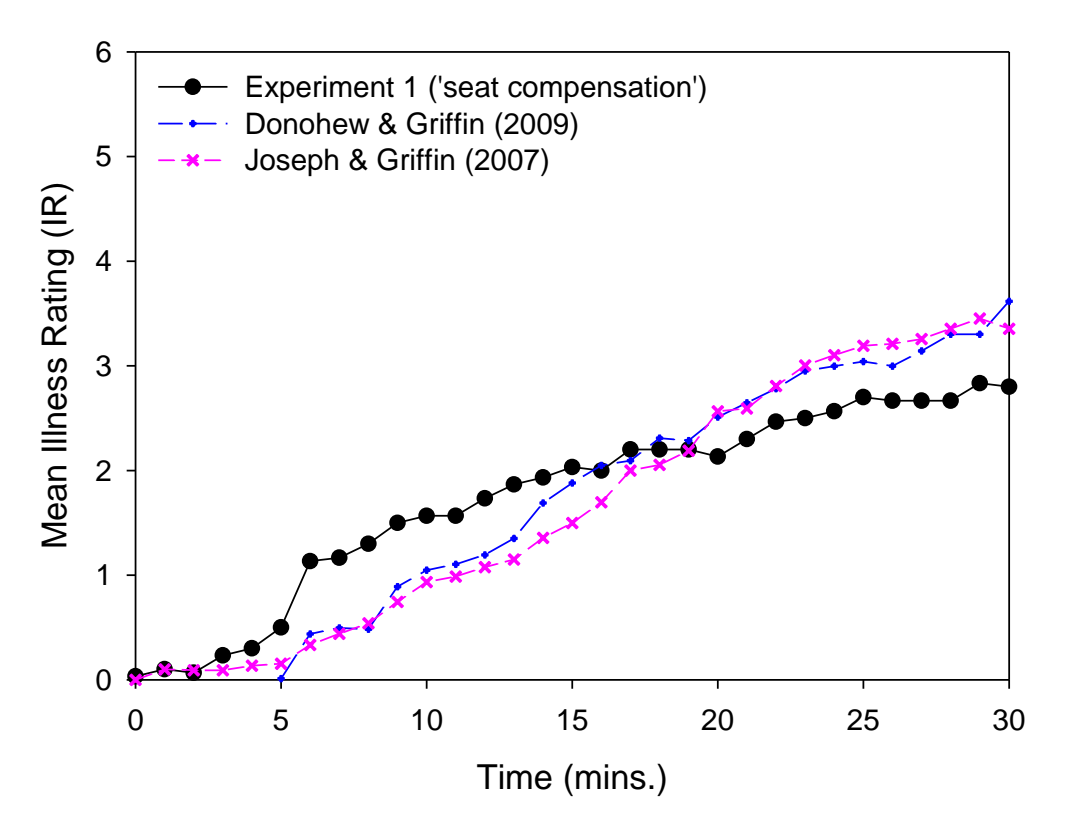


Figure 9.1 Comparison of mean illness ratings during 30-minute exposures to fully roll-compensated sinusoidal lateral oscillation at 0.2 Hz.

In Experiment 1, the development of motion sickness was also assessed with 0.2-Hz fully roll-compensated lateral oscillation where the position of full roll-compensation was at approximate head height; a condition equivalent to 88% roll-compensated lateral oscillation with the position of full roll-compensation at the seat surface. The effect of compensation on motion sickness caused by 0.2-Hz roll-compensated lateral oscillation where the position of full roll-compensation is at the seat surface may be assessed using this condition and those reported previously (see Figure 9.2). It appears there is a tendency for mean illness ratings to decrease with decreasing compensation, except for 88% (i.e. the 'head compensation' condition in Experiment 1) where mean illness ratings were highest. Nominal motion quantities at the seat and at the head (assuming the approximate head height is 800 mm above the seat surface) during fully roll-compensated lateral oscillation are shown in Table 9.1. If the sensory rearrangement theory is correct (see Section 2.4.3) zero lateral acceleration at the head will result in greater conflict between the interpretation of vestibular nerve impulses from the otoliths and the semi-circular canals. This may explain the greater mean illness ratings seen with the 'head compensation' condition in Figure 9.2, however no statistically significant differences were

found between this condition and the 'seat compensation' condition in Experiment 1 (Chapter 4). Comparison with previous research shows support for the hypothesis examined in Experiment 1, but further research is required to substantiate this theory.

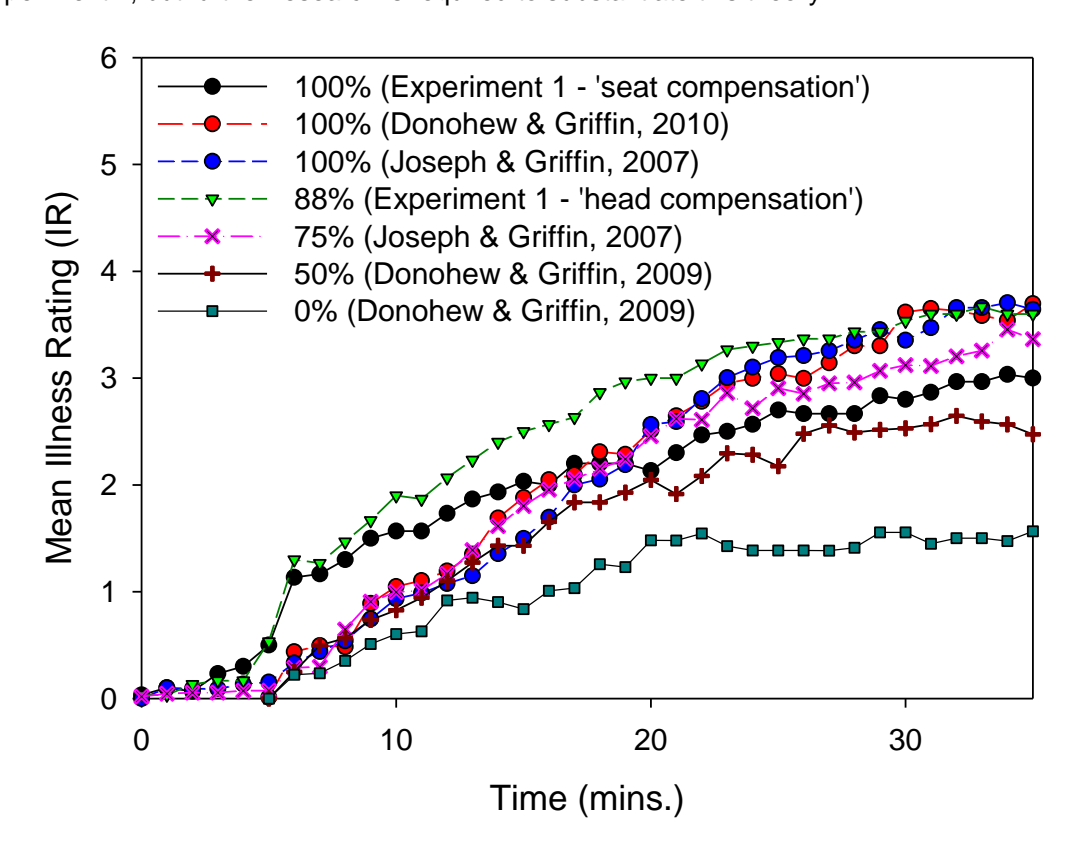


Figure 9.2 Effect of percentage compensation at the seat surface during 30-minute exposures to roll-compensated lateral oscillation at 0.2 Hz.

Previous research has shown that the likelihood of motion sickness caused by fully roll-compensated lateral oscillation increases with increasing frequency between about 0.05 and 0.2 Hz and then decreases at frequencies greater than this range (Donohew, 2006). The physical discomfort caused by fully roll-compensated lateral oscillation on a rigid seat with and without backrest (of varying heights) and on a foam seat without backrest has been established in Experiment 3 - 5 (Chapters 6 - 8). Figure 9.3 shows the mean equivalent comfort contours for all these conditions in comparison with previously reported mean illness ratings (Donohew, 2006). Equivalent comfort contours are approximately constant between 0.25 and 0.5 Hz and then decrease with increasing frequency above this range, suggesting greatest physical discomfort at 1 Hz. At around 0.25 Hz, there appears to be an 'optimum' for the least physical discomfort but a 'maximum' for motion sickness sensitivity.

Table 9.1 Nominal motion quantities at the seat surface and at the head* during roll-compensated lateral oscillations (* head assumed to be 800 mm above the seat surface).

Study	Earth-lateral acceleration (± ms ⁻²)	Roll displacement (±°)	Phase delay (°)	Acceleration at seat (± ms ⁻²)	Acceleration at head* (± ms ⁻²)	Compensation at seat (%)	Compensation at head* (%)
Experiment 1 'seat compensation'	1.26	7.3	0	0	0.15	100	112
Experiment 1 'head compensation'	1.41	7.3	0	0.17	0	88	100
Joseph &	1.26	7.3	0	0	0.15	100	112
Griffin (2007)	1.26	7.3	14.5	0.32	0.12	75	85
	1.26	7.3	0	0	0.15	100	112
Donohew & Griffin (2009)	1.26	3.7	0	0.63	0.08	50	56
Cililii (2000)	1.26	0	0	1.26	1.26	0	0

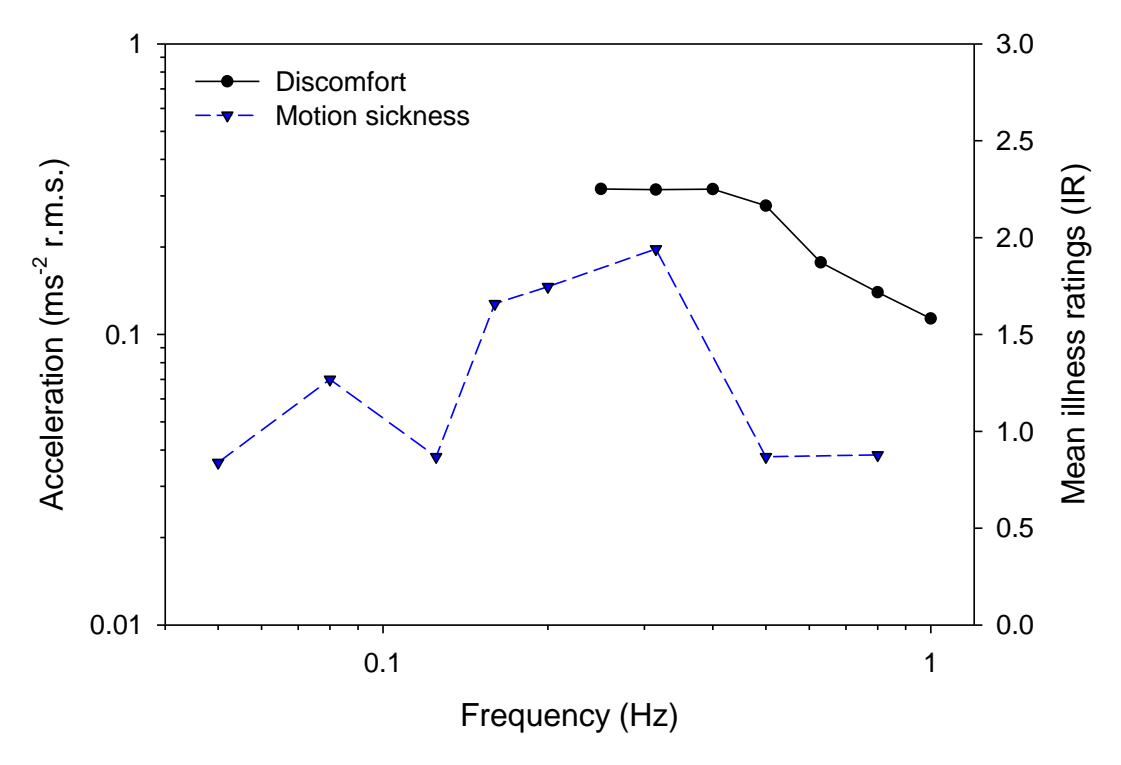


Figure 9.3 Components of Earth-lateral acceleration required to produce equivalent discomfort (solid line) and mean illness ratings (dotted line; Donohew, 2006) associated with fully roll-compensated lateral oscillation between 0.05 and 1 Hz. [Equivalent comfort contours calculated from the mean of all contours reported in Experiments 3, 4 and 5].

The frequency-dependence of motion sickness caused by uncompensated lateral oscillation is similar to that with fully roll-compensated lateral oscillation, but the severity of symptoms is greater with the latter motion (Donohew and Griffin, 2010). Conversely, the physical discomfort caused by 0.25-Hz uncompensated lateral oscillation is greater than that caused by 0.25-Hz fully roll-compensated lateral oscillation. This suggests that full roll-compensation of lateral oscillation at frequencies around 0.25 Hz increases the likelihood of motion sickness but decreases the physical discomfort (see Figure 9.4). At frequencies greater than 0.5 Hz, fully compensating lateral oscillation has little effect on motion sickness, but the physical discomfort is worsened.

Reducing the level of compensation may reduce the provocation of motion sickness (Donohew and Griffin, 2010; Figure 9.2), but further work is required to understand the effect of partially roll-compensated lateral oscillation on physical discomfort (see Section 9.6.2).

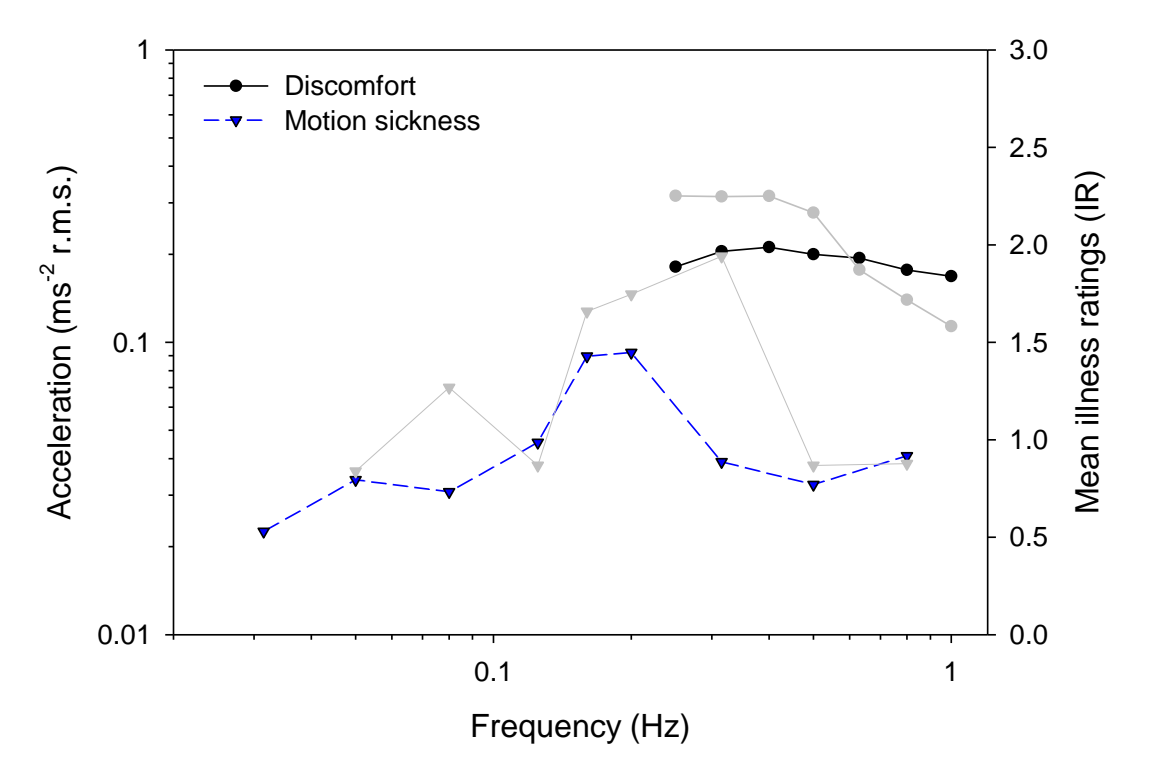


Figure 9.4 Effect of frequency of uncompensated lateral oscillation on motion sickness (Donohew and Griffin, 2004) and physical discomfort (Experiment 3, 4 and 5) (grey lines indicate fully roll-compensated motion).

9.2.1. Mechanisms of motion sickness and physical discomfort

The differences in the frequency-dependence of motion sickness and physical discomfort are grounded in differences in the mechanisms responsible for these sensations. The development of motion sickness is reliant on the vestibular system (Money, 1970). According to the sensory rearrangement theory (Reason and Brand, 1975), intra-sensory conflict within the vestibular system will occur with fully roll-compensated lateral oscillation, due to an unusual combination of stimulation of the otoliths and the semi-circular canals. A positive nerve impulse from the semi-circular canals triggered by the roll component of the motion is unaccompanied by the usual nerve impulse from the otoliths (because the gravitational component arising from the roll offsets the component arising from the lateral acceleration) (see Section 4.1). The 'maximal' sensitivity at frequencies around 0.2 Hz might be explained by a frequency-dependent phase discrepancy in the processing of motion stimuli by the two organs of balance (Golding *et al.*, 2001).

The posture and orientation of the body affect the stimulation of the otoliths and the semi-circular canals and thus the subsequent motion sickness; supine postures result in less sickness than seated upright postures (Golding and Kerguelen, 1992). The configuration of the seat may affect the level of motion sickness, with some evidence for greater sickness when seated with a low backrest than with a high backrest during fore-and-aft and lateral oscillation (Mills and Griffin, 2000). The height of a backrest affects the relative motion between the head and the seat (Brett and Griffin, 1991), so a high backrest may reduce the stimulation of the organs of balance resulting in less sickness.

Physical vibration discomfort is characterised as the extent to which individuals associate negative attributes to a given vibration stimulus. Discomfort of seated people may arise from a disturbance to sitting posture (requiring muscular effort to maintain an upright position) or from the transmission of vibration to localised areas of the body. At very low frequencies, vibration discomfort is likely to result from posture disturbance, whereas at higher frequencies discomfort may be more localised. Both sources of discomfort are affected by the configuration of the seat. A soft seat pan will reduce the pressure at the seat-body interface (i.e. the ischial tuberosities) increasing static comfort (Sprigle, Chung and Brubaker, 1990; Moxley *et al.*, 2011), but will reduce the stability of the seat during low frequency motion, decreasing dynamic comfort (Experiment 4 - Chapter 7). As the height of the backrest increases, the lateral support for the torso increases thereby reducing the muscular effort required to maintain an upright posture but increasing the transmission of motion to the upper body. The support of a backrest reduces discomfort at very low frequencies, but increases discomfort at higher frequencies (Experiment

5 - Chapter 8). The severity of discomfort is therefore dependent on the frequency of the motion, and the sensitivity of different parts of the body.

An understanding of the mechanisms responsible for human responses to motion facilitates the development of models of motion sickness and physical discomfort.

9.2.2. Model of motion sickness

Figure 9.5 presents a simplified model of the vestibular system and the central nervous system which attempts to explain the generation of motion sickness from lateral and roll acceleration presented in isolation or in combination. Part one of the model has been constructed on the basis of experimental findings reported in Chapter 4. Part two of the model is based on hypotheses formulated from previous literature, and has not been empirically tested.

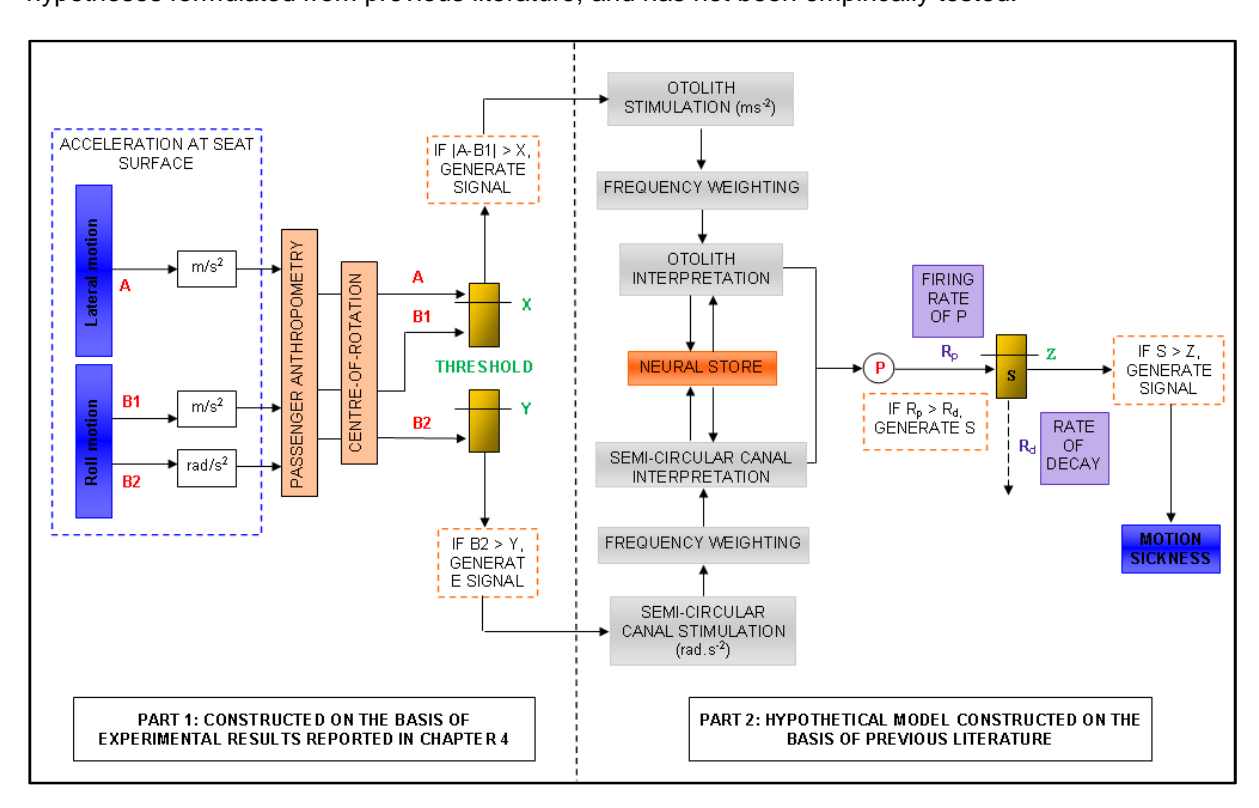


Figure 9.5 Conceptual model of motion sickness caused by combined lateral and roll oscillation.

There are three inputs to the model, defined as: lateral acceleration due to inertial lateral forces (A), lateral acceleration due to the gravitational forces associated with roll (B1) and roll acceleration due to inertial roll forces (B2). The stimulation of the organs of balance in the inner ear is mediated by: a) the frequency, magnitude and phase characteristics of the motion, and; b) passenger anthropometry and the position and orientation of the passenger relative to the

position of full roll-compensation (denoted the 'centre-of-rotation' in Figure 9.5). For example, stimulation of the otoliths will vary between a seated upright posture and a supine posture. Similarly, the translational stimulation of the otoliths will increase as the distance from the position of full roll-compensation increases (see Section 2.2.3). If the vector sum of A and B1 is greater than the otolithic threshold (X) then a change in the otolithic nerve impulse is registered by the central nervous system. Likewise, if B2 is greater than the semi-circular canal threshold (Y) then a change in the semi-circular canal nerve impulse is triggered.

The provocation of motion sickness which results from these nerve impulses is dependent on the frequency content of the motion (denoted as a frequency weighting in the model) and on previous 'knowledge' and experiences relevant to motion perception (denoted as the neural store in the model). Combination of the otolith signal and the semi-circular canal signal generates a provocation signal (P). In line with the sensory rearrangement theory (Reason and Brand, 1975), if the provocation signal (P) represents a conflicting interpretation of the motion, then a sickness response (S) is generated. If the neuronal firing rate of P is greater than the decay rate of S, then the sickness response (S) will increase with time (i.e. with continued exposure to the provocative motion). If S breaches the sickness perceptual threshold (Z), then motion sickness symptoms are generated.

9.2.3. Model of discomfort

The work reported in this thesis has shown that discomfort from fully roll-compensated lateral oscillation is highly dependent on the frequency of oscillation (see Figure 9.6).

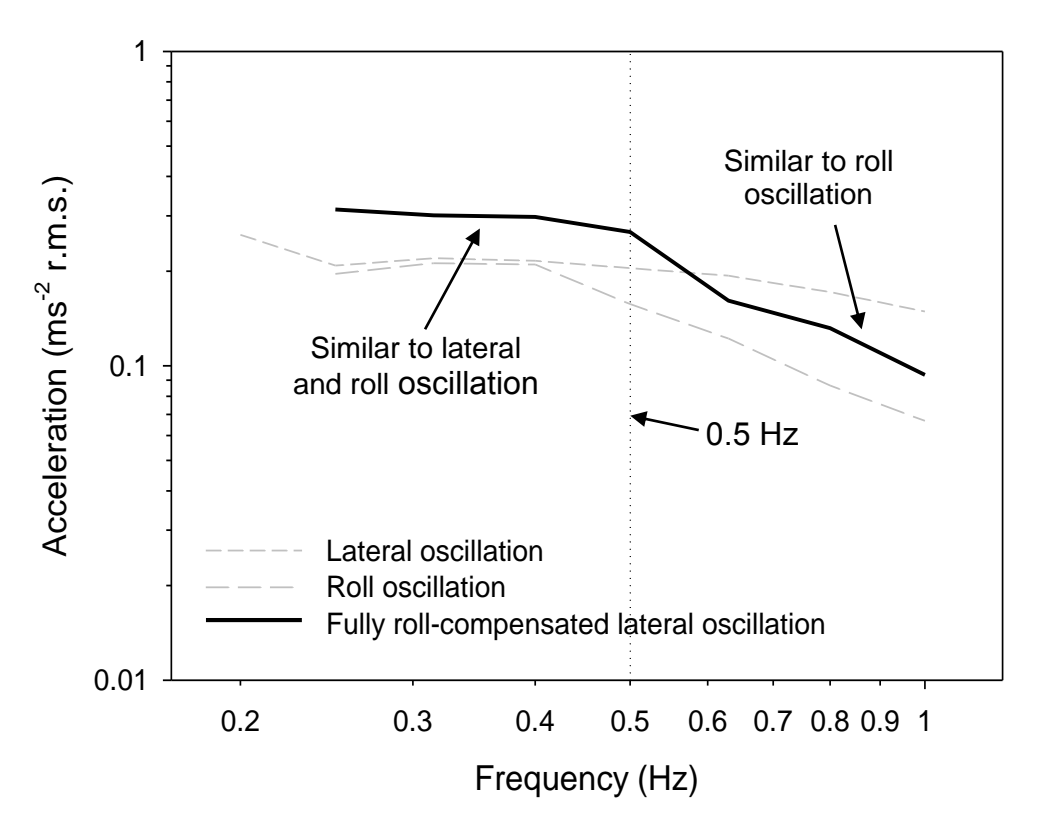


Figure 9.6 Equivalent comfort contours for lateral oscillation, roll oscillation (expressed as lateral acceleration in the plane of the seat, ms⁻² r.m.s.) and fully roll-compensated lateral oscillation (expressed as the Earth-lateral acceleration component, ms⁻² r.m.s.). Contours constructed from the mean of all equivalent comfort contours defined in Experiments 2 to 5.

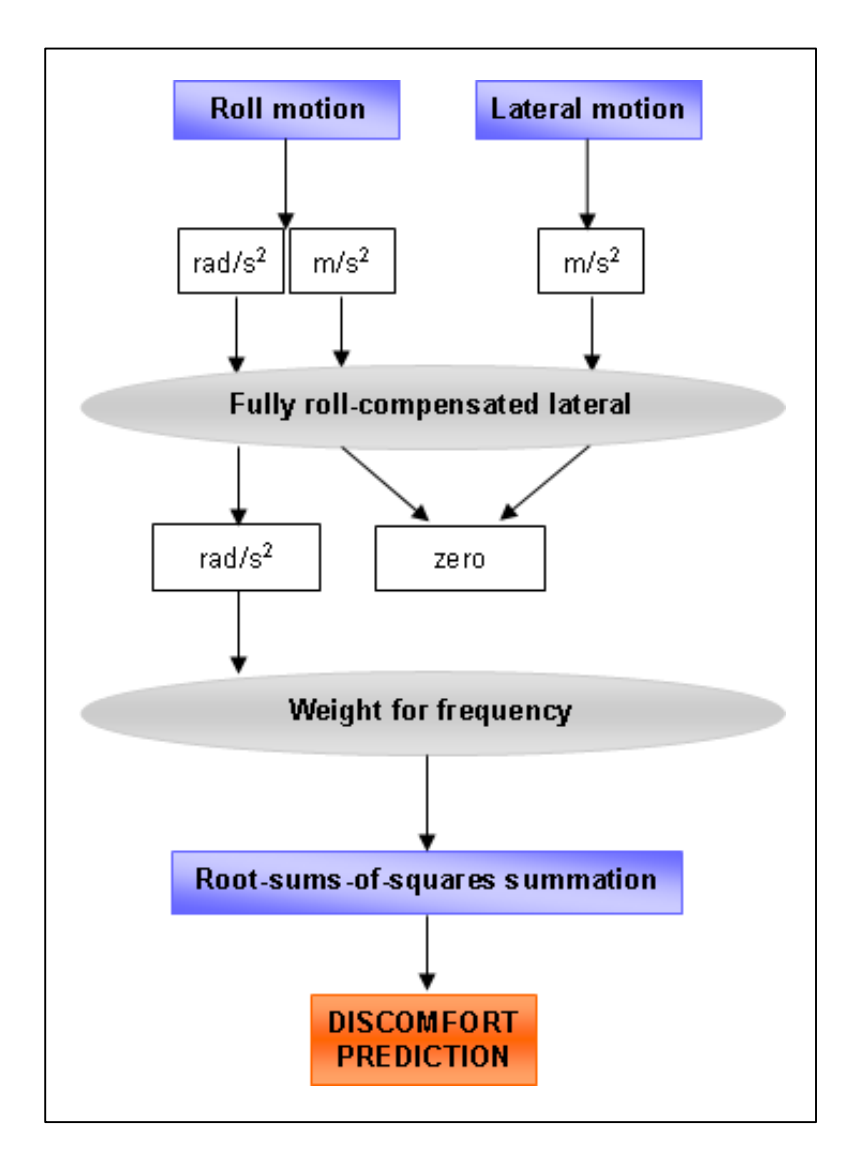


Figure 9.7 Model for predicting vibration discomfort with fully roll-compensated lateral oscillation.

At very low frequencies (below 0.5 Hz), the frequency-dependence of discomfort from roll-compensated lateral oscillation (expressed in terms of the Earth-lateral acceleration component, ms⁻² r.m.s.) is similar to that for both pure lateral oscillation and pure roll oscillation. At higher frequencies (above 0.5 Hz), the frequency-dependence of discomfort from roll-compensated lateral oscillation is similar to that for pure roll oscillation. Since the components of lateral acceleration in the plane of the seat associated with fully roll-compensated lateral oscillation are negligible (because the gravitational acceleration due to the roll offsets the inertial acceleration – see Section 2.2.4), it is logical that discomfort is dominated by components of roll acceleration. A model of the discomfort caused by fully roll-compensated lateral oscillation might therefore predict discomfort from the frequency-weighted roll acceleration measured at the seat

surface (see Figure 9.7). The basis for the model lies in the procedure for predicting discomfort documented in current vibration standards (BS 6841, 1987; ISO 2631-1, 1997; see Figure 2.32).

In Experiments 2, 4 and 5 (Chapters 5, 7 and 8), the discomfort of seated people was found to be highly dependent on the configuration of the seating and the subsequent sitting posture. When predicting discomfort from measured acceleration, the weightings must therefore account for these sensitivities. Current vibration standards offer weightings and axis multiplying factors for this purpose, but the work presented in Experiments 3 - 5 (Chapters 6 - 8) has established limitations of the standards over the frequency range 0.2 to 1.0 Hz. In light of these findings, recommendations for the standards are discussed in Section 9.3 in order to improve the accuracy of the current model of discomfort caused by low frequency motion.

9.3. Recommendations for vibration standards

9.3.1. Motion sickness dose value

The motion sickness dose value (MSDV) is used to predict the cumulative effect of motion frequency, magnitude and duration on the incidence of motion sickness, but current vibration standards (BS 6841, 1987; ISO 2631-1, 1997) only define a frequency weighting for predicting motion sickness with vertical oscillation (i.e. W_f). A frequency weighting for lateral oscillation is provided by Donohew and Griffin (2004); the weighting is similar to W_f but predicts greater sickness with lateral oscillation than vertical oscillation at frequencies less than about 0.1 Hz (see Section 2.5.1). Substantial roll-compensation of lateral acceleration (i.e. > 50% compensation) is known to increase motion sickness relative to uncompensated lateral acceleration (Donohew and Griffin, 2010), but there is currently no method for predicting motion sickness with roll-compensated motions.

Donohew and Griffin (2009) state that "motion sickness caused by combined lateral and roll oscillation cannot be predicted from a single independent variable" (p. 101), i.e. subject-lateral acceleration, Earth-lateral acceleration, or roll displacement. With fully roll-compensated lateral oscillation, the subject-lateral acceleration is effectively zero; meaning there is no quantity to be measured and weighted. Earth-lateral acceleration may not be representative of the passenger exposure to motion, and roll displacement, if presented alone, is not highly provocative of sickness (Howarth and Griffin, 2003). The current work presented in this thesis confirms the difficulties associated with quantitatively predicting roll-compensated motion sickness from measured acceleration quantities.

As discussed in Section 2.4.2.3, the *MSDV* may also be used to estimate the proportion of a population likely to vomit, such that:

Equation 9.1:
$$VI(\%) = MSDV \times K_m$$

where VI is the vomiting incidence (the percentage of people likely to vomit), and K_m is a constant dependent on the characteristics of the exposed population. International standard ISO 2631-1 (1997) states that K_m may be equal to 1/3 for a mixed population of unadapted male and female adults. Experiment 1 showed that a sample of Chinese, Indian or other Asian subjects was over 3 times as likely to experience mild nausea during fully roll-compensated lateral oscillation at 0.2 Hz than a sample of White British or other European subjects (see Chapter 4). If the 'European' subjects classified in Experiment 1 can be assumed to be similar to a 'mixed population of unadapted adults' (as defined in the standard), then this implies K_m should be approximately equal to 1 for the 'Asian' subjects. Further research with larger subject samples is required to validate the use of specific constants for the prediction of vomiting incidence (VI), but researchers should be aware of a 'hyper-susceptibility' to motion sickness in the Asian population (or conversely, a reduced susceptibility in the European population). It is recommended that such guidance is provided in appropriate vibration standards.

9.3.2. Discomfort from lateral acceleration

As discussed in Section 2.2, lateral acceleration in the plane of a seat may result from inertial horizontal forces or from the gravitational forces associated with rotation. The discomfort caused by both types of lateral acceleration has been investigated in Experiment 2 - 5 (Chapters 5 - 8).

Figure 9.8 shows ten equivalent comfort contours for lateral acceleration due to lateral displacement (i.e. inertial acceleration) on ten seating conditions studied in the Experiments 2 to 5. Likewise, Figure 9.9 shows six equivalent comfort contours for lateral acceleration due to roll displacement (i.e. gravitational acceleration) on six seating conditions. It is clear that sensitivity to lateral acceleration increases with increasing frequency between 0.2 and 1.0 Hz (with the exception of lateral acceleration on a foam seat without backrest), regardless of whether it is due to lateral displacement or rotation through the gravitational vector.

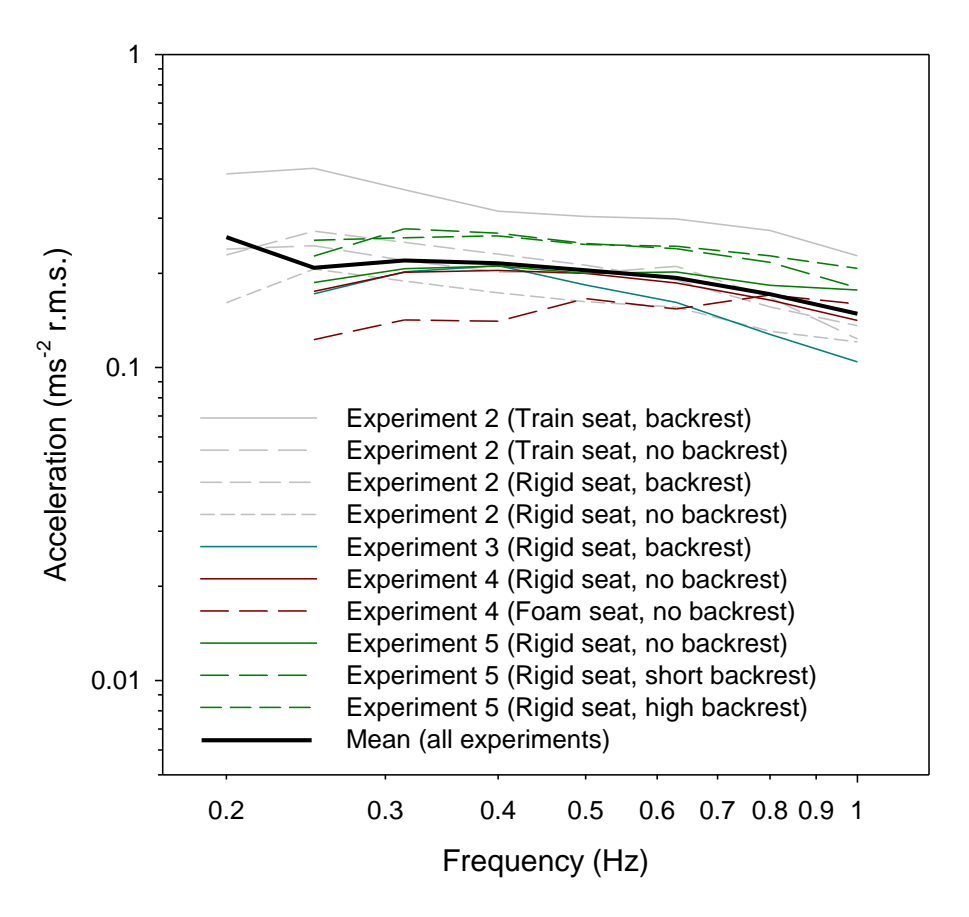


Figure 9.8 Equivalent comfort contours for inertial lateral acceleration (i.e. due to lateral displacement) from Experiments 2, 3, 4 and 5. [Mean equivalent comfort contour calculated across the ten conditions shown in bold].

All four discomfort experiments employed transient motion waveforms, but in Experiment 2 (Chapter 5) the motions were approximately constant duration (i.e. around 12 seconds) whereas in Experiment 3-5 (Chapter 6 to Chapter 8) the motions were 3.5 cycles and thus the duration varied with frequency. It might be expected that the longer duration stimuli used in Experiment 2 would lead to greater discomfort than the shorter exposures used in Experiment 3-5 (Griffin, 1990). Whilst the precise severity of the discomfort reported in each of the experiments cannot be compared, it can be seen from Figure 9.8 that the frequency dependence of lateral vibration discomfort determined in Experiment 2 is similar to that determined in Experiment 3-5.

Regardless of seating condition, the experiments reported in this thesis found that discomfort caused by inertial lateral acceleration (i.e. due to lateral displacement) and gravitational acceleration (i.e. due to roll displacement) is similar at frequencies less than about 0.5 Hz. At greater frequencies, the discomfort caused by the roll is worse than that caused by inertial

lateral acceleration. This finding has also been reported by Wyllie and Griffin (2007). Frequency weighting W_d appears to offer a close approximation to discomfort caused by inertial lateral acceleration at frequencies greater than about 0.4 Hz (and less than 1 Hz), but may not be representative of the frequency-dependence of discomfort caused by gravitational lateral acceleration in this range. Weighted values obtained using the realisable W_d weighting may be used to predict discomfort from both types of lateral acceleration at lower frequencies, however an extension of the high-pass filter defined in current standards to 0.2 Hz may improve the accuracy of this prediction (see Figure 9.11). The corresponding realisable weighting curve and the filter characteristics of such an adjustment to W_d are shown in Figure 9.11 and Table 9.2, respectively.

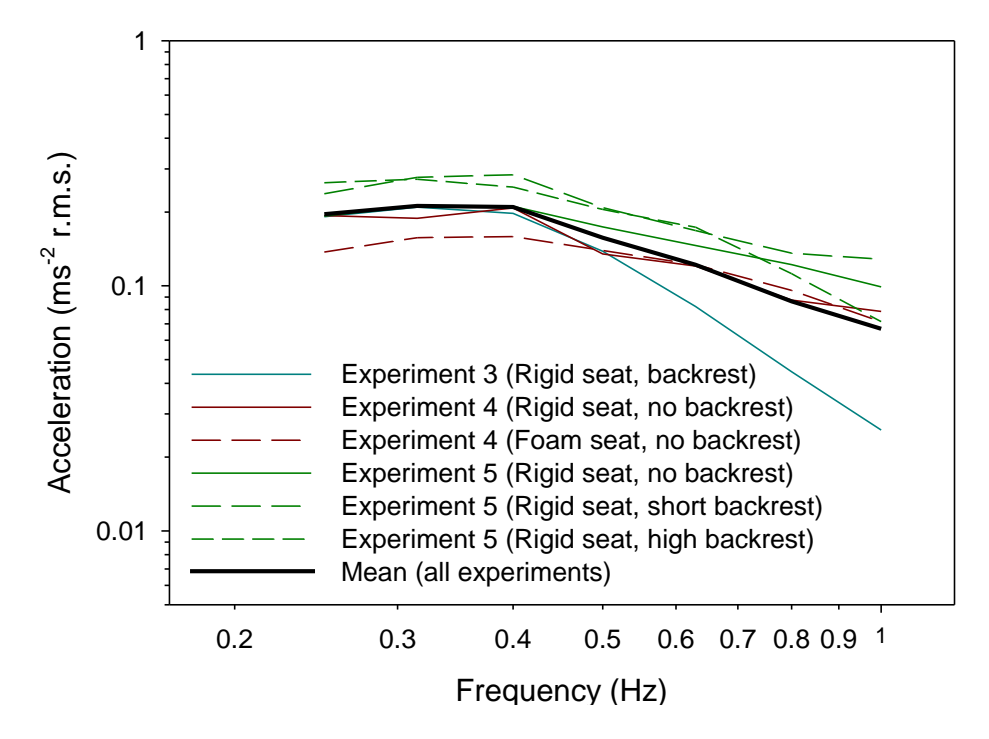


Figure 9.9 Equivalent comfort contours for gravitational lateral acceleration (i.e. due to roll displacement) from Experiment 3, 4 and 5. [Mean equivalent comfort contour calculated across the six conditions shown in bold].

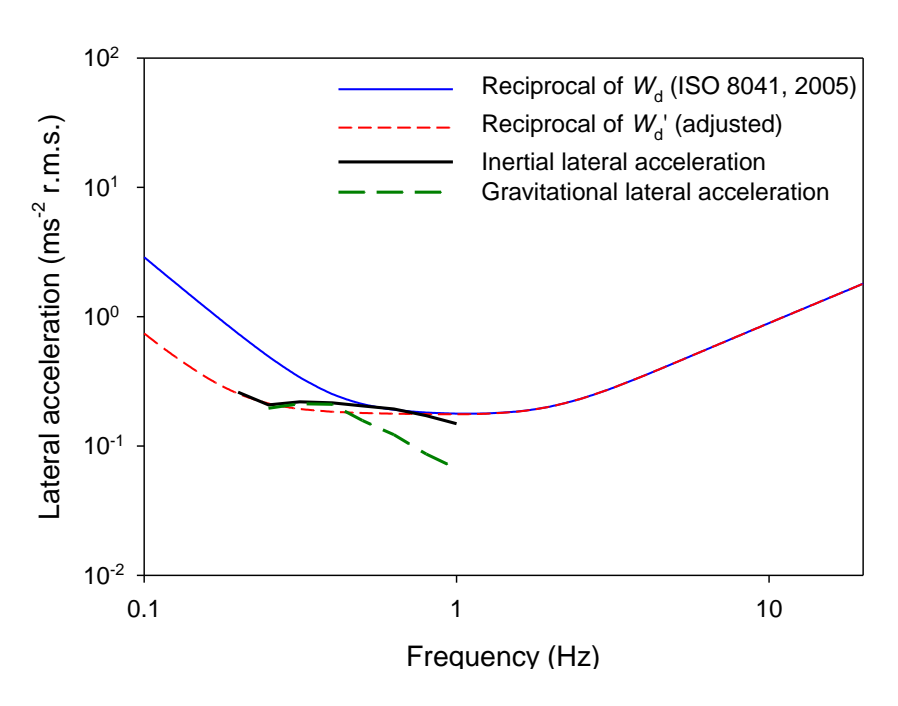


Figure 9.10 Mean equivalent comfort contours for inertial lateral acceleration (i.e. due to lateral displacement) and gravitational lateral acceleration (i.e. due to roll displacement) calculated across all conditions in Experiment 2, 3, 4 and 5, and normalised W_d (BS 6841, 1987) and W_d (adjusted) weightings.

Table 9.2 Parameters of the transfer functions for W_d (current weighting) and W_d (adjusted weighting) for lateral acceleration.³

Weighting		Band-limiting		Acceleration-velocity transition			Upward step			
	0 0	<i>f</i> ₁	f_2	<i>f</i> ₃	<i>f</i> ₄	Q_4	f ₅	Q_5	<i>f</i> ₆	Q_6
₩ _d	Current	0.4	100	2	2	0.63	∞	-	∞	-
<i>W</i> _d '	Adjusted	0.2	100	2	2	0.63	8	-	8	-

³ "The frequencies f_1 to f_6 and the resonant quality factors Q_4 to Q_6 are parameters of the transfer function which determine the overall frequency weighting (referred to acceleration as

the input quantity)". The 'acceleration-velocity transition' denotes "proportionality to acceleration at lower frequencies and proportionality to velocity at higher frequencies". The 'upward step' corresponds to a curve with steepness of approximately 6 dB per octave - proportional to jerk (ISO 2631-1, 1997, p. 18).

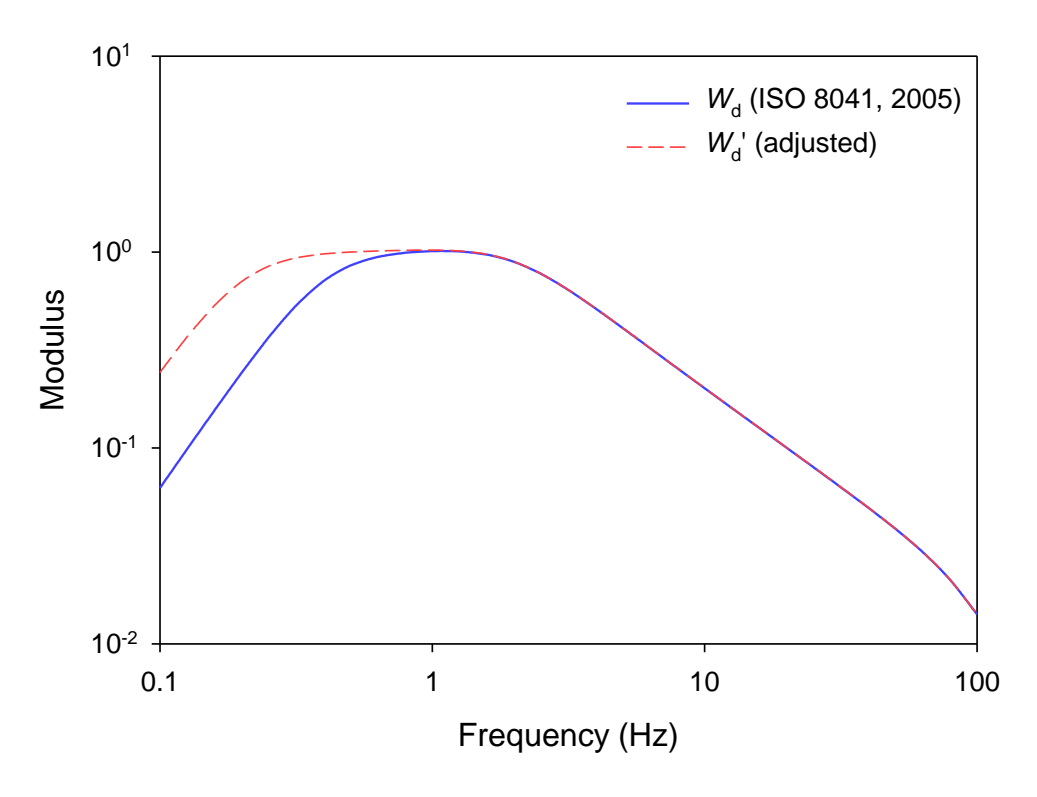


Figure 9.11 Standardised weighting W_d (ISO 8041, 2005) and adjusted weighting W_d ' for predicting discomfort from lateral acceleration. Weightings achieved with band-limiting filter defined in Table 9.2.

9.3.3. Discomfort from roll acceleration

Equivalent comfort contours for lateral acceleration caused by roll through the gravitational vector may also be defined in terms of roll acceleration. Figure 9.12 shows all six equivalent comfort contours for the six conditions of roll oscillation tested in Experiments 3, 4 and 5, expressed as rotational acceleration (rads⁻² r.m.s.), along with the mean contour for all experiments. It is clear that sensitivity to rotational acceleration tends to decrease with increasing frequency of oscillation between 0.2 and 1.0 Hz. Frequency weighting W_e (BS 6841, 1987) does not appear to offer a good approximation to the frequency-dependence of discomfort from roll acceleration at frequencies in the range 0.2 to 1.0 Hz (see Figure 9.13).

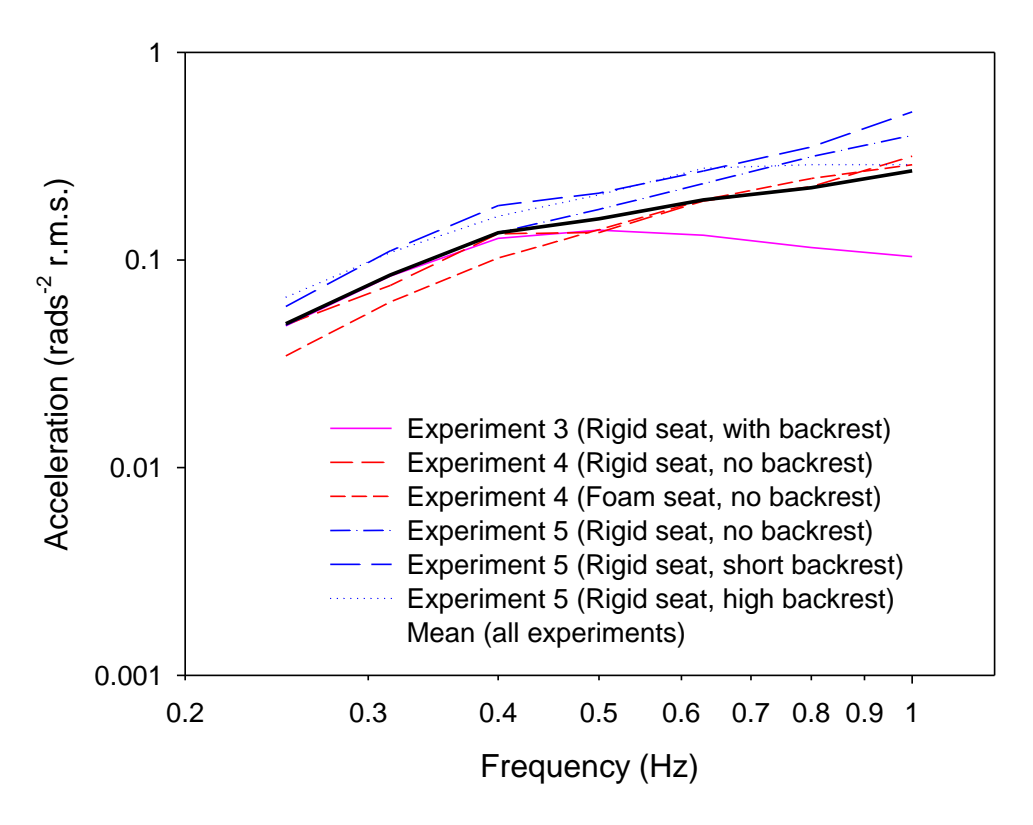


Figure 9.12 Equivalent comfort contours for roll acceleration from Experiment 3, 4 and 5. [Mean equivalent comfort contour calculated across the six conditions shown in bold].

With constant roll acceleration at all frequencies, the magnitude of rotational displacement decreases with increasing frequency of oscillation. A rotational displacement of sufficient magnitude is likely to cause disturbance to sitting posture, and in extreme cases could even be dangerous (i.e. causing a person to fall of their seat). Equivalent comfort contours between 0.2 and 1.0 Hz roughly approximate to constant rotational displacement when subjects are seated on a seat without backrest or with a short backrest, but when seated with a full height backrest (i.e. that tested in Experiment 3 and Experiment 5) there is some evidence that contours approximate to constant acceleration at frequencies greater than about 0.5 Hz (Figure 9.12). This may be due to a full-height backrest increasing discomfort with roll oscillation at the highest frequencies; predictions of the effect of seating are discussed in Section 9.3.5.

At frequencies less than about 0.5 Hz, lateral acceleration due to roll through the gravitational vector may be used to predict discomfort from roll oscillation, i.e. using frequency weighting W_d (see Section 9.3.2). This is not the case at higher frequencies, therefore adjustment of frequency weighting W_e is most important in the range 0.5 to 1.0 Hz. An extension of the high-pass filter and adjustment to the acceleration-velocity transition defined in current standards

may improve the discomfort prediction in this range (see Figure 9.13). The corresponding realisable weighting curve and the filter characteristics of such an adjustment to W_e are shown in Figure 9.14 and Table 9.3, respectively.

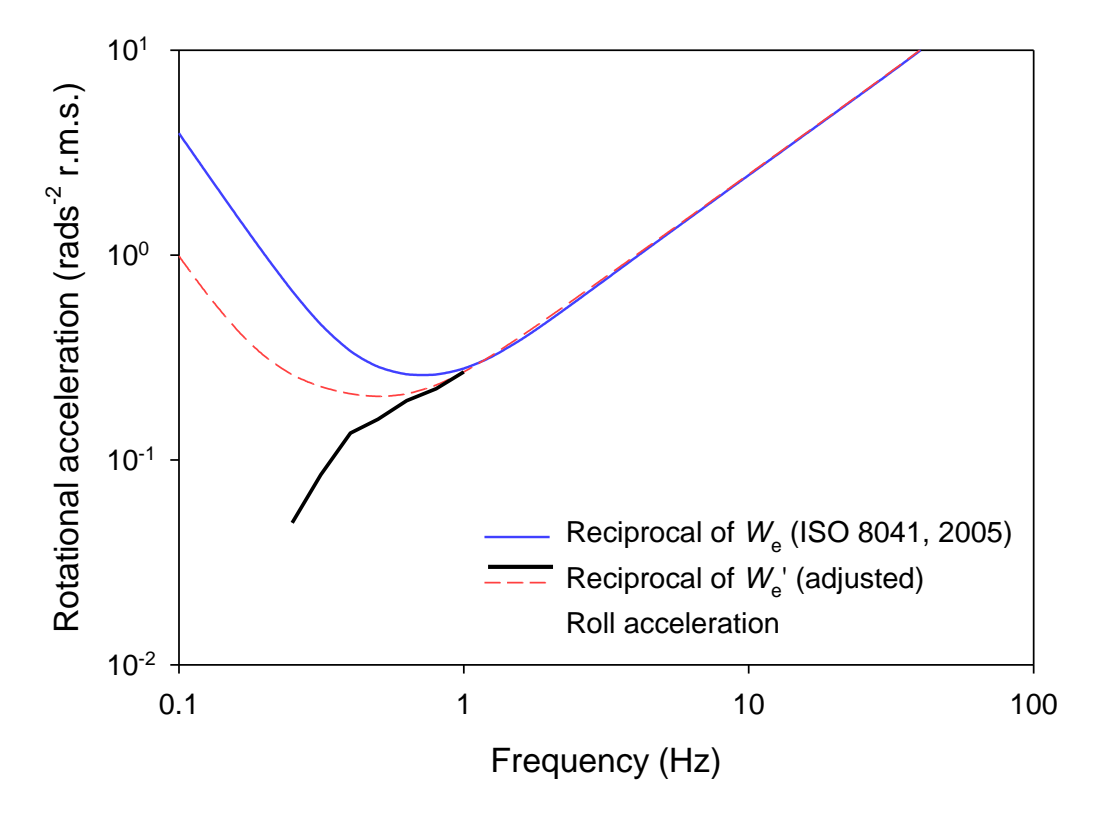


Figure 9.13 Mean equivalent comfort contours for roll acceleration calculated across all conditions in Experiment 3, 4 and 5, and normalised W_e (BS 6841, 1987) and W_e (adjusted) weightings.

Table 9.3 Parameters of the transfer functions for W_e (current weighting) and W_e (adjusted weighting) for roll acceleration.

Weighting		Band-I	imiting	Acceleration-velocity transition			Upward step			
		<i>f</i> ₁	f ₂	f ₃	f ₄	Q ₄	f 5	Q_5	f 6	Q_6
W e	Current	0.4	100	1.0	1.0	0.63	8	-	8	
We'	Adjusted	0.2	100	0.5	0.5	0.63	8	-	8	-

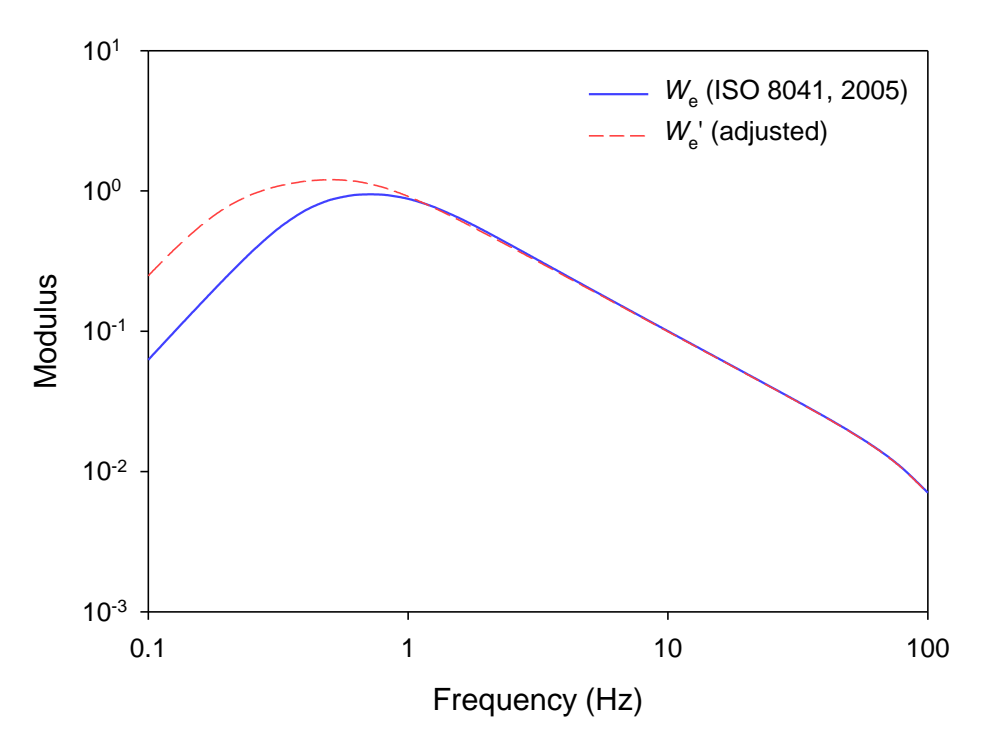


Figure 9.14 Standardised weighting W_e (ISO 8041, 2005) and adjusted weighting W_e for predicting discomfort from roll acceleration. Weightings achieved with band-limiting filter defined in Table 9.3.

9.3.4. Discomfort from roll-compensated lateral acceleration

The six equivalent comfort contours for fully roll-compensated lateral acceleration tested in the six conditions of Experiment 3, 4 and 5 are shown in Figure 9.15. Regardless of seating conditions, the sensitivity to fully roll-compensated lateral acceleration exhibits a similar frequency-dependence as pure roll oscillation in the range 0.25 to 1.0 Hz. (see Section 9.2.3). Between 0.5 and 1.0 Hz, the frequency-dependence of discomfort with fully roll-compensated lateral acceleration may be approximated using components of W_e '-weighted roll acceleration (see Figure 9.16). The reduced severity of discomfort with fully roll-compensated lateral acceleration compared to pure roll acceleration is represented by the negligible components of lateral acceleration included in the root-sums-of-squares prediction model with roll-compensated motions (see Section 9.4.3).

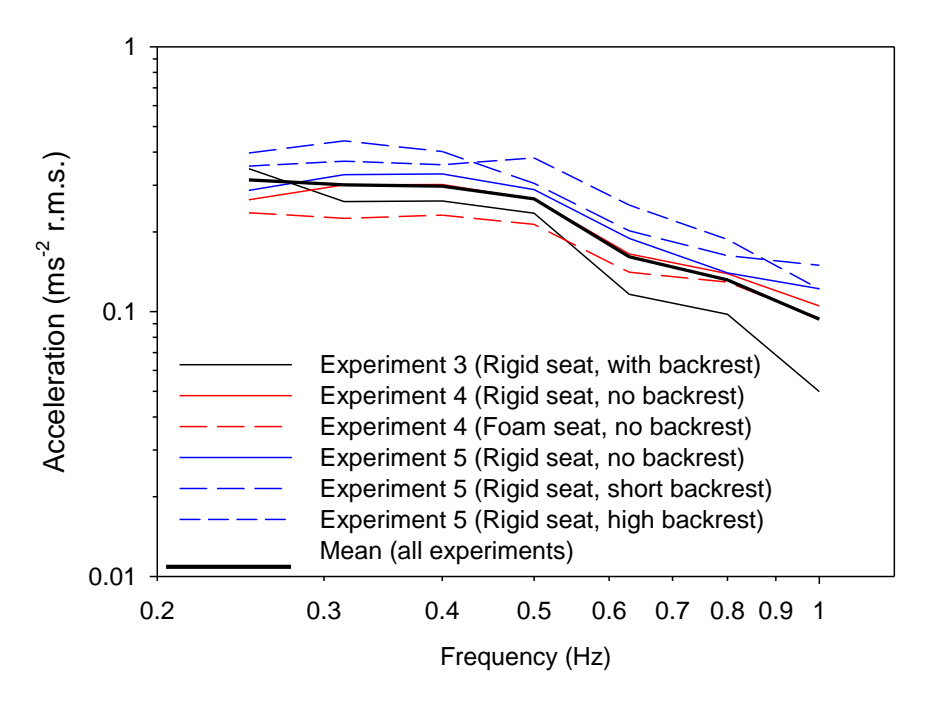


Figure 9.15 Equivalent comfort contours for fully roll-compensated lateral acceleration from Experiment 3, 4 and 5, expressed in terms of the component of Earth-lateral acceleration. [Mean equivalent comfort contour calculated across the six conditions shown in bold].

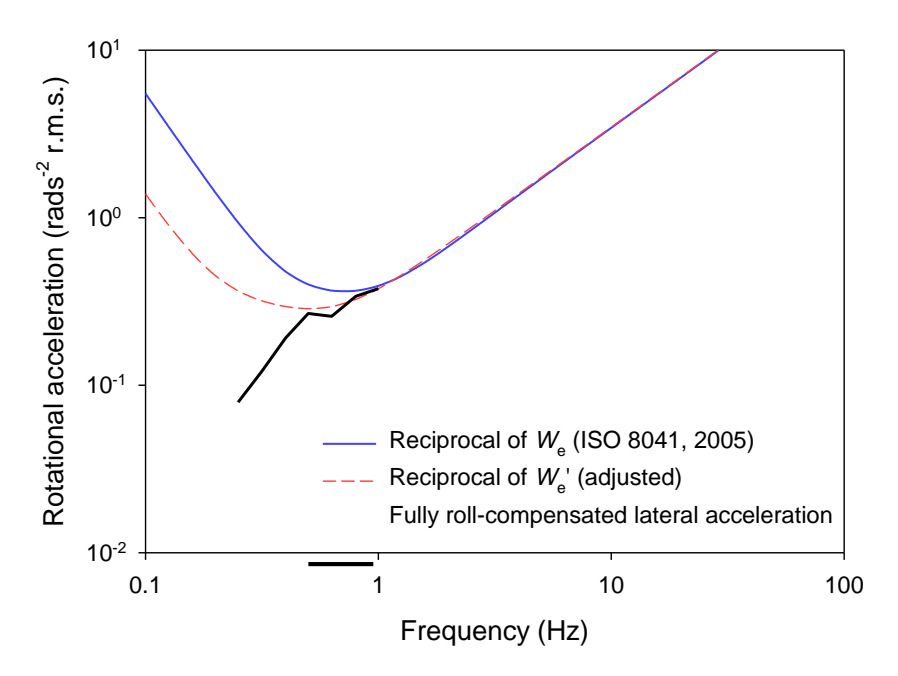


Figure 9.16 Mean equivalent comfort contours for fully roll-compensated lateral acceleration calculated across all conditions in Experiment 3, 4 and 5, and normalised W_e (BS 6841, 1987) and W_e (adjusted) weightings.

9.3.5. Passenger seating

The four discomfort experiments reported in Chapters 5 to 8 tested a total of ten seating conditions with various combinations of lateral, roll and fully roll-compensated lateral oscillation (see Table 9.4).

Vibration discomfort has been found to be highly dependent on the configuration of the seat. Soft foam seat pans may reduce the discomfort associated with the distribution of pressure at the seat-body interface (i.e. the ischial tuberosities), but may lower stability of the seat and increase the transmission of very low frequency oscillation to the body (Chapter 7). Current standards dictate that vibration is measured at the seat-body interfaces (i.e. between the floor and the feet, between the seat and the buttocks, and between the backrest and the back). Soft seats (e.g. with a stiffness of approximately 7.73 N/mm) are likely to worsen the vibration discomfort (due to poor postural stability) with lateral oscillations and roll oscillations at frequencies less than 1 Hz. The effects of seat pan stiffness on discomfort caused by these motions should be approximated by the standardised prediction methods.

ı	Motion direc	tion	
		Forther well	

Table 9.4 List of seating conditions tested in Chapters 5 to 8.

	Motion direction				
Experiment no.	Lateral	Roll Fully roll- compensated lateral Seat pan type		Backrest height (mm)	
2	✓	×	×	Rigid	0
4	✓	✓	✓	Rigid	0
5	✓	✓	✓	Rigid	0
2	✓	×	×	Foam A*	0
4	✓	✓	✓	Foam B*	0
5	✓	✓	✓	Rigid	295
3	✓	✓	✓	Rigid	550
2	✓	×	×	Rigid	570
5	✓	✓	✓	Rigid	650
2	✓	×	×	Foam B*	740

^{*} Foam A corresponds to cushioned train seat used in Experiment 2 (see Chapter 5), Foam B corresponds to foam block used in Experiment 4 (see Chapter 7)

The postural support offered to the upper body is determined by the characteristics of the backrest. A full-height backrest (i.e. > 550 mm) offers greater postural support than a shorter backrest or no backrest. Discomfort from inertial lateral acceleration (i.e. due to horizontal displacement) between 0.25 and 1.0 Hz is lower when seated with a full-height backrest than

with no backrest, with the benefits most notable at the lowest frequencies (Chapter 5 and 8). At frequencies less than about 0.63 Hz, discomfort from gravitational lateral acceleration (i.e. due to roll displacement) is lower when seated with a full-height backrest, but at higher frequencies comfort is worsened by a full-height backrest due to the increased horizontal displacement of the upper body and head (Chapter 8).

National and International vibration standards suggest frequency weighting W_d is used for both lateral acceleration at the seat surface and lateral acceleration at the back, but at the back the weighting is coupled with a multiplying factor of 0.5 (BS 6841, 1987; ISO 2631-1, 1997). Using the root-sums-of-squares summation method, it is therefore implied that the backrest has an additive effect on discomfort, with lateral acceleration at the back causing half as much discomfort as that caused by lateral acceleration at the seat surface (BS 6841, 1987; ISO 2631-1, 1997). The findings reported in this thesis suggest that this method is incorrect at very low frequencies. The standards advise that measured acceleration spectra are frequency-weighted with a single filter (e.g. W_d) and scaled with appropriate multiplying factors (i.e. 0.5 for a backrest). According to the findings of this thesis, ideally a positive multiplying factor for lateral vibration would be used for lateral acceleration at the backrest at frequencies greater than 1 Hz, but a negative multiplying factor would be used at frequencies less than 1 Hz. However this is inappropriate practically, since it would require measured acceleration spectra to be split into separate frequencies prior to frequency-weighting. Instead, it is recommended that guidance is issued to advise that a backrest is likely to reduce the discomfort caused by inertial lateral acceleration at frequencies less than 1.0 Hz, and that caused by gravitational lateral acceleration at frequencies less than about 0.63 Hz.

9.4. Assessment of adjusted weightings

Discomfort from lateral oscillation of a seat may result from three component ride values: lateral acceleration at the seat surface, the backrest and the foot support. In Chapters 6 to 8, it was shown that seven component ride values arising from roll oscillation of a seat may contribute to vibration discomfort: lateral acceleration at the seat surface, the backrest, and the foot support (due to these not being at the centre of roll), translational acceleration at the seat, the back, and the feet (arising from the gravitational component due to roll, $g.\sin\theta$), and rotational acceleration at the seat surface (Wyllie and Griffin, 2007).

Table 9.5 Frequency weightings at one-third octave centre frequencies. [Standardised weightings W_d and W_e (ISO 8041, 2005) and adjusted weightings W_d and W_e (Section 9.3)].

Frequency (Hz)	₩ _d	W ₀'	W e	W e'
0.1	0.0624	0.2427	0.0625	0.2483
0.125	0.0973	0.3642	0.0975	0.3771
0.16	0.1582	0.5399	0.1589	0.5699
0.2	0.2431	0.7088	0.2446	0.7670
0.25	0.3652	0.8453	0.3684	0.9442
0.315	0.5300	0.9326	0.5363	1.0811
0.4	0.7132	0.9785	0.7233	1.1713
0.5	0.8528	0.9998	0.8624	1.2039
0.63	0.9439	1.0125	0.9387	1.1694
0.8	0.9923	1.0209	0.9413	1.0594
1	1.0110	1.0231	0.8798	0.9144
1.25	1.0076	1.0125	0.7722	0.7617
1.6	0.9684	0.9701	0.6318	0.6082
2	0.8902	0.8909	0.5115	0.4911
2.5	0.7759	0.7762	0.4090	0.3947
3.15	0.6420	0.6421	0.3231	0.3140
4	0.5119	0.5119	0.2531	0.2476
5	0.4091	0.4091	0.2017	0.1982
6.3	0.3231	0.3231	0.1596	0.1574
8	0.2531	0.2531	0.1254	0.1240
10	0.2017	0.2017	0.1002	0.0992
12.5	0.1609	0.1609	0.0801	0.0794
16	0.1254	0.1254	0.0625	0.0620
20	0.1002	0.1002	0.0500	0.0496
25	0.0800	0.0800	0.0399	0.0396
31.5	0.0632	0.0632	0.0316	0.0313
40	0.0494	0.0494	0.0247	0.0245
50	0.0388	0.0388	0.0194	0.0193
63	0.0295	0.0295	0.0148	0.0146
80	0.0211	0.0211	0.0105	0.0104
100	0.0141	0.0141	0.0071	0.0070

Overall ride values may be calculated from these components using the root-sums-of-squares summation method and appropriate frequency weightings (BS 6841 1987, ISO 2631-1 1997; see Appendix A.10. for a list of equations relating to this method). Table 9.5 shows the moduli for standardised weightings W_d and W_e and adjusted weightings W_d and W_e at one-third octave

centre frequencies between 0.1 and 100 Hz. In this section, overall ride values are calculated from component ride values of lateral oscillation, roll oscillation and fully roll-compensated lateral oscillation which cause equal discomfort at all frequencies (i.e. using data from equivalent comfort contours constructed in Chapter 8). Overall ride values calculated using the weightings defined in current standards and the weightings defined in Section 9.3 are compared If the weightings are correct, overall ride values should be independent of frequency (i.e. predicting equal discomfort at all frequencies).

[Overall ride values are compared in Figure 9.17 to Figure 9.19. The separate weighted-components of lateral oscillation, roll oscillation and fully roll-compensated lateral oscillation for each seating condition can be found in the Appendices].

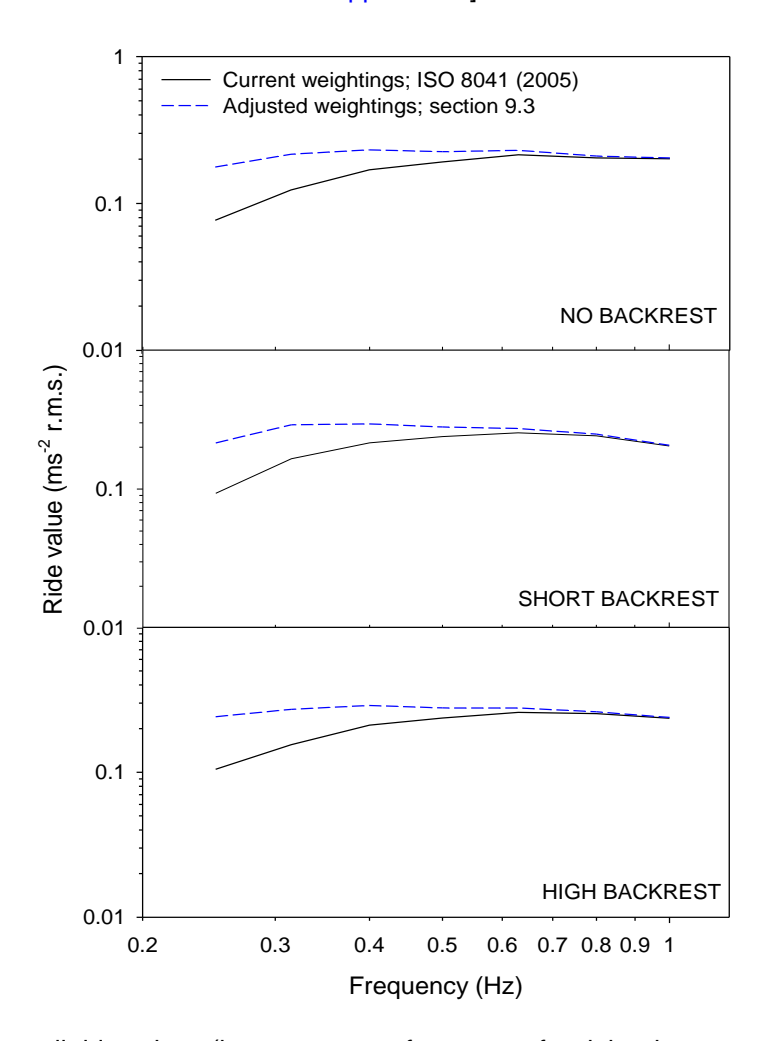


Figure 9.17 Overall ride values (i.e. root-sums-of-squares of weighted components) for lateral oscillation on a rigid seat with no backrest, with a short backrest and with a high backrest, frequency-weighted using current (ISO 8041, 2005) and adjusted (Section 9.3) weightings.

9.4.1. Lateral acceleration

Figure 9.17 shows 'overall ride values' for lateral oscillation on a rigid seat with no backrest, with a short backrest and with a high backrest (calculated from equivalent comfort contours constructed in Chapter 8), using current and adjusted frequency weightings (see Table 9.5). Using the adjusted weighting W_d ' for lateral acceleration instead of standardised weighting W_d , the overall ride values offer a closer approximation to discomfort caused by low frequency lateral oscillation between 0.25 and 0.63 Hz. The adjusted weighting W_d ' appears to improve the prediction of discomfort for all three seating conditions (no backrest, short backrest, and high backrest).

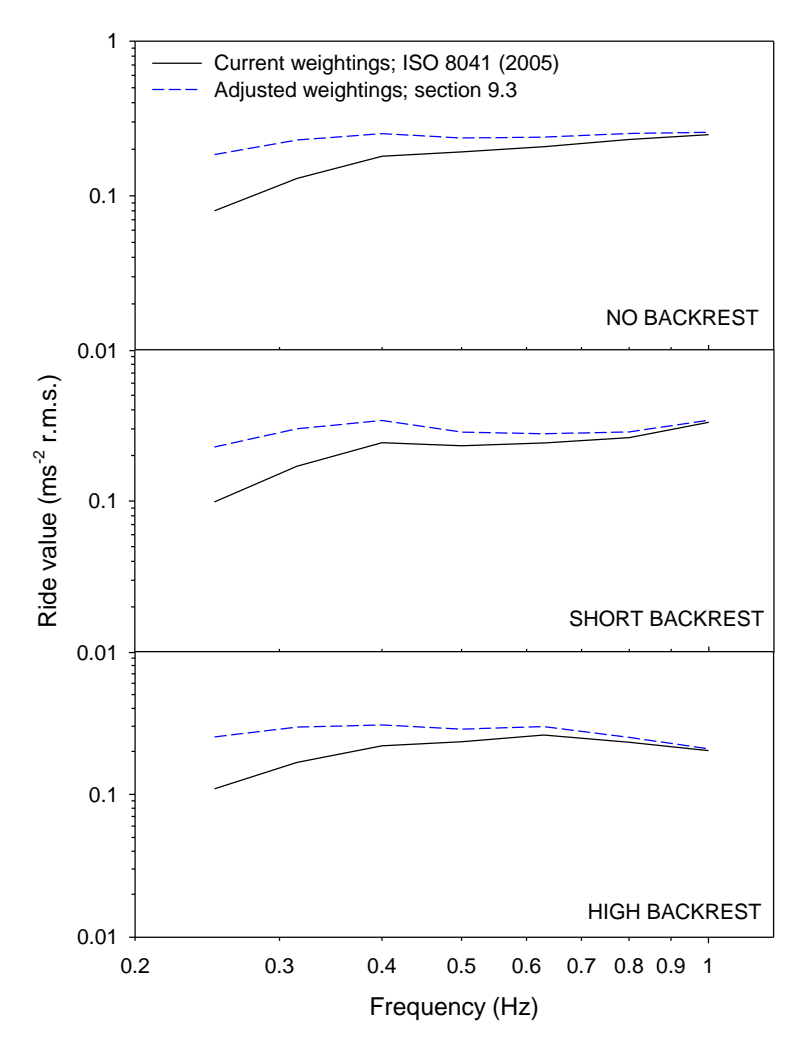


Figure 9.18 Overall ride values (i.e. root-sums-of-squares of weighted components) for roll oscillation on a rigid seat with no backrest, with a short backrest and with a high backrest, frequency-weighted using current (ISO 8041, 2005) and adjusted (Section 9.3) weightings.

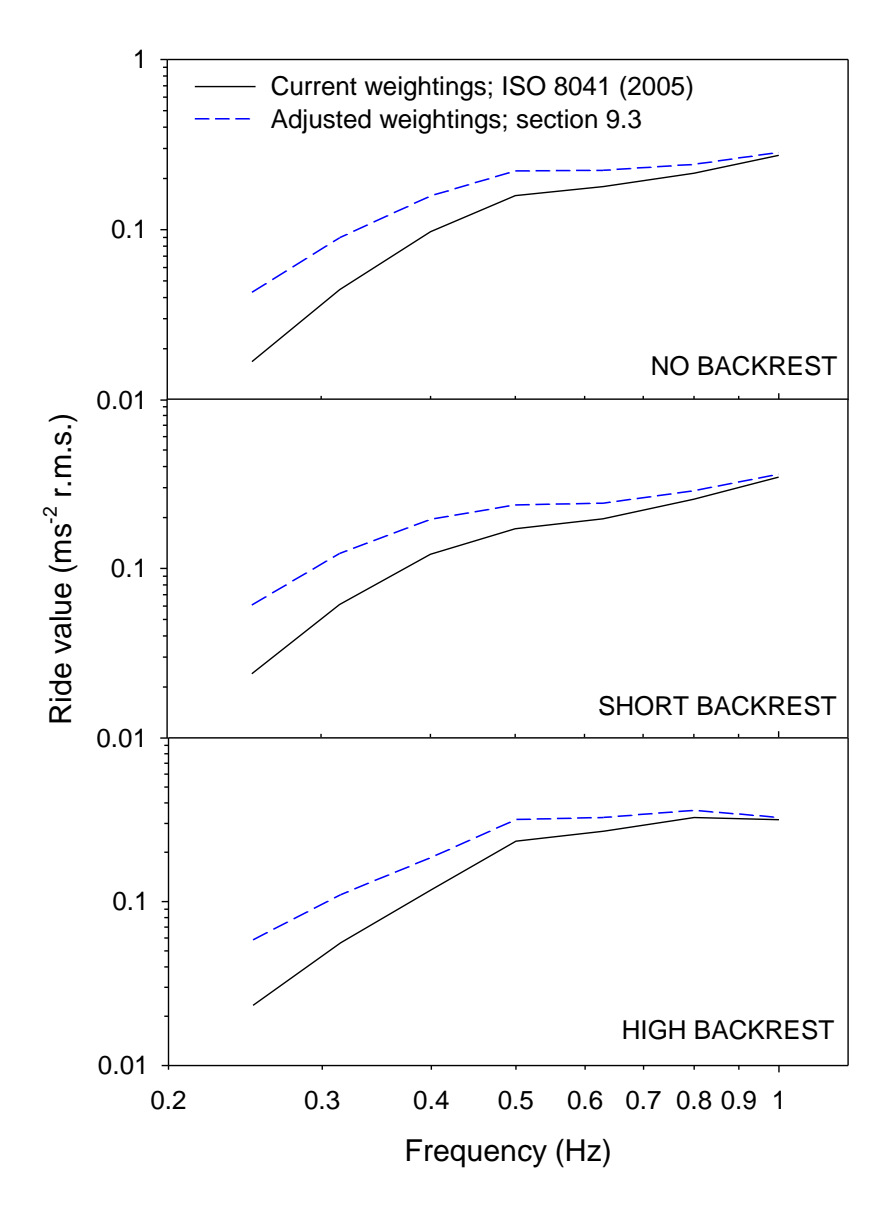


Figure 9.19 Overall ride values (i.e. root-sums-of-squares of weighted components) for fully roll-compensated lateral oscillation on a rigid seat with no backrest, with a short backrest and with a high backrest, frequency-weighted using current (ISO 8041, 2005) and adjusted (Section 9.3) weightings.

9.4.2. Roll acceleration

Figure 9.18 shows overall ride values for roll oscillation on a rigid seat with no backrest, with a short backrest and with a high backrest (calculated from equivalent comfort contours constructed in Chapter 8), using current and adjusted frequency weightings (see Table 9.5). Using the adjusted weightings W_d and W_e for

lateral acceleration and roll acceleration, respectively, the root-sums-of-squares of weighted components offer a closer approximation to discomfort caused by low frequency roll oscillation between about 0.25 and 0.8 Hz. The adjusted weightings appear to improve the prediction of discomfort for all three seating conditions (no backrest, short backrest, and high backrest) at the lowest frequencies, but do not account for increased sensitivity at the higher frequencies when sitting with a high backrest (see Chapter 8). The application of a single weighting for all magnitudes of roll acceleration on a seat with a full-height backrest may also be inappropriate (Chapter 8).

9.4.3. Fully roll-compensated lateral acceleration

As in Section 9.4.1 and 9.4.2, Figure 9.19 shows overall ride values for fully roll-compensated lateral oscillation on a rigid seat with no backrest, with a short backrest and with a high backrest, calculated using current and adjusted frequency weightings (see Table 9.5).

With the position of full roll-compensation at the seat surface, fully roll-compensated lateral oscillation results in zero lateral acceleration at the surface of the seat. Therefore, discomfort from this motion may arise from five component ride values: lateral acceleration at the backrest, and the foot support (due to these not being at the centre of roll), translational acceleration at the back, and the feet (arising from the gravitational component due to roll, $g.\sin\theta$), and rotational acceleration at the seat surface. The root-sums-of-squares summation of these five components appears to offer a reasonable approximation to discomfort caused by fully roll-compensated lateral oscillation between 0.5 and 1.0 Hz (Figure 9.19). This prediction is improved when using the adjusted frequency weightings $W_{\rm d}$ and $W_{\rm e}$ for lateral acceleration and roll acceleration, respectively.

Between 0.25 and 0.5 Hz, the overall ride values underestimate the discomfort caused by fully roll-compensated lateral oscillation. Since the translational components of fully roll-compensated lateral oscillation may be considered negligible, the prediction of discomfort relies on the frequency-weighted roll acceleration at the seat (i.e. $\rm rads^{-2}$). Adjusted frequency weighting $W_{\rm e}$ improves the prediction of discomfort from roll acceleration, but is only intended for use at frequencies greater than 0.5 Hz. At very low frequencies, the prediction of discomfort from fully roll-compensated lateral oscillation may require consideration of a weighting for rotational acceleration without gravity.

9.5. Research methodology

9.5.1. Absolute versus relative magnitude estimation

Vibration discomfort was assessed using the method of magnitude estimation with a 0.5-Hz lateral reference motion at 0.2 ms⁻² r.m.s. in Experiments 2 and 3 (Chapter 5 and 6), but in Experiments 4 and 5 (Chapter 7 and 8) the same method was used *without* a reference. The method of magnitude estimation without a reference (i.e. the absolute method) typically takes half as much time as magnitude estimation with a reference (i.e. the relative method), since it is not necessary to couple a reference stimulus with every exposure of a test stimulus. In the latter two experiments, the absolute method was therefore principally chosen because it was necessary to reduce the total duration of the experimental sessions. The validity of using magnitude estimation without a reference has been demonstrated previously (Green and Luce, 1974; Stevens, 1975; Zwislocki and Goodman, 1980), but it is also possible to compare directly absolute and relative methods using data from Experiments 2 to 5 (Chapters 5 to 8).

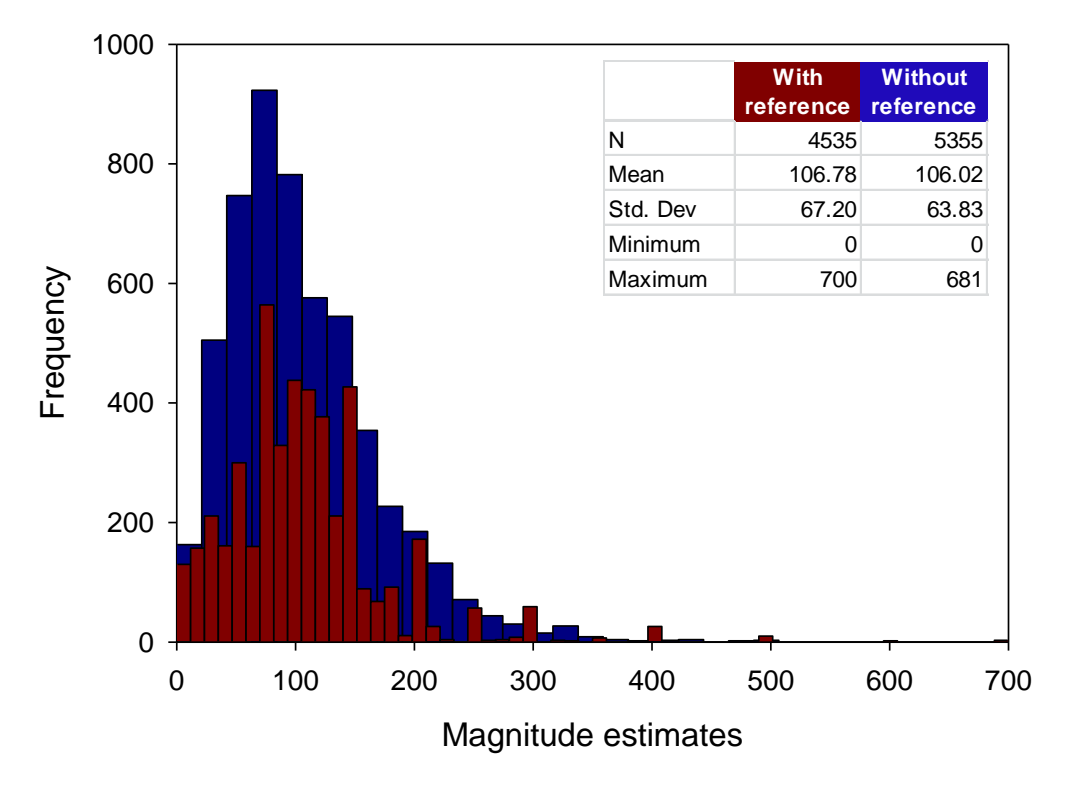


Figure 9.20 Distribution of lateral subjective magnitude estimates using the method of magnitude estimation with and without a reference (estimates reported without reference have been normalised), using all data collated from Experiments 2 to 5.

Stevens' power law (1975) affirms that the magnitude of subjective sensations (i.e. discomfort) can be related to the magnitude of physical stimuli (i.e. vibration acceleration) by a power function (see Section 3.4.2.2). This relationship is derived experimentally through least-squares regression of the logarithmic transformation of the power function (see Equation 3.4). Since the subjective magnitude estimates are integral to this process, a comparison of the absolute and relative methods can be made via assessment of the variation of magnitude estimates.

Figure 9.20 shows the distribution of magnitude estimates reported by subjects when exposed to lateral oscillation with a reference (Experiment 2 and 3) and without a reference (Experiments 4 and 5). (Magnitude estimates shown for the without reference condition have been normalised – see Section 7.2.5 and 8.2.5). There were a greater number of magnitude estimates collected during Experiments 4 and 5 (N = 5355), due to the greater number of experimental conditions tested, than during Experiments 2 and 3 (N = 4536). The range of values reported by subjects was similar for both absolute (M = 106.02, SD = 63.83, maximum = 681) and relative methods (M = 106.78, SD = 67.20, maximum = 700). Magnitude estimates were not significantly different between the two methods (p = 0.17; Mann-Whitney U).

When rating 'vibration comfort' of fore-and-aft oscillation between 0.8 and 12.5 Hz using the cross-modality matching method, Forta *et al.* (2012) reported greater rates of growth of discomfort than Schust *et al.* (2010) who used the same procedure and the same motions to rate 'vibration intensity'. The rates of growth of discomfort were also greater than those reported by Morioka and Griffin (2006a) who used the method of magnitude estimation with a 20 Hz reference to examine discomfort caused by fore-and-aft oscillation in a similar frequency range (Forta *et al.* 2012). It is possible that the type of subjective sensation (e.g. 'comfort' vs. 'intensity') and the choice of psychophysical method (e.g. cross-modality matching vs. magnitude estimation) influences the rate of growth of discomfort. For this work it is useful to assess whether the use of magnitude estimation with or without a reference influenced the rate of growth of discomfort.

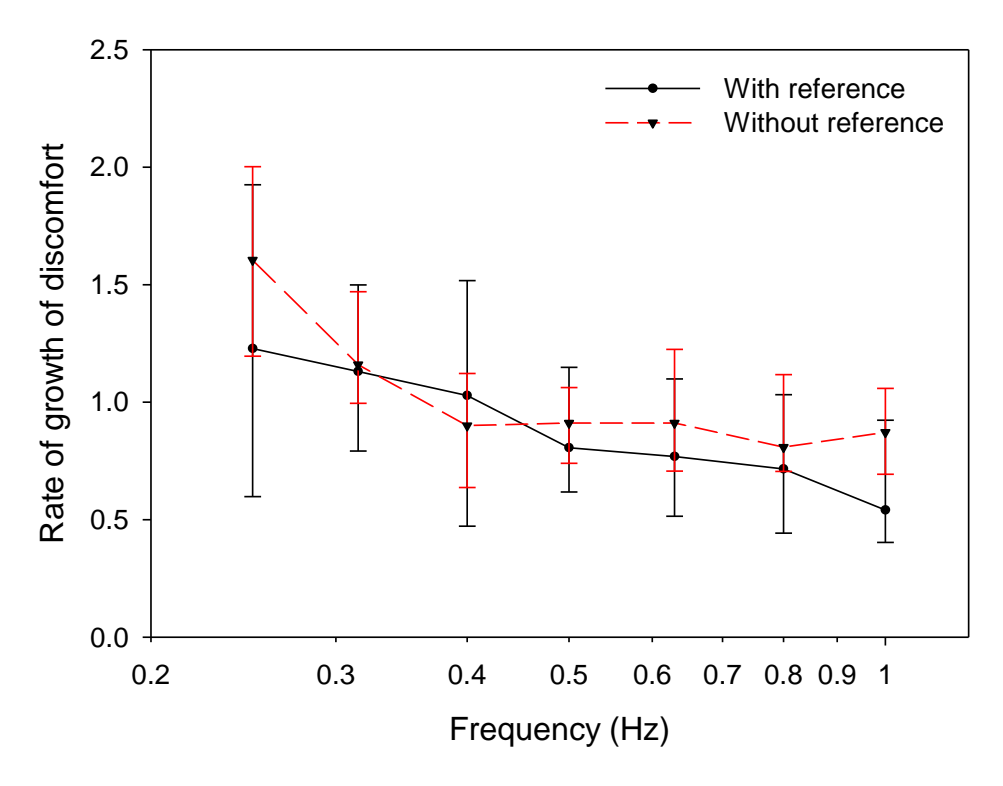


Figure 9.21 Median rates of growth of discomfort for lateral oscillation on a rigid seat with backrest obtained from magnitude estimates with a reference (Experiment 3) and without a reference (Experiment 5). Upper and lower error bars show 75th and 25th percentiles, respectively.

Figure 9.21 shows the median rates of growth of discomfort calculated from the subjective magnitude estimates for lateral oscillation on a rigid seat with a full-height backrest pooled from Experiment 3 (for magnitude estimation with reference) and Experiment 5 (for magnitude estimation without reference). [These data were chosen for the analysis because both the seating conditions, i.e. a full-height backrest, and the motion conditions, i.e. 3.5 cycle lateral oscillations, were comparable across the two experiments]. The pattern of decreasing rates of growth of discomfort with increasing frequency between 0.25 and 1.0 Hz was found with both relative and absolute magnitude estimation methods. No significant differences in the rates of growth of discomfort between the two methods were found at any frequency (p > 0.062; Mann-Whitney U).

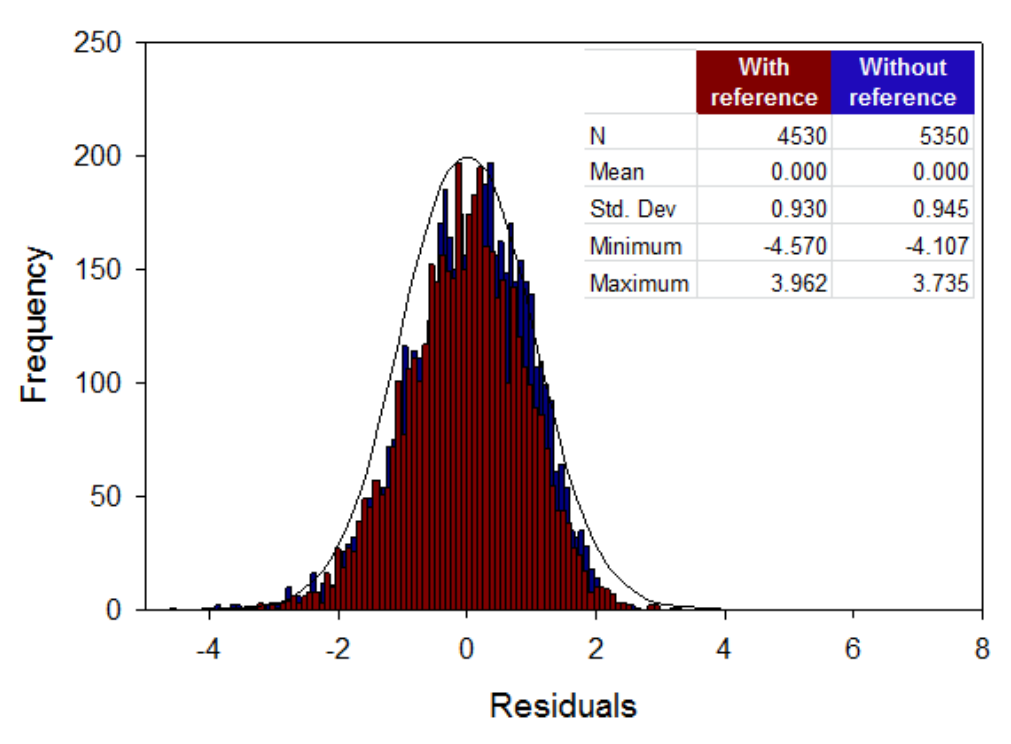


Figure 9.22 Distribution of standardised residuals when using magnitude estimation with and without reference, using all data collated from Experiments 2 to 5. Normal distribution indicated by solid line.

Linear least-squares regression relies on the assumption that standardised residuals are normally distributed (Osborne and Waters, 2002). Any inconsistency in magnitude estimates reported by individual subjects may increase the prevalence of outliers and thus increase the risk of violating this assumption. Some authors have argued that magnitude estimates are less vulnerable to variability when using a reference than when not using a reference (Mellers, 1983); therefore the distribution of standardised residuals may differ between absolute and relative magnitude estimation methods. Figure 9.22 shows the distribution of standardised residuals for least-squares regression performed between the subjective magnitudes and the acceleration magnitudes obtained when using magnitude estimation with and without a reference. There were no significant differences found between standardised residuals for absolute and relative magnitude estimation (p = 0.53; Mann-Whitney U), and it can be seen that the residuals for both methods approximate to a normal distribution.

In linear regression, the coefficient of determination (R²) describes the proportion of the response variable (i.e. subjective discomfort) which is explained by the predictor variable (i.e. acceleration magnitude). A weak (or nonlinear) relationship between subjective discomfort and

acceleration magnitude, as indicated by a small coefficient of determination (R^2), may result from large response variability. Therefore, if the response variability is greater when using magnitude estimation without a reference, as implied by Mellers (1983), then the value of the coefficients of determination should be smaller than that for magnitude estimation with a reference. In fact, it appears the opposite is true; Figure 9.23 shows larger R^2 values for magnitude estimation without a reference (p < 0.05, for all frequencies except 0.63 Hz; Mann-Whitney U). This is consistent with findings reported by Stevens (1975).

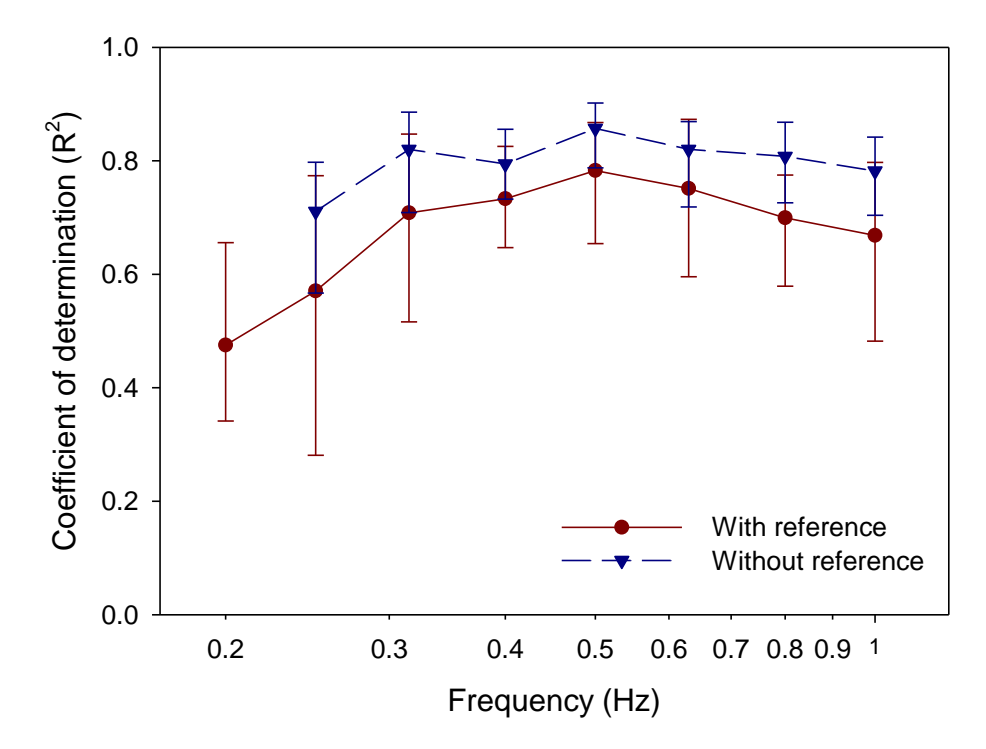


Figure 9.23 Median coefficients of determination (R^2) for least squares regression when using magnitude estimation with and without reference. Upper and lower errors bars indicate 75th and 25th percentiles, respectively.

9.5.2. Motion sickness bias

The experiment reported in Chapters 5 to 8 investigated the physical vibration discomfort caused by lateral, roll and fully roll-compensated lateral oscillations between 0.2 and 1.0 Hz. Horizontal and rotational oscillations in this frequency range may also cause motion sickness (e.g. Chapter 4, Donohew and Griffin, 2010), therefore it was important to ensure subjects could distinguish between the sensation of motion sickness and the sensation of vibration discomfort. Failure to separate the two sensations would greatly compromise the validity of the

experiments; subjective magnitude estimates would be biased by sensations of motion sickness.

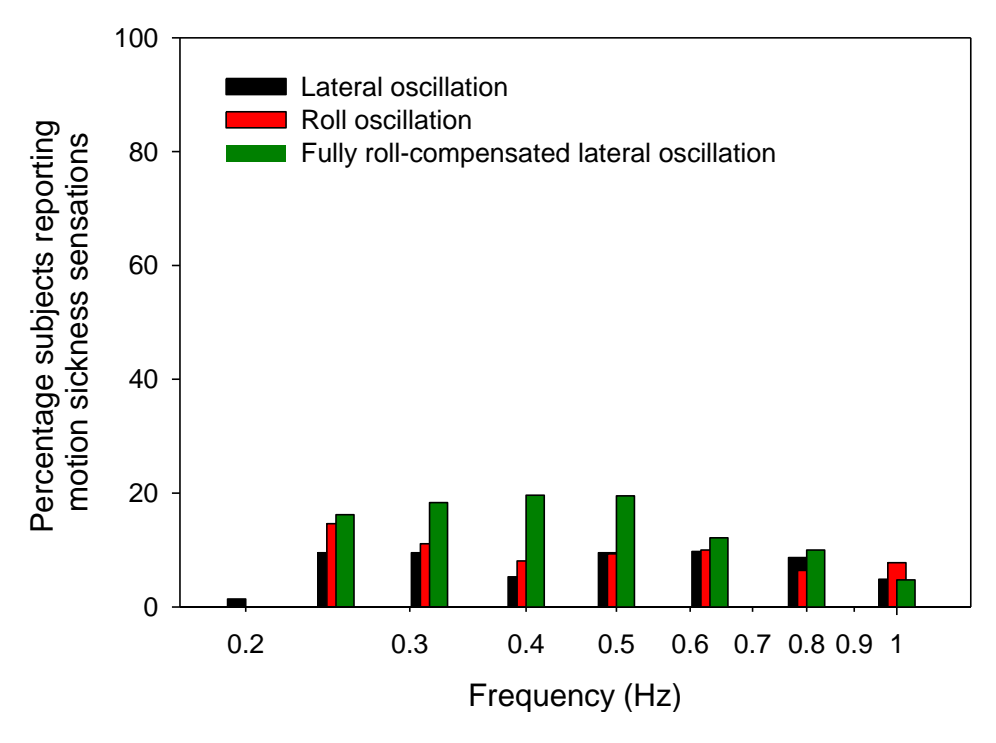


Figure 9.24 Percentage of subjects reporting sensations associated with motion sickness during exposure to lateral oscillation, roll oscillation and fully roll-compensated lateral oscillation (median values from Experiment 2, 3, 4 and 5).

To minimise the risk of motion sickness bias, subjects were instructed at the beginning of each experiment (see Appendices for a copy of the written instructions), with particular care given to the definition of vibration discomfort. Nevertheless, the degree of motion sickness experienced by subjects, and therefore the degree to which the sensation of motion sickness is likely to have influenced subjective magnitude estimates, can be assessed through analysis of the 'location of discomfort' data collected in Experiment 2 - 5 (Chapters 5 - 8). Subjects were asked to indicate the location of the body where they experienced discomfort during motion exposure, including any sensations associated with motion sickness such as vestibular stimulation or dizziness. Figure 9.24 shows the percentages of subjects who reported sensations associated with motion sickness during exposure to lateral, roll and fully roll-compensated lateral oscillation (median values collated from experiments 2 - 5).). The proportion of subjects reporting motion sickness sensations was maximal at frequencies less than $0.5 \, \text{Hz}$ (consistent with findings reported previously – Donohew, 2006; Chapter 4), but the physical discomfort reported by subjects was

minimal in this range (see Section 9.3.4). It is therefore unlikely that subjective magnitude estimates were influenced by a motion sickness bias.

9.5.3. Effects of fatigue

The duration of each experiment was limited to a maximum of 1.5 hours with frequent breaks, but it is possible that there was some subject fatigue. The order of presentation of all motion stimuli was fully randomised, and the order of specific experimental sessions were varied using a Latin square, therefore if there were no effects of fatigue then there should be no association between subjective responses and the order of presentation of motion stimuli. To test this conclusion, this section examines the effect of presentation order on subjective magnitude estimates collected in Experiments 3 to 5 for lateral oscillation at 0.5 Hz and 0.4 ms⁻² r.m.s. (Figure 9.25). For this magnitude and frequency of lateral oscillation, there was no strong relationship between presentation order and subjective magnitude estimates: Spearman's rank order correlation coefficient showed a non-significant, weak negative correlation between presentation order and subjective magnitude estimates (R = -0.033, p = 0.705). It can therefore be concluded that the order of presentation of motion stimuli had no effect on reported subjective magnitude estimates.

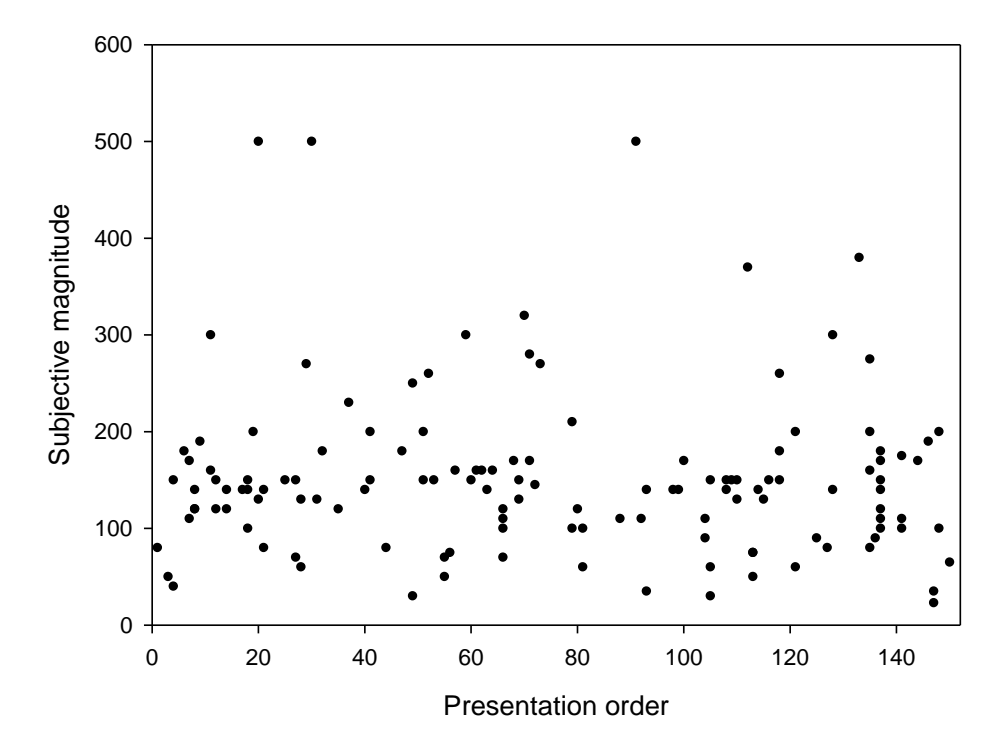


Figure 9.25 Effect of stimuli presentation order on subjective discomfort ratings obtained for lateral oscillation at 0.5 Hz and 0.4 ms⁻² r.m.s. in Experiments 3 – 5.

9.5.4. Order effects

When presenting pairs of motion stimuli, subjects may overestimate the discomfort caused by the second stimulus relative to the first stimulus (Griffin and Whitham, 1980). Experiments 2 and 3 (Chapters 5 and 6) used the method of magnitude estimation with a reference, therefore the discomfort ratings reported by participants in these studies may have been affected by this bias. To assess the degree of this bias, the distribution of 78 discomfort responses to test motions identical to the reference motion (i.e. 0.5 Hz lateral oscillation at 0.2 ms⁻² r.m.s.) is shown in Table 9.6 and Figure 9.26 (using data from Experiment 2 and 3).

Table 9.6 Distribution of 78 discomfort responses to test motions equivalent to a subjective magnitude of 100 (i.e. equivalent to the reference motion) reported by subjects during Experiment 2 and 3.

Discomfort response	Frequency	Percentage
50	2	2.6
70	1	1.3
75	1	1.3
80	5	6.4
85	1	1.3
90	6	7.7
95	3	3.8
100	27	34.6
105	4	5.1
110	10	12.8
115	2	2.6
120	4	5.1
125	3	3.8
130	2	2.6
150	4	5.1
180	1	1.3
200	1	1.3
280	1	1.3
< 100	19	24.4
> 100	32	41.0

The reference motion was given a subjective magnitude of 100, therefore if no bias is present the distribution of discomfort ratings below 100 should be similar to that for discomfort ratings above 100. With a mean discomfort rating of 107.44 and a standard deviation of 30.31, 41% of

subjects overestimated discomfort and 24% of subjects underestimated discomfort caused by the test stimulus relative to the reference stimulus. When judging pairs of motion stimuli, it seems there was a slightly greater sensitivity to the second stimulus, consistent with Griffin and Whitham (1980).

Section 9.5.1 compared the method of magnitude estimation with and without reference as used in Experiment 2 to 5. It was concluded that there were no substantial differences in the distribution of discomfort ratings produced by these two methods, but absolute magnitude estimation produced slightly greater coefficients of determination. It is clear that using the method of magnitude estimation without a reference also has other benefits, such as a faster experimental procedure and reduced risk of bias due to order effects.

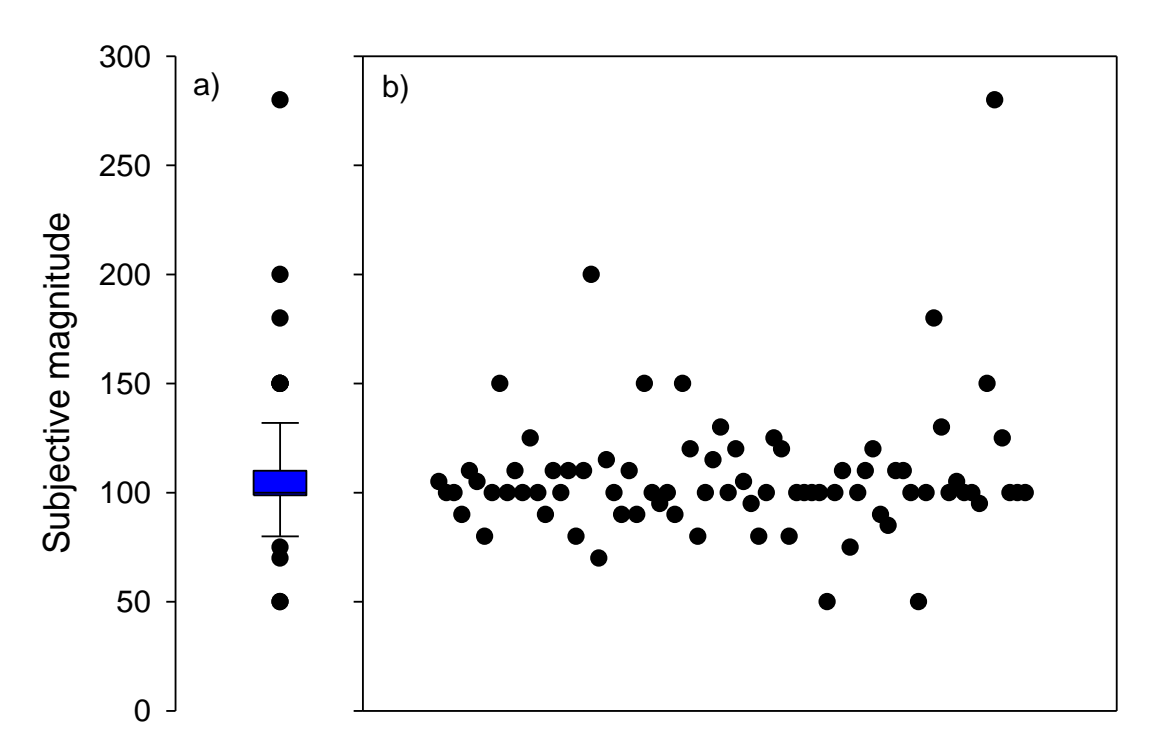


Figure 9.26 Distribution of discomfort responses to test motions equivalent to a subjective magnitude of 100 (i.e. equivalent to the reference motion); a) boxplot showing median and interquartile range, and; b) scatterplot showing 78 individual responses.

9.5.5. Range effects

In Experiments 2, 3, 4 and 5, the range of acceleration magnitudes was limited to 0.08-0.40 ms⁻² r.m.s. due to restrictions with motion simulation equipment (see Section 3.2). When using magnitude estimation, there is some evidence that increasing the range of stimulus magnitudes

reduces the rate of growth of sensation, i.e. the exponent in Stevens' power law, and thus the subsequent shape and level of equivalent comfort contours (Teghtsoonian and Teghtsoonian, 1978; Suzuki, 1998).

The nonlinearity of the human body response to vibration magnitude is such that the frequency dependence of discomfort may be different with different magnitudes of vibration (e.g. Griffin, 1990; Morioka and Griffin, 2006a). This nonlinearity, coupled with the effects of the range of stimulus magnitudes, means that rates of growth of discomfort and equivalent comfort contours for lateral oscillation, roll oscillation and fully roll-compensated lateral oscillation between 0.25 and 1.0 Hz may differ from those reported in this thesis if the magnitudes of vibration are increased above 0.40 ms⁻² r.m.s. Since it is possible that accelerations in transport vehicles may occur at magnitudes greater than studied here, further research is required to offer a complete understanding of subjective responses to low frequency lateral and roll oscillations.

9.6. Recommendations for future research

9.6.1. Centre-of-rotation⁴

Chapter 4 describes an experiment which investigated the effect of the vertical position of the centre-of-rotation on motion sickness caused by 0.2 Hz fully roll-compensated lateral oscillation. Whilst there were no statistical differences between the 'seat compensation' and 'head compensation' conditions reported in Experiment 1, there was a trend for a marginally greater incidence of motion sickness when the centre-of-rotation was at head height. Larger differences in the position of the centre-of-rotation (i.e. greater than the 0.8 m difference studied here) are likely to elicit different results. Furthermore, the influence of the centre-of-rotation on motion sickness is likely to vary with the frequency and the magnitude of roll-compensated lateral oscillation.

The position of the centre-of-rotation may also affect the discomfort caused by fully roll-compensated lateral oscillation. As the distance from the centre-of-rotation increases from 80 to 240 mm, there is an increase in sensitivity to roll and pitch oscillation between 2 and 16 Hz (Parsons and Griffin, 1978). Equivalent comfort contours became more similar to those produced by translation as the distance from the centre-of-rotation increases. This suggests the translational component of the rotation (see Section 2.2.3) becomes more important for

⁴ In this section, the term 'centre-of-rotation' refers to either: a) the point in space about which an object rotates, in the absence of translational movement, or; b) the position of full roll-compensation with combined lateral and roll motion.

discomfort. In tilting rail vehicles, differences in the position of the centre-of-rotation may be far greater than 240 mm (e.g. Hitachi, 2009), therefore it is of importance to vehicle manufacturers and passengers to understand the effect of the location of the centre-of-rotation on discomfort with roll-compensated lateral oscillations.

Table 9.7 Effect of distance from centre-of-rotation* on nominal lateral accelerations at the seat and the head+.

Direction	Frequency (Hz)	Earth-lateral acceleration (± ms ⁻²)	Roll displacement (± °)	Distance from centre-of-rotation* (m)	Acceleration at seat (± ms ⁻²)	Acceleration at head ⁺ (± ms ⁻²)
		0.5	0	0	0.5	0.5
	0.2	0.5	0	0.8	0.5	0.5
		0.5	0	1.6	0.5	0.5
		0.5	0	0	0.5	0.5
Lateral	0.5	0.5	0	0.8	0.5	0.5
		0.5	0	1.6	0.5	0.5
		0.5	0	0	0.5	0.5
	1	0.5	0	0.8	0.5	0.5
		0.5	0	1.6	0.5	0.5
		0	2.92	0	0.5	0.56
	0.2	0	2.92	0.8	0.56	0.63
		0	2.92	1.6	0.63	0.70
	0.5	0	2.92	0	0.5	0.90
Roll		0	2.92	0.8	0.90	1.31
		0	2.92	1.6	1.31	1.71
		0	2.92	0	0.5	2.11
	1	0	2.92	0.8	2.11	3.72
		0	2.92	1.6	3.72	5.33
		0.5	2.92	0	0	0.06
	0.2	0.5	2.92	0.8	0.06	0.13
		0.5	2.92	1.6	0.13	0.19
100% roll-		0.5	2.92	0	0	0.40
compensated	0.5	0.5	2.92	0.8	0.40	0.80
lateral		0.5	2.92	1.6	0.80	1.21
		0.5	2.92	0	0	1.61
	1	0.5	2.92	0.8	1.61	3.22
		0.5	2.92	1.6	3.22	4.83

^{*} centre-of-rotation at seat surface, * head assumed to 800 mm above the seat

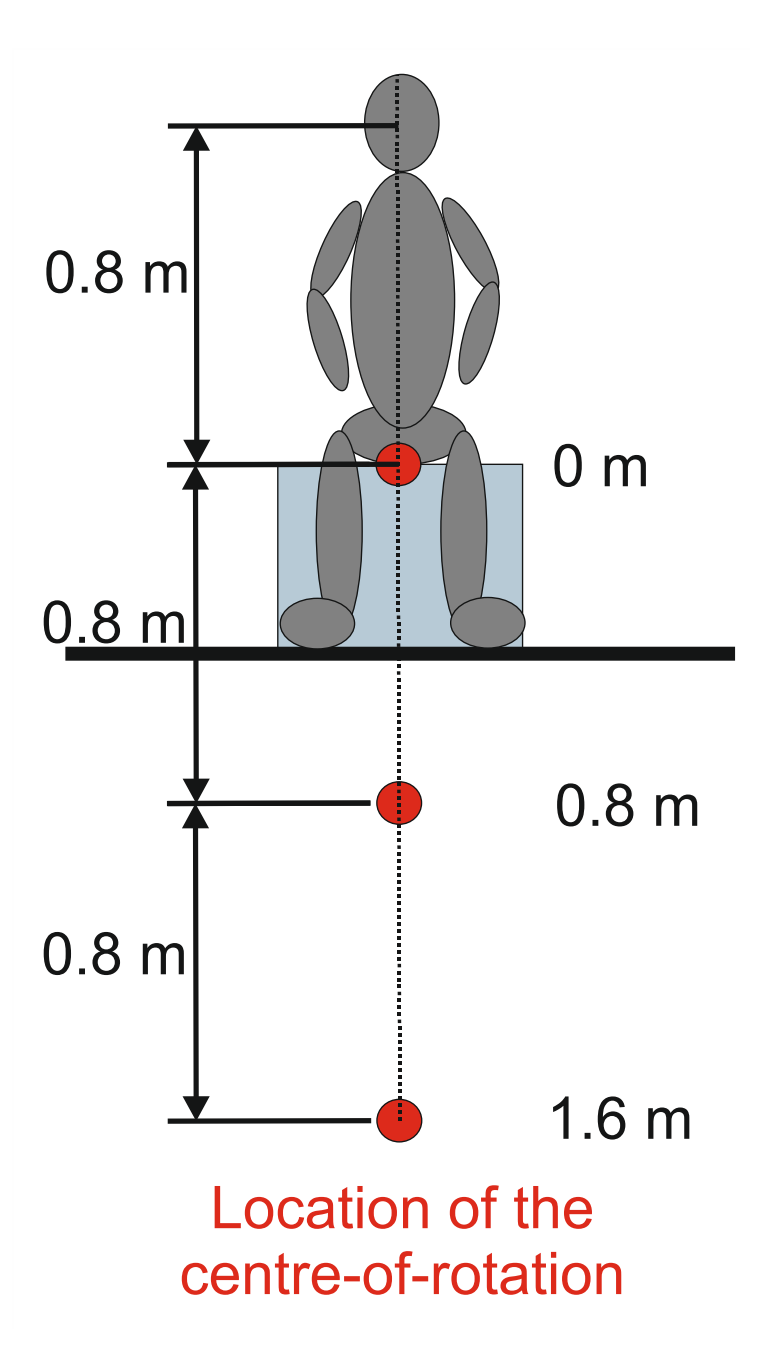


Figure 9.27 Illustration of the position of the centre-of-rotation relative to a seated subject used to calculate nominal quantities given in Table 9.7.

Nominal motion quantities for three frequencies (0.2, 0.5 and 1.0 Hz) of lateral, roll and fully roll-compensated lateral oscillation with a centre-of-rotation at three different heights are shown in Table 9.7 (an illustration of locations of the centre-of-rotation is shown in Figure 9.27). As shown by Table 9.7, the resultant lateral accelerations at the seat and the head are unaffected by the

position of the centre-of-rotation during lateral oscillation, but increase with increasing distance from the centre-of-rotation during roll and fully roll-compensated lateral oscillation (due to the translational components associated with the roll – see Section 2.2.3). This suggests that the discomfort will increase with increasing distance from the centre-of-rotation – Figure 9.28 shows predictions of equivalent comfort contours for roll and fully roll-compensated lateral oscillation at 0.8 and 1.6 m from the centre-of-rotation (as shown in Figure 9.27) superimposed on experimental contours for lateral, roll and fully roll-compensated lateral oscillation established in Chapter 6, 7 and 8. Further experimental work is required to test these predictions.

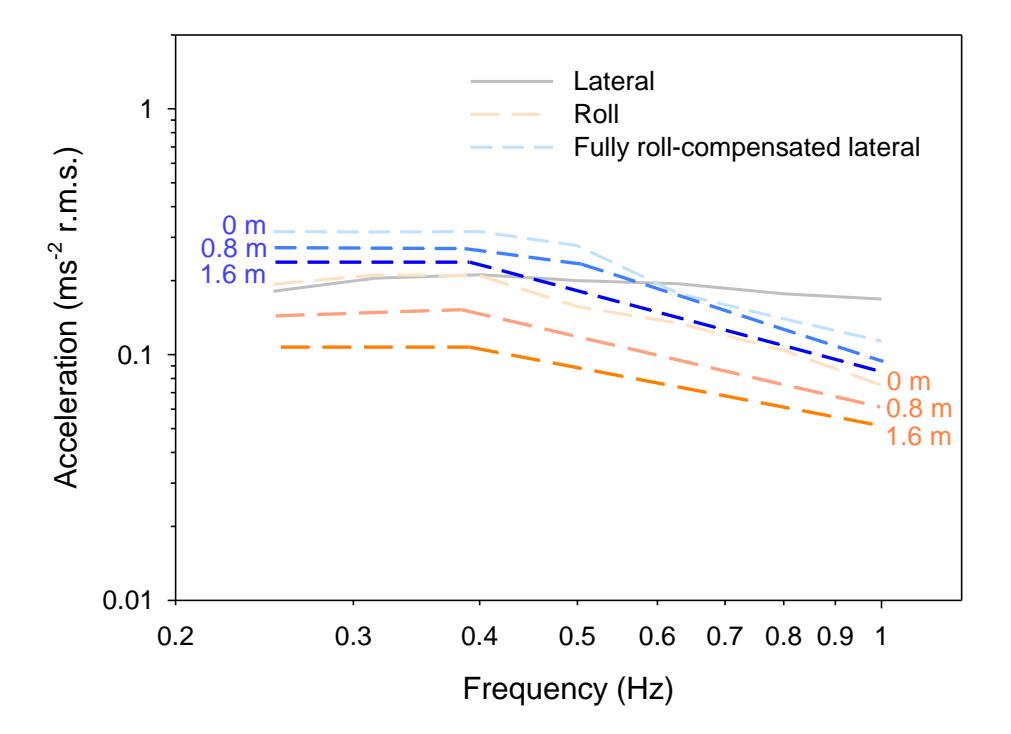


Figure 9.28 Nominal predictions of the effect of increasing the vertical height of the centre-ofrotation from 0 to 1.6 m above the seat surface on the level of equivalent comfort contours for lateral oscillation, roll oscillation and fully-roll compensated lateral oscillation.

9.6.2. Percentage compensation

Previous work has investigated the effect of percentage compensation on motion sickness caused by roll-compensated lateral oscillation (Donohew and Griffin, 2010). The work presented in this thesis investigated the physical discomfort caused by 100% roll-compensated lateral oscillation at frequencies between 0.25 and 1.0 Hz, but other levels of roll-compensation were not tested.

Table 9.8 Effect of percentage compensation on nominal accelerations at the seat and the head during roll-compensated lateral oscillation.

Frequency (Hz)	Earth-lateral acceleration (± ms ⁻²)	Roll displacement (± °)	Percentage compensation	Acceleration at seat (± ms ⁻²)	Acceleration at head+ (± ms-2)			
	Constant Earth-lateral acceleration (± ms ⁻²)							
	0.50	0	0	0.50	0.50			
	0.50	0.73	25	0.38	0.02			
0.2	0.50	1.46	50	0.25	0.03			
	0.50	2.19	75	0.13	0.05			
	0.50	2.92	100	0.00	0.06			
	0.50	0	0	0.50	0.50			
	0.50	0.73	25	0.38	0.10			
0.5	0.50	1.46	50	0.25	0.20			
	0.50	2.19	75	0.13	0.30			
	0.50	2.92	100	0.00	0.40			
	0.50	0	0	0.50	0.50			
	0.50	0.73	25	0.38	0.40			
1	0.50	1.46	50	0.25	0.81			
	0.50	2.19	75	0.13	1.21			
	0.50	2.92	100	0.00	1.61			
	Constant roll displacement (± °)							
	0	2.92	0	0.50	0.50			
	0.13	2.92	25	0.38	0.43			
0.2	0.25	2.92	50	0.25	0.31			
	0.38	2.92	75	0.13	0.18			
	0.50	2.92	100	0	0.06			
	0	2.92	0	0.50	0.50			
	0.13	2.92	25	0.38	0.77			
0.5	0.25	2.92	50	0.25	0.65			
	0.38	2.92	75	0.13	0.52			
	0.50	2.92	100	0	0.40			
	0	2.92	0	0.50	0.50			
	0.13	2.92	25	0.38	1.98			
1	0.25	2.92	50	0.25	1.86			
	0.38	2.92	75	0.13	1.73			
	0.50	2.92	100	0	1.61			

With a constant Earth-lateral acceleration, the percentage compensation will decrease with a decreasing magnitude of roll displacement – meaning the motion will become similar to uncompensated lateral oscillation as the percentage compensation approaches zero. With a constant roll displacement, the percentage compensation will decrease with a decreasing magnitude of Earth-lateral acceleration – meaning the motion will become similar to pure roll oscillation as the percentage compensation approaches zero. This relationship is illustrated by the nominal motion quantities presented in Table 9.8 and the subsequent predictions of equivalent comfort contours shown in Figure 9.29 and Figure 9.30. The figures show predictions of equivalent comfort contours for combined lateral and roll oscillation with 75%, 50% and 25% compensation where the Earth-lateral acceleration is held constant (Figure 9.29) and where the roll displacement is held constant (Figure 9.30), superimposed on experimental contours for uncompensated and fully roll-compensated lateral oscillation established in Chapter 6, 7 and 8. Further experimental work is required to test these predictions and to assist the optimisation of roll-compensated lateral motions in terms of both motion sickness and discomfort.

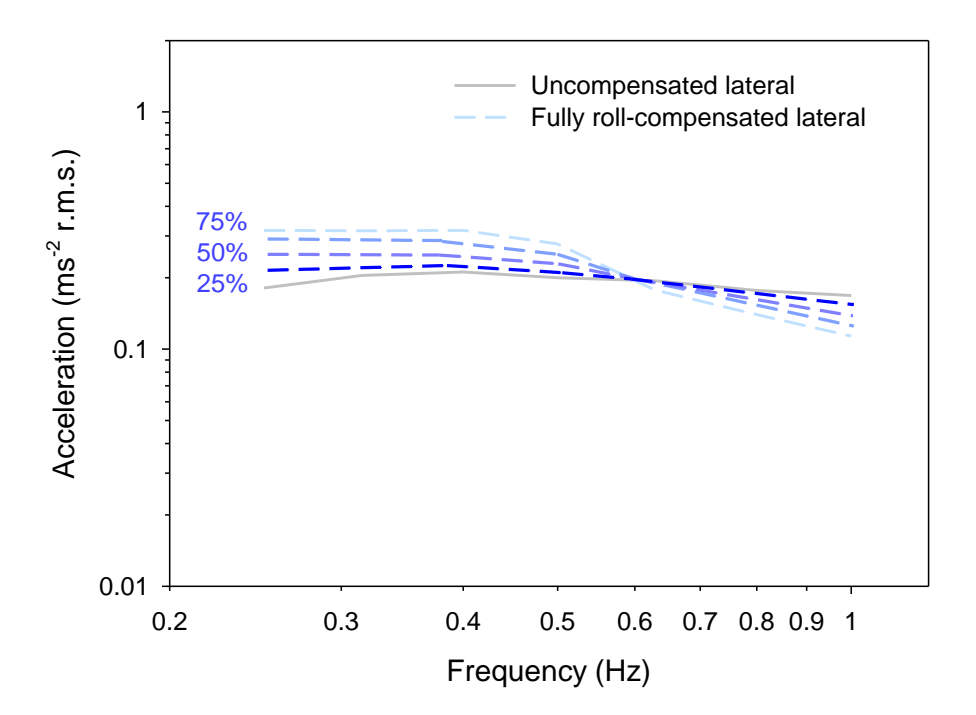


Figure 9.29 Nominal predictions of the frequency-dependence of equivalent comfort contours for uncompensated lateral oscillation and 25%, 50%, 75% and 100% roll-compensated lateral oscillation (with constant Earth-lateral acceleration).

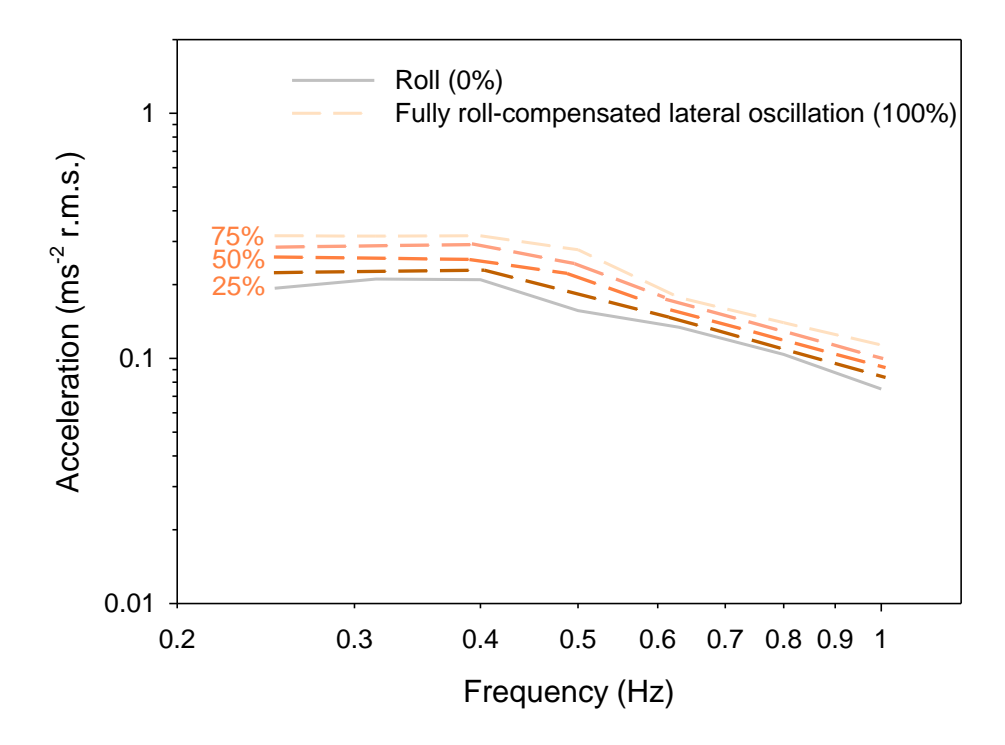


Figure 9.30 Nominal predictions of the frequency-dependence of equivalent comfort contours for roll oscillation and 25%, 50%, 75% and 100% roll-compensated lateral oscillation (with constant roll displacement).

9.6.3. The semantics of discomfort

As discussed in Section 2.9, the semantic expression of vibration discomfort varies considerably across the population and is context dependent. A vibration at a magnitude perceived to be typical for a car would likely be appalling in a building. British Standard 6841 (1987) and International Standard ISO 2631-1 (1997) provide some guidance on the interpretation of frequency- and axis-weighted vibration total values in terms of the 'likely comfort reaction' of exposed persons in transport (see Table 9.9), but the guidance is limited and unspecific. An investigation into the 'estimated comfort level' associated with various magnitudes of weighted motion in a variety of vehicles would be useful for quantifying the context-dependency of vibration discomfort.

Table 9.9 Effect of the magnitude of vibration total values of estimated comfort levels, as provided by ISO 2631-1 (1997).

VTV (ms ⁻²)	Estimated comfort level
< 0.315	not uncomfortable
0.315 - 0.63	a little uncomfortable
0.5 - 1.0	fairly uncomfortable
0.8 - 1.6	uncomfortable
1.25 - 2.5	very uncomfortable
> 2.0	extremely uncomfortable

9.6.4. Phase

The level of roll-compensation of lateral acceleration is dependent on the ratio between the roll displacement and the Earth-lateral acceleration (see Section 9.6.2) and the relative phase between the roll motion and the lateral motion. The effect of phase delay (where the roll supersedes the lateral motion) and phase advance (where the roll precedes the lateral motion) on the development of motion sickness has been investigated previously (Joseph and Griffin, 2007). There was greatest sickness with a phase delay of 0° (equivalent to 100% compensation) and decreasing sickness with increasing phase delay between 14.5° (75% compensation) and 29° (50% compensation), showing support for previous research into the effects of percentage compensation on motion sickness (e.g. Forstberg *et al.*, 1998; Donohew and Griffin, 2010). However, a 29° phase advance was found to be less provocative of motion sickness than a 29° phase delay, despite offering the same level of compensation (i.e. 50%). The phase between the lateral component and the roll component during roll-compensated lateral oscillation will affect the motion of the body, therefore it is might be expected that the level of discomfort caused by this motion is influenced by the phase relationship. Further experimental work is required to understand these effects.

Chapter 10

Conclusion

This thesis describes five experiments designed to investigate the effects on motion sickness or physical discomfort of lateral oscillation, roll oscillation and fully roll-compensated lateral oscillation at frequencies less than 1.0 Hz, with a variety of seating conditions (Chapter 4 to 8). Analysis of the subjective data obtained in these experiments informed the construction of a conceptual model of motion sickness, a conceptual model of physical discomfort, and recommendations for current vibration standards for predicting physical discomfort with low frequency lateral and roll oscillations (Chapter 9).

Previous research determined that the motion sickness caused by fully roll-compensated lateral oscillation is greatest at about 0.2 Hz and decreases with increasing frequency (with the Earth-lateral jerk held constant). The work reported in this thesis has found that the physical discomfort caused by fully-roll compensated lateral oscillation is smallest at 0.25 Hz and *increases* with increasing frequency (with the Earth-lateral acceleration held constant). The optimum motion conditions for minimising motion sickness are therefore different from those required to minimise physical discomfort. At frequencies less than about 0.5 Hz, fully roll-compensated lateral acceleration causes less discomfort than the same magnitude of uncompensated lateral acceleration. But at higher frequencies (0.5 to 1.0 Hz), full roll-compensation of lateral acceleration worsens discomfort due to the components of rotational acceleration. The consequence of employing roll-compensation techniques to reduce passenger exposure to lateral accelerations (such as in tilting trains) is therefore dependent on the motion frequency.

Passenger comfort is also dependent on factors other than the frequency of oscillation. The design of tilting trains differs between countries, with some adopting active-tilting mechanisms and others passive-tilting. Differences in the height of the position of full roll-compensation between these designs are unlikely to cause great differences in the incidence of sickness in passengers, but the prevalence of motion sickness may be dependent on inherent

characteristics of the passenger population. For example, susceptibility to tilting-train sickness may be greater in Asian populations than in European populations.

Vehicle seating determines the transmission of vehicle motion to the human body and the postural support offered to the body. Some soft foam seat cushions may provide poor stability for passengers, leading to lateral and roll floor-to-seat transmissibilities greater than unity at frequencies less than 1 Hz. The discomfort associated with maintaining postural stability during low frequency lateral oscillation may be reduced with the addition of an appropriate backrest, but these benefits are dependent on the motion frequency, the motion direction, and the height of the backrest. A short backrest reduces discomfort with lateral oscillations at frequencies less than 0.5 Hz, whilst a full-height backrest is beneficial for comfort at frequencies up to 1 Hz. With roll oscillation about a centre-of-rotation at the seat surface, a full-height backrest reduces discomfort at frequencies less than 0.5 Hz, but worsens comfort at higher frequencies because of the translational components above the seat. With fully roll-compensated lateral oscillation, a full-height backrest is beneficial for comfort between 0.4 and 0.63 Hz.

The prediction of discomfort using currently standardised methods may be improved through adjustment of the frequency-weightings for lateral acceleration and roll acceleration. An extension of the high-pass filter defined for W_d and W_e (BS 6841, 1987; ISO 2631-1, 1997: ISO 8041, 2005) from 0.4 to 0.2 Hz will improve the prediction of discomfort with low frequency lateral acceleration and roll acceleration, respectively. In addition, adjustment to the acceleration-velocity transition defined for W_e is also recommended. Using the proposed model, discomfort from fully roll-compensated lateral oscillation between 0.5 and 1.0 Hz may be approximated through analysis of the frequency-weighted component of roll acceleration.

Appendices

A.1. Subject consent form

FRONT PAGE

Consent form to be completed by adult subjects who are being paid for their participation in an experiment (Adults are 18 years of age or older).

Human Experimentation Safety & Ethics Approval Number:
Exposure Number:
Vibration Experiment Exposure and Consent Form
Before completing this form, please read the 'Information for Subjects' on the reverse side of this sheet.
(i) Name
(ii) Do you have any of the conditions listed on the reverse side of this form?
(iii) Have you ever suffered any serious illness or injury?
(iv) Are you under medical treatment or suffering disability affecting your daily life?
If your answer is 'YES' to questions (ii), (iii) or (iv), please give details to Experimenter.
I understand that for my participation in this experiment I am to be paid the sum of £ for the sum of £
my attendance on o ccasions.
DECLARATION
I volunteer to be a subject in a vibration experiment. My replies to the above questions an correct to the best of my belief, and I understand that they will be treated by the experimenter a confidential. I understand that I may at any time withdraw from the experiment and that I an under no obligation to give reasons for withdrawal or to attend again for experimentation.
I undertake to obey the regulations of the laboratory and instructions of the Experimente regarding safety, subject only to my right to withdraw declared above. The purpose and method of the research have been explained to me and I have had the opportunity to ask questions.
Signature of Subject
I confirm that I have explained to the subject the purpose and nature of the investigation which has been approved by the Human Experimentation Safety and Ethics Committee.
Signature of Experimenter
Medical assistance is available if required.
Cont/

This form must be submitted to the Secretary of the Human Experimentation Safety and Ethics

Committee on completion of the experiment.

BACK PAGE

Information for Subjects

Persons with any of the following conditions are usually considered unfit for vibration experiments

Active disease of respiratory system including recent history of coughing-up blood or chest pain.

Active disease of the gastro-intestinal tract: including internal or external hemia, peptic ulcer, recent gall-bladder disease, rectal prolapse, anal fissure, haemonhoids or pilonidal sinus.

Active disease of the genito-urinary system including kidney stones, urinary incontinence or retention or difficulty in micturition.

Active disease of the cardiovascular system including hypertension requiring treatment, angina of effort, valvular disease of the heart, or haemophilia.

Active disease of the musculo-skeletal system including degenerative or inflammatory disease of the spine, long bones, or major joints or a history of repeated injury with minor trauma.

Active or chronic disease or disorders of the nervous system including eye and ear disorders and any disorder involving motor control, wasting of muscles, epilepsy or retinal detachment.

Pregnancy: any woman known to be pregnant should not participate as a subject in a vibration experiment.

Mental Health: subjects must be of sound mind and understanding and not suffering from any mental disorder that would raise doubt as to whether their consent to participate in the experiment was true and informed.

Recent trauma and surgical procedures; persons under medical supervision following surgery or traumatic lesions (e.g. fractures) should not participate in vibration experiments.

Prosthesis: persons with internal or external prosthetic devices normally should not participate in vibration experiments (although dentures need not exclude participation in experiments with low magnitudes of vibration).

Other:	
(For completion by experiment	ter)
To be completed by the Exp	erimenter:

MBRATOR:

<u>DESCRIPTION OF VIBRATION</u>: State <u>levels</u>, <u>frequencies</u>, <u>axes</u>, <u>durations</u> etc. (If subject is in direct or indirect control of the vibration level, also state maximum vibration level for each condition.) Indicate subject posture, seat type, etc. and any other factors affecting subject exposure. Description must be sufficient to enable reader to reproduce a similar exposure pattern.

COMMENTS: (Ifmore space is required, please attach a continuation sheet.)

A.2. Motion sickness susceptibility questionnaire

Exposure no
Subject no
Condition no
Experiment no

MOTION SICKNESS SUSCEPTIBILITY QUESTIONNAIRE

INSTRUCTIONS

This questionnaire is primarily concerned with: (i) your susceptibility to motion sickness and, (ii) what types of motion are most effective in causing this sickness.

Please read the questions carefully and answer them ALL by either TICKING or FILLING IN the boxes which most closely correspond to you as an individual.

All the information you give is CONFIDENTIAL and will be used for research purposes only.

Thank you very much for your co-operation.

NAME		AGE	<u> </u>	ETHNIC	ORIGIN _		
SUBJECT NUMBER	R	BODY	WEIGHT		_ HEIGH	г	-
In the past Y the following			es have y	ou travell	led ASA F	PASSEN	GER in
CARS BUSES COACHES SMALL BOATS SHIPS AEROPLANES TRAINS	NEVER	1	2-3	4-15	16-63	64-255	256+
2. In the past Y PASSENGE					whilst trav	elling AS	A
CARS BUSES COACHES SMALL BOATS SHIPS AEROPLANES TRAINS	NEVER	1	2	3	4-7	8-15	16+
3. In the past YEAR, how many times have you VOMITED whilst travelling AS A PASSENGER in the following types of transport?							
CARS BUSES COACHES SMALL BOATS SHIPS AEROPLANES TRAINS	NEVER	1	2	3	4-7	8-15	16+

4. Do you EVER feel HOT or SWEAT whilst travelling AS A PASSENGER in the following types of transport?						
	NEVER	OCCASIONALLY	OFTEN	ALWAYS		
CARS BUSES COACHES SMALL BOATS SHIPS AEROPLANES TRAINS						
5. Do you EV	ER suffer fron wing types of t	n HEADACHES whilst to ransport?	ravelling AS A	PASSENGER		
	NEVER	OCCASIONALLY	OFTEN	ALWAYS		
CARS						
BUSES COACHES						
SMALL BOATS						
SHIPS AEROPLANES						
TRAINS						
		n LOSS/CHANGE OF S ASSENGER in the follo				
	NEVER	OCCASIONALLY	OFTEN	ALWAYS		
CARS						
BUSES COACHES						
SMALL BOATS						
SHIPS AEROPLANES						
TRAINS						

	NEVER		0.555	
	PASSENGER in the follo	owing types of transport?	•	
1.	Do you EVER Suiter from	IIMOUTH WATERING W	misctravenin	g A S A

	NEVER	OCCASIONALLY	OFTEN	ALWAYS
CARS BUSES COACHES SMALL BOATS SHIPS AEROPLANES TRAINS				

Do you ${\bf EVER}$ feel DROWSY whilst travelling ${\bf AS}$ ${\bf A}$ ${\bf PASSENGER}$ in the following types of transport? 8.

	NEVER	OCCASIONALLY	OFTEN	ALWAYS
CARS BUSES COACHES SMALL BOATS SHIPS AEROPLANES TRAINS				

Do you EVER feel DIZZY whilst travelling AS A PASSENGER in the following 9. types of transport?

	NEVER	OCCASIONALLY	OFTEN	ALWAYS
CARS BUSES COACHES SMALL BOATS SHIPS AEROPLANES TRAINS				

10. Do you EVER suffer from NAUSEA (stomach discomfort, feeling sick) whilst travelling AS A PASSENGER in the following types of transport?							
CARS BUSES COACHES SMALL BO SHIPS AEROPLAI TRAINS	ATS	NEVER	000	ASIONALL	Y	OFTEN	ALWAYS
11. Hav	e you EV wing type	ER VOMIT es of transp	TED whilstoort?	travelling	AS A P	ASSENG	GER in the
CARS BUSES COACHES SMALL BO SHIPS AEROPLAI TRAINS	ATS	NO		YES	DOM	N'T KNO	w
	ıld you av ness?	oid any of	the follow	ing types	of transp	ort beca	use of motion
CARS BUSES COACHES SMALL BO SHIPS AEROPLA TRAINS	ATS	NEVER	000	ASIONALL	Y (OFTEN	ALWAYS

13. Which of the following best describes your SUSCEPTIBILITY to motion sickness?
MUCH LESS THAN AVERAGE LESS THAN AVERAGE AVERAGE MORE THAN AVERAGE MUCH MORE THAN AVERAGE
14. Have you ever suffered from any serious illness or injury?
YES NO
15. Are you under medical treatment or suffering a disability affecting daily life?
YES NO
16. Have you participated in a motion sickness experiment before?
YES NO
If yes, when? Please tick one of the following:
In the last 6 weeks:
In the last year:
In the last 2 years:

A.3. Subject information questionnaire

SUBJECT INFORMATION QUESTIONNAIRE

Anonymity

Your participation in this experiment is anonymous. In all discussions of this work and publications relating to it you will only be identified by subject number. Any data we hold will be managed in accordance with the Data Protection Act.

Section 1 – About You					
	Subject ID				
	Name				
	Age				
	Ethnic orig	in			
	Occupation	n	Staff \ Student		
	Email addr	ess			
Section 2 – I	nvitation to part	icipate in further t	<u>rials</u>		
If you would be willing for us to contact you to invite you, without obligation, to volunteer for further trials, please answer YES to the question below:					
I wish to rec	wish to receive information about further trials YES \ NO				
Section 3 – Anthropometric Data					
Body v	veight		Buttock-popliteal		
Sitting	weight		Sitting knee height		
Standi	ng height		Shoulder breadth		
Sitting	height		Hip breadth		

A.4. Subject instructions

A.4.1. Experiment 1

INSTRUCTION SHEET FOR SUBJECTS

You will be taking part in an experiment investigating the effect of low frequency oscillation on motion sickness.

- A vibration exposure consent and screen form and motion sickness susceptibility questionnaire should be completed.
- If you are wearing a watch, please remove it before entering the cabin.
- When seated in the simulator, please strap yourself in using the belt provided. Please assume a relaxed but upright posture, keeping your hands in your lap and your feet flat on the floor.
- Please put on the headphones and the blindfold supplied.
- When you are ready, the experiment will commence. The experimenter will ask you how you feel
 every minute during the experiment. You should answer with a number selected from the table
 below that corresponds to your feelings. If a rating of 1 or higher is given, the experimenter will
 ask you to indicate what symptoms you are feeling, using the list of motion sickness symptoms
 shown below.

ILLNESS RATING SCALE AND SYMPTOM CHECKLIST

RATING	CORRESPONDING FEELINGS	
0	No symptoms	
1	Any symptoms, however slight	
2	Mild symptoms	
3	Mild nausea	
4	Mild to moderate nausea	
5	Moderate nausea but can continue	
6	Moderate nausea and want to stop	

SYMPTOMS				
YAWNING	DIZZY			
COLD SWEATING	BODILY WARMTH			
NAUSEA	HEADACHE			
STOMACH	INCREASED			
AWARENESS	SALIVATION			
DRY MOUTH	DROWSY			

• The motion will stop either after 30 minutes, or when you have reached a rating of 6.

YOU ARE ABLE TO TERMINATE THE EXPERIMENT AT ANY TIME WITHOUT GIVING A REASON:

The experiment can be stopped using the emergency stop button or by signalling verbally.

- After the motion has stopped, you should remain still. The experimenter will continue to monitor your illness ratings every minute for 15 minutes.
- At the end of the experiment you will be asked to fill out a form asking you which symptoms you felt whilst you were in the cabin.

IF YOU FEEL NAUSEOUS OR UNSTEADY AFTER THE EXPERIMENT, YOU SHOULD NOT DRIVE OR OPERATE MACHINERY UNTIL YOU FEEL ABLE TO DO SO SAFELY.

A.4.2. Experiment 2

INSTRUCTION SHEET FOR SUBJECTS

Thank you for agreeing to take part in this research project. The experiment has been approved by the Human Experimentation Safety and Ethics Committee of the Institute of Sound and Vibration Research at the University of Southampton.

This research aims to investigate the effect of low frequency oscillation on physical discomfort across two seating conditions and two sitting postures. There will be four sessions conducted on four separate days and each session will comprise three tests: equivalent comfort contours (Test 1); relative discomfort (Test 2), and location of discomfort (Test 3). Each session will use one of the following seat arrangements: rigid seat (with backrest), rigid seat (no backrest), train seat (with backrest), train seat (no backrest).

Please read the following instructions carefully.

Preparation phase

- Complete the consent form and health questionnaire
- · Complete motion sickness susceptibility questionnaire
- Complete the training to familiarise yourself with the test procedure

Exposure phase

- Sit comfortably in the seat as guided by the experimenter
- It is important that you maintain a comfortably upright posture with your feet flat on the floor, your hands in your lap and your head pointing straight in front of you
- When you are seated with your back against the backrest please ensure the whole of your back is in contact with the backrest
- Please wear the headphones supplied
- Hold the emergency stop button (this can be pressed at any time during the experiment to stop the motion if you wish, or alternatively you may signal to the experimenter that you wish to stop)

Test 1

- 16-second motion stimuli will be presented in pairs (a reference motion, followed by a test motion), with 5-second intervals between each stimulus.
- The reference motion represents discomfort of 100.
- Your task is to rate the DISCOMFORT caused by the second stimulus (test motion) relative to the discomfort caused by the reference motion (i.e. 100). The reference motion will be the same throughout the session.
- For example, if the test motion causes twice as much discomfort as the reference, then you should assign a value of 200. Likewise, if the test motion causes half as much discomfort as the reference, then you should assign a value of 50.

Test 2

Test 2 will follow the same procedure as test 1, however you will be required to adjust your
posture or seating conditions between the reference (e.g. sitting upright with no backrest contact)
and the test motion (e.g. sitting back against the backrest). The experimenter will provide
guidance for this part of the test.

Test 3

 Here you will be required to indicate the location of the body where you felt the MOST DISCOMFORT for a series of 16-second motion stimuli. A body map is provided for guidance.

A.4.3. Experiment 3

INSTRUCTION SHEET FOR SUBJECTS

Thank you for agreeing to take part in this research project. The experiment has been approved by the Human Experimentation Safety and Ethics Committee of the Institute of Sound and Vibration Research at the University of Southampton.

This research aims to investigate the effect of low frequency lateral, roll and fully-roll compensated lateral oscillation on **PHYSICAL DISCOMFORT**. There will be one session only, which will comprise of two tests: equivalent comfort contours (Test 1); and location of discomfort (Test 2). During the session you will be asked to sit on rigid seat with backrest.

Please read the following instructions carefully.

Preparation phase

- · Complete the consent form and health questionnaire
- Complete motion sickness susceptibility questionnaire
- · Complete the training to familiarise yourself with the test procedure

Exposure phase

- Sit comfortably in the seat as guided by the experimenter
- It is important that you maintain a comfortably upright posture with your feet flat on the floor, your hands in your lap and your head pointing straight in front of you
- Please ensure the whole of your back is in contact with the backrest
- Please wear the headphones supplied
- Please keep your eyes closed throughout the experiment
- Hold the emergency stop button (this can be pressed at any time during the experiment to stop the motion if you wish, or alternatively you may signal to the experimenter that you wish to stop)

Test 1

- Motion stimuli will be presented in pairs (a reference motion, followed by a test motion).
- The reference motion represents discomfort of 100.
- Your task is to rate the DISCOMFORT caused by the second stimulus (test motion) relative to the DISCOMFORT caused by the reference motion (i.e. 100). The reference motion will be the same throughout the session.
- For example, if the test motion causes **twice** as much discomfort as the reference, then you should assign a value of **200**. Likewise, if the test motion causes *half* as much discomfort as the reference, then you should assign a value of *50*.

Test 2

Here you will be required to indicate the LOCATION(S) of the body where you felt DISCOMFORT
for a series of motion stimuli. A body map is provided for guidance. Please state each location
where discomfort is felt, with a corresponding number between 1 and 10 indicating the severity of
discomfort at each location (1 indicates mild discomfort, 10 indicates extreme discomfort).

A.4.4. Experiment 4

INSTRUCTION SHEET FOR SUBJECTS

Thank you for agreeing to take part in this research project. The experiment has been approved by the Human Experimentation Safety and Ethics Committee of the Institute of Sound and Vibration Research at the University of Southampton.

This research aims to investigate the effect of low frequency lateral, roll and fully-roll compensated lateral oscillation on **PHYSICAL DISCOMFORT**. There will be two sessions which will comprise of four tests: equivalent comfort contours (Test 1); location of discomfort (Test 2), relative discomfort (Test 3), objective measurements (Test 4). One session will involve sitting on a rigid seat, and the other will involve sitting on a foam seat.

Please read the following instructions carefully.

Preparation phase

- Complete the consent form and health questionnaire
- Complete the training to familiarise yourself with the test procedure

Exposure phase

- · Sit comfortably in the seat as guided by the experimenter
- It is important that you maintain a comfortably upright posture with your feet flat on the floor, your hands in your lap and your head pointing straight in front of you
- Please wear the headphones supplied
- · Please keep your eyes closed throughout the experiment
- Hold the emergency stop button (this can be pressed at any time during the experiment to stop the motion if you wish, or alternatively you may signal to the experimenter that you wish to stop)

Test 1

- A series of individual motion stimuli will be presented in turn.
- Your task is to rate the DISCOMFORT caused by each of the motion stimuli by assigning a numerical value.
- It is important that your ratings are proportional to the discomfort experienced for each stimulus.
- For example, if you feel that one motion caused twice as much discomfort as another, then the ratings should reflect this (i.e. the motions may be rated as 100 and 200).
- You may use any number you feel is appropriate, but it is advised that 100 should be taken as the 'mid-point' value.

Test 2

Here you will be required to indicate the LOCATION(S) of the body where you feel
DISCOMFORT for a series of motion stimuli. A body map is provided for guidance. Please state
each location where discomfort is felt.

Test 3

 This will follow the same procedure as test 1, but two different seats will be tested in the same session.

Test 4

• This will follow the same procedure as test 1, but some objective measurements of rotational acceleration at the seat-body interface will be taken at the same time.

A.4.5. Experiment 5

INSTRUCTION SHEET FOR SUBJECTS

Thank you for agreeing to take part in this research project. The experiment has been approved by the Human Experimentation Safety and Ethics Committee of the Faculty of Engineering and the Environment at the University of Southampton.

This research aims to investigate the effect of low frequency lateral and roll oscillations on **PHYSICAL DISCOMFORT**. There will be three sessions on separate days, which will comprise of three tests: equivalent comfort contours (Test 1); relative discomfort (Test 2); location of discomfort (Test 3). In each session you will be seated on a rigid seat with either no backrest, a low backrest or a high backrest. Please read the following instructions carefully.

Preparation phase

- Complete the consent form and health questionnaire
- Complete the training to familiarise yourself with the test procedure

Exposure phase

- Sit comfortably in the seat as guided by the experimenter
- It is important that you maintain a comfortably upright posture with your feet flat on the floor, your hands in your lap and your head pointing straight in front of you
- Please wear the headphones supplied
- Please keep your eyes closed throughout the experiment
- Hold the emergency stop button (this can be pressed at any time during the experiment to stop the motion if you wish, or alternatively you may signal to the experimenter that you wish to stop)

Test 1

- A series of individual motion stimuli will be presented in turn.
- Your task is to rate the **DISCOMFORT** caused by each of the motion stimuli by assigning a numerical value.
- It is important that your ratings are **proportional** to the discomfort experienced for each stimulus.
- For example, if you feel that one motion caused twice as much discomfort as another, then the ratings should reflect this (i.e. the motions may be rated as 100 and 200).
- You may use any number you feel is appropriate, but it is advised that 100 should be taken as the 'mid-point' value.

Test 2

• This will follow the same procedure as test 1, but two different sitting postures will be tested in the same session (i.e. with backrest and without backrest).

Test 3

Here you will be required to indicate the LOCATION(S) of the body where you feel
 DISCOMFORT for a series of motion stimuli. A body map is provided for guidance. Please state
 each location where discomfort is felt.

Thank you for taking part in this experiment

A.5. MATLAB scripts: Motion generation

A.5.1. 12-m tilting and translating cabin

LONGSTROKESIGNAL.M

```
%longstrokesignal - issue 2.0 (20/05/10) - HVLab HRV Toolbox
%-----
%Script to create equalised horizontal and rotational input motions
for
% HFRU 12m simulator using HVLab HRV toolbox functions. Requires
% hvlongstrokesignal.m and hvlstiltdrive.m.
% Written by CHL (03/03/2010).
% Modified by CHL (03/03/2010) to use the new function hvlstiltdrive.m
      which incorporates fnlcalc.m
F = input('Oscillation frequency [Hz] = {0.2} ');
if isempty(F), F = 0.2; end
Amax = input('Peak acceleration [m/s^2] = \{1.0\}');
if isempty(Amax), Amax = 1.0; end
Dmax = Amax / ((2*pi*F)^2);
% Dmax = input('Peak displacement [m] = {1.5} ');
% if isempty(Dmax), Dmax = 1.5; end
Tfinal = input('Signal duration [minutes] = {30.0} ');
if isempty(Tfinal), Tfinal = 30.0; end
Fs = input('Sample rate [samples/sec] = {50} ');
if isempty(Fs), Fs = 50; end
% H = input('Roll height = {0.4} ');
% if isempty(H), C = 0.4; end
C = input('Proportion of compensation = {1.0} ');
if isempty(C), C = 1.0; end
C = max(C, 1.0);
outfile = input('Drive signal filename = {driveSig} ');
if isempty(outfile), outfile = 'driveSig'; end
HV.TINCREMENT = 1/Fs;
Tm = 1.5;
                       % duration of test signal
Tscale = 2.1;
                      % initial translational scaling factor (V/ms^-
                       % initial scaling factor for gears and pinion
Rscale = 0.0245;
[drive, target] = hvlongstrokesignal(F, C, Dmax, Tm, Fs, Tscale,
Rscale); % generate 2min test signal
% response = input('*****ENABLE TRANSLATION AND PRESS ENTER TO OUTPUT
TEST MOTION *****');
% indata = hvdata(0, drive, 1);
[incr, len] = hvxstats(drive(1));
HV.DURATION = len + 0.25;
hvwrite('drive.das', drive);
hvdatawin;
```

```
response = input('**** ENABLE TRANSLATION, OUTPUT drive.das & INPUT
indata.das *****');
response = input('************** PRESS ENTER TO CONTINUE
indata = hvread('indata.das');
infilt = indata(1);
infilt(2) = hvweight(indata(1), 'wf');
infilt(3) = hvlobutter(indata(1), F*1.4142, 10);
infilt(4) = hvhibutter(indata(1), F*1.4142, 10);
infilt(5) = hvlobutter(target(3), F*1.4142, 10);
inrms = hvstats(infilt);
Tscale = Tscale * inrms(5) / inrms(3)
HVFUNPAR ('ACQUIRED TRANSLATIONAL ACCELERATION SIGNAL');
HVFUNPAR('-----');
HVFUNPAR('target r.m.s. acceleration', inrms(5), 'm/s^2');
HVFUNPAR('unfiltered r.m.s. acceleration', inrms(1), 'm/s^2');
HVFUNPAR('fundamental r.m.s. acceleration', inrms(2), 'm/s^2');
HVFUNPAR('distortion', 100*inrms(4)/inrms(3), '%');
HVFUNPAR('Revised Tscale', Tscale , 'V/ms^-2');
HVFUNPAR('=======');
hvgraph(infilt);
% response = input('*****ENABLE ROTATION AND PRESS ENTER TO OUTPUT
TEST MOTION ** * * * ');
% indata = hvdata(0, drive, 1);
[incr, len] = hvxstats(drive(2));
HV.DURATION = len + 0.25;
hvwrite('drive.das', drive);
% hvdatawin;
response = input('***** ENABLE ROTATION, OUTPUT drive.das & INPUT
indata.das ******');
indata = hvread('indata.das');
infilt = hvcreate(asin(indata(2).y./9.81)*360/(2*pi), indata(2).x,
'est. angle', 'deg', 's')
infilt(2) = hvweight(infilt, 'wf');
infilt(3) = hvlobutter(infilt(1), F*1.4142, 10);
infilt(4) = hvhibutter(infilt(1), F*1.4142, 10);
infilt(5) = hvlobutter(target(2), F*1.4142, 10);
inrms = hvstats(infilt);
Rscale = Rscale * inrms(5) / inrms(3)
HVFUNPAR ('ACQUIRED TILT SIGNAL');
HVFUNPAR('=======');
HVFUNPAR('target r.m.s. angle', inrms(5), 'deg');
HVFUNPAR('unfiltered r.m.s. acceleration', inrms(1), 'deg');
HVFUNPAR('fundamental r.m.s. acceleration', inrms(2), 'deg');
HVFUNPAR('distortion', 100*inrms(4)/inrms(3), '%');
HVFUNPAR('Revised Rscale', Rscale);
HVFUNPAR('-----');
```

```
hvgraph(infilt);
response = input('*****PRESS ENTER TO CREATE DRIVE SIGNALS*****');
[drive, target] = hvlongstrokesignal(F, C, Dmax, Tm, Fs, Tscale,
Rscale); % generate 2min test signal
hvwrite([outfile ' cal' '.das'], drive);
[drive, target] = hvlongstrokesignal(F, C, Dmax, Tfinal, Fs, Tscale,
Rscale); % generate full test signal
hvwrite([outfile '.das'], drive);
[incr, len] = hvxstats(drive(1));
HV.DURATION = len + 0.25;
```

HVLONGSTROKESIGNAL.M

```
%hvlongstrokesignal - issue 2.0 (20/05/10) - HVLab HRV Toolbox
%[drivesig, targetSig] = hvlongstrokesignal(frequency, pcomp, dmax,
duration, srate, tscale, rscale);
% Creates horizontal and rotational input motions for 12m horizontal
% simulator according to user specifications. Requires hvlstiltdrive.m
t.o
% calculate the tilt drive.
% drivesig = name of two-channel HVLab data structure:
               chnl 1 contains the translational drive signal in
응
volts
              chnl 2 contains the rotational drive signal in volts
% targetOut = name of four-channel HVLab data structure [Dt, Dr, At,
% frequency = oscillation frequency in Hz
% pcomp = proportion of compensation (between 0 and 1)
% dmax = peak displacement in translation in m
% duration = duration of signals in minutes
% srate = sampling rate in s/s
% tscale = translational scaling factor (Volts/(m/s))
% rscale = rotational scaling factor
function [driveSig, targetSig] = hvlongstrokesignal(F, C, Dmax, Tm,
Fs, Tscale, Rscale)
global HV; %allow access to global parameter structure
if nargin < 1, F = 0.16; end
if nargin < 2, C = 1.0; end
if nargin < 3, Dmax = 1.0; end
if nargin < 4, Tm = HV.DURATION/60; end</pre>
if nargin < 5, Fs = 1/HV.TINCREMENT; end</pre>
if nargin < 6, Tscale = 2.0; end</pre>
if nargin < 7, Rscale = 0.0245; end</pre>
%Force the signal to an integer number of wavelengths, W
           % Nominal duration in s
T = 60 * Tm;
W = ceil(T*F);
                       % Number of whole wavelengths
T = W/F;
                       % Duration of signal corrected to whole
wavelengths
```

```
N = round(T*Fs);
                       % No. of samples in padded signal
Fs = N/T;
                       % Sampling rate corrected to whole samples
Drms = Dmax/sqrt(2);
                      % RMS amplitude
taperLen = 5/(2*F);
                      % Duration of cosine tapers
% Generate displacement signal
Dt = hvsine(F, T, Drms, 1/Fs, 'translation displacement', 'm', 's',
taperLen);
% Pad ends with 1s of zeroes
Dt = hvpad(Dt, Fs, Fs, 'points'); % add 1s of zero padding to ends
% Differentiate to get velocity signal
Vt = hvdifferentiate(Dt);
Vt.title = 'translation velocity';
% Differentiate to get acceleration signal
At = hvdifferentiate(Vt);
At.title = 'translation acceleration';
% Generate tilt belt drive signal
%[Vrbelt, Dr, As] = hvlstiltdrive(At, C, H);
[Vrbelt, Dr, As] = hvlstiltdrive(At, C);
% Apply scaling to get drive signals
driveSig(1) = hvprod(Vt, Tscale); % Trans scaling factor = 2.0
Volts/(m/s)
driveSig(1).yunit = 'V';
driveSig(1).title = 'translation drive signal';
driveSig(2) = hvdiv(Vrbelt, Rscale); % 0.0245 = scaling factor for
gears and pinion etc.
driveSig(2).yunit = 'V';
driveSig(2).title = 'rotation drive signal';
HVFUNPAR('');
HVFUNPAR ('DETAILS OF GENERATED SIGNAL');
HVFUNPAR('=========;);
HVFUNPAR('Frequency of signal', F, 'Hz');
HVFUNPAR('Duration of signal', T, 's');
HVFUNPAR('Corrected sampling rate', Fs, 's/s');
HVFUNPAR('Peak transln displacement', max(Dt.y), 'm');
HVFUNPAR('Peak transln velocity', max(Vt.y), 'm/s');
HVFUNPAR('Peak transln acceleration', max(At.y), 'm/s^2');
HVFUNPAR('Compensation', 1.035*100, '%');
HVFUNPAR('Peak angular displacement', max(Dr.y), 'degrees');
HVFUNPAR('=======');
sig = [Dt Dr driveSig(1) driveSig(2) At As ];
hvgraph(sig);
targetSig = [Dt Dr At As ];
HVLSTILTDRIVE.M
```

```
%hvlstiltdrive - issue 1.0 (15/03/10) - HVLab HRV Toolbox
%-----
%[dasVbelt, dasDr, dasAs] = hvlstiltdrive(dasAt, hcr)
%Creates a rotational drive signal for the HFRU 12m simulator so as to
```

```
% provide a given degree of acceleration compensation for the
translational
% trolley acceleration
   dasVbelt = new HVLab data structure containing the belt velocity
           = new HVLab data structure containing rotational
displacement
               in radians
             = new HVLab data structure containing the subjective
   dasAs
              acceleration in m/s^2
            = single-channel HVLab data structure containing the
  dasAt
             translational trolley acceleration in m/s^2
% pcomp
            = proportion of acceleration compensation (0-1)
  hcr
            = height of centre-of-roll above table (defaults to
0.5296)
% Written by CHL (15/03/2010) based on original functions by Barney
Donohew
function [dasVbelt, dasDr, dasAs] = hvlstiltdrive(dasAt, pcomp, hcr)
error (HVFUNSTART ('GENERATE ROTATIONAL DRIVE FOR 12m SIMULATOR',
dasAt)); % show header and abort if input is not a valid structure
if length(dasAt) > 1; error('Input must be a single-channel data
structure'); end;
if nargin < 3; hcr = 0.5296; end; % default centre-of-roll height
xincr = dasAt.x(2) - dasAt.x(1);
% Generate rotational displacement signal
alpha = atan(dasAt.y / 9.81);
ar = sqrt(dasAt.y .* dasAt.y + 9.81^2);
dr = asin((1-1.035)*dasAt.y./ar) - alpha; % rotational displacement
in radians
dasDr = HVMAKESTRUCT('rotation angle', 'deg', 's', 1, 0, [1/xincr 0 0
0 0 0], dasAt.x);
dasDr.y = dr.*360/(2*pi);
% Generate velocity drive signal
dasVbelt = HVMAKESTRUCT('rotation belt velocity', 'm', 's', 1, 0,
[1/xincr 0 0 0 0 0], dasAt.x);
dasVbelt.y = gradient(fnlcalc(hcr, dr), xincr); % belt velocity
% Compute subject lateral acceleration
dasAs = HVMAKESTRUCT('subjective acceleration', 'm/s^2', 's', 1, 0,
[1/xincr 0 0 0 0 0], dasAt.x);
dasAs.y = dasAt.y + 9.81*sin(dr);
HVFUNPAR('Height of roll centre', hcr, 'm');
HVFUNPAR('Duration of signal', dasAt.x(length(dasAt.x)), 's');
HVFUNPAR('Sampling rate', 1/xincr, 's/s');
HVFUNPAR('Peak transln acceleration', max(dasAt.y), 'm/s^2');
HVFUNPAR('Acceleration compensation', 1.035*100, '%');
HVFUNPAR('Peak angular displacement', max(dasDr.y), dasDr.yunit);
HVFUNPAR('Peak subjective acceleration', max(dasAs.y), dasAs.yunit);
```

return

```
$_____
=====
function dl = fnlcalc(h, ang)
%Calculates change in belt length, dl, required for a given rotational
%displacement, ang
a = 0.962;
b = -0.6503;
c = 0.3022;
r = sqrt(a^2+h^2);
theta = ang + atan(a/h);
x0 = c;
x1 = a;
x2 = r*sin(theta);
y0 = b;
y1 = 0;
y2 = -r*cos(theta) + h;
deltaX1 = x1 - x0;
deltaX2 = x2 - x0;
deltaY1 = y1 - y0;
deltaY2 = y2 - y0;
11 = sqrt(deltaX1^2 + deltaY1^2);
12 = sqrt(deltaX2.^2 + deltaY2.^2);
d1 = 12 - 11;
return
```

A.5.2. 1-m horizontal simulator

```
% Create 1-channel motion signals for 1-m horizontal simulator
% Written by George F. Beard (November, 2010)
clear;
hvlab
load fr la; % matrix containing desired frequency, magnitude,
duration, taper and padding information
sr = 512; % sample rate
scales = ones(6,1);
scales = scales*10; % scaling factor
units = 'm/s^2'; % it has to be noticed that VERTCAT does not allow to
have different length columns
names = 'Acceleration Y'; % channel name
comments = 'na';
Signals = zeros(length(fr_la), 5); % matrix for motion statistics
% Generate lateral motion signals
for n = 1:length(fr la) % number of motion stimuli required
```

```
A = hvpad(hvsine(fr la(n,1), fr la(n,4), fr la(n,7), 1/sr, 'y-
input', 'm/s^2', 's'), fr la(n,6), fr la(n,6)); % pure sine wave
    B = hvpad(hvsine(fr la(n,5), fr la(n,4), 1, 1/sr, 'y-input',
'm/s^2', 's'), fr_la(n,6), fr_la(n,6)); % half-sine
    Sig = hvprod(A, B); % product of A and B gives transient waveform
    At = hvprod(A, B);
    Vt = hvintegrate(At); % calculate velocity waveform
    Dt = hvintegrate(Vt); % calculate displacement waveform
    [~, maximum, minimum, ~, rms, ~] = hvstats(At); % calculate
acceleration statistics
    if maximum > abs(minimum);
       peak = maximum;
    elseif maximum < abs(minimum);</pre>
        peak = abs(minimum);
    end
    Signals (n,1) = fr la(n,1); % save acceleration statistics
    Signals(n,2) = peak;
    Signals(n,3) = rms;
    [~, maximum, minimum, ~, rms, ~] = hvstats(Vt); % calculate
velocity statistics
    if maximum > abs(minimum);
       peak = maximum;
    elseif maximum < abs(minimum);</pre>
        peak = abs(minimum);
    end
    Signals(n,4) = peak; % save velocity statistics
    [~, maximum, minimum, ~, rms, ~] = hvstats(Dt); % calculate
displacement statistics
    if maximum > abs(minimum);
        peak = maximum;
    elseif maximum < abs(minimum);</pre>
        peak = abs(minimum);
    end
    Signals(n,5) = peak; % save displacement statistics
    savefile1 = 'Signals';
    save(savefile1, 'Signals'); % save statistics matrix
    savefile2 = ['LAT ' num2str(fr la(n,1)) 'Hz ' num2str(fr la(n,2))
'rmsacc.mat' ];
    save(savefile2, 'Sig');
    out = zeros(length(Sig.y), 1); % as many rows as the length of
signal y axis, one coloumn for y input (only one channel needed).
```

```
out(:,1) = Sig.y;

filename = ['LAT_' num2str(fr_la(n,1)) 'Hz_' num2str(fr_la(n,2))
'rmsacc.sef' ]; % file naming system
   WriteFile(filename, sr, names, scales, units, out(:,:), comments);
   hvexportsef(filename, Sig, scales, comments); % export motion
signal as .sef format
end
```

A.5.3. 6-axis simulator

```
% Create 6-channel motion signals for generating lateral motion
% Written by George F. Beard (February 2011)
clear;
load tran3; % matrix containing desired frequency, magnitude,
duration, taper and padding information
sr = 512; % sample rate
scales = ones(6,1);
scales = scales*10; % scaling factor
units = ['m/s^2';'m/s^2';'m/s^2';'r/s^2';'r/s^2']; % it has to
be noticed that VERTCAT does not allow to have different length
columns
names = ['Acceleration X'; 'Acceleration Y'; 'Acceleration Z';
'Acceleration R'; 'Acceleration P'; 'Acceleration W']; % channel names
comments = 'na';
% [signal] = hvsine(frequency, duration, magnitude, increment, title,
yunit, xunit, taperlen)
LATERAL = zeros(length(tran3),6);
% Generate lateral motion signals
for n = 1:length(tran3) % number of motion stimuli required
    A = hvpad(hvsine(tran3(n,2), tran3(n,10), 0, 1/sr, 'x-input',
'm/s^2', 's'), tran3(n,11), tran3(n,11)); % x-channel (zero)
   B1 = hvpad(hvsine(tran3(n,2), tran3(n,10), tran3(n,4), 1/sr, 'y-
input', m/s^2', s'), tran3(n,11), tran3(n,11)); % pure sine wave
    B2 = hvpad(hvsine(tran3(n,13), tran3(n,10), 1, 1/sr, 'y-input',
'm/s^2', 's'), tran3(n,11), tran3(n,11)); % half sine
    B = hvprod(B1, B2); % y-channel
    C = hvpad(hvsine(tran3(n,2), tran3(n,10), 0, 1/sr, 'z-input',
'm/s^2', 's'), tran3(n,11), tran3(n,11)); % z-channel (zero)
    D = hvpad(hvsine(tran3(n,2), tran3(n,10), 0, 1/sr, 'roll-input',
'r/s^2', 's'), tran3(n,11), tran3(n,11)); % roll-channel (zero)
   E = hvpad(hvsine(tran3(n,2), tran3(n,10), 0, 1/sr, 'pitch-input',
'r/s^2', 's'), tran3(n,11), tran3(n,11)); % pitch-channel (zero)
```

```
F = hvpad(hvsine(tran3(n,2), tran3(n,10), 0, 1/sr, 'yaw-input',
'r/s^2', 's'), tran3(n,11), tran3(n,11)); % yaw-channel (zero)
    out(1) = A; % assign channels
    out(2) = B;
    out(3) = C;
    out(4) = D;
    out(5) = E;
    out(6) = F;
    filename = ['LAT ' num2str(tran3(n,1)) '' ]; % file naming system
    hvexportsef(filename, out, scales, comments) % export motion
signal as .sef format
    [~, maximum, minimum, ~, rms, ~] = hvstats(out(2)); % calculate
acceleration statistics
    if maximum > abs(minimum);
        peak acc = maximum;
    else peak acc = abs(minimum);
    end
   LATERAL(n,1) = tran3(n,1); % save acceleration statistics
   LATERAL(n,2) = tran3(n,2);
   LATERAL(n,3) = peak acc;
   LATERAL (n, 4) = rms;
   velocity = hvintegral(out(2)); % calculate velocity waveform
    [~, maximum, minimum, ~, ~, ~] = hvstats(velocity(2)); % calculate
velocity statistics
    if maximum > abs(minimum);
       peak vel = maximum;
    else peak vel = abs(minimum);
    end
    LATERAL(n,5) = peak vel;
    displacement = hvintegral(velocity); % calculate displacement
waveform
    [~, maximum, minimum, ~, ~, ~] = hvstats(displacement(2)); %
calculate displacement statistics
    if maximum > abs(minimum);
       peak disp = maximum;
    else peak disp = abs(minimum);
    end
    LATERAL(n,6) = peak disp; % save displacement statistics
    savefile1 = 'LATERAL';
```

```
save(savefile1, 'LATERAL'); % save statistics matrix
end
clear;
hvlab
load tran3; % matrix containing desired frequency, magnitude,
duration, taper and padding information
sr = 512; % sample rate
scales = ones(6,1);
scales = scales*10; % scaling factor
units = ['m/s^2';'m/s^2';'m/s^2';'r/s^2';'r/s^2']; % it has to
be noticed that VERTCAT does not allow to have different length
columns
names = ['Acceleration X'; 'Acceleration Y'; 'Acceleration Z';
'Acceleration R'; 'Acceleration P'; 'Acceleration W']; % channel names
comments = 'na';
% [signal] = hvsine(frequency, duration, magnitude, increment, title,
yunit, xunit, taperlen)
ROLL = zeros(length(tran3),6);
% Generate roll motion signals
for n = 1:length(tran3) % number of motion stimuli required
    A = hvpad(hvsine(tran3(n,2), tran3(n,10), 0, 1/sr, 'x-input',
'm/s^2', 's'), tran3(n,11), tran3(n,11)); % x-channel (zero)
   B = hvpad(hvsine(tran3(n,2), tran3(n,10), 0, 1/sr, 'y-input',
'm/s^2', 's'), tran3(n,11), tran3(n,11)); % y-channel (zero)
    C = hvpad(hvsine(tran3(n,2), tran3(n,10), 0, 1/sr, 'z-input',
'm/s^2', 's'), tran3(n,11), tran3(n,11));
    D1 = hvpad(hvsine(tran3(n,2), tran3(n,10), tran3(n,4), 1/sr,
'roll-input', 'd', 's'), tran3(n,11), tran3(n,11)); % pure sine wave
   D2 = hvpad(hvsine(tran3(n,13), tran3(n,10), 1, 1/sr, 'roll-input',
'd', 's'), tran3(n,11), tran3(n,11)); % half sine
   D3 = hvprod(D1, D2);
    D4 = tran3(n,8); % Correction factor
    D5 = hvprod(D3, 1/D4);
    D = hvprod(D5, -tran3(n, 14)); % roll-channel
    D.title = 'roll-input';
    D.yunit = 'r/s^2';
    E = hvpad(hvsine(tran3(n,2), tran3(n,10), 0, 1/sr, 'pitch-input',
'r/s^2', 's'), tran3(n,11), tran3(n,11)); % pitch-channel
    F = hvpad(hvsine(tran3(n,2), tran3(n,10), 0, 1/sr, 'yaw-input',
'r/s^2', 's'), tran3(n,11), tran3(n,11)); % yaw-channel
    out(1) = A; % assign channels
    out(2) = B;
    out(3) = C;
    out(4) = D;
    out(5) = E;
    out(6) = F;
```

```
filename = ['ROLL ' num2str(tran3(n,1)) '' ]; % file naming
system
    hvexportsef(filename, out, scales, comments) % export motion
signal as .sef format
    [\sim, maximum, minimum, \sim, rms roll, \sim] = hvstats(out(4)); %
calculate acceleration statistics
    if maximum > abs(minimum);
       peak roll = maximum;
    else peak roll = abs(minimum);
    end
    ROLL(n,1) = tran3(n,1); % save acceleration statistics
    ROLL(n,2) = tran3(n,2);
    ROLL(n,3) = peak_roll;
   ROLL(n,4) = rms roll;
    velocity = hvintegral(out); % calculate velocity waveform
    [~, maximum, minimum, ~, ~, ~] = hvstats(velocity(2)); % calculate
velocity statistics
    if maximum > abs(minimum);
       peak vel = maximum;
    else peak vel = abs(minimum);
    end
   ROLL(n,5) = peak_vel;
    displacement = hvintegral(velocity); % calculate displacement
waveform
    [~, maximum, minimum, ~, ~, ~] = hvstats(displacement(2)); %
calculate displacement statistics
    if maximum > abs(minimum);
        peak disp = maximum;
    else peak disp = abs(minimum);
    ROLL(n,6) = peak disp; % save displacement statistics
    savefile1 = 'ROLL';
    save(savefile1, 'ROLL'); % save statistics matrix
end
clear;
hvlab
load tran3; % matrix containing desired frequency, magnitude,
duration, taper and padding information
```

```
sr = 512; % sample rate
scales = ones(6,1);
scales = scales*10; % scaling factor
units = ['m/s^2';'m/s^2';'m/s^2';'r/s^2';'r/s^2']; % it has to
be noticed that VERTCAT does not allow to have different length
columns
names = ['Acceleration X'; 'Acceleration Y'; 'Acceleration Z';
'Acceleration R'; 'Acceleration P'; 'Acceleration W']; % channel names
comments = 'na';
% [signal] = hvsine(frequency, duration, magnitude, increment, title,
yunit, xunit, taperlen)
% For Combined lateral and roll signals
COMB = zeros(length(tran3),12);
% [signal] = hvsine(frequency, duration, magnitude, increment, title,
yunit, xunit, taperlen)
% [sdev, maximum, minimum, mean, rms, duration] = hvstats(datastruct)
% [At, Vt, Dt] = hvtransient(cycles, frequency, accel, increment,
title)
for n = 1:length(tran3) % number of motion stimuli required
    A = hvpad(hvsine(tran3(n,2), tran3(n,10), 0, 1/sr, 'x-input',
'm/s^2', 's'), tran3(n,11), tran3(n,11)); % x-channel (zero)
   B1 = hvpad(hvsine(tran3(n,2), tran3(n,10), tran3(n,4), 1/sr, 'y-
input', m/s^2', s'), tran3(n,11), tran3(n,11)); % pure sine wave
    B2 = hvpad(hvsine(tran3(n,13), tran3(n,10), 1, 1/sr, 'y-input',
'm/s^2', 's'), tran3(n,11), tran3(n,11)); % half sine
    B = hvprod(B1, B2); % y-channel
    C = hvpad(hvsine(tran3(n,2), tran3(n,10), 0, 1/sr, 'z-input',
'm/s^2', 's'), tran3(n,11), tran3(n,11));
    D1 = hvpad(hvsine(tran3(n,2), tran3(n,10), tran3(n,4), 1/sr,
'roll-input', 'd', 's'), tran3(n,11), tran3(n,11)); % pure sine wave
   D2 = hvpad(hvsine(tran3(n,13), tran3(n,10), 1, 1/sr, 'roll-input',
'd', 's'), tran3(n,11), tran3(n,11)); % half sine
    D3 = hvprod(D1, D2);
    D4 = tran3(n,8); % Correction factor
    D5 = hvprod(D3, 1/D4);
    D = hvprod(D5, -tran3(n, 14)); % roll-channel
    D.title = 'roll-input';
    D.yunit = 'r/s^2';
    E = hvpad(hvsine(tran3(n,2), tran3(n,10), 0, 1/sr, 'pitch-input',
'r/s^2', 's'), tran3(n,11), tran3(n,11)); % pitch-channel
    F = hvpad(hvsine(tran3(n,2), tran3(n,10), 0, 1/sr, 'yaw-input',
'r/s^2', 's'), tran3(n,11), tran3(n,11)); % yaw-channel
    out(1) = A; % assign channels
    out(2) = B;
    out(3) = C;
    out(4) = D;
    out(5) = E;
    out(6) = F;
```

```
filename = ['COMB ' num2str(tran3(n,1)) '' ]; % file naming
system
    hvexportsef(filename, out, scales, comments) % export motion
signal as .sef format
   [~, maximum, minimum, ~, rms, ~] = hvstats(out(2)); % calculate
lateral acceleration statistics
    if maximum > abs(minimum);
       peak acc = maximum;
    else peak acc = abs(minimum);
    end
    COMB(n,1) = tran3(n,1); % save lateral acceleration statistics
    COMB(n,2) = tran3(n,2);
    COMB(n,3) = peak_acc;
    COMB(n,4) = rms;
    velocity = hvintegral(out(2)); % calculate lateral velocity
waveform
    [~, maximum, minimum, ~, ~, ~] = hvstats(velocity); % calculate
lateral velocity statistics
    if maximum > abs(minimum);
       peak vel = maximum;
    else peak vel = abs(minimum);
    end
    COMB(n, 5) = peak_vel;
    displacement = hvintegral(velocity); % calculate lateral
displacement waveform
    [~, maximum, minimum, ~, ~, ~] = hvstats(displacement); %
calculate lateral displacement statistics
    if maximum > abs(minimum);
       peak_disp = maximum;
    else peak disp = abs(minimum);
    end
    COMB (n, 6) = peak disp; % save lateral displacement statistics
    [~, maximum, minimum, ~, rms roll, ~] = hvstats(out(4)); %
calculate roll acceleration statistics
    if maximum > abs(minimum);
       peak roll = maximum;
    else peak roll = abs(minimum);
    end
```

```
COMB(n,7) = tran3(n,1); % save roll acceleration statistics
    COMB (n, 8) = tran3(n, 2);
    COMB(n, 9) = peak_roll;
    COMB(n, 10) = rms roll;
    velocity2 = hvintegral(out(4)); % calculate roll velocity waveform
    [~, maximum, minimum, ~, ~, ~] = hvstats(velocity2); % calculate
roll velocity statistics
    if maximum > abs(minimum);
       peak vel = maximum;
    else peak vel = abs(minimum);
    end
    COMB(n,11) = peak vel;
    displacement2 = hvintegral(velocity2); % calculate roll
displacement waveform
    [~, maximum, minimum, ~, ~, ~] = hvstats(displacement2); %
calculate roll displacement statistics
    if maximum > abs(minimum);
       peak disp = maximum;
    else peak disp = abs(minimum);
    end
    COMB(n,12) = peak_disp; % save roll displacement statistics
    savefile1 = 'COMB';
    save(savefile1, 'COMB'); % save statistics matrix
```

end

A.6. Subject demographics

Experiment number	Subject number	Gender (M = male, F = female)	Age (years)	Height (m)	Weight (kg)	Ethnicity	
1	1.1	М	26	1.70	60.0	European/Asian	
1	1.2	M	28	1.71	56.0	Chinese	
1	1.3	M	25	1.65	63.0	Chinese	
1	1.4	M	30	1.75	90.0	White Greek	
1	1.5	M	26	1.78	62.0	Chinese	
1	1.6	M	24	1.74	63.0	Chinese	
1	1.7	M	30	1.73	70.0	White Italian	
1	1.8	M	22	1.98	80.0	White British	
1	1.9	M	22	1.71	65.0	Asian	
1	1.10	M	23	1.88	88.0	White British	
1	1.11	M	25	1.68	64.0	Asian	
1	1.12	M	26	1.65	50.0	Chinese	
1	1.13	M	22	1.77	85.0	White British	
1	1.14	M	24	1.72	75.0	Asian	
1	1.15	M	24	1.76	81.0	European	
1	1.16	M	21	1.77	73.0	White British	
1	1.17	M	21	1.85	82.0	White British	
1	1.18	M	23	1.82	62.0	Indian	
1	1.19	M	29	1.67	87.0	White Greek	
1	1.20	M	21	1.77	70.0	White British	
1	1.21	M	21	1.75	81.0	Indian	
1	1.22	M	22	1.77	76.0	White British	
1	1.23	M	23	1.78	67.0	White British	
1	1.24	M	23	1.75	65.0	Asian	
1	1.25	M	25	1.72	63.0	White British	
1	1.26	M	23	1.83	85.0	White British	
1	1.27	M	22	1.67	70.0	White British	
1	1.28	M	23	1.70	55.0	Indian	
1	1.29	M	24	1.67	64.0	Asian	
1	1.30	M	28	1.72	55.0	Chinese	
1	1.31	M	24	1.79	72.0	European	
1	1.32	M	28	1.67	62.0	Indian	

1	1.33	M	24	1.76	59.0	Indian
1	1.34	M	23	1.70	65.0	Asian
1	1.35	M	25	1.70	65.0	Chinese
1	1.36	М	21	1.76	73.0	White European
1	1.37	М	26	1.63	55.0	Chinese
1	1.38	М	23	1.84	74.0	Chinese
1	1.39	М	23	1.70	70.0	Chinese
1	1.40	М	23	1.80	70.0	Chinese
1	1.41	М	27	1.63	60.0	Chinese
1	1.42	М	24	1.69	61.0	White European
1	1.43	М	25	1.80	70.0	White British
1	1.44	М	27	1.71	65.0	Chinese
1	1.45	М	24	1.67	54.0	Pakistani
1	1.46	М	27	1.73	72.0	Chinese
1	1.47	М	22	1.93	70.0	Sri Lankan
1	1.48	М	25	1.83	67.0	Chinese
1	1.49	М	28	1.77	77.5	Chinese
1	1.50	М	26	1.80	70.0	Chinese
1	1.51	M	23	1.98	130.0	Chinese
1	1.52	М	25	1.71	58.0	Chinese
1	1.53	М	21	1.88	85.0	Chinese
1	1.54	M	24	1.78	80.0	Chinese
1	1.55	M	29	1.80	94.0	White/Middle-Eastern
1	1.56	M	28	1.76	70.0	Taiwan
1	1.57	М	24	1.97	160.0	Chinese
1	1.58	M	24	1.76	65.0	Chinese
1	1.59	M	25	1.75	70.0	Indian
1	1.60	M	28	1.63	56.0	Chinese
2	2.1	M	26	1.63	61.0	Chinese
2	2.2	M	29	1.70	56.0	Chinese
2	2.3	M	26	1.78	60.0	Chinese
2	2.4	M	27	1.73	67.0	Chinese
2	2.5	M	24	1.93	105.0	White British
2	2.6	M	22	1.76	74.8	White Mixed
2	2.7	M	26	1.67	60.0	Asian
2	2.8	M	25	1.73	82.0	Indian

2	2.9	М	24	1.84	85.0	White Spanish
2	2.10	М	19	1.78	85.0	White British
2	2.11	М	19	1.85	66.7	White British
2	2.12	М	30	1.67	75.0	Mixed Greek
3	3.1	F	22	1.69	58.0	White French
3	3.2	М	24	1.93	105.0	White British
3	3.3	F	25	1.67	77.0	White Irish
3	3.4	М	30	1.67	75.0	Mixed Greek
3	3.5	F	27	1.63	52.0	Chinese
3	3.6	М	29	1.70	56.0	Chinese
3	3.7	F	24	1.59	65.3	White British
3	3.8	М	30	1.73	63.0	Iranian
3	3.9	F	30	1.66	50.0	Iranian
3	3.10	М	28	1.64	48.0	Chinese
3	3.11	F	30	1.68	51.0	Polish
3	3.12	F	28	1.76	74.0	White Italian
3	3.13	М	27	1.73	67.0	Chinese
3	3.14	F	19	1.73	66.0	White British
3	3.15	М	24	1.65	60.2	White British
3	3.16	М	22	1.86	78.4	White European
3	3.17	F	20	1.66	58.3	Black British
3	3.18	F	28	1.66	59.0	White European
3	3.19	F	28	1.50	47.5	Asian Pakistani
3	3.20	М	27	1.75	67.0	White European
3	3.21	F	30	1.71	57.0	Asian
3	3.22	М	27	1.70	60.0	Mixed Asian/European
3	3.23	М	30	1.76	86.0	White Russian
3	3.24	F	26	1.56	60.0	White Russian
3	3.25	F	26	1.62	55.0	Chinese
3	3.26	F	23	1.64	65.0	White Irish
3	3.27	М	29	1.72	84.0	Chinese
3	3.28	М	22	1.82	83.0	White British
3	3.29	М	26	1.67	60.0	Asian
3	3.30	М	24	1.77	73.4	White British
4	4.1	М	23	1.82	63.0	White British
4	4.2	М	30	1.67	67.7	Greek

4	4.3	М	27	1.78	49.4	Chinese	
4	4.4	М	20	1.82	71.2	White British	
4	4.5	М	25	1.93	83.0	White British	
4	4.6	М	29	1.78	63.0	White British	
4	4.7	М	24	1.82	61.0	Asian/Malay	
4	4.8	М	26	1.72	63.5	Indian	
4	4.9	М	28	1.67	34.4	Chinese	
4	4.10	М	23	1.73	55.7	Chinese	
4	4.11	М	27	1.84	78.0	Brazilian	
4	4.12	М	26	1.72	62.1	Chinese	
4	4.13	М	29	1.72	49.7	Chinese	
4	4.14	М	28	1.80	66.2	Italian	
4	4.15	М	18	1.80	42.7	White British	
4	4.16	М	20	1.88	84.6	Greek	
4	4.17	М	21	1.83	73.3	White British	
4	4.18	М	29	1.70	47.6	Chinese	
4	4.19	М	19	1.80	101.5	White British	
4	4.20	М	32	1.77	63.1	Korean	
5	5.1	М	24	1.72	76.5	Chinese	
5	5.2	М	22	1.80	87.7	White Irish	
5	5.3	М	30	1.70	64.3	Chinese	
5	5.4	М	27	1.68	73.4	Chinese	
5	5.5	М	31	1.67	85.0	Greek	
5	5.6	М	24	1.71	76.9	White British	
5	5.7	М	26	1.76	79.5	Indian	
5	5.8	М	22	1.83	92.0	White British	
5	5.9	М	19	1.75	58.7	White British	
5	5.10	М	33	1.75	71.9	Korean	
5	5.11	М	26	1.69	61.5	Chinese	
5	5.12	М	21	1.87	74.5	White British	
5	5.13	М	29	1.65	47.7	Chinese	
5	5.14	М	20	1.73	69.9	White British	
5	5.15	М	32	1.78	70.7	Bangladeshi	
5	5.16	М	21	1.83	83.0	White British	
5	5.17	М	27	1.78	62.4	Chinese	
5	5.18	М	24	1.83	82.7	Malaysian	

Αı	ope	ndid	es
\neg	JPE	HUIL	,53

5	5.19	M	19	1.76	61.5	White British
5	5.20	M	32	1.76	72.2	Taiwanese
5	5 21	М	25	1 96	112 0	White British

A.7. Load-deflection curve for foam cushion used in Experiment 4

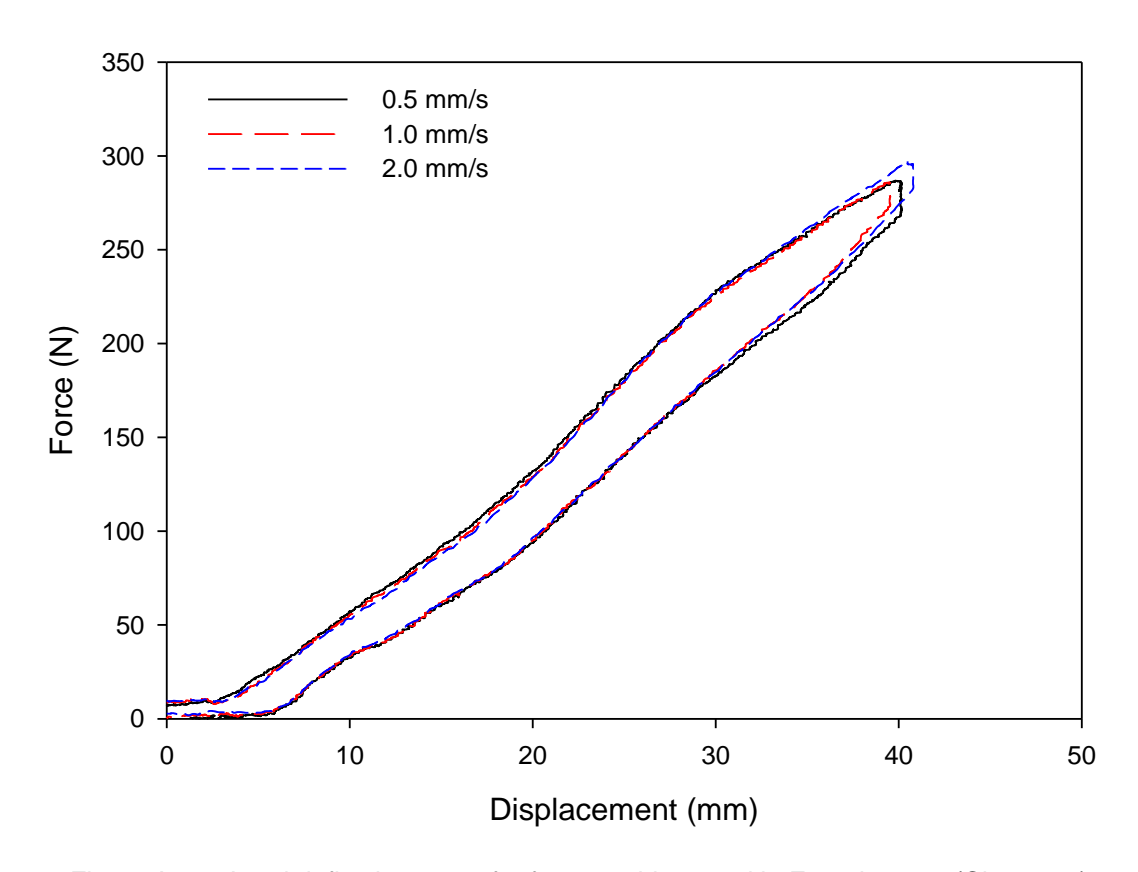


Figure A.8.1. Load deflection curve for foam cushion used in Experiment 4 (Chapter 7). Measurement made with 40% compression at three loading speeds; 0.5, 1.0 and 2.0 mm/s, according to ISO 2439 (2008).

A.8. Frequency-weighted components of lateral, roll and fullyroll compensated lateral motion

In section 9.3, the adjusted weightings W_d and W_e for lateral acceleration and roll acceleration, respectively, were validated through analysis of the root-sums-of-squares of weighted components of lateral oscillation, roll oscillation and fully roll-compensated lateral oscillation. The following figures display the weighted components calculated in order to perform this analysis.

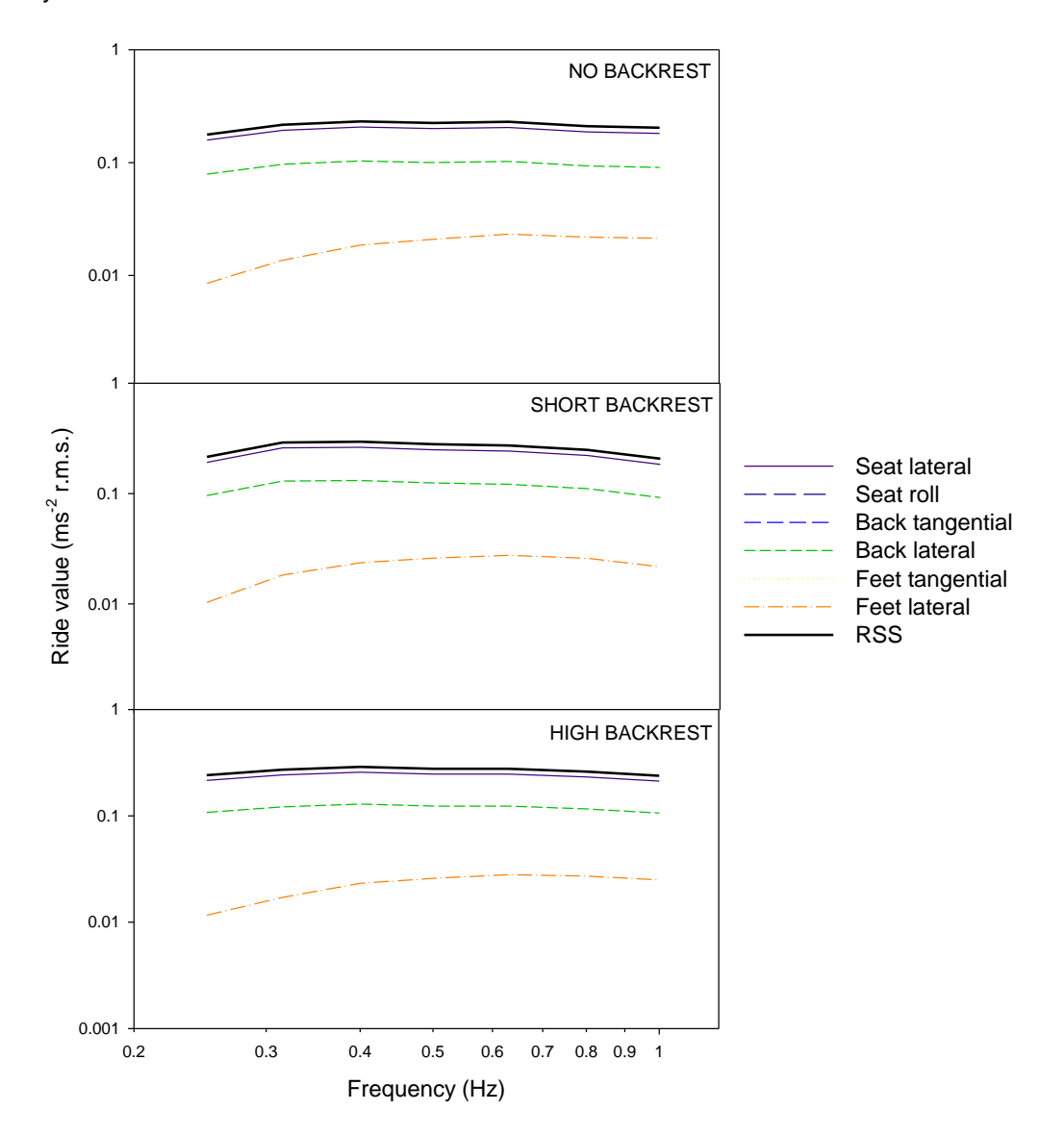


Figure A.8.1. Frequency-weighted components of equivalent comfort contours for lateral oscillation on a seat with no backrest, a short backrest and a high backrest. Data from Experiment 5 (Chapter 8). Components weighted using adjusted weightings $W_{\rm d}$ ' and $W_{\rm e}$ ' defined in section 9.3.

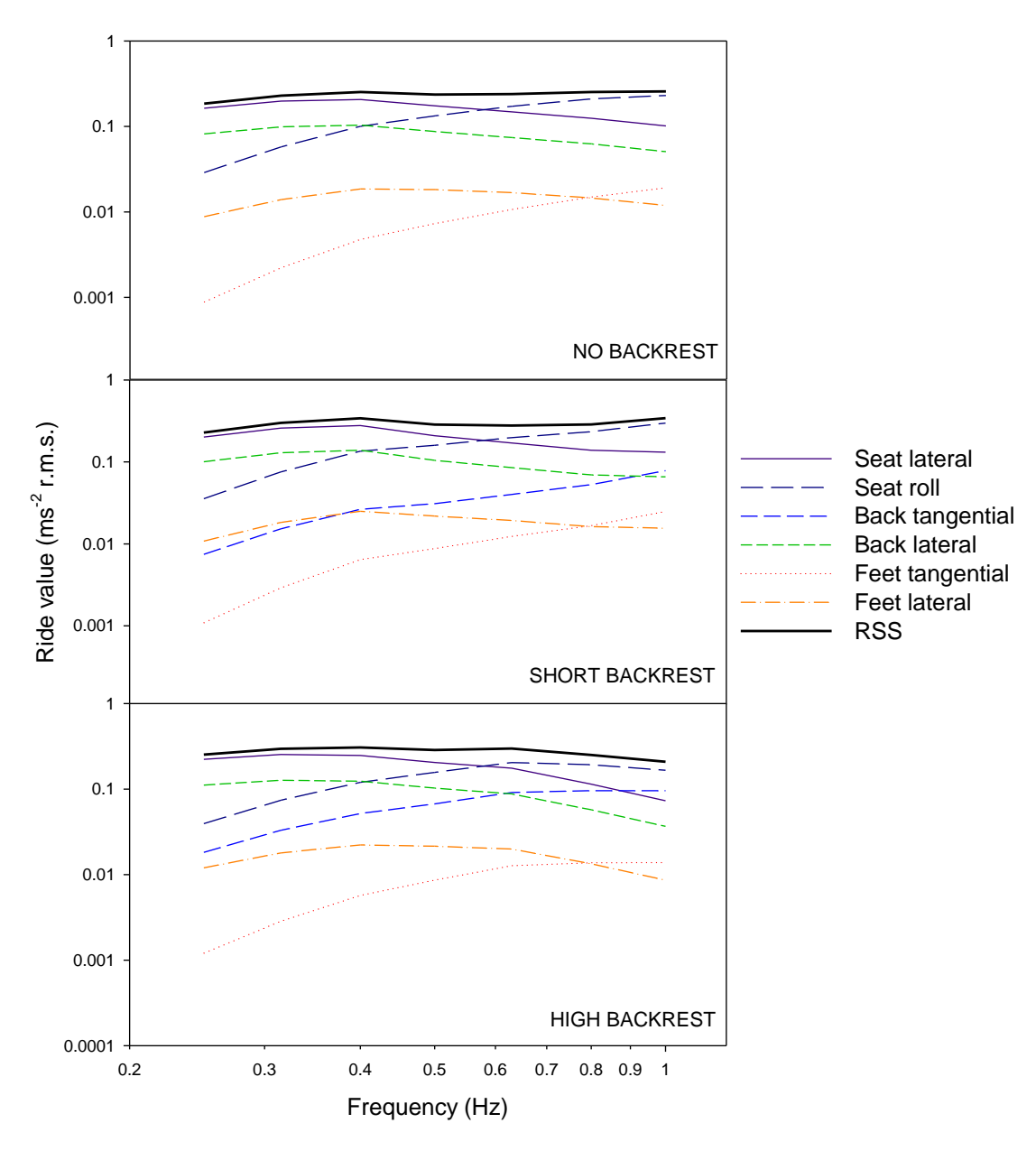


Figure A.8.2. Frequency-weighted components of equivalent comfort contours for roll oscillation on a seat with no backrest, a short backrest and a high backrest. Data from Experiment 5 (Chapter 8). Components weighted using adjusted weightings $W_{\rm d}$ ' and $W_{\rm e}$ ' defined in section 9.3.

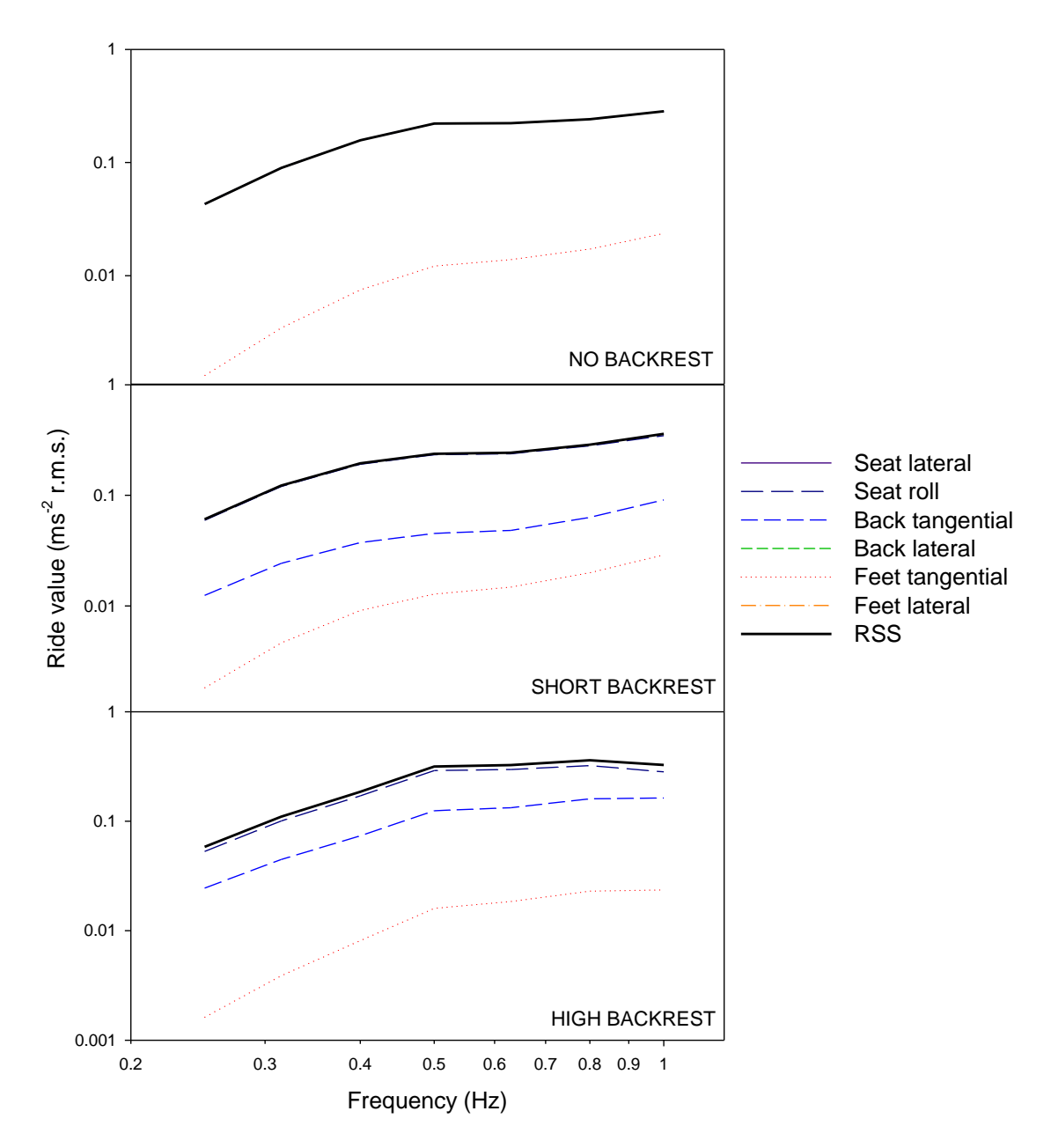


Figure A.8.1. Frequency-weighted components of equivalent comfort contours for fully roll-compensated lateral oscillation on a seat with no backrest, a short backrest and a high backrest. Data from Experiment 5 (Chapter 8). Components weighted using adjusted weightings $W_{\rm d}$ and $W_{\rm e}$ defined in section 9.3.

A.9. Experimental designs

This section provides additional detail on the experimental design for each of the five experiments described in Chapter 4 to Chapter 8.

A.9.1. Experiment 1

Experiment 1 tested 60 subjects in one experimental session only using an independent samples design.

Subjects were assigned alternately to one of the experimental conditions ('seat compensation' or 'head compensation'). Subjects were also classified as 'Asian' or 'European' based on their self-reported ethnic origin. The breakdown of the subject sample into each of these experimental groups is shown in Table A.9.1.

The total duration of each experimental session was approximately one hour.

Total subject sample	Experimental condition	Subject ethnicity		
		Asian		
	Seat compensation	n=20		
n=60 (all male, aged 18-35)	n=30	European		
		n=10		
		Asian		
	Head compensation	n=20		
	n=30	European		
		n=10		
Notes	Subjects assigned alternately to each condition	Ethnicity self-reported by subjects		

Table A.9.1. Breakdown of subject sample used in Experiment 1.

A.9.2. Experiment 2

Experiment 2 tested a total of 12 subjects in four experimental sessions using a repeated measures design. Subjects participated in a single experimental session per day. The breakdown of the subject sample is shown in Table A.9.2.

Each experimental session comprised of three parts. A description of each of these parts is shown in Table A.9.3. The order of the four experimental sessions was balanced using a Latin square (see Table A.9.4.).

The total duration of each experimental session was approximately one hour.

Table A.9.2. Breakdown of subject sample used in Experiment 2.

Total subject sample	Experimental condition			
	Train seat, with backrest (TB)			
	n=12			
	Train seat, no backrest (TN)			
n=12 (all male, aged	n=12			
18-35)	Rigid seat, with backrest (RB)			
,	n=12			
	Rigid seat, no backrest (RN)			
	n=12			
Notes	All subjects exposed to all 4 conditions, across 4 experimental sessions conducted on 4 different days. Order of experimental sessions varied using a Latin square.			

Table A.9.3. Description of part 1, 2 and 3 of each experimental session used in Experiment 2. (TB = Train seat, with backrest; TN = Train seat, no backrest; RB = Rigid seat, with backrest; RN = Rigid seat, no backrest).

Experimental session								
Part 1	Part 2	Part 3						
Equivalent comfort contours constructed using magnitude estimation with reference.	Correction factor calculated using magnitude estimation with reference on two different seats.	Location of discomfort determined using body map diagram.						
One of the 4 conditions tested (TB, TN, RB or RN).	Reference condition: RB.	Experimental condition same as that used in part 1.						
Same condition used for reference and test.	Test condition: same as part 1.							

Table A.9.4. Order of experimental sessions for each of the 12 subjects tested in Experiment 2. (See Table A.9.5. for the key to this table).

0.1.1							Session	numbei	•					
Subject no.	1	2	3	4		1	2	3	4		1	2	3	4
		Par	t 1				Pa	rt 2				Pai	rt 3	
1	ТВ	TN	RB	RN		TBTN	RBTN	RBTB	RBRN		ТВ	TN	RB	RN
2	RN	ТВ	TN	RB		RBRN	TBTN	RBTN	RBTB		RN	ТВ	TN	RB
3	RB	RN	ТВ	TN		RBTB	RBRN	TBTN	RBTN		RB	RN	ТВ	TN
4	TN	RB	RN	ТВ		RBTN	RBTB	RBRN	TBTN		TN	RB	RN	ТВ
5	ТВ	TN	RB	RN		TBTN	RBTN	RBTB	RBRN		ТВ	TN	RB	RN
6	RN	ТВ	TN	RB		RBRN	TBTN	RBTN	RBTB		RN	ТВ	TN	RB
7	RB	RN	ТВ	TN		RBTB	RBRN	TBTN	RBTN		RB	RN	ТВ	TN
8	TN	RB	RN	ТВ		RBTN	RBTB	RBRN	TBTN		TN	RB	RN	ТВ
9	ТВ	TN	RB	RN		TBTN	RBTN	RBTB	RBRN		ТВ	TN	RB	RN
10	RN	ТВ	TN	RB		RBRN	TBTN	RBTN	RBTB		RN	ТВ	TN	RB
11	RB	RN	ТВ	TN		RBTB	RBRN	TBTN	RBTN		RB	RN	ТВ	TN
12	TN	RB	RN	ТВ		RBTN	RBTB	RBRN	TBTN		TN	RB	RN	ТВ
	Note: E	ach su	bjects	partic	ipa	ted in a n	naximum	of one e	xperimen	tal	sessio	n per d	lay.	

Table A.9.5. Key for codes used in Table A.9.4.

Code	Condition			
TB	Train seat, backrest			
TN	Train seat, no backrest			
RB	Rigid seat, backrest			
RN	Rigid seat, no backrest			
TBTN	Reference: TB, Test: TN			
RBTN	Reference: RB, Test: TN			
RBTB	Reference: RB, Test: TB			
RBRN	Reference: RB, Test: RN			

A.9.3. Experiment 3

Experiment 3 tested a total of 30 subjects in a single experimental session using a repeated measures design. The breakdown of the subject sample is shown in Table A.9.6.

Each experimental session comprised of two parts. A description of each of these parts is shown in Table A.9.7.

The total duration of each experimental session was approximately one hour 30 minutes.

Table A.9.6. Breakdown of subject sample used in Experiment 3.

Total subject sample	Seating condition
n=30 (15 male, 15 female, all	Rigid seat with backrest.
aged 18-35)	n=30

Table A.9.7. Description of part 1 and 2 of each experimental session used in Experiment 3.

Experimental session								
Part 1	Part 2							
Equivalent comfort contours constructed using magnitude estimation with reference.	Location of discomfort determined using body map diagram.							

A.9.4. Experiment 4

Experiment 4 tested a total of 20 subjects in two experimental sessions using a repeated measures design. Subjects participated in a single experimental session per day. The breakdown of the subject sample is shown in Table A.9.8.

Each experimental session comprised of four parts. A description of each of these parts is shown in Table A.9.9. The order of the two experimental sessions was balanced using a Latin square (see Table A.9.10.).

The total duration of each experimental session was approximately one hour.

Table A.9.8. Breakdown of subject sample used in Experiment 4.

Total subject sample	Experimental condition
	Rigid seat, no backrest
n=20	n=20
(all male, aged 18-35)	Foam cushion, no backrest
	n=20
Notes	All subjects exposed to both experimental conditions, across 2 experimental sessions on 2 different days. Order of experimental sessions varied using a Latin square.

Table A.9.9. Description of part 1, 2, 3 and 4 of each experimental session used in Experiment 4. (R = Rigid seat, no backrest; F = Foam cushion, no backrest).

	Experime	ntal session	
Part 1	Part 2	Part 3	Part 4
Equivalent comfort contours constructed using magnitude estimation without reference.	Location of discomfort determined using body map diagram.	Correction factor calculated using magnitude estimation without reference on two seats.	Objective measurements of lateral and roll transmissibility.
One of the 2 conditions tested (R or F).	Experimental condition same as that used in part 1.	Both experimental conditions tested sequentially.	Foam cushion only.

Table A.9.10. Order of experimental sessions for each of the twenty subjects tested in Experiment 4. (R = Rigid seat, no backrest; F = Foam cushion, no backrest; R>F = Rigid seat first, Foam cushion second; F>R = Foam cushion first, Rigid seat second).

Subject		Sess	ion 1			Sess	ion 2	
Subject no.	Part	Part	Part	Part	Part	Part	Part	Part
110.	1	2	3	4	1	2	3	4
1	R	R	R>F	F	F	F	F>R	
2	F	F	F>R		R	R	R>F	F
3	R	R	R>F	F	F	F	F>R	
4	F	F	F>R		R	R	R>F	F
5	R	R	R>F	F	F	F	F>R	
6	F	F	F>R		R	R	R>F	F
7	R	R	R>F	F	F	F	F>R	
8	F	F	F>R		R	R	R>F	F
9	R	R	R>F	F	F	F	F>R	
10	F	F	F>R		R	R	R>F	F
11	R	R	R>F	F	F	F	F>R	
12	F	F	F>R		R	R	R>F	F
13	R	R	R>F	F	F	F	F>R	
14	F	F	F>R		R	R	R>F	F
15	R	R	R>F	F	F	F	F>R	
16	F	F	F>R		R	R	R>F	F
17	R	R	R>F	F	F	F	F>R	
18	F	F	F>R		R	R	R>F	F
19	R	R	R>F	F	F	F	F>R	
20	F	F	F>R		R	R	R>F	F
Notes	Ea	ch sub,		rticipate ession			um of c	one

A.9.5. Experiment 5

Experiment 5 tested a total of 21 subjects in three experimental sessions using a repeated measures design. Subjects participated in a single experimental session per day. The breakdown of the subject sample is shown in Table A.9.11.

Each experimental session comprised of three parts. A description of each of these parts is shown in Table A.9.12. The order of the three experimental sessions was balanced using a Latin square (see Table A.9.13.).

The total duration of each experimental session was approximately one hour.

Table A.9.11. Breakdown of subject sample used in Experiment 5.

Total subject sample	Experimental condition		
	Rigid seat, no backrest (NB)		
	n=21		
n=21	Rigid seat, short backrest (SB)		
(all male, aged 18-35)	n=21		
	Rigid seat, high backrest (HB)		
	n=21		
Notes	All subjects exposed to all 3 experimental conditions, across 3 experimental sessions on 3 different days		

Table A.9.12. Description of part 1, part 2 and part 3 of each experimental session used in Experiment 5. (NB = Rigid seat, no backrest; SB = Rigid seat, short backrest; HB = Rigid seat, high backrest).

Exp	erimental sess	ion		
Part 1	Part 2	Part 3		
Equivalent comfort contours constructed using magnitude estimation without reference.	Correction factor calculated using magnitude estimation on two seats.	Location of discomfort determined using body map diagram.		
One of the 3 conditions tested (NB, SB or HB).	Two experimental conditions tested sequentially.	Experimental condition same as that used in part 1.		

Table A.9.13. Order of experimental sessions for each of the twenty-one subjects tested in Experiment 5. (NB = No backrest; SB = Short backrest; HB = High backrest; NB>NB = No backrest first, No backrest second; SB>NB = Short backrest first, No backrest second; NB>HB = High backrest first, No backrest second).

						Session					
Subject no.	1	2	3		1	2	3		1	2	3
110.	Part 1						Part 3		3		
1	NB	SB	НВ		NB>NB	SB>NB	HB>NB		NB	SB	НВ
2	НВ	NB	SB		HB>NB	NB>NB	SB>NB		НВ	NB	SB
3	SB	НВ	NB		SB>NB	HB>NB	NB>NB		SB	НВ	NB
4	NB	SB	НВ		NB>NB	SB>NB	HB>NB		NB	SB	НВ
5	НВ	NB	SB		HB>NB	NB>NB	SB>NB		НВ	NB	SB
6	SB	НВ	NB		SB>NB	HB>NB	NB>NB		SB	НВ	NB
7	NB	SB	НВ		NB>NB	SB>NB	HB>NB		NB	SB	НВ
8	НВ	NB	SB		HB>NB	NB>NB	SB>NB		НВ	NB	SB
9	SB	НВ	NB		SB>NB	HB>NB	NB>NB		SB	НВ	NB
10	NB	SB	НВ		NB>NB	SB>NB	HB>NB		NB	SB	НВ
11	НВ	NB	SB		HB>NB	NB>NB	SB>NB		НВ	NB	SB
12	SB	НВ	NB		SB>NB	HB>NB	NB>NB		SB	НВ	NB
13	NB	SB	НВ		NB>NB	SB>NB	HB>NB		NB	SB	НВ
14	НВ	NB	SB		HB>NB	NB>NB	SB>NB		НВ	NB	SB
15	SB	НВ	NB		SB>NB	HB>NB	NB>NB		SB	НВ	NB
16	NB	SB	НВ		NB>NB	SB>NB	HB>NB		NB	SB	НВ
17	НВ	NB	SB		HB>NB	NB>NB	SB>NB		НВ	NB	SB
18	SB	НВ	NB		SB>NB	HB>NB	NB>NB		SB	НВ	NB
19	NB	SB	НВ		NB>NB	SB>NB	HB>NB		NB	SB	НВ
20	НВ	NB	SB		HB>NB	NB>NB	SB>NB		НВ	NB	SB
21	SB	НВ	NB		SB>NB	HB>NB	NB>NB		SB	НВ	NB
Note: S	Subject	s part	icipate	ed in a	a maximui	n of one e	xperiment	al ses	sion _l	oer da	ay.

A.10. Equations for calculating ride values

This section provides details of the equations used to calculate the ride values listed in this thesis. W_d , W_e and W_b correspond to the frequency weightings given in ISO 2631-1 (1997).

Equation A.10.1. Seat lateral (SL) =
$$a_y$$
 at seat surface $\times W_d$

where SL is lateral acceleration at the seat surface multiplied by the frequency weighting W_d .

Equation A.10.2. Seat roll (RL) =
$$a_{Ry}$$
 at seat surface $\times W_e \times 0.63$

where RL is roll acceleration at the seat surface multiplied by the frequency weighting W_e .

Equation A.10.3. Back lateral (BL) =
$$a_y$$
 at seat surface $\times W_d \times 0.5$

where BL is lateral acceleration at the backrest multiplied by the frequency weighting W_d .

Equation A.10.4. Back tangential
$$(BT) = a_{ty}$$
 at seat surface $\times W_d \times 0.5$

where BT is tangential lateral acceleration at the backrest, caused by rotation about the seat surface, multiplied by the frequency weighting W_d .

Equation A.10.5. Feet lateral
$$(FL) = a_y$$
 at feet $\times W_b \times 0.25$

where FL is lateral acceleration at the backrest multiplied by the frequency weighting W_b .

Equation A.10.6. Feet tangential
$$(FT) = a_{ty}$$
 at feet $\times W_b \times 0.25$

where FT is tangential lateral acceleration at the backrest, caused by rotation about the seat surface, multiplied by the frequency weighting W_b .

Equation A.10.6. Ride value (RSS) =
$$\sqrt{SL^2 + SR^2 + BL^2 + BT^2 + FL^2 + FT^2}$$

where the ride value is equal to the root-sums-of-squares of the six components (*SL*, *SR*, *BL*, *BT*, *FL*, *FT*).

A.11. Normalisation procedures

This section provides additional detail on the procedure used to normalise subjective magnitude estimates in Experiment 4 and 5 (Chapter 7 and Chapter 8). The data handling procedure is defined below in four steps. Figure A.11.1 and Figure A.11.2 show an example work through of these four steps using nominal data for 2 dummy subjects.

STEP 1

- For each subject, for each direction and for each frequency of oscillation, perform a
 separate linear regression on the logarithm of the subjective magnitude estimates
 (Log₁₀(Ψ)) and the logarithm of the acceleration magnitudes (Log₁₀(φ)).
- Use the resulting exponent (n) and constant (k) values, calculate the subjective magnitude (Ψ) which corresponds to the chosen reference (in this case, 0.5 Hz lateral oscillation at 0.2 ms⁻² r.m.s.
 - o i.e. $\Psi = k \times 0.2^n$
- Use the resulting value of Ψ to calculate a correction factor (*CF*) for normalisation.
 - o i.e. $CF = 100/\Psi$
- Calculate normalised subjective magnitude estimates (Ψ_n), by applying the correction factor to all subjective magnitude estimates for that subject, such that the reference motion (i.e. 0.5 Hz, 0.2 ms⁻² r.m.s. lateral oscillation) corresponds to a value of 100.

o i.e.
$$\Psi_n = CF \times \Psi$$

STEP 2

- For each subject, for each direction and for each frequency of oscillation, perform a separate linear regression on the logarithm of the **normalised** subjective magnitude estimates (Log₁₀(Ψ_n)) and the logarithm of the acceleration magnitudes (Log₁₀(φ)).
- Use the resulting exponent (n) and constant (k) values, calculate the acceleration magnitude (φ) which corresponds to a subjective magnitude of 100.

o i.e.
$$\varphi = (100/k) \wedge (1/n)$$

STEP 3

 Within each frequency and direction of oscillation, across all subjects, calculate the median acceleration magnitude (φ) which corresponds to a subjective magnitude (Ψ) of 100.

STEP 4

Use the median values of φ to plot equivalent comfort contours for each frequency and direction of oscillation.

						! ! !		ST	EP 1		
Raw data for two subjects						Normalisation procedure					
Subject no.	Frequency (Hz)	Acceleration magnitude, ms ⁻² r.m.s. (φ)	Discomfort magnitude (Ψ)	Log ₁₀ (φ)	Log₁₀(Ψ)	Exponent (n)	Intercept (Log 10(k))	k = 10^(Log ₁₀ (k))	Reference $(\varphi) = 0.2$, $\Psi = ?$	Correction factor (CF = 100 / Ψ)	Normalised discomfort magnitude (Ψ _n = Ψ * CF)
		0.08	25			!					13
		0.1	40			ļ					21
		0.125	75			i					39
1	0.4	0.16	90			Correction	factor calcul	lated based on	chosen refe	rence of 0.5	47
1	0.4	0.2	95			i	H	z, 0.2 ms ⁻² r.m.	.s. \		50
		0.25	120			!			\	Ī	63
		0.315	140			ł					73
		0.4	180			i					94
		0.08	30	-1.097	1.477		2.857	719.890	191	0.52	16
		0.1	50	-1.000	1.699	i					26
		0.125	75	-0.903	1.875	2.000 2.041 0.823					39
1	1 0.5	0.16	100	-0.796	2.000						52
'	0.5	0.2	110	-0.699	2.041						58
		0.25	150	-0.602	2.176						78
		0.315	180	-0.502	2.255	ī					94
		0.4	220	-0.398	2.342	!					115
		0.08	25			i					16
		0.1	40			!					26
		0.125	75								48
2	0.4	0.16	90			Correction	57				
2	0.4	0.2	95			Hz, 0.2 ms ⁻² r.m.s.					61
		0.25	120								77
		0.315	140			<u> </u>	\				
		0.4	180			<u>i</u>			\		115
		0.08	50	-1.097	1.699	!			1	$\overline{}$	32
		0.1	90	-1.000	1.954	ŀ				\	57
		0.125	100	-0.903	2.000	<u>i</u>				🔏 [64
2	0.5	0.16	145	-0.796	2.161	0.970	2.873	745.910	157	0.64	93
4	0.5	0.2	150	-0.699	2.176	0.970	2.073	745.910	137	0.04	96
		0.25	190	-0.602	2.279	2.279				[121
		0.315	220	-0.502	2.342	i		1		1	140
		0.4	300	-0.398	2.477	Ì	l	l	l	i [191

Figure A.11.1 Data handling procedure used for constructing equivalent comfort contours (part 1). [Worked example using nominal data for two dummy subjects].

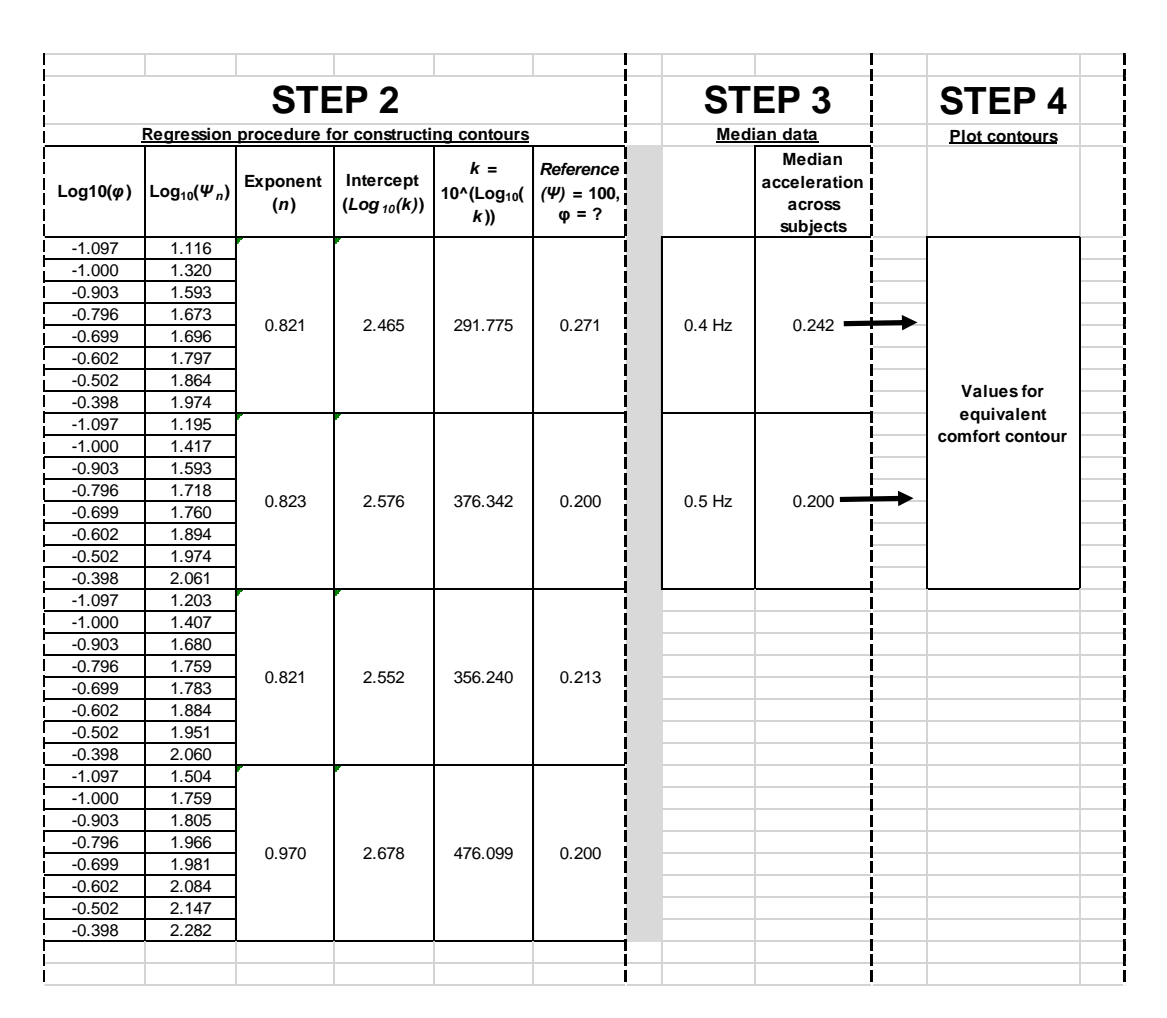


Figure A.11.2 Data handling procedure used for constructing equivalent comfort contours (part 2). [Worked example using nominal data for two dummy subjects].

References

Abdul-Jalil, N.A. and Griffin, M.J. (2007). Fore-and-aft transmissibility of backrests: effect of backrest inclination, seat-pan inclination, and measurement location. Journal of Sound and Vibration, 299, 99-108.

Basri, B. and Griffin, M.J. (2011). The vibration of inclined backrests: perception and discomfort of vibration applied normal to the back in the x-axis of the body. Journal of Sound and Vibration, 330, 4646-4659.

Basri, B. and Griffin, M.J. (2012). Equivalent comfort contours for vertical seat vibration: effect of vibration magnitude and backrest inclination. Ergonomics. DOI: 10.1080/00140139.2012.678390.

Beard, G.F. and Griffin, M.J. (2012a). Motion sickness caused by roll-compensated lateral acceleration: effects of centre-of-rotation and subject demographics. Proceedings of the Institution of Mechanical Engineers, Part F: Journal of Rail and Rapid Transit. DOI: 10.1177/0954409712460981.

Beard, G.F. and Griffin, M.J. (2012b). Discomfort during lateral acceleration: Influence of seat cushion and backrest. Applied Ergonomics. http://dx.doi.org/10.1016/j.apergo.2012.11.009.

Beard, G.F. and Griffin, M.J. (2012c). Discomfort caused by low frequency lateral oscillation, roll oscillation, and fully roll-compensated lateral oscillation. Ergonomics. DOI: 10.1080/00140139.2012.729613.

Bos, J.E. and Bles, W. (2002). Theoretical considerations on canal-otolith interaction and an observer model. Biological Cybernetics, 86, 191-207.

Bos, J.E., Damala, D., Lewis, C., Ganguly A. and Turan, O. (2007). Susceptibility to seasickness. Ergonomics, 50 (6), 890-901.

Branton, P. (1984). Backshapes of seated persons – how close can the interface be designed? Applied Ergonomics, 15 (2), 105-107.

Brett, M.W. and Griffin, M.J. (1991). Effect of height of backrest support on head motion during exposure to low frequency lateral vibration. In, Proceedings of the Ergonomics Society's 1991 Annual Conference, Southampton, England, 16-19 April 1991.

British Standards Institution. (1987). Measurement and evaluation of human exposure to whole-body mechanical vibration and repeated shock. BS 6841. British Standards Institution, London.

British Standards Institution. (1995). Acoustics. Frequency weighting "A" for noise measurement BS ISO 10845. British Standards Institution, London.

British Standards Institution. (2004). Acoustics—Determination of Sound Emission from Sound Sources Placed Close to the Ear—Part 2: Technique Using a Manikin. BS EN ISO 11904-2. British Standards Institution, London.

British Standards Institution. (2008). Flexible cellular polymeric materials – Determination of hardness (indentation technique). BS EN ISO 2439. British Standards Institution, London.

British Standards Institution. (2009). Railway applications. Ride comfort for passengers. Measurement and evaluation. BS EN 12299. British Standards Institution, London.

Bromberger, L. (1996). Pourquoi vous avez mal au coeur. La Vie du Rail, 2556. Paris, France

Butler, C.A. (2008). Motion sickness with fore-and-aft and pitch oscillation: Effect of visual scene. PhD Thesis, University of Southampton, Southampton, United Kingdom.

Butler, C.A. and Griffin, M.J. (2006). Motion sickness during fore-and-aft oscillation: Effect of the visual scene. Aviation, Space and Environmental Medicine, 77, 1236-1243.

Carcone, S.M. and Keir, P.J. (2007). Effects of backrest design on biomechanics and comfort during seated work. Applied Ergonomics. 38, 755-764.

Coelho, D.A. and Dahlman, S. (1999). A pilot evaluation of car seat side support; Leading to a redefinition of the problem. International Journal of Industrial Ergonomics, 24, 201-210.

Cohen, B., Dai, M., Ogorodnikov, D., Laurens, J., Raphan, T., Muller, P., Athanasios, A., Edmaier, J., Grossenbacher, T., Stadtmuller, K., Brugger, U., Hauser, G. and Straumann, D. (2011). Motion sickness on tilting trains. The FASEB Journal: Research Communication, 25, 3765-3774.

Corbridge, C. and Griffin, M.J. (1986). Vibration and comfort: vertical and lateral motion in the range 0.5 to 5.0 Hz. Ergonomics, 29 (2), 249-272.

Corlett, E.N. and Eklund, J.A.E. (1984). How does a backrest work? Applied Ergonomics. 15 (2), 11-114.

Crowell, B. (1998). Light and Matter. Fullerton: California.

Darwin, E. (1796). Zoonomia; or, The laws of organic life. Volume 1, Second Edition. Retrieved 1 September 2012, from: http://www.gutenberg.org/files/15707/15707-h/15707-h.htm#sect_VII

Donati, P., Grosjean, A., Mistrot, P. and Roure, L. (1983). The subjective equivalence of sinusoidal and random whole-body vibration in the sitting position (an experimental study using the 'floating reference vibration' method). Ergonomics 26, 251–273.

Donohew, B.E. (2006). Motion sickness with lateral and roll oscillation. PhD Thesis, University of Southampton, Southampton, United Kingdom.

Donohew, B.E. and Griffin, M.J. (2004). Motion sickness: Effect of the frequency of lateral oscillation. Aviation, Space and Environmental Medicine, 75, 649-656.

Donohew, B.E. and Griffin, M.J. (2007). Low frequency motions and motion sickness on a tilting train. Proceedings of the Institution of Mechanical Engineers, Part F: Journal of Rail and Rapid Transit, 221, 125-133.

Donohew, B.E. and Griffin, M.J. (2009). Motion sickness with fully roll-compensated lateral oscillation: Effect of oscillation frequency. *Aviation, Space and Environmental Medicine*, 80, 94-101.

Donohew, B.E. and Griffin, M.J. (2010). Motion sickness with combined lateral and roll oscillation: effect of percentage compensation. Aviation, Space and Environmental Medicine, 81 (1), 22-29.

Ebe, K. and Griffin, M.J. (2000a). Qualitative models of seat discomfort including static and dynamic factors. Ergonomics, 43 (6), 771-790.

Ebe, K. and Griffin, M.J. (2000b). Quantitative prediction of overall seat discomfort. Ergonomics. 43 (6), 791-806.

Fairley, T.E. and Griffin, M.J. (1988). Predicting the discomfort caused by simultaneous vertical and fore-and-aft whole-body vibration. Journal of Sound and Vibration, 124 (1), 141-156.

Fairley, T.E. and Griffin, M.J. (1990). The apparent mass of the seated human body in the fore-and-aft and lateral directions. Journal of Sound and Vibration, 139 (2), 299-306.

Farah, G., Petit-Boulanger, C., Hewson, D.J. and Duchêne, J. (2006). Surface electromyography as a tool to assess the responses of car passengers to lateral accelerations. Part II: Objective comparison of vehicles. Journal of Electromyography and Kinesiology. 16 (6), 677-684.

Finley, J.C. Jr., O'Leary, M., Wester, D., MacKenzie, S., Shepard, N., Farrow, S. and Lockette W. (2004). A genetic polymorphism of the alpha2-adrenergic receptor increases autonomic responses to stress. Journal of Applied Physiology, 96 (6), 2231-2239.

Forta, N.G., Schust, M., von Lewis, P., Kaiser, H. and Kreisel, A. (2012). Subjective comfort of fore-and-aft whole-body vibration measured with the cross-modality matching method. Presented at the 47th United Kingdom Conference on Human Responses to Vibration, held at ISVr, University of Southampton, Southampton, England, 17-19 September 2012.

Förstberg, J. (2000). *Ride comfort and motion sickness in tilting trains: Human responses to motion environments in train experiment and simulator experiments*. TRITA-FKT Report 2000:28. Stockholm: KTH Railway Technology.

Förstberg, J., Andersson, E. and Ledin, T. (1998). Influence of different conditions for tilt compensation on symptoms of motion sickness in tilting trains. Brain Research Bulletin, 47 (5), 525-535.

Fothergill, L.C. and Griffin, M.J. (1977). The evaluation of discomfort produced by multiple frequency whole-body vibration. Ergonomics, 20 (3), 263-276.

Gallais, C.H.R. (2007). Effect of the frequency of fore-and-aft sinusoidal whole-body vibration on neck muscle activity. Presented at the 42nd United Kingdom Conference on Human Responses to Vibration, held at ISVR, Southampton, Hampshire, England, 10-12 September 2007.

Goldberg, J. M. and Fernández, C. (2011). The Vestibular System. Comprehensive Physiology. 977–1022. Retrieved, 14 August 2012, from:

http://www.comprehensivephysiology.com/WileyCDA/CompPhysArticle/refld-cp010321.html

Golding, J.F. (1998). Motion sickness susceptibility questionnaire revised and its relationship to other forms of sickness. Brain Research Bulletin, 47 (5), 507-516.

Golding, J.F. and Kerguelen, M. (1992). A comparison of the nauseogenic potential of low-frequency vertical versus horizontal linear oscillation. Aviation, Space and Environmental Medicine, 63, 491-497.

Golding, J.F. and Markey, H.M. (1996). Effect of frequency of horizontal linear oscillation on motion sickness and somatogravic illusion. Aviation, Space and Environmental Medicine, 67, 121-126.

Golding, J.F., Bles, W., Bos, J.E., Haynes, T. and Gresty, M.A. (2003). Motion sickness and tilts of the inertial force environment: Active suspension systems vs. active passengers. Aviation, Space and Environmental Medicine, 74, 220-227.

Golding, J.F., Finch, M.I. and Stott, J.R.R. (1997). Frequency effect of 0.35-1.0 Hz horizontal translational oscillation on motion sickness and the somatogravic illusion. Aviation, Space and Environmental Medicine, 68, 396-402.

Golding, J.F., Markey, H.M. and Stott, J.R.R. (1995). The effects of motion direction, body axis, and posture on motion sickness induced by low frequency linear oscillation. Aviation, Space and Environmental Medicine, 66, 1046-1051.

Golding, J.F., Mueller, A.G. and Gresty, M.A. (2001). A motion sickness maximum around the 0.2 Hz frequency range of horizontal translational oscillation. Aviation, Space and Environmental Medicine, 72, 188-92.

Green, D.M. and Luce, R.D. (1974). Variability of magnitude estimates: A timing theory analysis. Perception and psychophysics. 15 (2). 291-300.

Griffin, M.J. (1975). Vertical vibration of seated subjects: effects of posture, vibration level, and frequency. Aviation, Space and Environmental Medicine, 46 (3), 269-276.

Griffin, M.J. (1990). Handbook of human vibration. London: Academic Press.

Griffin, M.J. (2007). Discomfort from feeling vehicle vibration. *Vehicle System Dynamics*, 45 (7), 679-698.

Griffin, M.J. and Howarth, H.V.C. (2000). Motion sickness history questionnaire. Institute of Sound and Vibration Research Technical Report No. 283. Institute of Sound and Vibration Research, University of Southampton, England.

Griffin, M.J. and Mills, K.L. (2002a). Effect of frequency and direction of horizontal oscillation on motion sickness. Aviation, Space and Environmental Medicine, 73 (6), 537-543.

Griffin, M.J. and Mills, K.L. (2002b). Effect of magnitude and direction of horizontal oscillation on motion sickness. Aviation, Space and Environmental Medicine, 73 (7), 640-646.

Griffin, M.J. and Whitham, E.M. (1980). Discomfort produced by impulsive whole-body vibration. Journal of Acoustical Society of America, 68 (5), 1277-1284.

Griffin, M.J., Parsons, K.C. and Whitham, E.M. (1982b). Vibration and comfort IV. Application of experimental results, Ergonomics, 25 (7), 721–739.

Griffin, M.J., Whitham, E.M. and Parsons, K.C. (1982a). Vibration and comfort I. Translational seat vibration, Ergonomics, 25 (8), 603–630.

Hacaambwa, T.M. and Giacomin, J. (2007). Subjective response to seated fore-and-aft direction whole-body vibration. International Journal of Industrial Ergonomics, 37, 61-72.

Harris, N.R., Schmid, F. and Smith, R.A. (1998). Introduction: theory of tilting train behaviour. Proceedings of the Institution of Mechanical Engineers, Part F: Journal of Rail and Rapid Transit, 212 (1), 1-5.

Haslwanter, T. (2008). Vestibular system. Retrieved 16 Aug 2012, from: http://commons.wikimedia.org/wiki/File:VestibularSystem.gif

Heeger, D.J. and Simoncelli, E.P. (1993). Model of visual motion sensing. In, Harris, L. and Jenkin, M. (Eds.), Spatial Vision in Humans and Robots, 267-392. Cambridge University Press.

Helander, M., Czaja, S., Drury, C., Cara, J. and Burri, G. (1987). An ergonomic evaluation of office chairs. Office: Technology and People. 3, 247–262.

HFRU. (2012a). Tilting and translating cabin. Human Factors Research Unit. Retrieved 1 Jul 2012, from: http://www.southampton.ac.uk/hfru/lab_facilities/low_frequency.html

HFRU. (2012b). 1-m horizontal simulator. Human Factors Research Unit. Retrieved 1 Jul 2012, from: http://www.southampton.ac.uk/hfru/lab facilities/horizontal vibrator.html

HFRU. (2012c). 6-axis simulator. Human Factors Research Unit. Retrieved 1 Jul 2012, from: http://www.southampton.ac.uk/hfru/lab_facilities/6_axis.html

Hitachi. (2009). Comparison between the Japanese and European system. Retrieved 4 April 2010, from http://www.hitachi-rail.com/products/rv/tilting/features/index 5.html.

Holmes, S.R. (1996) Heart rate variability as a predictor of individual motion sickness susceptibility on exposure to yaw oscillation. Paper presented at the UK Informal Group Meeting on Human Response to Vibration held at MIRA, England, 18th - 20th September.

Holmes, S.R. (1997) Electrogastric activity during a control condition and as a measure of motion sickness on exposure to yaw oscillation. Paper presented at the UK Informal Group Meeting on Human Response to Vibration held at ISVR, University of Southampton, England, 17th - 19th September.

Holmes, S.R. (1998) Heart rate and motion sickness incidence during exposure to nauseogenic optokinetic stimulation. Paper presented at the UK Informal Group Meeting on Human Response to Vibration held at the Health and Safety Executive, Buxton, Derbyshire, England, 16th - 18th September.

Horseman, B.G., Macauley, M.W.S. and Barnes, W.J.P. (2011). Neuronal processing of translational optic flow in the visual system of the shore crab Carcinus maenas. Journal of Experimental Biology, 214, 1586-1598.

Howarth, H.V.C. (1999) Laboratory study of the effect of frequency of roll motion on motion sickness. Paper presented at the United Kingdom Group Meeting on Human Response to Vibration held at Ford Motor Company, Dunton, Essex, England, 22th - 24th September.

Howarth, H.V.C. and Griffin, M.J. (2003). Effect of roll oscillation frequency on motion sickness. Aviation, Space and Environmental Medicine, 74, 326-331.

Howarth, H.V.C., Martino, M.M. and Griffin, M.J. (1999) Laboratory study of the effect of visual scene on motion sickness caused by lateral oscillation. Paper presented at the United Kingdom Group Meeting on Human Response to Vibration held at Ford Motor Company, Dunton, Essex, England, 22nd - 24th September.

International Organization for Standardization. (1997). Mechanical vibration and shock - evaluation of human exposure to whole-body vibration - Part 1: General requirements. International Standard, ISO 2631-1.

International Organization for Standardization. (2005). Human response to vibration – Measuring instrumentation. EN ISO 8041.

Jacobson, G.P., Newman, C.W. and Kartush, J.M. (1993). Handbook of Balance Function Testing. London: Singular Publishing Group, Inc.

Jang, H.K. and Griffin, M.J. (1999). The effect of phase of differential vertical vibration at the seat and feet on discomfort. Journal of Sound and Vibration, 223 (5), 785-794.

Jang, H.K. and Griffin, M.J. (2000). Effect of phase, frequency, magnitude and posture on discomfort associated with differential vertical vibration at the seat and feet. Journal of Sound and Vibration, 229 (2), 273-286.

Joseph, J.A. (2008). Motion sickness with Earth-horizontal translational and rotational oscillation presented in isolation and in combination. PhD Thesis, University of Southampton, Southampton, United Kingdom.

Joseph, J.A. and Griffin, M.J. (2007). Motion sickness from combined lateral and roll oscillation: Effect of varying phase relationships. Aviation, Space and Environmental Medicine, 78 (10), 944-950.

Joseph, J.A. and Griffin, M.J. (2008a). Motion sickness: Effect of magnitude of roll and pitch oscillation. Aviation, Space and Environmental Medicine, 79 (4), 390-396.

Joseph, J.A. and Griffin, M.J. (2008b). Motion sickness: Effect of changes in magnitude of combined lateral and roll oscillation. Aviation, Space and Environmental Medicine, 79 (11), 1019-1027.

Kamp, I., Kilincsoy, Ü. and Vink, P. (2011). Chosen postures during specific sitting activities. Ergonomics, 54 (11), 1029-1042.

Kaplan, I. (1964). Motion sickness on railroads. Industrial Medicine and Surgery, 33, 648-651.

Kennedy, R.S., Dunlap, P. and Fowlkes, J.E. (1990). Prediction of motion sickness susceptibility: A taxonomy and evaluation of relative predictor potential. In: Crampton, G.H., (ed.), Motion and space sickness (pp. 179-215). Boca Raton, FL: CRC Press.

Klauser, P. (2005). Operating at high cant deficiency. The Journal of Wheel/Rail Interaction. Retrieved 16 August 2011, from: http://www.interfacejournal.com/features/09-05/cant/1.html

Klosterhalfen, S., Kellerman, S., Pan, F., Stockhorst, U., Hall, G. and Enck, P. (2005). Effects of ethnicity and gender on motion sickness susceptibility. Aviation, Space and Environmental Medicine, 76 (11), 1051-1057.

Klosterhalfen, S., Pan, F., Kellerman, S. and Enck, P. (2006). Gender and race as determinants of nausea induced by circular vection. Gender Medicine, 3 (3), 236-242.

Kyung, G. and Nussbaum, M.A. (2008). Driver sitting comfort and discomfort (part II): Relationships with and prediction from interface pressure. International Journal of Industrial Ergonomics, 38, 526-538.

Kyung, G., Nussbaum, M.A. and Babski-Reeves, K. (2008). Driver sitting comfort and discomfort (part I): Use of subjective ratings in discriminating car seats and correspondence among ratings. International Journal of Industrial Ergonomics, 38, 516-525.

Lawther, A. and Griffin, M.J. (1986). The motion of a ship at sea and the consequent motion sickness amongst passengers. Ergonomics, 29 (4), 535-552.

Lawther, A. and Griffin, M.J. (1987). Prediction of the incidence of motion sickness from the magnitude, frequency, and duration of vertical oscillation. Journal of Acoustical Society of America, 82 (3), 957-966.

Lawther, A. and Griffin, M.J. (1988). A survey of the occurrence of motion sickness amongst passengers at sea. Aviation, Space and Environmental Medicine, 59, 399-406.

Lawther, A. and Griffin, M.J. (1989). Studies of the individual variability in susceptibility to motion sickness. ISVR Technical Memorandum, No 687. University of Southampton, Southampton, United Kingdom.

Liu, L., Yuan, L., Wang, H.B., Yu, L.S., Zheng, J., Luo, C.Q., and Wang, Y. (2002). The human alpha (2A)-AR gene and the genotype of site -1296 and the susceptibility to motion sickness [In Chinese]. Sheng Wu Hua Xue Yu Sheng Wu Wu Li Xue Bao (Shanghai), 34 (3), 291⁻²97.

Lobb, B. (1999) Effect of waveform of lateral motion on motion sickness: a comparison of sinusoidal and octave band random motion waveforms. Paper presented at the United Kingdom Group Meeting on Human Response to Vibration held at Ford Motor Company, Dunton, Essex, England, 22nd - 24th September.

Mandapuram, S.C., Rakheja, S., Ma, S., Demont, R.G. and Boileau, P. (2005). Influence of back support conditions on the apparent mass of seated occupants under horizontal vibration. Industrial Health, 43, 421-435.

Matsumoto, Y., Griffin, M.J. (2005) Nonlinear subjective and biodynamic responses to continuous and transient whole-body vibration in the vertical direction. Journal of Sound and Vibration, 287 (4-5), 919-937.

McCauley, M. E., Royal, J. W., Wylie, C. D., O'Hanlon, J. F., and Mackie, R. R. (1976). Motion sickness incidence: exploratory studies of habituation, pitch and roll, and the refinement of a mathematical model. Human Factors Research Inc. Technical Report 1733-2.

Mellers, B.A. (1983) Evidence against "absolute" scaling. Perception and Psychophysics, 33 (6), 523-526.

Mills, K.L. and Griffin, M.J. (2000). Effect of seating, vision and direction of horizontal oscillation on motion sickness. Aviation, Space and Environmental Medicine, 71, 996-1002.

Miwa, T. (1967). Evaluation methods for vibration effect. I. Measurements of threshold and equal sensation contours of whole-body for vertical and horizontal vibrations. Industrial Health, 5, 183–205.

Money, K.E. (1970). Motion sickness. Physiology Review, 50, 1-39.

Morioka, M. and Griffin, M.J. (2006a). Magnitude-dependence of equivalent comfort contours for fore-and-aft, lateral and vertical whole-body vibration. Journal of Sound and Vibration, 298, 755-772.

Morioka, M. and Griffin, M.J. (2006b). Magnitude-dependence of equivalent comfort contours for hand-transmitted vibration in three axes. Journal of Sound and Vibration, 295, 633–648.

Moxley, P.R., Morioka, M. and Griffin, M.J. (2011). Discomfort during lateral whole-body vibration: influence of seat pan form. Presented at the 46th United Kingdom Conference on Human Response to Vibration, held at the Health and Safety Laboratory and the Health and Safety Executive, Buxton. 20 - 22 September 2011.

Moxley, P.R., Morioka, M. and Griffin, M.J. (2012). On the importance of vision in determining perception thresholds for whole-body vibration in the fore-and-aft and lateral axes. Presented at the 47th United Kingdom Conference on Human Responses to Vibration, held at ISVR, University of Southampton, Southampton, England, 17 - 19 September 2012.

NASA. (2002). The effects of space flight on the human vestibular system. National Aeronautics and Space Administration. Retrieved 1 Aug 2012 from:

http://weboflife.ksc.nasa.gov/learningResources/humanVestibularSystem.htm

NDBC. (2012). National Dizzy and Balance Center - Anatomy of the Vestibular System.

Retrieved 1 Aug 2012 from: http://www.stopdizziness.com/resources_vestibular_anatomy.asp

Neimer, J., Eskiizmirliler, S., Dominey-Ventre, J. and Darlot, C. (2001). Trains with a view to sickness. Current Biology, 11 (14), R549–R550.

O'Hanlon, J.F. and McCauley, M.E. (1973). Motion sickness incidence as a function of the frequency and acceleration of vertical sinusoidal motion. Technical Report, Office of Naval Research, Goleta, CA, United States of America: Human Factors Research, Inc.

Oborne, D.J. (1976). Examples of the use of rating scales in ergonomics research. Applied Ergonomics, 7 (4), 201-204.

Oborne, D.J. (1978a). The stability of equal sensation contours for whole-body vibration. Ergonomics, 21, 651–658.

Oborne, D.J. (1978b). Techniques available for the assessment of passenger comfort. Applied Ergonomics, 9 (1), 45-49.

Oborne, D.J. (1978c). The ergonomics of passenger comfort: Passenger comfort – an overview. Applied Ergonomics, 9 (3), 131-136.

Oborne, D.J. (1978d). Vibration and passenger comfort: Can data from subjects be used to predict passenger comfort? Applied Ergonomics, 9 (3), 155-161.

Oborne, D.J. and Boarer, P.A. (1982). Subjective response to whole-body vibration: The effects of posture. Ergonomics, 25 (7), 673-681.

Oborne, D.J. and Clarke, M.J. (1975). The effect of rating scale parameters on the assessment of vibration intensity. Ergonomics, 18 (1), 67-79.

Oborne, D.J., Boarer, P. and Heath, T.O. (1981). Variations in response to whole-body vibration: intensity dependent effects. Ergonomics, 24 (7), 523-530.

Oborne, D.J., Heath, T.O. and Boarer, P. (1981). Variation in human response to whole-body vibration. Ergonomics, 19, 719-726.

Osborne, J. and Waters, E. (2002). Four assumptions of multiple regression that researchers should always test. *Practical Assessment, Research & Evaluation*, 8 (2). Retrieved September 5, 2012 from http://PAREonline.net/getvn.asp?v=8&n=2

Paddan, G.S. and Griffin, M.J. (1988). The transmission of translational seat vibration to the head – II. Horizontal seat vibration. Journal of Biomechanics, 21 (3), 199-206.

Paddan, G.S. and Griffin, M.J. (1992). Transmission of roll and pitch seat vibration to the head. Ergonomics, 37, 1513-1531.

Paddan, G.S., Mansfield, N.J., Arrowsmith, C.I., Rimell, A.N., King, S.K. and Holmes, S.R. (2012). The influence of seat backrest angle on perceived discomfort during exposure to vertical whole-body vibration. Ergonomics. DOI:10.1080/00140139.2012.684889.

Park, S., Gianna-Poulin, C., Black, F.O., Wood, S. and Merfeld, D.M. (2006). Roll rotation cues influence roll tilt perception assayed using a somatosensory technique. Journal of Neurophysiology, 96, 486-491.

Parsons, K.C. and Griffin, M.J. (1978). The effect of the position of the axis of rotation on the discomfort caused by whole-body roll and pitch vibrations of seated persons. Journal of Sound and Vibration, 58 (1), 127-141.

Parsons, K.C. and Griffin, M.J. (1982). Vibration and comfort. II. Rotational seat vibration. Ergonomics, 25 (7), 631-644.

Parsons, K.C., Griffin, M.J. and Whitham, E.M. (1982). Vibration and comfort. III. Translational vibration of the feet and back. Ergonomics, 25 (8), 705-719.

Persson, R. (2008). Tilting trains: Technology, benefits and motion sickness. Licentiate thesis, Royal Institute of Technology (KTH), Stockholm, Sweden.

Persson, R. (2010). Tilting trains: Benefits and motion sickness. *Proceedings of the Institution of Mechanical Engineers, Part F: Journal of Rail and Rapid Transit*, 224, 513-522.

Persson, R., Goodall, R.M., and Sasaki, K. (2009). Carbody tilting – technologies and benefits. Vehicle System Dynamics, 47 (8), 949-981.

Pheasant, S. (1996). Bodyspace: anthropometry, ergonomics and the design of work, Second ed. London: Taylor and Francis.

Porter, J.M., Gyi, D.E. and Tait, H.A. (2003). Interface pressure data and the prediction of driver discomfort in road trials. Applied Ergonomics. 34, 207-214.

Reason, J.T. (1978). Motion sickness adaptation: A neural mismatch model. Journal of Royal Society of Medicine, 71, 819–829.

Reason, J.T. and Brand, J.J. (1975). Motion sickness. London: Academic Press.

Reavley, C.M., Golding, J.F., Cherkas, L.F., Spector, T.D. and MacGregor, A.J. (2006). Genetic influences on motion sickness susceptibility in adult women: A classical twin study. Aviation, Space and Environmental Medicine, 77 (11), 1148-1152.

Reid, F.R. (1991) A comprehensive study of motion sickness and its influencing factors. B.Eng. Project (Part III), ISVR, University of Southampton, England. Unpublished.

Richards, L.G. (1980). On the psychology of passenger comfort. In: Human Factors in Transport Research, D.J. Oborne, and J.A. Lewis, (Eds.), Vol. 2, pp. 15-23. London: Academic Press.

RNIB. (2011). How the eye works – Royal National Institute of Blind People. Retrieved 2 Aug 2012, from: http://www.rnib.org.uk/eyehealth/eyeconditions/pages/how_eye_works.aspx

Robertson, C.D. and Griffin, M.J. (1989). Laboratory studies of the electromyographic response to whole-body vibration. ISVR Technical Report 184. University of Southampton, Southampton UK.

Rolnick, A. and Bles, W. (1989). Performance and well-being under tilting conditions: the effects of visual reference and artificial horizon. Aviation, Space and Environmental Medicine, 60 (8), 779-785.

Ronan, P. (2007). Electromagnetic spectrum. Retrieved 1 Aug 2012, from: http://en.wikipedia.org/wiki/File:EM_spectrum.svg

Sari, M. and Griffin, M.J. (2010). Effect of hand support on discomfort or difficulty when walking and perturbed by lateral oscillation. 45th United Kingdom Conference on Human Responses to Vibration, held at Institute of Naval Medicine, Alverstoke, Gosport, PO12 2DL, England, 6 - 8 September 2010.

Seidel, H. (1988). Myoelectric reactions to ultra-low frequency and low-frequency whole body vibration. European Journal of Applied Physiology, 57, 558-562.

Schust, M., Kreisel, A., Seidel, H. and Blüthner, R. (2010). Examination of the frequency-weighting curve for accelerations measured on the seat and at the surface supporting the feet during horizontal whole-body vibrations in x- and y-directions. Industrial Health, 48, 725-742.

Schust, M., Hinz, B., Menzel, G., Pinto, I., Hofmann, J. and Bovenzi, M. (2012). Comparison of different methods for detecting multiple shocks in vibration time histories. Presented at the 47th United Kingdom Conference on Human Responses to Vibration, held at ISVR, University of Southampton, Southampton, England, 17-19 September 2012.

Society of Automotive Engineers (SAE) Standard. (2008). Devices for use in defining and measuring vehicle seating accommodation. SAE J826. Society of Automotive Engineers, Warrendale, Pennsylvania, United States of America.

Sprigle, S., Chung, K.C. and Brubaker, C.E. (1990). Reduction of sitting pressure with custom contoured cushions. Journal of Rehabilitation Research and Development, 27 (2), 135-140.

Stern, R.M., Hu, S., LeBlanc, R. and Koch, K.L. (1993). Chinese hyper-susceptibility to vection-induced motion sickness. Aviation, Space and Environmental Medicine, 64, 827-830.

Stern, R.M., Hu, S., Uijtdehaage, S.H., Muth, E.R., Xu, L.H. and Koch, K.L. (1996). Asian hypersusceptibility to motion sickness. Human Heredity, 46 (1), 7-14.

Stevens, S. S. (1975). *Psychophysics: introduction to its perceptual, neural, and social prospects*. Oxford: Transaction Publishers.

Suzuki, H. (1998a). Effects of the range and frequency of vibrations on the momentary riding comfort evaluation of a railway vehicle. Japanese Psychological Research, 40 (3), 156-165.

Suzuki, H. (1998b). Research trends on riding comfort evaluation in Japan. Proceedings of the Institution of Mechanical Engineers, Part F: Journal of Rail and Rapid Transit, 212, 61-72.

Suzuki, H. (2001). Effect of compensated lateral acceleration on the riding comfort in tilt train. Presented at the Japan Group Meeting on Human Response to Vibration held at Mito, Japan, 25-27 July 2001.

Suzuki, H., Shiroto, H. and Tezuka, K. (2005). Effect of low frequency vibration on train motion sickness. Quarterly Report of Railway Technical Research Institute, 46 (1), 35–39.

Suzuki, H., Shiroto, H., Tanaka, A., Tezuka, K. and Nakagawa, S. (1999). Effects of Vibrational Factors on the Riding Comfort Evaluation of Tilting Train Passing Curve Transitions. Proceedings of the World Congress of Railway Research, 1999, Tokyo, Japan, RTRI: Tokyo. p.42.

Suzuki, H., Shiroto, H., Tanaka, A., Tezuka, K. and Takai, H. (2000). Psychophysical evaluation of railway vibrational discomfort on curved sections. Quarterly Review of Railway Technical Research Institute, 41 (3), 106-111.

Teghtsoonian, R. and Teghtsoonian, M. (1978). Range and regression effects in magnitude scaling. Perception and Psychophysics, 24 (4), 305-314.

Thuong, O. (2011). Predicting the vibration discomfort of standing passengers in transport. PhD Thesis, University of Southampton, Southampton, United Kingdom.

Thuong, O. and Griffin, M.J. (2011). The vibration discomfort of standing persons: the effect of body supports. Proceedings of the Institution of Mechanical Engineers, Part F: Journal of Rail and Rapid Transit. 225 (2), 228-235.

Toward, M.G.R. and Griffin, M.J. (2010). Apparent mass of the human body in the vertical direction: Inter-subject variability. Journal of Sound and Vibration, 330, 827-841.

Treisman, M. (1977). Motion sickness: An evolutionary hypothesis. Science, 197, 493-495.

Tsuchitani, C. (1997). Chapter 2: Somatosensory Systems. Neuroscience Online, University of Texas Health Science Center at Houston. Retrieved 23 July 2011, from: http://neuroscience.uth.tmc.edu/s2/chapter02.html Turner, M. and Griffin, M.J. (1999a). Motion sickness in public road transport: The relative importance of motion, vision and individual differences. British Journal of Psychology, 90, 519-530.

Turner, M. and Griffin, M.J. (1999b). Motion sickness in public road transport: passenger behaviour and susceptibility. Ergonomics, 42 (3), 444-461.

Turner, M., Griffin, M.J. and Holland, I. (2000). Airsickness and aircraft motion during short-haul flights. Aviation, Space and Environmental Medicine, 71, 1181-1189.

Ueno, M., Ogawa, T., Nakagiri, S., Arisawa, T., Mino, Y., Oyama, K., Kodera, R., Taniguchi, T., Kanazawa, S., Ohta, T., and Aoyama, H. (1986). Studies on motion sickness caused by high curve speed railway vehicles. Japanese Journal of Industrial Health, 28 (4), 266-274.

Vos, G.A., Congleton, J.J., Moore, J.S., Amendola, A.A. and Ringer, L. (2006). Postural versus chair design impacts upon interface pressure. Applied Ergonomics, 37 (6), 619-628.

Webb, N.A. (1997). Comparison of vection and motion sickness in a real and virtual reality optokinetic drum. Presented at the UK Group Meeting on Human Response to Vibration held at the Institute of Sound and Vibration Research, University of Southampton, Southampton, SO17 1BJ, England, 17th -19th September 1997.

Webb, N.A. (1998). Motion sickness with normal and degraded vision. Presented at the UK Group Meeting on Human Response to Vibration held at the Health and Safety Executive, Buxton, Derbyshire, England, 16th -18th September 1998.

Webb, N.A. (1999). Motion sickness with corrected and uncorrected vision. Paper presented at the United Kingdom Group Meeting on Human Response to Vibration held at Ford Motor Company, Dunton, Essex, England, 22nd - 24th September.

Whitham, E.M. and Griffin, M.J. (1977). Measuring vibration on soft seats. Society of Automotive Engineers, SAE Paper 770253, International Automotive Engineering Congress and Exposition, Detroit, 28 February - 4 March 1977.

Whitham, E.M. and Griffin, M.J. (1978). The effects of vibration frequency and direction on the location of areas of discomfort caused by whole-body vibration. Applied Ergonomics. 9 (4), 231-239.

Woodman, P.D. and Griffin, M.J. (1997) Effect of direction of head movement on motion sickness caused by Coriolis stimulation. Aviation, Space, and Environmental Medicine, 68 (2), 93-98.

Wyllie, I.H. (2007). Effect of posture on discomfort caused by low frequency roll and pitch oscillation. Presented at the 42nd UK Conference on Human Responses to Vibration, held at ISVR, University of Southampton, Southampton, England, 10-12 September 2007.

Wyllie, I.H. (2008). The discomfort arising from exposure to low frequency rotational and translational vibration. PhD Thesis, University of Southampton, Southampton, United Kingdom.

Wyllie, I.H. and Griffin, M.J. (2007). Discomfort from sinusoidal oscillation in the roll and lateral axes at frequencies between 0.2 and 1.6 Hz. Journal of the Acoustical Society of America, 121, (5), 2644-2654.

Wyllie, I.H. and Griffin, M.J. (2009). Discomfort from sinusoidal oscillation in the pitch and fore-and-aft axes at frequencies between 0.2 and 1.6 Hz. Journal of Sound and Vibration, 324, 453-467.

Zwislocki, J.J. and Goodman, D.A. (1980). Absolute scaling of sensory magnitudes: A validation. Perception and psychophysics. 28 (1), 28-38.